DOCTOR OF PHILOSOPHY

Numerical modelling of the spatiotemporal variability of environmental factors and their influences on oil transport in a tide-dominated estuary

Eke, Chijioke David

Award date:
2020

Awarding institution:
Coventry University

Numerical Modelling of the Spatiotemporal Variability of Environmental Factors and their Influences on Oil Transport in a Tide-Dominated Estuary

By

Chijioke D. Eke

September 2019

Coventry University

A thesis submitted in partial fulfilment of the University's requirements for the Degree of Doctor of Philosophy

Content removed on data protection grounds

Certificate of Ethical Approval

Applicant:

Chijioke Eke

Project Title:

Assessing the influence of spatiotemporal variability of environmental factors on oil spill dynamics in the Humber estuary.

This is to certify that the above named applicant has completed the Coventry University Ethical Approval process and their project has been confirmed and approved as Low Risk

Date of approval:

22 October 2018

Project Reference Number:

P76065

ABSTRACT

Oil spills in estuaries are less studied and less understood than their oceanic counterparts. Despite the significant risk oil spills present to estuaries, its dynamics in estuarine environments present a gap in academic literature. To address this gap, this study undertakes a numerical analysis of the influence of environmental factors on oil spill transport in tide-dominated estuaries.

This study develops and analyses a range of numerical simulations for the Humber Estuary, uing TELEMAC3D (a coupled hydrodynamic and oil spill model). For modelling studies such as this, there are multiple combinations of variables that can be considered, however, this study focuses on the influence of seasonal fluvial discharge variations, projected climatic conditions (sea level rise and projected river flow) and varying lateral points of release on oil spill transport in tide-dominated estuaries. Consequently, the influence of other variables (e.g. sediment transport and morphology, flooding and storm events) on oil slick transport is not considered in this study.

The key findings were: (a) there is a statistically significant ($P<0.05$) difference in the influence of hydrodynamic conditions on oil slick impacted area, length and distance travelled; (b) the influence of seasonal discharge on oil slick spreading is dependent on the time of release within a tidal cycle; (c) the influence of sea level rise and projected changes in river flow on oil slick transport dynamics is relatively insignificant; (d) water current magnitude is the key determinant of the differences in dynamics between oil slicks released along the estuary length; and (e) the differences in the dynamics of oil slick released along the estuary width is strongly determined by differences in lateral

current speed and direction. It is the first time that these dynamics have been illustrated and advanced.

The implications of these findings for operational oil spill response are the need to: (a) take cognisance of time of oil release within a tidal period; (b) understand how the interaction of river discharge and tidal range influences oil slick dynamics, as this will aid responders in assessing the likely oil trajectories; (c) be aware of axial and lateral variations in current magnitude and direction in the estuary and how it affects oil slicks from a release location; (d) take cognisance of the interaction between oil slick and estuary bank and how it influences oil slicks overall travel distance; and (e) understand the interaction between oil release location, the geometry of the estuary and current magnitude and direction to effectively deal with oil slicks in a tide-dominated estuary. Considering the complexity of estuaries, findings from this study may be unique to tide-dominated estuaries.

ACKNOWLEDGEMENT

I would like to express my deepest gratitude to Jesus in whom I found the strength to complete this work.

My profound gratitude goes to my family. To my parents Graham and Gracia Eke and my siblings Ada, Ifedinma and Ruthy, for your prayers and well wishes throughout my studies, I am grateful.

To Bukola Bolade, my greatest support, thank you for your constant encouragement especially in times when it seemed like my research was at a dead end.

I would like to appreciate my supervisory team. I am exceptionally grateful to my Director of Studies, Dr Babatunde Anifowose who believed in me and my ability to successfully undertake a PhD. His continuous support and refusal to settle for less were instrumental in completing this work. I am grateful to Dr Marco Van De Wiel and Dr Michiel Knaapen who provided a wealth of knowledge in the areas of estuaries and numerical modelling. Also to Prof. Damian Lawler for his invaluable contribution.

I would like to appreciate the Faculty of Engineering, Environment and Computing, Coventry University who funded this research.

I am grateful to Hailiang Shen, Ph.D., P.Eng. for developing the script used to visualise the TELEMAC oil spill output on Blue Kenue.

I am also grateful to the Association of British Ports for the provision of Humber estuary bathymetry data; the British Oceanographic Data Centre (BODC) for provision of tidal data at Immingham station as well as salinity data; the UK Meteorological Office for wind data at Donna Nook; the UK Environmental Agency for the provision of stage data as well as water quality (temperature and salinity) data; and the Met Office Hadley Centre for provision of the UKCP18 sea level data. The data were provided on a non-commercial license. FES2014 was produced by Noveltis, Legos and CLS Space Oceanography Division and distributed by Aviso, with support from Cnes (http://www.aviso.altimetry.fr/).

TABLE OF CONTENTS

CHAPTER 1

1 INTRODUCTION

1.1 BACKGROUND

Oil spills are a source of worldwide marine pollution (Kang et al. 2016a) due to growing energy demand and consumption which drive the production of petroleum as well as marine transportation (Chen et al. 2015; Kang et al. 2016b). Oil spills cause considerable harm to the ecosystem (Bernabeu et al. 2016); as well as adverse environmental, social and economic impacts (Bernabeu et al. 2016; Kankara et al. 2016). The impacts of oil spill include damage to fisheries, water supplies, beaches and the ecosystem (Liu and Sheng 2014). Furthermore, oil spills present health hazards (Noh et al. 2019; Sharpe et al. 2019) as prolonged exposure impacts lung health (Liu et al. 2016a) and it introduces hydrocarbons which have mutagenic and carcinogenic effects (Khaustov and Redina 2012). The unpredictability of oil spills presents considerable oil spill risk around regions surrounding production platforms and along tanker routes (Vethamony et al. 2007). Considering the adverse economic, environmental and social impacts, it is no surprise that oil spills are regarded as one of the worst types of marine pollution (Guo et al. 2018). Understanding the oil travel path and oil travel time to receptors is important to mitigate the impact of oil spills (Al-Rabeh et al. 2000; Berry et al. 2012; Amir-Heidari and Raie 2018). Consequently, numerical oil spill models are employed to understand oil spill behaviour, as a way to minimize oil pollution impacts (Guo et al. 2018). An effective approach is by simulating an ensemble of hypothetical spill scenarios thereby providing a statistical measure of oil spill impact (Amir-Heidari and Raie 2018). Over the last three decades, numerous studies have employed numerical modelling tools to improve our understanding of oil slick behaviour in the marine environment (e.g. ASCE 1996; Reed et al. 1999; Wang et al. 2005; Guo and Wang 2009; Mendes et al. 2009; Berry et al. 2012; Cucco et al. 2012; Yan et al. 2012; Spaulding 2017). However, the study of oil slick behaviour in estuarine environment presents a gap in academic literature.

The estuarine environment is unique because its hydrodynamics is significantly influenced by both marine and fluvial processes (i.e. the driving forces of tide, waves and river; Dai et al. 2014; Zhang et al. 2018). Estuaries hold ecological, recreational and economic value given their free connection to the open sea and they are rich in biological and ecological resources (McLusky and Elliott 2004; Rehitha et al. 2017). As a result, estuaries are often centres of human activities, which can increase the risk of environmental problems (Woodroffe et al. 2006; Syvitski and Saito 2007). The burgeoning coastal population is expected to: further threaten estuarine ecosystem (Kennish 2002); result in deterioration of wetland system, reduction of freshwater systems and coastal flooding; and alter hydrodynamic processes, environmental gradients and morphological patterns (Syvitski 2008; Zhu et al. 2016; Zhang et al. 2017). On the other hand, estuarine processes are influenced by tidal regime and range, seasonal freshwater discharge, sea-level rise and storm-events (Pye and Blott 2014; Robins et al. 2016). Yet, there is no evidence that the influence of these interacting factors on oil slick transport have been assessed.

This study, therefore, aims to assess the spatiotemporal variability of environmental factors and present the first detailed analysis of their influence on oil spill transport focusing on a tide-dominated estuary.

1.2 RESEARCH GAP

Most estuaries, because of the services they can provide, increasingly host shipping vessels of different sizes (Pezy et al. 2017). These vessels include crude and refined oil carriers, with potential risks of oil spill during routine processes such as engine maintenance, transfer of contents, and tank cleaning (Williams et al. 2017). There is also the risk of accidents, such as grounding and collision which can be major sources of oil spill (Vidmar and Perkovič 2018; Chen et al. 2019). These raise significant concerns as oil is considered one of the most detrimental sources of anthropogenic pollution in estuaries (Kennish 2002; Anifowose et al. 2016).

Despite the significant risks that oil spills present to estuaries, a survey of oil spill literature since 1968 reveal that estuaries have received much less research attention than coastal and pelagic environments (Murphy et al. 2016). This claim was substantiated by searching the Scopus database using chosen keywords (Table 1.1). The search result yielded 10 published papers relating to numerical oil spill modelling in estuaries (Table 1.1). Review of these articles indicated that, despite the term "estuary" being featured in their titles (3 papers) or abstracts (7 papers), only Yan et al.'s (2012) study actually focused on an estuarine environment. Their paper looks at the impact of wind and time of release (with respect to peak ebb and flood) on oil spill trajectory. However, they do not consider the influence of river discharge in their study. Considering the significant risks that oil spills present to estuaries and the gap in academic literature, it is important to better understand the influences of both tidal flows and seasonal freshwater discharges on oil spill transport in estuaries. Furthermore, no known study has ever investigated has investigated (a) the impact of projected climatic conditions on oil spill transport; and (b) the influence of varying lateral points of release on oil spill transport. Hence, this study aims to bring novel understanding of:

a) the influence of the relative role of tidal currents and seasonal river flow on oil spill transport;
b) the influence of seasonal river discharge variability on oil spill transport;
c) the influence of projected climatic conditions on oil spill transport; and
d) the influence of lateral points of release on oil spill dynamics in the tide-dominated Humber Estuary.

The novelty of this study is the characterisation of the influence of environmental factors particularly seasonal fluvial discharge variations, projected climatic conditions and varying points of release on oil spill dynamics in tide-dominated estuaries. Hence, an in-depth assessment of the spatiotemporal variability of environmental factors in a tide-dominated estuary could engender answers to the following research questions:

1. How will seasonal variability of river discharge influence oil spill trajectory in a tide-dominated estuary?
2. What will be the influence of projected climatic condition on oil spill trajectory in a tide-dominated estuary?
3. How will varying lateral points of release influence oil spill trajectory in a tide-dominated estuary?

1.2.1 Study Aim and Objectives

Therefore, this study aims to assess the spatiotemporal variability of environmental factors and present the first detailed analyses of their influence on oil spill transport on water surface by focusing on a tide-dominated estuary. The objective is to:

1. examine the temporal variability of hydraulics in the Humber Estuary.
2. assess the influence of seasonal variability of river discharge on oil spill trajectory in a tide-dominated estuary using numerical modelling tools.
3. analyse the influence of projected climatic conditions (sea-level rise and projected river flow) on oil spill trajectory in a tide-dominated estuary using numerical modelling tools.
4. appraise the influence of varying lateral points of release on oil spill trajectory in a tide-dominated estuary using numerical modelling tools.

Geographically, tide-dominated estuaries (Section 2.1.4) are common around the globe (Bárcena et al. 2015). Among others, these include: Bonny Estuary, Nigeria (Dublin-Green 1994); Caravelas Estuary, Brazil (Schettini and Miranda 2010); Hudson Estuary, USA (Warner et al. 2005); Narmada Estuary, India (Bhakta et al. 2018); Pungwe Estuary; Mozambique (Nzualo et al. 2018); Seine Estuary, France (Tessier et al. 2012), Suances Estuary, Spain (Bárcena et al. 2012); and Yangtze Estuary, China (Hori et al. 2001). Fulfilling the research aim could have a worldwide impact, enabling adequate management and control, and sustainable development in tide-dominated estuaries.

Table 1.1: Summary of Scopus search results for "oil spill" and "numerical oil spill modelling" studies based on article title and abstract

Environment	Oil spill		Numerical oil spill modelling	
	Result	Keywords	Result	Keywords
Coastal	2,078	(TITLE (coastal AND "oil spill") OR ABS (coastal AND "oil spill"))	107	(TITLE (coastal AND "oil spill" AND numerical AND model) OR ABS (coastal AND "oil spill" AND numerical AND model))
Estuary	263	(TITLE (estuary AND "oil spill") OR ABS (estuary AND "oil spill"))	10	(TITLE (estuary AND "oil spill" AND numerical AND model) OR ABS (estuary AND "oil spill" AND numerical AND model))
Ocean	1,358	(TITLE (ocean AND "oil spill") OR ABS (ocean AND "oil spill"))	114	(TITLE (ocean AND "oil spill" AND numerical AND model) OR ABS (ocean AND "oil spill" AND numerical AND model))

Sea	2,078	(TITLE (sea AND "oil spill") OR ABS (sea AND "oil spill"))	194	(TITLE (sea AND "oil spill" AND numerical AND model) OR ABS (sea AND "oil spill" AND numerical AND model))

1.3 STUDY AREA – THE HUMBER ESTUARY

Tide-dominated estuaries are commonly funnel-shaped as a result, tidal energy is hypersynchronous in nature making them complex to characterise (Dalrymple and Choi 2007; Nelson et al. 2013). To meet the research aim and objectives, the Humber Estuary was adopted as the case study. Being a tide-dominated estuary with a funnel-shaped configuration, the Humber Estuary is representative of tide-dominated estuaries (Pye and Blott 2014; Wu and Parson 2019). The Humber Estuary was also considered as a suitable case study because of the availability of background data and the potential risks of an oil spill to the estuary.

The Humber Estuary, located on the northeast coast of the UK, is one of the largest estuarine systems in the UK with a mean fluvial flow of ~250 m^3/s (and high flow of 1600 m^3/s), with Q10 and Q95 (i.e. 10^{th} and 95^{th} percentile flows) of 610 and 58 m^3/s respectively, over the period 1980 – 2015 (Townend and Whitehead 2003; Fujii 2007; Robins et al. 2018). These volumes are delivered from several rivers (including the R. Trent and the R. Ouse), with a combined catchment area of 24,240 km^2 (draining approximately 20% of England's landmass) (Yamanaka et al. 2010). Several smaller rivers such as the R. Hull, R. Ancholme and R. Freshney, also discharges into the Humber Estuary. The estuary meets the North Sea at Spurn Head, located approximately 62 km downstream from the Ouse-Trent confluence at Trent Falls (Boyes and Elliott 2006) (Figure 1.1). The distance of tidal influence extends from the mouth to 120 km on the River Ouse and 147 km on the River Trent (Mitchell 2013; Skinner et al. 2015). The width of the Humber Estuary is approximately 8 km at the mouth (Spurn Head) and is less than 0.5 km upstream of Ouse-Trent confluence, making it a funnel-shaped estuary (Fujii 2007; Pye and Blott 2014). The large semi-diurnal macro-tidal estuary has a range that varies between 3.2 m (mean neap tidal range) and 6.4 m (mean spring tidal range) at Immingham, near the mouth of the Humber (Mitchell et al. 2003a; van der Wal et al. 2010). The tidally averaged water depth of the Humber Estuary varies between 3 m and 8 m in the inner estuary and at the mouth respectively (Cave et al. 2003). A summary of the characteristics of the Humber Estuary is listed in Table 1.2.

Table 1.2: Summary of the characteristics of the Humber Estuary

Parameter	**Values**
Length	Approximately 62 km (Trent Falls to Spurn Head)
Tidal extend	120 km on River Ouse 147 km on River Trent
Minimum and maximum tidal range at Immingham	3.2 m (mean neap tidal range) 6.4 m (mean spring tidal range)
Width	8 km at the mouth (Spurn Head) <0.5 km at the head (Trent Falls)
Mean freshwater flow	250 m^3/s
Mean water depth	3 m (at the tidal limit); 8 m (at the mouth)
Channel depth	11m (inner estuary); 16 m (outer estuary)

The Humber Estuary has one of the UK's biggest constellation of oil refining industries (Edwards and Winn 2006; Humber Nature Partnership 2015). In the outer Humber Estuary is the Tetney Monobuoy from which crude oil is unloaded and transferred through underground pipelines to the ConocoPhillips Ltd's Humber refinery (Cave et al. 2003). Furthermore, three marine terminal facilities, are located at the Southbank of the Humber (South Killingholme Jetty, Immingham gas jetty and Immingham oil terminal), which provide services to two oil refineries at Immingham (Humber Nature Partnership 2015). Consequently, the Humber Estuary plays host to oil tankers which berth at the oil terminals (Cave et al. 2003). In 2001, over 40 million tonnes of oil and chemicals were transported in and out of the Humber (English Nature 2003) which makes it the main east coast port for crude hydrocarbon landing in the UK (Cave 2003). The estuary thus is prone to oil spill risk, and several incidents have occurred in the past. The Sivand tanker incident, which occurred on September 1983, spilled 6,000 tonnes of Nigerian light crude into the Humber Estuary (Little 1985). Also, 46 tonnes of crude oil spills from 9 different incidents have been recorded on the Humber Estuary between 1989 and 1997 (Cave et al. 2003). These oil spill records and the presence of oil refineries and transport along the Humber Estuary highlight the significance of this study.

Several hydrodynamic models of the Humber have been developed. Falconer and Owens (1990) and Lin and Falconer (1995) developed a 2D finite-difference model to simulate suspended sediment fluxes in the Humber Estuary; Lin and Falconer (1997) developed a 3D model of the Humber estuarine flow including flooding and drying; Wu et al. (1999) developed a 3D model to simulate cohesive sediment fluxes in the Humber Estuary; ABPmer and WL|Delft Hydraulics (2002) developed a 3D hydrodynamic model to simulate the hydrodynamic conditions of the Humber Estuary. While the objectives of these studies were achieved, Falconer and Owens (1990), Lin and Falconer (1995) and Lin and Falconer (1997) study only considered the outer

Humber Estuary (i.e. from the seaward boundary to Hull region) (Figure 1.1). As a result, these models did not account for river inputs. Wu et al. (1999) study considered a wider model domain (Seaward boundary to Trent Falls), consideration was still not given to river inputs. Furthermore, these studies were carried out on a short timescale. ABPmer and WL|Delft Hydraulics (2002) study considered a single-neap cycle. A more recent study undertaken by Skinner et al. (2015) employed a 2D inertia based model with the aim of simulating tidal and storm surge hydraulics in the Humber Estuary. The current study, therefore, is the first study to employ numerical modelling tools to understand oil spill transport in the Humber Estuary.

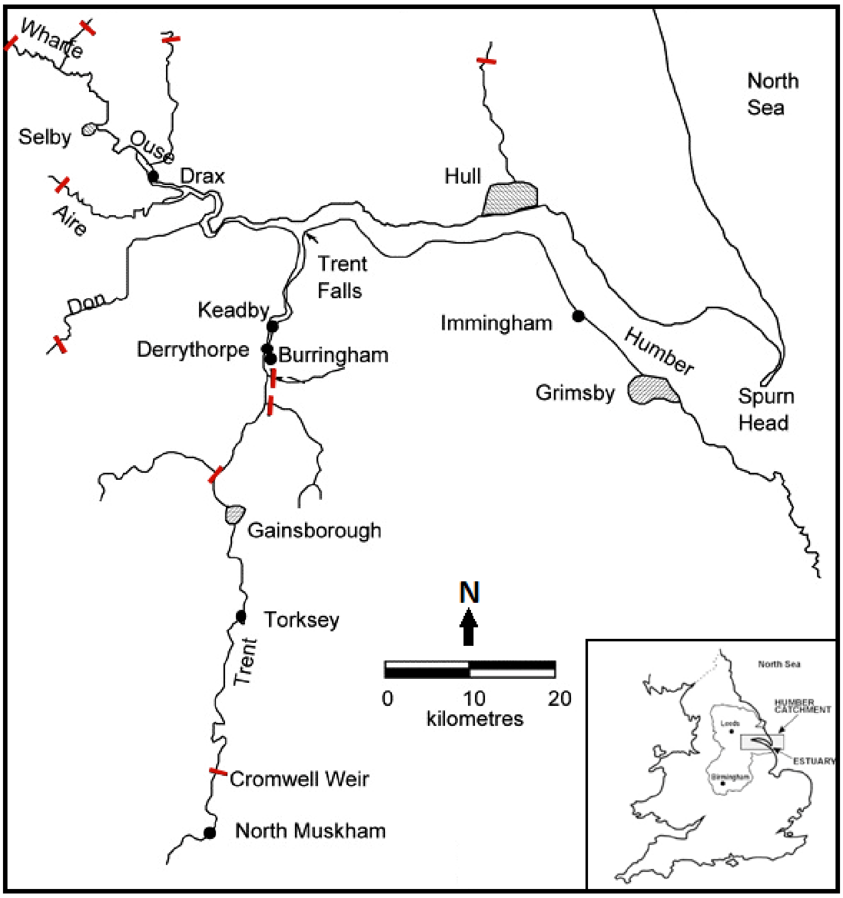

Figure 1.1: The Humber Estuary system. Inset shows the location of the Humber Estuary in the UK (Mitchell et al. 2003a; Edwards and Winn 2006). Tidal limits are indicated as red bars crossing the channel.

1.4 RESEARCH SCOPE AND ACTIVITIES

The research scope and activities, as well as the chapters in which these activities are undertaken, are highlighted and justified in Table 1.3.

Table 1.3: Scope of research activities and justification

S/N	Activities	Justification	Section
1	Classification of estuaries	This section evaluates the various classification of estuaries to highlight the diversity of estuaries and provide an indication of the environment where this study may be deemed applicable.	Chapter 2
2	Transportation of oil slicks	Oil slicks are driven by a complex transport mechanism. This section discusses the forces of advection that drive oil slick, thereby determining oil slick dynamics.	Chapter 2
3	Evaluate the weathering of oil slicks.	This section highlights the processes that possibly contribute to oil slick weathering in estuaries.	Chapter 2
4	Modelling estuarine processes	This section determines the state of the art in hydrodynamic modelling and highlights the suitability of TELEMAC3D hydrodynamic modelling tool for this study.	Chapter 2
5	Oil spill modelling.	This section discusses the state of oil spill modelling and highlights	Chapter 2

		the suitability of the TELEMAC oil spill modelling tool for this study.	
6	Assessing temporal variability of hydraulics in the Humber Estuary.	This section examines the temporal variability of environmental factors in the Humber Estuary to understand the hydraulics of the estuary and ascertain its suitability for assessing the influence of seasonal discharge variability on oil slick dynamics, thereby fulfilling objective 1.	Chapter 3
7	Assessing the influence of seasonal freshwater discharge variability on oil slick dynamics in tide-dominated estuaries.	Season variation plays a critical role in the control of estuarine hydrodynamics and processes. Furthermore, seasonal variations in river discharge are common around the globe. This chapter aims to assess the influence of seasonal freshwater discharge variation on oil slick transport to aid effective preparation for, and response to, oil spills in tide-dominated estuaries, thereby achieving objective 2. This chapter will also improve our	Chapter 3

		understanding of the relative role of tidal currents; and the impact time of release within a tidal cycle has on oil spill transport.	
8	Assessing the influence of projected on oil slick dynamics in tide-dominated estuaries.	Sea level and river flow variability have been identified as stressors to estuaries (Merrifield et al. 2011; Pye and Blott 2014; Robins et al. 2016). Sea level rise is projected to increase over the 21st century in the UK. Furthermore, river flow in the UK is expected to decrease in summer and slightly increase in winter. This chapter seeks to understand how these projected climatic conditions will influence oil slicks dynamics, thereby fulfilling objective 3.	Chapter 4
9	Sensitivity analysis on oil slicks point of release in tide-dominated estuaries.	Arbitrary oil spill points are employed in Chapters 3 and 4. Chapter 5 assesses the influence of varying lateral points of release on oil slick transport. Findings will aid	Chapter 5

		effective preparation for, and response to, oil spills.	
10	Summary of the project findings and suggestions for further studies	To present This Chapter presents the research findings and its application in a global context. Furthermore, this Chapter will provide areas for further studies.	Chapter 6

1.5 METHODOLOGY FLOWCHART

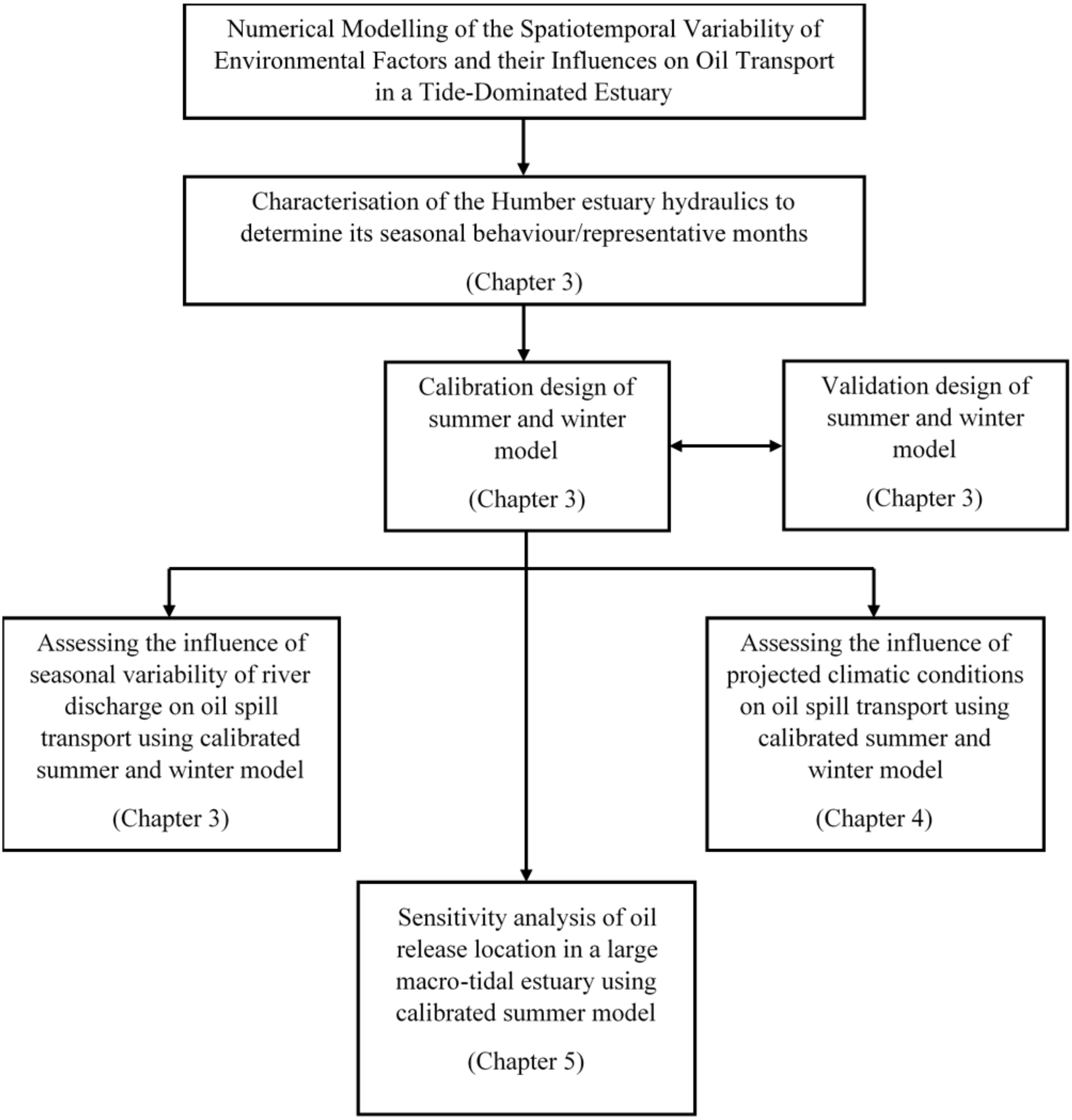

Figure 1.2: Flowchart showing the thesis methodology and commonality between between the three empirical chapters.

This thesis adopts a non-traditional structure. The thesis structure consists of introduction (Chapter 1), literature review (Chapter 2), three empirical chapters (Chapter 3 – 5) and conclusion and recommendation (Chapter 6). The three empirical chapters each have their specific methodology and are designed to address an identified research gap (Section 1.2; Table 1.3).

Chapter 1 discusses the research gaps, as well as the aim and objectives of this study. Chapter 2 further justifies the research gaps identied in Section 1.2, highlights the diversity of estuaries, provides an indication of the environment where this study may be deemed applicable and provides justification for modelling parameters employed in subsequent chapters. Chapter 3 asseses the influence of seasonal freshwater discharge variation on oil spill dynamics in a tide-dominated estuary. To address this gap, calibration and validation design of summer and winter models for the Humber Estuary are undertaken (Figure 1.2). The summer and winter models developed in Chapter 3 are employed in Chapter 4 to assess the influence of projected climatic conditions on oil slick transport in a tide-dominated estuary (Figure 1.2). Considering the choice of arbitrary oil spill release points in Chapter Chapters 3 and 4, Chapter 5 assesses the influence of varying points of release on oil slick transport employing the hydrodynamic model developed in Chapter 3 (Figure 1.2). Based on findings (from Chapter 3 – 5), Chapter 6 will provide answers to the research questions (Section 1.2) and propose recommendations for advanced research.

CHAPTER 2

2 NUMERICAL MODELLING OF OIL SPILL IN ESTUARIES

This chapter highlights various classifications of estuaries to highlight their diversity as well as to provide an indication of estuarine environments where this study may be applicable. The transportation and weathering of oil slicks are also discussed to highlight the mechanisms that govern these processes, thereby providing insight into the factors that determine oil slick travel direction and time, and alteration of its chemical and physical properties. Furthermore, the modelling of estuarine flow processes is discussed to determine the current state-of-the-art of hydrodynamic modelling in estuaries, identifying challenges and areas that require development. Next, the current state-of-the-art of hydrodynamic modelling tools is discussed. Finally, the current generation of oil spill modelling tools is discussed. This will provide insight into the current state of oil spill modelling and aid in the identification of a suitable oil spill modelling tool for this study.

2.1 CLASSIFICATION OF ESTUARIES

Estuaries can be defined as semi-enclosed bodies of water in which incoming saline ocean water is diluted by freshwater (Kim et al. 2017). While it appears that there is substantial study on oil spills in estuaries, literature review reveals that many authors in this field have considered the term “estuary” to be synonymous with “bay”, “inlet”, “lagoon” and “sound” (Pye and Blott 2014). While estuaries, bays, lagoons and sounds are all sea inlets, they are different. Unlike estuaries, bays do not have significant input from freshwater (Savenije 2005). While lagoons are separated from the sea by barriers and are shallower in comparison to estuaries (Miththapala 2013). While flow dynamics in estuaries are characterised as fast and strong, flow dynamics in Lagoons are characterised as sluggish (Miththapala 2013). A sound is the part of the sea, between two bodies of land. The generalisation of these water bodies as estuaries supports Murphy et al.'s (2016) claim that estuaries have received less research attention in terms of oil spill studies. Estuary forms and dynamics vary widely across the globe. The diversity of estuaries have resulted in several classifications:

a) water circulation (salt-wedge, highly stratified, partially mixed or well-mixed);
b) connection to the sea (open or closed);
c) tidal range (micro-tidal, meso-tidal or macro-tidal); and
d) dominant influence (tide-dominated or wave-dominated)

The complexity of estuaries is further increased by irregular coastlines, channels, shoals, islands and anthropogenic structures and dredging operations (Hu et al. 2009) as well as the fact that many estuaries do not fall into any simple category (Pye and Blott 2014). This diversity indicates the challenge of attempting to understand estuary dynamics.

2.1.1 Classification of Estuaries by Water Circulation

Transport and circulation in estuaries are tide-driven, wind-driven and density-driven (Nguyen 2008). These processes are influenced by the relative effects of river input and tidal mixing (Pinet 2019). Based on the degree of mixing between freshwater and saline water (Table 2.1: Classification of Estuaries by Water Circulation (Adapted from Martin and McCutcheon 1999; Dolgopolova and Isupova 2010)), Pritchard (1955) and Cameron and Pritchard (1963) classified estuaries into:

a) salt-wedge estuaries: characterised by large river discharge compared to weak tidal forcing (Dolgopolova and Isupova 2010).
b) highly stratified estuaries: characterised by moderate to large river discharge and weak to moderate tidal forcing (Valle-Levinson 2010).
c) partially mixed (weakly stratified) estuaries: characterised by weak to moderate river discharge and moderate to strong tidal forcing (Valle-Levinson 2010).
d) well-mixed estuaries: characterised by the interaction of weak river discharge and strong tidal forcing (Kowalewska-Kalkowska and Marks 2015).

Stratification (which is as a result of mixing between freshwater and saline water) gives rise to vertical acceleration as a result of the buoyancy effect caused by the density differential between freshwater and saline water (Martin and McCutcheon 1999; Zhou 2013). Stratification in estuaries is enhanced by increased river discharge and reduced by tidal forcing. Likewise, an increase in tidal flow weakens stratification by enhancing turbulent mixing (Pinet 2019). It is worth noting that the degree of stratification in estuaries can vary spatially and temporally (Prandle 2009). Furthermore, estuaries can change from one type to another as a result of variations in tidal forcings or river discharge, as well as, change in estuary width or depth (Pinet 2019; Kowalewska-Kalkowska and Marks 2015). Savenije (2005) points out that river discharge is the main driver of gravitational circulation (density-driven circulation) in estuaries as it provides potential energy (through buoyant freshwater). This explains why density-driven circulation can be considered as negligible in well-mixed estuaries (Cheng et al. 2010; Valle-Levinson 2010). Considering the influence of stratification on vertical acceleration, different modelling approaches may be required to understand the processes within the estuary (Table 2.1; Section 2.4). For example, in stratified estuaries or studies where vertical acceleration is important, three-dimensional models would be better suited to model flow and transport dynamics (Parsapour-Moghaddam and Colin 2014). The Humber Estuary is a well-mixed estuary (Fujii 2007), consequently, this study's choice of the Navier-Stokes equation with hydrostatic pressure approximation to model the Humber Estuary (Section 3.2.2.1) will not have any significant impact of the reliability of the results.

Table 2.1: Classification of Estuaries by Water Circulation (Adapted from Martin and McCutcheon 1999; Dolgopolova and Isupova 2010)

Estuary characteristics	**Fluid dynamics principles**	**Criteria for model selection**
Salt wedge estuary	$R/V \geq 1$	
Highly stratified estuary	$R/V \sim 0.1 - 1.0$	Include the vertical dimension in at least two-layer model
partially mixed (weakly stratified) estuary	$R/V \sim 0.005 - 0.1$	Can include the vertical dimension in a multi-layered model
Well-mixed estuary	$R/V < 0.005 - 0.1$	Neglect vertical dimension, unless water quality process dictate vertical resolution

where:

R is runoff volume of freshwater entering the estuary during high tide; and *V* is runoff volume of saltwater entering the estuary during high tide.

2.1.2 Classification of Estuaries by Connection to the Sea

By connection to the sea, estuaries can be characterised as open or intermittently open/closed estuaries (Cooper 2001). Most studies have been undertaken in open estuaries compared to intermittently open/closed estuaries (Nozais et al. 2001; Gobler wt al. 2005). Intermittently open/closed estuaries are abundant in South Africa (71% of its 258 estuaries) (Scharler 2012) and Australia (Griffiths 2001; Young and Potter 2002). Similar systems exist in Brazil, Uruguay (Bonilla et al. 2005), India, Mexico and the U.S. (Gobler wt al. 2005; Slinger 2017). Intermittently open/closed estuaries are characterised by extended periods of sand bars across the estuary mouth, thereby cutting it off from the sea (Cowley et al. 2001). This feature is due to changes in seasons where longshore sand movement in the marine nearshore combines with low or no river inflow (Nozais et al. 2001). Compared to open estuaries, intermittently open/closed estuaries are more susceptible to accumulation of pollutant (Nozais et al. 2001), exhibit greater fluctuations in nutrient balance and salinity (Griffiths 2001; Young and Potter 2002; Lawrie et al. 2010) and are characterised by significant reduction in water levels when closed (Froneman et al. 2004).

2.1.3 Classification of Estuaries by Tidal Range

By tidal range, estuaries are usually classified according to Davies (1964) system of classification. The three classes of estuaries are micro-tidal (tidal range < 2m), meso-tidal (2 – 4 m) and macro-tidal (> 2m). Micro-tidal and macro-tidal estuaries are typically characterised by the dominant hydrodynamic force. Micro-tidal estuaries are wave-dominated and macro-tidal estuaries are tide-dominated system (Cooper 2002; Tessier et al. 2012). Flemming (2012) asserts that a mixture of wave- and tide-dominated regimes occur in estuaries at the upper and lower end of the micro-tidal and macro-tidal range respectively. Some studies further classify estuaries with a tidal range greater than 6 m as hyper-tidal (Archer 2013; Bolaños et al. 2014). In undertaking a comparative study, Archer (2013) further subdivided hyper-tidal estuaries into 2 m intervals (ranging from hyper-tidal-A to hyper-tidal-E). Tidal range significantly influences the biological and physio-chemical processes (salinity regime, geomorphology, sedimentology, residence times, tidal water movements, turbidity and intertidal area) in estuaries (Tweedley et al. 2016). Meso-tidal and macro-tidal estuaries are likely to be partially mixed or well-mixed as a large tidal range induces strong turbulent mixing (Pye and Blott 2014). The Humber Estuary employed in this study has a mean spring tidal range of 5.7 m, making it a macro-tidal estuary (Skinner et al. 2015).

2.1.4 Classification of Estuaries by Dominant Influence

By dominant influence, estuaries are generally classified as wave- or tide-dominated (Billy et al. 2012; Reynaud et al. 2018). The dominant influence of an estuary was defined by Dalrymple et al. (1992) as the degree to which waves, river or tidal discharge influences the sediment dynamics. Wave-dominated estuaries are relatively easier to understand due to the monotonic trend of wave energy (Dalrymple and Choi 2007). Tide-dominated estuaries are commonly funnel-shaped, therefore, tidal range increases as tides enter the estuary because of the progressive decrease in cross-sectional area (Nelson et al. 2013; Pittaluga et al. 2015). As a result of the estuary geometry, tidal energy is hypersynchronous in nature making them complex to understand (Dalrymple and Choi 2007). Wave-dominant estuaries are characterised by coarse-grained coastal barriers in the outer zone, fine-grained deposits mostly originating from fluvial sources in the central zone and bay-head delta formed from coarser fluvial sediments concentrate at the estuary head in the inner zone (Tessier 2012). Tide-dominated estuaries consist of a braided system of longitudinal tidal bars at the mouth, followed landward by complex networks of tidal channels and bars (Dalrymple and Choi 2007; Tessier 2012). Cooper (2002) points out that the degree of river and tide dominance in estuaries can vary due to seasonal variations while Billy et al. (2012) suggest that estuaries can be mixed wave- and tide-dominated (e.g. The Gironde Estuary, France). Hence, using the Humber Estuary as a case study, this study will help better understand oil spill dynamics in tide-dominated estuaries.

2.2 TRANSPORTATION OF OIL SLICKS

The horizontal and vertical movement of oil slicks is governed by advection (Lee and Jung 2015; Faghihard and Badri 2016), turbulent diffusion and buoyancy (Wang and Shen 2010; Liu and Sheng 2014; Tkalich and Chan 2002) (Figure 2.1). In estuaries, the interaction of the driving forces (i.e. river, tide, wind and wave) results in a complex transport mechanism which is subject to a large spatial and temporal variability (Mantovanelli et al. 2004; Zhang et al. 2018). Understanding the behaviour of oil slicks is important to ascertain oil slick travel direction and travel time to key receptors (Al-Rabeh et al. 2000; Berry et al. 2012; Özgökmen et al. 2016), thereby, contributing to efficient control and response operations (Wang et al. 2008).

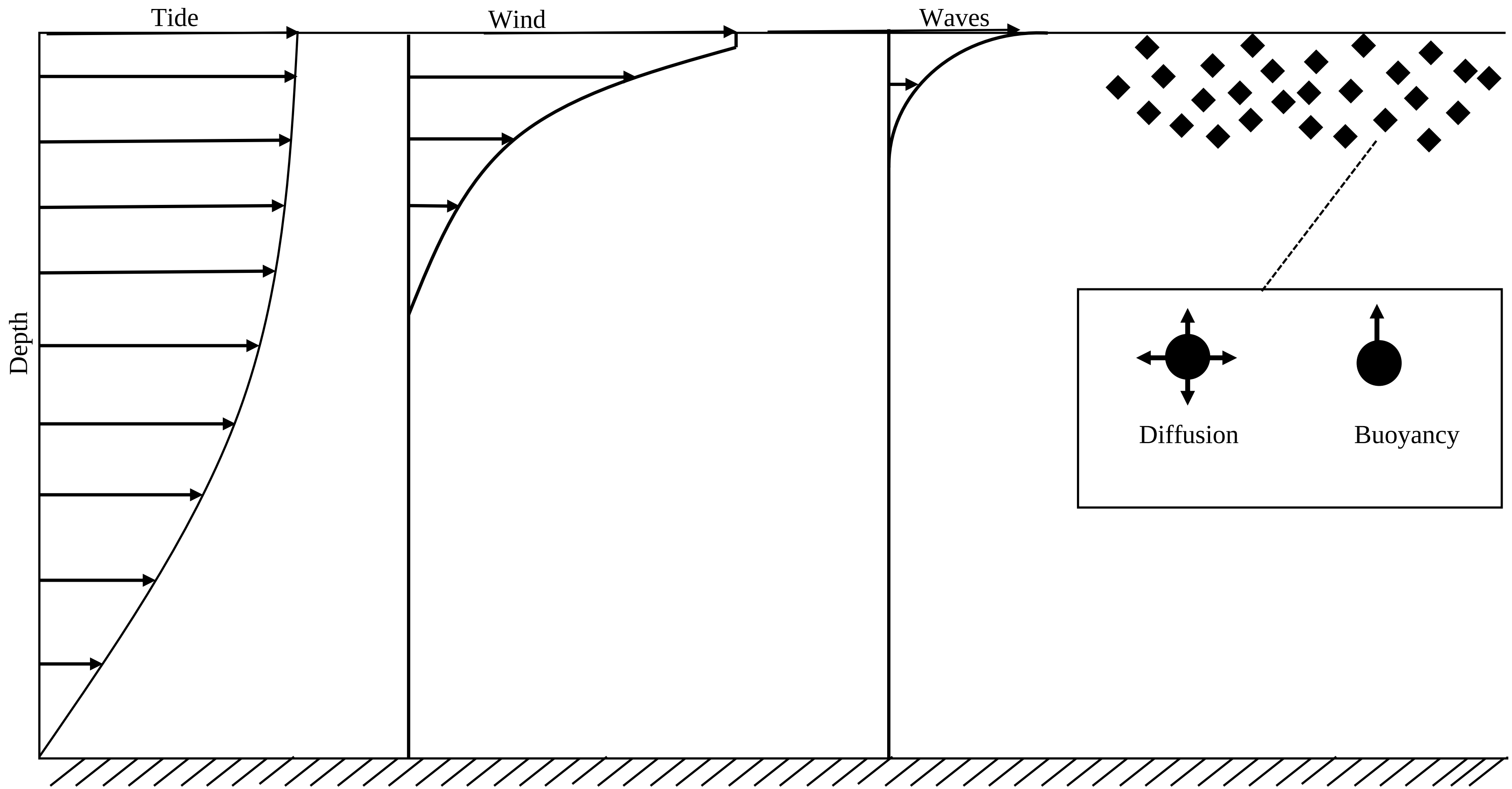

Figure 2.1: Schematic representation of the mechanisms that govern oil slick transportation: advection, diffusion and buoyancy (Adapted form Elliot 1986).

2.2.1 Advection

The movement of oil slicks on water is mainly governed by advection i.e. transport due to the water movement (Badejo and Nwilo 2004, Wang et al. 2008). This process is dominated by current, wind and waves, which can act independently (i.e. in the same or opposite direction) and concurrently on oil slick transport (Wang et al. 2008; Guo et al. 2009). The total advection velocity of an oil slick can be obtained by the sum of the various components (Guo et al. 2014; Liu et al. 2015):

$$\vec{\boldsymbol{U}}_{\mathrm{a}} = \vec{\boldsymbol{U}}_{\mathrm{cr}} + \mathrm{C}_{\mathrm{wind}}\mathrm{D}_{\mathrm{wind}}\vec{\boldsymbol{U}}_{\mathrm{wind}} + \vec{\boldsymbol{U}}_{\mathrm{wave}} \tag{2.1}$$

where:

> $\vec{U}_a$ is advection velocity; $\vec{U}_{cr}$ is the velocity of water current; C_{wind} is the wind drift factor; D_{wind} is a transformative matrix used to account for wind deviation angle; $\vec{U}_{wind}$ is the velocity of wind 10m above the sea surface; and $\vec{U}_{wave}$ is the wave-induced velocity (wave stokes drift).

2.2.1.1 Current

Current is the main driver of an oil slick (Abascal et al. 2017). Oil slicks migrate at a current drift factor of 1, i.e. they migrate at 100% the current velocity (Chao et al. 2001; Faghihifard and Badri 2016; Fingas 2013) when wind speed is less than 10 km/hr (Fingas 2011). Accurate numerical simulation of current patterns in estuaries requires solutions to several complex challenges, such as sudden bathymetry changes, boundary effects, and wetting and drying processes due to intertidal environments (Abascal et al. 2017). While it is generally agreed that oil slicks migrate at a current drift factor of 1, Sotillo et al (2008) and Abascal et al. (2009) point out that differences may exist between numerical and actual current. As a result, current drift factor may be included to account for uncertainties in numerical current during calibration of oil spill models. This explains the current drift factor of 0.52 employed by Sotillo et al (2008), 0.26 employed by Abascal et al. (2009) and 1.1 employed by Wang and Shen (2010) in their study. The use of current data obtained from numerical model results explains the inclusion of current drift factor in Abascal et al.'s (2009) study. This present study employed TELEMAC to develop a range of oil spill models (Section 2.5.5). The TELEMAC oil spill model was employed for this study because of its ready integration within the TELEMAC3D hydrodynamic model (Section 2.4.1). Consequently, the hydrodynamic models developed with TELEMAC will provide the current required to drive oil slick transport.

2.2.1.2 Wind

The contribution of wind velocity to oil slick movement is influenced by the wind drift factor and wind deviation angle (Guo et al. 2016) (Equation 2.1). The wind correction factors (wind drift factor and wind deviation angle) are usually employed to reproduce surface Ekman currents as numerical models might not accurately resolve local wind effects (Coppini et al. 2011; Janeiro et al. 2014). Wind drift factor C_{wind} (Equation 2.1) employed as only a fraction of the wind velocity (De Dominicis et al. 2016) influences the oil slick movement due to surface shear stress (Samuels et al. 1982). As a rule-of-thumb, the wind drift factor is assumed to be 3% (Simecek-Beatty 2011). However, observational and experimental results of oil spills indicate that wind drift factor ranges from 1% to 6%. Lehr and Simecek-Beatty (2000) attribute this variation to other physical factors affecting oil slicks or poor data collection techniques. The TELEMAC oil spill model employs a wind drift factor of 3.6% (Joly et al. 2014). The wind drift factor was computed by theoretically examining the force acting on a floating body with constant flow velocity (Joly et al. 2014).

The wind deviation angle is normally assumed to range between 0^0 and 25^0 (De Dominicis et al. 2016). The wind-induced direction of oil spill motion is at a non-zero angle (known as deflection angle) to the wind direction as a result of Coriolis forces (Wang and Shen 2010). This factor is taken into consideration by employing the transformation matrix D_{wind}, which allows the introduction of a deviation angle. Samuels et al. (1982) reviewed thirty-two studies which presented the various formula to resolve the deflection angle, indicating that there is no accepted way to estimate deflection angle (Sebastião and Guedes Soares 2007). However, a review of recent studies (Wang et al. 2005; Sebastião and Guedes Soares 2007; Wang and Shen 2010; Cucco et al. 2012; Xu et al. 2012; Guo et al. 2014; Liu et al. 2015) indicates that in oil spill modelling the transformation matrix is commonly given as Equation 2.2 where the deflection angle θ is often calculated in one of two ways.

$$D_{wind} = \begin{pmatrix} \cos\theta & \sin\theta \\ -\sin\theta & \cos\theta \end{pmatrix} \tag{2.2}$$

The first is the formula of Samuels et al. (1982) (Equation 2.3):

$$\theta = 25^0 \exp(-10^{-8}W^3/vg) \tag{2.3}$$

where:

θ is the deflection angle (degrees, clockwise in Northern Hemisphere); W is the wind speed; v is the kinematic viscosity of the seawater; and g is the gravitational acceleration.

The second is the formula of Zhang et al. (1991) (Equation 2.4):

If wind speed is less than 25 m/s,

$$\beta = 40^0 - 8\sqrt[4]{w_x^2 + w_y^2}. \quad (2.4)$$

While for greater wind speeds, $\beta = 0$.

where:

β is the deflection angle; w_x and w_y are the components of wind speed.

Sebastião and Guedes Soares (2007) allude that the choice of formula is dependent on the formula that presents good agreement with the field observation. However, with the development of state-of-the-art hydrodynamic models, the Ekman current is sufficiently resolved, thus rendering the application of deviation angle obsolete (Coppini et al. 2011; De Dominicis et al. 2016).

While wind generally plays a secondary role in oil slick transport (Fingas 2011), Fingas (2013) points out that in open sea at a speed greater than 20 km/hr, wind dominates oil slick movement in place of other factors. Regarding estuaries, Llebot et al. (2014) point out that the effect of wind is more important in micro-tidal estuaries, where tide is not a dominant driving force (Section 2.1).

2.2.1.3 Waves

The contribution of waves to oil slick advection is less well investigated compared to current and wind, mainly because wave-induced drift is generally considered to be of smaller magnitude (Guo et al. 2014). However, studies show that waves can significantly influence oil slick advection (Tkalick and Chen 2002; Wang and Shen 2010). As waves are the resultant effect of the wind blowing over the water surface, its size is dependent on the duration, magnitude and fetch length of the wind (Badejo and Nwilo 2004). Wind-waves can contribute to advection through wave drift, i.e. the net movement in the wave propagation direction (Wang and Shen 2010), through wave radiation stresses, i.e. the forcing of nearshore currents due to wave-induced stresses (Janeiro et al. 2014), or through breaking waves, i.e. by injecting turbulent kinetic energy into the upper ocean layer (Tkalich and Chan 2002; Janeiro et al. 2014).

Wave action contributes to oil slick advection by transferring fine droplets of oil into the water column resulting in natural dispersion (Boufadel et al. 2007; Fingas 2013). While both non-breaking and breaking waves are responsible for natural dispersion (Guo et al. 2014), significant dispersion occurs mainly under significant wave action i.e. breaking waves, which arises when wind speed exceeds 5 m/s^2 (Lehr and Simecek-Beatty 2000; Singsaas et al. 2000).

Castanedo et al. (2006) purport that wave drift factor ranges from 0.05 to 1.5%, while Sobey and Barker (1997) estimate this to be 0.015 (1.5%). Both studies indicate that the estimated wave drift is dependent on the sea state. These estimates generally indicate that the contribution of waves to oil slick advection is of much smaller magnitude compared to current and wind. However, this assumption may be invalid in wave-dominated regions where waves have been observed to equally contribute to advection (Guo et al. 2014) or have been the most important factor of advection (Castanedo et al. 2006). Hydrodynamic Eulerian models do not model wave drift (De Dominicis et al. 2016). However, in scenarios where the wave propagation is in the same direction as the local wind, it is appropriate to add the wave drift to the wind drift (Sobey and Barker 1997; Abascal et al. 2009; Guo et al. 2014). The mean current forced by waves can only be modelled by coupling a hydrodynamic model with a wave model (De Dominicis et al. 2016). This study does not consider the contribution of waves to oil slick behaviour in the Humber Estuary. The exclusion of the effects of waves on oil behaviour will not have any significant effect on the reliability of the results as the Humber Estuary is tide-dominated (Section 2.1.4). An overview of wave modelling tools is presented in Appendix A.

2.2.2 Turbulent Diffusion

The horizontal and vertical displacements (dispersion) of oil slicks are influenced by turbulent diffusion (Chao et al. 2001; Korotenko et al. 2004; Liu et al. 2015). Increasing turbulent diffusion will increase oil spreading in both the horizontal and vertical directions (Boufadel et al. 2007). The process of turbulent diffusion is poorly understood and inadequately represented in models and as a result, it can be considered as the “ignorant coefficient” (Simecek-Beatty 2011:287). Pan and Gu (2016) point out that turbulent mixing, as one of the most important dynamics in estuaries plays a significant role in the dispersion of pollutants. A common approach in oil spill modelling is to use a constant diffusion coefficient value (Simecek-Beatty 2011), which typically can be specified by the user or obtained from the hydrodynamic model (Spaulding 2017). However, Simecek-Beatty and Lehr (2016) point out that the appropriate diffusion coefficient is based on the location of the spill, the scale of the spill and model prediction, while Sayed et al. (2008) purport that water depth and local shear velocity are the determinants on the diffusion coefficient in rivers. In estuaries, the diffusion coefficient should be a function of tides, river flow and bathymetry, and may potentially be influenced by state variables (e.g. salinity gradients) (MacCready and Geyer 2010). This presents a drawback in oil spill models that employ a constant diffusion coefficient value as the modelling outputs may not be reliable therefore might negatively impact response decision-making. In scenarios where model output does not match the observation of the oil distribution, Simecek-Beatty and Lehr (2016) recommend that the oil spill modeller adjust the turbulent mixing term between model runs.

Guo et al. (2009) highlight that since Johansen (1982) and Elliott et al. (1986) put forward the hypothesis that oil slick movement can be modelled using a random walk technique, numerous models have adopted it due to its easier implementation. Hence, turbulent diffusion within models is usually computed by a random walk procedure (Chao et al. 2001). The random walk procedures most commonly employed in oil slick modelling are the Csandy’s (1973) random walk technique (Zelenke et al. 2012; Marta-Almeida et al. 2013; Otero et al. 2014), the Fischer et al.’s (1979) random walk technique (Wang et al. 2005; Wang and Shen 2010; Xu et al. 2012; Cucco et al. 2012) and the Al-Rabeh et al.’s (1989) random walk technique (Chao et al. 2001; Berry et al. 2012; Guo et al. 2014). An advantage of the random walk technique is the breaking of oil slick into Lagrangian elements, where specific attributes such as age, density, size etc. can be assigned to each particle (Elliott et al. 1986; Hunter 1987; Cekirge et al. 1995). However, a shortcoming of the random walk technique is that the number of particles must be restricted as a result of computational power demand (Guo and Wang 2009).

2.2.3 Buoyancy

Advancement in oil spill modelling has led to the consideration of processes such as buoyancy (Zheng and Yapa 2000; Liu and Sheng 2014). Buoyancy is the rise velocity of the oil droplets (Guo et al. 2014) and contributes to the vertical displacement of oil slicks (Wang and Shen 2010; Yan et al. 2012; Liu et al. 2016b) (Figure 2.1). The volume of oil that will remain dispersed depends on the equilibrium between shear stresses and buoyancy (Azevedo et al. 2014). During dispersion, larger droplets tend to resurface due to higher buoyancy compared to smaller droplets which stay suspended in the water column (Zeinstra-Helfrich et al. 2016; Azevedo et al. 2014; Li et al. 2016b). In estuaries, buoyancy is due to the joint effect of stratification and the gravity force (Dolgopolova and Isupova 2010). Buoyancy in estuaries is influenced by seasonal freshwater inflows, contraction in estuary basin size due to increased deposition of riverine sediment and modification of tidal channel at its mouth (Hearn and Largier 1997; Schettini et al. 2017). Llebot et al. (2014) purport that buoyancy in estuaries is also influenced by wind, as the direction and magnitude of the wind affect freshwater inflows. Wang and Shen (2010) suggest that oil droplet's buoyancy velocity is dependent on the water viscosity, oil droplet size and density difference between oil droplets and seawater. Models that do not consider oil transport in the water column fail to consider buoyancy which is important in understanding the behaviour of oil spills (Liu and Sheng 2014). Considering TELEMAC is a two-dimensional oil spill model (Section 2.5.5), it is also unable to compute oil slick dispersion.

2.3 WEATHERING OF OIL SLICK

Once crude oil is spilt, it begins to degrade as it undergoes concurrent natural processes characterised as oil weathering processes (OWP) (Mishra and Kuma 2015) which alter the chemical and physical properties of the oil slick (Fingas 2013). The OWP include spreading, evaporation, emulsification, dispersion, dissolution, photo-oxidation, sedimentation and biodegradation (Ranieri et al. 2013a); some of which occur at the sea surface and others throughout the water column (Azevedo et al. 2014) (Figure 2.2). While photo-oxidation, sedimentation and biodegradation are long-term OWP the other OWP are important in the early stages of the oil spill (Toz and Koseoglu 2018). OWP act simultaneously, are self-competing and complex and have been observed to have significant impacts on the viscosity and density of oil slick (Mishra and Kuma 2015); and by extension, on oil slick movement.

Figure 2.2: Oil Weathering Processes (ITOPF 2002)

To understand the weathering processes, it is important to understand the prevailing meteorological and ocean conditions, as well as the quantity and type of oil, as the OWP are dependent on these factors (Wang et al. 2013; Zhang et al. 2015). Knowledge of the fate of oil slicks aid oil spill contingency planning, clean-up operations and understanding the likely impact the spill could have on environmental receptors (Fingas 2015; Afenyo et al. 2016a; Afenyo et al. 2016b).

2.3.1 Spreading

During an oil spill occurrence, the area of the surface slick influences all mass transfer phenomena, making spreading one of the most important weathering processes (Goeury et al. 2014). Immediately after an oil spill occurs, spreading governs the horizontal expansion of the oil on the estuary surface, resulting in a thin layer called oil slick (Guo et al. 2009; Yan et al. 2012). The spreading of oil particularly depends on mechanical forces such as oil viscosity, surface tension, inertia and gravity (Guo et al. 2009; Goeury et al. 2014). Modelling of oil slick spreading is predominantly based of Fay (1971) formulation (Table 2.2), which points out that spreading involves the gravity–inertia, gravity–viscous and viscous–surface tension regimes.

Table 2.2: Spreading Laws of Oil Slicks (adapted from Fay 1971)

Regimes	One-dimensional	Axisymmetric
Gravity – Inertia	$l = k_{1i}(\Delta gAt^2)^{1/3}$	$r = k_{2i}(\Delta gVt^2)^{1/4}$
Gravity – Viscous	$l = k_{1v}(\frac{\Delta gA^2t^{\frac{3}{2}}}{\nu^{\frac{1}{2}}})^{1/4}$	$r = k_{2v}(\frac{\Delta gV^2t^{\frac{3}{2}}}{\nu^{\frac{1}{2}}})^{1/6}$
Viscous – Surface tension	$l = k_{1t}(\frac{\sigma^2t^3}{\rho^2\nu})^{1/4}$	$r = k_{2t}(\frac{\sigma^2t^3}{\rho^2\nu})^{1/4}$

where:

A is volume of oil per unit length normal to *x*; *g* is acceleration due to gravity; *k* is proportionality constant (see Table 2.3); *l* is length of one-dimensional oil slick; *r* is maximum radius of axisymmetric oil slick solubility; *t* is time since initiation of spread; *V* is the volume of oil in axisymmetric spread; *x* is dimension in the direction of one-dimensional spread; σ is spreading coefficient or interfacial tension (with subscript); ν is kinematic viscosity of water; density of water; Δ is ratio of density between water and oil to density of water.

Regarding the subscripts:

1 is one-dimensional spread; *2* is two-dimensional (axisymmetric) spread; *i* is inertia spread; *t* is surface tension spread; and *v* is viscous spread.

Table 2.3: Spreading Law Coefficient (Fay 1971)

	One-dimensional	Axisymmetric
Gravity – Inertia	$k_{1i} = 1.5$	1.14
Gravity – Viscous	$k_{1v} = 1.5$	1.45
Viscous – Surface tension	$k_{1t} = 1.33$	2.30

However, spreading in most models solely consider only the gravity-viscosity regime, as viscous–surface tension regime only occurs when the thickness of the oil slick is less than 0.1 mm and gravity–inertia regime occurs relatively rapidly i.e. within 10 minutes to 1 hour of the spill (Azevedo et al. 2014). This indicates that the lifespan of the oil slick is mostly in the gravity–viscous regime (Mishra and Kuma 2015). A drawback on Fay (1971) formulation is the failure to consider the influence of wind and turbulence on spreading (Sebastião and Guedes Soares 2007). As a result, several studies have modified Fay (1971) formulation to include these processes (Chao et al. 2001; Lehr et al. 2002; Guo and Wang 2009). Sebastião and Guedes Soares (1995) and Fingas (2013) agree that the direction of oil slick spreading is dependent on the direction of current and wind. In this study, computation of oil slick spreading was based on Fay's formulation. Like most models, TELEMAC only considers the gravity-viscosity regime (Joly et al. 2014).

2.3.2 Evaporation

Concerning the mass transfer process of oil slick, evaporation can be considered as the most important process (Goeury et al. 2014; Chiu et al. 2018) as it accounts for the most volume of oil lost; most of which occur in the first 48 hours (Fingas 2013; Azevedo et al. 2014). In the first 48 hours, 80% of the total oil mass lost to evaporation occurs (Fingas 2011). However, the volume of oil lost due to the evaporation process is influenced by the water temperature, wind speed, size of the oil slick and oil type (Lehr et al. 2002; Ranieri et al. 2013a). This explains the difference in the estimate of the volume of oil lost to evaporation in various studies. Azevedo et al. (2014) posit 25 – 40% of the total oil mass is lost to evaporation, Lehr et al. (2002) writes that 25 – 33.3% of the total oil mass loss is due to evaporation while Villoria et al. (1991) and Scholz et al. (1999) estimate the total oil mass loss due to evaporation lie between 20 – 40%. Douglas et al. (2002) study indicate that evaporation can account for up to 45% of the total oil mass lost.

Three main methods have frequently been employed for modelling evaporation of oil slick (Reed et al. 1999; Azevedo et al. 2014), these include:

1. Analytical method (evaporative exposure) (Stiver and Mackay 1984);

2. Pseudo-components method (Payne et al. 1983; Jones 1997); and
3. Fingas formulation (empirical method) (Fingas 1997; 1998; 2004)

Azevedo et al. (2014) compared the three methods using light, medium and heavy crude. The results from the study agreed with Jones' (1997) claim that the evaporative exposure method overestimates the evaporation rate. Azevedo et al. (2014) purport that while the Fingas formulation is suitable for operational systems due to its low data requirement (as it is only dependent on distillation percentage at 180 ^{o}C and water temperature), it tends to produce different results due to failure to consider other factors that influence evaporation. This drawback was pointed out by Reed et al. (1999) and Jones (1997). While the Reed et al. (1999) and Azevedo et al. (2014) agree that the Pseudo-components method is the most reliable, they also note that it requires a vast amount of input data and computational intensity, and as a result, it is not suitable for operational forecast systems. This explains why Stiver and Mackay's (1984) analytical method is the most frequently employed equation to model evaporation (Guo and Wang 2009). However, the TELEMAC oil spill model (Section 2.5.5) employed in this study utilises an evaporation model based on a pseudo-component approach (Goeury et al. 2012). The choice of evaporation model will not have any significant effect on the reliability of the results as this study does not focus on oil spill weathering (Section 2.5.5).

2.3.3 Emulsification

Water surface turbulence and breaking waves give rise to emulsification (Mishra and Kumar 2015). While the oil-in-water formation may be observed during oil spills, emulsification refers to the formation of water-in-oil emulsion sometimes called "mousse" or "chocolate mousse" (Fingas and Fieldhouse 2004:1). Emulsification as a dominant weathering process (Wei et al. 2003), plays a significant role in determining the behaviour of oil slicks (Xie et al. 2007; Kollo et al. 2017). Emulsification has been observed to drastically change the physiochemical properties of oil slicks (Xie et al. 2007; Li et al. 2016a), resulting in a 2 to 5 times increase in the original oil slick volume and 500 to 1000 increase in the oil slick's viscosity (Fingas and Fieldhouse 2012). Furthermore, emulsification results in an increase in the oil slick density due to the incorporation of water in the oil (ITOPF 2002; Wei et al. 2003).

Water-in-oil emulsion can be classified into 4 types of emulsion: unstable, entrained, meso-stable and stable (Spaulding 2017) based on the Stability Index (SI) proposed by Fingas and Fieldhouse (2009) and Fingas (2011). Fingas and Fieldhouse (2009) point out that each of the classes of emulsion has distinct physical properties (Table 2.4). Not all oil emulsify (Chui et al. 2018); the stability of emulsion is dependent on the asphaltene and resin contents of the oil as well as its starting viscosity (Fingas and Fieldhouse 2004; 2006), which is significantly influenced by evaporation as it results in an increase in oil viscosity as well as the asphaltene and resin percentage (Fingas 2011). The viscosity of the oil determines to what extent water will enter the oil (Fingas 2011). Furthermore, as asphaltene is formed around the water droplets in oil, the water-in-oil emulsion is stabilized while resin facilitates the asphaltene emulsion stability by acting as asphaltene solvents (Fingas and Fieldhouse 2009). Observations indicate that resin (R) should slightly exceed asphaltene (A) for greater stability, while the emulsion is destabilised by excess resin content ($A/R < 0.6$) (Fingas and Fieldhouse 2012). The TELEMAC oil spill model does not compute emulsification. The exclusion of the effects of emulsifiaction will not have any significant effect on the reliability of the results as this study does not focus on oil spill weathering (Section 2.5.5).

Table 2.4: Types of water-in-oil emulsion and their properties (Fingas 2013)

Types	Mechanism	Starting Oil Characteristics	Requirement	After Water Uptake		Typical Viscosity Increase	Typical Water Uptake
				Colour	Typical Lifetime		
Soluble Oil	Solubility	Most		Same	Years	1	<1%
Unstable or does not uptake water	None	Many oils		Same		1	-
Meso-stable	Viscous entrainment and A/R interaction	Moderate viscosity and some A/R	Sea energy	Reddish until broken	3 to 6 days	50	50% to 70%
Stable	Viscous entrainment and A/R interaction	Moderate viscosity and some A/R	Sea energy	Reddish	Months	800 to 1000	60% to 80%
Entrained	Viscous entrainment		Sea energy	As oil	2 to 10 days	2 to 5	30% to 40%

Note: A/R: Asphaltenes and Resins; Viscosity increase from starting oil

2.3.4 Dispersion

Dispersion results in the vertical mixing of oil droplets within the water column (Tkalich and Chan 2002) and the breakup of oil into droplets (Zeinstra-Helfrich et al. 2016). Oil dispersion is dependent on the oil properties and estuary state (Fingas 2011;

Li et al. 2016a). Regarding the influence of oil properties on dispersion, low viscosity of oil is easily dispersed compared to more viscous oil (Reed et al. 2009). The influence of viscosity supports Reed et al. (1999) claim that emulsification has a significant negative effect on dispersion as it results in an increase in viscosity and in oil slick thickness as a result of water entrainment. Furthermore, low resin and asphaltene content with high saturate content result in significant dispersion of light crude (Fingas 2013).

Regarding the water state, the influence of waves (especially breaking waves) on dispersion is discussed in Section 2.2.1.3. When dispersion occurs, the ratio of the upward buoyancy force (Figure 2.1) and downward wave mixing determines the oil mass that will remain dispersed (entrained). This explains the contribution of dispersion to the elongated shape observed in an oil spill as entrained oil droplets of various sizes will gradually resurface, forming a tail of thin-film behind the oil slick's thicker area (Reed et al. 1999). It is important to understand the dispersion process, as it is a key determinant of the oil slick's mass balance (Azevedo et al. 2014). Considering TELEMAC is a two-dimensional oil spill model (Section 2.5.5), it is unable to compute oil slick dispersion.

2.3.5 Dissolution

The contribution of dissolution to oil slick mass balance is negligible compared to evaporation and dispersion (Wang et al. 2005; Azevedo et al. 2014). The maximum effect dissolution has on oil mass balance is estimated to be 5% of the total oil mass, within the first 1 – 2 days of a spill (Azevedo et al. 2014). As evaporation and dissolution are competitive processes (Spaulding 2017), most of the oil components that may have undergone dissolution are lost to evaporation which is a faster process (Mishra and Kumar 2015). ITOPF (2002) estimates that evaporation is 10 to 1000 times faster than dissolution. However, under low evaporation i.e. from ice-covered surfaces and dispersed oil droplets, dissolution is significant (Spaulding 2017). Whereas the influence of dissolution on oil mass balance is negligible, it is critical to Environmental Impact Assessment as it introduces significant toxic compounds into the environment that are detrimental to marine biological life (Wang et al. 2005; Guo and Wang 2009; Azevedo et al. 2014; Goeury et al. 2014; Mishra and Kumar 2015). TELEMAC employs a Eulerian formulation to compute dissolution of the soluble oil component (Joly et . 2014))

2.3.6 Viscosity and Density

Viscosity and density of oil slicks are altered as a result of evaporation, emulsification and water temperature (Lehr et al. 2002; Berry et al. 2012). However, the effect that these parameters have on density is of a lesser extent compared to the effect on viscosity (Lehr et al. 2002; Fingas 2013). Viscosity and density tend to decrease when exposed to higher temperatures and increase with weathering (Ranieri et al. 2013b). It is important to understand the changes in oil slick viscosity and density as they influence the behaviour of oil slicks (Table 2.5).

Table 2.5: Influence of viscosity and density on oil slick behaviour (adapted from Ranieri et al. 2013b)

Oil Slick Behaviour	Viscosity	Density
Sinking	No identified effect	Oil slick will sink when its density exceeds the water density.
Spreading	The more viscous the oil, the slower it will spread.	In the early stages, the denser the oil slick, the faster it will spread.
Dispersion	Highly viscous oil is more resistant to dispersion	Denser oil will stay entrained more easily.
Emulsion	Viscous oils form stable emulsions	More dense oil increases the stability of emulsions.

2.3.7 Oil-Sediment Aggregates

Under the influence of advection, suspended sediment can interact with dispersed oil within an open water body resulting in the formation of oil-sediment aggregate (OSA) (Lee et al. 2003; Johnson et al. 2018). This natural process has several terminologies such as oil mineral aggregates (OMA), oil-fines interaction, oil-clay flocculation, oil-particle aggregate (OPA) and oil-sediment aggregate (OSA) (Lee 2002; Muschenheim and Lee 2002; Omotoso et al. 2002; Bandara et al. 2011; Johnson et al. 2018). When sediments carry oil particles with them, the fate and transportation of oil spill can undergo significant change (Bandara et al. 2011). The size of the OSA is dependent on the oil viscosity, the water turbulence and the oil interfacial tension (Zhao et al. 2014).

The density of the OSA formed will determine if it will float on the surface, settle on the seabed or remain suspended within the water column (Figure 2.3) (Sterling et al. 2004). The knowledge of the OSA formation has significantly influenced oil spill countermeasure strategies (Lee 2002; Gong et al. 2014). This study does not consider the suspended sediment or how they can interact with oil slicks. An overview of sediment transport modelling tools is presented in Appendix B.

Figure 2.3: Formation and movement of various types of OSAs (Gong et al. 2014)

2.4 MODELLING ESTUARINE PROCESSES: HYDRODYNAMIC MODELS

Generally, oil spill modelling consists of two models: a hydrodynamic model and oil transport model (Choi et al. 2013). Hydrodynamic models aid in the prediction of circulation patterns of water bodies (North et al. 2015) making them the foundation of oil spill trajectory prediction (Guo and Wang 2009; Yang and You 2016). This indicates that the reliability of oil spill predictions is significantly dependent on the reliability of the hydrodynamic models (Cheng et al. 2011; Michel et al. 2012). The Navier-Stokes equations are generally employed to model water flow (Broomans 2002). However, free surface flow in large shallow water area (lake, rivers, estuaries, coastal areas and shallow seas) is classically simulated in hydrodynamic models by solving the unsteady shallow-water equations (Lesser et al. 2004; Brière et al. 2007). The shallow-water equations assume that flow is dominated by the horizontal movement as a result vertical acceleration is negligible (Geveler et al. 2010). The shallow-water equations are derived from the Navier-Stokes equations by reducing the vertical momentum equation to the hydrostatic pressure equation (Fernández-Nieto et al. 2010; Zhao et al. 2017). This makes the shallow-water equations easier to solve than the Navier-Stokes equations (Zhao et al. 2017). The 3D shallow-water equations calculate the vertical velocity from the continuity equation while the 2D shallow-water equations do not consider vertical velocity (which is as a result of sudden bottom topography variations and buoyancy effect) (Lesser et al. 2004; Zhou 2013). As a result, Zhou (2013) purports that 2D shallow-water models are unable to predict vertical separation and 3D unable to accurately predict it. (Section 2.1.1). However, the hydrostatic pressure assumption is valid for regions where bed slopes and vertical acceleration caused by the pressure gradients are small (Robins et al. 2014). Literature review reveals that popular hydrodynamic models that employ the Navier-Stokes equations with the hydrostatic pressure approximation also include the Boussinesq approximation (Lesser et al. 2004; Mellor 2004; Haidvogel et al. 2008; Zhang and Baptista 2008; Pham et al. 2016). Consequently, vertical acceleration is not totally ignored neither is pressure assumed to be hydrostatic as the density variations are taken into account as buoyant forces (Hervouet 2007).

Non-hydrostatic modelling enables the study of small scale ocean processes (scales *L* < 1 km) such as dispersion of short waves, flow on steep slopes or over trenches (Marshall et al. 1997; Candy 2017) while the hydrostatic pressure approximation is suitable for large scale processes (e.g. internal tides) (Kanarska et al. 2007; Vitousek and Finger 2014). The modelling of small scale phenomena makes non-hydrostatic pressure models more accurate than the widely employed hydrostatic pressure approximation (Marshall et al. 1997). However, Botelho et al (2009) and Liu et al. (2016c) point out that non-hydrostatic computation requires more computation efficiency compared to hydrostatic models. To modify the hydrostatic equation to non-hydrostatic equation, the total pressure is derived (Lai et al. 2010). A common approach adopted in non-hydrostatic models entails breaking down the total pressure into a hydrostatic and non-hydrostatic component (dynamic component) (Marshall et al. 1997; Kanarska and Maderich 2003; Lai et al. 2010; Liu et al. 2016c). This approach is advantageous as it reduces the computational cost directly incurred from directly solving the 3D Poisson equation of total pressure (Kanarska et al. 2007). Furthermore, the rate of change, advection and diffusion of the vertical velocity is computed in the non-hydrostatic equations (Lai et al. 2010) as the hydrostatic pressure approximation does not account for vertical acceleration. The present study employed TELEMAC3D to develop the hydrodynamic model of the Humber Estuary. Considering the estuary is well-mixed (Section 2.1.1), vertical acceleration (due to variation of density) can be considered as negligible. Hence, to compute the estuarine circulation this study will adopt the Navier-Stokes equations with hydrostatic pressure approximation. Furthermore, adopting the hydrostatic pressure approximation will save computational cost without having any significant effect on the reliability of the results.

Based on grid structure, hydrodynamic models can be categorized into structured grid (which employs a finite-difference method) or unstructured grid (which employs a finite-volume or finite-element method) (Priya et al. 2012; Seenath et al. 2016). The main challenge to a cross-scale circulation model is to resolve complex bathymetry and geometry commonly observed in rivers, tidal flats, estuaries and coast in a robust, efficient and adequate way without compromising the deep ocean resolution (Zhang and Baptista 2008). To resolve this challenge, hydrodynamic models based on an unstructured grid are suitable (Zhang and Baptista 2008; Wang and Shen 2010). Some finite-difference model employs curvilinear orthogonal coordinates to resolve complex bathymetry as it is capable of following the boundary lines to a certain extent (Darby et al. 2002; Moffatt and Nichol 2005; Hervouet 2007). Compared to structured grid, setting up unstructured grid can be time-consuming and pre-processing tools employed in the model development becomes critical (Moffatt and Nichol 2005). Furthermore, structured grid produces a computationally simpler model (Seenath et al. 2016). While finite-element and finite-volume model can be employed in unstructured grid modelling, finite volume models require a lot of complex computations and their calibration large amounts of data (Priya et al. 2012). TELEMAC3D is a finite-element model (Section 2.4.1). This makes it ideal for resolving the complex bathymetry and geometry of the Humber Estuary.

Hydrodynamic modelling tools solving in 3 dimensions resolve the vertical coordinates using the Z-model, isopycnal models or terrain-following (sigma) model. Z-models are best suited to resolve the upper mixed layer; isopycnal ($\rho - coordinates$) models are best suited for deep stratified ocean as it resolves the vertical coordinate using the potential density; and terrain-following ($\sigma - coordinates$) models are best suited for coastal regions (Chassignet et al. 2006; Mehra and Rivin 2010) (Figure 2.4).

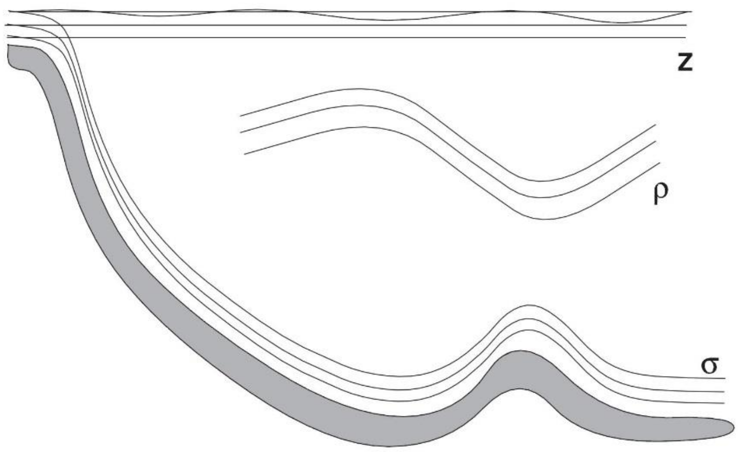

Figure 2.4: The three regimes for resolving the vertical coordinates (Griffes et al. 2000)

The terrain-following model is popular for resolving the vertical coordinates in coastal engineering applications, as well as regional and basin-wide studies, as it provides a good representation of the bottom topography as well as the equation of state with the associated thermodynamic effect (Griffes et al. 2000). Furthermore, the sigma coordinate provides a good adaptation to the free surface and bathymetry as it provides an equal number of levels in deep and shallow water (Abascal et al. 2017). However, its main drawback is the difficulty in computing internal pressure gradient especially over a steep topography (Shchepetkin and McWilliams 2003; Berntsen et al. 2015). In hydrodynamic modelling, hybrid coordinates can be employed to resolve the vertical coordinates as it enables the optimal simulation of ocean circulation features as the pros of the various coordinate types can be combined (Chassignet et al. 2007, Schiller and Kourafalou 2010). However, the transition between the various coordinates can adversely attenuate momentum (Zhang et al. 2015). TELEMAC3D employs a sigma coordinate to resolve the vertical direction (Section 2.4.1). Hence, it is capable of providing a good representation of the bottom topography of the Humber Estuary. An overview of TELEMAC3D and other popular hydrodynamic modelling tools employed in estuary modelling is further discussed in Appendix C.

2.4.1 TELEMAC3D

The present study employed TELEMAC3D (v7p0) to implement the hydrodynamic model of the Humber Estuary. TELEMAC3D is a three-dimensional open-source finite element model (Villaret et al. 2013) that solves the Navier Stokes equations with or without hydrostatic pressure approximation (Guillou et al. 2016; Stansby et al. 2016). The main originality of TELEMAC, which lies in the flexibility and efficiency its finite element algortihms, makes it stand out in comparison to other comprehensive modelling systems (Hervouet 2007; Villaret et al. 2013; Jia et al. 2015). In addition, it provides ready integration with an oil spill model (Pham et al. 2016). TELEMAC3D employs a semi-implicit scheme (Violeau et al. 2002; Stansby et al. 2016). TELEMAC3D uses a sigma transformation to resolve the vertical direction and unstructured triangular grid in the horizontal direction (Moulinec et al. 2011; Villaret et al. 2013). It provides a wide variety of numerical options to solve various processes within the model (Standby et al. 2016). The hydrodynamic model also provides users with numerous turbulence models; these include (1) constant viscosity; (2) mixing length model; (3) Smagorinsky model; (4) k-ε turbulent closure model (Pham et al. 2016). However, the difference in result from the comparison of the four vertical turbulence models within TELEMAC3D by Rahman and Venugopal (2017) was observed to be negligible. Furthermore, TELEMAC3D provides users with the option to construct all the density variations within the model while still taking the active tracers (temperature, salinity etc.) into account (Pham, Goeury and Joly 2016). Examples of estuarine hydrodynamic models developed with TELEMAC3D include the Nile Estuary, Egypt (Mahgoub et al. 2015), Yangtze Estuary, China (Pu et al. 2016), Scheldt Estuary, France (Smolders et al. 2014), Gironde Estuary, France (Ross and Sottolichio 2016), and Loire Estuary, France (Cheviet et al. 2014) (Table A.1). The theoretical aspects of TELEMAC3D with the hydrostatic pressure approximation are (Hervouet 2007):

The hydrostatic pressure hypothesis consists of simplifying the equation for vertical velocity W, while neglecting diffusion, the source terms and acceleration, to obtain:

$$\frac{\partial p}{\partial z} = -\rho g \tag{2.5}$$

Or even, by writing ρ as $\rho = \rho_o + \Delta\rho$:

$$\frac{\partial p}{\partial z} = -\rho_o g\left(1 + \frac{\Delta\rho}{\rho_o}\right) \tag{2.6}$$

From which one obtains the expression for pressure at elevation z:

$$p = p_{atm} + \rho_o g(Z_s - z) + \rho_o g \int_z^{Z_s} \frac{\Delta\rho}{\rho_o} dz' \tag{2.7}$$

The pressure at one point only depends on the atmospheric pressure on the surface and on the weight of the column of water above it

Boussinesq approximation: The difference in density $\Delta\rho$ in relation to a reference value ρ_o is supposedly small. The equation of state has the form:

$$\frac{\Delta\rho}{\rho_o} = f(T_1, \dots, T_i, \dots, T_n) \tag{2.8}$$

Where:

> T_i is the ith active tracer transported. The increase in density is proportional to the difference in concentration, by the intermediary of volumetric dilatation coefficient β_i:

$$\frac{\Delta\rho}{\rho_o} = -\sum_i \beta_i (T_i - T_i^0)_i \tag{2.9}$$

Where:

> β_i can be positive (temperature) or negative (salinity, sediment in suspension; T_i^0 is the reference value of the tracer i.

The pressure gradient term in the first two momentum equations is the developed to first order:

$$-\frac{1}{\rho}\frac{\partial p}{\partial x} \approx \frac{1}{\rho_o}\left(1 - \frac{\Delta\rho}{\rho_o}\right)\frac{\partial p}{\partial x} \tag{2.10}$$

$$-\frac{1}{\rho}\frac{\partial p}{\partial y} \approx \frac{1}{\rho_o}\left(1 - \frac{\Delta\rho}{\rho_o}\right)\frac{\partial p}{\partial y} \tag{2.11}$$

Which gives by using Equation 2.7:

$$-\frac{1}{\rho}\frac{\partial p}{\partial x} \approx \frac{1}{\rho_o}\left(1 - \frac{\Delta\rho}{\rho_o}\right)\frac{\partial p_{atm}}{\partial x} - g\left(1 - \frac{\Delta\rho}{\rho_o}\right)\frac{\partial Z_s}{\partial x} - g\frac{\partial}{\partial x}\left(\int_z^{Z_s}\frac{\Delta\rho}{\rho_o}dz'\right) \tag{2.12}$$

$$-\frac{1}{\rho}\frac{\partial p}{\partial y} \approx \frac{1}{\rho_o}\left(1 - \frac{\Delta\rho}{\rho_o}\right)\frac{\partial p_{atm}}{\partial y} - g\left(1 - \frac{\Delta\rho}{\rho_o}\right)\frac{\partial Z_s}{\partial y} - g\frac{\partial}{\partial y}\left(\int_z^{Z_s}\frac{\Delta\rho}{\rho_o}dz'\right) \tag{2.13}$$

These two gradients are broken down into a slope effect of the free surface $-g\nabla(Z_s)$ and into two source terms due to buoyancy, the first one called barotropic and the second baroclinic, which can be written along x:

$$g\frac{\Delta\rho}{\rho_o}\frac{\partial Z_s}{\partial x} - g\frac{\partial}{\partial x}\left(\int_z^{Z_s}\frac{\Delta\rho}{\rho_o}dz'\right) \tag{2.14}$$

And along y:

$$g\frac{\Delta\rho}{\rho_o}\frac{\partial Z_s}{\partial y} - g\frac{\partial}{\partial y}\left(\int_z^{Z_s}\frac{\Delta\rho}{\rho_o}dz'\right) \tag{2.15}$$

And to which is added the effect of atmospheric pressure. They are subsequently integrated in the source terms F_x and F_y.

In view of these hypothesis and conventions, the Navier-Stokes equations with hydrostatic hypothesis as follows:

Mass conservation:

$$\frac{\partial U}{\partial x} + \frac{\partial V}{\partial y} + \frac{\partial W}{\partial z} = 0 \tag{2.16}$$

Momentum equation:

$$\frac{\partial U}{\partial t} + U\frac{\partial U}{\partial x} + V\frac{\partial U}{\partial y} + W\frac{\partial U}{\partial z} = g\frac{\partial Z_s}{\partial x} + v\Delta(U) + F_x \tag{2.17}$$

$$\frac{\partial V}{\partial t} + U\frac{\partial V}{\partial x} + V\frac{\partial V}{\partial y} + W\frac{\partial V}{\partial z} = g\frac{\partial Z_s}{\partial y} + v\Delta(V) + F_y \tag{2.18}$$

Pressure:

$$p = p_{atm} + \rho_o g(Z_s - z) + \rho_o g \int_z^{Z_s} \frac{\Delta\rho}{\rho_o} dz' \quad (2.19)$$

where:

> U, V, W are 3D components of velocity (m/s); x and y are planform dimensions (m); z is the vertical dimension (m); t is time (s); g is acceleration due to gravity (m/s^2); Z_s is the free surface elevation (m); ν represents velocity and tracer diffusion coefficients (m^2/s); F_x and F_y are source terms (m/s^2); p is pressure; p_{atm} is atmospheric pressure; ρ_0 represents a reference density; $\Delta\rho$ denotes density variation around the reference density; T is a passive or active tracer (^{o}C, g/L…); and Q is the tracer source of sink (tracer unit).

2.5 OIL SPILL MODELLING

Oil spill modelling has developed over the past five decades (Wang et al. 2008), evolving from first, second to third-generation models (Berry et al. 2012). The current generation of oil spill modelling tools (subsequently discussed) mostly uses Lagrangian formulation (Lynch et al. 2015) to compute transport (advection and dispersion) and utilises individual formulations to compute weathering processes (Spaulding 2017). Guo et al. (2018) assert that the use of a range of parameters in oil spill modelling is partly evidence of a lack of knowledge of the underlying mechanisms behind oil complex behaviour. The Lagrangian approach involves the representation of oil slicks by a number of constituents (particles) that are transported by advection and dispersion (De Dominicis et al. 2016). In contrast, some oil spill models are based on Eulerian approach (Tkalich et al. 2003; Di Martino and Peybernes 2007) which either apply the mass and momentum equation to the oil slick layer or apply a convection-diffusion equation (Delgado et al. 2006; Nagheeby and Kolahdoozan 2010). In general, Lagrangian models are more popular in oil spill modelling because complexities that arise from irregular and discontinuous oil slick shapes are more easily simulated than with Eulerian models (Durgut and Reed 2017). Furthermore, dispersion phenomena are not directly resolved by Eulerian models, thereby resulting in numerical diffusion (Guo and Wang 2009). Compared to Eulerian models, the Lagrangian approach is more efficient and cost-effective (Toz and Koseoglu 2018). A combination of Eulerian/Lagrangian approaches complements the simulation of particles on water, whereby terms that contribute to advection can be avoided (Eke and Anifowose 2017). The Telemac oil spill model (Section 2.5.5) uses a combined Eulerian/Lagrangian approach to compute oil slick transport (Pham et al. 2016). The Deepwater Horizon oil spill have driven state-of-the-art oil spill models to include the simulation of the rise of buoyant oil plume from the seabed to the sea surface (Özgökmen et al. 2016). To address the research gap (Section 1.2), this study employs TELEMAC to develop a range of oil spill models (Section 2.5.5). An overview of the current generation of oil spill modelling tools is discussed.

2.5.1 GNOME

GNOME (General NOAA Operational Modeling Environment) is a two-dimensional state-of-the-art oil spill modelling tool developed by NOAA/ERD (National Oceanic and Atmospheric Administration/Emergency Response Division) for hind- and forecast application (Cheng et al. 2011; Farzingohar et al. 2011; Zelenke et al. 2012). GNOME employs a combined Eulerian-Lagrangian approach to compute oil slick transport (Eke and Anifowose 2017). The hybrid particle tracking (Eulerian-Lagrangian) approach prevents the explicit treatment of the advection terms, as the transport equation can be decoupled into two parts (advection and diffusion) and solved separately (Guo and Wang 2009; Souli and Benson 2010). GNOME can provide users with the best guess solution and minimum regret solution (Marta-Almeida et al. 2013; Xu et al. 2013). The best guess solution is the trajectory developed under the assumption that all the model inputs are error-free (Beegle-Krause 2001), while the minimum regret solution considers uncertainties in model input (current, wind etc.) (Marta-Almeida et al. 2013). To account for uncertainties, input parameters can be varied to derive the minimum regret trajectory (Mearns et al. 2011). Processes that result in the movement of pollutants (e.g. oil) on water are known as "movers" and these are generally current, wind and diffusion (Prasad et al. 2014:18). Uncertainty in current is taken into account by activating the "cross current uncertainty" and "along current uncertainty" which represents the uncertainty in right ($\beta > 0$) and left ($\beta < 0$) direction and the uncertainty in currents forward ($\alpha > 0$) and backward ($\alpha < 0$) direction respectively (Zelenke et al. 2012). Zelenke et al. (2012) recommend that "along current uncertainty" and "cross current uncertainty" be set at 50% and 25% respectively. Furthermore, uncertainty in wind speed and direction, as well as diffusion, can be activated in GNOME (Eke and Anifowose 2017).

The evolution of oil slick movement in GNOME is represented by "splots" (spill dots or also known as Lagrangian Elements - LEs) (Xu et al. 2013:110). GNOME tracks the velocity and position of each splot by assigning longitude and latitude coordinates enabling GNOME to predict if splots leave the modelling space domain, beach or remain on the water (Cheng et al. 2011; Zelenke et al. 2012). GNOME is capable of simulating oil slick movement of various oil types as well as simulating some weathering processes (Liu and Sheng 2014). However, Zelenke et al. (2012) point out that GNOME is not suitable for simulating weathering as the oil types and oil weathering are very rudimentary. To this effect, Zelenke et al. (2012) suggest that oil slick weathering should be simulated using ADIOS2 (Section 2.5.2). GNOME supports various kinds of users. Based on the users required degree of automation, it can be operated in Standard Mode (most automated mode), GIS Output Mode and Diagnostic mode (NOAA 2002). While GNOME is capable of simulating various types of sea surface oil spill, it is not capable of simulating subsurface spills (Marta-Almeida et al. 2013; Eke and Anifowose 2017). Compared to other oil spill models, GNOME requires fewer parameters and is suitable anywhere in the world (Cheng et al. 2011). GNOME is freely made available by NOAA/ERD (Xu et al. 2013), it is robust, efficient and fully relocatable (Marta-Almeida et al. 2013).

2.5.2 ADIOS2

ADIOS2 (Automated Data Inquiry for Oil Spills) is an oil spill modelling tool developed by NOAA/ERD to forecast oil slick weathering characteristics, processes and clean-up strategies (Table 2.6) (Lehr et al. 2002; Azevedo et al. 2014). ADIOS2 is unable to simulate long term oil slick weathering processes such as biodegradation and photo-oxidation (Eke and Anifowose 2017). Furthermore, ADIOS2 is limited to a 5-day simulation time (Stronach and Hospital 2014). ADIOS2 incorporates the properties of over a thousand refined product and crude oil in its database (Janeiro et al. 2008). Eke and Anifowose (2017) illustrate that custom oil can be created in ADIOS2.

Table 2.6: Processes and Properties modelled or tracked in ADIOS2 (Lehr et al. 2002)

PROCESSES	**PROPERTIES**
Evaporation	Viscosity
Dispersion	Density
Spreading	Benzene hazard
Emulsification	Water fraction
Skimming	
In-situ burning	
Leak rate	
Smoke plume	
Beaching	

Existing oil within ADIOS2 can be also be modified (Lehr et al. 2002). While not an object-oriented software, ADIOS2 computational engine which contains the weathering algorithm is isolated from the oil database and the platform-dependent user interface in accordance to certain object-oriented protocols (Figure 2.5) (Overstreet et al. 1995, Lehr et al. 2002). ADIOS2 is made freely available by NOAA/ERD and GNOME's weathering limitation is removed when jointly executed with ADIOS2 (Zelenke et al. 2012, Korsah and Anifowose 2014). The development of WebGNOME combines GNOME and ADIOS2 functionalities (NOAA 2017).

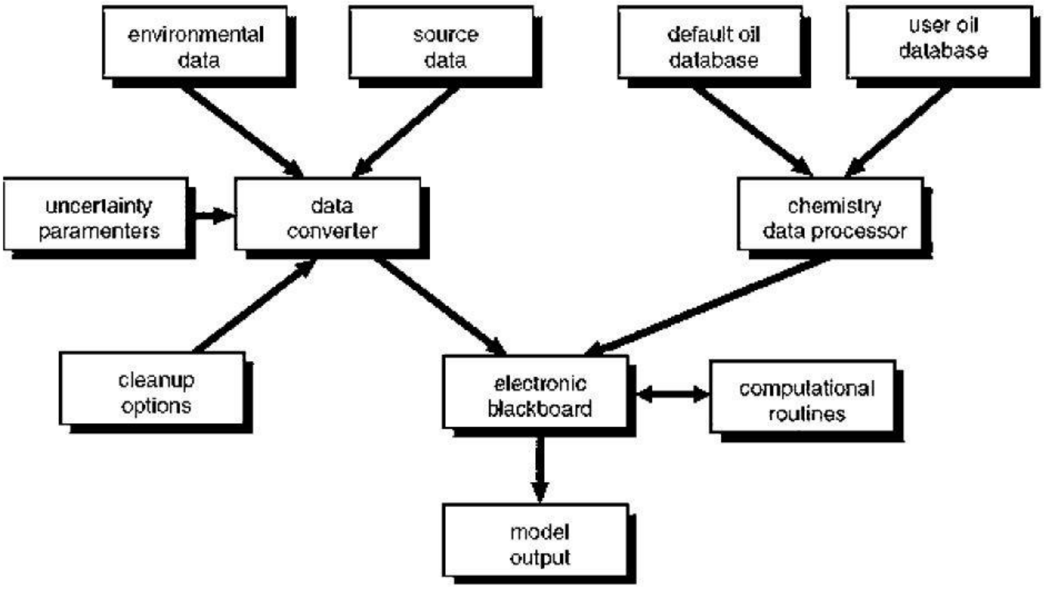

Figure 2.5: Overview of ADIOS2 system (Lehr et al. 2002)

2.5.3 OSCAR

OSCAR (Oil Spill Contingency and Response) is a three-dimensional state-of-the-art oil spill modelling tool developed by SINTEF for oil spill transport and fate prediction (Afenyo et al. 2016a). OSCAR provides a tool for analysis of different oil spill response strategies as well as for hind- and forecasting (Abascal et al. 2010; Faksness et al. 2016). OSCAR is made up of various components: Fates, SINTEF Oil Weathering Model (SINTEF OWM), Oil Spill Combat (Figure 2.6) (Reed et al. 1995a) and more recently DeepBlow model (for blowouts and deep-sea drilling simulation) (Socolofsky et al. 2015). Wirtz et al. (2007) point out that OSCAR also incorporates exposure models for marine animals, birds, meroplankton and fish.

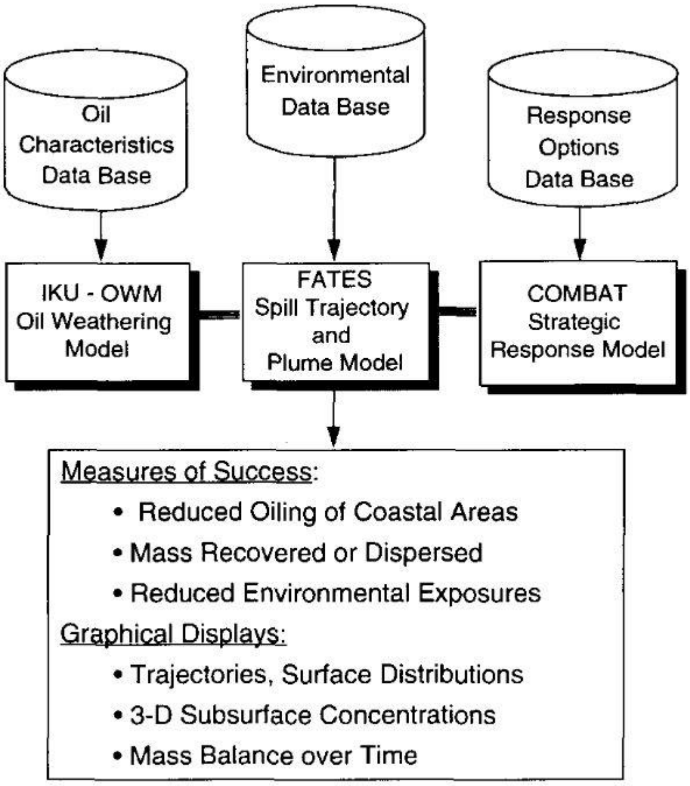

Figure 2.6: Overview of the OSCAR system (Reed et al. 1995a)

OSCAR computes the distribution of the pollutant in various environmental compartments including water column, water surface, sediments, shoreline and atmosphere (Liu and Wirtz 2009). OSCAR computes a three-dimensional generalized transport equation based on Lagrangian particle-tracking (Reed et al. 1995b; Nepstad et al. 2015). OSCAR is capable of simulating dissolution, emulsification, evaporation, dispersion, water-in-oil, oil-in-water, sedimentation, stranding, response action and long term processes such as biodegradation (Lamine and Xiong 2013). The OSCAR database has grown from five oil types with different oil properties to nearly 200 oil types (Fakness et al. 2016). OSCAR as a proprietary (commercial) software (Nelson et al. 2015) can be employed for stochastic simulations as well as deterministic modelling

(Iazeolla et al. 2016). However, OSCAR is unable to model the backtracking of an oil spill (Fernandes et al. 2013).

2.5.4 OILMAP

OILMAP is a state-of-the-art three-dimensional oil spill modelling tool developed by Applied Science Asoociates Inc. (ASA) for hind and forecast modelling (Lima et al. 2003). OILMAP was designed in a modular fashion to incorporate diverse types of oil spill model within the basic system without influencing the user interface complexity (Reynolds et al. 2009). The components of OILMAP v7 suite highlight the functionalities of the modelling tool (Table 2.7).

Table 2.7: Summary of OILMAP (version 7.0) suite (RPS 2016a)

Modules	**Function**
Surface module	Simulate the behaviour of surface oil spills
Subsurface module	Simulate oil release below the water surface
Land module	Evaluate the behaviour of oil released on land reaching the river network
Airmap module	Computes atmospheric dispersion of the lighter oil fractions from a spill
Deep module	Simulates oil spills from the seabed (blowouts and dispersant application)

Stochastic module	Computes the probabilistic distribution of oiling in water and onshore
Backtrack module	Evaluate the oil spill source

OILMAP is based on Lagrangian approach, representing an oil slick as a large number of individuals elements called “spillets” (Howlett et al. 2008:6) to simulate trajectory and contains a number of algorithms for spreading, evaporation, entrainment, emulsification, oil-reed bed, oil-ice, and oil-shoreline interaction (King et al. 2010; RPS ASA 2017). OILMAP also models dissolution, photo-oxidation, encapsulation and sedimentation (Lei and He 2017). OILMAP provides oil spill response option assessment for mechanical (skimming and booming) and dispersant application (from aircraft and vessel resources) (Howlett et al. 2008; RPS ASA 2017). In addition to the up-to-date oil database within OILMAP, users can create new oil, as well as copy, edit and adjust oil from the Master oil database (RPS 2016a). OILMAP as a proprietary (commercial) software (Nelson et al. 2015), provides implementation options for users which includes: OILMAP desktop (Windows-based model system), OILMAP on the cloud (a cloud-based version of OILMAP), OILMAPWeb (a web-based GIS version) and OILMAP ArcGIS Extension (RPS 2016b). Zigic (2004) points out that OILMAP is the world’s most popular oil spill model employed by the government, research institutes, oil companies and consultants worldwide. However, a literature search reveals that there are very limited OILMAP studies available in the public domain.

2.5.5 TELEMAC

Integrated into TELEMAC3D is a two-dimensional oil spill model (similar to GNOME; Section 2.5.1) for short-term forecasting of oil spill behaviour in continental waters (lakes, rivers and estuaries) (Goeury 2012; Goeury et al. 2014). The oil spill model uses a combined Eulerian/Lagrangian approach to compute oil slick transport (advection-diffusion) (Pham et al. 2016). TELEMAC accounts for advection, diffusion, wind, spreading, dissolution and evaporation processes (Goeury et al. 2012). TELEMAC3D employs the Eulerian model to simulate soluble oil component dissolution in water while the Lagrangian model simulates surface oil slick transport (Goeury et al. 2014). A set of hydrocarbon particles, considered as a mixture of discrete non-interacting hydrocarbon components (soluble and insoluble components), represent the oil slick (Joly et al. 2014), while the TELEMAC3D hydrodynamic model (Section 2.4.1) provides the required hydrodynamic data. TELEMAC's capability for simulating oil spill transport was validated by Goeury (2012) using the ERIKA oil spill incident that occurred in the Bay of Biscay in December 1999. Full description of the validation of TELEMAC oil spill processes is detailed in Goeury (2012) and Goeury et al. (2014). Consequently, the subsequent lack of oil spill validation in this study does not influence the reliability of the oil spill results as a the Telemac oil spill model has been extensively validated. While TELEMAC accounts for spreading, evaporation and dissolution of the oil spill, it does not model other key short term weathering processes such as dispersion, emulsification, viscosity, density and buoyancy (Section 2.3). Similar to GNOME (Section 2.5.1), the TELEMAC oil spill model can, therefore, be considered as rudimentary with regards to modelling oil weathering processes. Consequently, the focus of this study is on oil spill transport in tide-dominated estuarine environment. The TELEMAC oil spill model was employed for this study because of its ready integration within the TELEMAC3D hydrodynamic model and its combined Lagrangian/ Eulerian approach. The theoretical aspects of TELEMAC are discussed in Section 3.2.3 and an overview is presented in Table 2.8.

2.5.6 MEDSLIK-II

MEDSLIK-II is an open-source two-dimensional Lagrangian oil spill modelling tool for simulating oil slick transportation and weathering processes (Samaras et al. 2014). MEDSLIK-II represents oil slicks in three state variables: the particle, the slick and the structural state variables (De Dominicis et al. 2013a). Transport and diffusion processes are represented by the particle state variable, transformation processes (i.e. weathering) are represented by the slick state variable, and the oil concentration in water is computed by the structural state variables (combination of the particle and the slick state variables) (De Dominicis et al. 2013b; Samaras et al. 2014).

MEDSLICK-II accounts for Stokes drift in computing oil slick transportation using Hasselmann et al. (1973) model, as a result, a separate wave model may not be required (De Dominicis et al. 2016). However, MEDSLICK-II does not consider swell waves and assumes wave and wind are aligned (Sorgente et al. 2016). Furthermore, MEDSLIK-II tends to overestimate Stokes drift (De Dominicis et al. 2016). De Dominicis et al. (2013a) recommend running a wave model with MEDSLIK-II to provide Stokes drift. Regarding weathering processes, MEDSLIK-II simulates spreading, evaporation, dispersion and water-in-oil emulsification (Liubartseva et al. 2016). While MEDSLIK-II is a fully deterministic model (Al Shami et al. 2017), a variant of MEDSLIK-II has been developed (CranSLIK) to predict surface oil spill movement and spread via stochastic approach (Rutherford et al. 2015). The capabilities of the various oil spill modelling tools and their algorithms are summarised in Table 2.8.

Table 2.8: Processes modelled by oil spill modelling tools and associated algorithm (adapted from Reed et al. 1995b; Reed et al. 2000; Lehr et al. 2002; Reynold et al. 2009; Zelenke et al. 2012; De Dominicis et al. 2013b; Horn and French McCay 2014; Joly et al. 2014)

	GNOME	**ADIOS2**	**OSCAR**	**OILMAP**	**TELEMAC**	**MEDSLIK**
Model type	Deterministic	Deterministic	Deterministic and Stochastic	Deterministic and Stochastic	Deterministic	Deterministic
Advection-Diffusion	Two dimensional	-	Three dimensional	Three dimensional	Two dimensional	Two dimensional
Stokes drift	-	-	✓	-	-	Hasselmann et al. (1973) model
Backtracking	-	-	-	✓	-	-
Beaching	✓	-	✓	✓	✓	✓
Blowout	-	-	✓	✓	-	-

Spreading	-	Extension of Fay (1971) model as suggested by Ahlstrom (1975)	Mackay et al. (1980; 1982) approach	Mackay et al. (1980; 1982) approach	Fay (1971) model; Layer averaged Navier-Stokes formulation proposed by Warluzel and Benque (1981); and Constant Area	Mackay et al. (1979; 1980) model
Evaporation	3-phase evaporation algorithm by Boehm et al. (1982)	Pseudo-component evaporation model by Jones (1997)	✓	Evaporative exposure (Mackay et al. 1980; 1982)	Based on Pseudo-component evaporation model	Mackay et al. (1980) algorithm

Dispersion	-	Delvigne and Sweeney (1988) hydraulic model	Delvigne and Sweeney (1988) formulation	Delvigne and Sweeney (1988) formulation	-	Mackay et al. (1979) empirical formulas
Emulsification	-	Based on Fingas, et al. (1996) study	✓	Mackay et al. (1980; 1982) approach	-	Mackay et al. (1979)
Dissolution	-	-	Delvigne and Sweeney (1988) hydraulic model	Mackay and Leinonen (1977) model for surface oil and French-McCay et al. (1996) model for subsurface oil.	Based on Whitman's (1923) theory	-
Benzene Fraction	-	Evaporation algorithm and	-	-	-	-

		vapour dispersal model based on boundary layer				
Photo-oxidation	-	-	✓	✓	-	-
Biodegradation	-	-	Based on transformation rates derived by Brakstad and Fakness (2000)	First-order decay algorithm (French-McCay et al. 1999)	-	-
Smoke plume	-	Bent plume concept (Briggs 1984)	-	-	-	-
Response strategies	-	-In-situ burning -Skimming	- Skimming	- Skimming	-	-

			- Booms - Dispersant application	- Booms - Dispersant application		
Oil-ice interaction	-	-	✓	✓	-	-
Oil-sedimentation interaction	-	-	✓	Kirstein et al. (1987) model and French-McCay et al. (1994)	-	-
Oil-shoreline interaction	Based on half-life of Lagrangian Element	-	✓	Reed, Gundlach and Kana (1989) model	Considered if: -The slick thickness is greater than the water level under the oil slick; or	-

					-The size of the bottom roughness is greater than the water level.	
	GNOME	**ADIOS2**	**OSCAR**	**OILMAP**	**TELEMAC**	**MEDSLIK-II**

✓ Indicates the process is modelled within the oil spill modelling tool

2.6 CONCLUSION

This chapter provides insight into the complexities of estuary classification and factors that govern the transport and weathering of oil spills in the estuarine environment. Also, the current state of hydrodynamic modelling of estuarine processes and oil spill modelling were discussed. A review on the application of hydrodynamic models reveals that there is limited research on oil spill dynamics in estuaries (Table A.1). This emphasises the significance of this research, as this study will present the first detailed analysis of oil slicks in an estuarine environment, specifically a large well-mixed macro-tidal estuary. This chapter highlighted some useful insights, including:

(a) the class of estuary (based on stratification) influences the modelling approach required to understand flow and vertical acceleration in the estuary (Section 2.1.1).

(b) further studies required to understand the influence of turbulent diffusion on oil slicks and incorporate it into oil spill models (Section 2.2.2).

(c) non-hydrostatic hydrodynamic models are not as common as hydrostatic models due to the computational cost (Section 2.4);

(d) resolving complex bathymetry and geometry has driven the evolution of hydrodynamic models (Section 2.4);

(e) evolution of hydrodynamic models has also been driven by the resolution of the external (barotropic) mode resulting in the evolution from explicit to semi-implicit models (Section 2.4);

(f) the internal pressure gradient error, especially over steep topography when the sigma coordinate system is employed to resolve the vertical computation grid, is still a challenge in hydrodynamic modelling (Section 2.4);

In view of the diversity of estuaries (Section 2.1), this study will be applicable in a large well-mixed tide-dominated estuary. Tide-dominated estuaries are common around the globe (Section 1.2.1), some of which are faced with a significant risk of oil spills e.g. the Bonny Estuary, Nigeria (Snowden and Ekweozor 1987; Anifowose et al. 2014). Consequently, the research findings are expected to have global implications on oil spill response planning in this type of estuarine environment.

To develop the hydrodynamic model for the Humber Estuary, this study will employ the Navier Stokes equations with hydrostatic pressure approximation, due to the intense computational power demanded by non-hydrostatic pressure models (Section 2.4). Regarding the reliability of the model, the impact of using hydrostatic pressure approximation is expected to be relatively insignificant; as the Humber Estuary is a well-mixed estuary (Section 2.1.1; 2.4). Also, as there is no indication that the processes (small scale ocean processes) emphasised by the use of non-hydrostatic pressure models influence oil slick transportation. TELEMAC3D is a finite-element modelling tool (Section 2.4.1), hence, it is ideal for resolving complex bathymetry and geometry in a robust, efficient and adequate way without compromising the deep ocean resolution (Section 2.4). This study does not consider the impact of waves on oil slick transport. Considering the type of estuarine environment and the contribution of waves to oil slick advection (Section 2.1.4; 2.2.1.3), the reliability of the research findings are not expected to be significantly affected.

The TELEMAC oil spill model (Section 2.5.5) was employed for this study because of its ready integration within the TELEMAC3D hydrodynamic model (Section 2.4.1). While TELEMAC accounts for spreading, evaporation and dissolution, it does not model other key short term weathering processes such as dispersion, emulsification, viscosity, density and buoyancy (Section 2.3). Like GNOME (Section 2.5.1), the TELEMAC oil spill model can, therefore, be considered as rudimentary with regards to modelling oil weathering processes. Consequently, the focus of this study is on oil spill transport in tide-dominated estuarine environment.

With the aid of numerical modelling tools, subsequent chapters of this study will assess the relative influence of advection mechanisms, tidal flows, seasonal freshwater discharge variability, projected climatic conditions on oil spill dynamics in tide-dominated estuaries. Also, a sensitivity analysis will be undertaken to understand how the varying lateral points of oil slick release could influence oil dynamics in a tide-dominated estuary.

CHAPTER 3

3 THE INFLUENCE OF SEASONAL FRESHWATER DISCHARGE VARIATION ON OIL SPILL DYNAMICS IN A TIDE-DOMINATED ESTUARY

Oil spills in estuaries are less studied and less understood than their oceanic counterparts. To address this gap, this chapter presents a detailed analysis of estuarine oil spill dynamics. The temporal variability of environmental factors (discharge, stage height, wind, temperature and salinity) in the Humber Estuary is examined to understand the hydraulics of the estuary and ascertain its suitability for assessing the influence of seasonal discharge variability on oil slick dynamics, thereby fulfilling objective 1. Furthermore, a range of simulations for the Humber Estuary is developed and analysed, using coupled hydrodynamic and oil spill models. Because of limited high-resolution discharge data, the hydrodynamic models are driven by constant river discharge at the river boundaries and 15-minute tidal height data at the offshore boundary. In the absence of current data, the models are calibrated and validated with water level during the representative seasons. The oil spill model simulates a range of oil spill scenarios in the tide-dominated Humber Estuary. The prediction models will aid in understanding how seasonal freshwater discharge variation influences oil slick transport to aid effective preparation for, and response to, oil spills in tide-dominated estuaries, thereby achieving objective 2.

3.1 BACKGROUND

Estuaries exhibit complex hydrodynamics because of the combined action of marine and fluvial processes i.e. the driving forces of tide, waves and river (Jia et al. 2015).

The interaction of these driving forces significantly influences estuary characteristics (Dai et al. 2014; Zhang et al. 2018). River discharge, as a driving force of estuarine hydrodynamics, is significantly influenced by seasonal variations (Pontee et al. 2004; Robin et al. 2014). It is important to understand the influence of seasonal variations, as it plays a critical role in the control of estuarine hydrodynamics and processes. It is worth noting that the effect of seasonal variations in river discharge is relevant worldwide e.g. Yangtze River estuary, China (Guo et al. 2015), Pearl River Estuary, China (Zhai et al. 2015), Columbia River, USA (Kärnä et al. 2015), Tana estuary, Kenya (Kitheka et al. 2005) and Hudson River estuary, USA (Woodruff et al. 2001). Also, a study of ten rivers in Columbia revealed strong seasonal freshwater discharge variations (Restrepo et al. 2014).

The effect of seasonal freshwater discharge variations on estuarine processes has piqued interest. Several studies have explored the impact of seasonal variation on freshwater flow within estuaries, to better understand the biological and physio-chemical characteristics of estuaries such as: estuarine morphology (Guo et al. 2015), spatial distribution of sedimentation (Woodruff et al. 2001), hydrodynamics and sediment dynamics (van Maren and Hoekstra 2004; Purnachandra et al., 2011), flow turbidity (Uncles et al., 1998a; Mitchell et al., 1998; Lawler 2016), siltation (Pontee et al., 2005), river plume (Dong et al. 2004) and dissolved nutrients (Uncles et al. 1998a; 1998b; Sigleo and Frick 2007). But no known study has investigated (i) the influence of seasonal river discharge variability on oil spill transport; and (ii) the implications of interacting tidal currents and riverine flows on oil spill transport in a tide-dominated estuary.

Because of the complexities of estuaries, numerical models have become essential tools to understand the processes occurring within them (Hu et al. 2009; Gichamo et al. 2012; van Griensven et al. 2013). This chapter, therefore, employs numerical models to assess: (a) the impact of seasonal freshwater flow variation on oil slick transport; and (b) the implication of interacting tidal currents and riverine flows on oil slick transport in the tide-dominated Humber Estuary. Considering the worldwide occurrence of tide-dominated estuaries influenced by seasonal freshwater discharge variations, the findings of this study are expected to have worldwide relevance.

3.2 MATERIALS AND METHODS

3.2.1 Data Collection

3.2.1.1 Bathymetry

The Association of British Ports (ABP) provided the bathymetry data for the Humber Estuary, collected in 2008. The point data covered the Humber Estuary, extending from Blacktoft on the River Ouse and Keadby on the River Trent to the entrance of the Humber Estuary. All positions are aligned to the UK Ordnance Survey National Grid (OSGB) 1936/British national grid and depth with reference to chart datum (Figure 3.1). Each data set is referenced using a local chart datum; a local reference level. This datum varies over the area (and sometimes over time). To get a consistent reference level, all data is converted to ODN (Ordnance Datum Newlyn), which is the UK's national reference level. (Section 3.2.2.1.1).

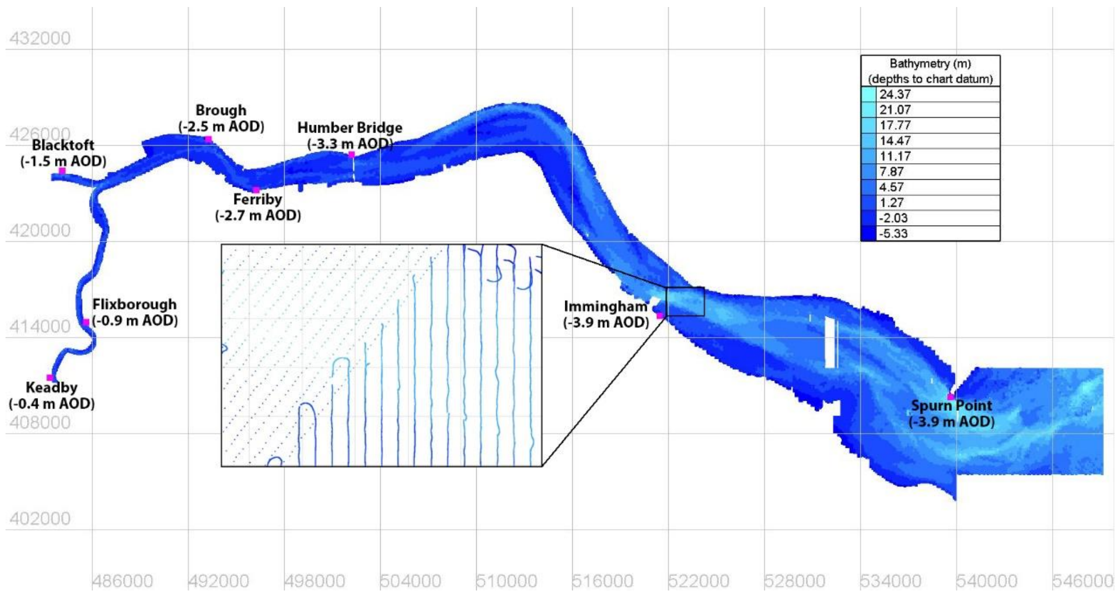

Figure 3.1: Bathymetry data relative to Chart Datum for the Humber Estuary showing metres Above Ordnance Datum (m ODN) at various locations. Inset shows XYZ measurement points.

3.2.1.2 Fluvial data

Several rivers drain into the Humber Estuary. The largest freshwater discharge comes from Rivers Ouse and Trent (Morris and Mitchell, 2013; Wang and Townend, 2012), for which discharge data is available. For the many smaller tributaries, no data is available. Therefore, this study only considers river input from Rivers Ouse and Trent. The impact of neglecting other freshwater sources is expected to be insignificant. Cave et al. (2003), for example, point out that River Hull contributes approximately 1% of the freshwater input while River Ancholme freshwater contribution is less than River Hull.

To characterise the estuary's seasonality this study examines the temporal variability of fluvial discharge from the Rivers Ouse and Trent over an 11-year period (2007 – 2017).

The UK Environment Agency provided high-resolution discharge data recorded at 15-minute intervals from the year 2007 to 2017 on Rivers Ouse at Skelton (456845; 455373) which lies 17 km from Naburn (Walling et al. 1999) and Trent at North Muskham (480430; 360560) which lies 0.75 km from Cromwell Weir (Skidmore et al. 1998; Figure 1.1). Constant discharge at Blacktoft on the River Ouse and Keadby on the River Trent was obtained from literature to drive the fluvial boundaries (Section 3.2.2.1.2).

High-resolution 15-minutes stage height data at Blacktoft on the River Ouse and Keadby on the River Trent from the year 2007 to 2017 was also provided by the UK Environmental Agency. Stage height data from Keadby station (483540, 411310) was recorded with respect to Ordnance Datum. While stage data from Blacktoft station (484238, 424156) was recorded with respect to Station Datum (–0.06 m ODN). To ensure consistency, stage height data at Blacktoft was corrected to Ordnance Datum.

3.2.1.3 Tidal height data

Considering the unavailability of recorded tidal height measurements at the mouth of the Humber Estuary, 15-minutes tidal height data from the FES2014 model is used for setting the boundary conditions along the offshore input. Mean tidal height data from the interaction of 34 tidal components (Appendix D) at the estuary's mouth was extracted from the FES2014 model (at 541049, 402468 and 540841, 409420) (Appendix E). FES2014 is the most recent version of the Finite Element Solution (FES) global tidal model following the FES2012 (Carrère et al. 2013) and FES2004 versions (Lyard et al. 2006). FES2014 is based on hydrodynamic modelling with assimilation data (Zawadzki et al. 2016) and takes advantage of more accurate ocean bathymetry, improved modelling and data assimilation techniques, better altimeter standards and longer altimeter time series and a refined mesh in most shallow water regions (Lei et al. 2017). Ranji et al. (2017) and Seifi et al. (2019) compared eight different tide models in the Persian Gulf and Great Barrier Reef, Australia respectively. These models include: the DTU10 (Cheng and Anderson 2011); Empirical Ocean Tide model (EOT11a) (Savcenko and Bosch 2012); FES2012; FES2014; Goddard/Grenoble Ocean Tide (GOT4.8) (Ray 1999); Hamburg direct data Assimilation Methods for TIDEs (HAMTIDE 11 & 12) (Taguchi et al. 2014); OSU12 (Fok 2012); and TOPEX/POSEIDON global tidal model (TPX08) (Egbert and Erofeeva 2002). Both studies agree that FES2014 presents the best tidal prediction for coastal regions. Tidal harmonics obtained from the FES model have compared favourably with model outputs of the Irish Sea (Robins et al. 2013) and the European Shelf (Neil and Hashemi 2013); and has been employed to successfully develop a hydrodynamic model for the Conwy Estuary, UK (Robins et al. 2014).

Corresponding high-resolution 15-minutes tidal height data at Immingham station located at National Grid Reference 520049, 416473 (Figure 3.1) was provided by the British Oceanographic Data Centre (BODC). Tidal height data at Immingham was recorded with respect to Chart Datum (-3.9 m ODN). To ensure consistency, the tidal height data was corrected to Above Ordnance Datum (-3.9 m ODN).

3.2.1.4 Wind data

The UK Meteorological Office provided hourly wind speed and direction data at Donna Nook station near the Humber's mouth (National Grid Reference 542900; 399700) recorded from the year 2007 to 2016. Wind data was measured at an altitude of 8 m over the sea surface. For use in this study, wind data was converted from knots to m/s (the ratio is 0.514 m/s).

3.2.1.5 Temperature and salinity

Temperature and salinity data were obtained from the "UK Environmental Agency water quality archive". The water quality archive contains water quality samples taken from various sampling points around England. The Humber Estuary water quality data was obtained from the Lincolnshire and Northamptonshire area and the Yorkshire area. Temperature and salinity measurements taken around the mouth of the Humber Estuary were extracted from the datasets. Due to the absence of salinity measurements for several months, supplementary data was also obtained from the British Oceanographic Data Centre (BODC). Salinity data obtained from the BODC was recorded during the Land Ocean Interaction Study (LOIS) and Joint Nutrient Study I (JoNuS) from the year 1990 to 1995. Table 3.1 is a summary of the temperature and salinity data employed.

Table 3.1: Description of temperature and salinity data collected around the Humber's mouth

Month	**Temperature measurements**		**Salinity measurements**	
	No. of samples	**Sources**	**No. of samples**	**Sources**
January	10	Environmental Agency	171	Environmental Agency; JoNuS

February	34	Environmental Agency	61	Environmental Agency; LOIS; JoNuS
March	13	Environmental Agency		
April	11	Environmental Agency	61	Environmental Agency; LOIS
May	38	Environmental Agency	27	Environmental Agency
June	37	Environmental Agency	33	Environmental Agency
July	30	Environmental Agency	27	Environmental Agency
August	30	Environmental Agency	31	Environmental Agency
September	33	Environmental Agency	30	Environmental Agency
October	21	Environmental Agency	93	Environmental Agency; LOIS; JoNuS
November	25	Environmental Agency	243	Environmental Agency; LOIS; JoNuS

December	19	Environmental Agency	83	Environmental Agency; LOIS

3.2.1.6 Oil spill properties

To understand oil spill transport, Brent blend properties (Table 3.2) required by TELEMAC's oil spill model (Section 3.2.3) were extracted from BP (2011) crude oil assay report. The Brent blend was chosen due to its proximity to the Humber Estuary, as it is located in the North Sea off the United Kingdom's coast. Because of limited data, this study only considered the insoluble component of the Brent crude oil. This will have no influence on the quality of the results as this study is not focused on oil spill toxicity i.e. dynamics of soluble oil component dissolution (Joly et al. 2014).

Table 3.2: Summary of oil properties required for the oil spill simulation

Parameters	**Values**	
	Mass fraction (% wt)	Boiling point of each component (K)
Insoluble component parameters	8.66	368.15
	10.52	422.15
	5.18	448.15
	9.19	505.15
	20.98	615.15

	4.48 22.12 4.42 14.45	642.15 782.15 823.15 858.15
Oil density (kg/m^3)	836.9	
Oil viscosity (m^2/s)	0.000006377	

3.2.2 Hydrodynamic Model

3.2.2.1 TELEMAC3D

The hydrodynamics of the Humber Estuary were computed with TELEMAC3D (Section 2.4.1). This study employs the hydrostatic pressure approximation due to the intense computational power demanded by non-hydrostatic pressure models (Section 2.4). Furthermore, the impact of using hydrostatic pressure approximation on the reliability of the model is expected to be relatively insignificant; as there is no indication that the processes (small scale ocean processes) emphasised by the use of non-hydrostatic pressure models (Section 2.4) influence oil slick transportation.

Here, the model was implemented with 5 equidistant σ-coordinate layers in the vertical. The application of 5 σ-coordinate levels is sufficient and efficient for developing an operational oil spill system (Abascal et al. 2017). In addition, the Humber Estuary is a well-mixed estuary, which does not necessitate multi-layers to resolve the vertical direction (Table 2.1). Horizontal turbulence was resolved using the Smagorinsky model because it is best suited for tidal systems that involve highly non-linear flow (Rahman and Venugopal 2017). Vertical turbulence was resolved using Nezu and Nakagawa mixing length model as it offers a good representation of wind drift (Rahman and Venugopal 2017). Chezy's law of bottom friction was employed as it is more suited for TELEMAC3D models applying the equidistant layer (Rahman and Venugopal 2017). In an analysis of over 15 estuaries, Savenije (2001; 2005) indicate that the Chezy friction coefficient typically ranges from 45 – 70 $m^{0.5}/s$. In this study, the Chezy friction coefficient is a calibration parameter, although TELEMAC3D's default value of 60 $m^{0.5}/s$ is initially employed. A simulation time step of 45 seconds was employed which satisfies the Courant-Friedrichs-Lewy criterion. To take into account possible dry zones in the domain, TELEMAC3D's "Tidal Flats" option was activated in this study. Coriolis force was also taken into account in this study as it influences discharge in the Humber Estuary (Pietrzak et al. 2011). Furthermore, Coriolis force influences oil slick transportation (Zanier et al. 2017). Coriolis coefficient of $1.172E^{-4}$ was derived (Equation 3.1). The initial conditions of the hydrodynamic models were defined in the steering file, a CASsette file (.cas) that describes the configuration of the simulation (Gifford-Miears and Leon, 2013; Rahman and Venugopal, 2015) (Appendix F).

$$C = 2\omega sin(\lambda) \qquad (3.1)$$

where:

C is the Coriolis coefficient; ω is the Earth's rotational velocity of 7.27×10^{-5} rad/s; and λ is the model's average latitude estimated to be 53.72.

3.2.2.2 Blue Kenue

Blue Kenue is a software developed by the Hydraulic Canadian Centre which proposes a powerful mesh generation and user-friendly pre- and post-processing tool (Pham et al. 2016). Mesh generated by Blue Kenue can be used by finite-element modelling software such as TELEMAC and ADCIRC (NRC Canada 2011). This study employed Blue Kenue to develop the geometry file (a SERAFIN file (.slf) which contains the information on the model mesh); and the boundary condition file (a command-line user interface file (.cli) which describes the domain's boundary condition) (Gifford-Miears and Leon, 2013; Rahman and Venugopal, 2015).

3.2.2.2.1 Geometry file

The point dataset provided by ABP (Figure 3.1) was loaded into Blue Kenue to develop the computational mesh for the Humber Estuary. A closed line was drawn around the Humber Estuary boundary, creating an outline of the computational domain of interest (Figure 3.2). The computational domain of interest extended from Blacktoft on the River Ouse and Keadby on the River Trent to the entrance of the Humber Estuary. The *T3 mesh generator* within Blue Kenue was employed to develop a two-dimensional scalar triangular (unstructured) mesh with edge length (mesh resolution) set to 50 m. Brown and Davies (2009) indicate that a high-resolution mesh ranges between 20 – 100 m as this allows high resolution of the significant bathymetric features. Furthermore, an edge length of 50 m is sufficient to adequately capture flow propagation (Rahman and Venugopal 2017). The choice of mesh size was also influenced by computational power demand as the computational system employed in this study could not cope with the computational demand of edge length less than 50 m (Azevedo et al. 2014; Guo et al. 2014). A sensitivity analysis using edge length of 50 m, 75 m and 100 m suggested that there is no significant difference of the choice of edge length on oil spill transport in the Humber Estuary (Appendix G). The resulting computational domain consisted of 92,369 nodes and 183,925 elements, with a mean edge length of 54.57 m varying from 11 m to 803 m (Figure 3.3). The mesh was interpolated with the point dataset to develop the bathymetric mesh. The geometry file was created by using the *New SELAFIN object*, where the bathymetric mesh was assigned the child-object mesh *bottom* and stored as a geometry file (Figure 3.4). To ensure consistency, it was required that the depths be corrected to Ordnance Datum because the depth conversion values from Chart Datum and Ordnance Datum vary along the estuary (Figure 3.1). Based on the difference between chart datum and Ordnance datum along the estuary's length, an interpolated grid of values (Appendix H) was used to apply the correction to the geometry file within MATLAB environment (Figure 3.5).

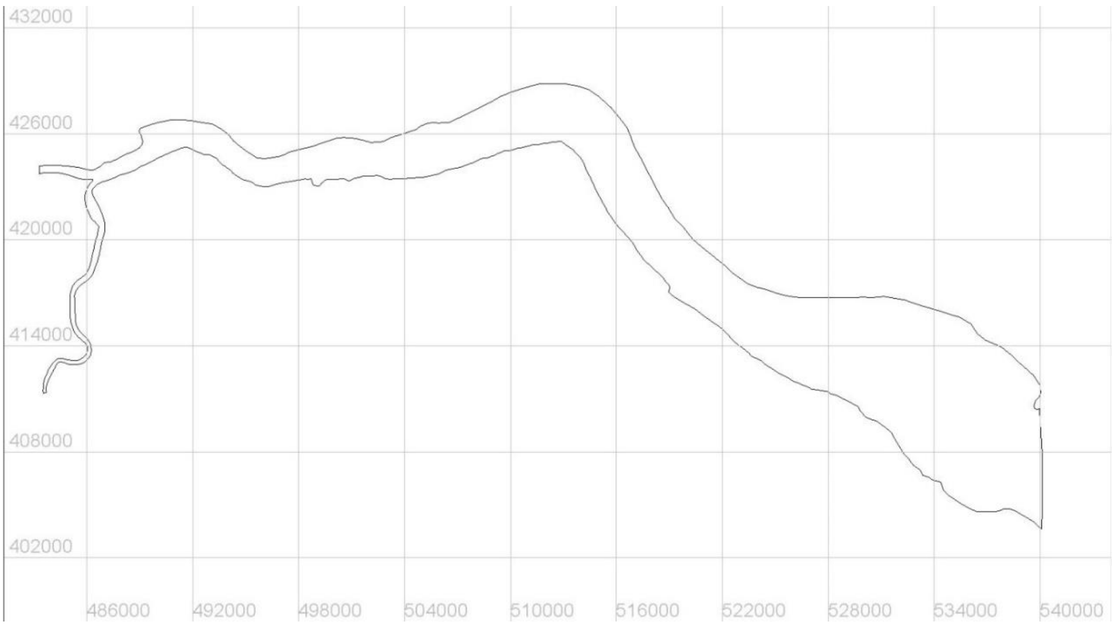

Figure 3.2: Outline of the computational domain.

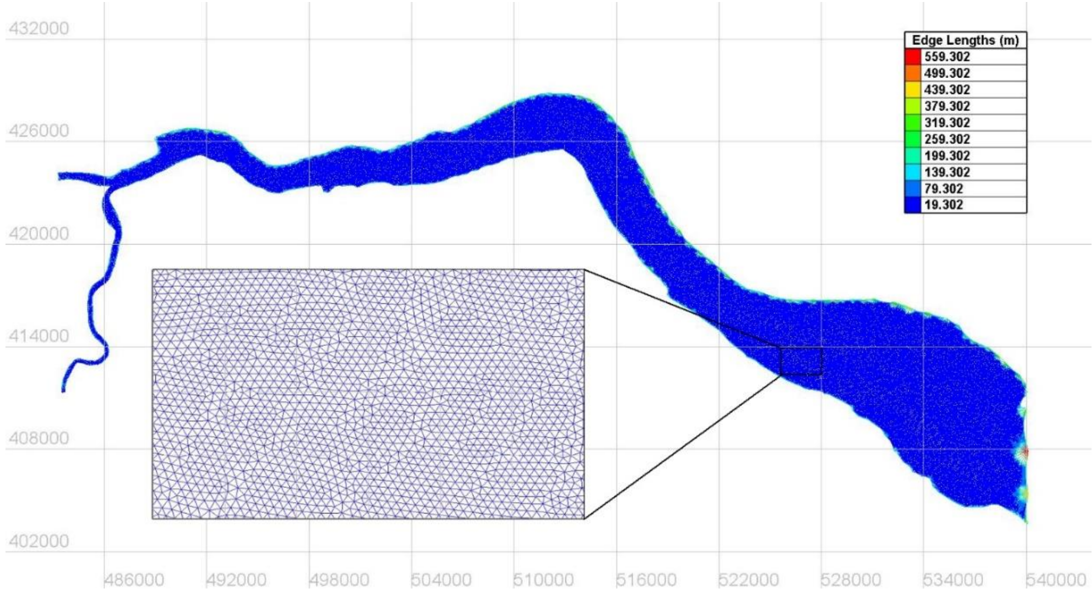

Figure 3.3: The bathymetric mesh for the Humber Estuary simulations. Inset shows the detail of the computational mesh.

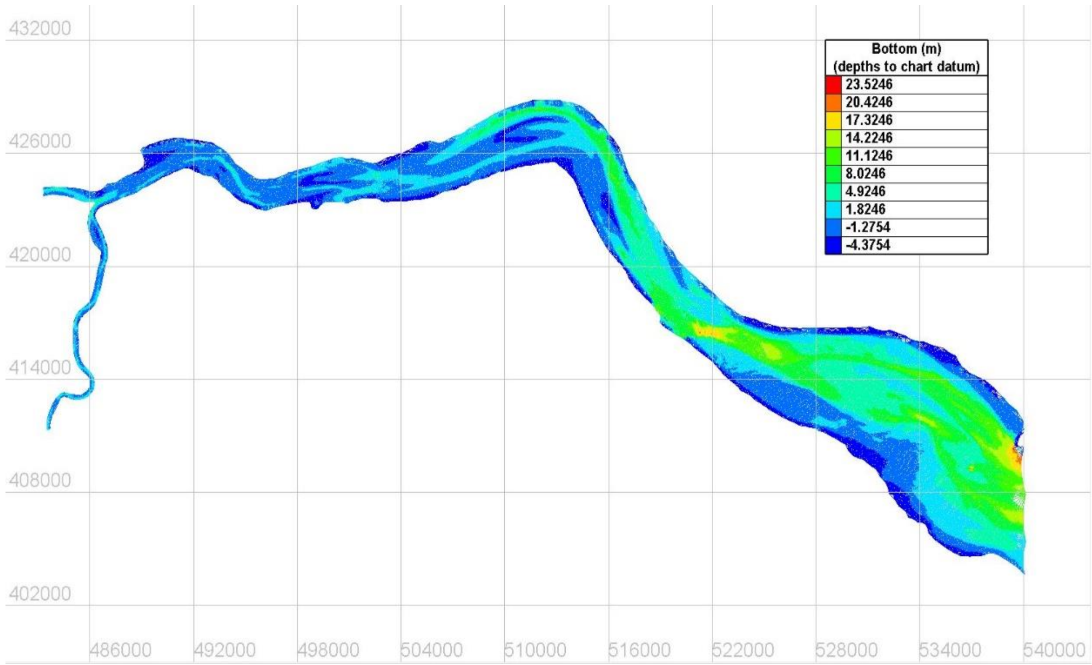

Figure 3.4: The computational domain for the Humber Estuary after interpolation with point dataset; all depths to chart datum.

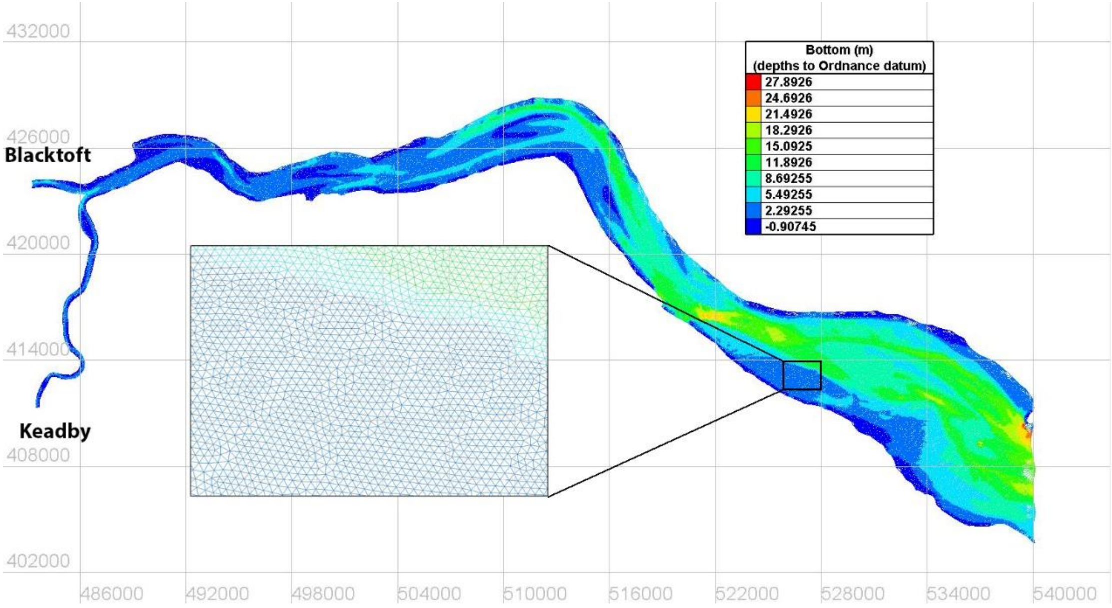

Figure 3.5: The computational domain for the Humber Estuary after correction of datum; all depths to ordnance datum. Inset shows the detail of the computational mesh.

3.2.2.2.2 Boundary condition file

Blue Kenue was employed to develop the boundary condition file required for the simulation. Boundary conditions can be applied to inlets and outlets to determine which factors will supply the required forcing to drive the hydrodynamics of the Humber Estuary (Magnier et al. 2013). The boundary conditions can be defined as solid (default) or liquid boundaries (Pérez-Ortiz et al. 2013). This study employed liquid boundaries as time-varying boundary condition values were specified (Ata et al. 2014). In TELEMAC3D, boundary conditions can only be defined for the horizontal velocities *U* and *V*, flowrates *Q*, water depth *H* and tracers. Pérez-Ortiz et al. (2013) pointed out that TELEMAC3D defines the data associated with the boundaries as Blue Kenue is only capable of defining the boundary type and location. The data associated with the boundaries are defined in the liquid boundary file. Within Blue Kenue, the type of boundary employed is represented by a specific code and colour (Table 3.3). Open river boundary with prescribed *Q* was placed at the fluvial inputs (Rivers Ouse and Trent) while open offshore boundary with prescribed *H* and prescribed tracer was placed at the Humber Estuary mouth (Figure 3.6). Hence, the open river boundary was driven by river discharge while the open offshore boundary was driven by tidal height data extracted from the FES2014 model (Section 3.2.1.3). The boundary conditions can also be edited using Fudaa-Prepro software or a text editor (see Pham et al. 2016 for more details).

Table 3.3: Boundary segment codes and colour (NRC Canada 2011)

Boundary Type	**Code**	**Colour**
Closed boundary (wall)	222	Brown
Open boundary with prescribed Q	455	Blue
Open boundary with prescribed H	544	Green
Open boundary with prescribed Q and H	555	Cyan
Open boundary with prescribed UV	466	Red
Open boundary with prescribed UV and H	566	Orange
Open boundary with incident waves	111	Yellow

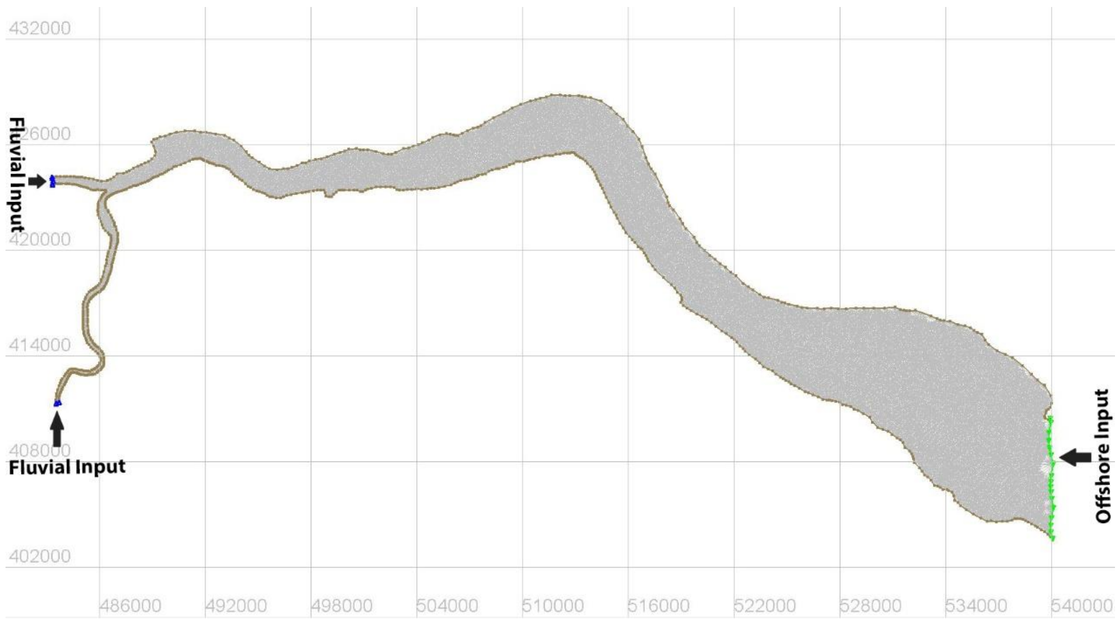

Figure 3.6: Boundaries set up for the hydrodynamic model.

3.2.3 Oil Trajectory Model

The TELEMAC oil spill model (Figure 3.7) was employed for this study (Section 2.5.5). Advection of an oil slick can be expressed as (Equation 3.2):

$$U_{oil} = U_c + \beta U_w \tag{3.2}$$

where:

> U_{oil} represents the oil slick velocity vector, U_w represents wind velocity vector above the water surface, represents the drift of the surface slick due to the wind ($\beta = 0.036$; Joly et al. 2014), and U_c represents the current velocity vector at the free surface.

A stochastic approach is employed to account for turbulent diffusion (Joly et al. 2014). The depth-averaged definition of the turbulent diffusion equation can be expressed as:

$$\frac{\partial C}{\partial t} + U\nabla(C) = \frac{1}{h}\nabla.\left(\frac{h\nu_t}{\sigma_c}\nabla C\right) \tag{3.3}$$

where:

C represents a depth-averaged pollutant concentration, U represents the depth-averaged velocity vector replaced by U_{oil}, h represents water depth computed from TELEMAC3D, and ν_t represents turbulent viscosity computed from TELEMAC3D.

In addition to the TELEMAC3D input files (geometry file, boundary condition file, modified steering file (Appendix I) and liquid boundary file), the oil spill simulation also required: an oil spill steering file (Appendix J) which contained the oil characteristics (Table 3.2); and the modified FORTRAN file which indicates the oil release time step and position (Appendix K). Within the oil spill steering file, computation of oil slick was set to Fay's spreading formulation. Due to computational demand, the number of oil slick particles (*NUMBER OF DROGUES*) was set to 2500. Using the *PRINTOUT PERIOD FOR DROGUES* keyword, the position of the particles was stored at fifteen-minute intervals. In modelling large oil spill transport around the UK, Legrand (2015) assumed a spill volume of 10,000 m^3 released of Brent light crude from 7 locations around the North Sea and English Channel. Consequently, this study employed a hypothetical oil spill volume to 10,000 m^3 as this spill size represents a major oil spill and a more probable spill size which is large enough to illustrate the scale of response required for a major marine oil spill (DeCola et al. 2012). Constant wind speed and direction in time and space were applied to the oil spill simulation. The reliability of the result is not significantly affected by the assumption of constant wind speed, as the influence of wind speed on oil slick transport is approximately 3.6% of the wind speed (Joly et al. 2014; Section 2.2.1.2).

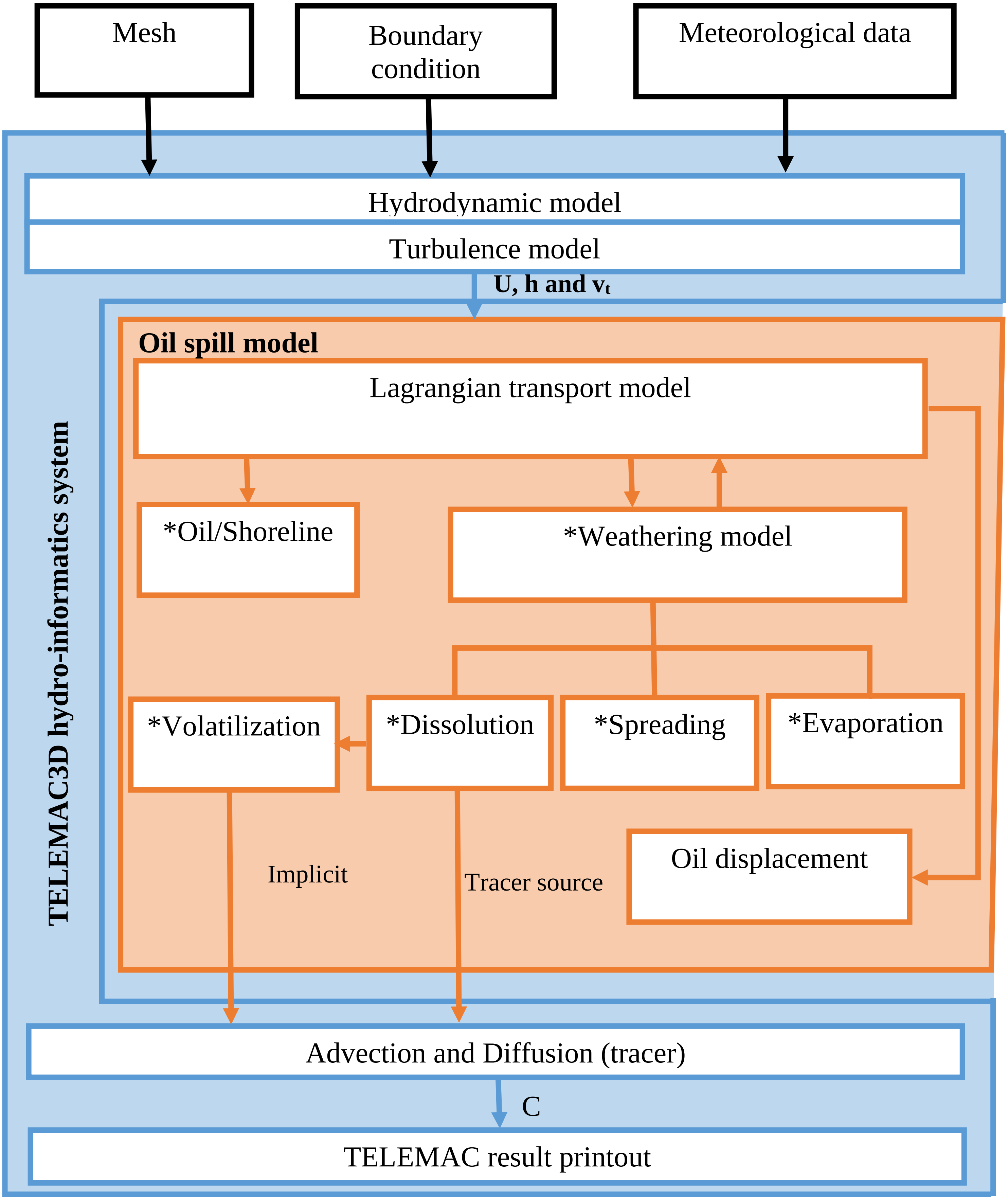

Figure 3.7: TELEMAC hydrodynamic and oil spill model interaction (Joly et al. 2014)

*oil weathering components, hence, not considered in this study.

3.2.4 Temporal Variability of Environmental Factors in the Humber Estuary

The temporal variability of environmental factors in the Humber Estuary was examined to understand the hydraulics of the estuary and characterise its seasonality. These factors included discharge, stage height, wind, temperature and salinity.

3.2.4.1 Freshwater discharge

The temporal variability of discharge from the Rivers Ouse and Trent over an 11-year period (2007 – 2017) was examined from high-resolution 15-minutes flow data at Skelton station on the River Ouse (Figure 3.8) and North Muskham Station on the River Trent (Figure 3.9). At Skelton, the mean monthly discharge from 2007 to 2017 was 56.78 m^3/s, while at North Muskham it was 89.20 m^3/s (Table 3.4). Analyses of discharge data at Skelton and North Muskham reveals that both Rivers Ouse and Trent relatively exhibit strong seasonal discharge variations, with the highest discharge in the winter and lowest in the summer (Table 3.4, Figure 3.10).

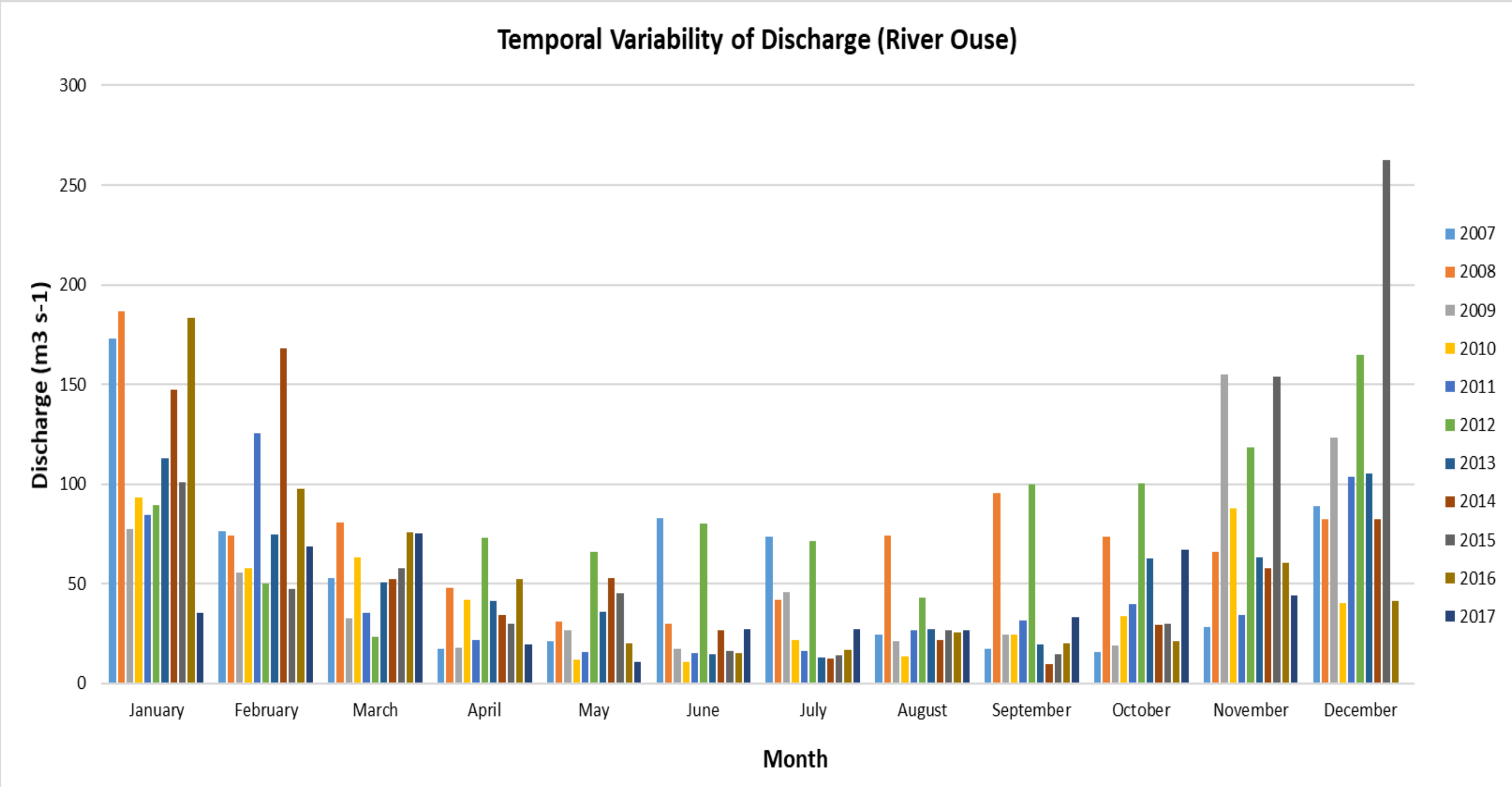

Figure 3.8: Temporal variability of discharge at Skelton station on River Ouse from 2007 – 2017.

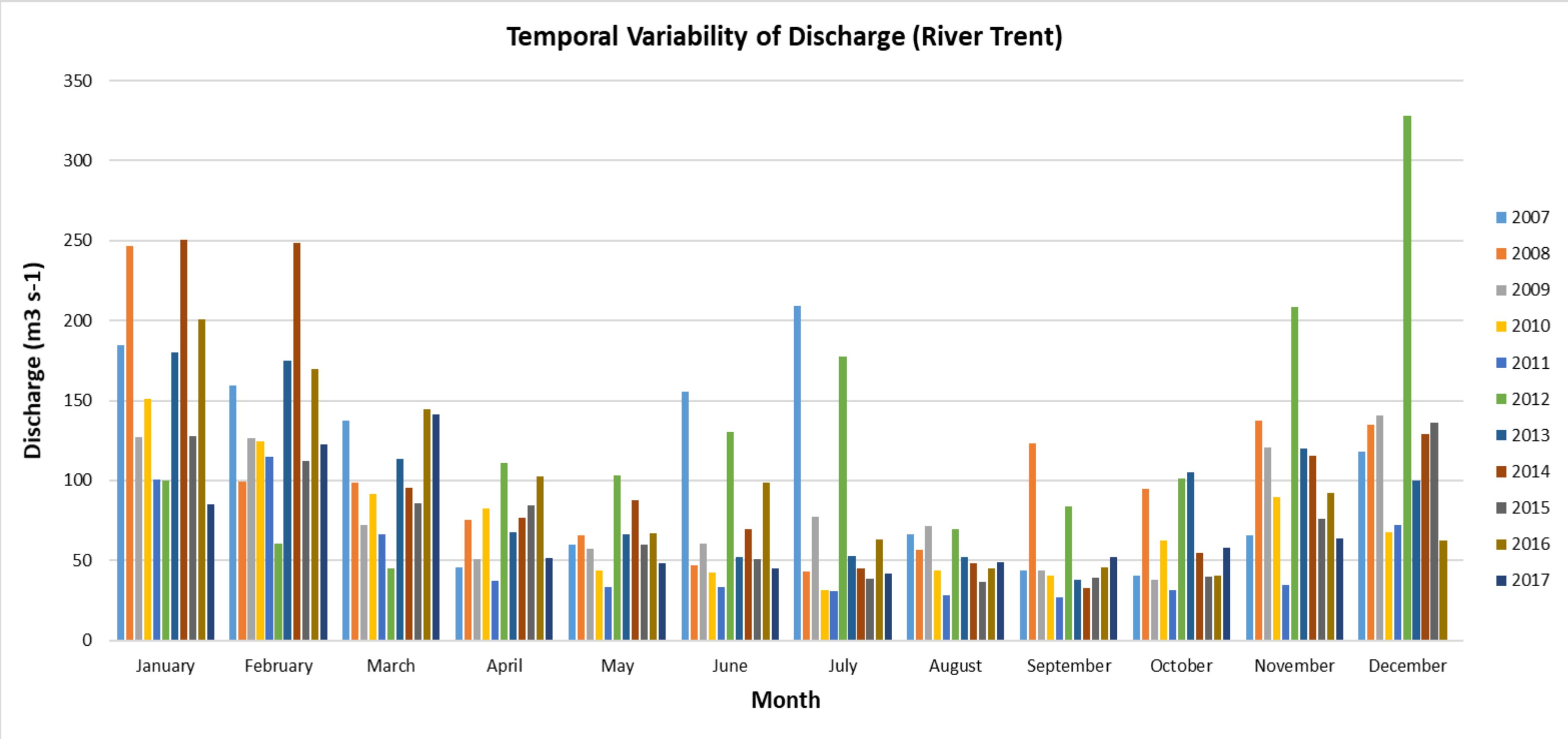

Figure 3.9: Temporal variability of discharge at North Muskham Station on River Trent from 2007 – 2017.

Table 3.4: Seasonal mean discharges (m^3/s) in the period 2007 – 2017

Season	River Ouse (at Skelton station)	River Trent (at North Muskham Station)
Summer (JJA)	30.95	65.53
Autumn (SON)	53.13	71.43
Winter (DJF)	102.60	141.98
Spring (MAM)	40.45	77.85
Average	56.78	89.20

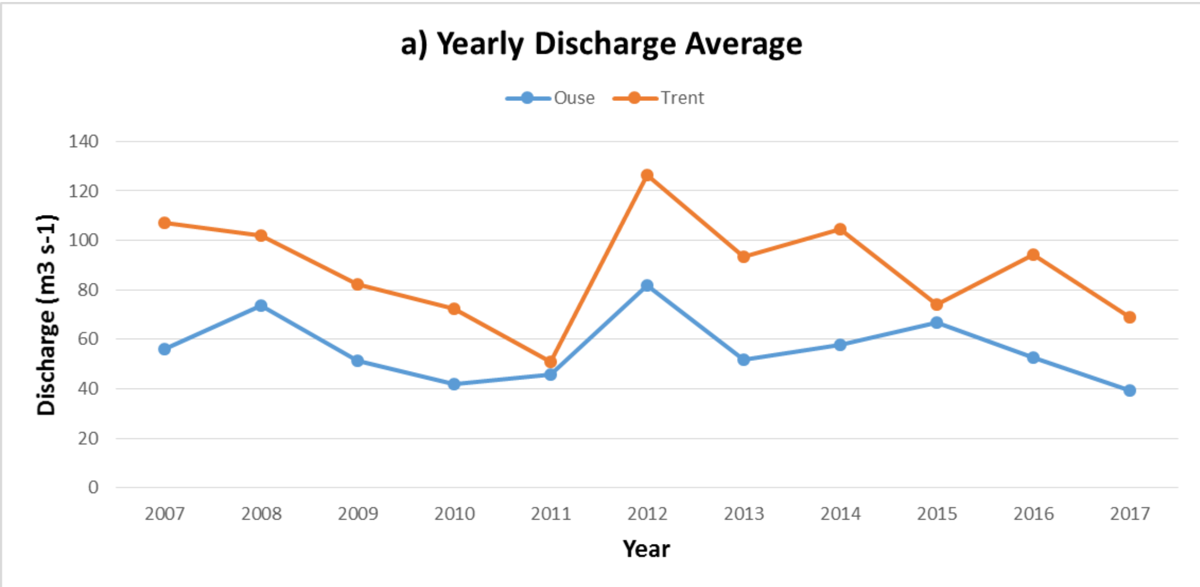

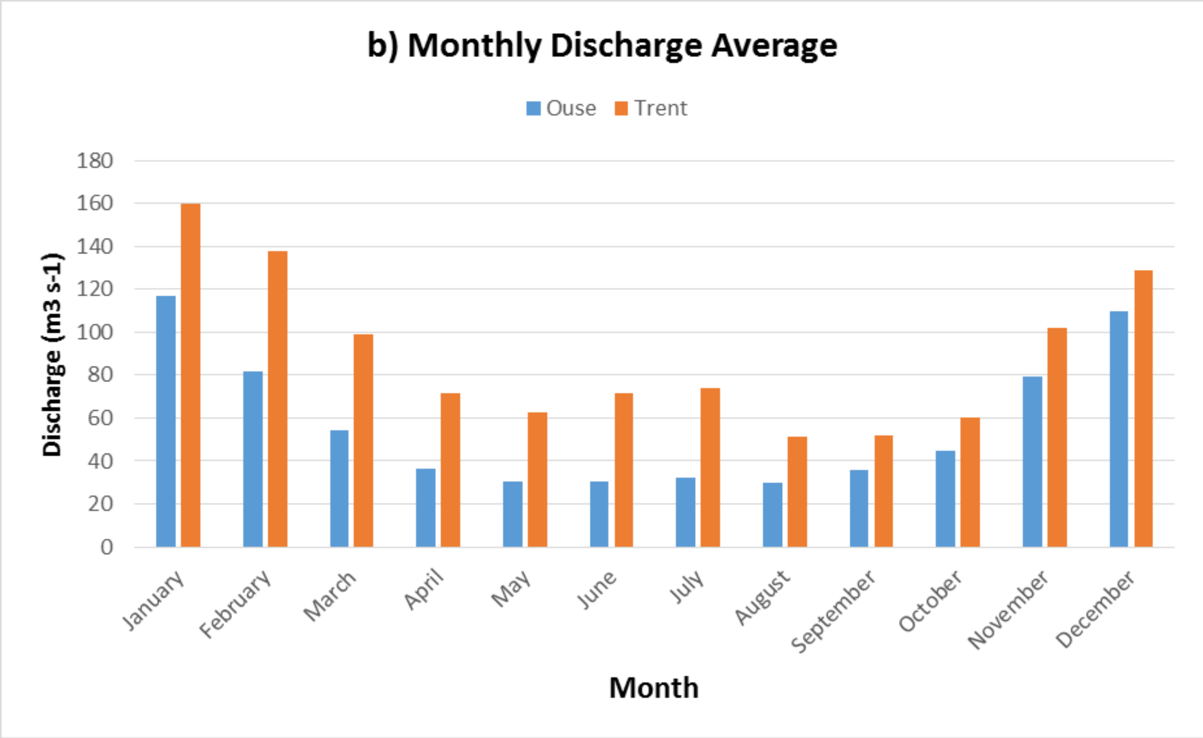

Figure 3.10: a) Yearly discharge averages for Rivers Ouse and Trent; b) Monthly discharge averages for Rivers Ouse and Trent (2007 – 2017).

3.2.4.2 Stage height

Stage height data was examined from 2007 – 2017 at Blacktoft on River Ouse (Figure 3.11) and at Keadby on River Trent (Figure 3.12). The mean monthly stage height from 2007 to 2017 was 0.81 m (above Ordnance Datum) at Blacktoft while at Keadby it was 1.20 m (above Ordnance Datum). Analyses of stage height at Blacktoft and Keadby indicates that the influence of seasonality on stage height (Table 3.5; Figure 3.13). The influence of seasonality reaches Blacktoft and Keadby, however, for a better understanding of the temporal variability of stage height, measurements can be taken further upstream as Blacktoft and Keadby stations are under tidal influence. The lowest stage height was observed in the summer at both stations, while the highest stage height was observed in autumn and winter at Blacktoft and Keadby respectively.

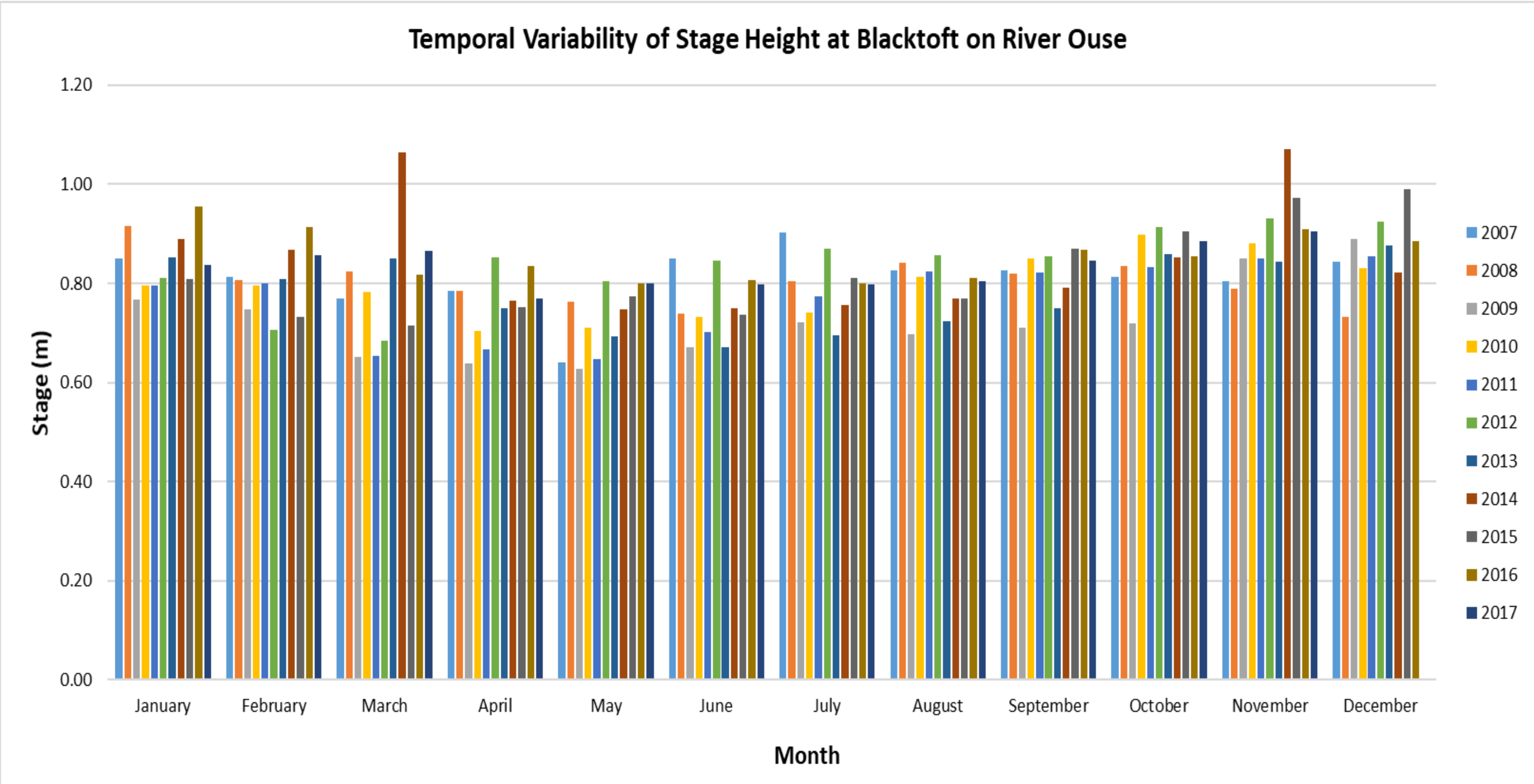

Figure 3.11: Temporal variability of stage height (with respect of Ordnance Datum) at Blacktoft station on River Ouse from 2007 – 2017.

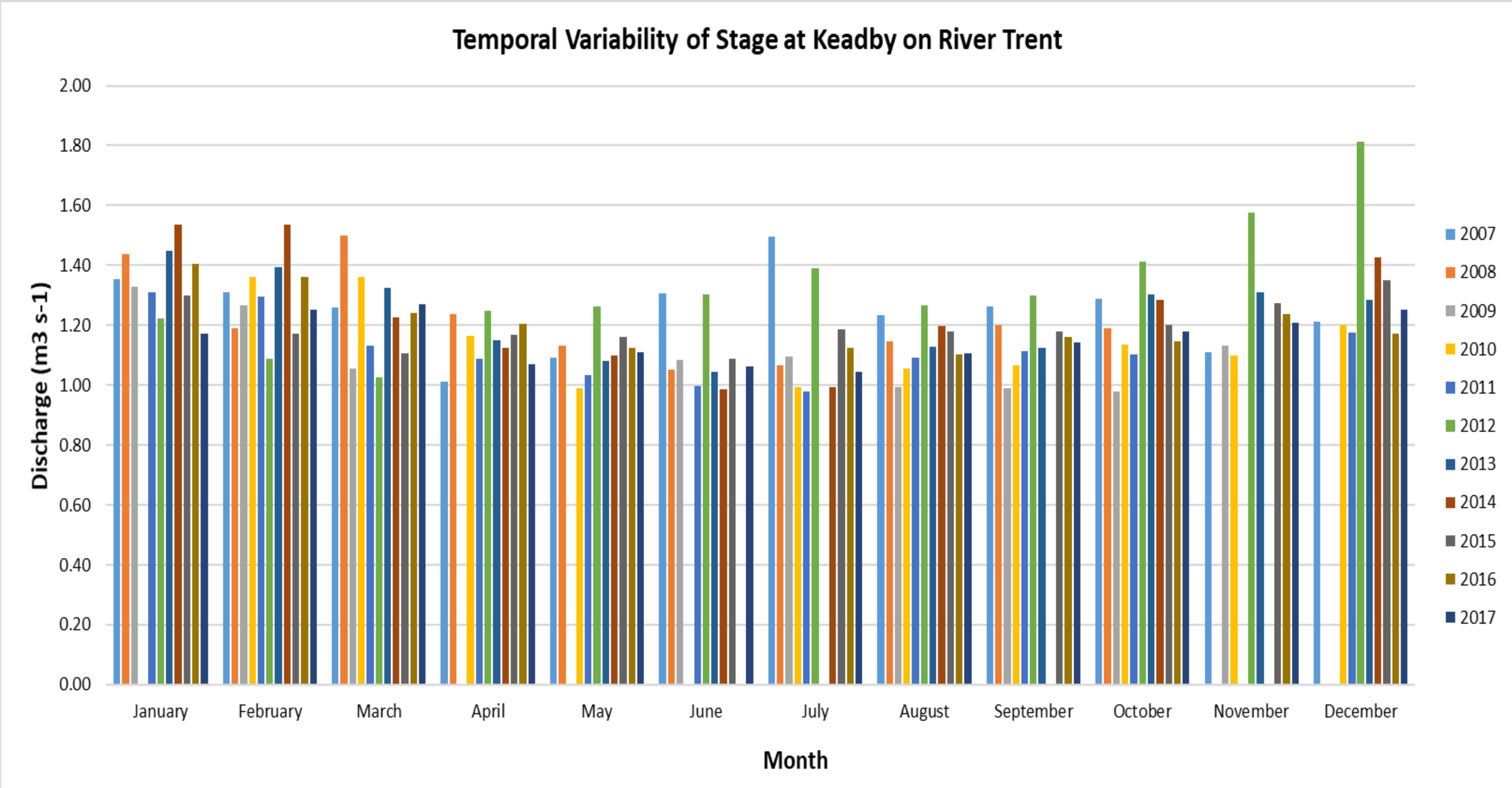

Figure 3.12: Temporal variability of stage height (with respect of Ordnance Datum) at Keadby station on River Trent from 2007 – 2017.

Table 3.5: Seasonal mean stage height (m) in the period 2007 – 2017

Season	River Ouse (at Blacktoft station)	River Trent (at Keadby Station)
Summer (JJA)	0.78	1.12
Autumn (SON)	0.85	1.20
Winter (DJF)	0.84	1.32
Spring (MAM)	0.78	1.16
Average	**0.81**	**1.20**

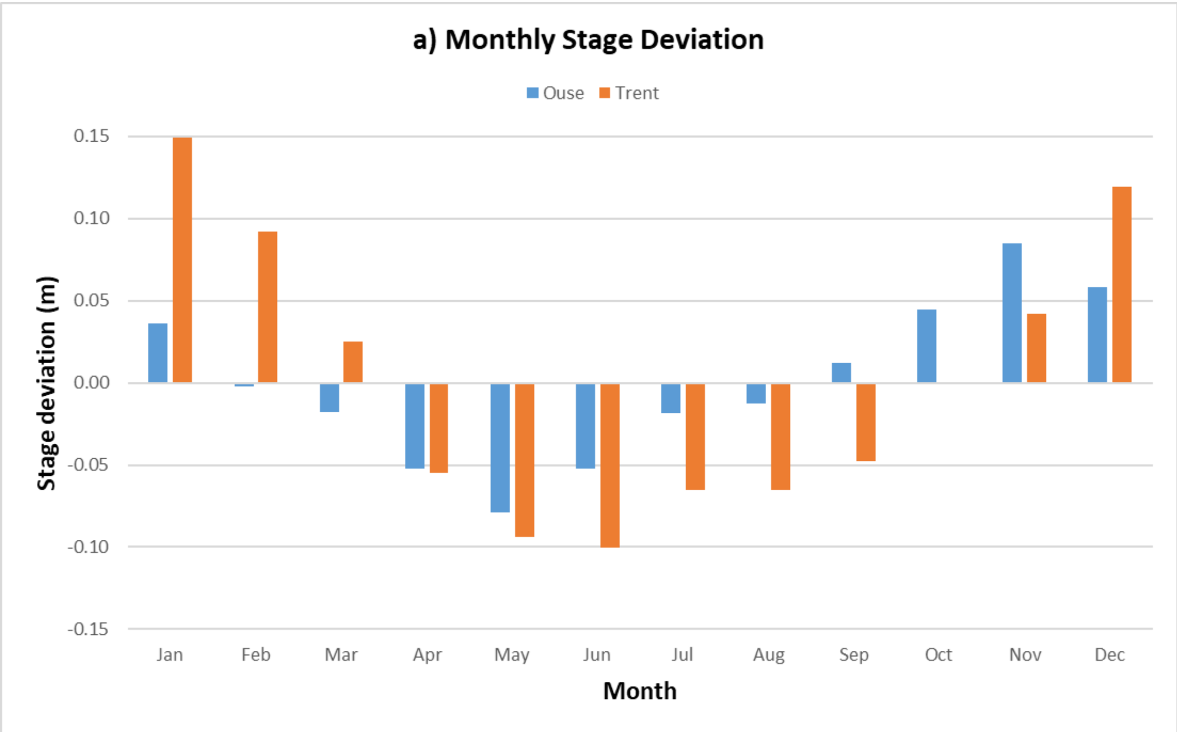

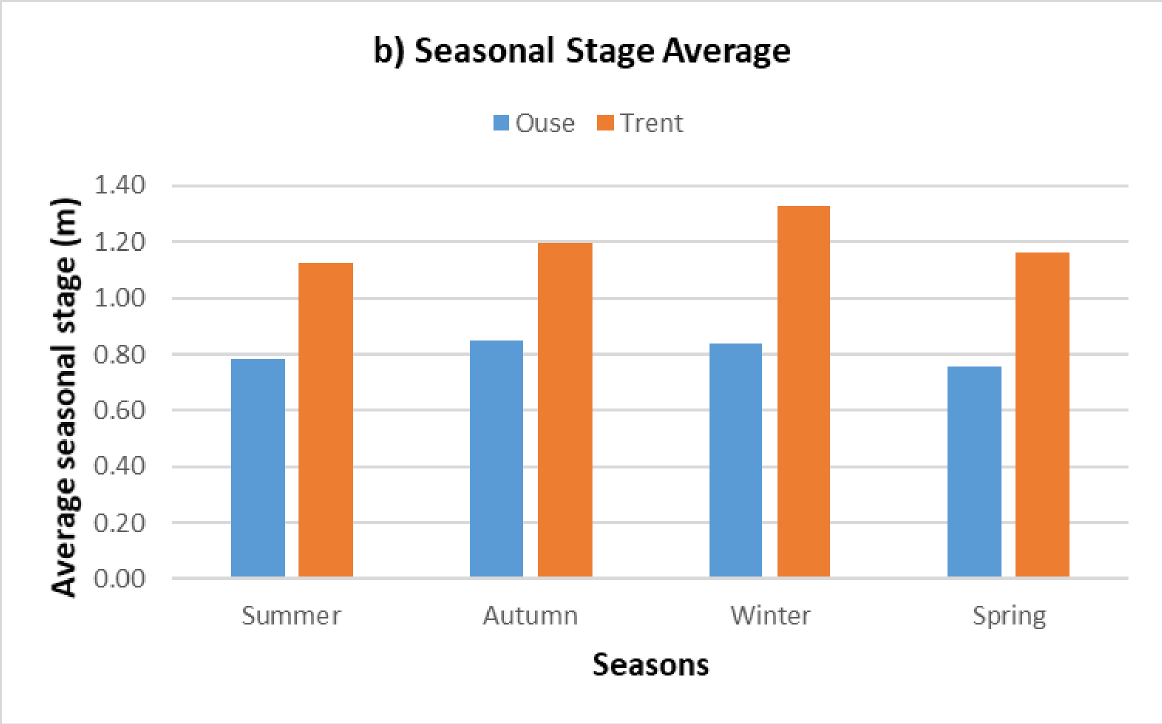

Figure 3.13: a) Average monthly deviations from annual stage averages at Blacktoft (River Ouse) and Keady (River Trent) from 2007 to 2017; b) Seasonal stage averages at Blacktoft and Keadby (2007 – 2017).

3.2.4.3 Wind

Hourly wind data at the Donna Nook station was also examined (Figure 3.14). Analyses of wind data from 2007 – 2016 indicate that wind in the Humber Estuary exhibits seasonal variations (Figure 3.15; Table 3.6). The strongest wind speed was recorded in the winter while weakest wind speed was recorded in the summer.

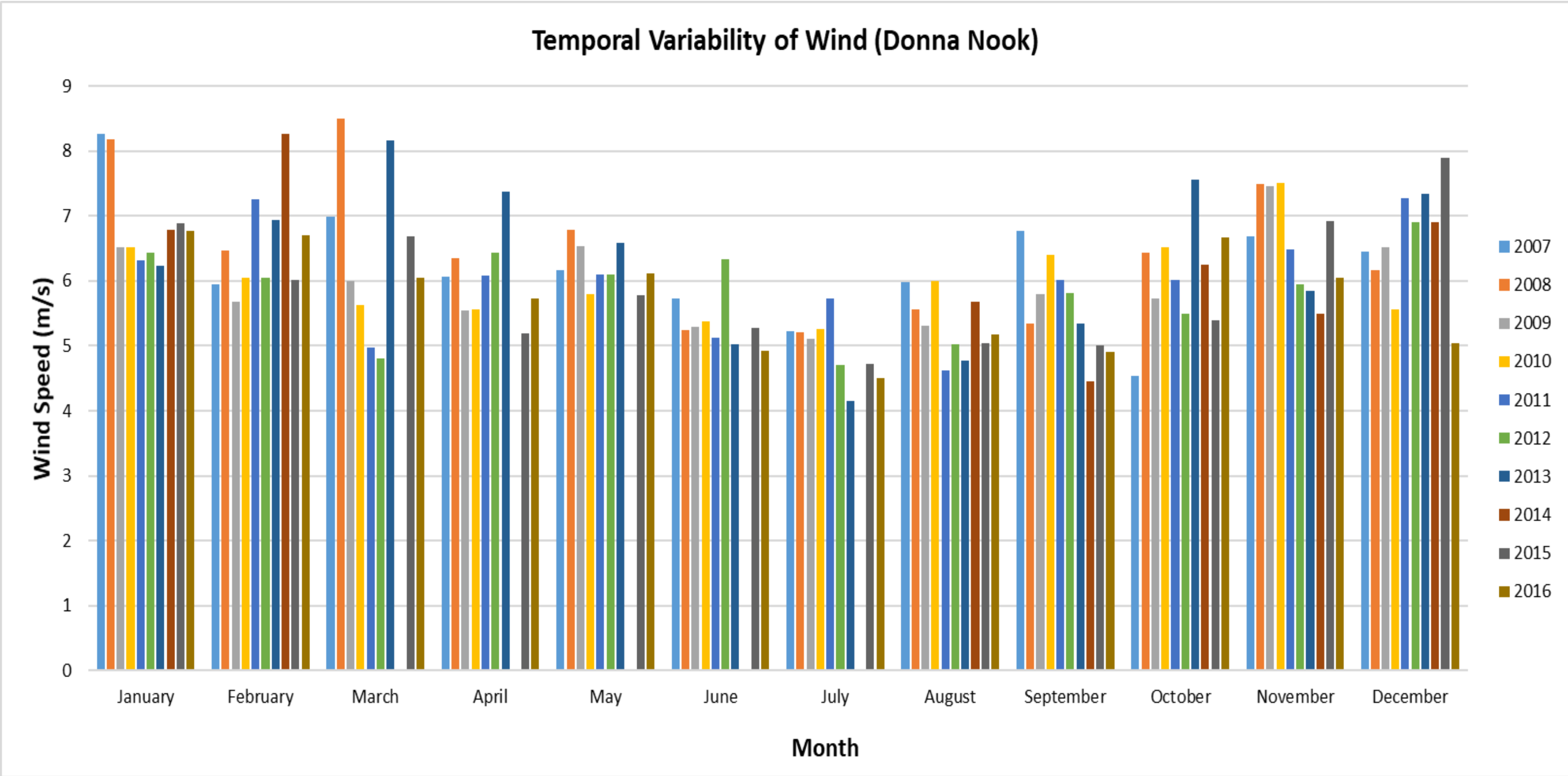

Figure 3.14: Temporal variability of wind at Donna Nook station from 2007 – 2016.

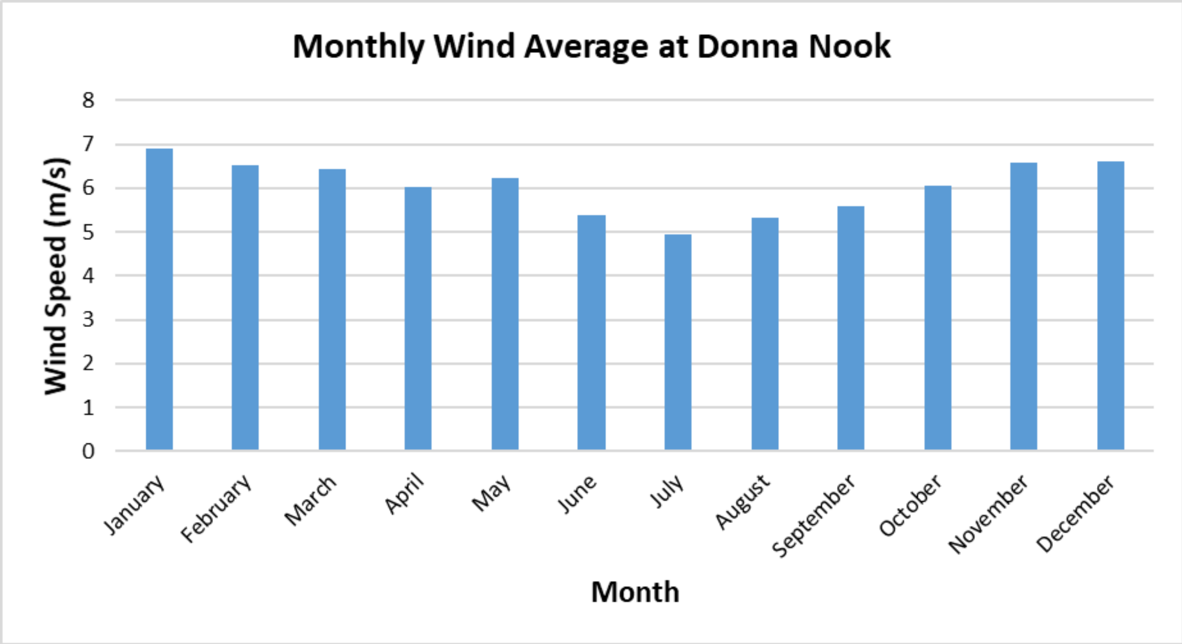

Figure 3.15: Temporal variability of wind at Donna Nook station from 2007 – 2016.

Table 3.6: Seasonal mean wind speed (m/s) in the period 2007 – 2016

Season	**Wind Speed (m/s)**
Summer (JJA)	5.21
Autumn (SON)	6.08
Winter (DJF)	6.68
Spring (MAM)	6.23
Average	6.05

3.2.4.4 Temperature and salinity

Temperature data from 2007 – 2017 was examined alongside salinity data from 1990 – 1995 and 2007 – 2017. Analyses of water temperature data revealed that the highest temperature occurs in the summer while the lowest temperature occurs in the winter (Figure 3.16). While evaluation of salinity data revealed that the highest water salinity occurs in the autumn and lowest water salinity occurs in the spring (Figure 3.17; Table 3.7).

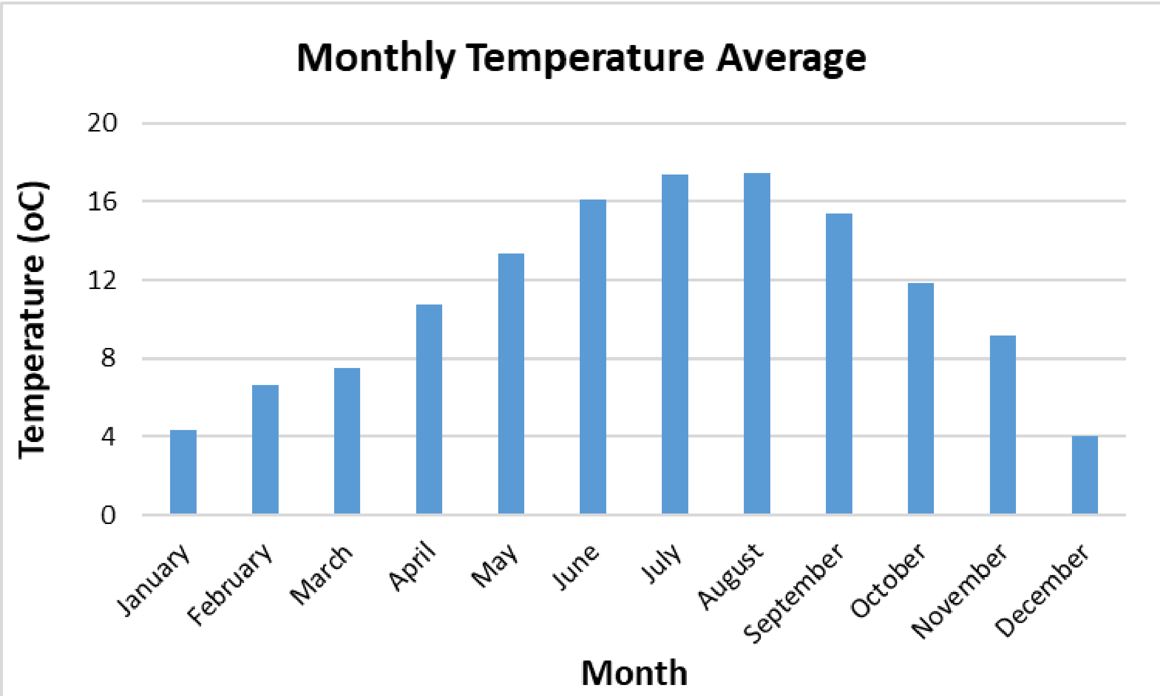

Figure 3.16: Average monthly temperature of the Humber Estuary.

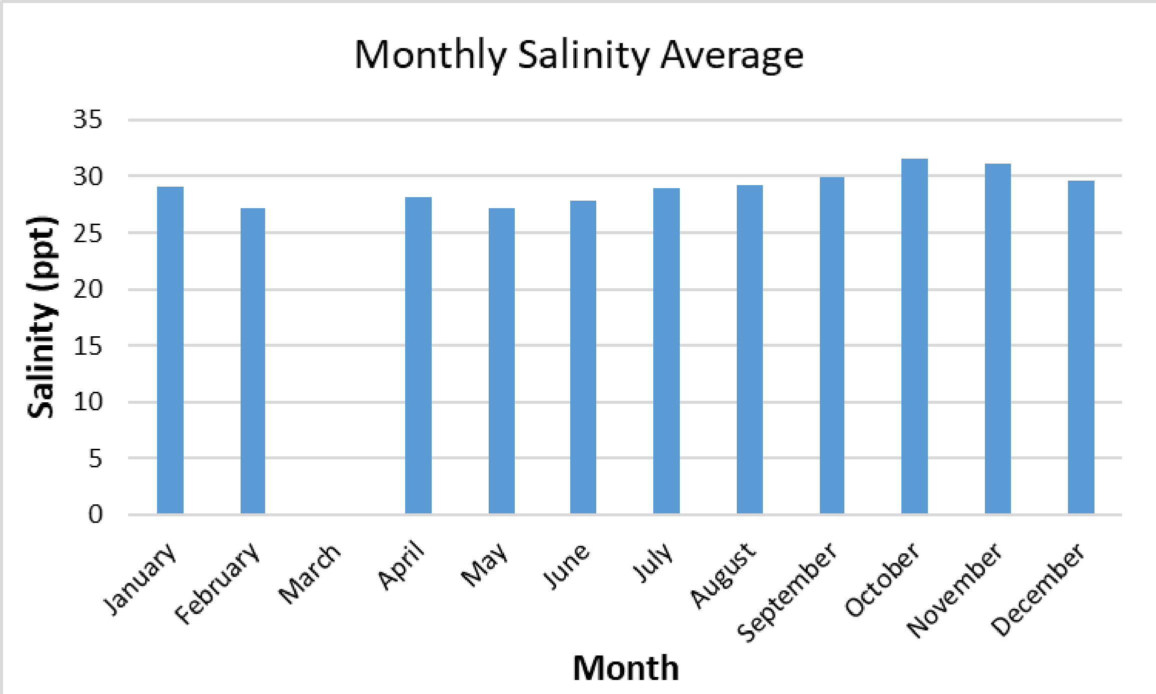

Figure 3.17: Average monthly salinity of the Humber Estuary. Note: No salinity data was available for the month of March.

Table 3.7: Seasonal mean temperature and salinity of the Humber Estuary

Season	**Temperature (°C)**	**Salinity (ppt)**
Summer (JJA)	16.96	28.74
Autumn (SON)	12.15	30.84
Winter (DJF)	5.00	28.65
Spring (MAM)	10.52	27.72
Average	11.16	28.99

Analyses of the various environmental factors in the Humber Estuary indicate that the hydraulics in the estuary is governed by seasonal variability. This makes the Humber

Estuary an ideal case study to assess the influence of seasonal discharge variability on oil spill dynamics in a tide-dominated environment.

3.2.5 Calibration and Validation Design

In this section, hydrodynamic model scenarios were developed for summer and winter conditions in the Humber Estuary. In selecting a typical summer and winter month, it is important to pick a representative month for comparison with real-life data. Consequently, stage data available at the river boundary points were analysed to determine the best representative summer and winter months for the hydrodynamic models. Because of limited high-resolution discharge data, the models were driven by constant river discharge at the river boundaries and 15-minute tidal height data at the offshore boundary. In the absence of current data, the models were calibrated and validated with water level during the representative summer and winter months.

3.2.5.1 Seasonal variability of discharge

Numerical modelling tools were employed to assess the influence of seasonal discharge variability on oil spill transport. Rather than simulate a full decade of fluvial and tidal fluxes through the estuary, full 28-day semi-diurnal tidal cycles combined with two river flow conditions, representative of summer and winter were simulated. To determine the latter, the monthly stage height averages for each season at Blacktoft and Keadby were compared (using standard deviation) to find the month that best represents the flow seasonal condition (Figure 3.18). For each season, the average monthly stage height and stage height variability were calculated (Figure 3.18). Subsequently, from the observed data was selected the month which most resembles the seasonal average using standard deviation. This procedure results in representative seasonal data (Table

3.8). Consequently, the fidelity and variability of the observed empirical data in not lost, and compatibility with observed tidal data for the selected periods is maintained.

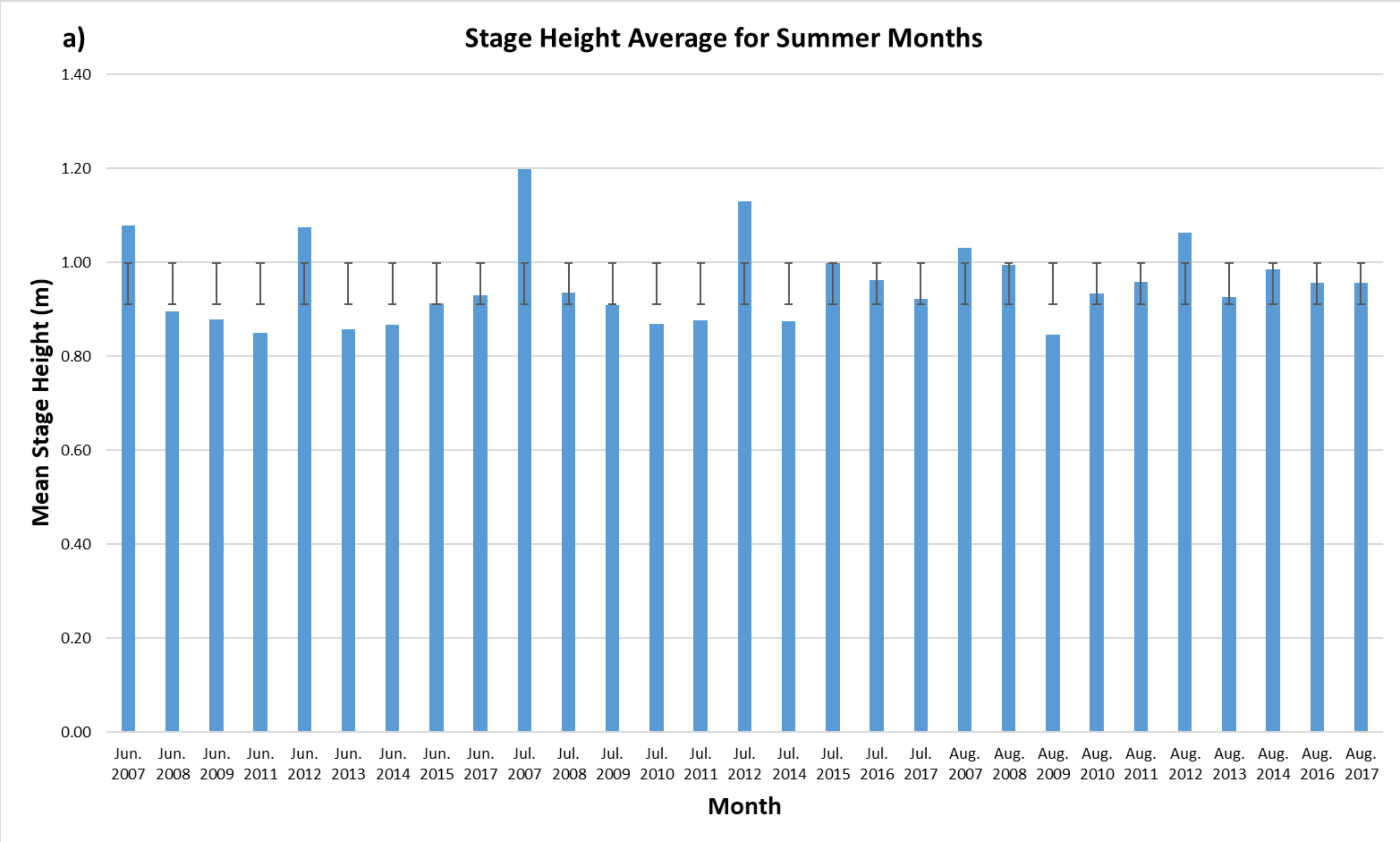

Figure 3.18a: Average monthly stage height and stage height variability (standard deviation) for summer

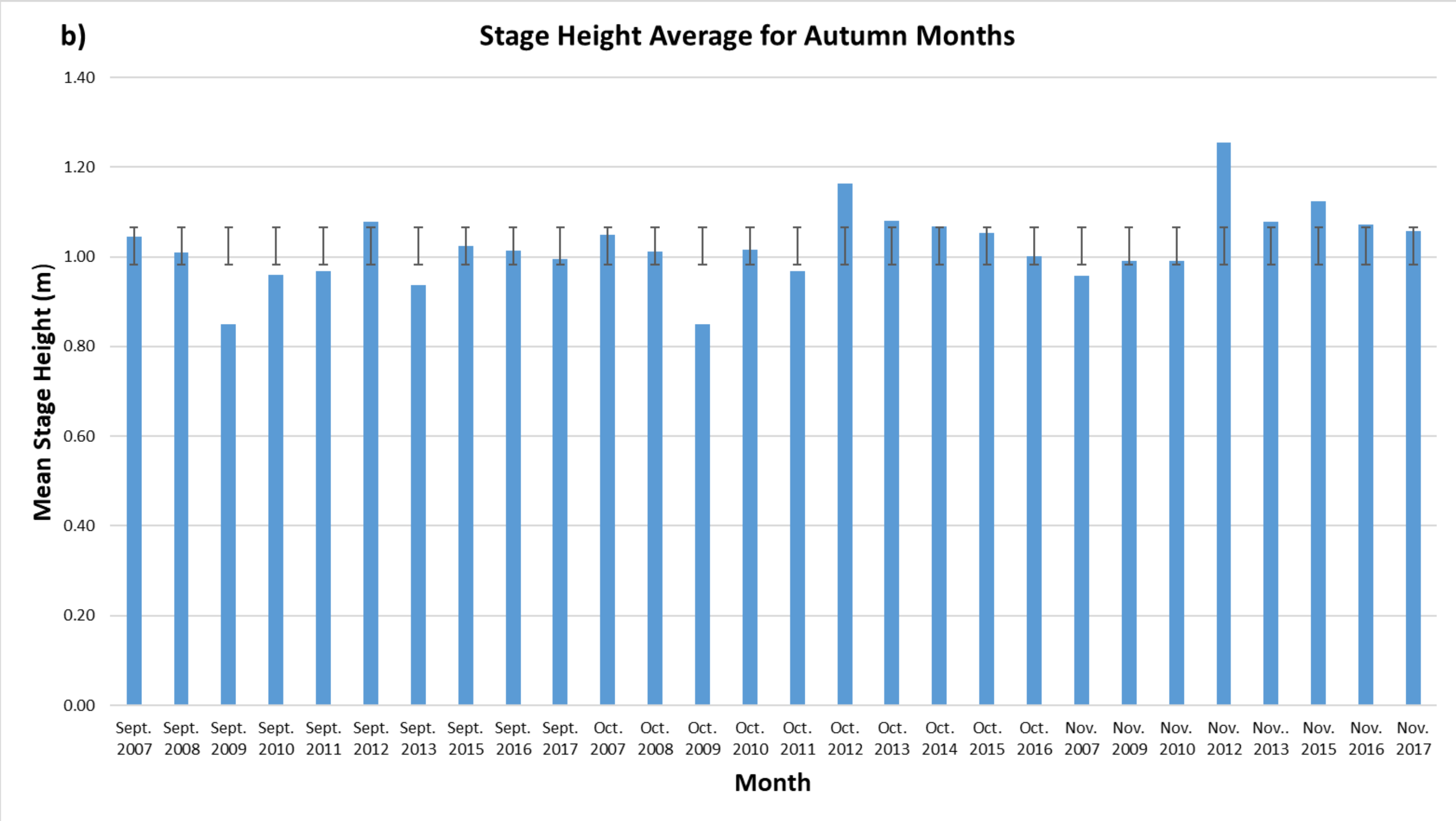

Figure 3.18b: Average monthly stage height and stage height variability (standard deviation) for autumn

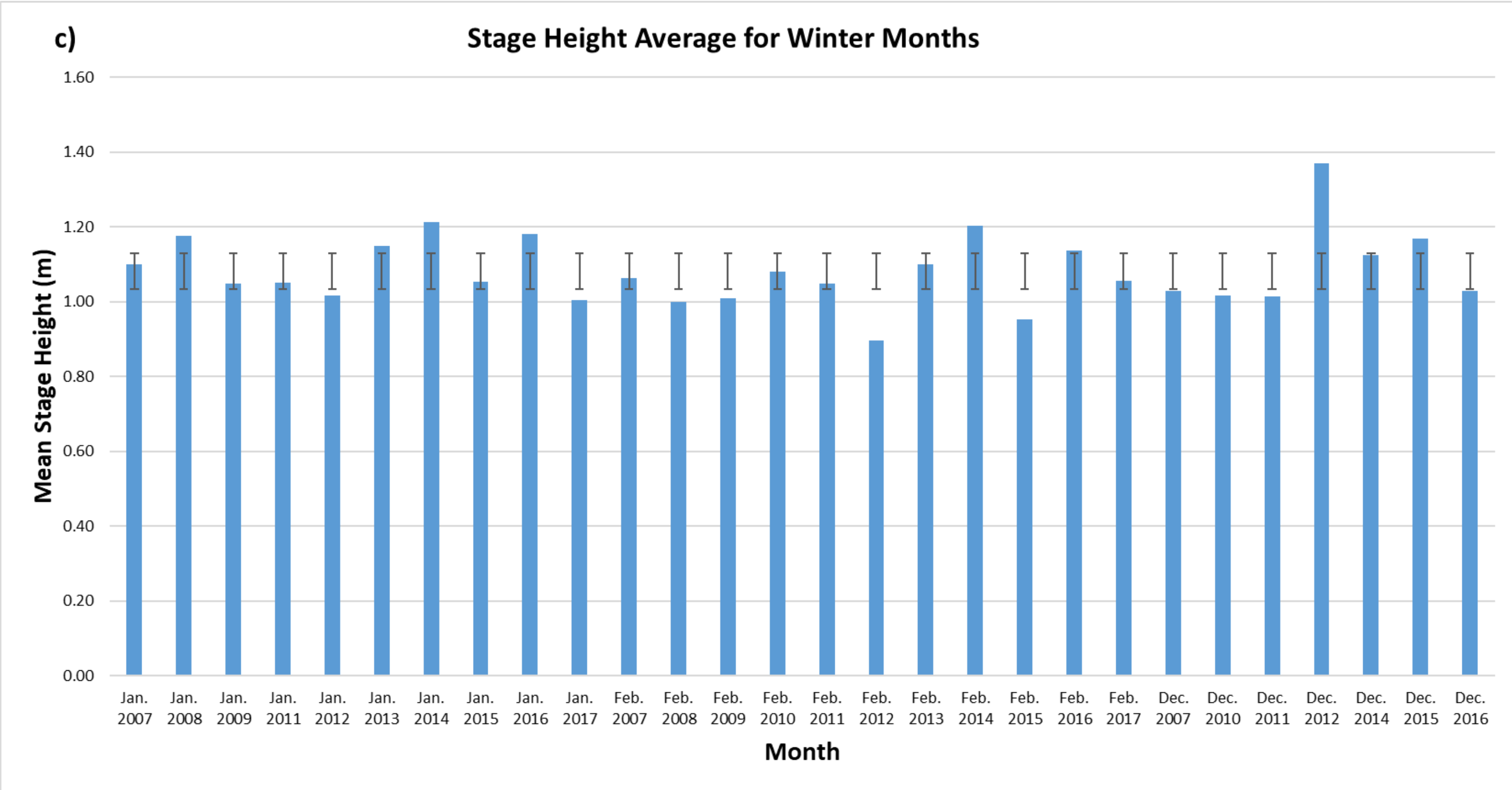

Figure 3.18c: Average monthly stage height and stage height variability (standard deviation) for winter

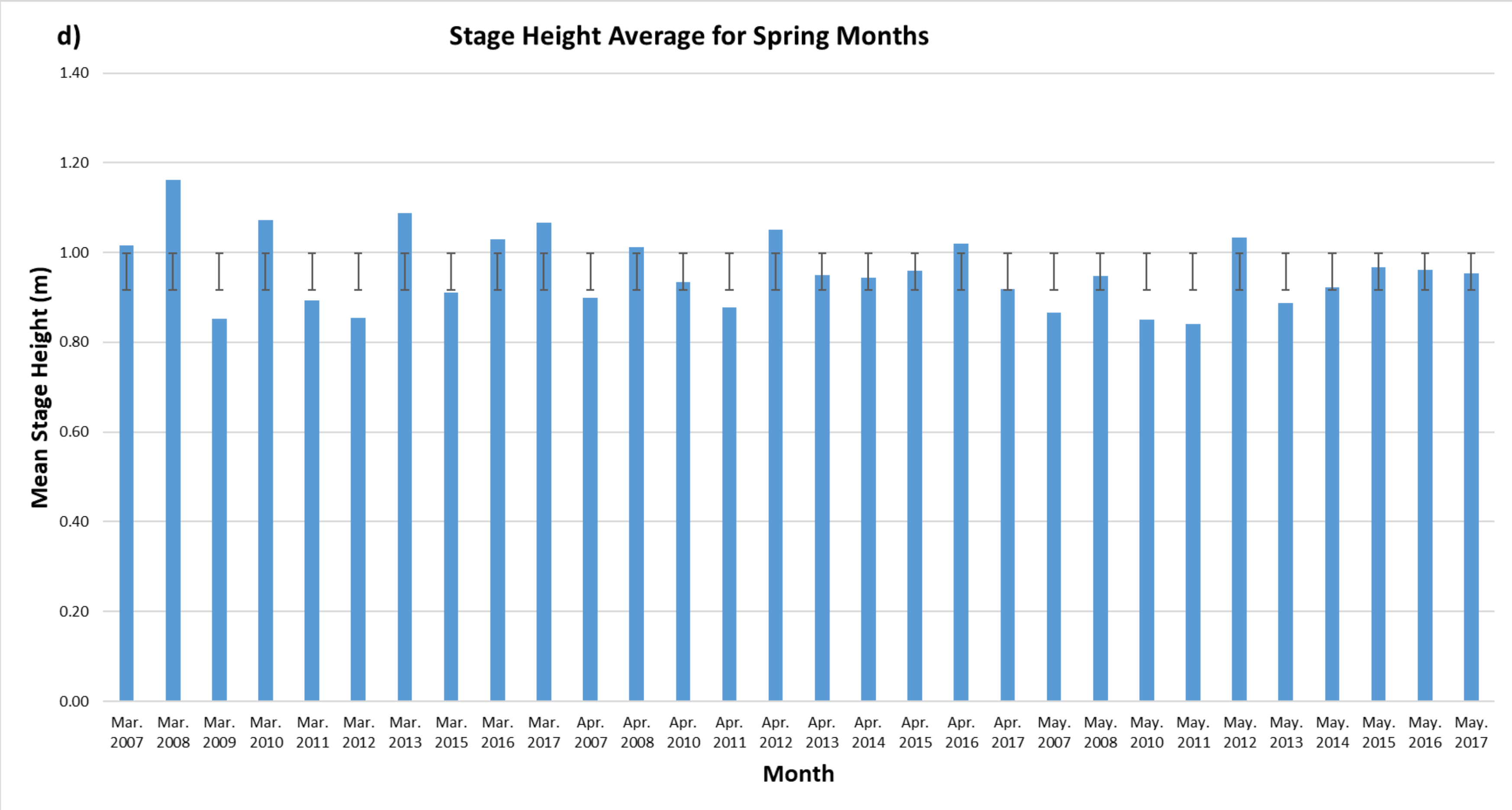

Figure 3.18d: Average monthly stage height and stage height variability (standard deviation) for spring

Table 3.8: Ideal period to develop hydrodynamic models for various seasons and associated average wind speed and direction applied to the oil spill model

Season	Representative Simulation Period			Second Most Representative Simulation Period (validation)		
	Period	Wind Speed (m/s)	Wind Direction (degree)	Period	Wind Speed (m/s)	Wind Direction (degree)
Summer	August 2017	4.75	211	August 2016	5.18	195
Autumn	September 2015	5.00	202	October 2010	6.51	191
Winter	February 2010	6.05	167	February 2013	6.95	175
Spring	April 2015	5.19	185	May 2017	6.12	209

Because of limited high-resolution discharge data at the fluvial inputs (Blacktoft on the River Ouse and Keadby on the River Trent), constant discharge obtained from literature was employed to drive the open fluvial boundary (Table 3.9). Also, this study only considered summer and winter season due to lack of typical discharge data for autumn and spring season. This is not expected to impact the study aim as the assessment of temporal variability in the estuary suggests that summer and winter conditions represent the extreme of hydraulic characteristics in the Humber Estuary (Section 3.2.4). The open offshore boundary was driven by 15-minute tidal height data extracted from the

FES2014 model (Section 3.2.1.3). Constant temperature and salinity for the representative seasons were assumed along the open offshore boundary (Table 3.7).

Table 3.9: Typical freshwater flows under high and low conditions from Rivers Ouse and Trent (Mitchell et al. 1999; 2003b)

River	Station	Winter (m^3/s)	Summer (m^3/s)
Ouse	Blacktoft	800	25
Trent	Cromwell	400	30

3.2.5.2 Model calibration and validation scenarios

Calibration is typically achieved by qualitatively comparing short time series of output data (e.g. current velocity or water level) by the numerical model with in-situ data from identical location and period (Vale and Dias 2011). The hydrodynamic models were calibrated against 15-minute tidal height data for Immingham station. In large estuaries, reasonable reproduction of the depth-averaged currents can be achieved if accurate bathymetry is employed and tidal elevation is accurately simulated (Prandle 2009). Model calibration was undertaken for a single point due to limited data collectection. Bottom friction (i.e. Chezy's friction coefficient) is an important and sensitive TELEMAC3D model parameter (Jia et al. 2015; Rahmann and Venugopal 2017) and formed the main focus of the model calibration. The calibrations were done independently for each representative month in each season (Table 3.8) to allow for seasonal variation in optimal parameter values.

Validation of the models was carried out to prove that the calibrated models are capable of simulating another time period to which they were not calibrated (Ganju et al. 2009).

The hydrodynamic models were also validated against 15-minute tidal height data for Immingham station. Model validation was undertaken by comparing model results with observed data from Immingham station, for the second most representative month for each season (Table 3.8).

3.2.5.3 Model performance indicators

Model performance was evaluated using three statistical measures: regression coefficient, *b*; coefficient of determination, R^2; and Root Mean Square Error, RMSE. The regression coefficient was employed to evaluate the statistical closeness of the measured and predicted data. A regression coefficient close to 1 suggests statistical closeness between the compared data (Adeboye et al. 2019). The coefficient of determination (Equation 3.4) is popularly employed to evaluate the goodness of fit in a linear regression model (Zhang 2017). A coefficient of determination ($0 \leq R^2 \leq 1$) close to 1 suggests a good fit between model output and measured data and that most of the variance in the measured data can be inferred from the model output (Adeboye et al. 2019). Cheng et al. (2014) point out that in scenarios where there is an error in the measured data, the derived statistical inference may be unreliable. To improve confidence, evaluation of metadata which was obtained alongside associated measured data was undertaken, to ensure that standard practice was adhered to. Root Mean Square Error (Equation 3.5) is appropriate to determine the agreement between model output and measured data for scalar quantities (e.g. water levels) (Brière et al. 2007; Lindim et al. 2011). The Root Mean Square Error value ranges from 0 to $+\infty$ (Adeboye et al. 2019). Ideally, if there is a perfect agreement between model output and measured data, Root Mean Square Error value will be zero (Umrao et al. 2018). Hence, lower Root Mean Square Error value indicates better model performance. The reliability of the

Root Mean Square Error improves with an increase in the number of values compared (Chai and Draxler 2014). To evaluate the model performance using the various statistical measures, 2,976 and 2,688 measured and predicted values were compared for summer and winter respectively. This comprised of 15-minutes free surface elevation data for the representative month.

$$R^2 = \left(\frac{\sum_{i=1}^{n}(A_i - \bar{A})(B_i - \bar{B})}{\sqrt{\sum_{i=1}^{n}(A_i - \bar{A})^2}\sqrt{\sum_{i=1}^{n}(B_i - \bar{B})^2}}\right)^2 \qquad (3.4)$$

$$RMSE = \sqrt{\frac{\sum_{i=1}^{n}(A_i - B_i)^2}{n}} \qquad (3.5)$$

where:

n is the number of observations; A_i is the measured values; and B_i is the predicted values.

A one-way ANOVA ($P < 0.05$) followed by Holm-Sidak test (Equation 3.6) was employed to understand the relative influence of hydrodynamic conditions (seasonal river discharge variation, water level and tidal range) on the oil slick impacted area on water surface, length of the oil slick over time (distance from one end of the slick to the other) and overall distance travelled (maximum upstream and downstream displacement from the point of release) (Section 3.2.6).

$$p = 1 - \left(\sqrt[(m+1=i)]{(1 - \alpha)}\right) \qquad (3.6)$$

where:

p is the p-value; m is the number of levels/comparisons; i is the rank i.e. position in the ordering according to Holm (1979); and α is the significance level (0.05).

3.2.6 Oil Spill Design

To investigate relative impacts of seasonal discharge variation and tidal flow on oil slick dynamics for the Humber Estuary a number of scenarios were simulated. Each scenario simulates an instantaneous oil release from one of two arbitrary locations, an upstream (in the upper half) and a downstream one (in the lower half) (L1 and L2; Figure 3.19). Considering the choice of arbitrary locations, the influence of oil release location on oil spill transport is undertaken in Chapter 5. Simulation sensitivity to the lateral position of the points is analysed in Chapter 5. The oil is released from these locations under eight scenarios, representing spring and neap tidal conditions at Immingham, during both high and low tide, under both summer and winter flows (Table 3.10). Immingham (Figure 3.1) was chosen as the reference point because of data availability. As a result, 16 oil spill scenarios are simulated in total. Each scenario simulates an instantaneous release of 10,000 m^3 of Brent Crude (Table 3.2), and the resulting simulated oil slick is monitored for a 48-hour period (over two semi-diurnal tidal cycles). To visualise the oil spill transport, a python script was utilised to convert the TELEMAC oil spill displacement output file (tecplot® .dat format) into an ArcMap readable (.xyz) format and to extract oil spill displacement at every time step (15 minutes interval) (Appendix L). Oil spill transport was visualised and analysed within ArcMap 10.5.1 software. The *measure tool* (Figure 3.20) within ArcMap was employed to measure, (a) the oil slick impacted area on water surface, (b) length of the oil slick over time (distance from one end of the slick to the other) and (c) overall distance travelled (maximum upstream and downstream displacement from the point of release).

These parameters are useful to understand the dynamics of oil slicks in the estuarine environment, which have not been studied before (Section 3.1). Furthermore, a one-way ANOVA ($P < 0.05$) followed by Holm-Sidak test was employed to understand the relative influence of hydrodynamic properties (seasonal river discharge variation, water level and tidal range) on these parameters. Here, oil beaching is defined as occurring when oil interacts with the edge of the computational grid. The length of the polluted estuary bank line was measured within ArcMap.

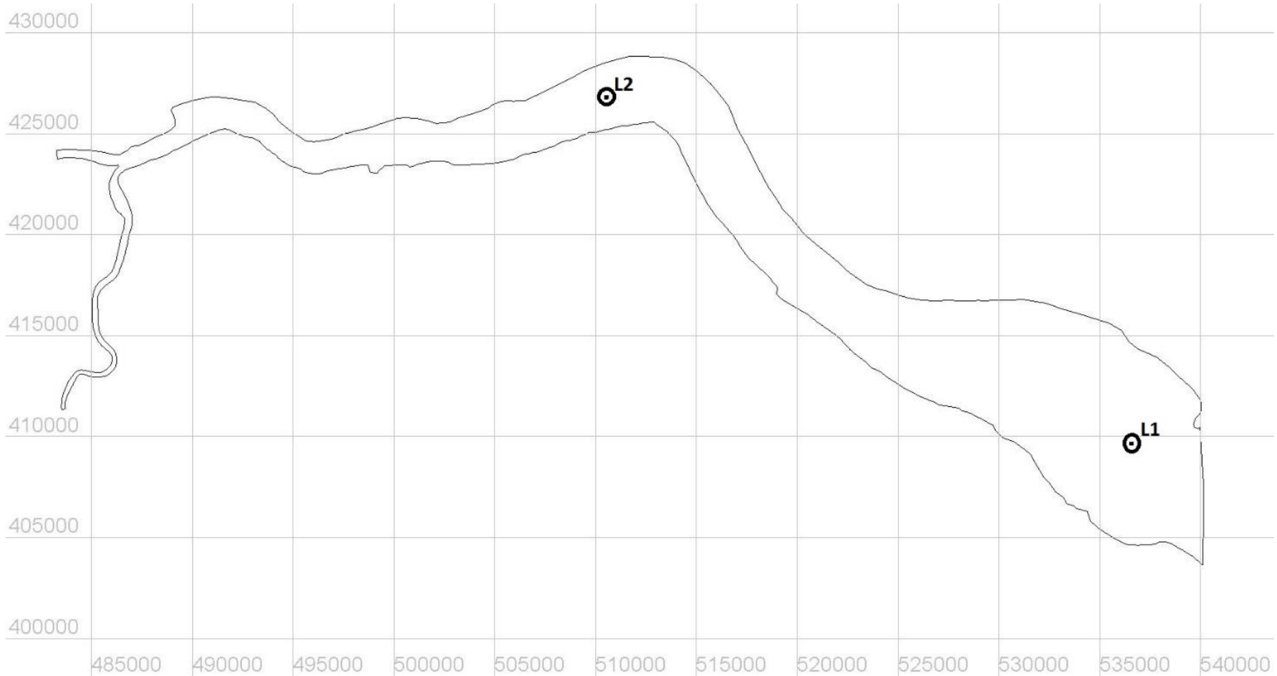

Figure 3.19: Outline for computational domain showing release points for oil spill scenarios at L1 (536528; 409627) and L2 (510498; 426777) (coordinates are in OSGB 1936).

Table 3.10: Summary of the oil slick release scenarios (tidal stage is with reference to Immingham station). Scenarios are repeated for both L1 and L2.

Scenario	**Oil release time**	
	Summer	**Winter**
HW NT	02/08/2017 (02:00)	07/02/2010 (23:15)
LW NT	01/08/2017 (18:45)	06/02/2010 (17:30)
HW ST	08/08/2017 (18:00)	01/02/2010 (19:30)
LW ST	08/08/2017 (00:15)	01/02/2010 (14:00)

Note: HW = high water; LW = low water; NT = neap tide; ST = spring tide.

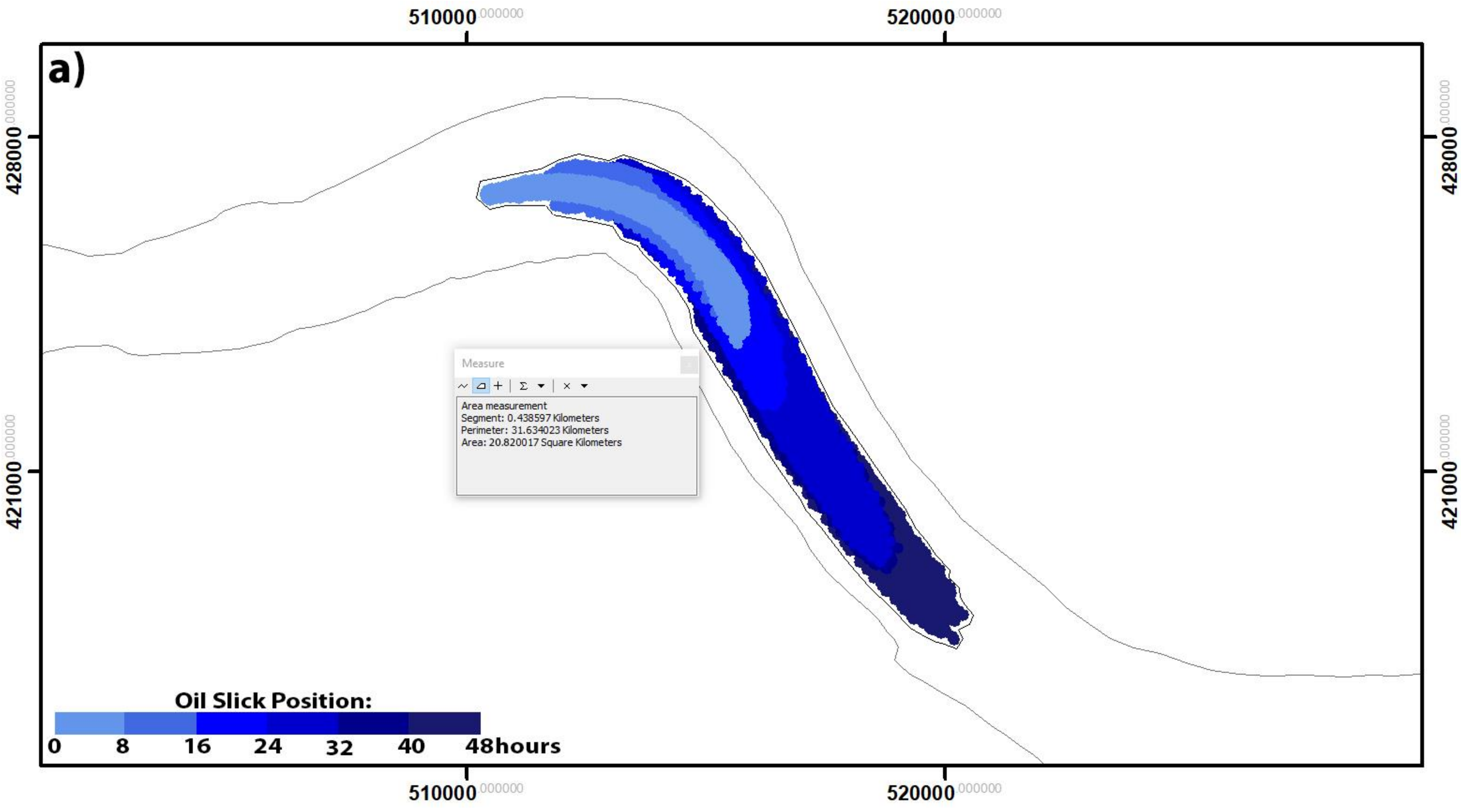

Figure 3.20a: Surrounding polygon to measure oil slick impacted area on water surface after 48 hours. Note: Trajectory shows oil released on the Humber Estuary at L2 high water neap in winter (Figure 3.34).

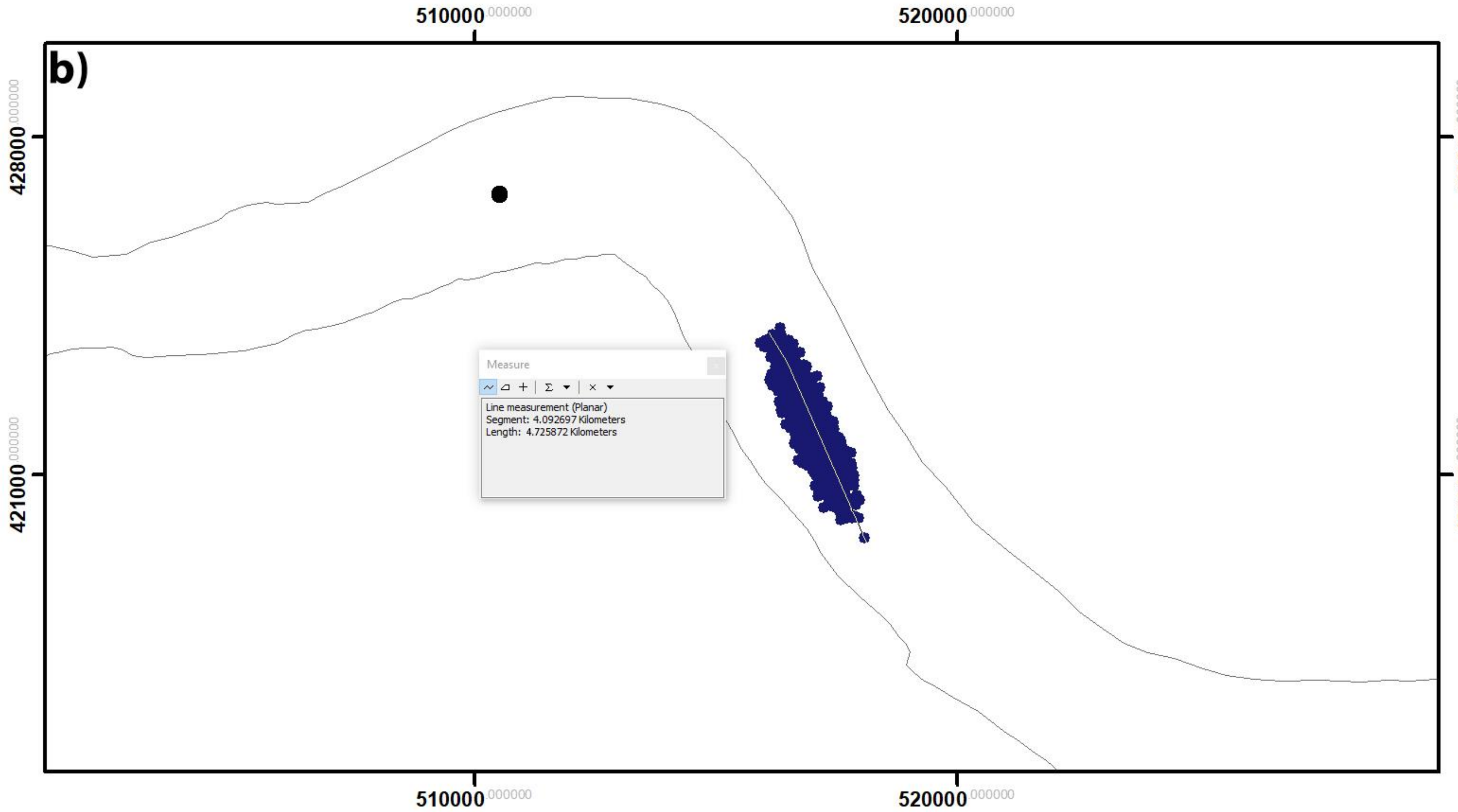

Figure 3.20b: Measurement of oil slick length after 48 hours; the black dot represents the point of release. Note: Trajectory shows oil released on the Humber Estuary at L2 high water neap in winter (Figure 3.34).

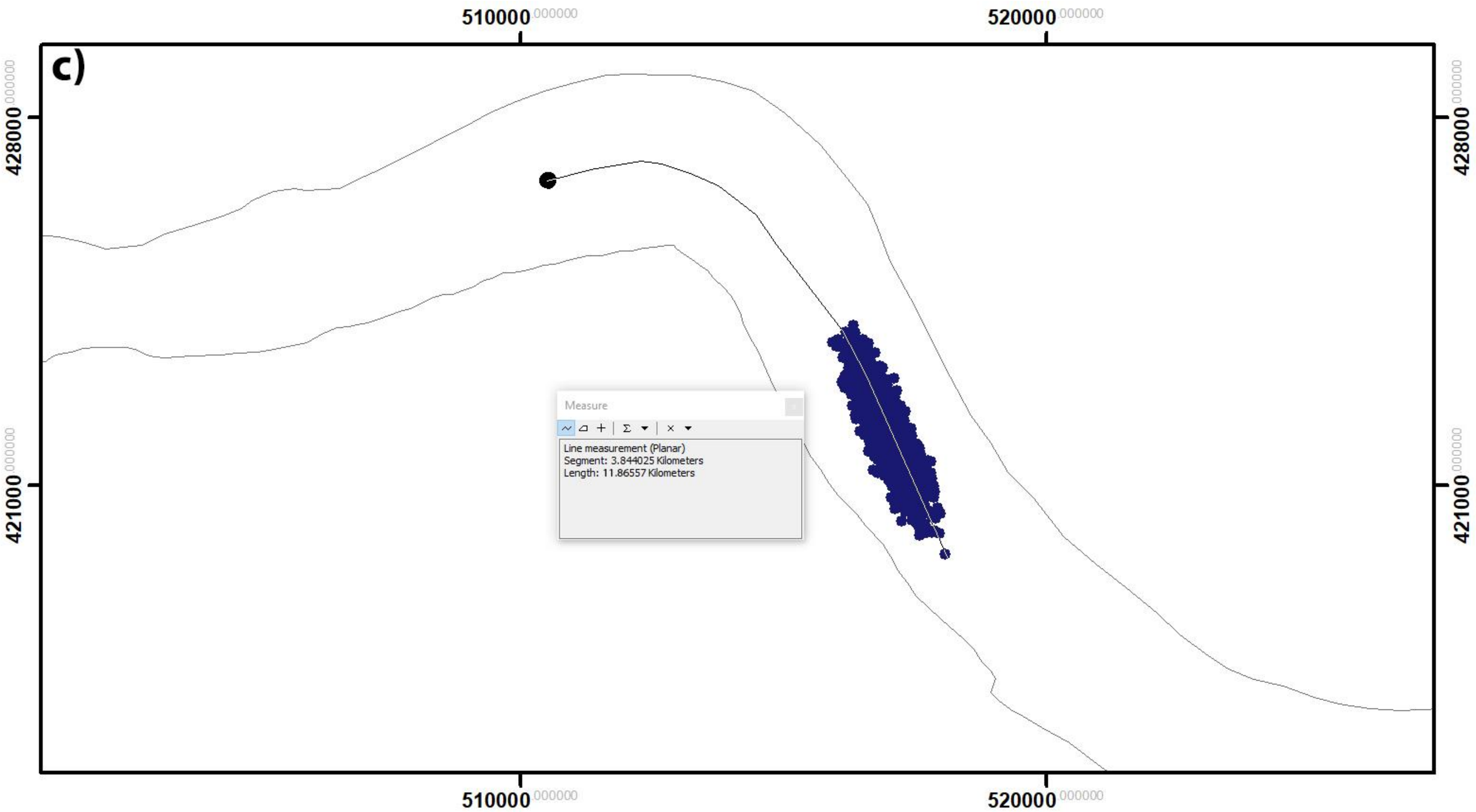

Figure 3.20c: Measurement of maximum downstream displacement from the point of release after 48 hours; the black dot represents the point of release. Note: Trajectory shows oil released on the Humber Estuary at L2 high water neap in winter (Figure 3.34).

3.3 RESULTS

3.3.1 Calibration

Calibration required adjusting the FES2014 tidal height data at offshore boundary by 10 days, a procedure recommended by Brown and Davies (2009). The calibrated results revealed that the best agreement between the measured data and model results was obtained with Chezy C of 70 $m^{0.5}/s$ and 75 $m^{0.5}/s$ in summer and winter respectively (Table 3.11). In all seasons, the model was able to replicate the observed tidal elevation cycles (Figure 3.21; 3.22).

Table 3.11: Calibration metrics comparing observed and simulated tidal heights for different seasons as a function of Chezy C. Best values for each metric are indicated as underlined italics.

Season (representative month)	**Chezy C**	**RMSE** (m)	**R^2**	**b**
Summer (August 2017)	60 (uncalibrated)	3.198	0.403	-0.674
	60	0.625	0.880	0.954
	70	<u>*0.623*</u>	<u>*0.883*</u>	0.966
	75	0.624	<u>*0.883*</u>	0.970
	80	0.628	<u>*0.883*</u>	0.973

	90	0.643	0.880	*0.976*
Winter (February 2010)	60 (uncalibrated)	3.046	0.283	-0.548
	60	0.713	0.848	0.922
	70	*0.709*	0.852	0.933
	75	*0.709*	0.852	0.937
	80	0.711	*0.853*	0.939
	90	0.722	0.851	*0.947*

a)

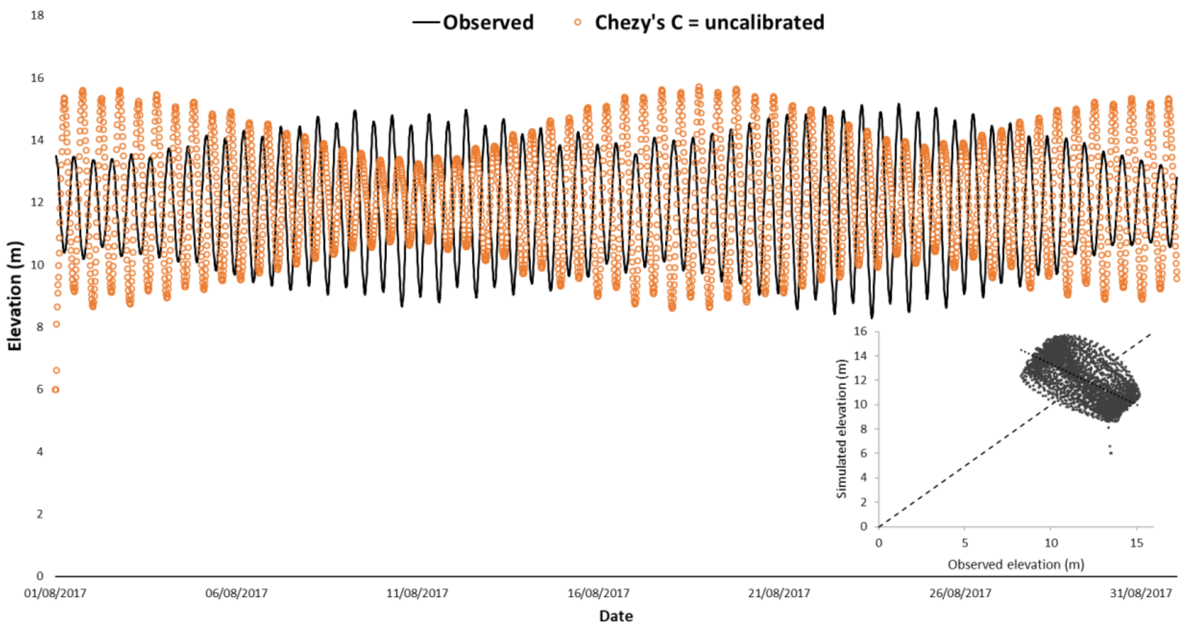

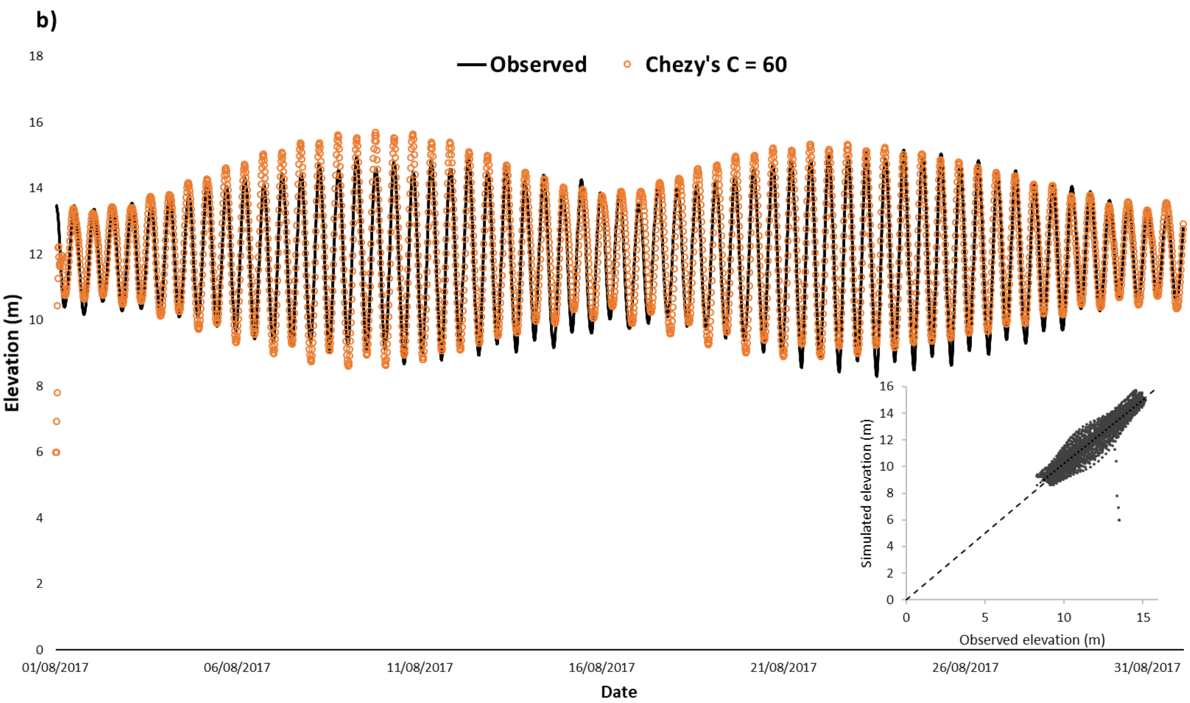
b)
Observed
Chezy's C = 60
Elevation (m)
Date
01/08/2017
06/08/2017
11/08/2017
16/08/2017
21/08/2017
26/08/2017
31/08/2017
Simulated elevation (m)
Observed elevation (m)

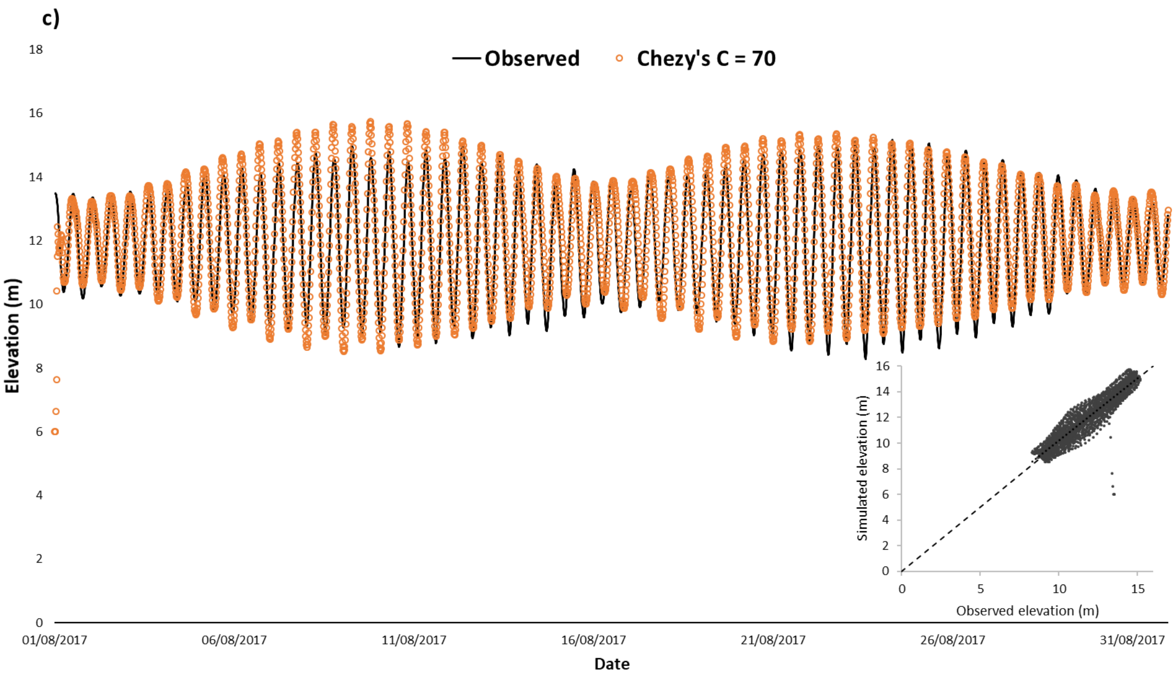
c)
Observed
Chezy's C = 70
Elevation (m)
Date
01/08/2017
06/08/2017
11/08/2017
16/08/2017
21/08/2017
26/08/2017
31/08/2017
Simulated elevation (m)
Observed elevation (m)

d)

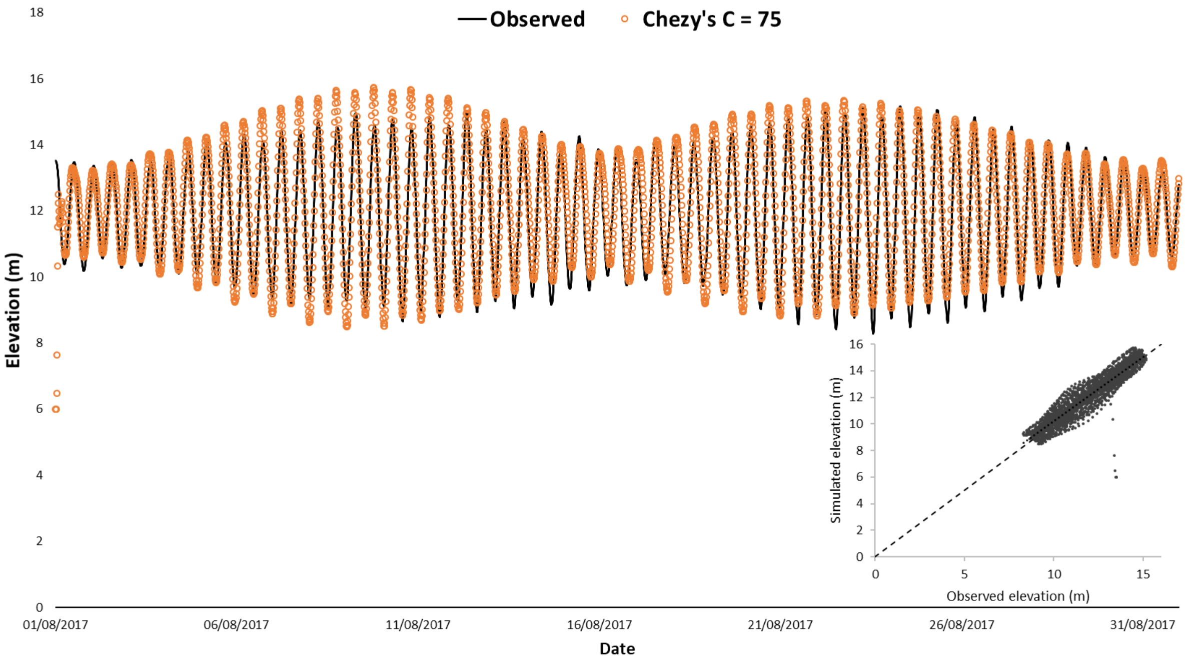
Observed
Chezy's C = 75
Elevation (m)
Date
01/08/2017
06/08/2017
11/08/2017
16/08/2017
21/08/2017
26/08/2017
31/08/2017
Simulated elevation (m)
Observed elevation (m)

e)

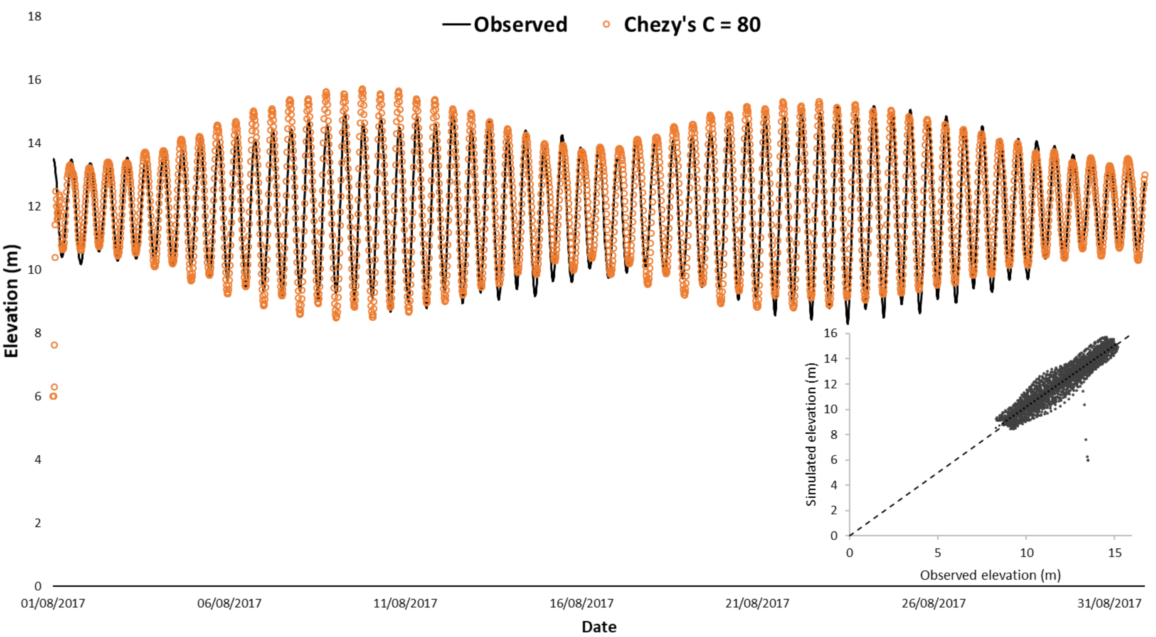
Observed
Chezy's C = 80
Elevation (m)
Date
01/08/2017
06/08/2017
11/08/2017
16/08/2017
21/08/2017
26/08/2017
31/08/2017
Simulated elevation (m)
Observed elevation (m)

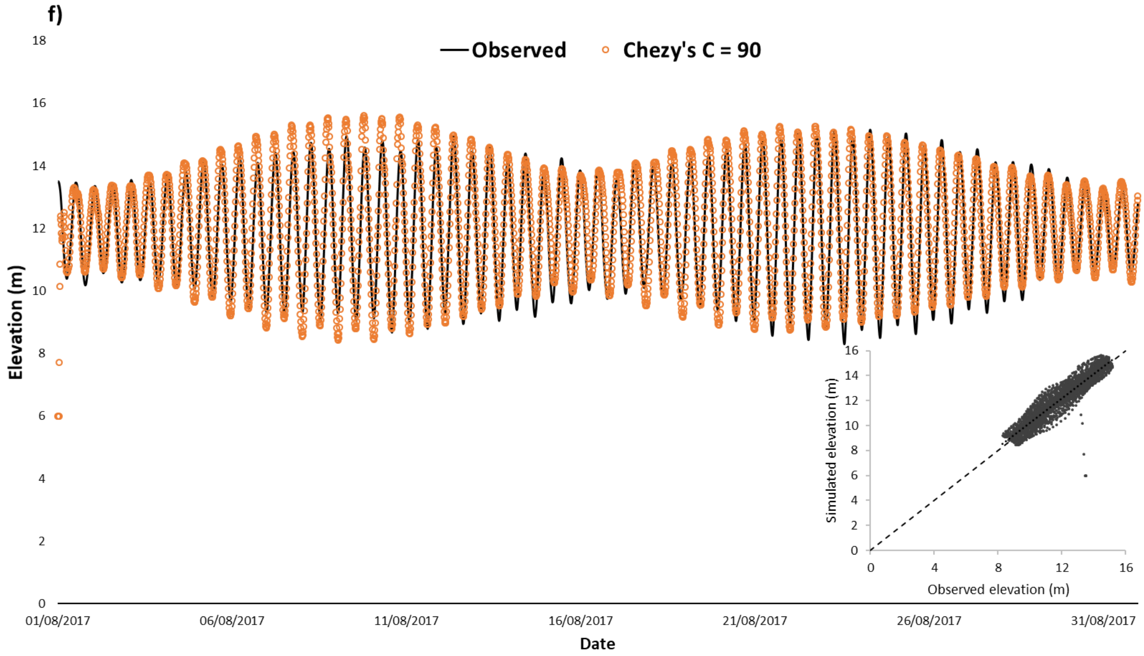

Figure 3.21: Observed (line) and simulated (points) free surface elevations at Immingham for a representative summer month (August 2017). Inset: Point correlation between observed and simulated free surface elevations at Immingham. (a) Chezy's C = 60 (uncalibrated); (b) Chezy's = 60; (c) Chezy's = 70; (d) Chezy's = 75; (e) Chezy's = 80; (f) Chezy's = 90.

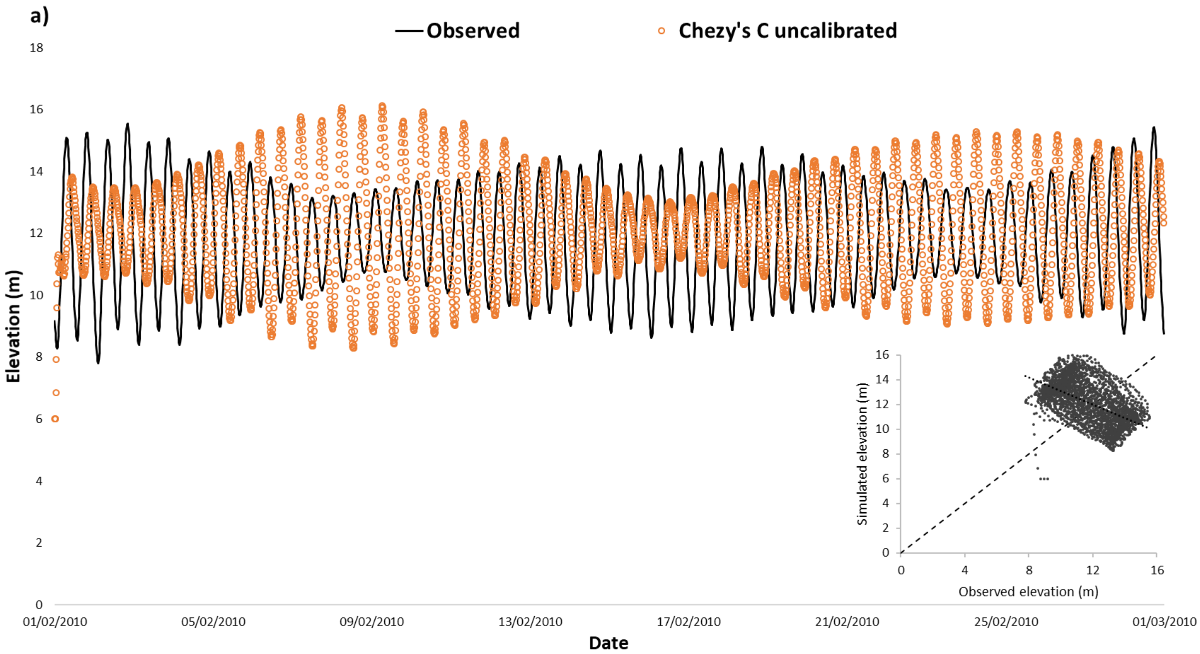
a)
Observed
Chezy's C uncalibrated
Elevation (m)
Date
01/02/2010
05/02/2010
09/02/2010
13/02/2010
17/02/2010
21/02/2010
25/02/2010
01/03/2010
Simulated elevation (m)
Observed elevation (m)

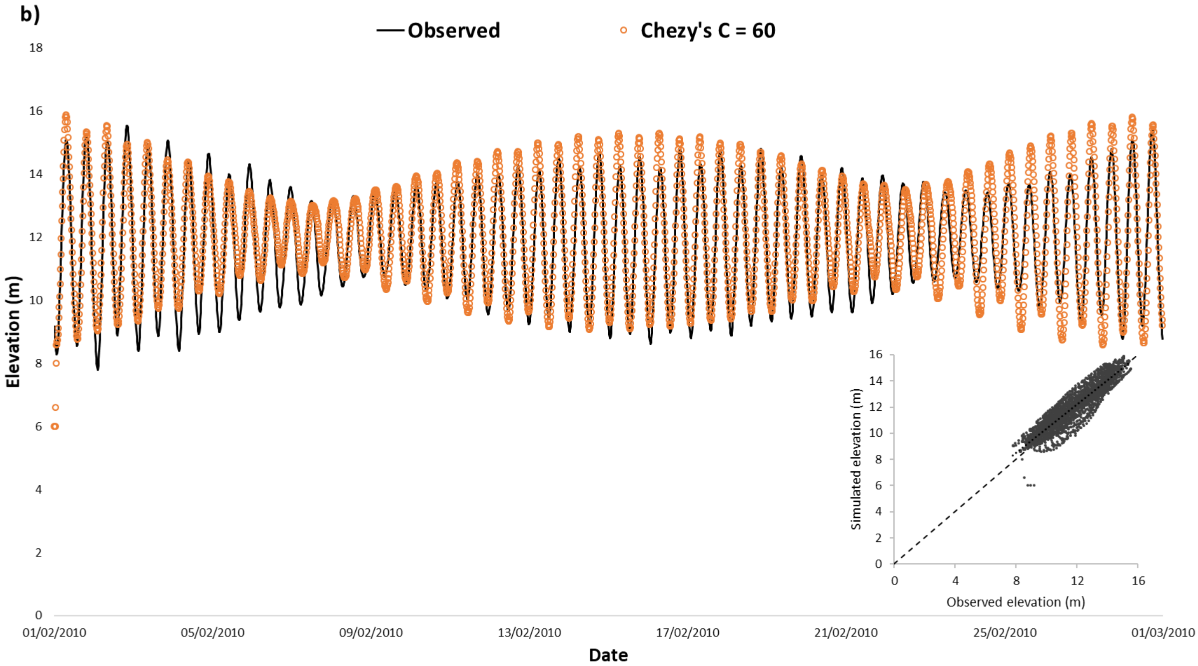
b)
Observed
Chezy's C = 60
Elevation (m)
Date
01/02/2010
05/02/2010
09/02/2010
13/02/2010
17/02/2010
21/02/2010
25/02/2010
01/03/2010
Simulated elevation (m)
Observed elevation (m)

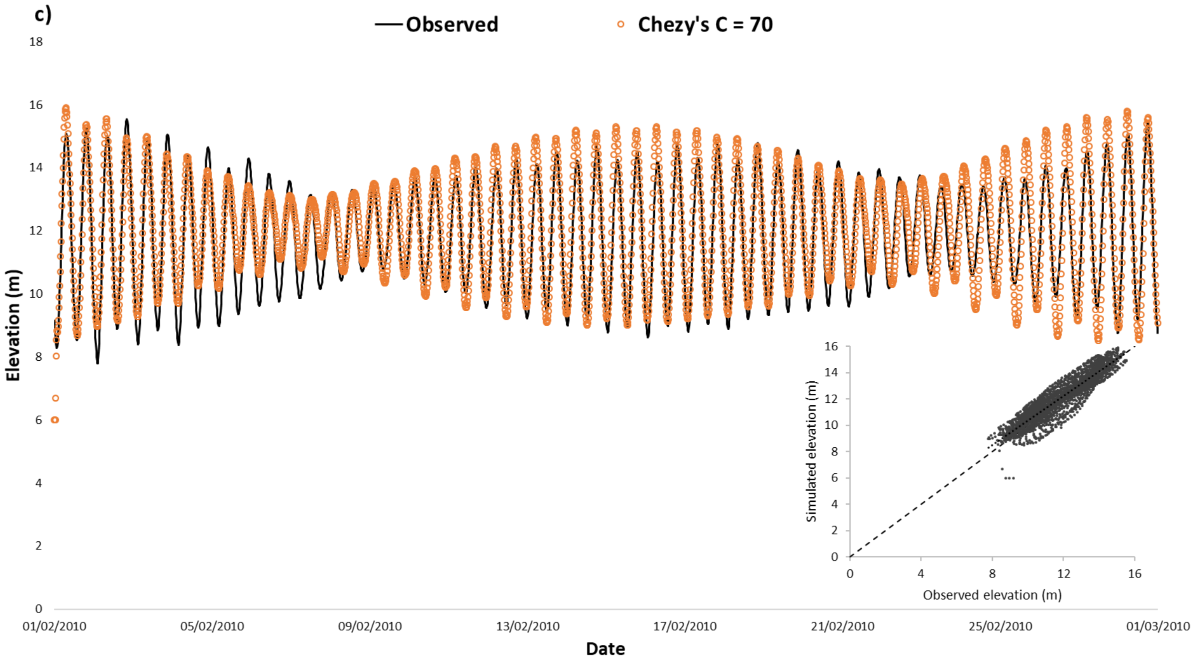
c)
Observed
Chezy's C = 70
Elevation (m)
Date
Simulated elevation (m)
Observed elevation (m)

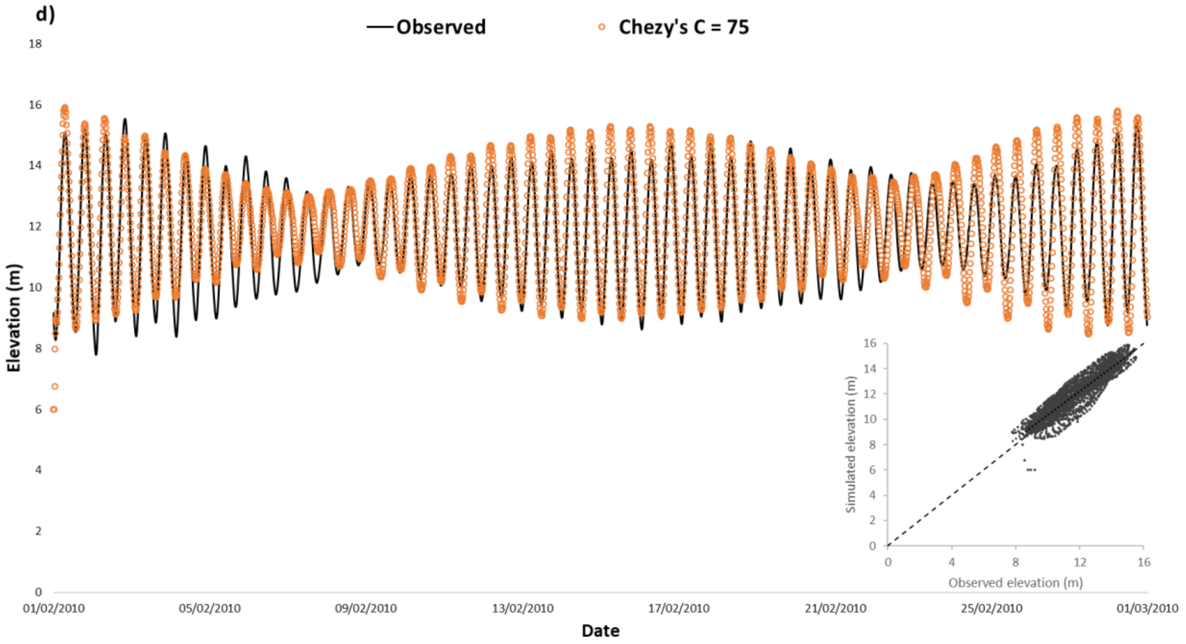
d)
Observed
Chezy's C = 75
Elevation (m)
Date
Simulated elevation (m)
Observed elevation (m)

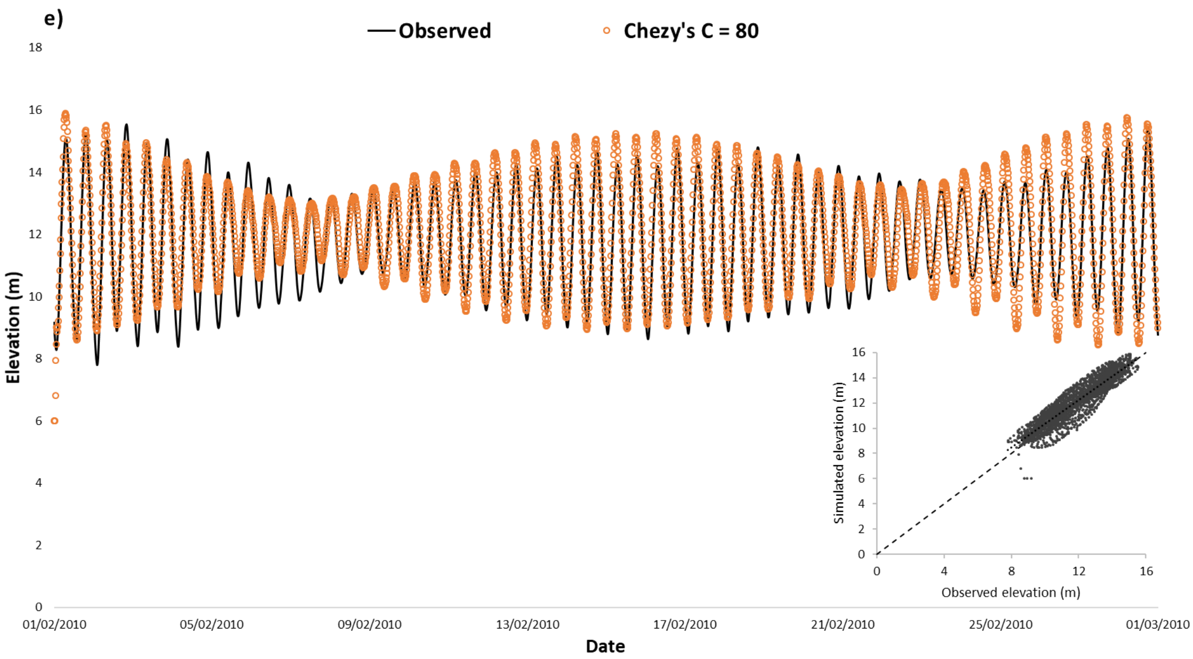

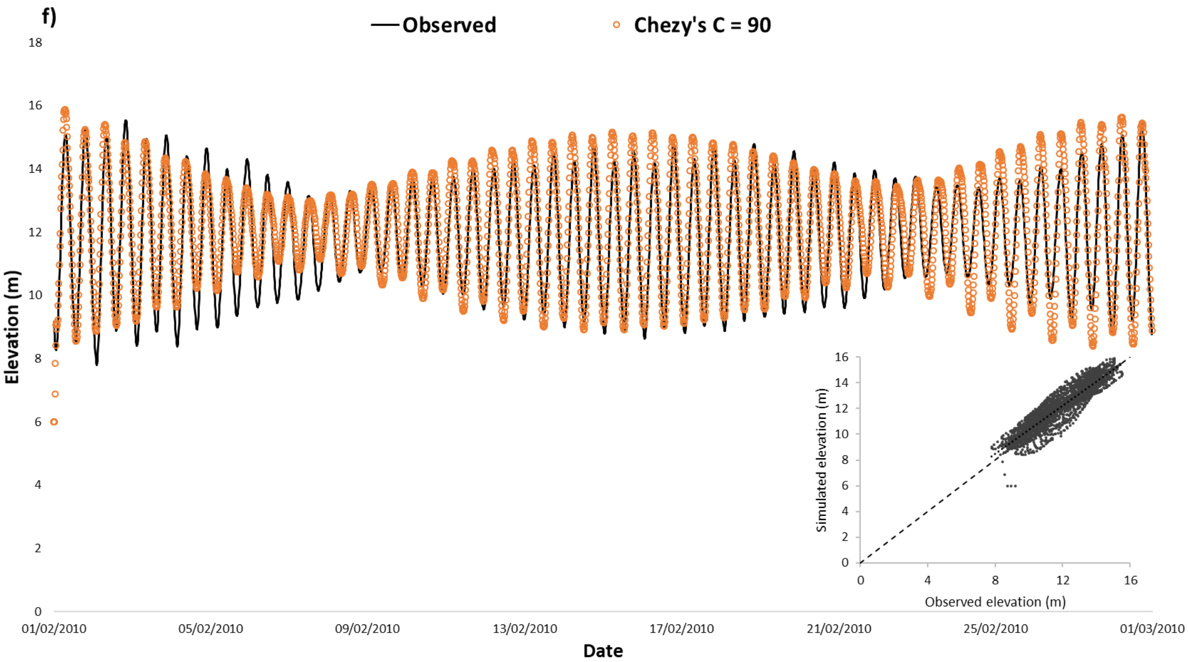

Figure 3.22: Observed (line) and simulated (points) free surface elevations at Immingham for a representative winer month (February 2010). Inset: Point correlation between observed and simulated free surface elevations at

Immingham. (a) Chezy's C = 60 (uncalibrated); (b) Chezy's = 60; (c) Chezy's = 70; (d) Chezy's = 75; (e) Chezy's = 80; (f) Chezy's = 90.

3.3.2 Validation

The validation was undertaken using different time periods for summer and winter (Table 3.8). The calibrated Chezy friction coefficients of 70 $m^{0.5}/s$ and 75 $m^{0.5}/s$ were employed in secondary summer and winter simulations respectively. Evans (1993) classified RMSE value that is 15% of the spring tidal range as satisfactory while Brown et al. (2011) and Skinner et al. (2015) agree that an RMSE value that is less than 20% of the tidal range is considered satisfactory. The simulated water level showed satisfactory agreement with the recorded data (Table 3.12; Figure 3.23; 3.24) resulting in an RMSE of 9.09% and 12.86% of the spring tidal range in summer and winter respectively. Minor discrepancies in simulated high and low tides might have been influenced by the exclusion of surges in the hydrodynamic model (Jones et al. 2016), the use of simulated tidal height data rather than measured data to drive the offshore boundary, and the use of constant discharge-driven boundary condition. To improve model performance, the computational domain can be extended upstream to reach a point where high-resolution water discharge measurement is available. Sensitivity analysis on the influence of river discharge on model performance indicates that discharge does does not significantly influence model performance (Appendix M)

Table 3.12: Validation metrics comparing observed and simulated tidal heights for different seasons as a function of Chezy C.

Season	**Chezy C**	**RMSE**	**R^2**	**b**

(validation month)		(m)		
Summer (August 2016)	70	0.582	0.912	0.996
Winter (February 2013)	75	0.823	0.848	0.933

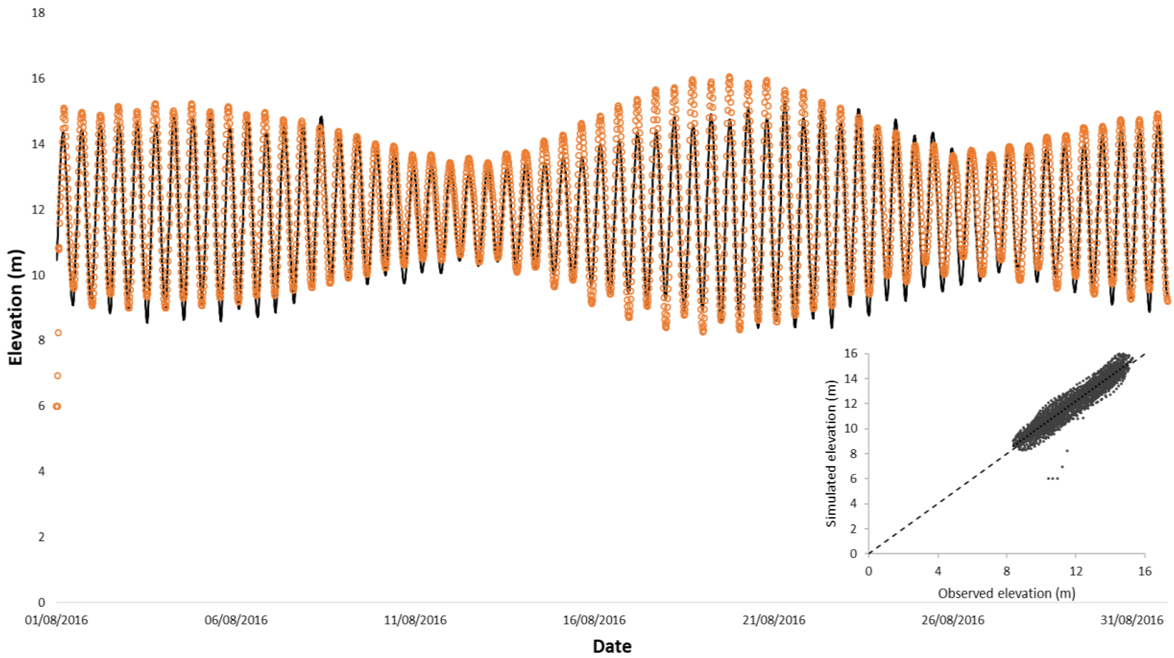

Figure 3.23: Observed (line) and simulated (points) free surface elevations at Immingham for the validation summer period (August 2016). Inset: Point correlation between observed and simulated tidal elevations (R^2 = 0.912).

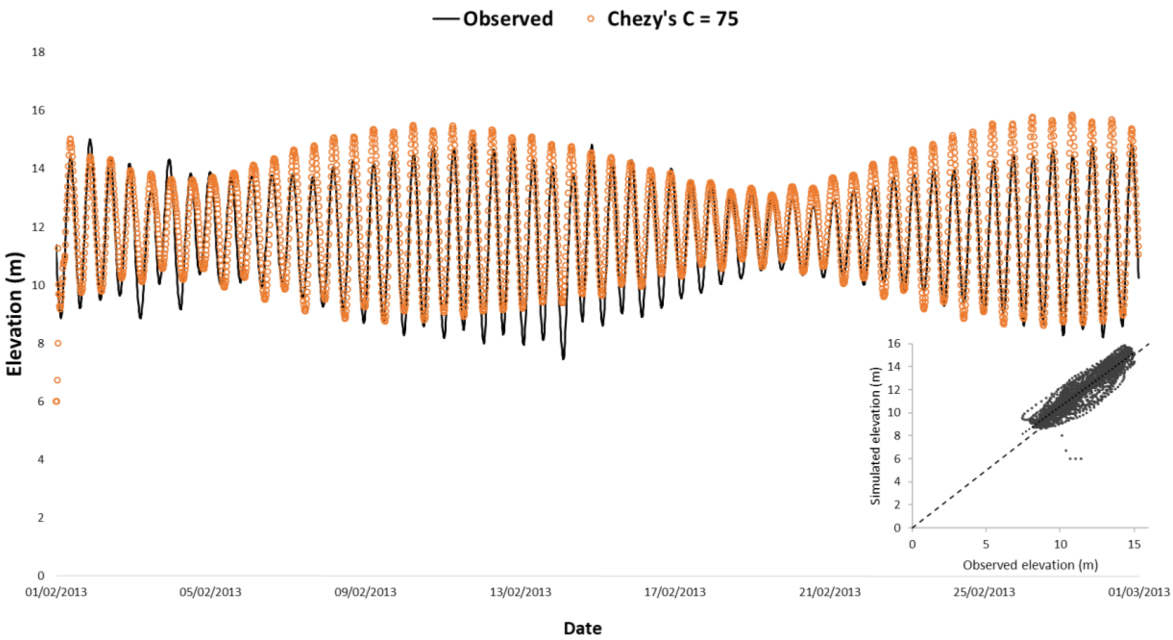

Figure 3.24: Observed (line) and simulated (points) free surface elevations at Immingham for the validation winter period (February 2013). Inset: Point correlation between observed and simulated tidal elevations (R^2 = 0. 848).

3.3.3 Oil Spill Scenarios

The calibrated and validated Chezy friction coefficients are used for all the oil spill scenarios. It is the first time that these dynamics have been illustrated and advanced. It can be asserted that there is a novelty in also simulating these expected behaviours, as they have not been formally and explicitly demonstrated until now.

Oil slicks are seen moving back and forth in the estuary as tides flood and ebb (Figure 3.25 – 3.40). The exceptions are oil spills released at L1 at high water, which leave the computational domain during the first tidal cycle (Figures 3.25, 3.26, 3.29, 3.30). Overall, oil slicks travel downstream over time. However, oil slicks released at low water first travel upstream as the tides come in (Figures 3.27; 3.28; 3.31; 3.32; 3.35;

3.36; 3.39; 3.40). The oil slicks spread over time. After 48 hours, i.e. after two semi-diurnal tidal cycles, the simulated oil slicks cover an area between 13.7 and 67.8 km^2 on the water surface, with an average of 37.8 km^2 (Table 3.13; Figures 3.41 – 3.44). However, within these overall results, there are systematic patterns and trends that relate to the scenario configurations. These nuances are discussed in detail in the next section.

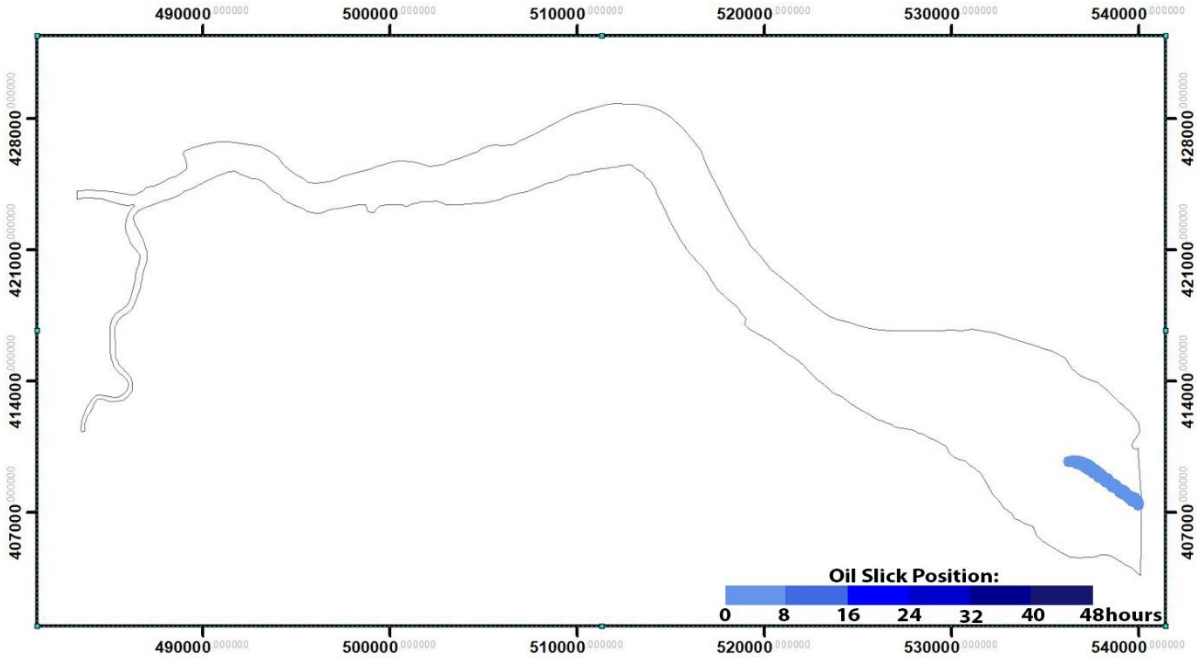

Figure 3.25: Trajectories of oil released on the Humber Estuary at L1 high water neap in summer

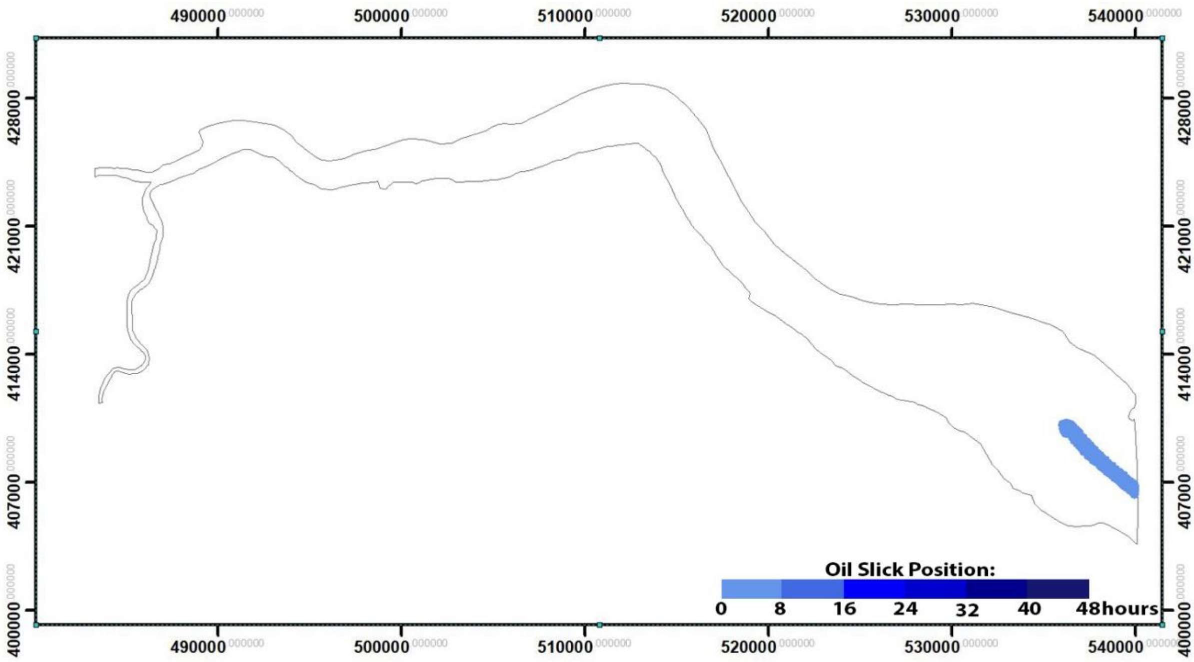

Figure 3.26: Trajectories of oil released on the Humber Estuary at L1 high water neap in winter

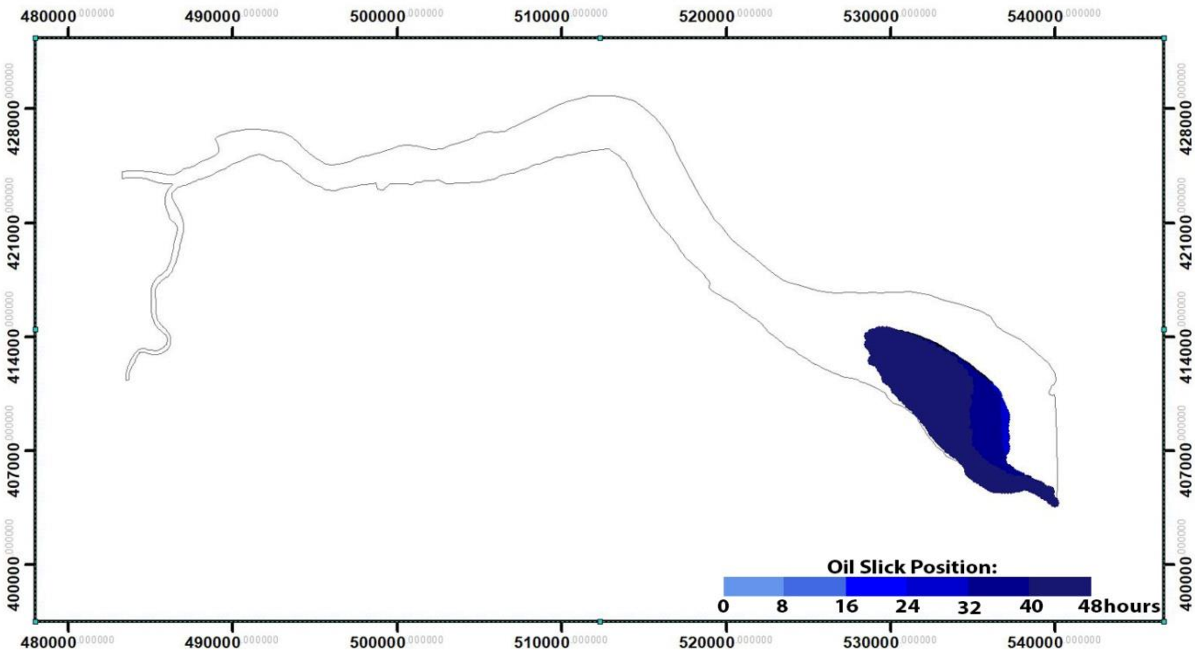

Figure 3.27: Trajectories of oil released on the Humber Estuary at L1 low water neap in summer

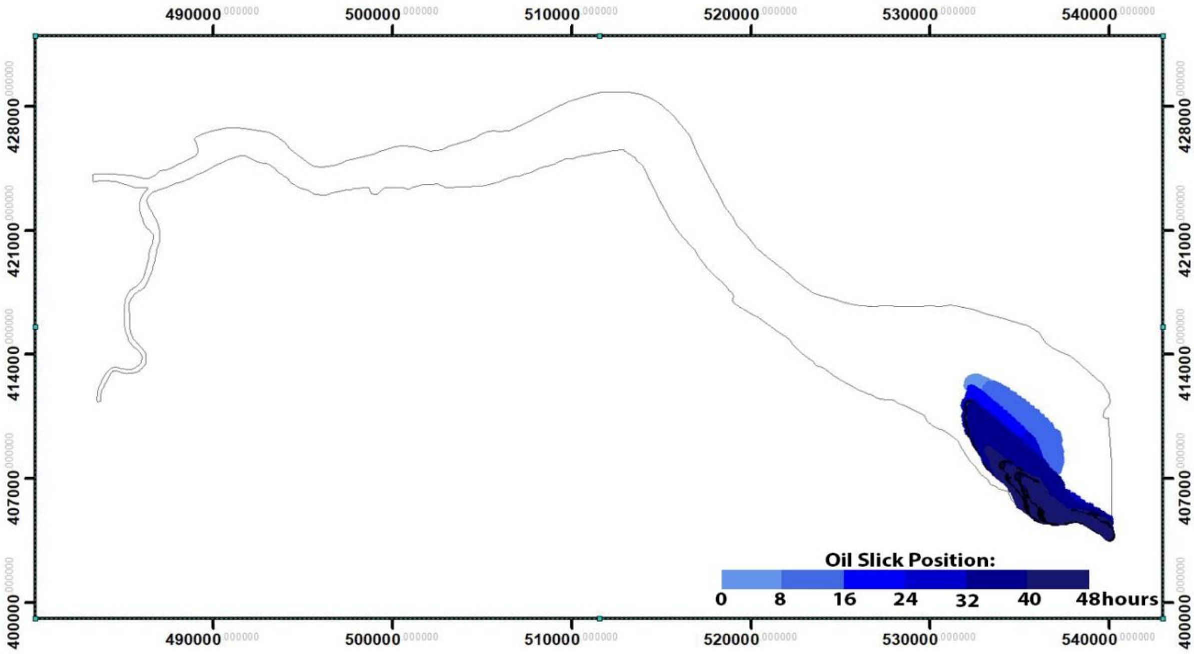

Figure 3.28: Trajectories of oil released on the Humber Estuary at L1 low water neap in winter

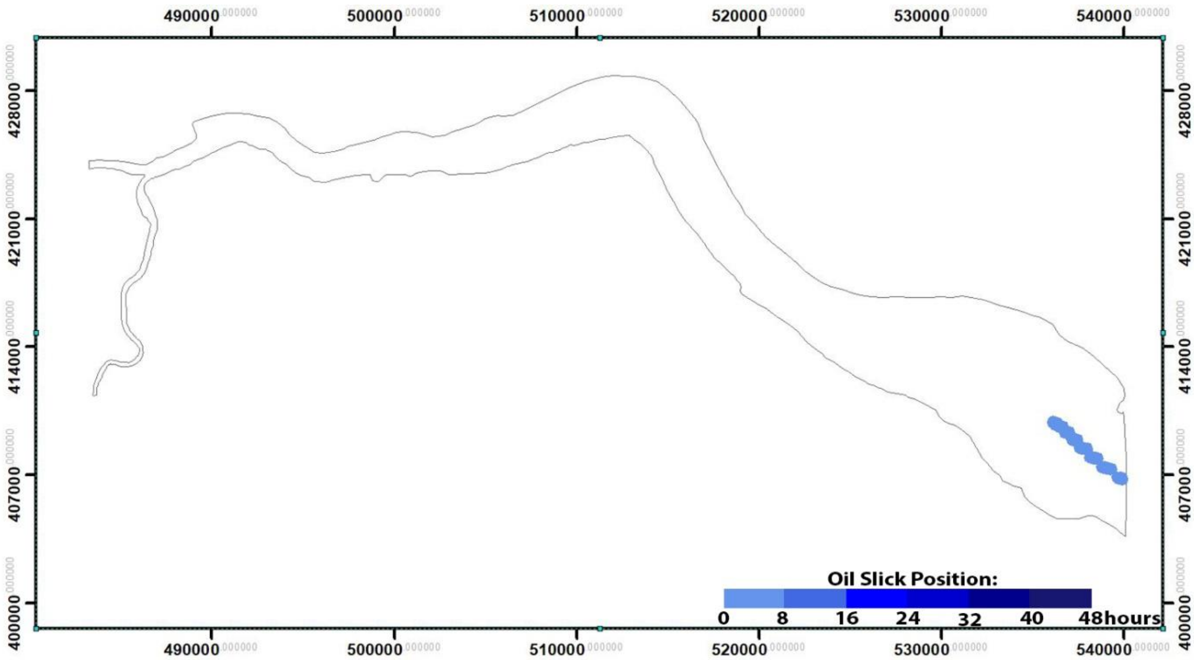

Figure 3.29: Trajectories of oil released on the Humber Estuary at L1 high water spring in summer

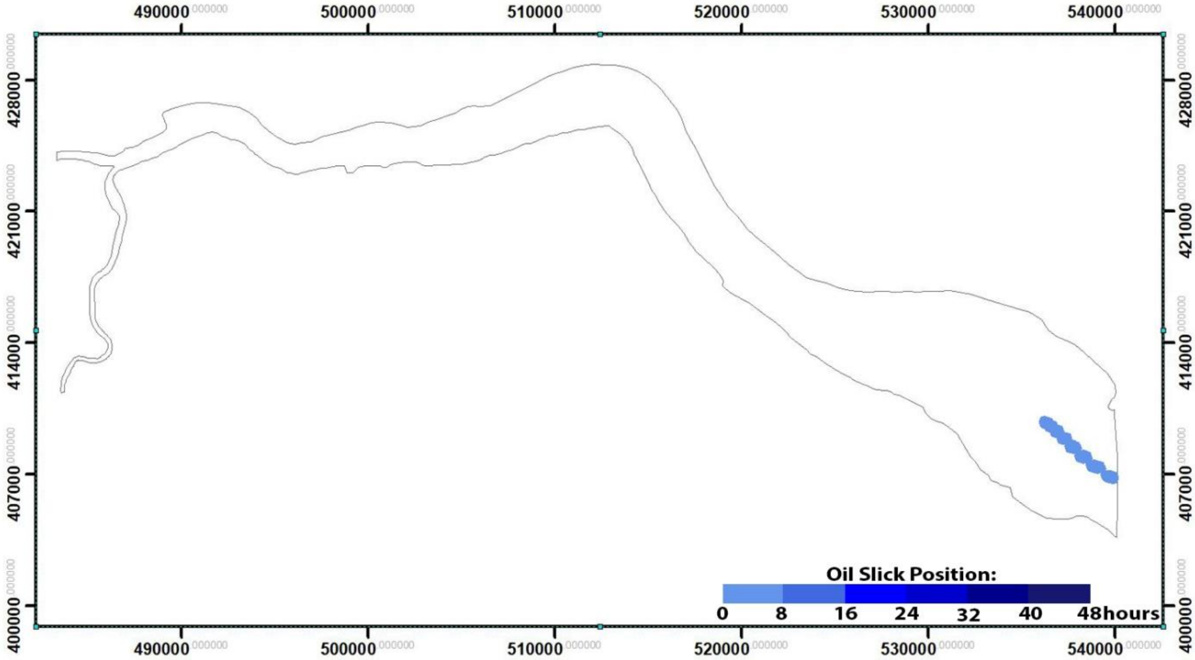

Figure 3.30: Trajectories of oil released on the Humber Estuary at L1 high water spring in winter

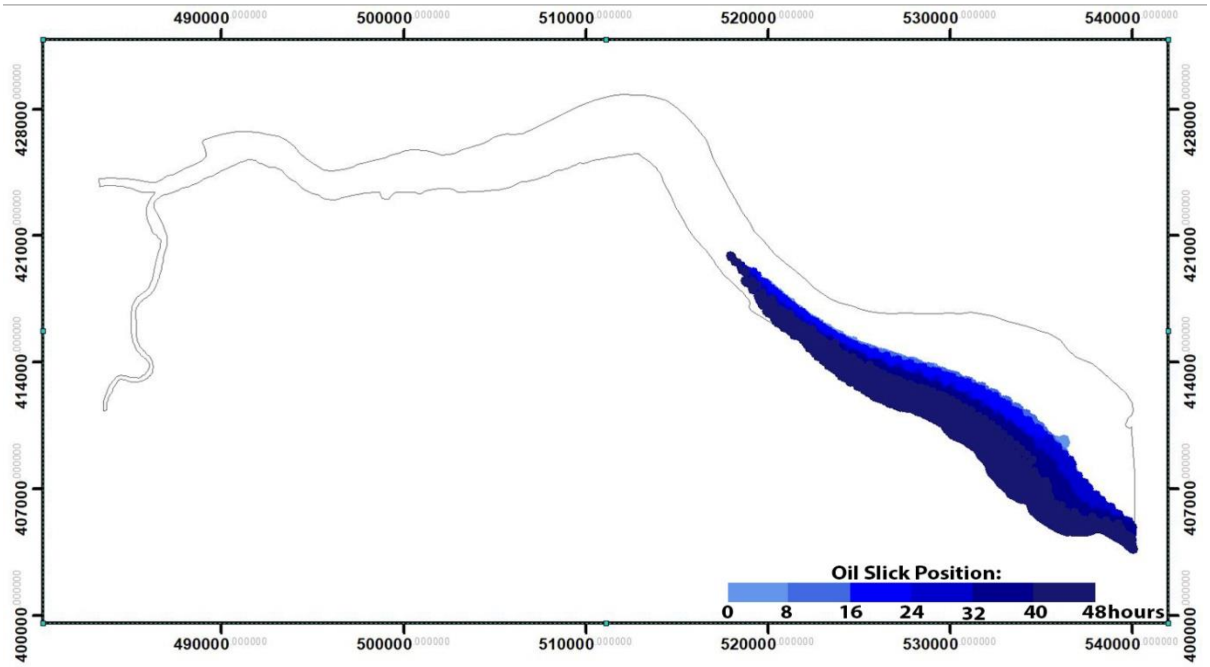

Figure 3.31: Trajectories of oil released on the Humber Estuary at L1 low water spring in summer

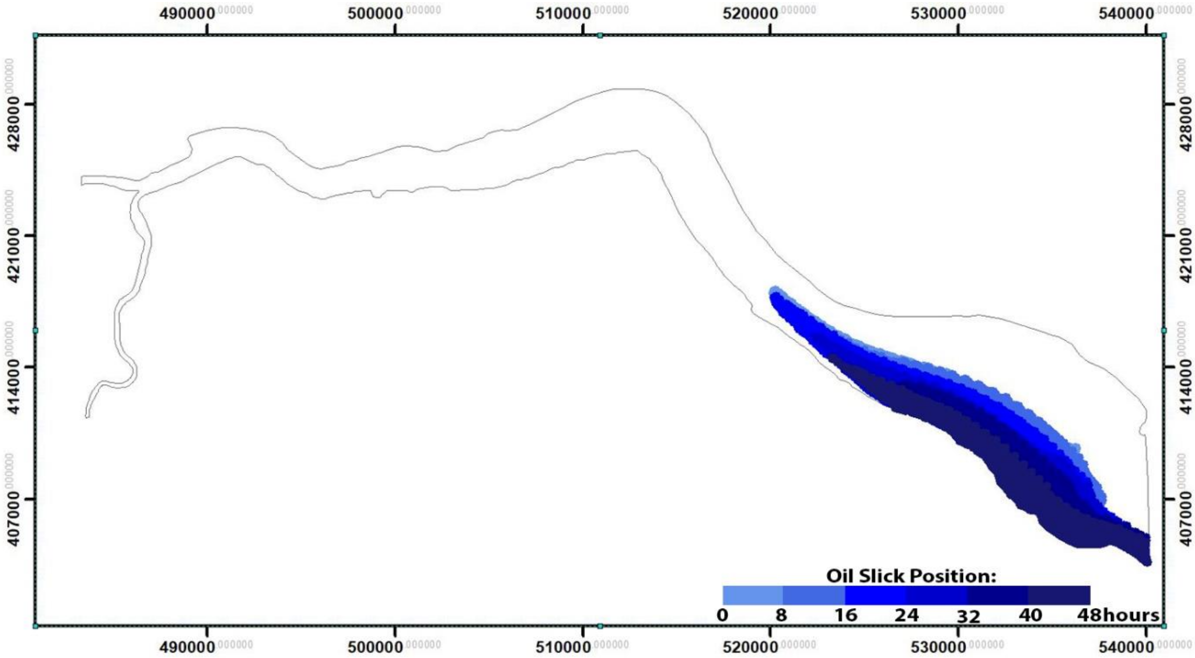

Figure 3.32: Trajectories of oil released on the Humber Estuary at L1 low water spring in winter

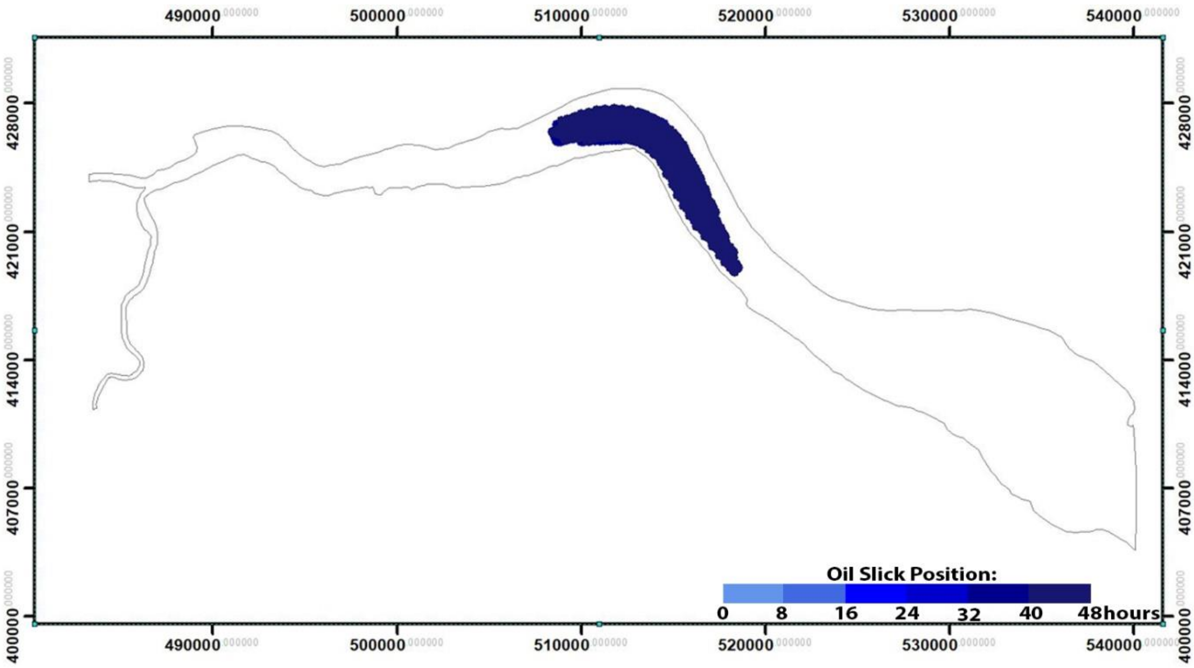

Figure 3.33: Trajectories of oil released on the Humber Estuary at L2 high water neap in summer

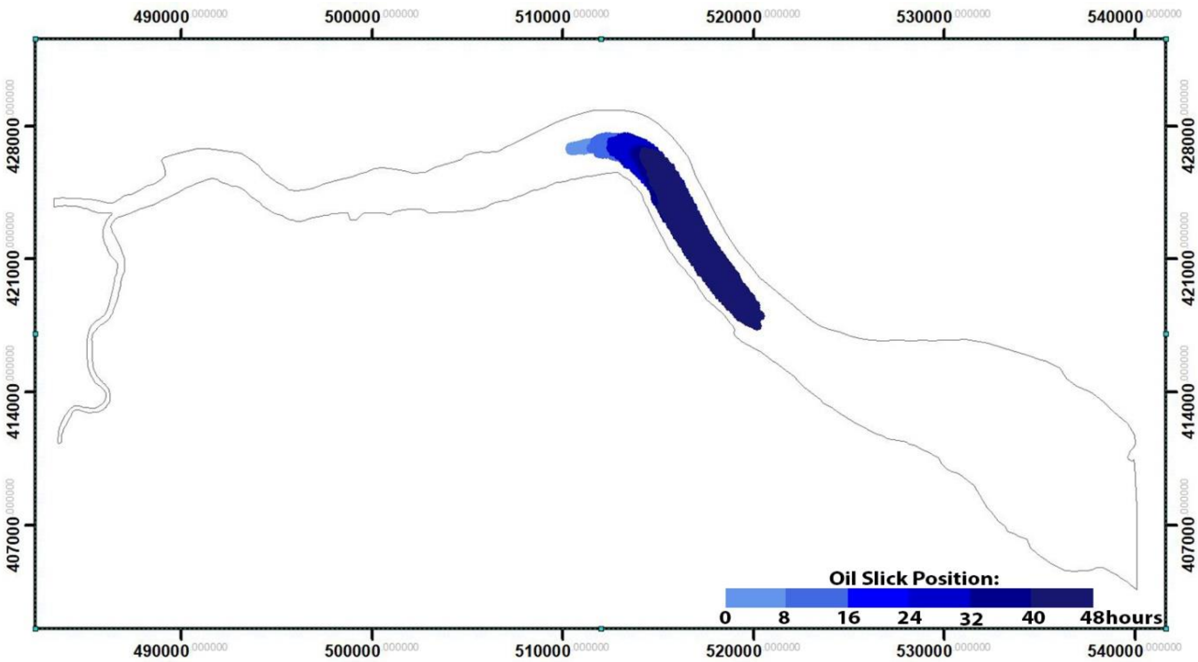

Figure 3.34: Trajectories of oil released on the Humber Estuary at L2 high water neap in winter

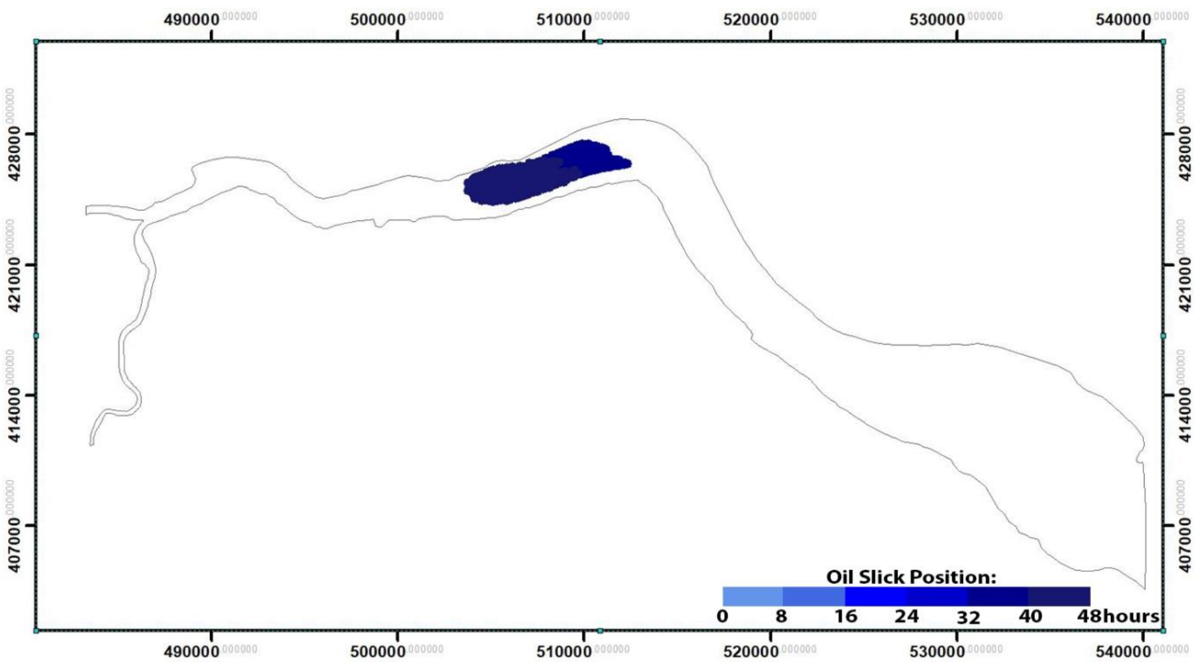

Figure 3.35: Trajectories of oil released on the Humber Estuary at L2 low water neap in summer

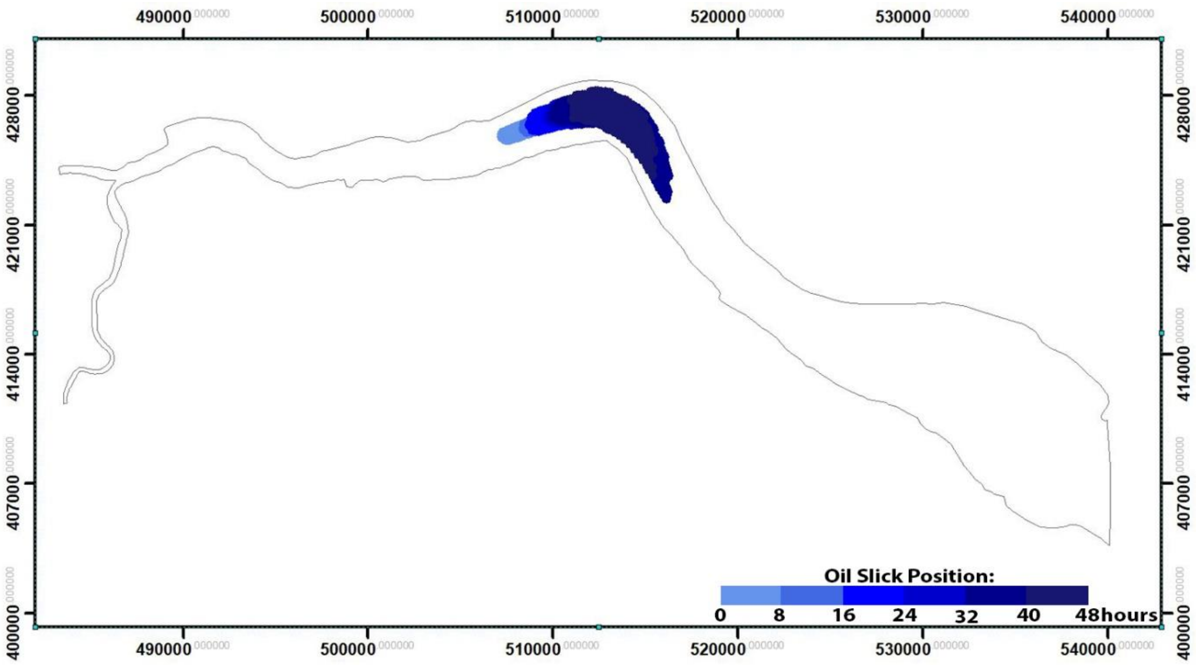

Figure 3.36: Trajectories of oil released on the Humber Estuary at L2 low water neap in winter

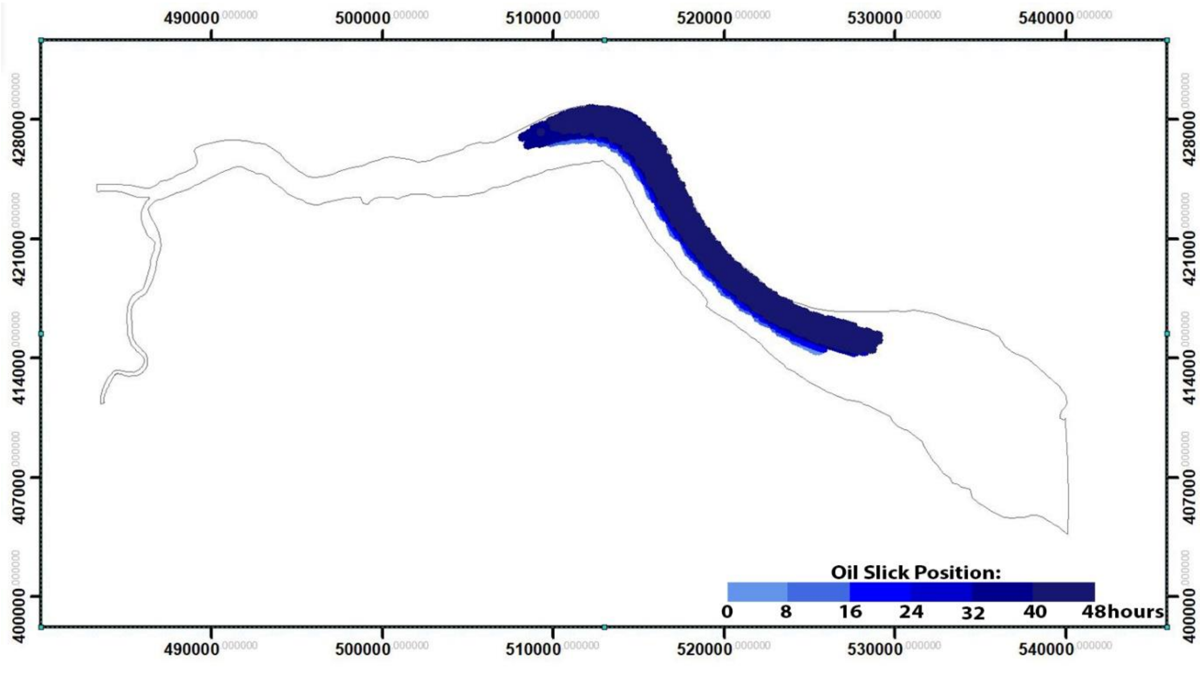

Figure 3.37: Trajectories of oil released on the Humber Estuary at L2 high water spring in summer

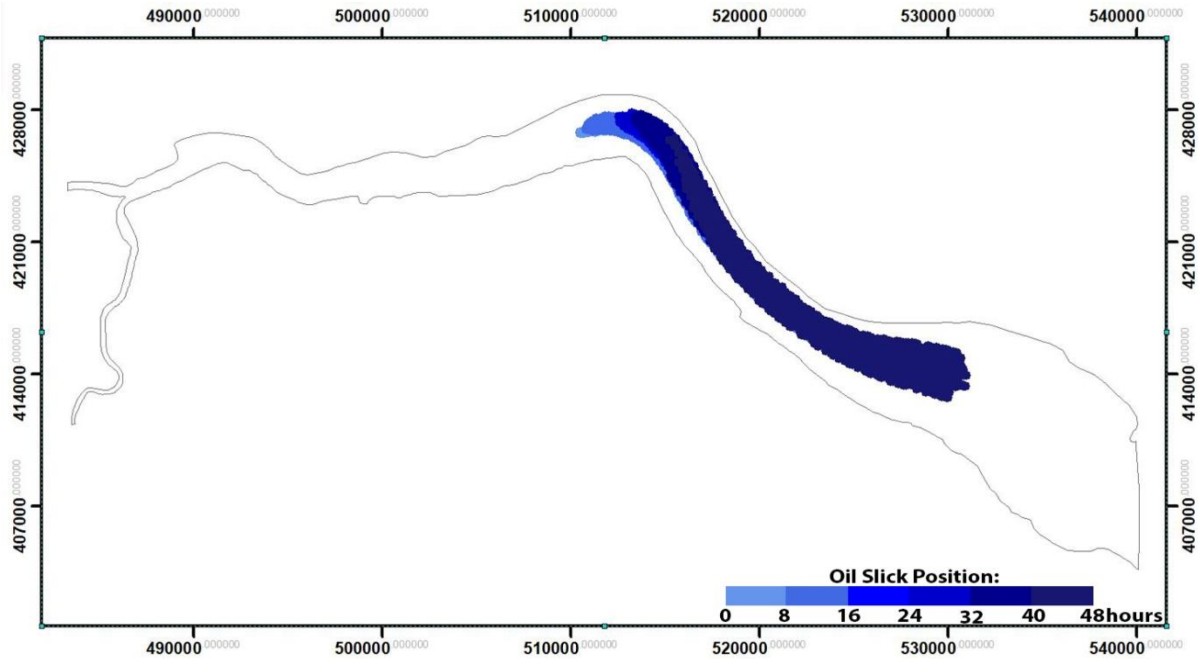

Figure 3.38: Trajectories of oil released on the Humber Estuary at L2 high water spring in winter

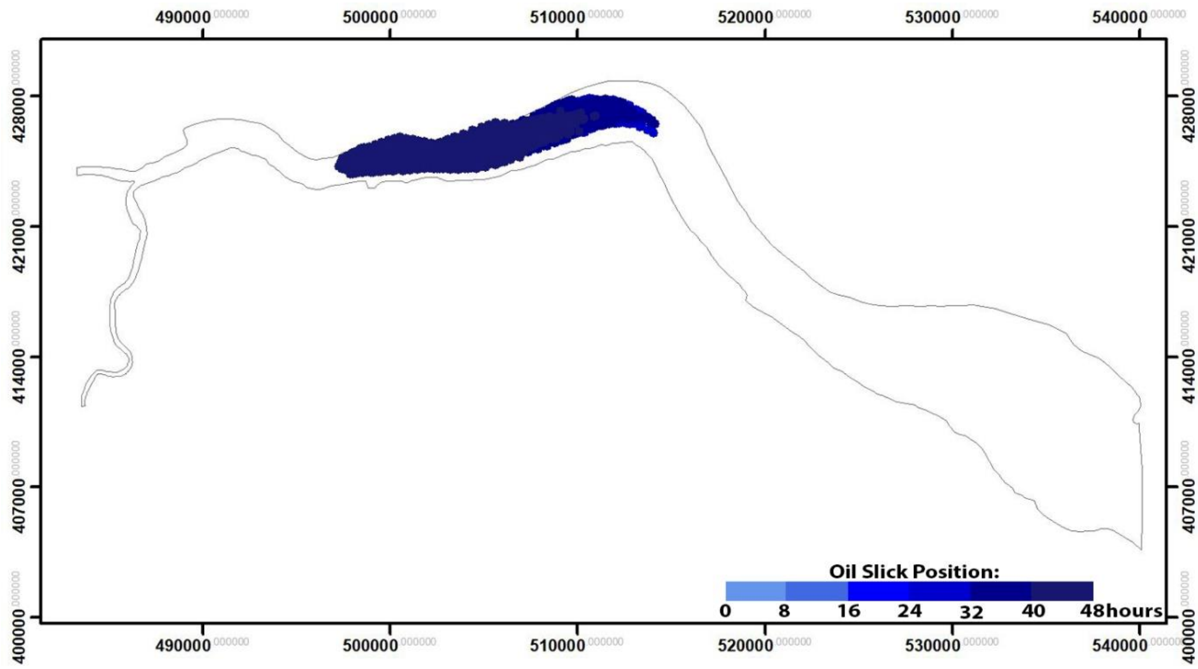

Figure 3.39: Trajectories of oil released on the Humber Estuary at L2 low water spring in summer

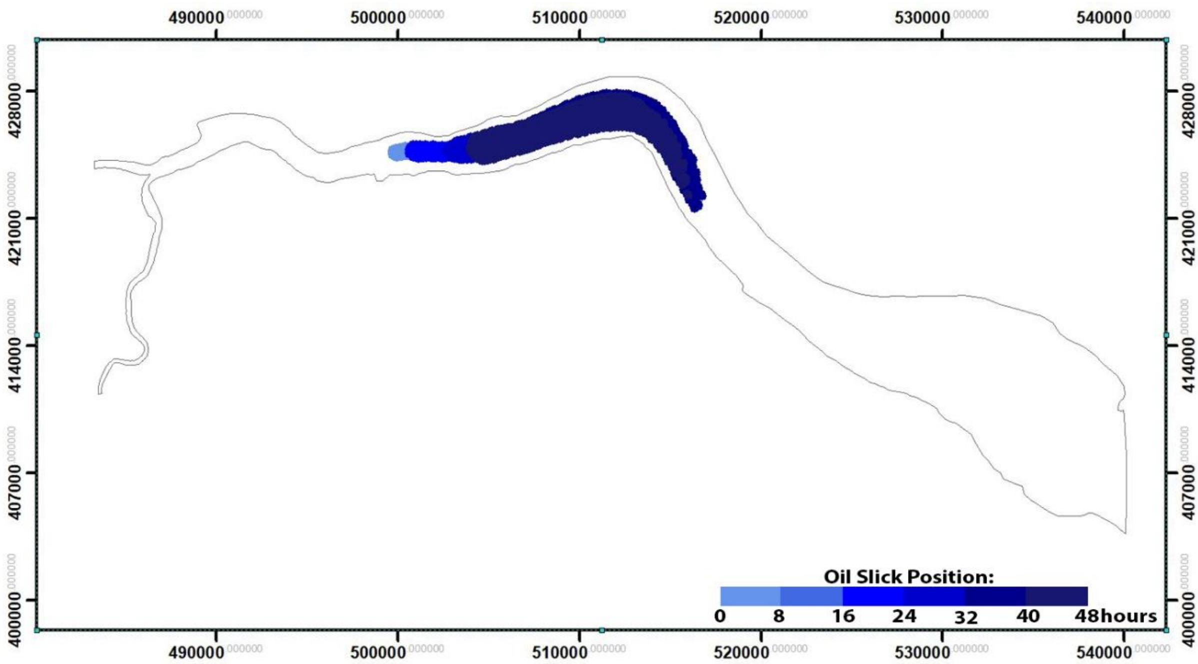

Figure 3.40: Trajectories of oil released on the Humber Estuary at L2 low water spring in winter

Table 3.13: Simulated oil slick area, A (sq. km), length of estuary bank line polluted, L (km), and oil travel time to reach estuary bank, T (hours), for different seasonal flow scenarios.

Scenarios	0 - 8h	8 - 16h	16 - 24h	24 - 32h	32 - 40h	40 - 48h	L	T
	A	A	A	A	A	A		
L1 HW NT summer	1.81	-	-	-	-	-	-	-
L1 HW NT winter	3.28	-	-	-	-	-	-	-
L1 LW NT summer	3.94	11.89	16.15	29.99	37.81	44.53	8.85	38.25
L1 LW NT winter	2.93	13.06	20.95	28.96	29.33	30.40	6.91	28.50

L1 HW ST summer L1 HW ST winter	2.43 2.34	- -	- -	- -	- -	- -	- -	- -
L1 LW ST summer L1 LW ST winter	11.11 13.81	35.65 48.35	54.37 63.43	66.25 65.57	66.74 66.00	67.76 67.22	24.60 18.40	25.75 15.75
L2 HW NT summer L2 HW NT winter	4.62 5.04	8.62 6.92	13.74 10.23	16.09 16.50	18.18 17.47	23.29 20.82	- -	- -
L2 LW NT summer L2 LW NT winter	3.44 2.20	5.78 6.32	7.95 7.30	10.33 9.18	11.47 15.25	13.77 16.90	- -	- -
L2 HW ST summer L2 HW ST winter	16.66 14.03	26.42 21.88	35.32 29.70	45.87 37.56	52.49 38.96	56.86 48.03	19.45 -	37.50 -
L2 LW ST summer L2 LW ST winter	7.47 6.95	13.59 15.07	19.84 19.48	27.03 23.35	29.77 30.34	32.67 31.39	13.21 -	20.00 -

Note: L1, L2 = release points; HW = high water; LW = low water; NT = neap tide; ST = spring tide.

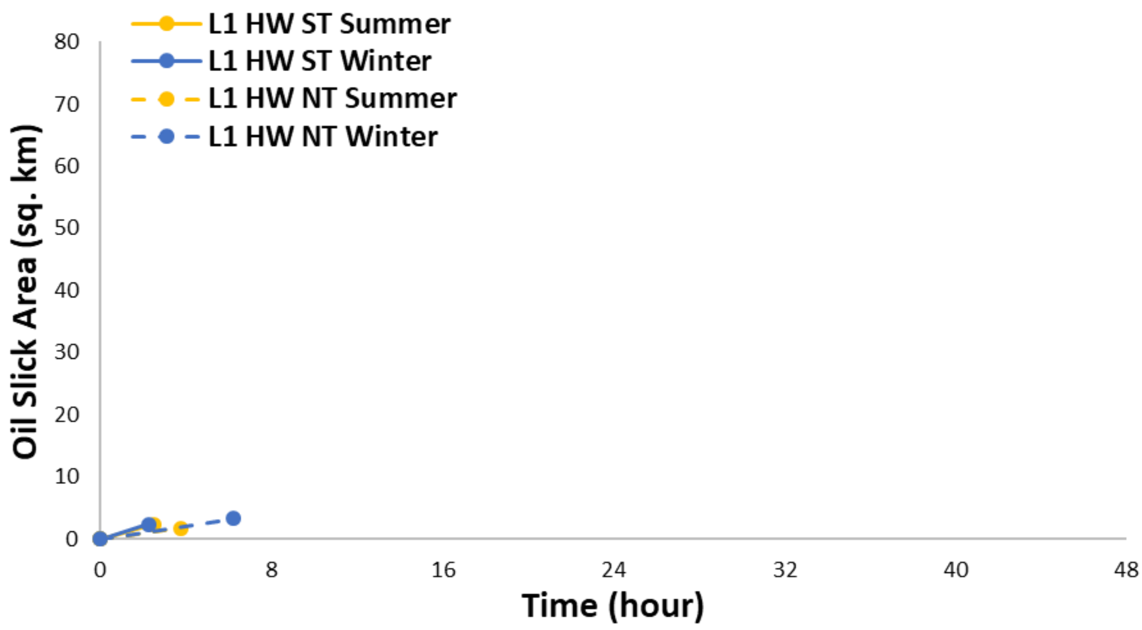

Figure 3.41: Area covered by simulated oil slick over time for a spill from L1 at high water

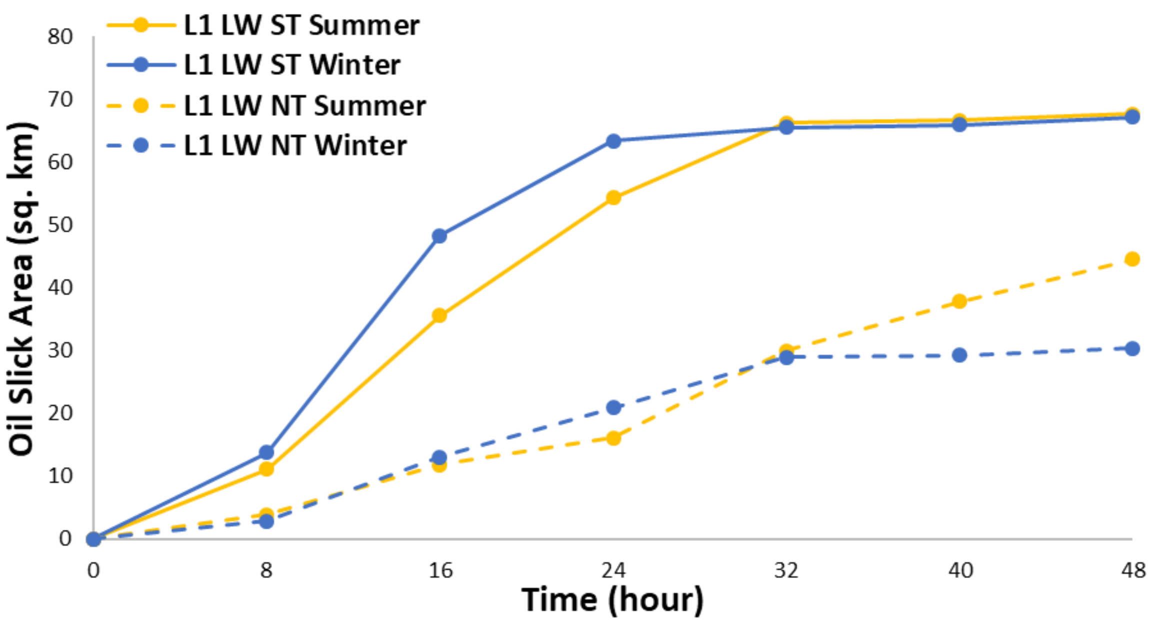

Figure 3.42: Area covered by simulated oil slick over time for a spill from L1 at low water

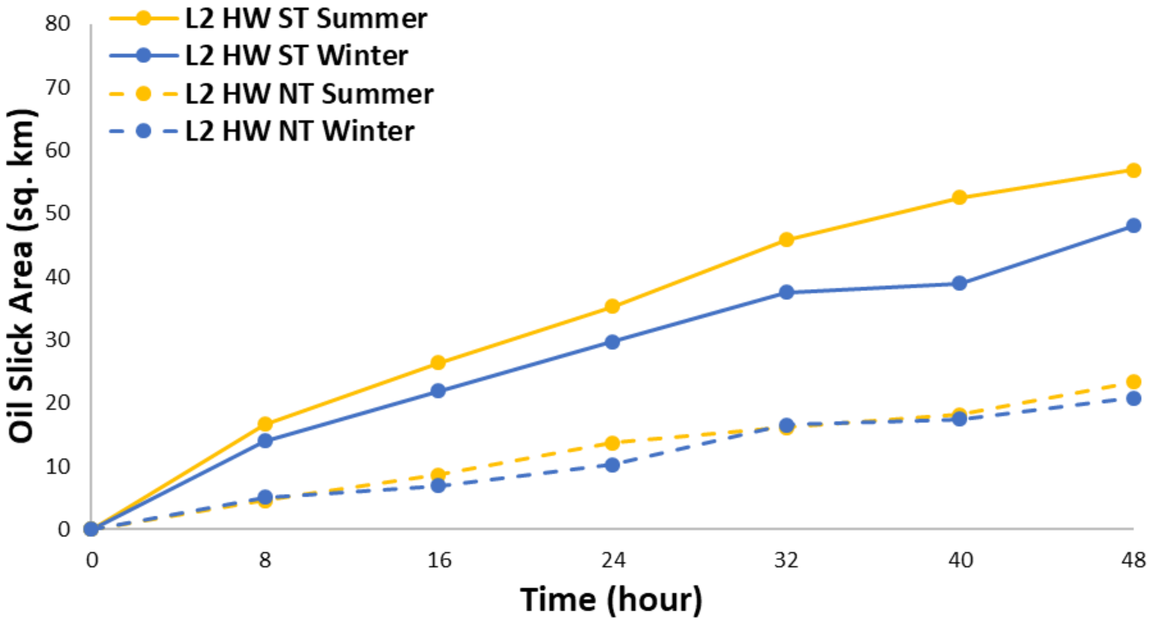

Figure 3.43: Area covered by simulated oil slick over time for a spill from L2 at high water

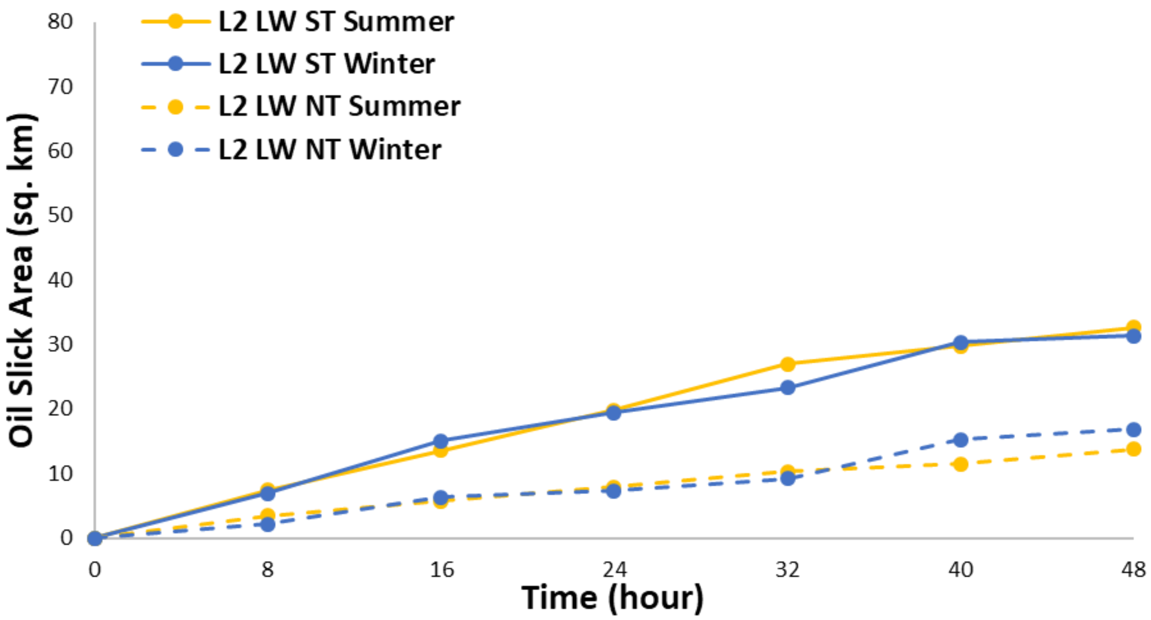

Figure 3.44: Area covered by simulated oil slick over time for a spill from L2 at low water

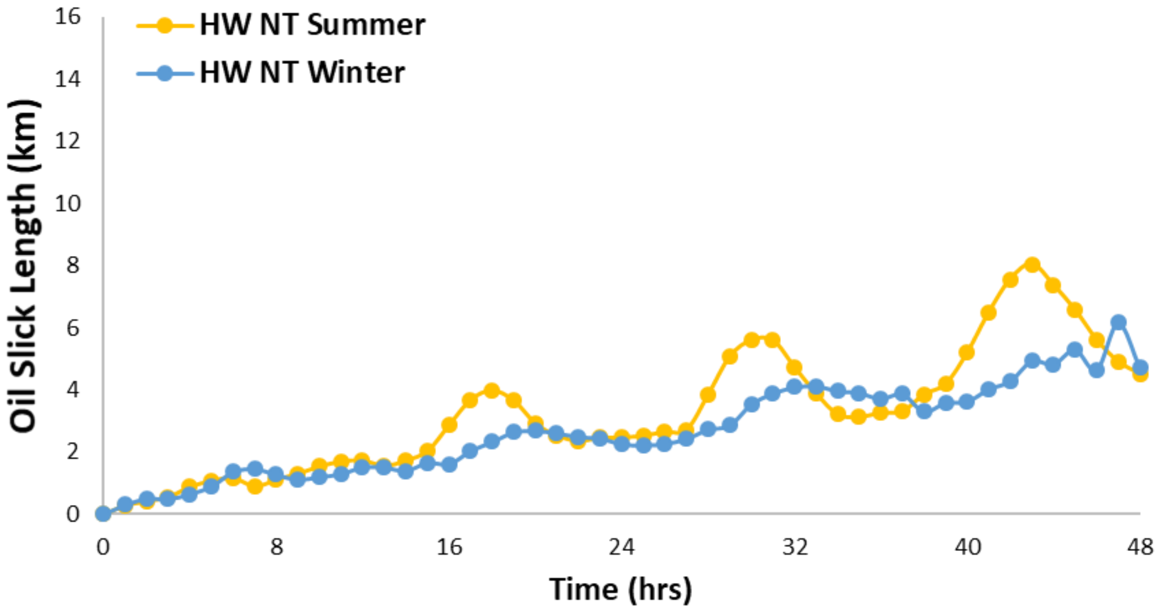

Figure 3.45: L2 oil slick length over time for a spill at high water during neap tide

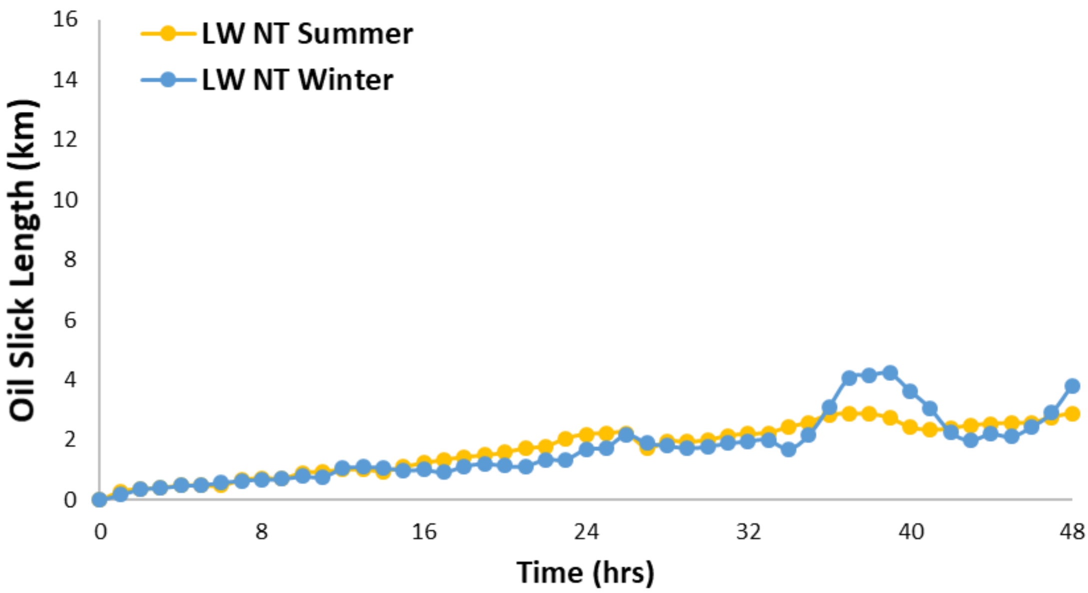

Figure 3.46: L2 oil slick length over time for a spill at low water during neap tide

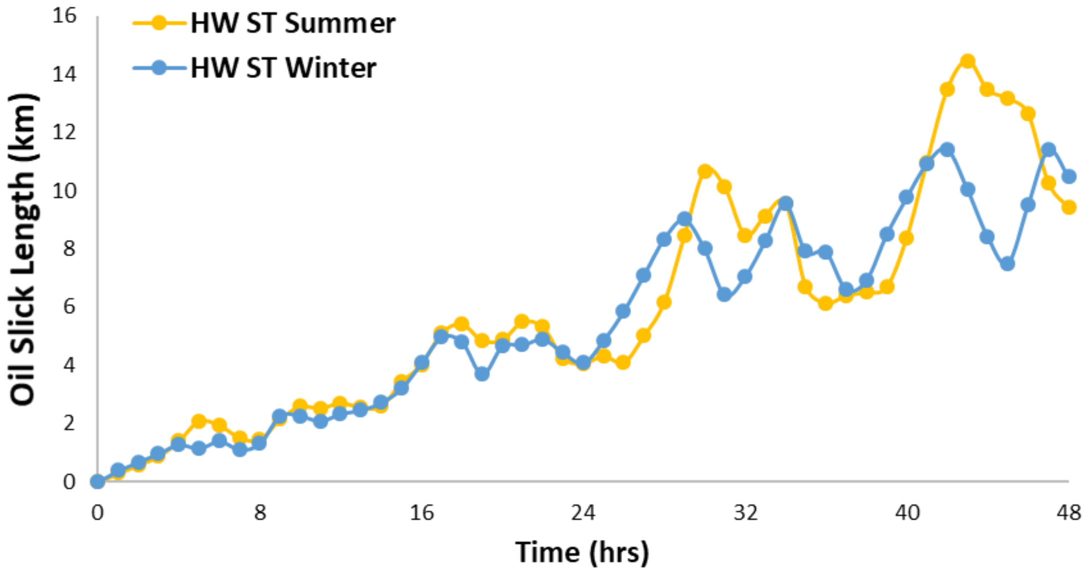

Figure 3.47: L2 oil slick length over time for a spill at high water during spring tide

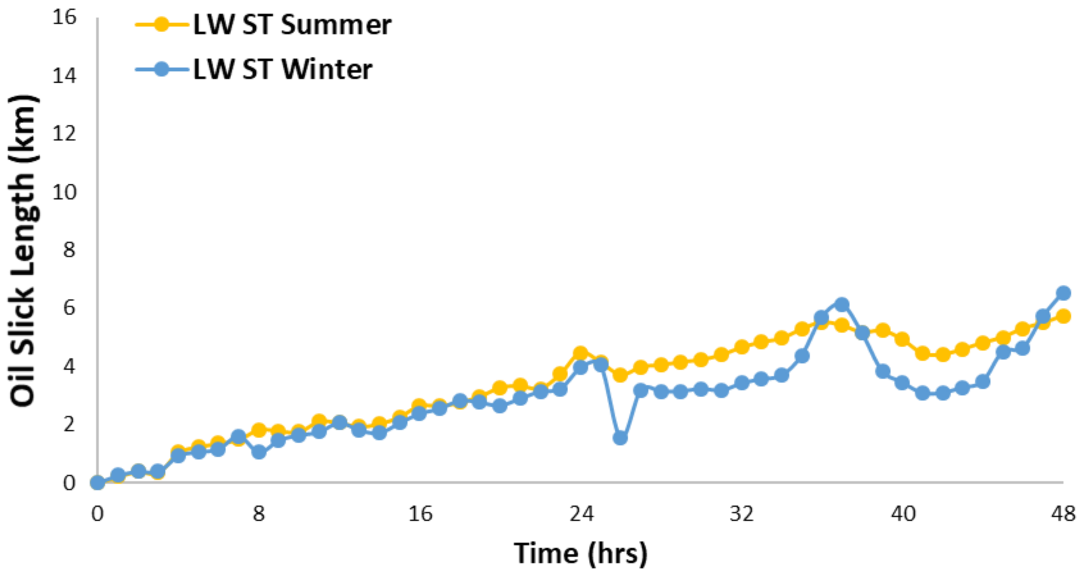

Figure 3.48: L2 oil slick length over time for a spill at low water during spring tide

3.4 DISCUSSION

3.4.1 Impact of Seasonal Discharge Variation (summer vs winter)

Simulated oil spills in the Humber Estuary were observed to drift with flood and ebb currents. Results show that oil slicks are likely to remain in the estuary within the first 48 hours (Figure 3.25 – 3.40). This is dependent on the point of release, as oil slicks released at L1 are observed to leave the computational domain (Figure 3.27; 3.28; 3.31; 3.32; 3.35; 3.36; 3.39; 3.40). Oil slicks released at L1 could re-enter the estuary on the flood tide, depending on North Sea current magnitudes and directions. However, this scenario is beyond the scope of this study.

Using the oil slicks released from L2 as the reference case, oil slick lengths were observed to increase over time, albeit not at a uniform rate (Figures 3.45 – 3.48). It was observed that the maximum oil slick lengths in summer were longer than the winter slicks for the two HW scenarios (Figure 3.45; 3.47), while maximum oil slick lengths in winter were longer than the summer slicks for the two LW scenarios (Figure 3.46; 3.48). This indicates that the influence of seasonal discharge on oil slick spreading is dependent on the time of release within a tidal cycle.

The oil slick impacted area, depends on the release point, time from oil release, neap/spring tide and high/low water scenario and the season (Figure 3.41 – 3.44). After 48 hours the oil slick impacted area is predominantly greater in the summer (by an average of 4%; Table 3.14). This contrasts with the findings that winter slicks were displaced (i.e. travelled) farther (by an average of 12% than summer slicks) after 48 hours (Table 3.14). Winter slicks thus are longer but narrower than summer slicks. This shows that seasonal river discharge significantly influences oil slick spreading in the tide-dominated Humber Estuary.

Table 3.14: Relative properties of comparable oil slicks released in the summer and winter (ratio = summer value / winter value), as measured 48 hours after the spill.

	Area ratio						Length ratio	Distance ratio
	8 h	16 h	24 h	32 h	40 h	48 h	48 h	48 h
L2 HW NT	0.92	1.25	1.34	0.98	1.04	1.12	0.96	0.98
L2 LW NT	1.56	0.91	1.09	1.13	0.75	0.81	0.76	0.73
L2 HW ST	1.19	1.21	1.21	1.22	1.35	1.18	0.90	1.01
L2 LW ST	1.07	0.90	1.02	1.16	0.98	1.04	0.88	0.83
Average	1.19	1.07	1.17	1.12	1.03	1.04	0.88	0.89

Overall, the distances travelled by winter slicks released at low water are 20.4% and 36.9% greater than those of summer slicks (Figure 3.53 – 3.60; Table 3.15). The differences in distance travelled under high water are less pronounced, as the distance covered by winter slicks is only 1.6% greater than summer slicks when released at high water (HW) neap tide (NT) (Figure 3.53; 3.54) while the distance travelled by summer slicks is only 0.7% greater than winter slicks when released at HW spring tide (ST) (Figure 3.57; 3.58; Table 3.14). However, these distances obscure an important qualitative difference in the oil slick trajectory. Oil slicks released under winter conditions were observed to travel further downstream compared to oil slick released under summer conditions. After 48 hours, the downstream displacement of winter slicks was, on average, 4.19 km further than summer slicks (Figure 3.53 – 3.60; Table 3.15). However, summer slicks reached an average of 2.51 km further upstream (Figure 3.53 – 3.60; Table 3.15). While winter slicks released at high water do not experience any upstream displacement, summer slicks were able to travel upstream over repeated tidal cycles (Figure 3.53 – 3.60; Table 3.15). We now know that seasonal river discharge variability has a key influence on upstream and downstream displacement of the oil slick.

Thus, there is a distinct difference in oil slick dynamics within the estuary, whereby summer spills tend to travel further upstream and winter spills tend to slowly migrate downstream (Figure 3.50 – 3.60). As a consequence, oil slicks released in winter are likely to leave the estuary more quickly than oil slicks released in summer. This dynamic can be attributed to the relatively higher ebb velocities as a result of higher freshwater flow in winter (Mitchell et al. 2003a). It also supports Townend and Whitehead (2003) who point out that in the Humber Estuary, flood asymmetry dominates in summer, while flow in winter months becomes ebb dominant as gravity flow dominates.

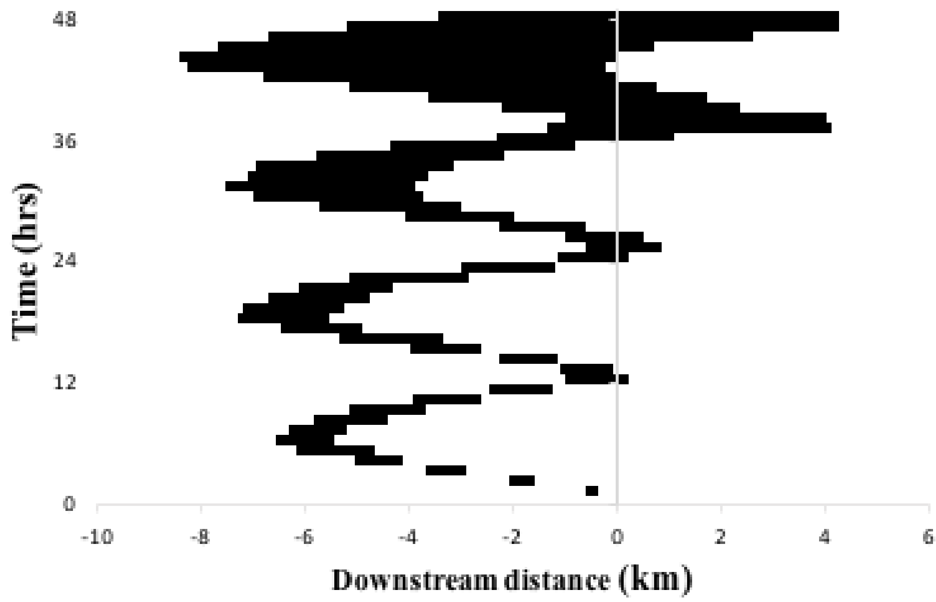

Figure 3.49: Longitudinal position and extent of L1 oil slicks over time at low water during neap tide in summer

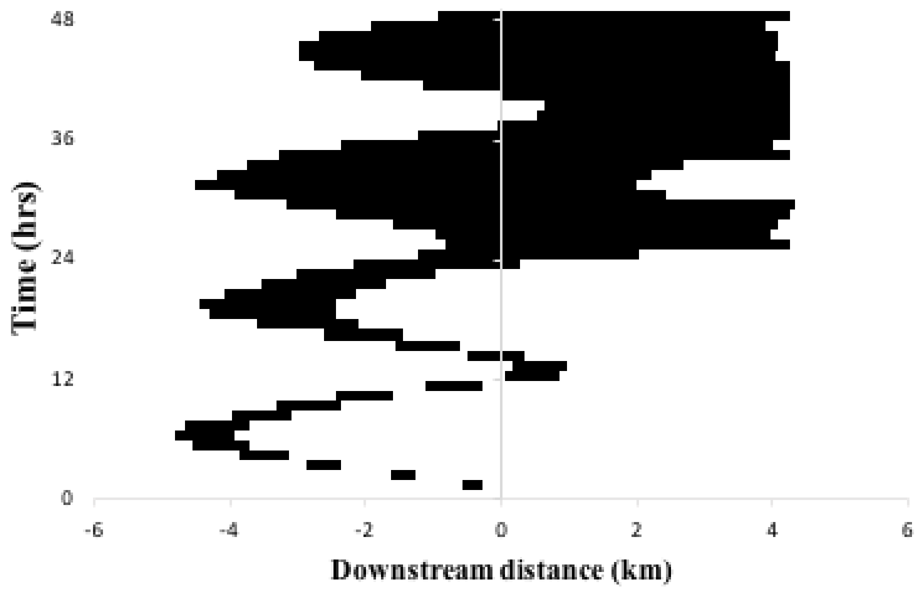

Figure 3.50: Longitudinal position and extent of L1 oil slicks over time at low water during neap tide in winter

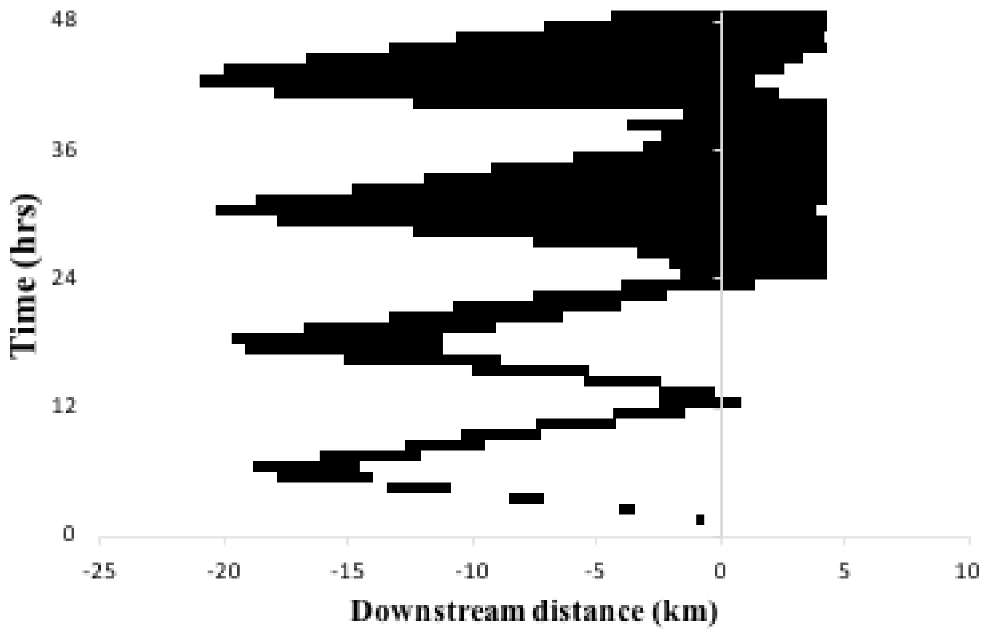

Figure 3.51: Longitudinal position and extent of L1 oil slicks over time at low water during spring tide in summer

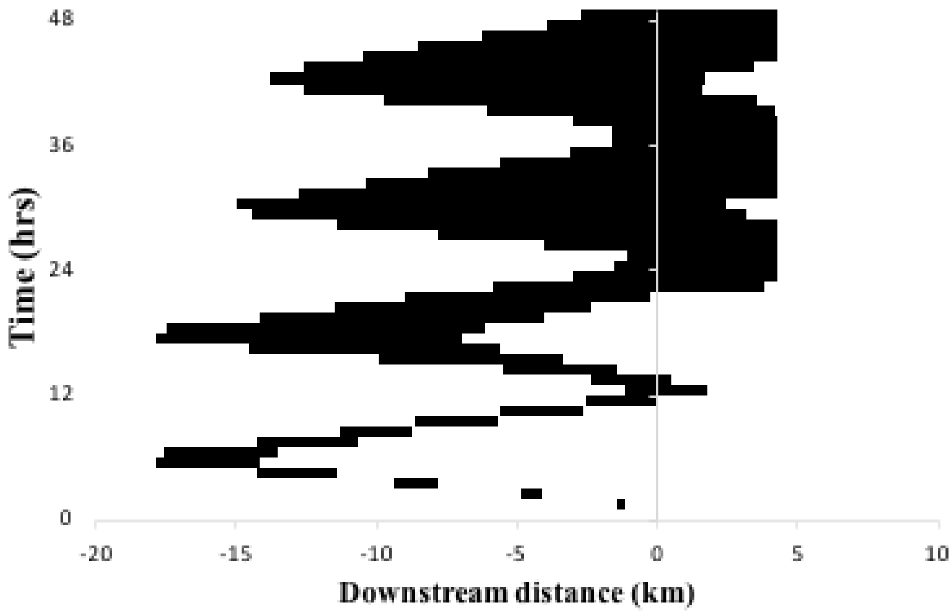

Figure 3.52: Longitudinal position and extent of L1 oil slicks over time at low water during spring tide in winter

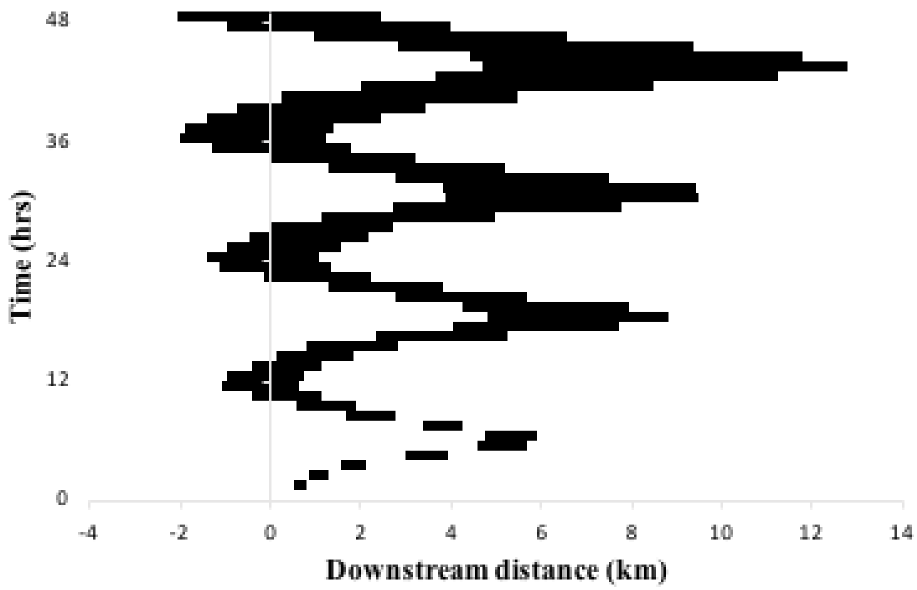

Figure 3.53: Longitudinal position and extent of L2 oil slicks over time at high water during neap tide in summer

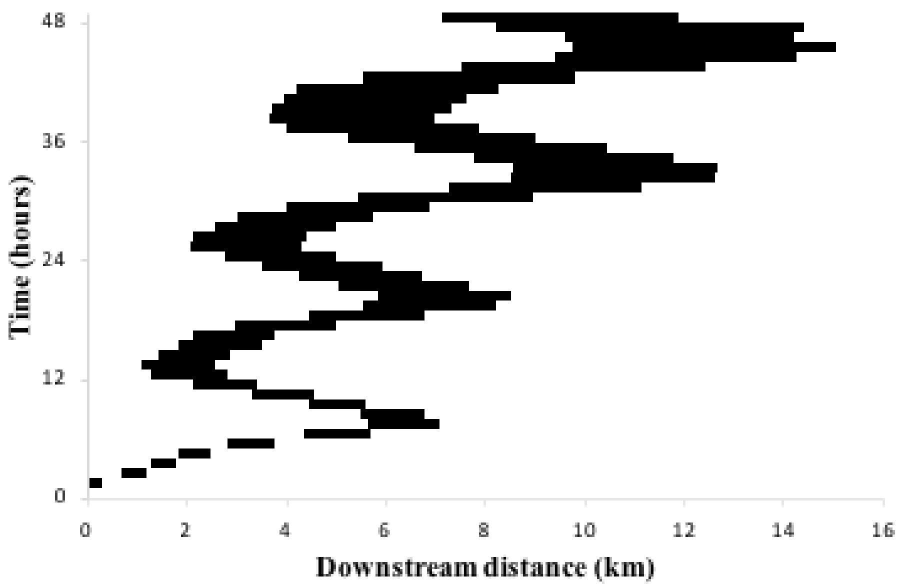

Figure 3.54: Longitudinal position and extent of L2 oil slicks over time at high water during neap tide in winter

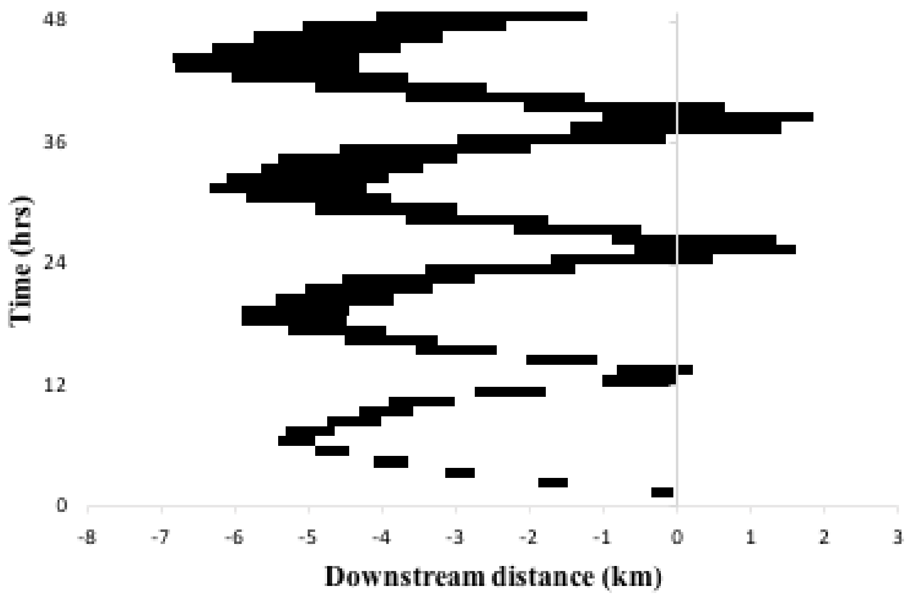

Figure 3.55: Longitudinal position and extent of L2 oil slicks over time at low water during neap tide in summer

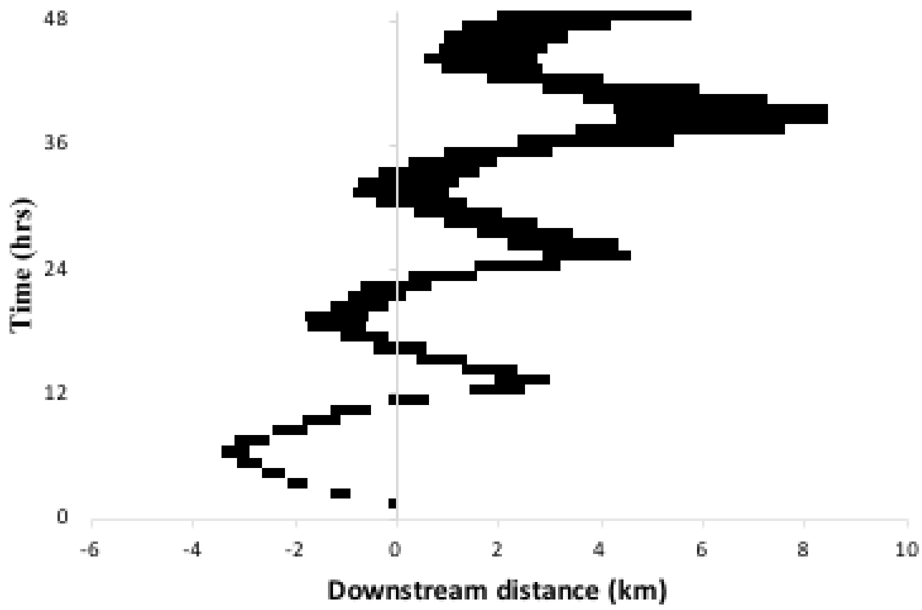

Figure 3.56: Longitudinal position and extent of L2 oil slicks over time at low water during neap tide in winter

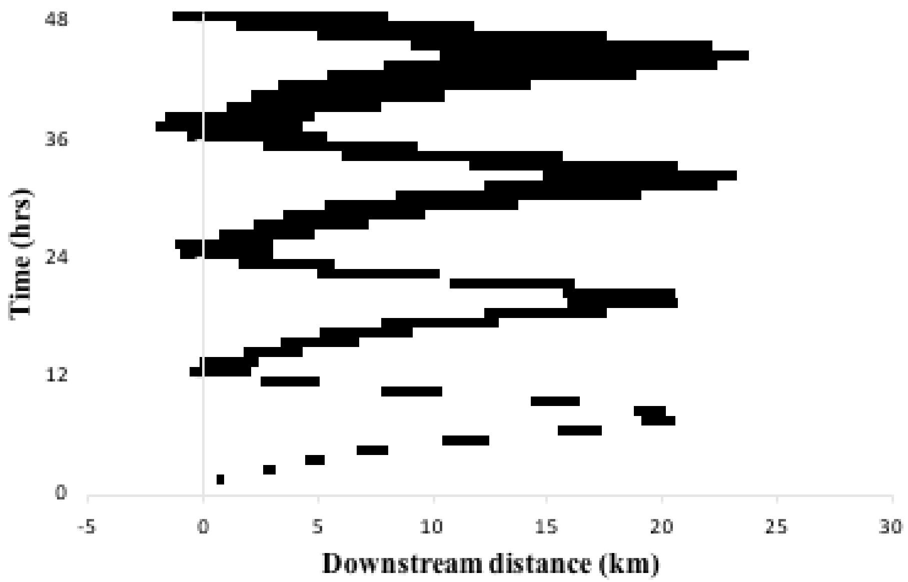

Figure 3.57: Longitudinal position and extent of L2 oil slicks over time at high water during spring tide in summer

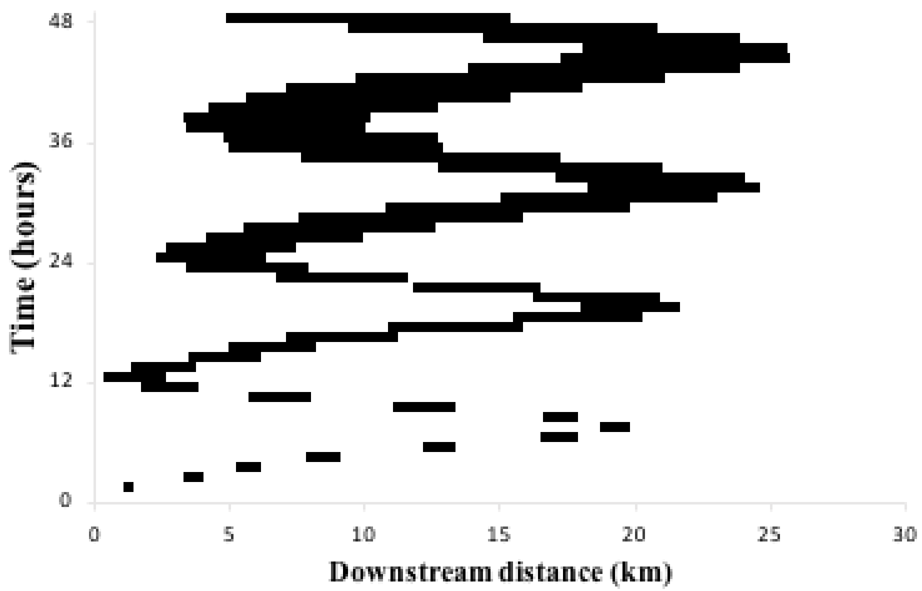

Figure 3.58: Longitudinal position and extent of L2 oil slicks over time at high water during spring tide in winter

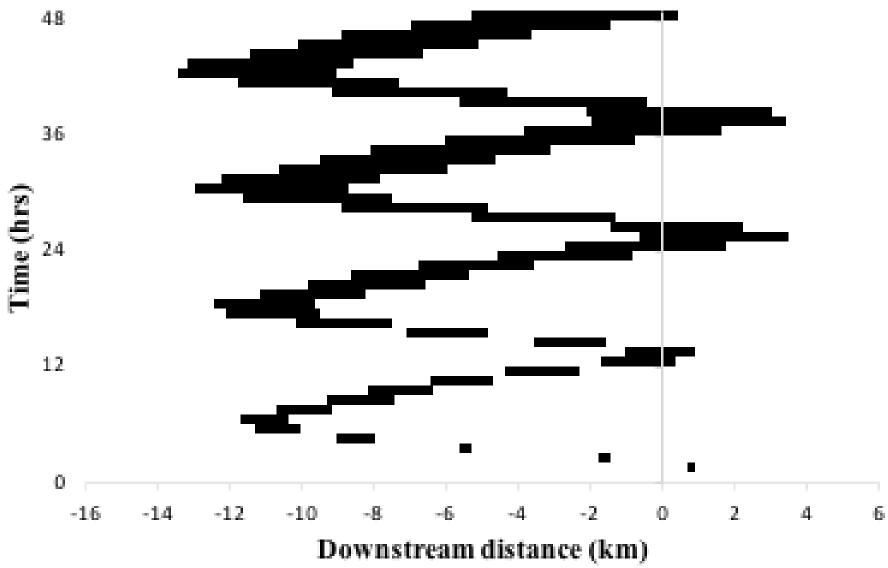

Figure 3.59: Longitudinal position and extent of L2 oil slicks over time at low water during spring tide in summer

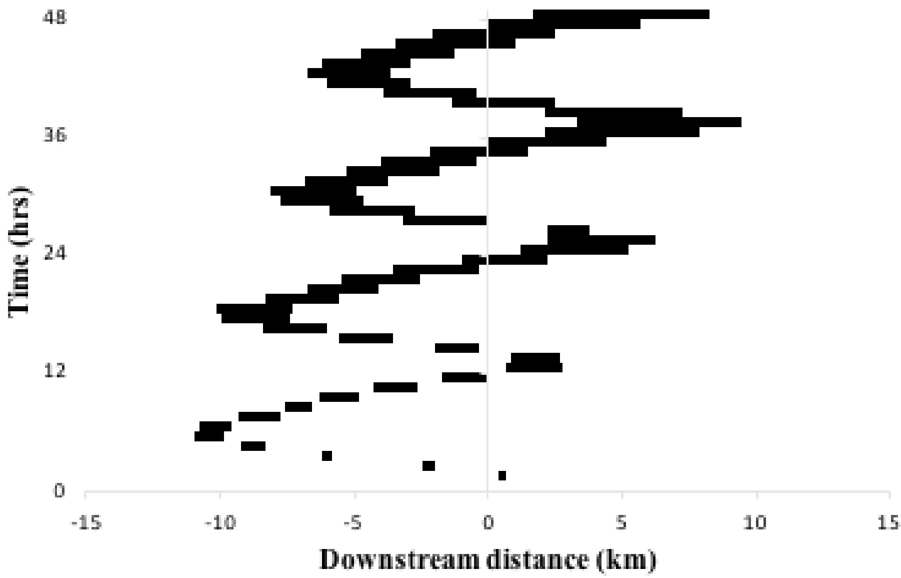

Figure 3.60: Longitudinal position and extent of L2 oil slicks over time at low water during spring tide in winter

Table 3.15: Summary of maximum oil slick displacement (km) from point of release.

	Upstream displacement (summer)	**Upstream displacement (winter)**	**Downstream displacement (summer)**	**Downstream displacement (winter)**
L2 HW NT	2.07	0	12.75	15.05
L2 LW NT	6.85	3.46	1.84	8.44
L2 HW ST	2.10	0	23.75	25.67
L2 LW ST	13.43	10.96	3.52	9.45

3.4.2 Impact of Tide (Spring Tide vs Neap Tide)

After 48 hours, oil slick impacted areas on water surface are between 86% and 144% larger under spring tide conditions than under neap tides, with an average of 125% (Table 3.16). This is due to the larger magnitudes of the currents driving the oil slick (Figure 3.61 – 3.64). Similarly, after 48 hours, the lengths of oil slicks released under spring tide were on average 100% longer than under neap tides (Figure 3.45 – 3.48; Table 3.16), whilst the total distance travelled by spring tide oil slicks was on average 78% greater than for neap tide oil slicks (Figure 3.53 – 3.60; Table 3.16). After 48 hours, the upstream displacement of oil slicks released under spring tide was on average 3.53 km further than under neap tide (Table 3.15). Similarly, after 48 hours, the downstream displacement of oil slicks released under spring tide was on average 6.08 km further than under neap tide (Table 3.15). Mendes et al. (2008) made similar findings in the Ria De Aveiro Lagoon, pointing out that compared to neap tides, spring tides have a larger influence on oil travel distance. These findings confirm that oil spills released under spring tide in an estuarine environment have a greater slick impacted area on water surface and distance travelled.

Table 3.16: Relative properties of comparable oil slicks released at spring and neap tides (ratio = ST value / NT value), as measured 48 hours after the spill.

	Area ratio						**Length ratio**	**Distance ratio**
	8 h	**16 h**	**24 h**	**32 h**	**40 h**	**48 h**	**48 h**	**48 h**
L2 HW summer	3.61	3.06	2.57	2.85	2.89	2.44	2.08	1.74
L2 HW winter	2.78	3.16	2.90	2.28	2.23	2.31	2.22	1.71
L2 LW summer	2.17	2.35	2.50	2.62	2.60	2.37	1.99	1.95
L2 LW winter	3.16	2.38	2.67	2.54	1.99	1.86	1.71	1.72
Average	2.93	2.74	2.66	2.57	2.43	2.25	2.00	1.78

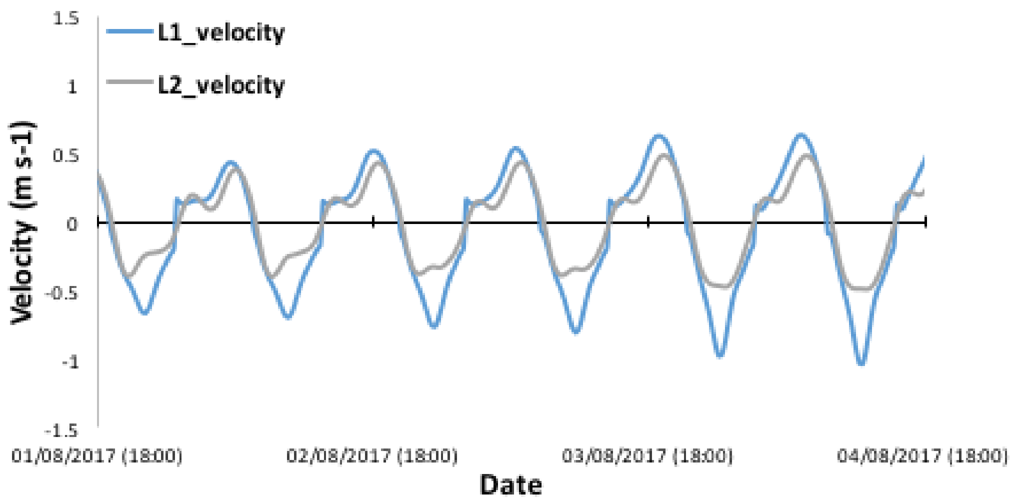

Figure 3.61: Simulated free surface velocities covering the duration of oil spill during neap tide summer. Note: negative current velocity indicates upstream movement while positive current velocity indicates downstream movement.

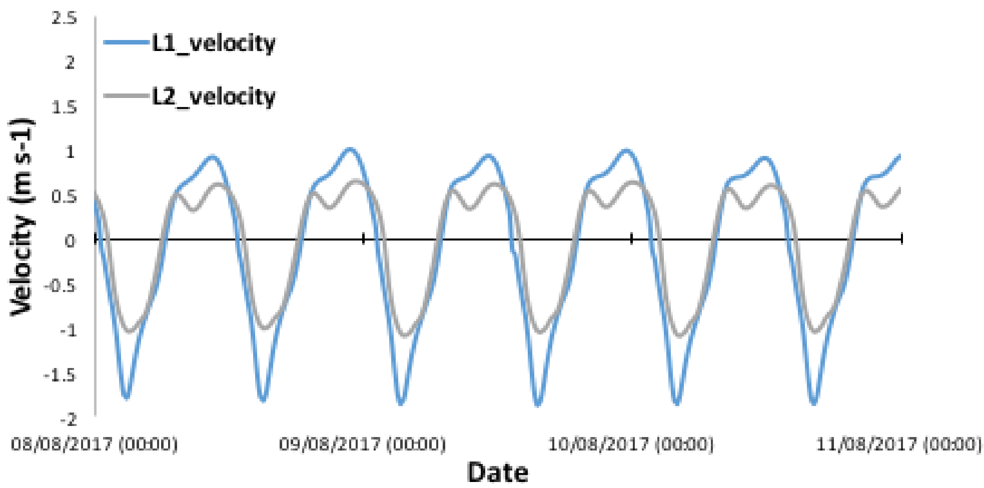

Figure 3.62: Simulated free surface velocities covering the duration of oil spill during spring tide summer Note: negative current velocity indicates upstream movement while positive current velocity indicates downstream movement.

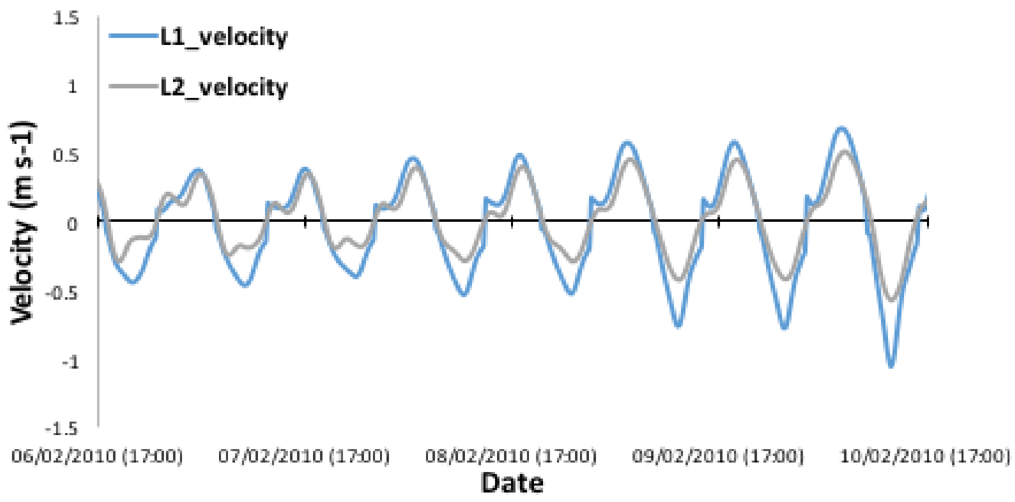

Figure 3.63: Simulated free surface velocities covering the duration of oil spill during neap tide winter Note: negative current velocity indicates upstream movement while positive current velocity indicates downstream movement.

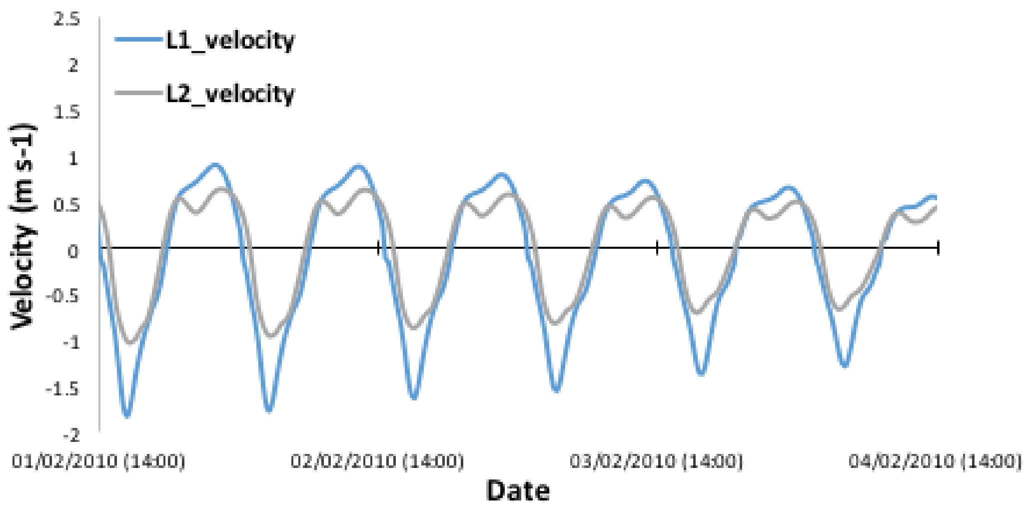

Figure 3.64: Simulated free surface velocities covering the duration of oil spill during spring tide winter Note: negative current velocity indicates upstream movement while positive current velocity indicates downstream movement.

3.4.3 Impact of Tidal Stage (High Water vs Low Water)

After 48 hours, oil slick impacted areas are between 23% and 74% larger when released at high water than at low water (Table 3.17). Similarly, after 48 hours, the lengths of oil slicks released at high water were on average 52% longer than at low water (Figure 3.45 – 3.48; Table 3.17). In agreement with Yan et al. (2012), this suggests that to efficiently deal with oil spills, responders will have to be made aware of the tidal stage at the time of oil release. Simulated oil slicks released at L2 high water were observed to travel further downstream compared to oil slicks released at low water, while oil slicks released at low water were observed to travel further upstream (Figures 3.25 – 3.40; 3.53 – 3.60). After 48 hours, the upstream migration of oil slicks released at low water was on average 7.63 km further than at high water. However, downstream displacement of oil slicks released at high water had migrated on average 13.49 km further than at low water (Table 3.15). This is likely due to the initial direction of displacement at the time of oil spill release caused by flood/ebb tides**.** The results suggest that oil slick upstream displacement at low water, and downstream displacement at high water, is enhanced during spring tides. This study discovers that the overall distances travelled by oil slicks released at high water were on average 44% greater than at low water (Figure 3.53 – 3.60; Table 3.17). We now know that oil spills released at high water have a greater oil slick impacted area on water surface and distance travelled, while oil spills released at low water present have a greater slick residence within the estuary since the oil slick will first move upstream with the incoming tide.

Table 3.17: Relative properties of comparable oil slicks released at high and low water (ratio = HW value / LW value), as measured 48 hours after the spill.

	Area ratio						Length ratio	Distance ratio
	8 h	**16 h**	**24 h**	**32 h**	**40 h**	**48 h**	**48 h**	**48 h**
L2 NT summer	1.34	1.49	1.73	1.56	1.59	1.69	1.57	1.71
L2 NT winter	2.29	2.29	1.40	1.80	1.16	1.23	1.24	1.26
L2 ST summer	2.23	1.94	1.81	1.70	1.76	1.74	1.64	1.53
L2 ST winter	2.02	1.45	1.52	1.61	1.28	1.53	1.61	1.26
Average	1.97	1.79	1.62	1.67	1.45	1.55	1.52	1.44

3.4.4 Relative Impacts of Season vs Tide vs Stage

Until now, no empirical comparison has been undertaken on the relative influence of hydrodynamic conditions (seasonal discharge variation, water level and tidal range) on oil slick impacted area, length and distance travelled. However, results indicate that the influence of time of release in a tidal cycle on oil slick dynamics is greater than seasonal flows. The above analyses (Sections 3.4.1; 3.4.2; 3.4.3) indicate that these differences are statistically significant ($P < 0.05$ in pairwise ANOVA using the Holm-Sidak method; Appendix N). This thus provides the first clear evidence that oil slick impacted area, length and distance travelled are predominantly affected by the tidal range (i.e. spring tide or neap tide) at the time of oil release, and that stage and season are only secondary influencing factors (Tables 3.14; 3.16; 3.17; Figure 3.65).

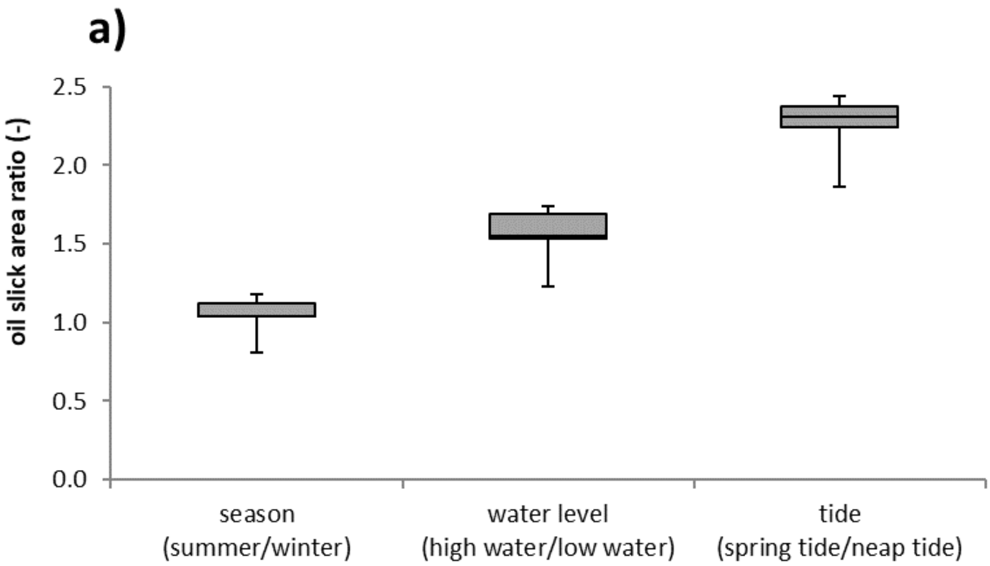
a)
oil slick area ratio (-)
2.5
2.0
1.5
1.0
0.5
0.0
season
(summer/winter)
water level
(high water/low water)
tide
(spring tide/neap tide)

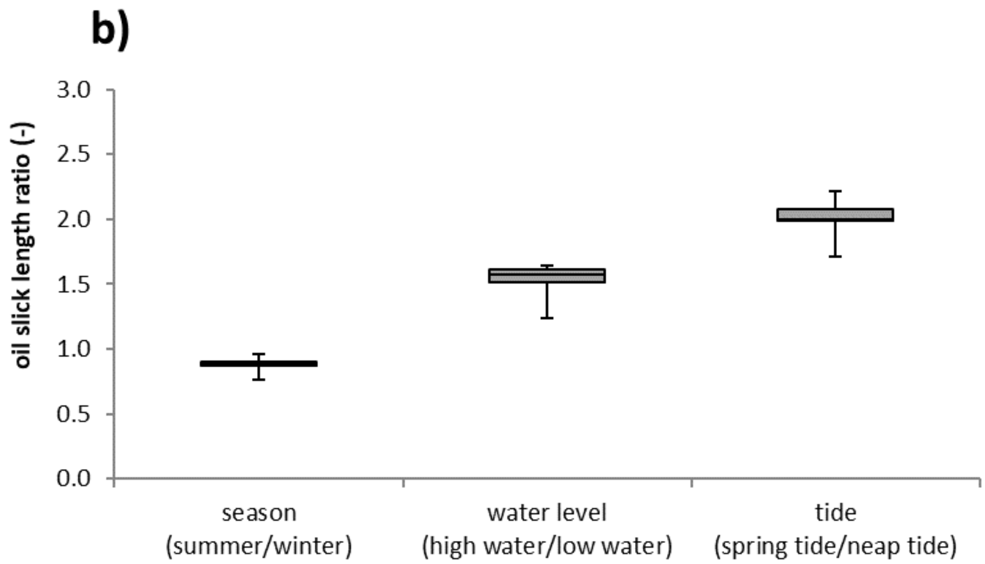
b)
oil slick length ratio (-)
3.0
2.5
2.0
1.5
1.0
0.5
0.0
season
(summer/winter)
water level
(high water/low water)
tide
(spring tide/neap tide)

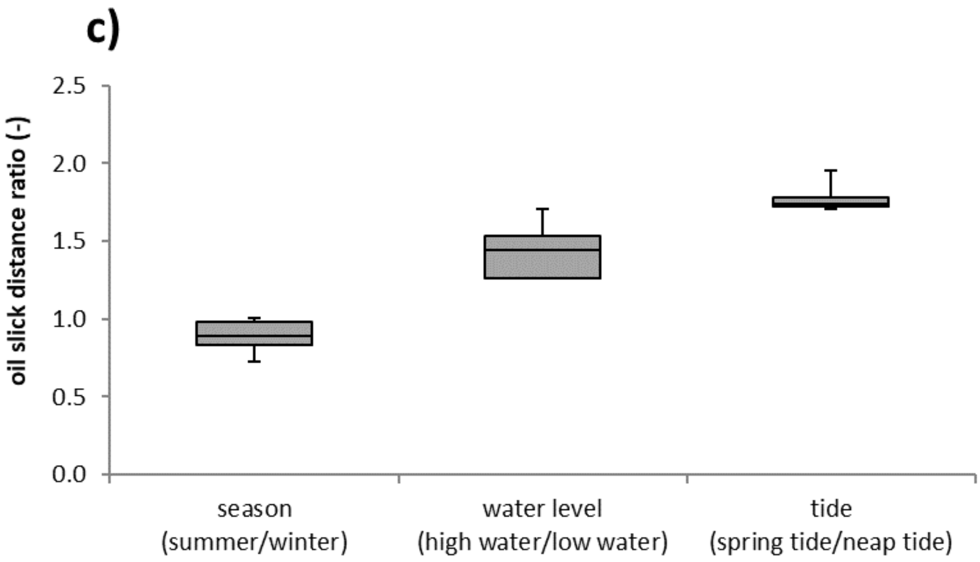

Figure 3.65: Boxplots of relative influences of hydrodynamic properties on a) oil slick impacted area; b) oil slick length; and c) oil slick distance, for spills released at L2 (Appendix O).

3.4.5 Oil Beaching

Here, oil beaching is defined as when oil interacts with the edge of the computational grid. The oil slick model shows the risk of an environmental disaster as oil may spread over the shallow intertidal/saltmarshes on the Southbank (as observed in the oil slicks released from L1) – Figure 3.27; 3.28; 3.31; 3.32, or on the densely populated north bank of the Humber Estuary (as observed in oil slicks released from L2) (Figure 3.35; 3.37; 3.39). The length of bank line affected and time of first contact (Table 3.13) suggests that although the oil slick reaches the estuary bank quicker in winter compared to summer, oil slick beaching covers a greater distance in summer. This is due to the differences in seasonal discharge. Oil slick beaching occurs in summer when released at L2 under spring tide conditions affecting 13.21 km and 19.45 km of the estuary bank line under low and high water respectively (Table 3.13). The absence of beaching in winter under the same scenario is likely related to the narrower slicks formed in winter.

However, the estuary bank affected by the oil slick is likely to depend on the cross-sectional location of the release point, which for this study was arbitrarily chosen. Further studies are needed to fully assess the impact of cross-sectional release point location.

3.5 LIMITATIONS

To achieve the study aim, instantaneous oil release was considered. However, there may be differences in the oil slick properties (i.e. the oil slick impacted area on water surface; length of the oil slick over time; and overall distance travelled) under continuous oil release. Further studies can be undertaken with continuous oil spill release. Due to limited data, this study employed the use of simulated tidal height data rather than measured data to drive the offshore boundary, constant discharge-driven boundary condition and did not consider surges in the hydrodynamic model,. This may have resulted in over- or under-prediction of oil spill transport. This study does not consider oil slick that leaves the computational domain into the North Sea. Oil slicks released at downstream could re-enter the estuary on the flood tide, depending on North Sea current magnitudes and directions. Findings from this study may be unique to tide-dominated estuaries. Considering the complexity of estuaries, further work can aim to extend results to other estuarine systems.

3.6 CONCLUSION

This study presents the first detailed analysis of oil spill dynamics in a large well-mixed macro-tidal estuary. Using the Humber Estuary as a case study, the influence of tidal cycles and seasonal freshwater discharge variability on the transport of hypothetical oil spills was assessed. This chapter also examined the temporal variability of environmental factors to understand the hydraulics of the Humber Estuary.

TELEMAC3D was employed to develop hydrodynamic models that represent the behaviour of the Humber Estuary in summer and winter. Satisfactory model performance (R^2 = 0.883 and 0.852 for summer and winter respectively) was attained using constant discharge at the river boundary. The models were validated against measured tidal height data at Immingham station for summer and winter, also with a satisfactory agreement (R^2 = 0.912 and 0.848 for summer and winter respectively). The two-dimensional oil spill model for the Humber Estuary was developed with the TELEMAC oil spill module.

To address the reseach gap (Section 1.2), this chapter assess the influence of seasonal river discharge variability on oil spill transport. We now know that, for this large well-mixed macro-tidal estuary:

(a) oil slicks are likely to remain in the estuary within the first 48 hours;
(b) lower summer discharges enable net upstream migration of oil slicks, while higher winter discharges encourage the downstream movement of oil slicks;
(c) because of seasonal variation in river discharge, winter slicks released at high water did not exhibit any upstream displacement over repeated tidal cycles,

while summer slicks travelled upstream into the estuary over repeated tidal cycles;

(d) there is a statistically significant ($P < 0.05$) difference in the influence of hydrodynamic conditions (seasonal discharge variation, water level and tidal range) on oil slick impacted area, length and distance travelled;

(e) the tidal range has a key influence on oil slick impacted area, with spring tide slicks being 125% bigger than neap tide slicks, on average;

(f) seasonal variations in river discharge have a significantly smaller impact on oil slick impacted area, with summer spills covering an area of only 4% larger than winter spills on average;

(g) although smaller in impacted area, winter slicks travel farther (12% on average) and are narrower than summer slicks;

(h) the influence of seasonal discharge on oil slick spreading is dependent on the time of release within a tidal cycle;

(i) oil spills released further downstream develop larger oil slicks and move over greater distances than oil spills released upstream;

(j) the farthest upstream displacement of the oil slick occurs for spills released at low water during summer spring tide conditions (e.g. 13 km for L2);

(k) the farthest downstream displacement of the oil slick occurs for spills released at high water during winter spring tide conditions (e.g. 26 km for L2); and

(l) the possibility of oil beaching on the banks of the estuary exposes environmental risks, with up to 24.6 km of shoreline affected in the simulations.

Some of these findings conform to intuitively expected dynamics, at least qualitatively. Others are arguably more surprising insights (e.g. c, d, e, f, h and l). However, all findings represent novel contributions in the sense that none had been formally and explicitly demonstrated or quantified, until now.

In general, oil spills released under spring tide have a greater oil slick impacted area on water surface and distance travelled. In addition, oil spills released at high water have form greater oil slick size, while oil spills released at low water have greater slick residence within the estuary since the oil slick will first travel upstream with the incoming tide.

It should be noted that this study investigated instantaneous oil slick releases in a large well-mixed macro-tidal estuary. To reliably generalize the findings, further studies should be undertaken, using continuous oil slick release and extending the analyses to other estuarine systems.

The implications of these findings for operational oil spill response are: a) the need to take cognisance of time of oil release within a tidal cycle; and (b) the need to understand how the interaction of river discharge and tidal range influences oil slick dynamics, as this will aid responders in assessing the likely oil trajectories.

Using the hydrodynamic models developed in this chapter, the next chapter (Chapter 4) will aim to access the influence of projected climatic conditions on oil slick transport in a tide-dominated estuary.

CHAPTER 4

4. INFLUENCE OF PROJECTED CLIMATIC CONDITIONS ON OIL SLICK TRANSPORT IN A TIDE-DOMINATED ESTUARY

The previous chapter investigates the implication of tidal currents and riverine flows on oil spill transport in a tide-dominated estuary, as well as, the influence of seasonal river discharge variability on oil slick transport. The findings from the previous chapter characterises oil spill transport under summer and winter conditions. This chapter assesses the potential influence of climate change-induced sea level rise and projected river flows on findings made in the previous chapter, thereby fulfilling objective 3 (Section 1.2.1). This is the first time that a range of simulation will be developed to address this gap. Consequently, there is a novelty in explicitly illustrating and demonstrating oil slick transport under these conditions (i.e. sea level rise and projected river flows).

4.1 BACKGROUND

Estuaries are significantly influenced by climate change because they respond to several types of forcing: momentum (i.e. wind stress); evaporation and precipitation (i.e. freshwater, heat and air-water fluxes of CO_2); streamflow quality and quantity; and sea-level changes (Najjar et al. 2010). This explains why projected climatic alterations, particularly changes in either river flow or mean sea level have been observed to have a critical impact on estuaries and its processes (Whitehead et al. 2009; Ranasinghe et al. 2012; Rice et al. 2012; Pye and Blott 2014; Robins et al. 2014; Wu and Parson 2019). Despite the increasing risks that oil spills present to estuaries (Kennish 2002; Anifowose et al. 2016) and the significant impact change in sea level and river flow has on estuarine functioning (Whitehead et al. 2009), the influence of projected future climatic conditions on oil spill transport in estuarine environment presents a gap in academic literature.

Sea level rise has garnered much attention because it is influenced by climate change and also because of its social, economic and environmental impact. The change of global sea level has been caused by ocean heat uptake and thermal expansion, glaciers, Greenland ice sheet, Antarctic ice sheet and water storage on land (anthropogenic activities) (Church et al. 2013). Sea level change was typically observed by tidal gauges until the 1990s when satellite altimetry was employed (Cazenave and Nerem 2004). The use of satellite altimetry to track sea level change has improved the sea level predictions (Ariana et al. 2017). Due to two main limitations, tidal gauges were less accurate: 1) being located only on ocean islands and continental margins, they had poor spatial distribution; 2) they are prone to vertical movement due to their attachment to land, as a result producing sea level change that is unrelated to climate variations (Nerem and Mitchum 2002).

In the last century, the global mean sea level has increased at a rate of +1 to +2 mm/year (Bindoff et al. 2007). However, since the use of satellite altimetry measurements, the upper range of global sea level rise has reached 3 mm/year (Bindoff et al. 2007; Robins et al. 2016). Observation of sea level in the 20th century indicates an increase of 1.4 mm/year around the UK (Lowe et al. 2018). To determine sea level change, Coupled Model Intercomparison Project (CMIP5) climate models and several emission scenarios known as Representative Concentration Pathways (RCPs) are employed (Table 4.1; Meinshausen et al, 2011). The recent UK climate projection 2018 (UKCP18) report does not consider RCP6.0 scenario as it presents similar sea level rise at 2100 to RCP4.5 and in comparison to other scenarios has poorer data availability in the CIMP5 database (Palmer et al. 2018). Mean sea level projection for the 21st century suggests sea level rise around the UK, although at spatially varying rates (Robins et al. 2014; Lowe et al. 2018).

Table 4.1: Details of the Representative Concentration Pathways (Moss et al. 2010).

Name	**Radiative forcing**	**Concentration (p.p.m)**	**Pathway**
RCP2.6	Peaks at ~3 W/m^2 before 2100 and the declines to 2.6 W/m^2 by 2100	Peaks at ~490 CO_2 before 2100 and the declines	Peak and decline
RCP4.5	~4.5 W/m^2 at stabilization after 2100	~650 CO_2 equivalent (at stabilization after 2100)	Stabilization without overshoot
RCP6.0	~6 W/m^2 at stabilization after 2100	~850 CO_2 equivalent (at stabilization after 2100)	Stabilization without overshoot
RCP8.5	>8.5 W/m^2 in 2100	>1,370 CO_2 equivalent in 2100	Rising

Much is known about the influence of sea level rise on flooding and inundation (Quinn et al. 2014), vertical mixing and salinity intrusion (Robins et al. 2016), sediment transport (Tessier et al. 2012), fluxes of nutrients (Robins et al. 2014; 2016) and behaviour of larger organisms (Chu-Agor et al. 2011; Fujii 2012) in tidal systems. It is critical to understand how projected sea level will influence oil slick transport.

The role of climate change on river discharge is poorly understood (Burn et al. 2012; Hannaford 2015). However, variations in rainfall and evapotranspiration due to climate change significantly impacts the hydrologic regime of water, particularly river discharge (Watts et al. 2015). The influence of increasing temperature to changes in rainfall through to river flow is a complex, non-linear process that is significantly influenced by catchment characteristics (Hannaford 2015). According to the UKCP18, the 21st century is expected to move towards hotter, drier summers and warmer wetter winters (Murphy et al. 2018). Robins et al. (2016) point out a relationship between increased UK winter rainfall and increased river flows in winter. Long trend analysis of UK river discharge (1961 – 2010) depicts higher discharge in winter compared to summer (Marsh and Dixon 2012; Hannaford 2015). Furthermore, Christierson et al.'s (2012) river catchment model predicts an increase and reduction in winter and summer discharge across the UK respectively from 2011 to 2040 respectively. In a review of observed trends and projected 21st century climate change to UK estuaries, Robins et al. (2016) assign medium confidence to increase in winter flow by up to 25% and decrease in summer mean flow by 40 – 80%. Several studies have been undertaken to explore the impact of projected river flow on solute transport (Robins et al. 2014); inlet-interrupted coastlines (Ranasinghe et al. 2012); and Anadromous fish (Ohlberger et al. 2018). Until now, the relative impact of projected sea level rise and river flow on oil spill transport dynamics in estuarine environments is poorly understood and there is no known study focusing on this important phenomenon; hence this study.

With the UK sea level projections expected to rise (Palmer et al. 2018) and river flow projected to decrease in summer and slightly increase in winter (Robins et al. 2016), it is important to understand how these factors will influence oil slick transport. Using the hydrodynamic models developed in the previous chapter (Section 3.2.2), this study is the first to assess the influence of projected river flow and sea level rise on oil slick dynamics in a tide-dominated estuary.

4.2 MATERIALS AND METHODS

4.2.1 Data Collection

4.2.1.1 Sea level data

Mean sea level data was provided by the Met Office Hadley Centre via the "UKCP user interface". The data was obtained from the "marine projections for the UK" data source using the same baseline (1981 – 2000) used to develop the recent UK climate projection 2018 report. Mean sea level for medium emission scenario (RCP4.5) was extracted from grid square latitude 53.5^{o}, longitude 0.08^{o} (538064; 402380; coordinates are in OSGB 1936) (Figure 4.1).

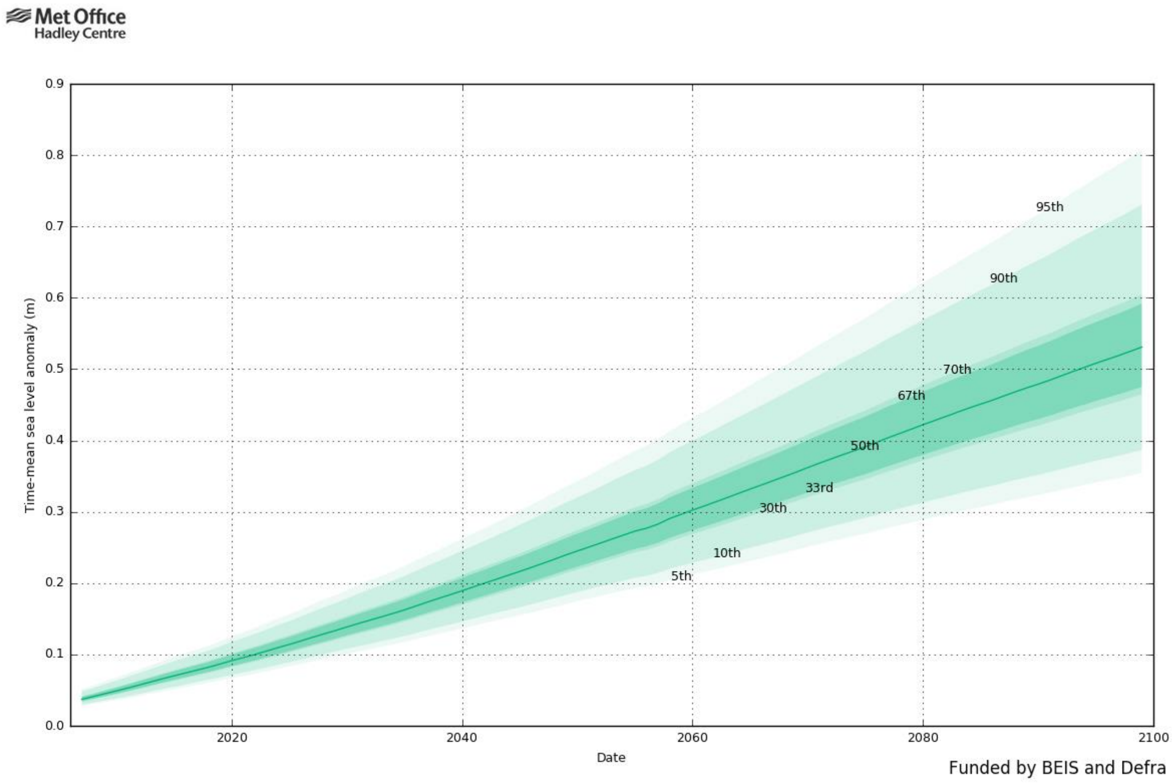

Figure 4.1: Time-mean sea level anomaly (m) for 2007 to 2100 for grid square 53.5º, 0.08º (538064; 402380), using baseline 1981 – 2000, and scenario RCP4.5, showing the 5th to 95th percentiles (Met Office Hadley Centre 2018).

4.2.1.2 Freshwater discharge data

Projected freshwater discharge data for the 21st century was obtained from literature. In a review of the impact of climate change on UK estuaries, Robins et al. (2016) project an increase of up to 25% in winter mean flow and decrease of 40 – 80% in summer mean flow by the year 2100. Consequently, an increase of 25% in winter mean flow and a decrease of 80% in summer mean flow is adopted for this study.

4.2.2 Oil Spill Design

Several scenarios were developed to assess the relative influence of projected climatic conditions on oil slick transport in a tide-dominated estuary. The influence of sea level rise and projected river flow was investigated using the hydrodynamic models developed for the representative summer and winter seasons (Table 3.7; Section 3.3.1). The open river boundary was driven by constant discharge obtained from literature (Table 3.8) while the open offshore boundary was driven by 15-minute tidal height data extracted from the FES2014 model (Section 3.2.1.3).

An instantaneous oil is released from an arbitrary location (L1; Figure 4.2) at high water during spring tide (Table 4.2). Considering the choice of arbitrary location, the influence of oil release location on oil spill transport is undertaken in Chapter 5. The oil is released under high water spring tide condition because it presents greater oil slick impacted area on water surface and distance travelled (Section 3.4.2; Section 3.4.3). Furthermore, the farthest downstream displacement of the oil slick occurs for spill released at this time (Section 3.4). The oil is released from this location under both representative summer and winter flows. Each scenario simulates an instantaneous release of 10,000 m^3 of Brent Crude (Table 3.2), and the resulting simulated oil slick is monitored for a 48-hour period. Visualisation of the oil slick transport and measurement of associated parameters (oil slick impacted area on water surface, length of the oil slick over time and overall distance travelled) were done within ArcMap 10.5.1 (Section 3.2.6; Figure 3.20).

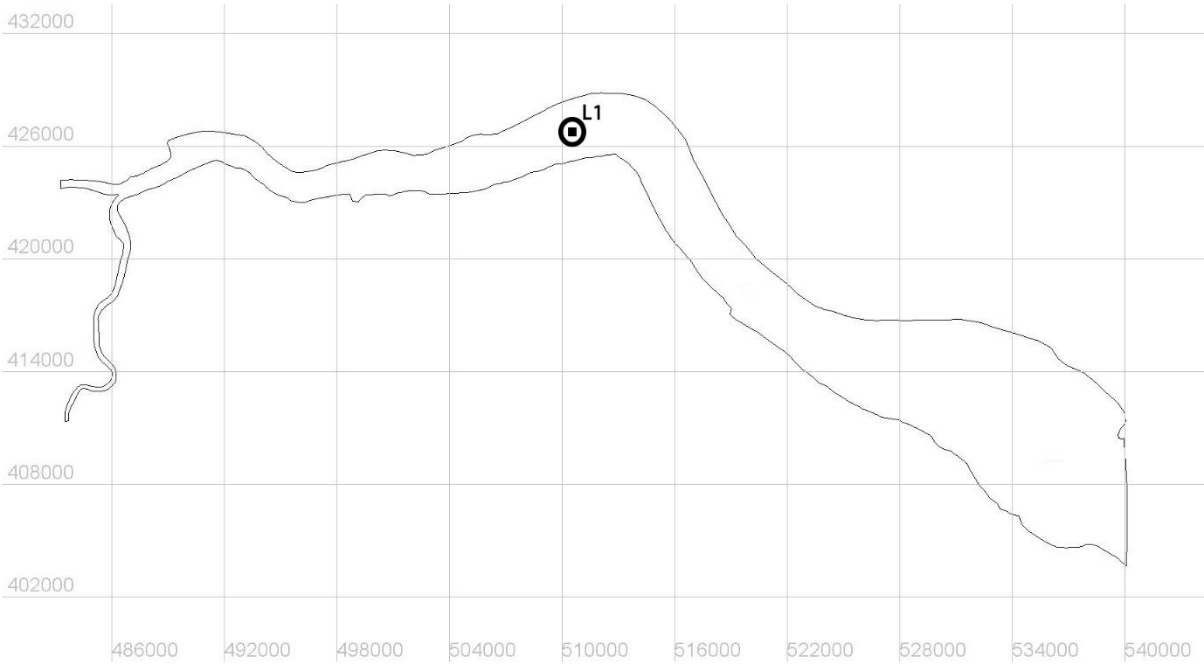

Figure 4.2: Outline for computational domain showing release points for oil spill scenarios at L1 (510498; 426777) (coordinates are in OSGB 1936).

Table 4.2: Summary of the oil slick release scenarios (tidal stage is with reference to release location)

Scenario	**Oil release time**
HW ST summer	08/08/2017 (06:00)
HW ST winter	01/02/2010 (19:15)

Note: HW = high water; ST = spring tide.

4.2.2.1 Sea level rise

In addition to oil slick transport simulations in the representative summer (August 2017) and winter (February 2010) months (Section 3.2.5.1), sea level projections for 2030, 2050 and 2100 were also simulated for both summer and winter. Considering winter scenario, global mean sea level is predicted to rise by 0.09 m between 2010 and 2030; 0.2 m between 2010 and 2050; and 0.48 m between 2010 and 2100 (Table 4.3). With regards to summer scenario (2017), sea level is predicted to rise by 0.06 m, 0.17 m and 0.45 m by 2030, 2050 and 2100 respectively (Table 4.3). In line with Robins et al. (2014) and Kumbier et al. (2018) methodology, the hydrodynamic models for February 2030, 2050 and 2100 were developed by linearly adding sea level rise values to the tidal height readings at the open offshore boundary (Table 4.4).

Table 4.3: Time-mean sea level (m) with respect to 1981 – 2000 for scenario RCP4.5, showing the 5th to 95th percentiles (Met Office Hadley Centre 2018).

Year	Time-mean sea level
2010	0.05 (0.04 – 0.07)
2017	0.08 (0.06 – 0.11)
2030	0.14 (0.10 – 0.19)
2050	0.25 (0.18 – 0.34)
2100	0.53 (0.36 – 0.81)

Table 4.4: Summary of oil spill simulations.

Run	Scenario	Flow input at river boundary (m^3/s)	Tidal height at offshore boundary (m)
1.1	Summer (August 2017)	Q	H
1.2	Winter (February 2010)	Q	H
2.1	Summer SLR 2030	Q	H + 0.06

2.2	Winter SLR 2030	Q	H + 0.09
2.3 2.4	Summer SLR 2050 Winter SLR 2050	Q Q	H + 0.17 H + 0.20
2.5 2.6	Summer SLR 2100 Winter SLR 2100	Q Q	H + 0.45 H + 0.48
3.1 3.2	Summer (SLR + Flow) 2100 Winter (SLR + Flow) 2100	Q – 80% Q + 25%	H + 0.45 H + 0.48
3.3 3.4	Summer Flow 2100 Winter Flow 2100	Q – 80% Q + 25%	H H

Note: *Q* is the typical freshwater flows from Rivers Ouse and Trent (Table 3.8); and *H* is the tidal height data extracted from the FES2014 model.

4.2.2.2 Projected river flow

In line with Robins et al. (2014) methodology, hydrodynamic models for projected river flow were developed by adding the projected flow values to freshwater discharge values at the open river boundaries (Table 4.4). The projected river flow for 2100 was simulated for both summer and winter. Also, projected river flow was simulated with corresponding sea level rise prediction for 2100 (Table 4.4).

4.3 RESULTS

4.3.1 Sea Level Rise Scenarios

The results for the 8 oil spill scenarios consisting of the representative summer and winter months and the corresponding sea level rise at 2030. 2050 and 2100 are presented (Figure 4.3 – 4.10; Table 4.5). While oil slicks exhibit similar dynamics despite sea level rise, certain behaviours associated with the scenario configurations were observed. These nuances are discussed in detail in the next section.

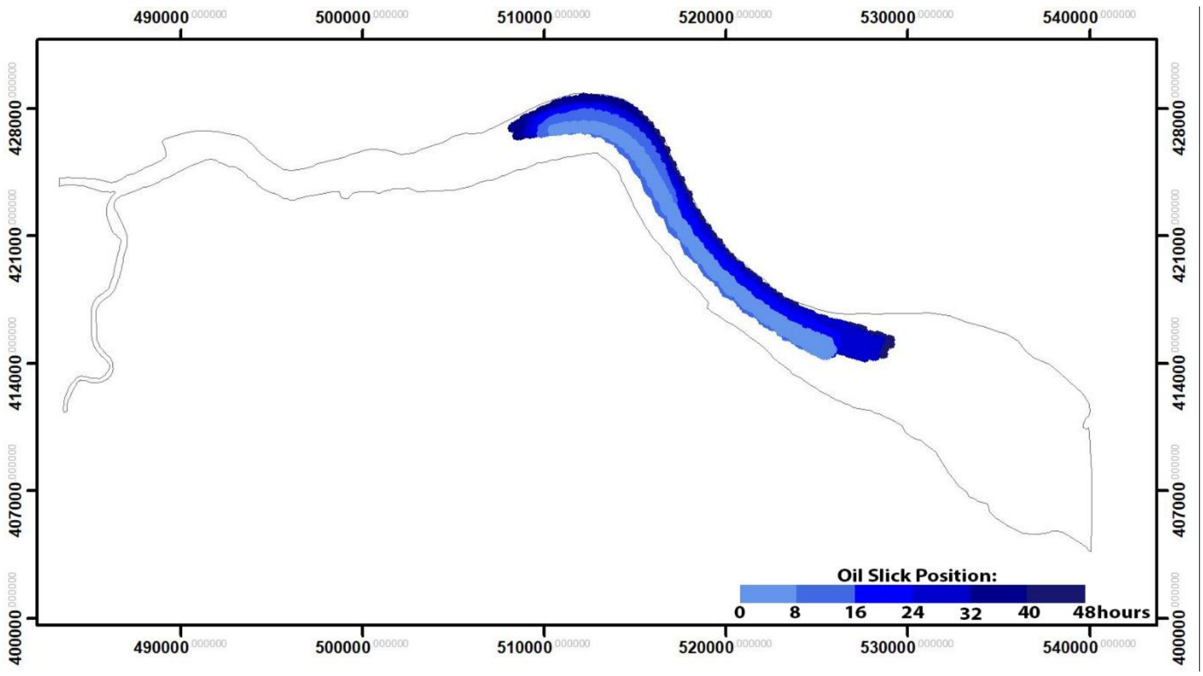

Figure 4.3: Simulated trajectories of oil released on the Humber Estuary at high water spring in summer with 2017 sea level.

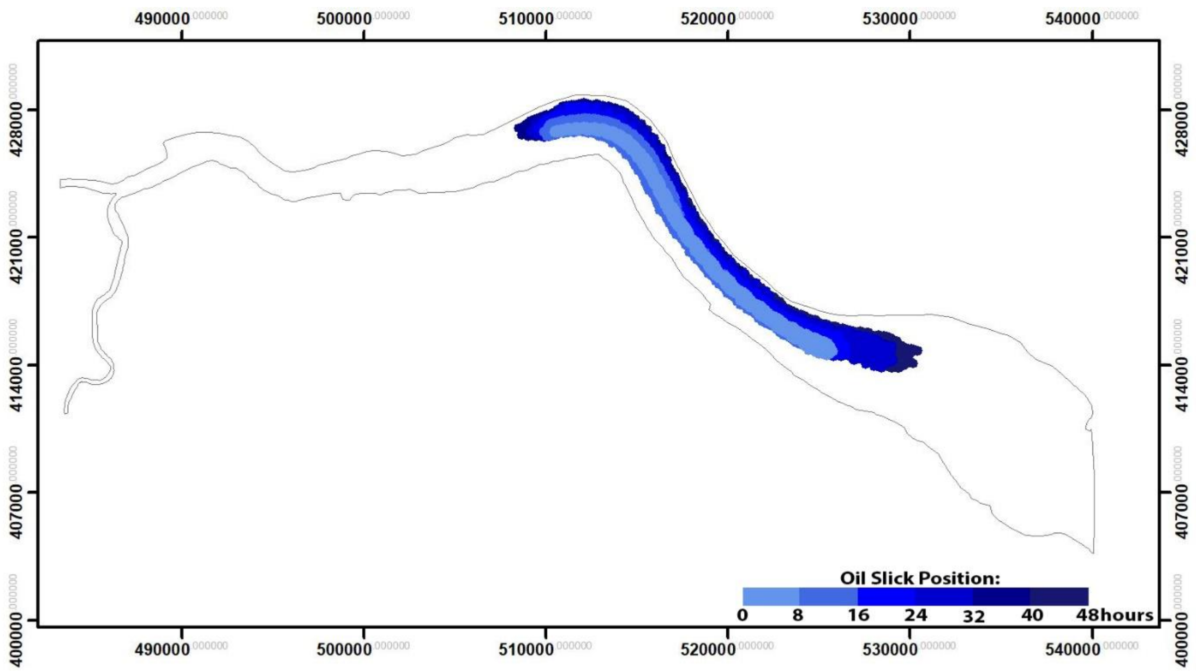

Figure 4.4: Simulated trajectories of oil released on the Humber Estuary at high water spring in summer with 2030 sea level.

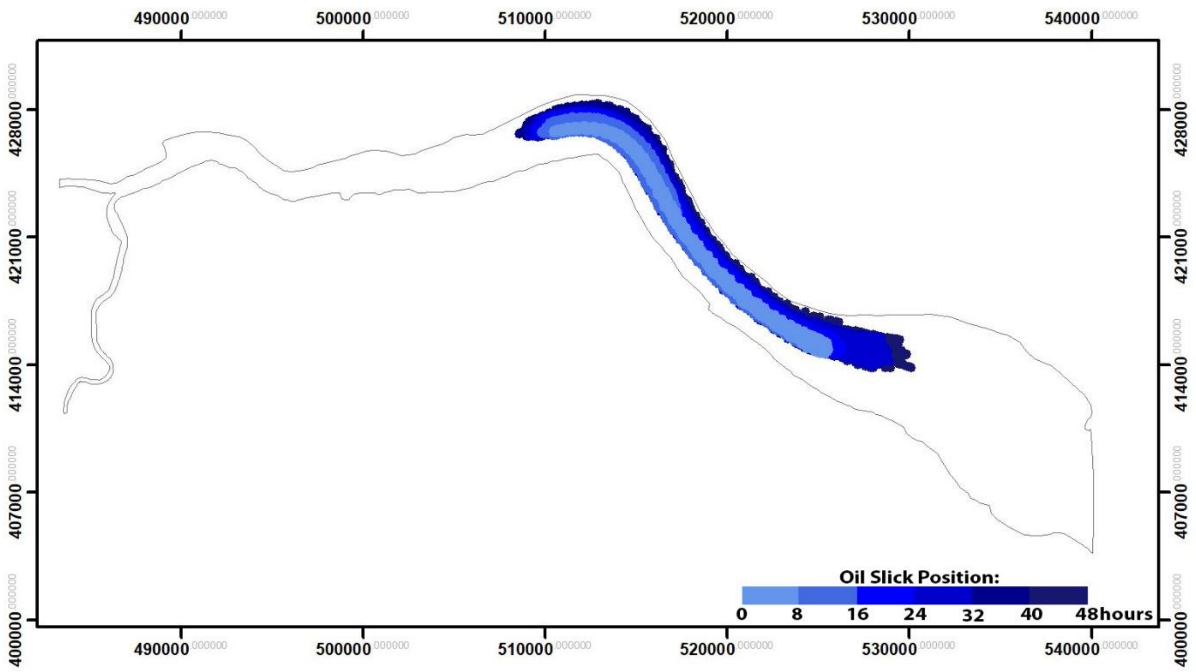

Figure 4.5: Simulated trajectories of oil released on the Humber Estuary at high water spring in summer with 2050 sea level.

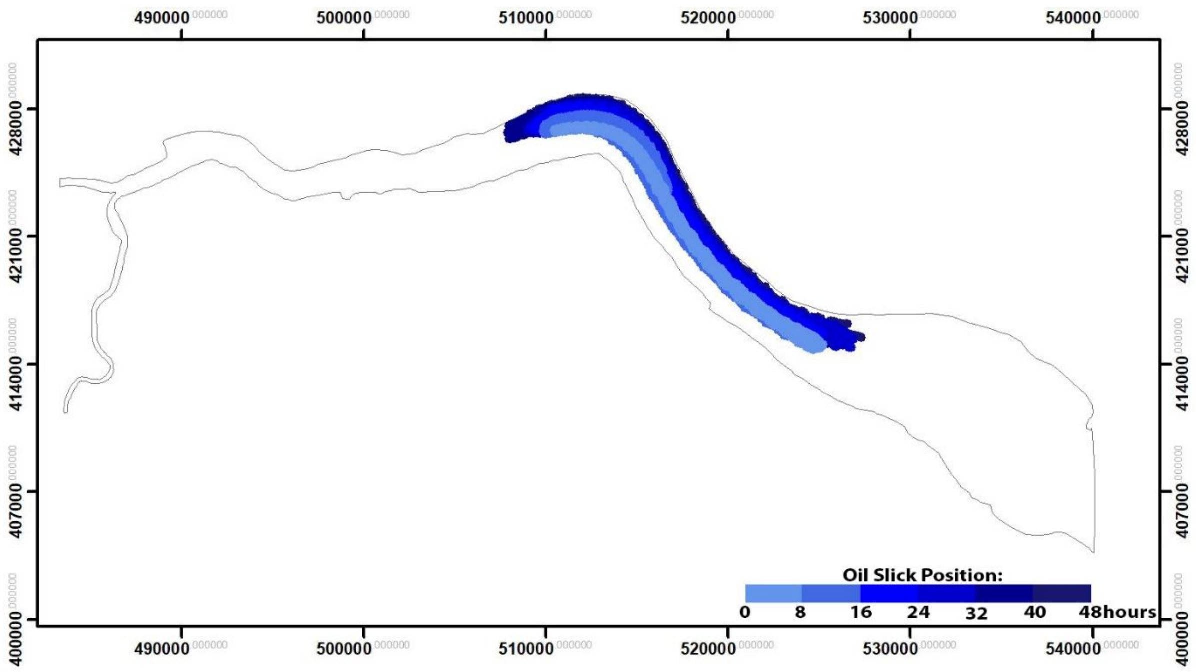

Figure 4.6: Simulated trajectories of oil released on the Humber Estuary at high water spring in summer with 2100 sea level.

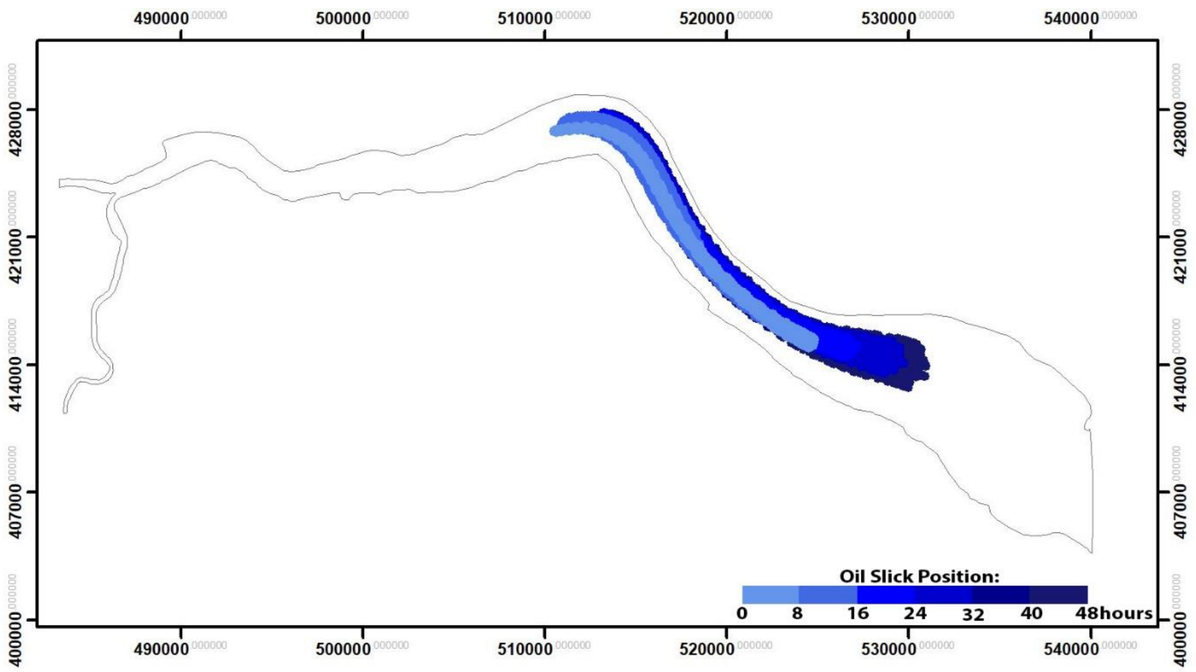

Figure 4.7: Simulated trajectories of oil released on the Humber Estuary at high water spring in winter with 2010 sea level.

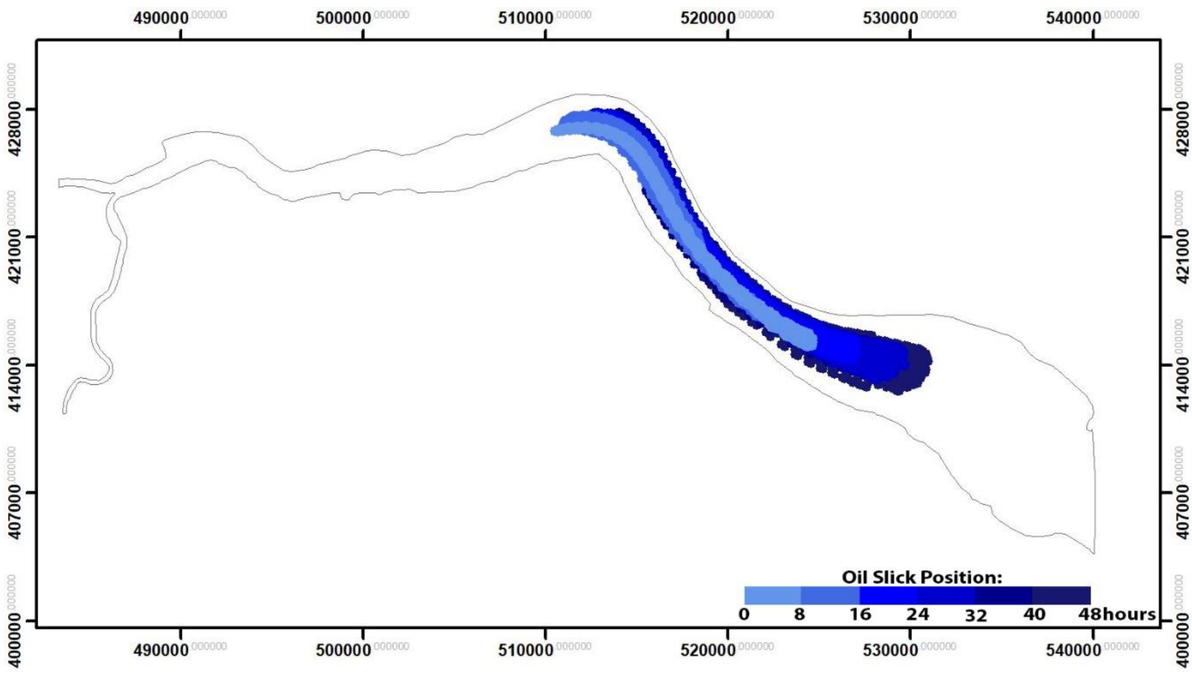

Figure 4.8: Simulated trajectories of oil released on the Humber Estuary at high water spring in winter with 2030 sea level.

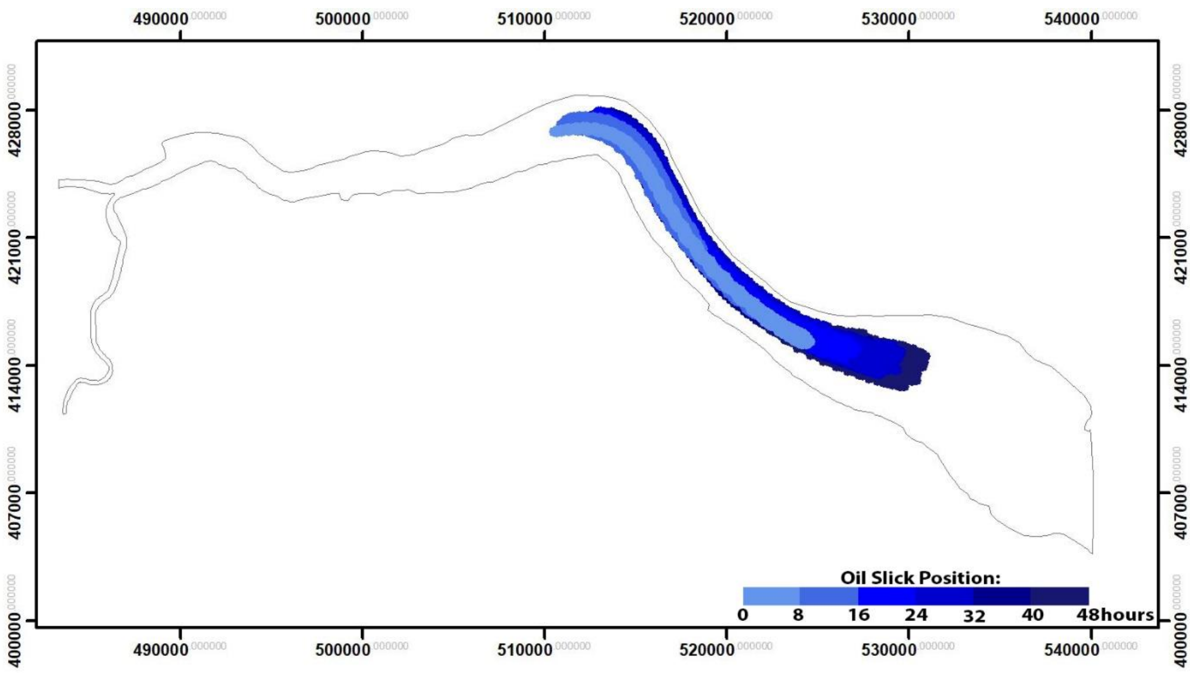

Figure 4.9: Simulated trajectories of oil released on the Humber Estuary at high water spring in winter with 2050 sea level.

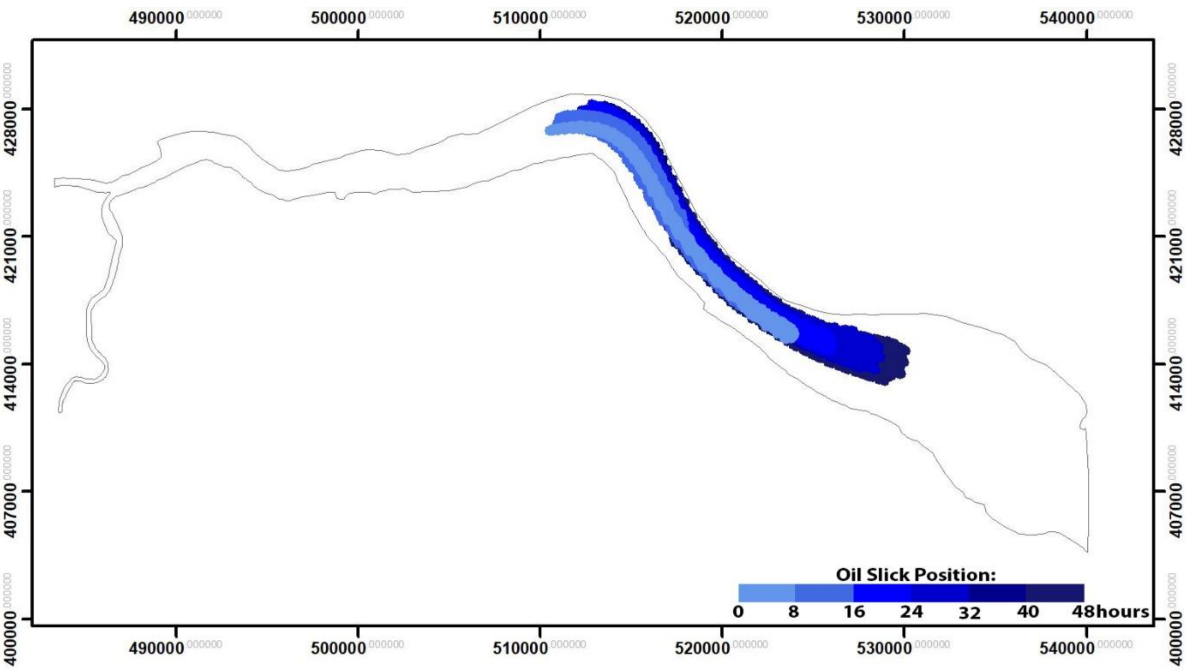

Figure 4.10: Simulated trajectories of oil released on the Humber Estuary at high water spring in winter with 2100 sea level.

Table 4.5: Simulated oil slick impacted area, A (sq. km) for different projected climate scenarios.

Scenarios	0 - 8h	8 - 16h	16 - 24h	24 - 32h	32 - 40h	40 - 48h
	A	A	A	A	A	A
Summer 2017	14.89	24.92	33.32	43.63	47.38	51.43
Summer SLR 2030	14.80	23.09	31.61	44.81	45.36	52.37
Summer SLR 2050	14.21	23.30	29.45	39.96	43.20	49.13
Summer SLR 2100	13.28	22.80	31.70	39.78	41.77	45.76

Winter 2010	13.69	22.19	29.01	38.64	38.76	46.37
Winter SLR 2030	13.17	22.82	29.74	41.42	43.57	53.48
Winter SLR 2050	11.49	20.66	27.19	36.69	40.33	46.81
Winter SLR 2100	13.35	20.74	29.09	38.86	39.29	46.45

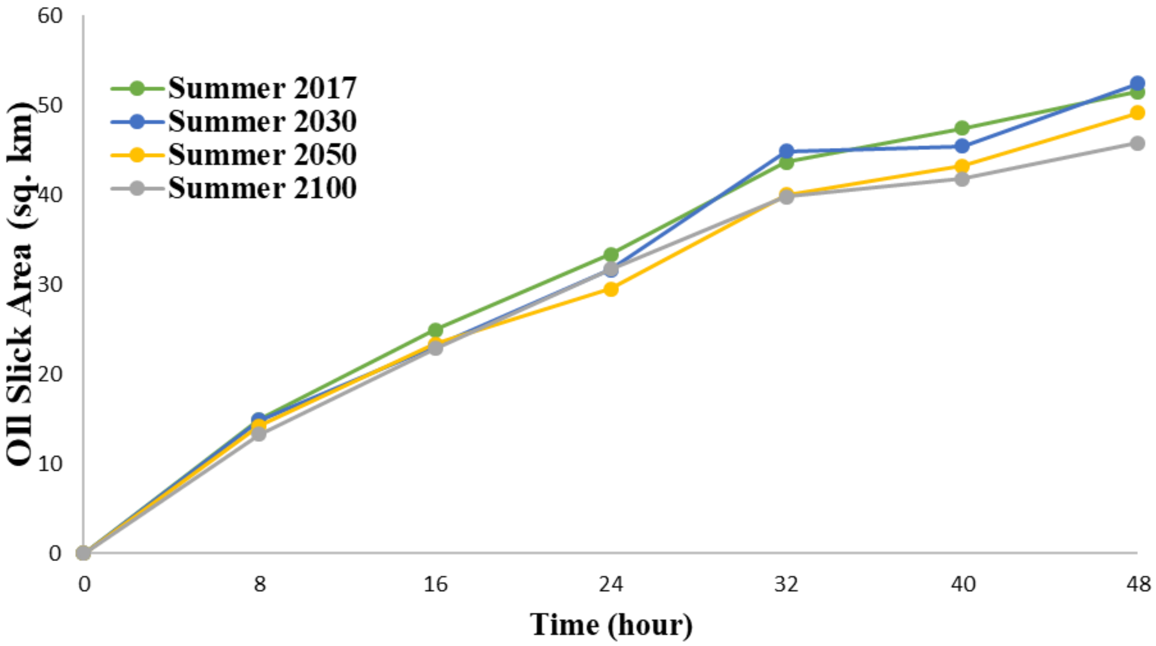

Figure 4.11: Area covered by simulated oil slicks over time for a spill at various summer sea levels.

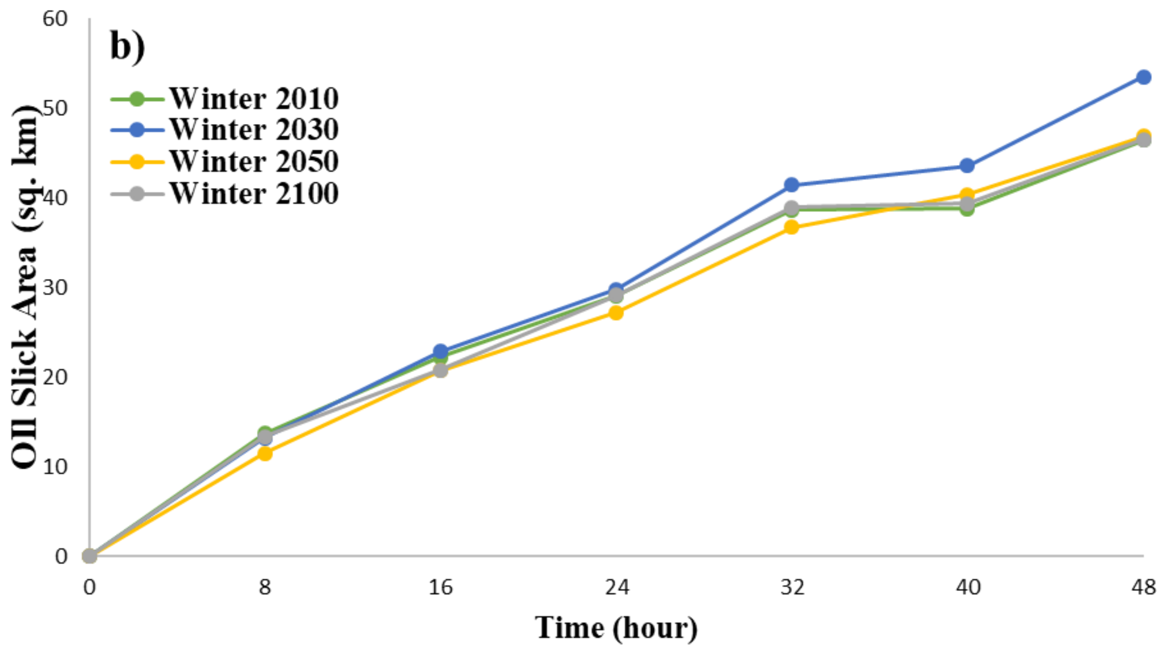

Figure 4.12: Area covered by simulated oil slick over time for a spill under various winter sea level

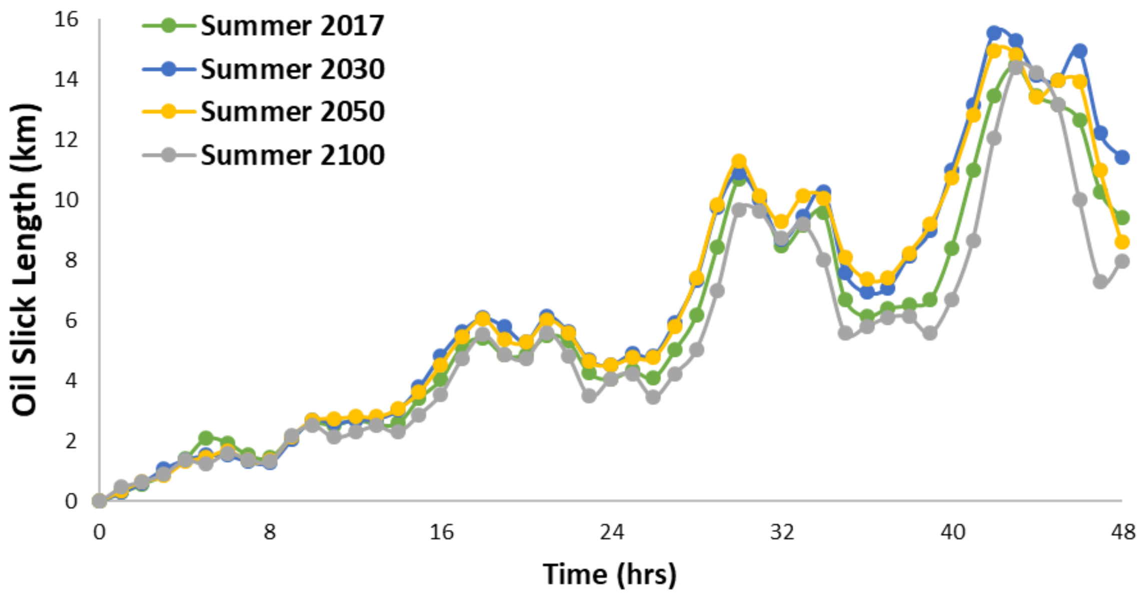

Figure 4.13: Simulated oil slick lengths over time for a spill under various summer sea levels.

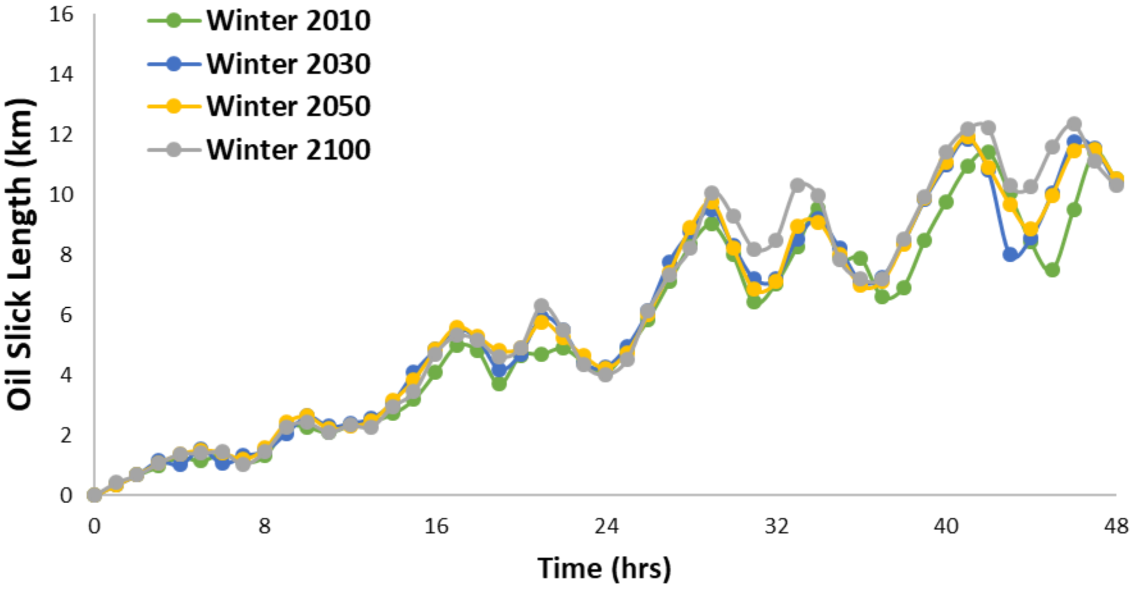

Figure 4.14: Simulated oil slick length over time for a spill under various winter sea level.

4.3.2 Projected River Flow Scenarios

The results for the 4 projected river flow scenarios are presented (Figure 4.15 – 4.18; Table 4.6). The results are discussed in the next section.

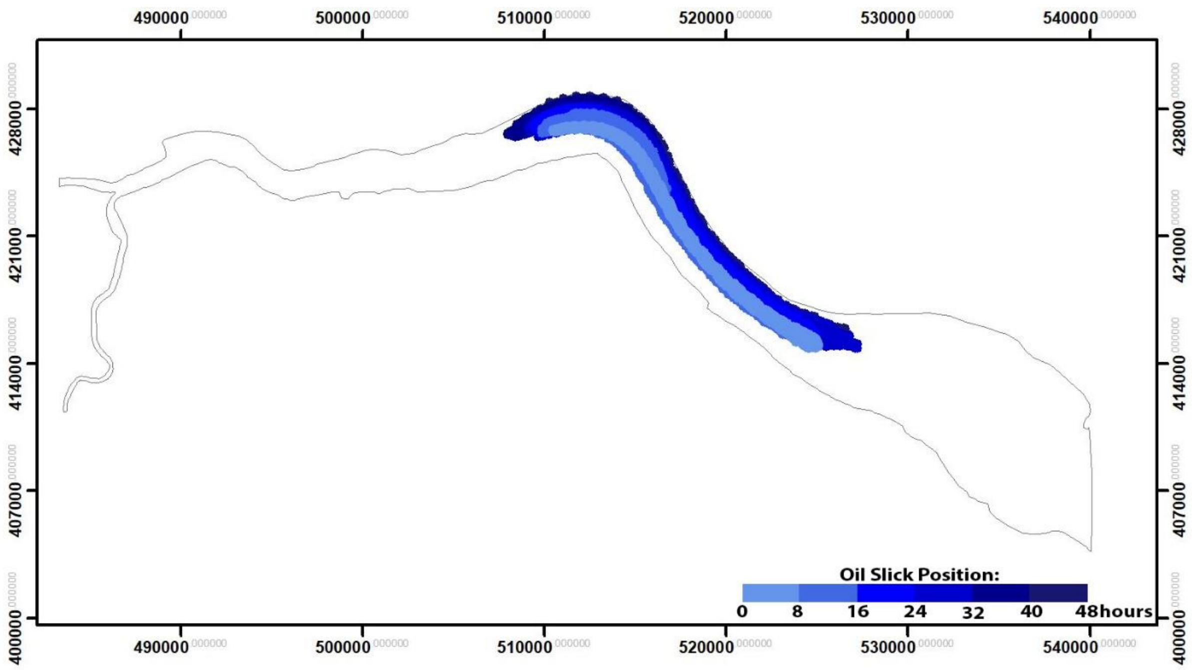

Figure 4.15: Simulated trajectories of oil released on the Humber Estuary at high water spring in summer with 2100 sea level and projected summer flow.

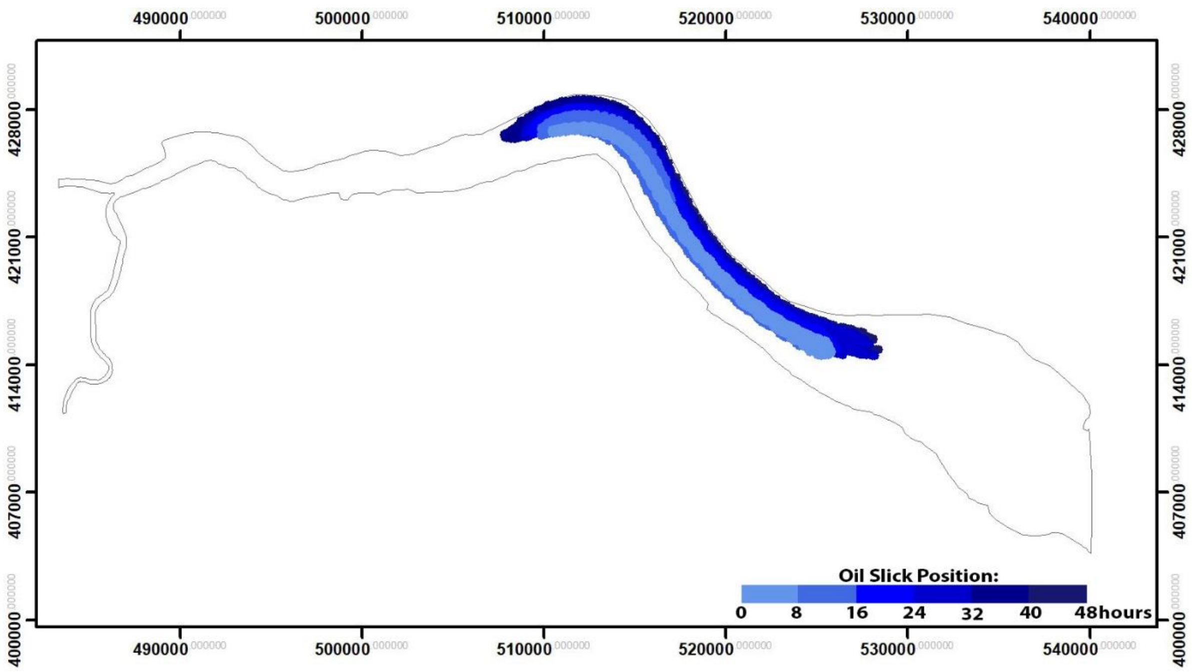

Figure 4.16: Simulated trajectories of oil released on the Humber Estuary at high water spring in summer with projected summer flow.

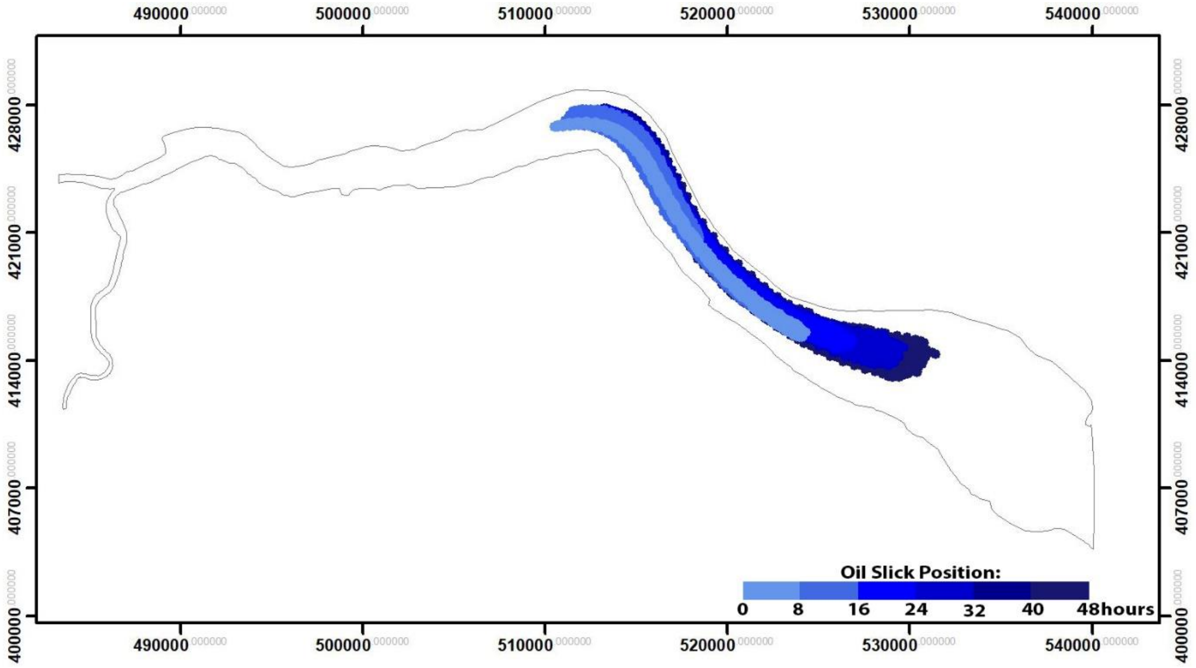

Figure 4.17: Simulated trajectories of oil released on the Humber Estuary at high water spring in winter with 2100 sea level and projected winter flow.

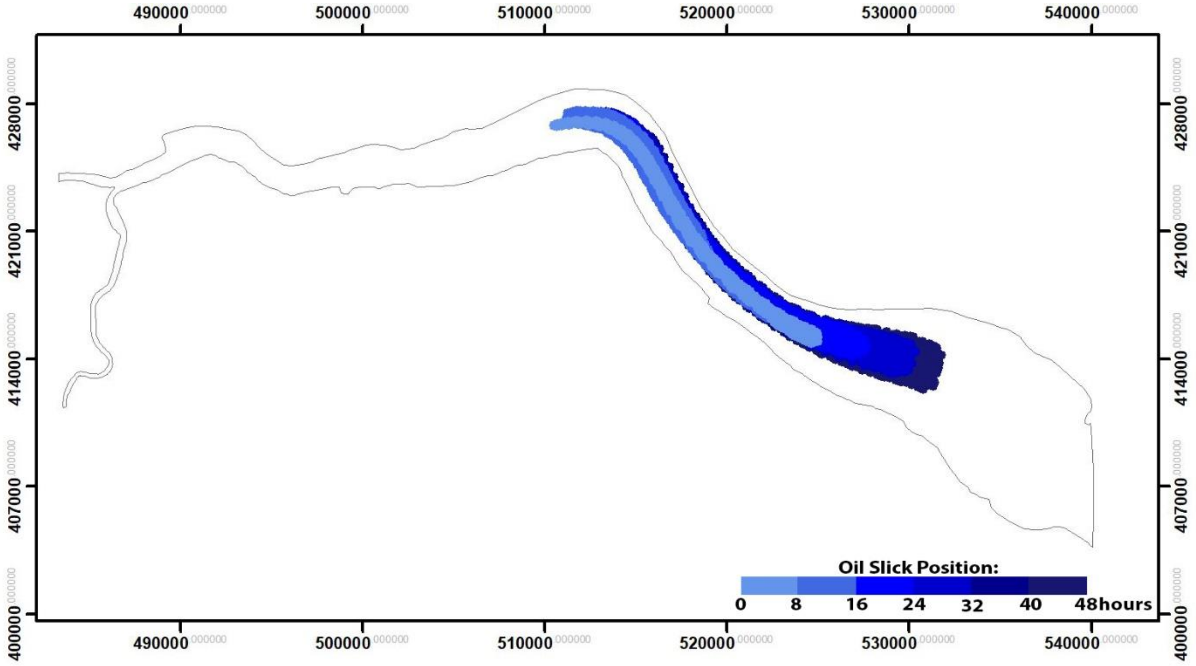

Figure 4.18: Simulated trajectories of oil released on the Humber Estuary at high water spring in winter with projected winter flow.

Table 4.6: Simulated oil slick impacted area, A (sq. km) for different projected climate scenarios.

Scenarios	0 - 8h	8 - 16h	16 - 24h	24 - 32h	32 - 40h	40 - 48h
	A	A	A	A	A	A
Summer (SLR + Flow) 2100	13.26	21.00	28.80	36.98	40.36	43.99
Summer Flow 2100	14.43	24.40	30.88	40.77	43.66	47.19
Winter (SLR + Flow) 2100	11.24	18.69	27.94	36.83	37.67	45.03
Winter Flow 2100	13.13	22.32	29.64	39.39	40.14	47.19

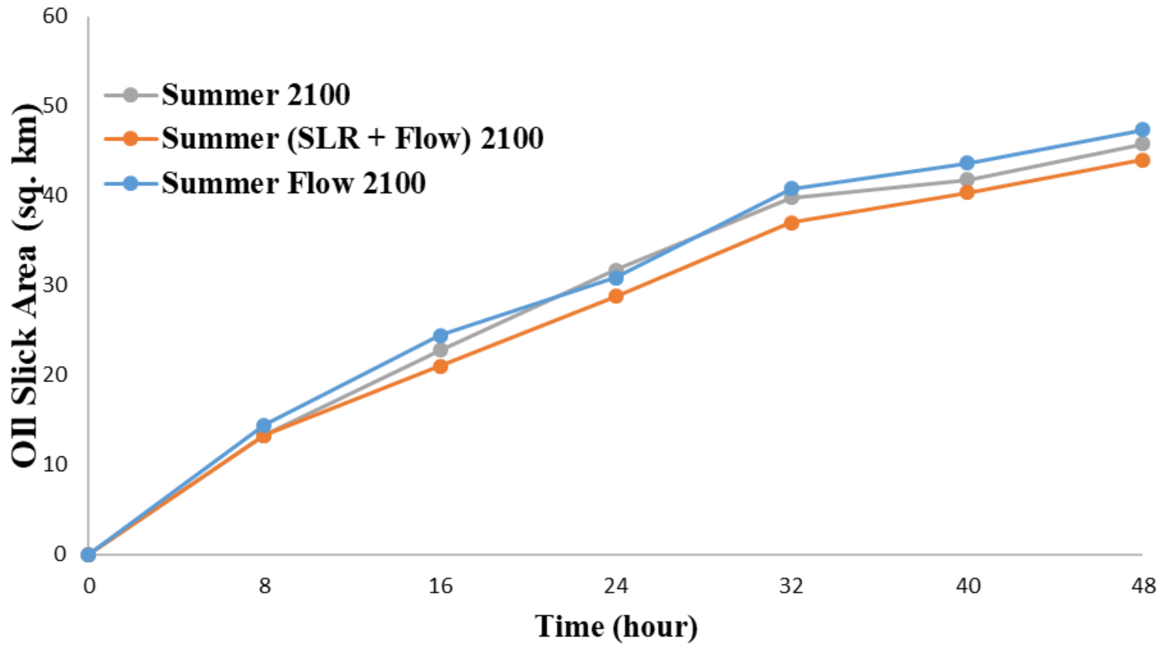

Figure 4.19: Area covered by simulated oil slick over time for a spill at various projected summer flow scenarios

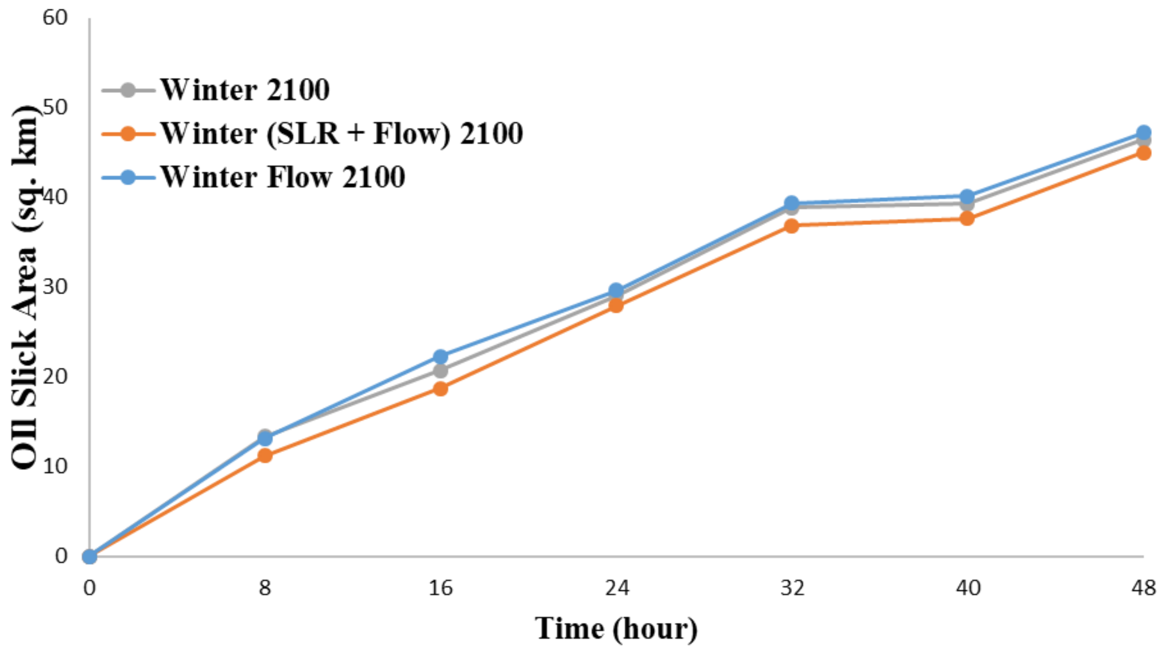

Figure 4.20: Area covered by simulated oil slick over time for a spill at various projected winter flow scenarios

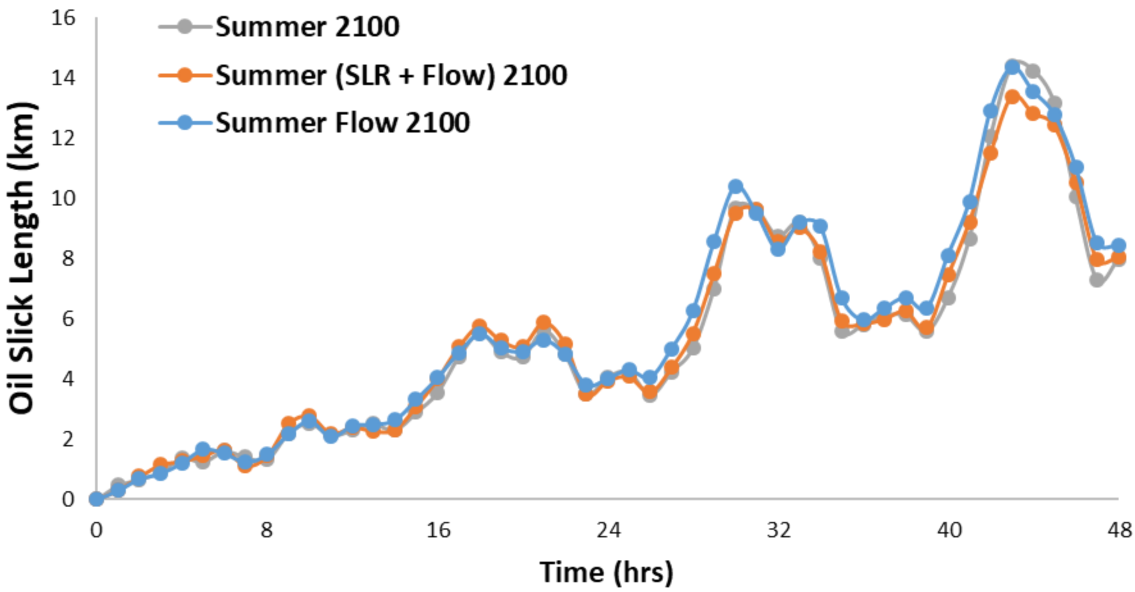

Figure 4.21: Simulated oil slick length over time for a spill under various projected summer flow scenarios

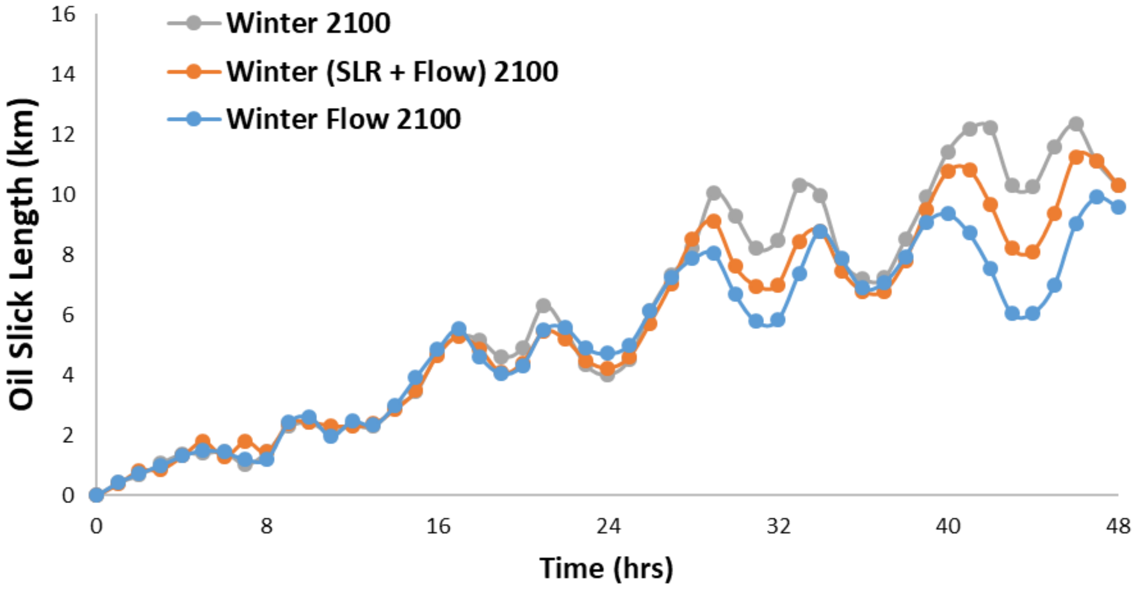

Figure 4.22: Simulated oil slick length over time for a spill under various projected winter flow scenarios

4.4 DISCUSSION

4.4.1 Impact of Sea Level Rise

The influence of sea level rise on oil slick transport was assessed. The influence of sea level rise on oil slick impacted area, length and distance travelled were analysed over the spill duration. Under summer conditions, maximum oil slick length was observed to peak at 2030 sea level spanning 15.55 km, slightly longer (8%) than the 2017 summer sea level scenario (Figure 4.13; Table 4.7). Under winter conditions, maximum oil slick length was observed to increase with sea level rise by an average of 5% by 2100 (Figure 4.14; Table 4.8). After 48 hours, the overall distance travelled by summer slicks peaked at 2030 sea level and by 2100 was about 3% less than the representative summer scenario (Table 4.7). While the overall distance travelled by winter slicks was an average of 2% less than the representative summer scenario by 2100 (Table 4.8). After 48 hours, the oil slick impacted area peaked at 2030 sea level by 2% and 15% in summer and winter respectively (Figure 4.11; 4.12). The impact of short term sea level rise is surprising, especially under winter conditions. This could possibly be due to the effect of sea level on tidal dynamics. Pelling et al. (2013) point out that the relationship between sea level and tidal dynamics can be non-linear. However, considering the overall influence of sea level rise on oil slick transport properties (Table 4.7; 4.8), it can be concluded that the influence of sea level rise on oil slick impacted area, length and overall distance travelled is relatively insignificant.

Table 4.7: Relative properties of comparable oil slicks released in summer 2030, 2050 and 2100 relative to summer 2017, as measured 48 hours after the spill.

Scenario	Impacted area ratio	Maximum length ratio	Distance ratio
Summer 2030	1.02	1.08	1.06
Summer 2050	0.96	1.03	1.06
Summer 2100	0.89	1.00	0.97
Average	0.96	1.04	1.03

Table 4.8: Relative properties of comparable oil slicks released in winter 2030, 2050 and 2100 relative to winter 2010, as measured 48 hours after the spill.

Scenario	Impacted area ratio	Maximum length ratio	Distance ratio
Winter 2030	1.15	1.04	0.99
Winter 2050	1.01	1.04	0.99
Winter 2100	1.00	1.08	0.96
Average	1.05	1.05	0.98

Although sea level does not significantly influence the area impacted by oil slick, oil slick length and distance travelled, the oil slick transport suggests that sea level influences upstream and downstream displacement to some degree (Figures 4.23; 4.24). Compared to summer slicks released under 2017 sea level, summer slicks released under 2030 and 2050 travelled further downstream, resulting in a displacement of 1.7 km and 1.6 km further downstream in 2030 and 2050 respectively (Figure 4.25 – 4.27). The difference in upstream displacement was negligible under 2030 and 2050 sea level respectively (Figures 4.25; 4.26; 4.27). Under 2100 sea level, summer slicks travelled further upstream (Figure 4.23). Compared to the 2017 summer scenario, downstream displacement was reduced by 1.3 km while summer slicks were displaced further upstream by 0.5 km (Figures 4.23; 4.28; Table 4.9). Summer slicks are expected to spread upstream over repeated tidal cycles, however, due to the time of release and relatively high river flow, there was no upstream displacement from the release point under winter conditions (Figures 4.29 – 4.32; Section 3.4.1). Downstream displacement of winter slicks was reduced by 0.2 km under 2030 and 2050 sea level and by 1.1 km under 2100 sea level (Figures 4.29 – 4.32). Results suggest that the influence of sea level rise on oil slicks displacement is influenced by seasonal variations. Under summer conditions, relatively short-term sea level rise (2030 and 2050) displaces oil slicks further downstream while long-term sea level rise displaces oil slicks further upstream (Figures 4.23; 4.24; Table 4.9). However, under winter conditions, oil slicks are displaced further upstream with sea level rise (Figures 4.23; 4.24; Table 4.9). A commonality in both seasons is the discouragement of downstream displacement by long-term sea level rise. This might be due to marine transgression, an effect on sea level rise on estuaries where the marine induced sedimentary environments and tidal limit moves upstream (Pye and Blott 2014).

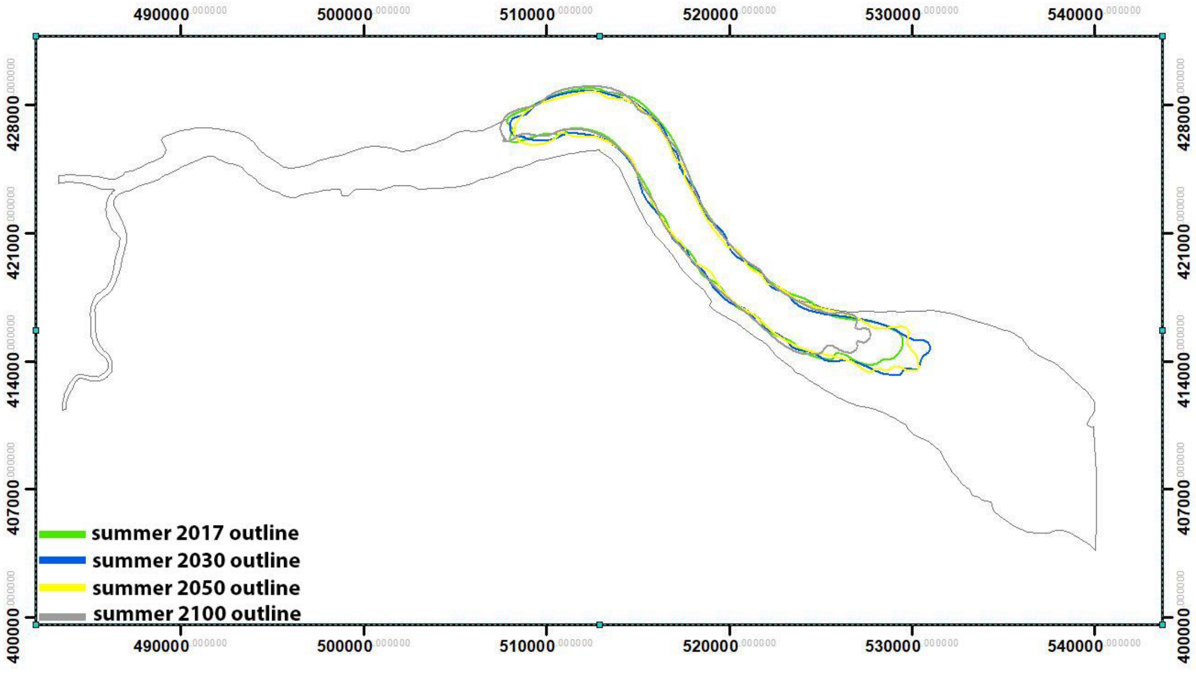

Figure 4.23: Outline of the area covered by oil slicks under different summer sea level scenarios

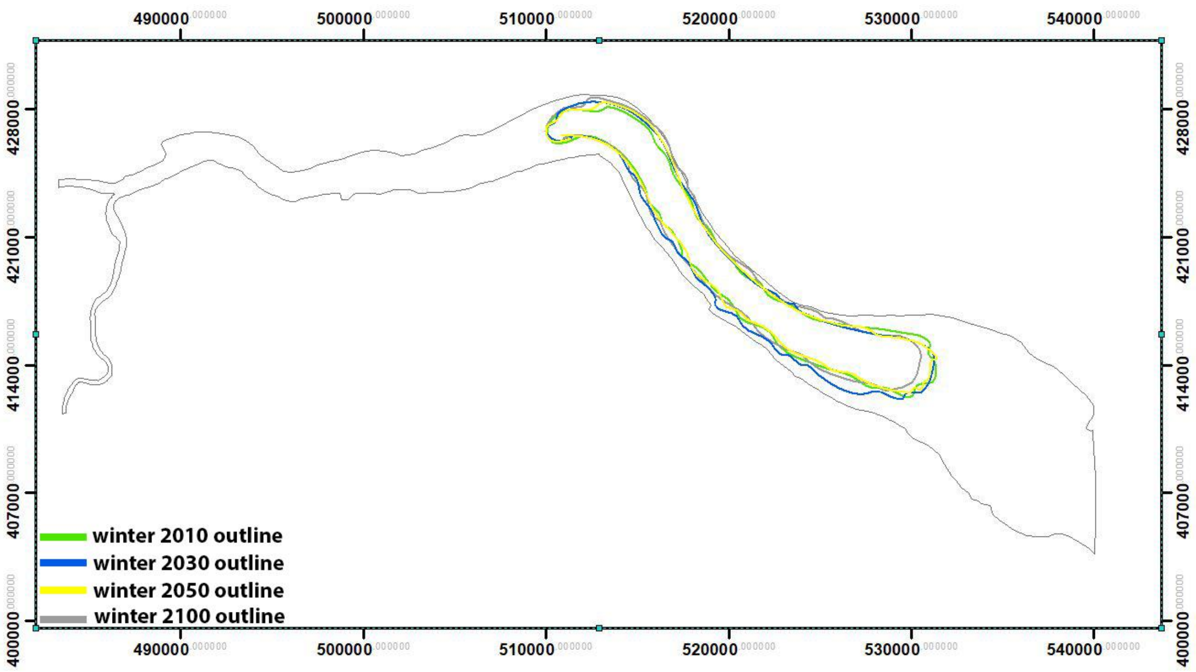

Figure 4.24: Outline of the area covered by oil slicks under different winter sea level scenarios

Table 4.9: Summary of maximum oil slick displacement (km) from point of release.

	upstream displacement (summer)	downstream displacement (summer)	upstream displacement (winter)	downstream displacement (winter)
Present-day	2.10	23.75	-	25.67
SLR 2030	2.06	25.42	-	25.47
SLR 2050	2.07	25.32	-	25.47
SLR 2100	2.56	22.45	-	24.59

SLR 2100 + Flow 2100	2.45	22.42	-	26.07
Flow 2100	2.73	23.61	-	26.35

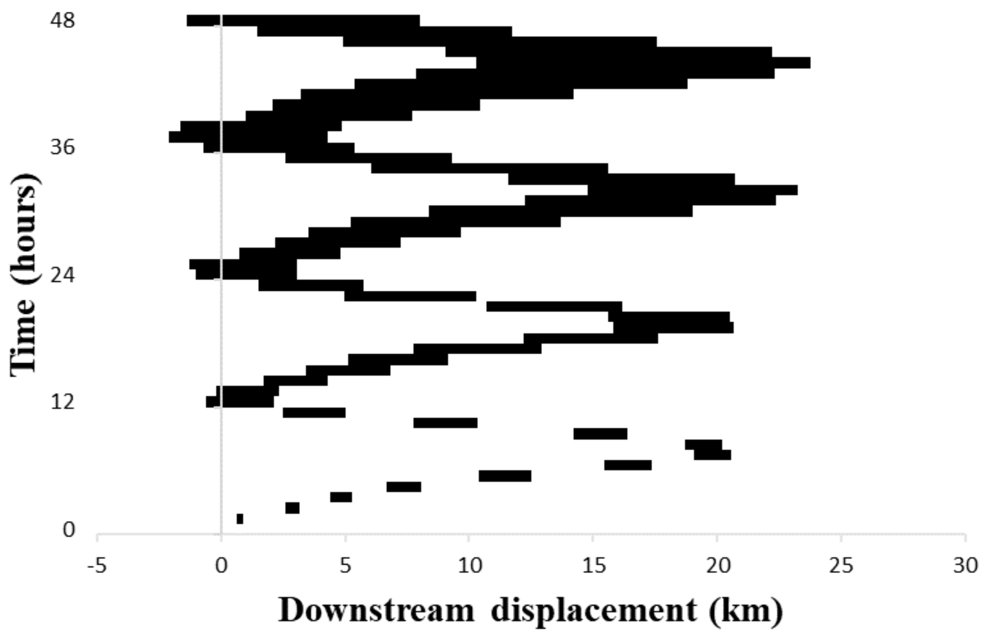

Figure 4.25: Longitudinal position and extent of oil slicks over time under summer 2017 scenario

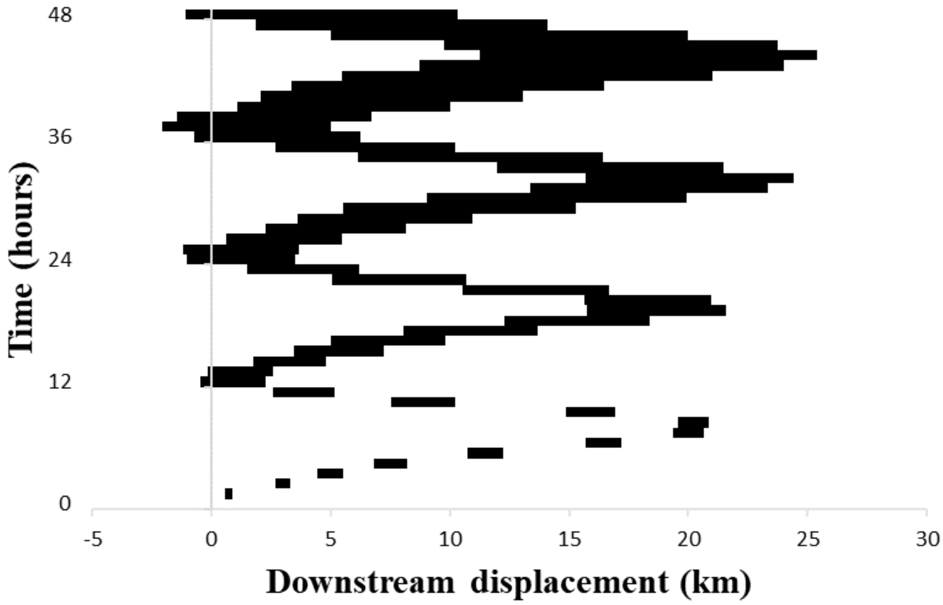

Figure 4.26: Longitudinal position and extent of oil slicks over time under summer 2030 scenario

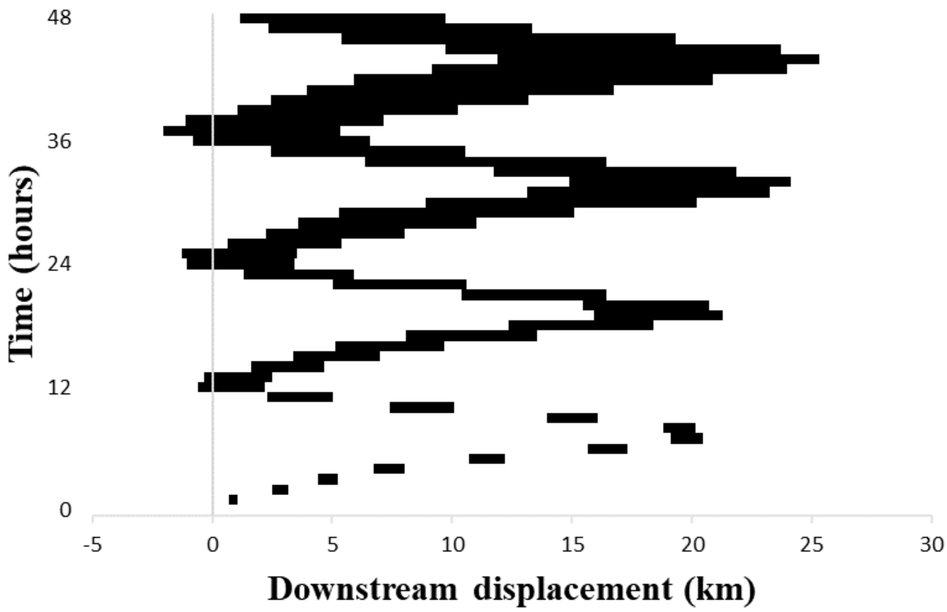

Figure 4.27: Longitudinal position and extent of oil slicks over time under summer 2050 scenario

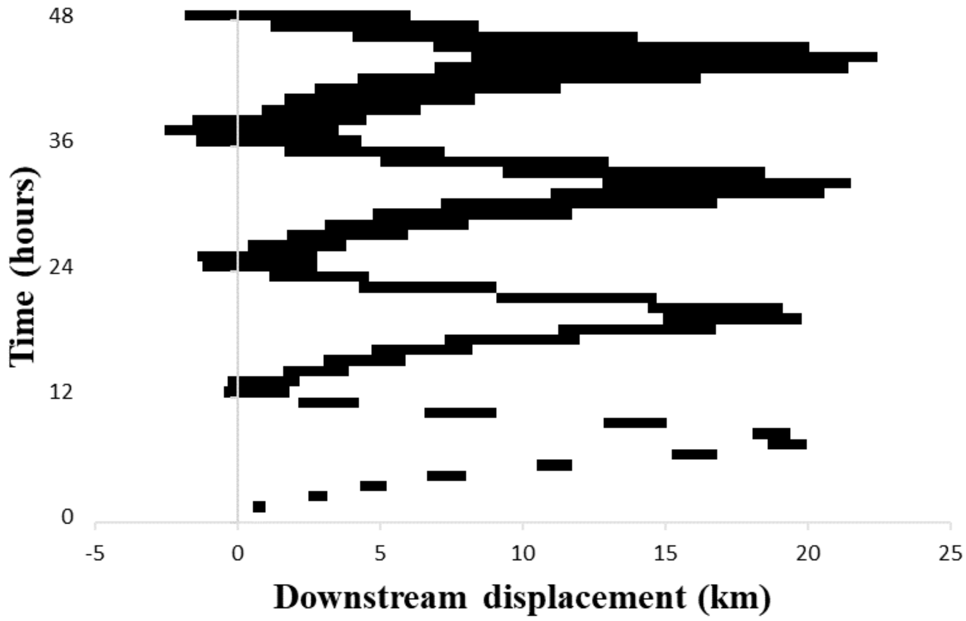

Figure 4.28: Longitudinal position and extent of oil slicks over time under summer 2100 scenario

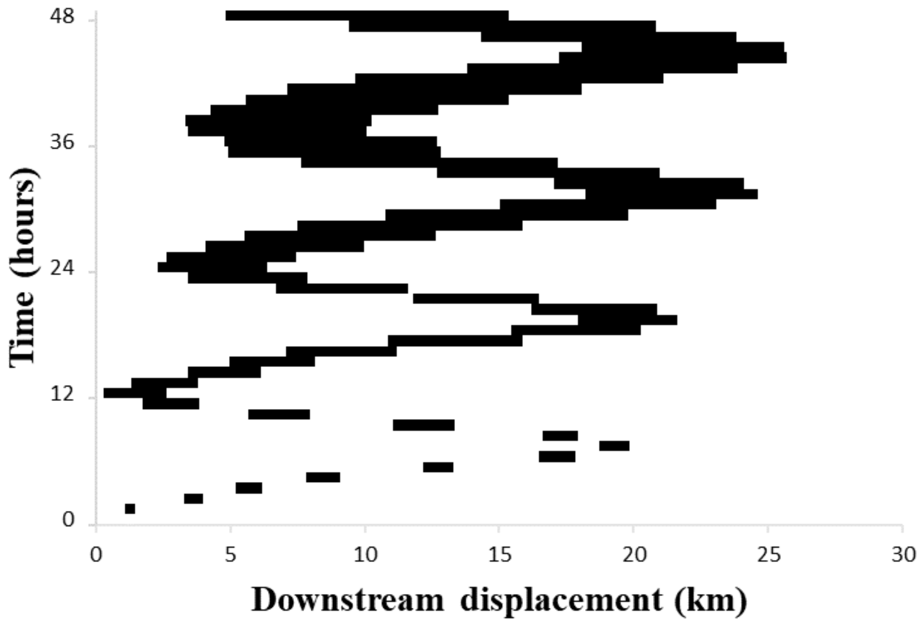

Figure 4.29: Longitudinal position and extent of oil slicks over time under winter 2010 scenario

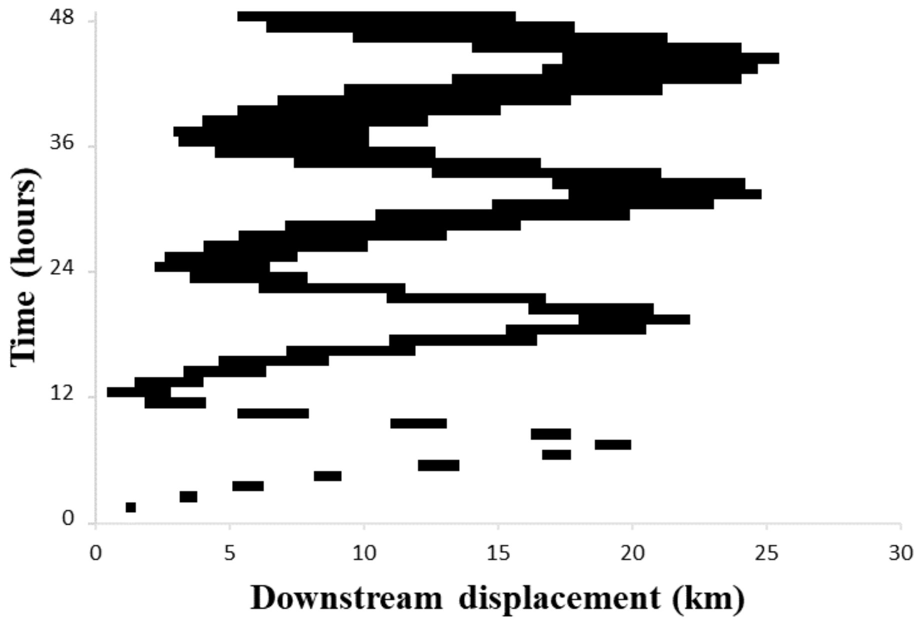

Figure 4.30: Longitudinal position and extent of oil slicks over time under winter 2030 scenario

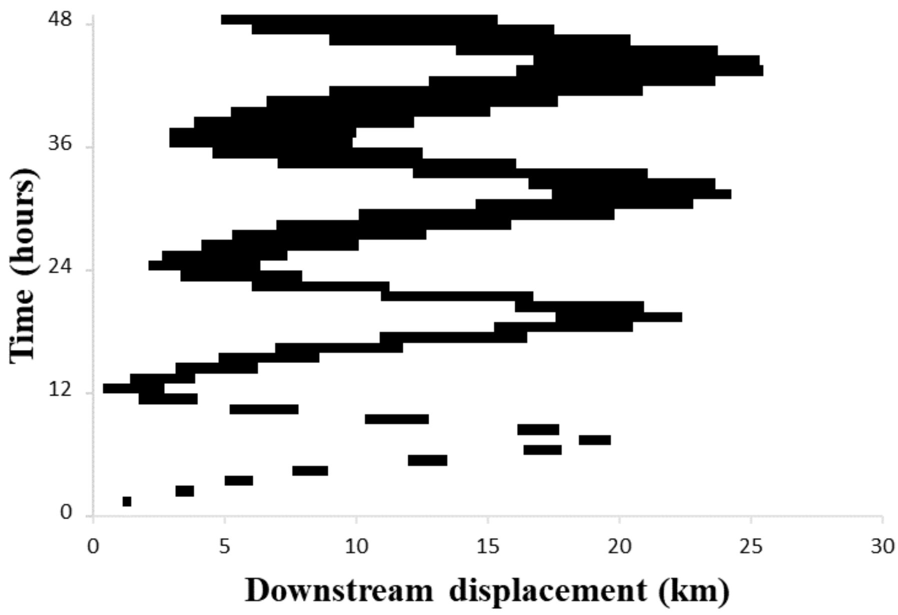

Figure 4.31: Longitudinal position and extent of oil slicks over time under winter 2050 scenario

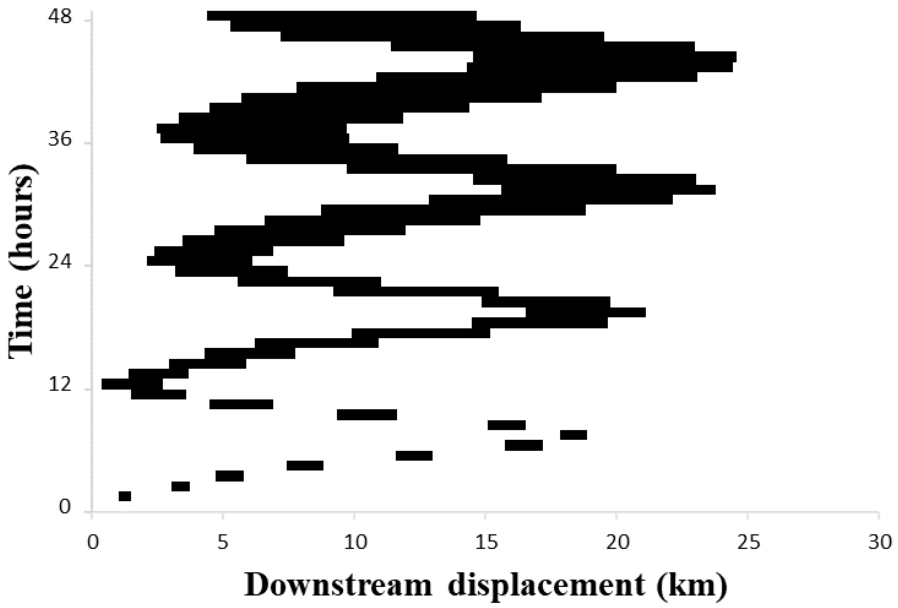

Figure 4.32: Longitudinal position and extent of oil slicks over time under winter 2100 scenario

4.4.2 Impact of Projected River Flow

The Humber Estuary is characterised by relatively low summer flows and relatively high winter flows. Alongside hotter drier summers and warmer wetter winters, river flows in the 21st century are projected to decrease in the summer and slightly increase in winter (Robins et al. 2016). It was observed that a decrease in river flow will encourage further upstream transport of summer slicks (Figure 4.33; Section 3.4.1). Considering summer conditions in the Humber Estuary, an 80% decrease in river flow led to oil slicks displacement of 0.6 km further upstream (Figure 4.34; Table 4.9). This was 0.2 km farther than when only sea level rise at 2100 was considered and also 0.3 km further than summer slicks released under a combination of decrease in river flow and 2100 sea level (Figure 4.35). Surprisingly, the summer (SLR + Flow) 2100 scenario (Figure 4.33; 4.35), exhibited less upstream displacement compared to under projected river flow (Table 4.9). This could possibly be due to the effect that combined sea level rise and decrease in river flow have on tidal asymmetry in the estuary. Decreases in river flow, sea level rise or a combination of both, restricted downstream displacement of summer slicks while resulting in an upstream transport of the entire oil slick (Table 4.7). Considering the upstream and downstream displacement, we now know that sea level rise acts as a mitigating factor on the effect of projected river flow on the spreading of summer slicks.

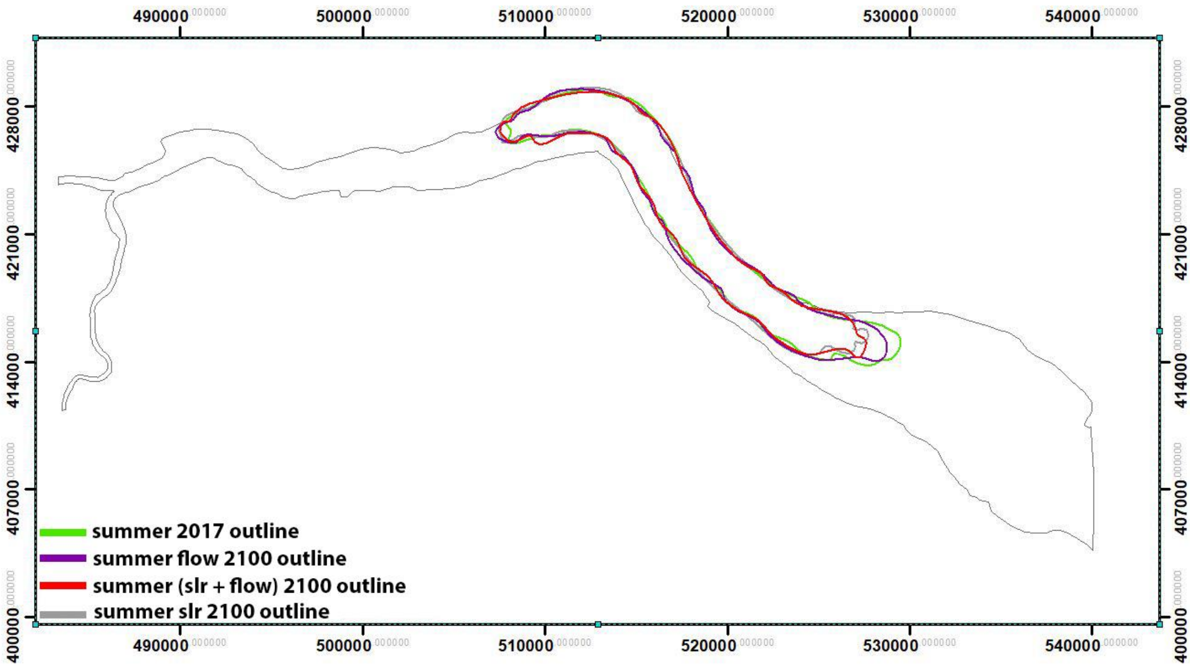

Figure 4.33: Outline of the area covered by oil slicks under projected summer flow scenarios

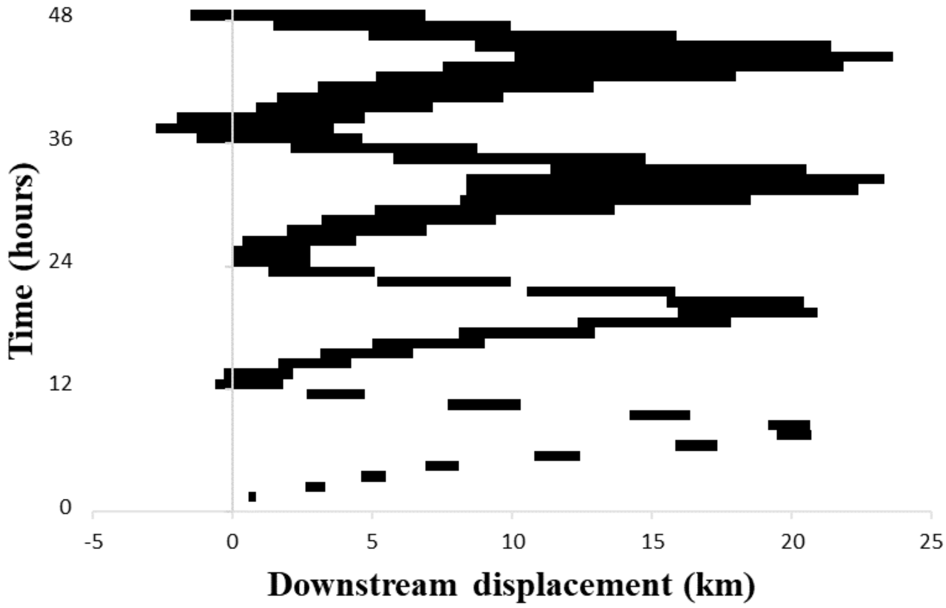

Figure 4.34: Longitudinal position and extent of oil slicks over time under projected summer flow

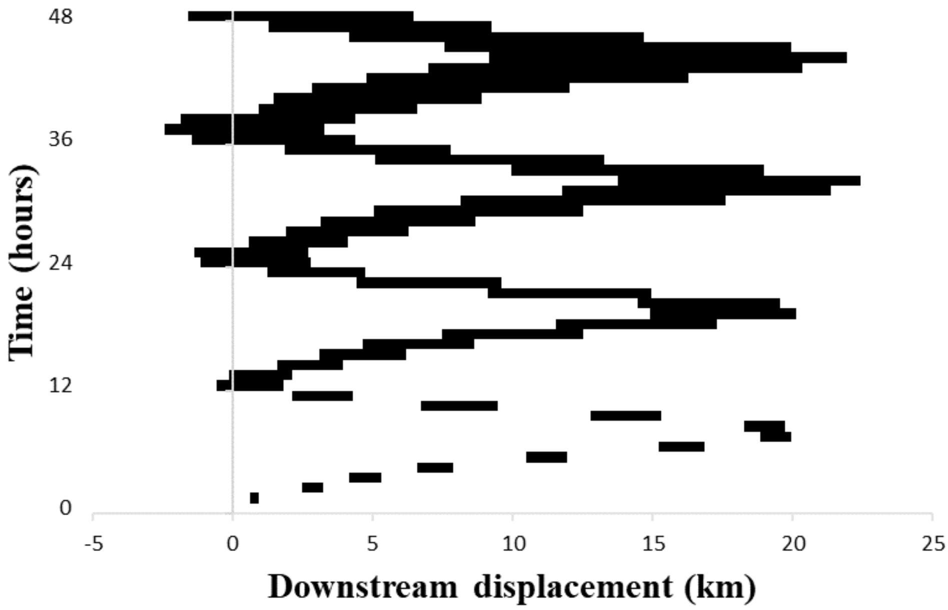

Figure 4.35: Longitudinal position and extent of oil slicks over time under projected summer flow with 2100 sea level

Under winter conditions, after 48 hours, 25% increase in river flows displaced oil slicks by 0.7 km further downstream (Figures 4.36; 4.37) while in the 2100 sea level scenario, downstream displacement of oil slick was reduced by 1.08 km (Table 4.9). However, the combination of increased river flow and sea level rise (SLR + Flow) displaced oil slicks by 0.4 km further downstream (Figure 4.38). Results suggest that while increased winter flow will increase the downstream displacement of oil slicks, sea level rise acts as a mitigating factor. In both seasons, overall distance travelled by oil slicks were greater solely based on flow variability; by about 2% and 4% in summer and winter respectively (Tables 4.10; 4.11). Overall distance was reduced when sea level rise was taken into account. Projected river flows have different effect on the area covered by summer and winter slicks. After 48 hours, the area covered by summer slicks is reduced by 8% while the area covered by winter slicks is increased by 2% (Tables 4.10; 4.11). However, the combination of projected sea level and river flow will reduce the area covered by both summer and winter slicks as well as the maximum oil slick length in both seasons (Tables 4.10; 4.11). Results suggest that projected river flow has a relatively insignificant impact on oil slick impacted area, length and overall distance travelled.

Table 4.10: Relative properties of comparable oil slicks released under summer projected river flow and projected river flow with 2100 sea level relative to summer 2017, as measured 48 hours after the spill.

Scenario	Impacted area ratio	Maximum length ratio	Distance ratio
Summer (SLR + Flow) 2100	0.86	0.93	0.96

Summer Flow 2100	0.92	0.99	1.02

Table 4.11: Relative properties of comparable oil slicks released under winter projected river flow and projected river flow with 2100 sea level relative to winter 2010, as measured 48 hours after the spill.

Scenario	Impacted area ratio	Maximum length ratio	Distance ratio
Winter (SLR + Flow) 2100	0.97	0.99	1.03
Winter Flow 2100	1.02	0.87	1.04

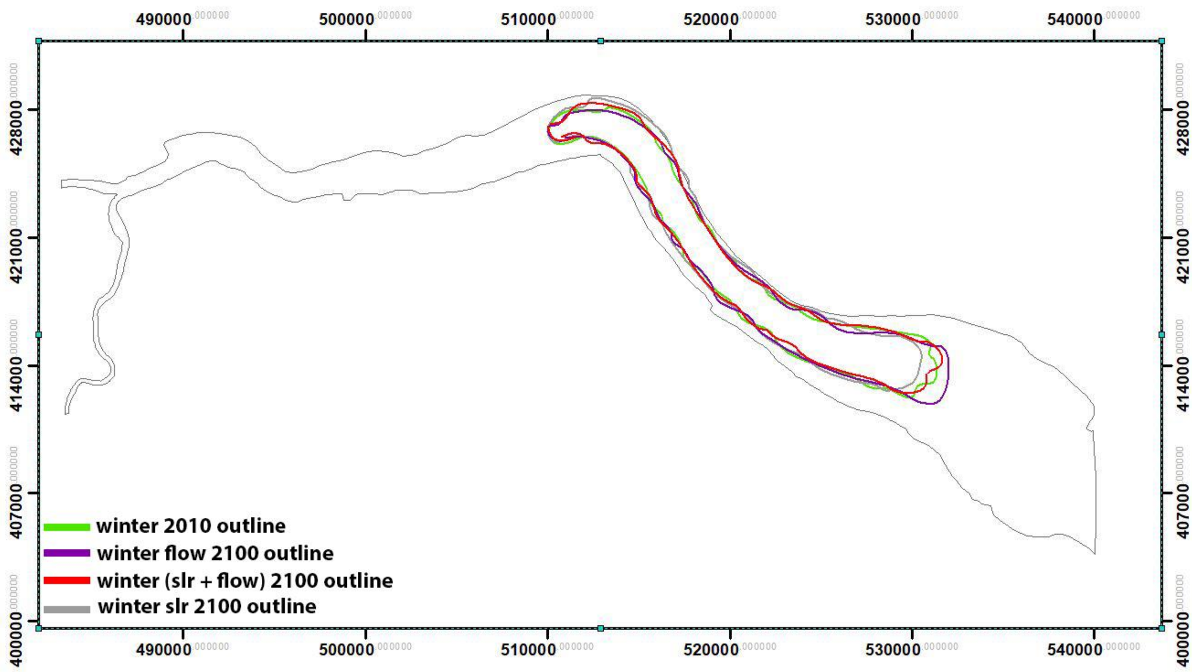

Figure 4.36: Outline of the area covered by oil slicks under projected winter flow scenarios

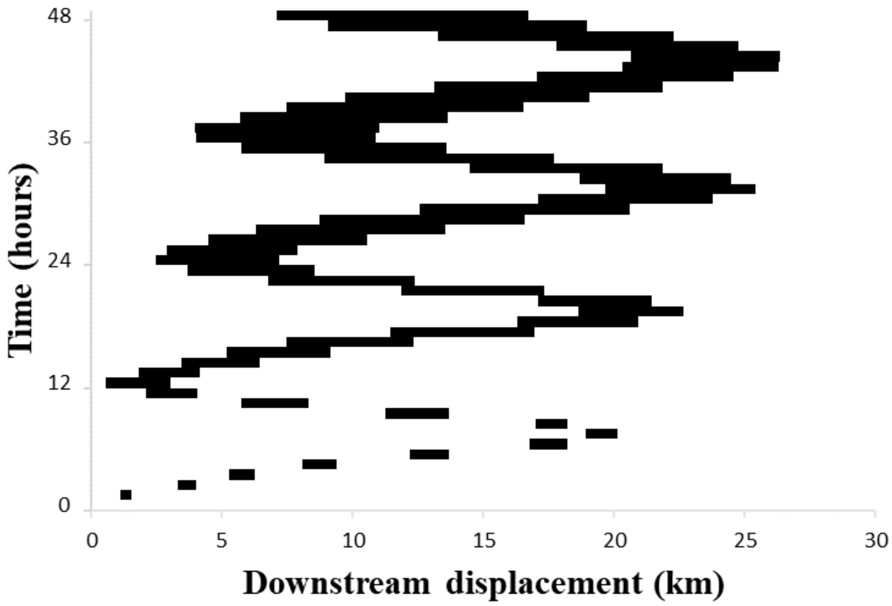

Figure 4.37: Longitudinal position and extent of oil slicks over time under projected winter flow

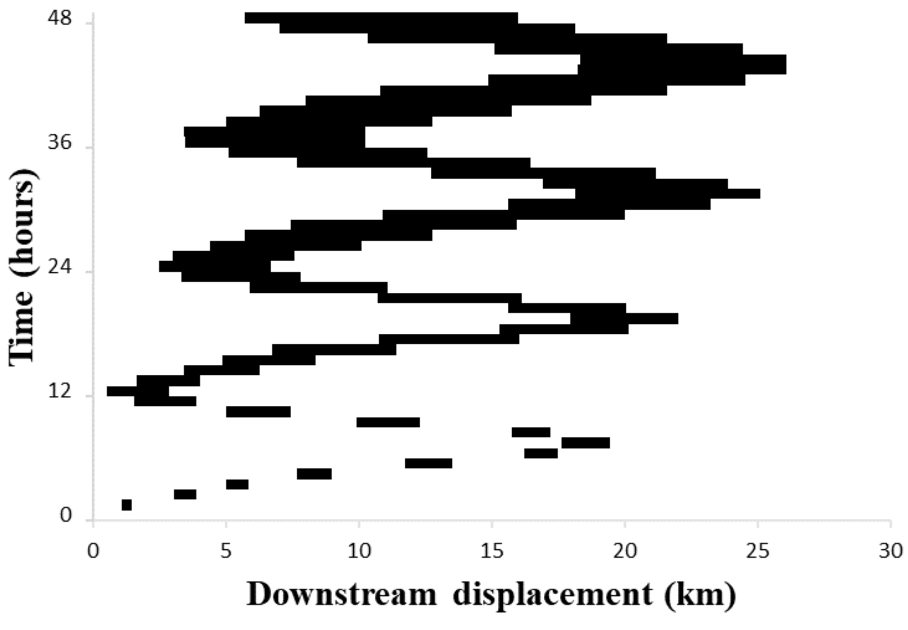

Figure 4.38: Longitudinal position and extent of oil slicks over time under projected winter flow with 2100 sea level

4.5 LIMITATIONS

Projected climatic conditions will drive changes in sea level, river discharge, wave conditions and storm surges (Ranasinghe et al. 2012; Robins et al. 2014). However, this study only considered projected sea level rise and river discharge on oil spill transport. Consequently, the findings in this chapter may not be suitable to understand the influence of storm surges and flooding on oil spill transport. The influence of flooding and storm events on oil slick transport can also be explored in future studies.

4.6 CONCLUSION

The impact of projected climatic conditions, particularly projected sea level and river flow on oil spills in an estuarine environment presents a gap in academic literature. To address this gap, for the first time, a range of numerical simulations was developed to understand the impact of sea level rise and projected river flows on oil spill transport. These novel simulations show that:

(a) the influence of sea level rise on oil slick impacted area, length and overall distance travelled is relatively insignificant;

(b) under summer conditions, long-term sea level rise (2100) transports the entire oil slick further upstream, thus encouraging upstream displacement and discouraging downstream displacement;

(c) under winter conditions, long-term sea level rise (2100) discourages further downstream displacement of oil sick;

(d) the influence of short-term sea level rise on oil slick displacement varies from the influence of long-term sea level rise under summer conditions. This could possibly be due to the effect of sea level on tidal dynamics. However, the influence of sea level rise on oil slick displacement is consistent under winter conditions, suggesting that the influence of sea level rise on oil slicks displacement is influenced by seasonal variations;

(e) projected changes in river discharge have relatively insignificant influence on oil slick impacted area, length and overall distance travelled;

(f) an 80% decrease in summer river flow led to oil slicks displacement of 0.6 km further upstream and reduced downstream displacement by 0.14 km;

(g) a 25% increase in winter river flows led to oil slicks displacement of 0.68 km further downstream;

(h) considering sea level rise and projected river flow (SLR + Flow) scenario, oil slicks were further displaced upstream by 0.35 km and downstream displacement was reduced by 1.33 km in summer while winter slicks were further displaced upstream by 0.4 km. In comparison to the projected flow scenarios, long-term sea level rise mitigates the impact of projected river flow on oil slick spreading.

These findings suggest that the overall impact of sea level rise and changes in river discharge is rather limited. Further studies can be undertaken to understand how flooding and storm events will influence oil slick transport in an estuarine environment.

Considering the choice of arbitrary oil spill release points in Chapter Chapters 3 and 4, the next Chapter 5 assesses the influence of varying lateral points of release on oil slick transport employing the hydrodynamic model developed in Chapter 3 (Figure 1.2). Findings made in this chapter will help responders understand how the results in the Chapter 3 and 4 may be influenced by oil release location.

CHAPTER 5

5. SENSITIVITY ANALYSIS OF OIL RELEASE LOCATION IN A LARGE MACRO-TIDAL ESTUARY

Previous chapters have established that the understanding of oil slick transport in estuarine environment presents a gap in academic knowledge. These chapters have employed simulations using arbitrary oil release locations to successfully understand the relative influence of advection mechanisms, seasonal freshwater discharge variations, sea level rise and projected river flows on oil spill transport in tide-dominated estuaries. Consequently, this chapter assesses the influence of varying lateral oil release locations on oil slick transport in this environment. Consequently, this chapter addresses this gap, thereby fulfilling research objective 4 (Section 1.2.1). Findings made in this chapter will help responders understand how the results in the previous chapters may be influenced by oil release location.

5.1 BACKGROUND

Oil significantly contributes to economic development, as a result, there is a continuous increase in the demand for crude oil and its derivatives (Wang et al. 2005; Chen et al. 2019). The production and transportation of crude and refined oil inevitably and undesirably leads to oil spills (Berry et al. 2012), making it a major contributor to marine pollution (Cheng et al. 2011; Kang et al. 2016). Consequently, oil spill models have been employed to predict the direction of oil travel, the time of arrival and its state upon arrival (Berry et al. 2012). The impact of oil spills have driven numerous studies, thus one can argue that much is known about the factors that influence oil spill transport and weathering (ASCE 1996; Reed et al. 1999; Spaulding 2017; Section 2.2; 2.3).

However, many aspects of oil complex behaviour are yet to be satisfactorily clarified (Guo et al. 2018). Considering the unpredictability of oil spills (Vethamony et al. 2007; Li et al. 2018) and the risks they present to estuaries, it is critical to understand the influence of lateral oil release locations on oil slick transport. This chapter presents the first detailed sensitivity analysis of lateral oil release location to ascertain its influence on oil slick transport in an estuarine environment.

5.2 EXPERIMENTAL DESIGN

The calibrated hydrodynamic model developed for the representative summer month (August 2017) (Table 3.7; Section 3.3.1) was employed to assess the influence of lateral oil release location on oil slick transport. Each scenario simulates an instantaneous oil release from one of 10 locations; 5 release locations placed upstream and downstream (Figure 5.1; Table 5.1). Oil slick release locations along L1 (L1_a; L1_b; L1_c; L1_d; and L1_e) and L2 (L2_a; L2_b; L2_c; L2_d; and L2_e) were situated 1,000 m and 350 m apart respectively. The difference in spacing was due to the funnel-shaped configuration of the estuary; a wide mouth of approximately 8 km that narrows to less than 0.5 km at the Ouse-Trent confluence (Fujii 2007). The oil was released under spring tidal conditions, during both high and low tide with reference to the release locations (Table 5.2). Spring tidal condition was chosen because it presents greater oil slick impacted area and distance travelled (Section 3.4.2). Each scenario simulates an instantaneous release of 10,000 m^3 of Brent Crude (Table 3.1), and the resulting simulated oil slick is monitored for a 48-hour period (over two semi-diurnal tidal cycles). Visualisation of the oil slick transport and measurement of its associated parameters (the oil slick impacted area on water surface, length of the oil slick over time and overall distance travelled) was done within ArcMap 10.5.1 (Section 3.2.6;

Figure 3.20). Here, oil beaching is defined as when oil interacts with the edge of the computational grid.

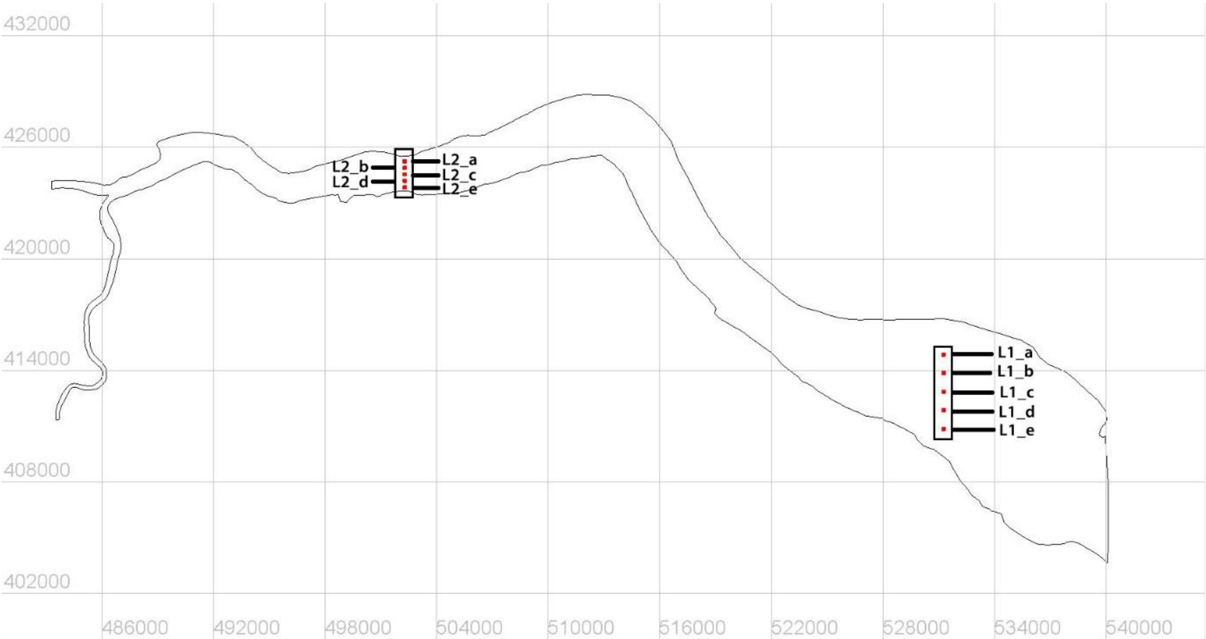

Figure 5.1: Outline for computational domain showing release location (red dots) for oil spill scenarios

Table 5.1: Coordinates (in OSGB 1936) for oil release location.

Oil release location	**Coordinates**
L1_a	531241.813; 414822.406
L1_b	531241.813; 413822.406
L1_c	531241.813; 412822.406
L1_d	531241.813; 411822.406
L1_e	531241.813; 410822.406
L2_a	502264.531; 425223.934
L2_b	502264.531; 424873.934

L2_c	502264.531; 424523.934
L2_d	502264.531; 424173.934
L2_e	502264.531; 423823.934

Table 5.2: Summary of the oil slick release scenarios (tidal stage is with reference to release location).

Scenario	**Oil release time**
L1 HW ST	08/08/2017 (18:00)
L1 LW ST	08/02/2010 (13:00)
L2 HW ST	08/08/2017 (18:00)
L2 LW ST	08/02/2010 (14:00)

Note: L1, L2 = release points; HW = high water; LW = low water; ST = spring tide.

5.3 RESULTS

Although governed by the same back and forth motions of flood and ebb currents, oil slicks exhibited different trend from the various release locations (Figure 5.2 – 5.21; Table 5.3). The results are discussed in detail in the next section.

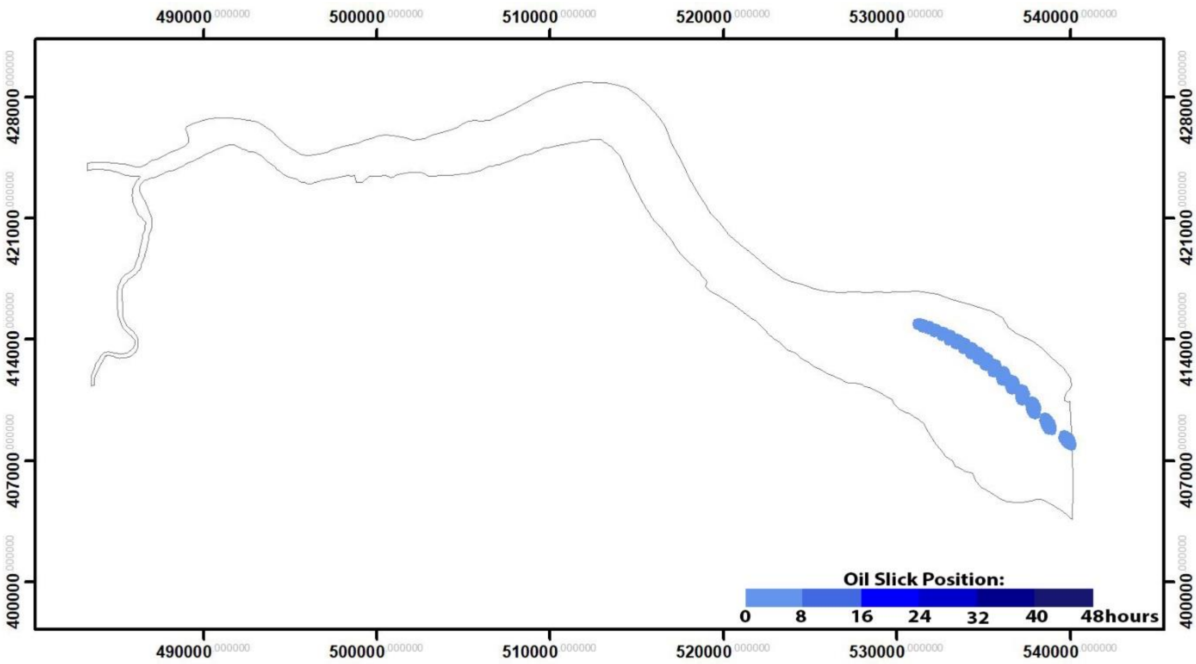

Figure 5.2: Trajectories of oil released on the Humber Estuary at L1_a at high water during a spring tide

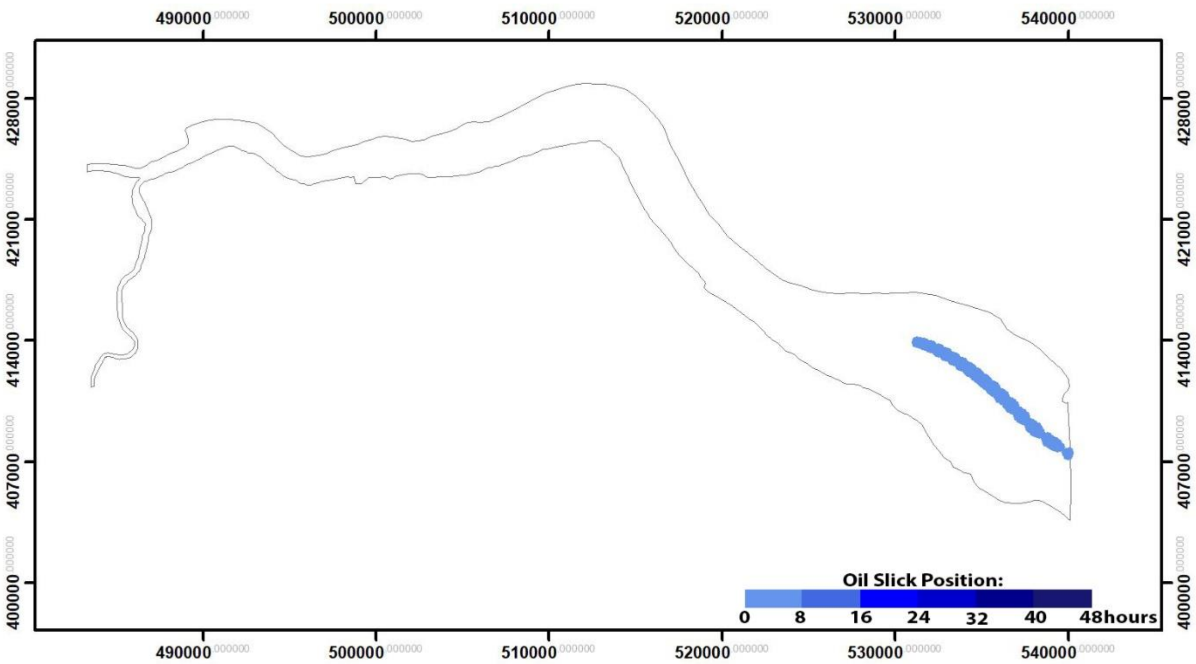

Figure 5.3: Trajectories of oil released on the Humber Estuary at L1_b at high water during a spring tide

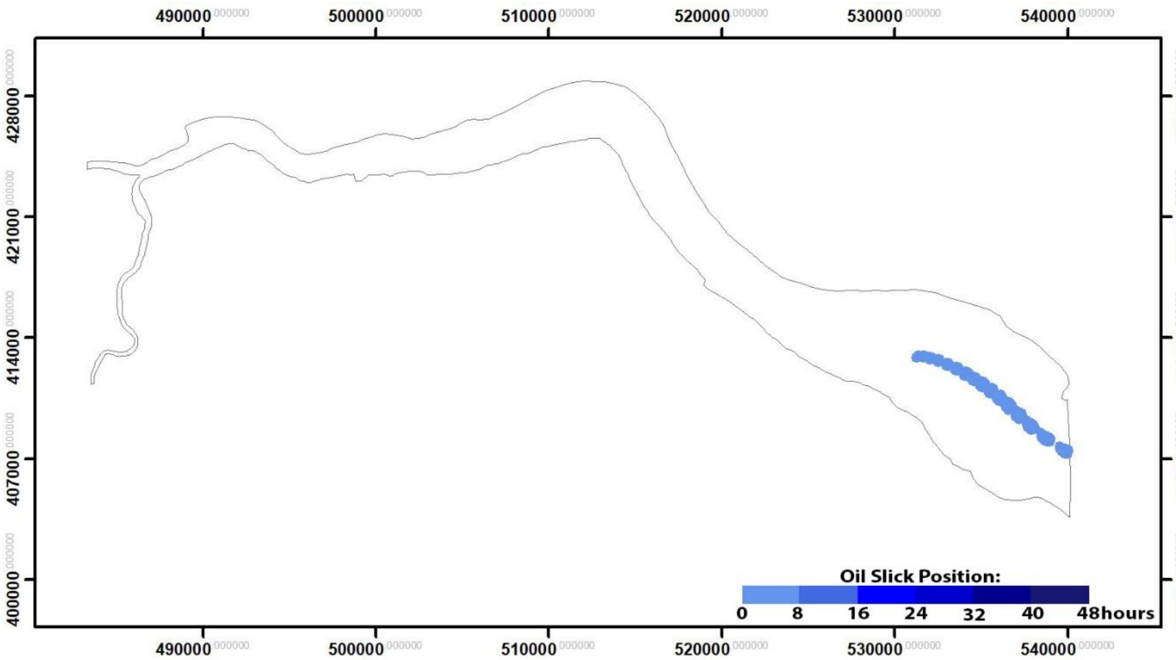

Figure 5.4: Trajectories of oil released on the Humber Estuary at L1_c at high water during a spring tide

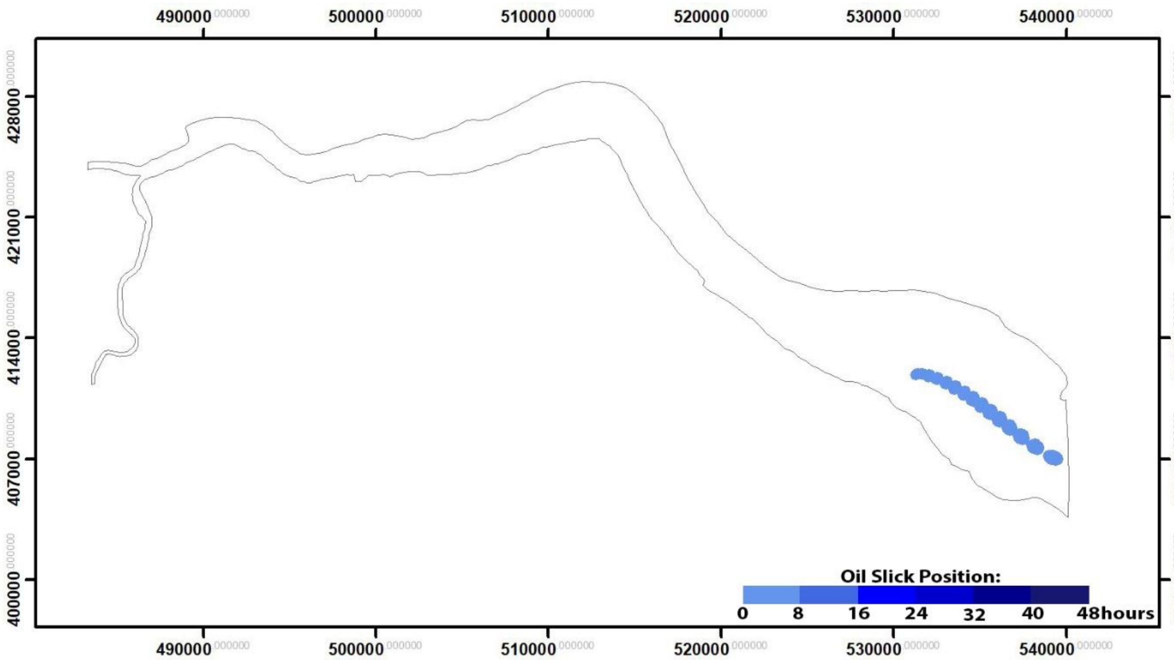

Figure 5.5: Trajectories of oil released on the Humber Estuary at L1_d at high water during a spring tide

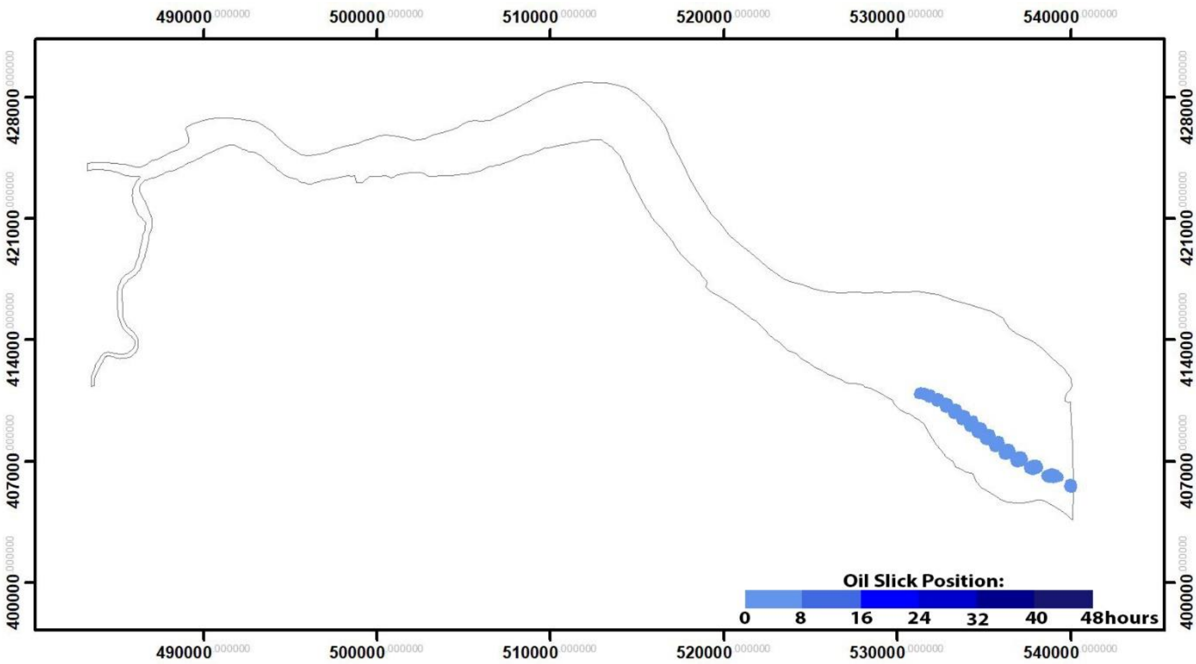

Figure 5.6: Trajectories of oil released on the Humber Estuary at L1_e at high water during a spring tide

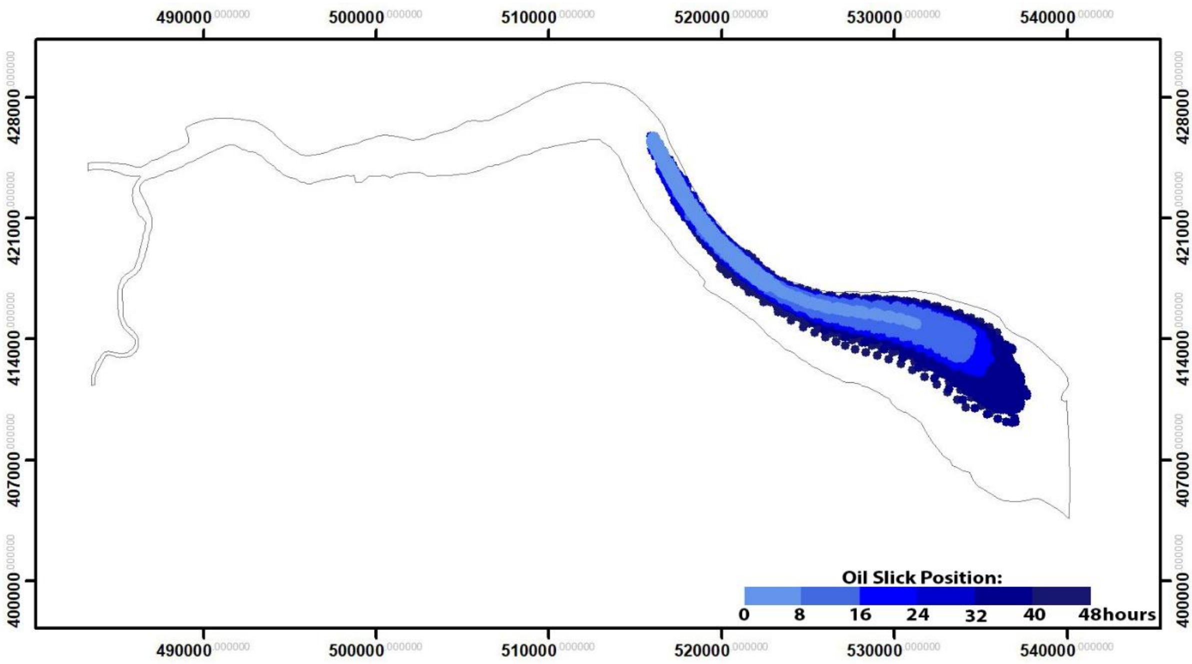

Figure 5.7: Trajectories of oil released on the Humber Estuary at L1_a at low water during a spring tide

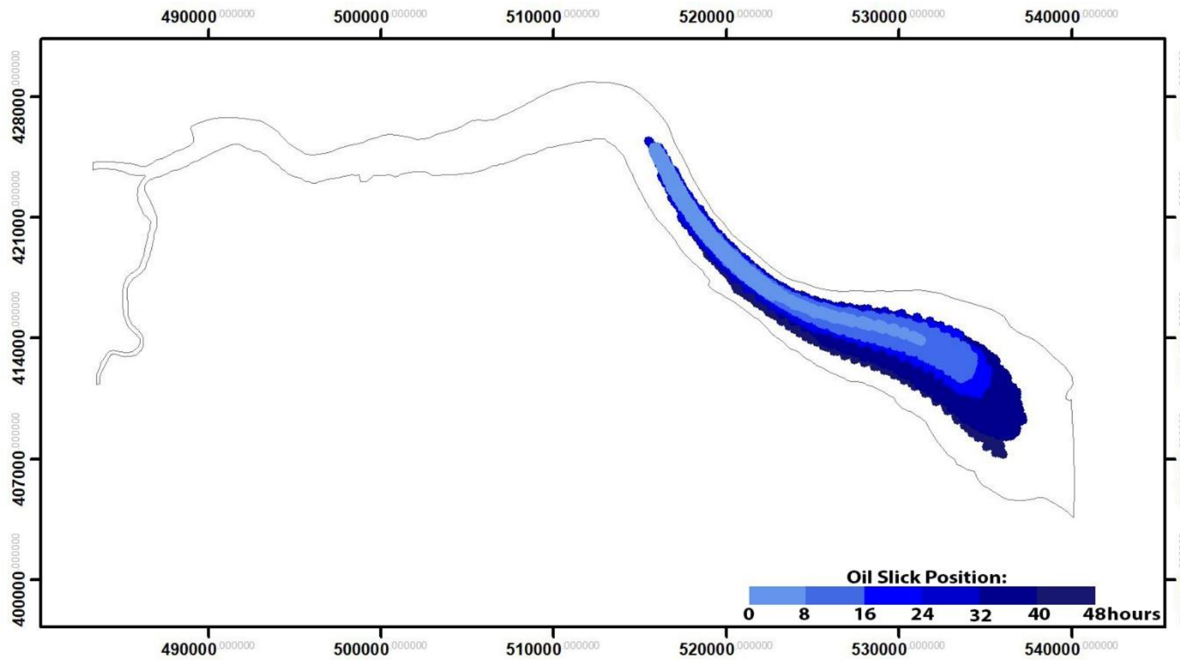

Figure 5.8: Trajectories of oil released on the Humber Estuary at L1_b at low water during a spring tide

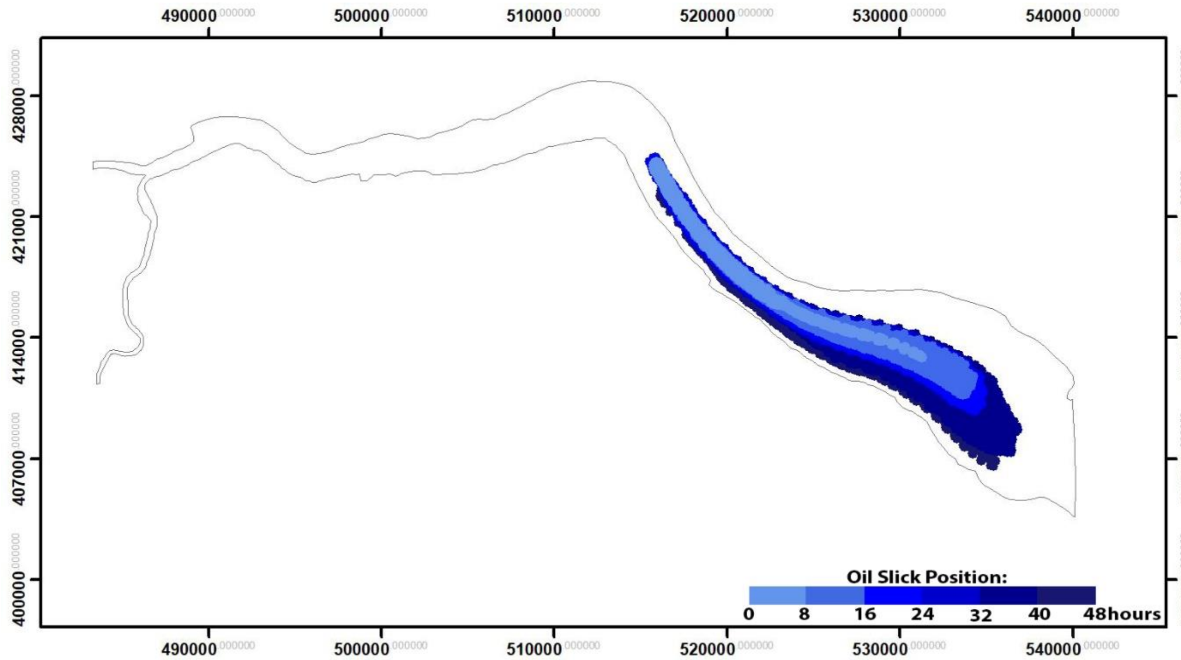

Figure 5.9: Trajectories of oil released on the Humber Estuary at L1_c at low water during a spring tide

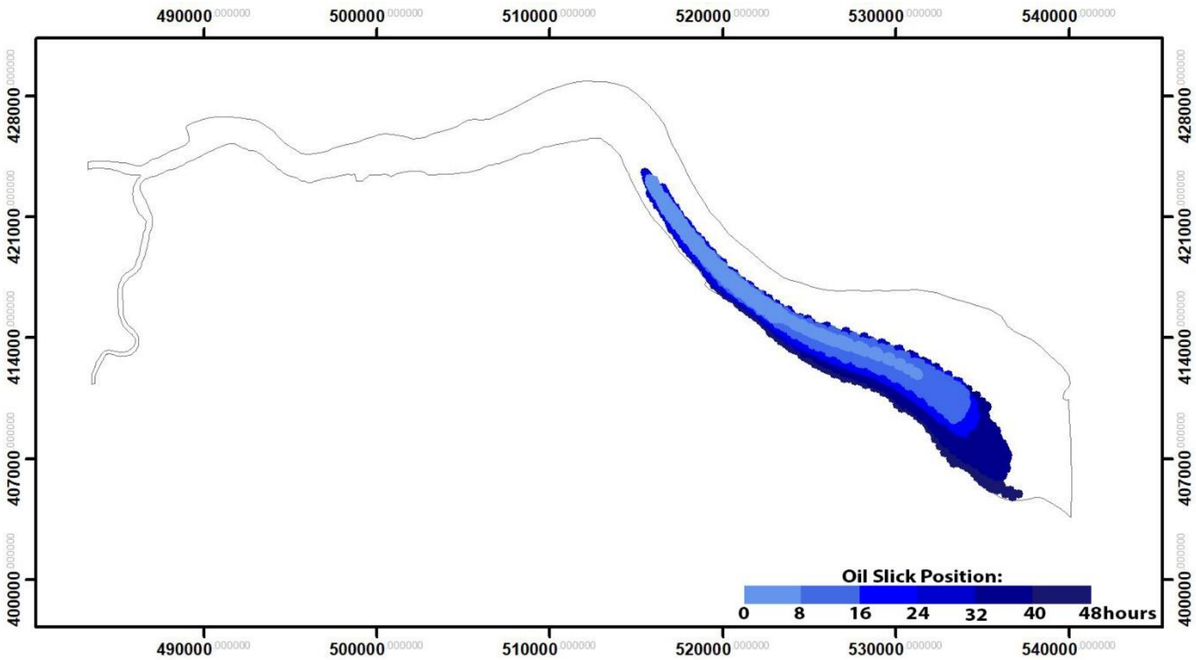

Figure 5.10: Trajectories of oil released on the Humber Estuary at L1_d at low water during a spring tide

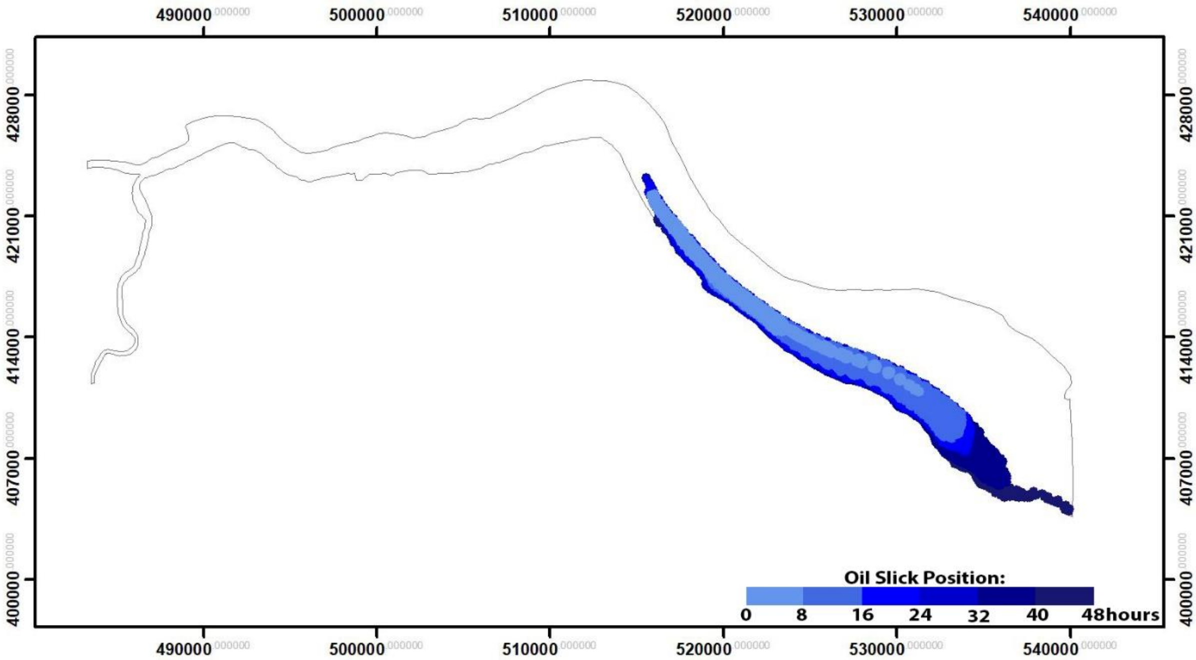

Figure 5.11: Trajectories of oil released on the Humber Estuary at L1_e at low water during a spring tide

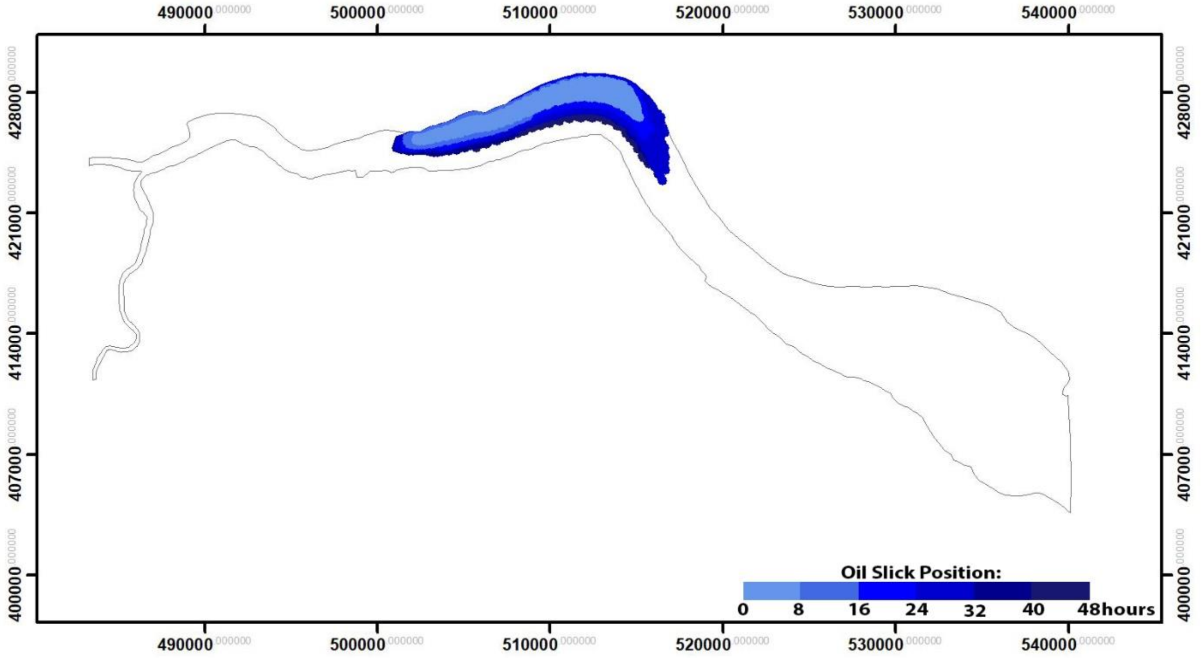

Figure 5.12: Trajectories of oil released on the Humber Estuary at L2_a at high water during a spring tide

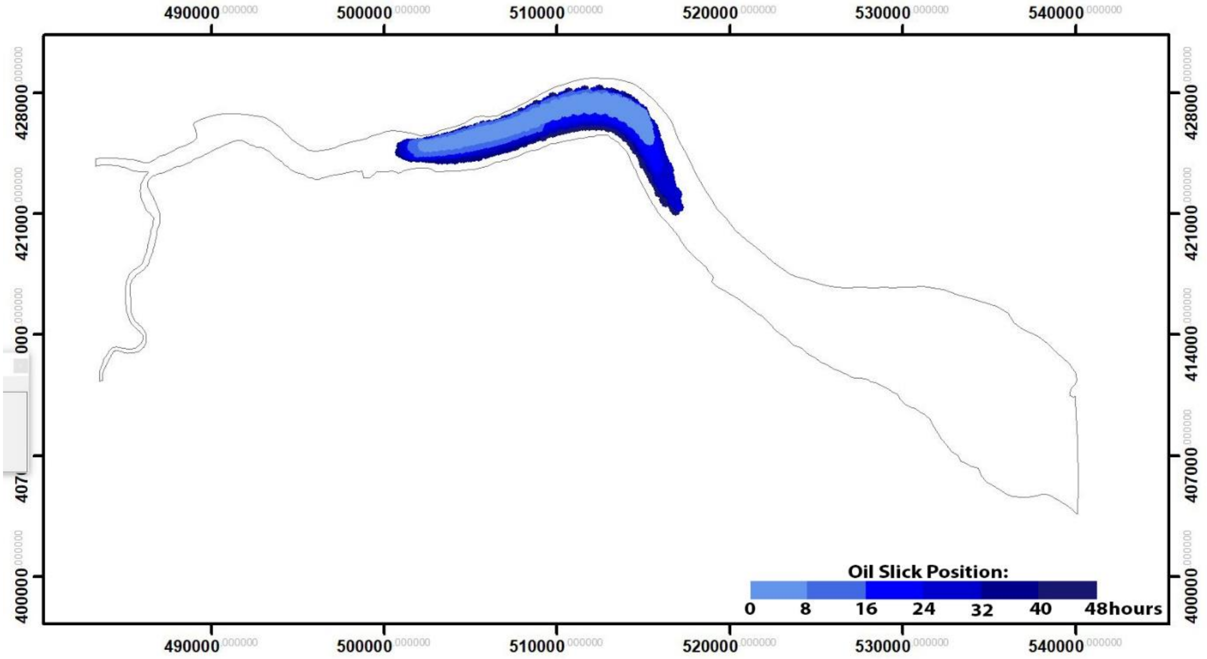

Figure 5.13: Trajectories of oil released on the Humber Estuary at L2_b at high water during a spring tide

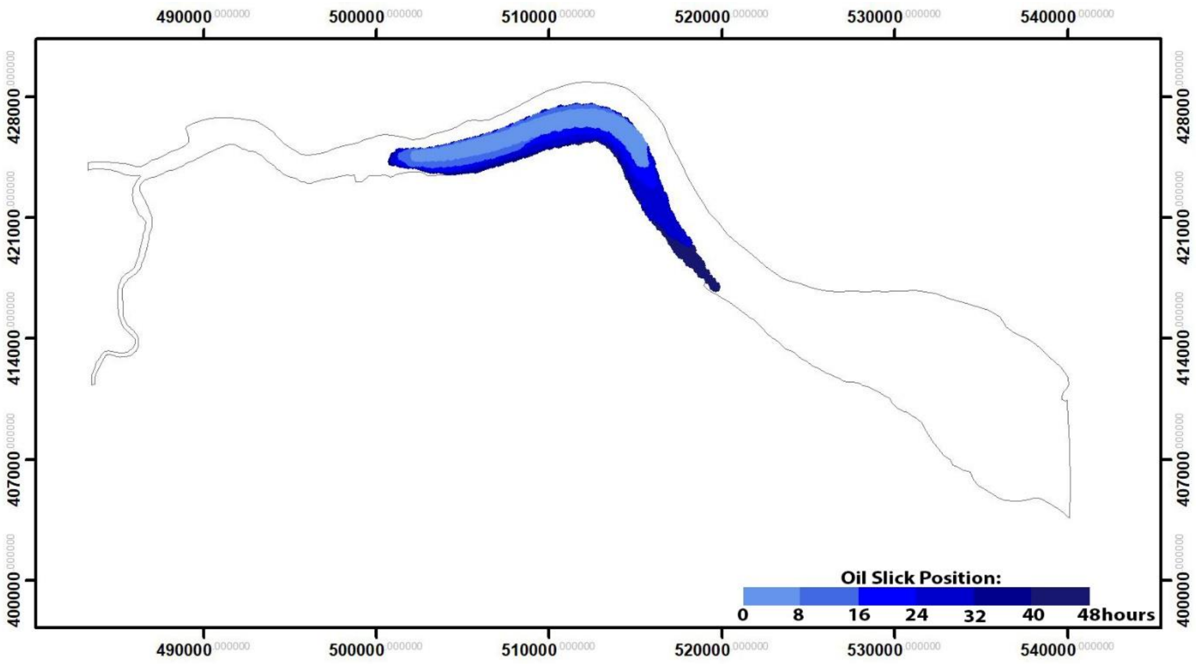

Figure 5.14: Trajectories of oil released on the Humber Estuary at L2_c at high water during a spring tide

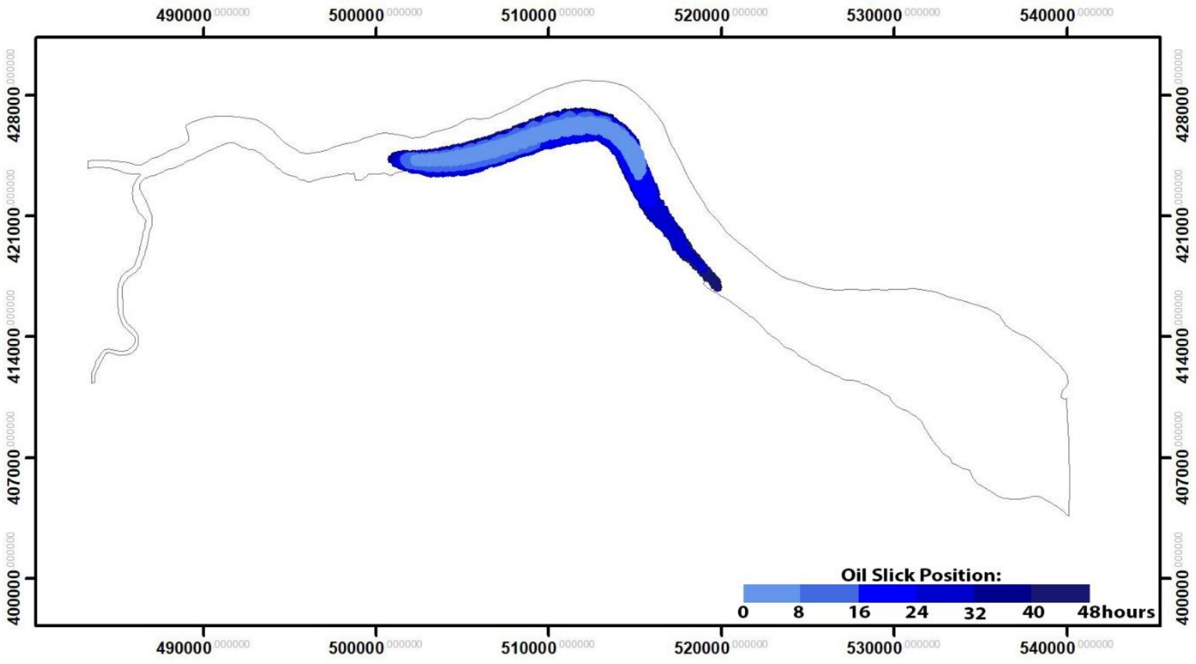

Figure 5.15: Trajectories of oil released on the Humber Estuary at L2_d at high water during a spring tide

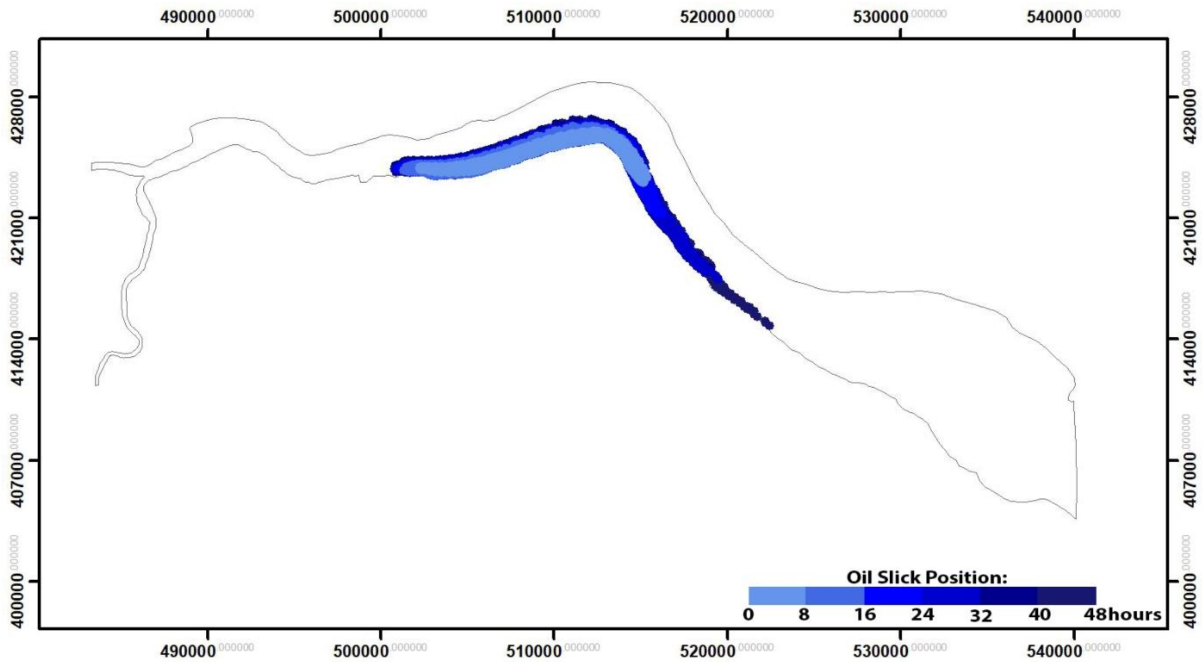

Figure 5.16: Trajectories of oil released on the Humber Estuary at L2_e at high water during a spring tide

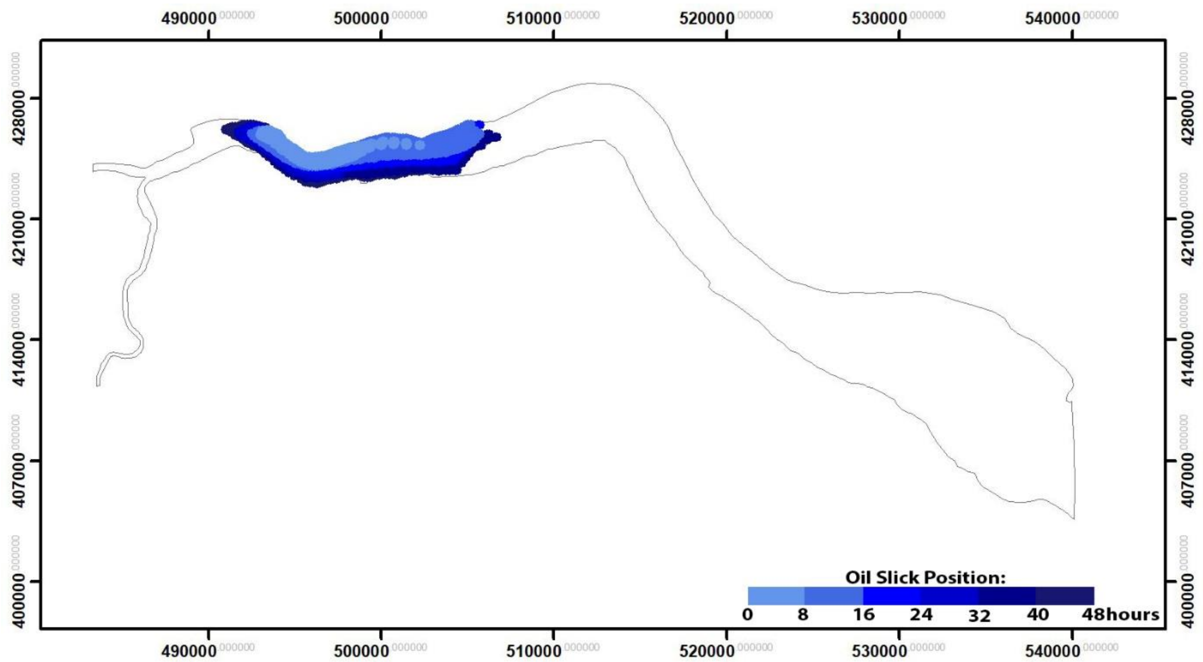

Figure 5.17: Trajectories of oil released on the Humber Estuary at L2_a at low water during a spring tide

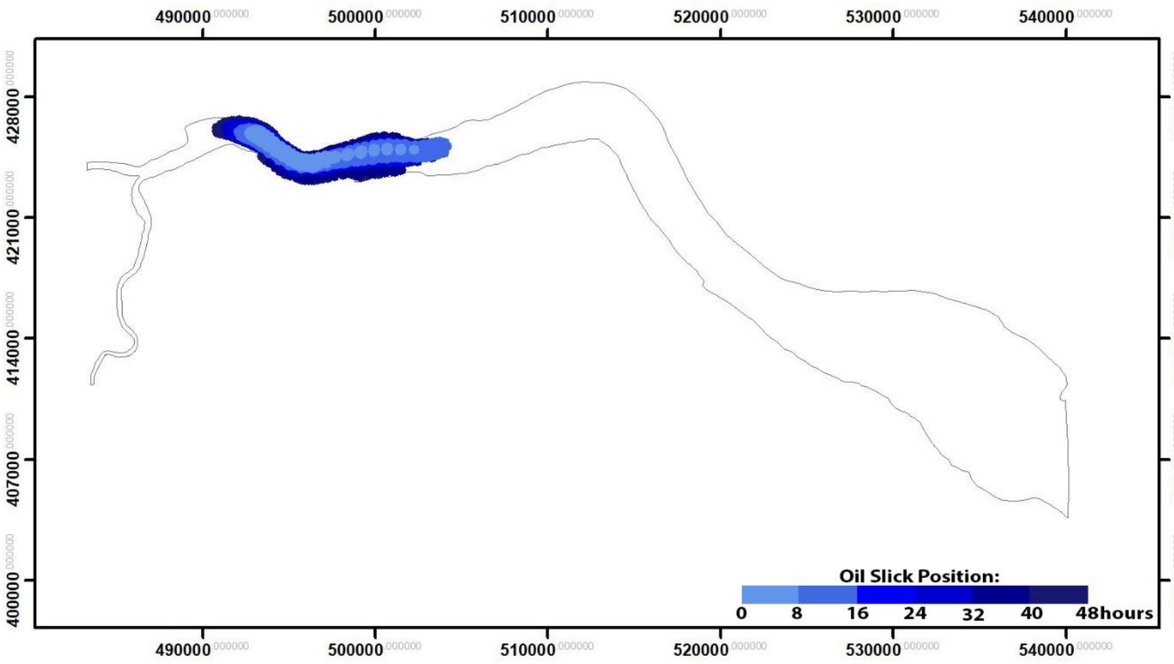

Figure 5.18: Trajectories of oil released on the Humber Estuary at L2_b at low water during a spring tide

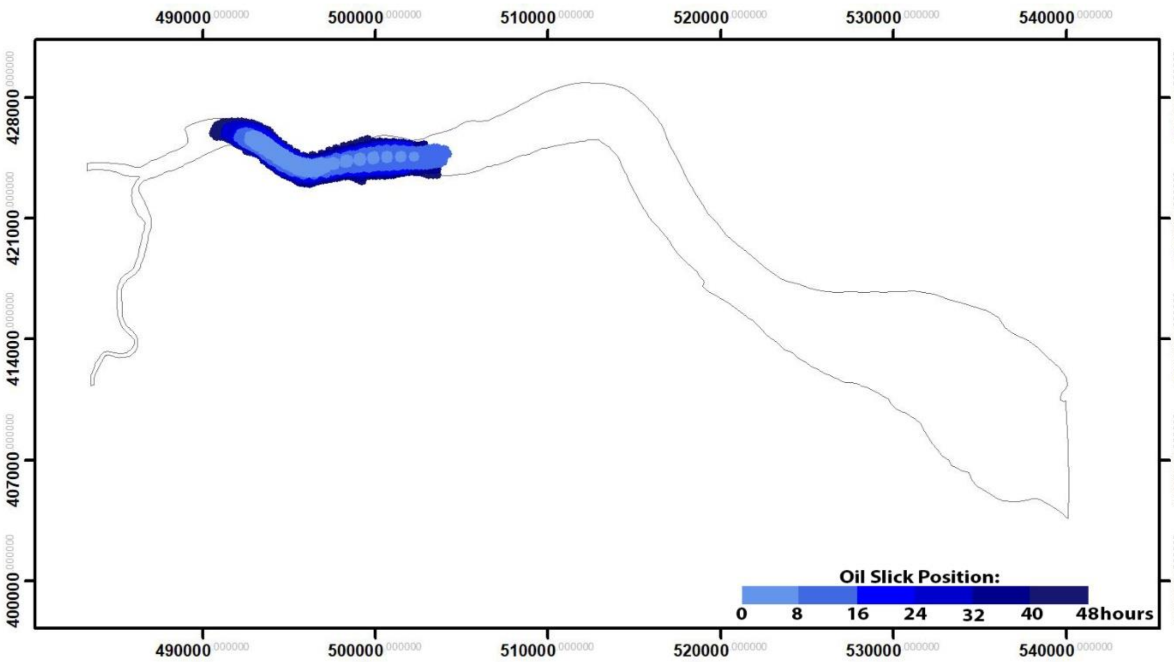

Figure 5.19: Trajectories of oil released on the Humber Estuary at L2_c at low water during a spring tide

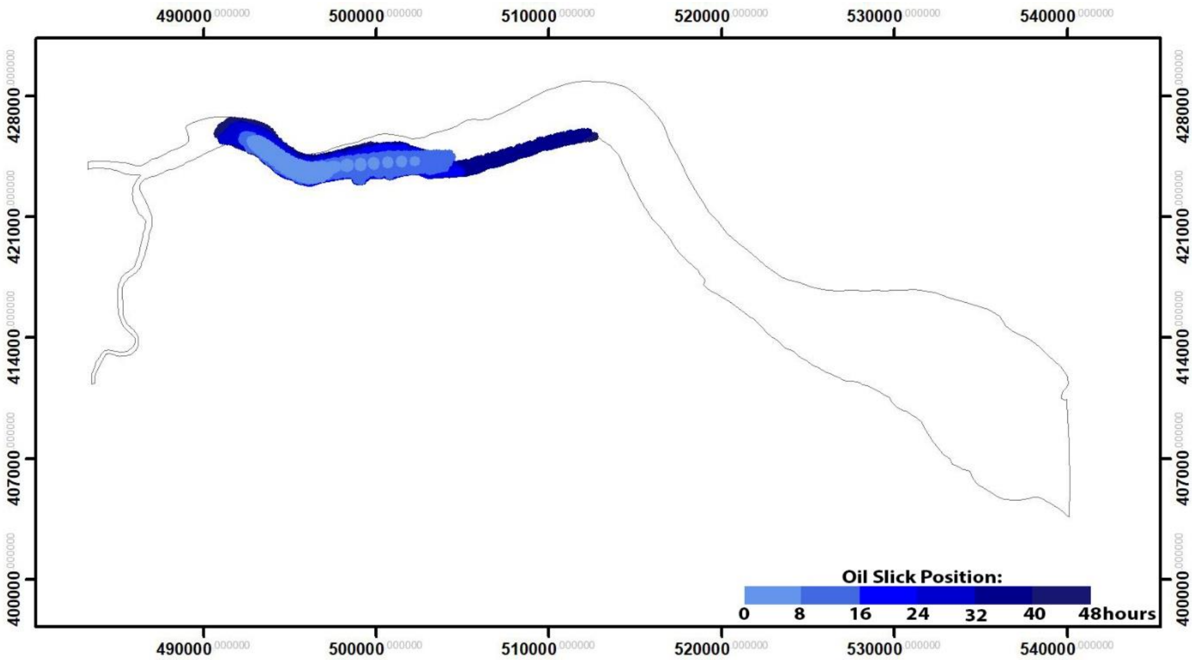

Figure 5.20: Trajectories of oil released on the Humber Estuary at L2_d at low water during a spring tide

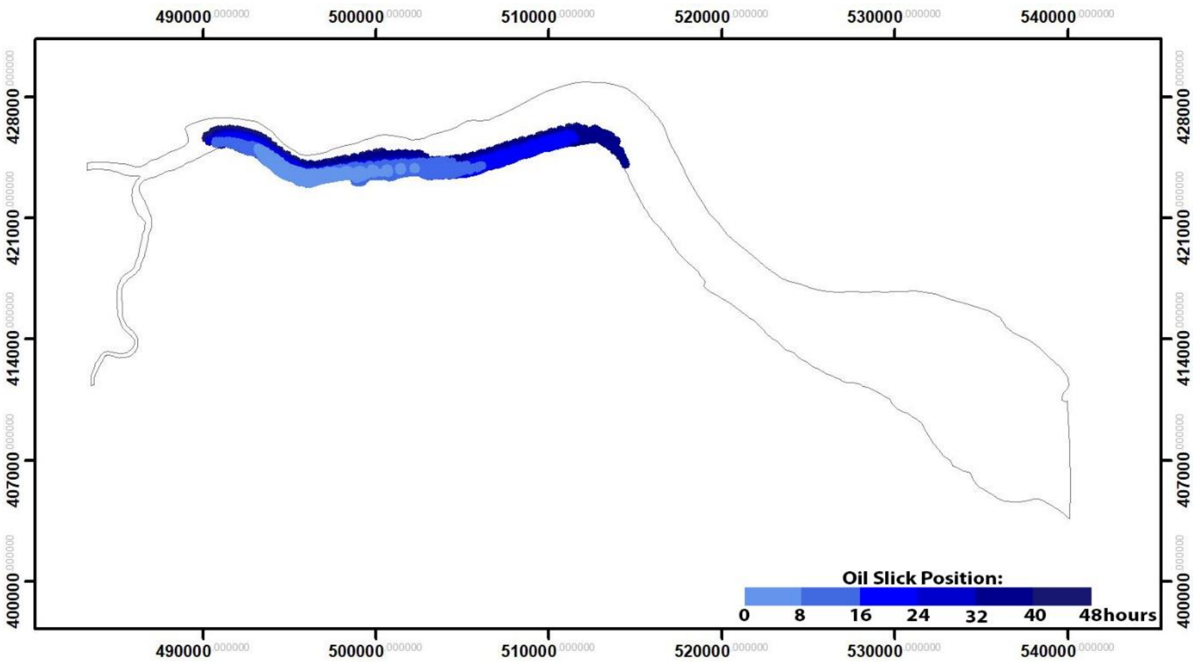

Figure 5.21: Trajectories of oil released on the Humber Estuary at L2_e at low water during a spring tide

Table 5.3: Simulated oil slick impacted area, A (sq. km), length of estuary bank line affected, L (km), and oil travel time to reach estuary bank, T (hours), for different release locations.

Scenarios	0 - 8h	8 - 16h	16 - 24h	24 - 32h	32 - 40h	40 - 48h	North bank		Southbank	
	A	A	A	A	A	A	L	T	L	T
L1_a HW	7.18	-	-	-	-	-	-	-	-	-
L1_b HW	5.46	-	-	-	-	-	-	-	-	-
L1_c HW	5.45	-	-	-	-	-	-	-	-	-
L1_d HW	5.43	-	-	-	-	-	-	-	-	-
L1_e HW	6.18	-	-	-	-	-	-	-	-	-
L1_a LW	14.36	31.78	40.06	42.75	65.74	75.11	12.89	17.50	-	-
L1_b LW	14.44	30.58	41.11	47.09	67.48	74.90	-	-	-	-
L1_c LW	14.32	32.23	39.91	43.65	63.42	71.12	-	-	-	-
L1_d LW	14.18	30.76	39.19	43.63	58.31	63.74	-	-	24.83	27.75
L1_e LW	14.40	29.40	34.37	35.12	42.29	46.09	-	-	31.16	3.75
L2_a HW	11.65	15.06	19.94	28.87	31.03	34.28	17.90	0.25	-	-
L2_b HW	10.99	15.37	20.84	26.92	30.16	33.61	-	-	-	-

L2_c HW	9.98	15.34	20.58	29.35	31.40	33.50	-	-	20.16	26
L2_d HW	9.82	15.31	20.70	25.02	26.54	28.12	-	-	21.99	12
L2_e HW	8.79	12.79	16.11	19.89	22.09	24.50	-	-	27.39	0.25
L2_a LW	5.85	13.56	17.26	20.17	25.30	27.41	15.16	0.25	11.72	27.25
L2_b LW	5.67	12.18	13.61	15.80	20.87	21.95	12.61	5.50	9.85	26.75
L2_c LW	5.70	12.72	15.50	18.07	20.83	22.83	9.64	18.50	13.50	14.50
L2_d LW	6.12	12.71	15.50	18.51	23.18	25.06	6.26	31.50	23.27	2.75
L2_e LW	4.84	9.96	14.99	16.35	23.63	26.24	-	-	25.52	0.25

Note: L1, L2 = release points; LW = high water; LW = low water.

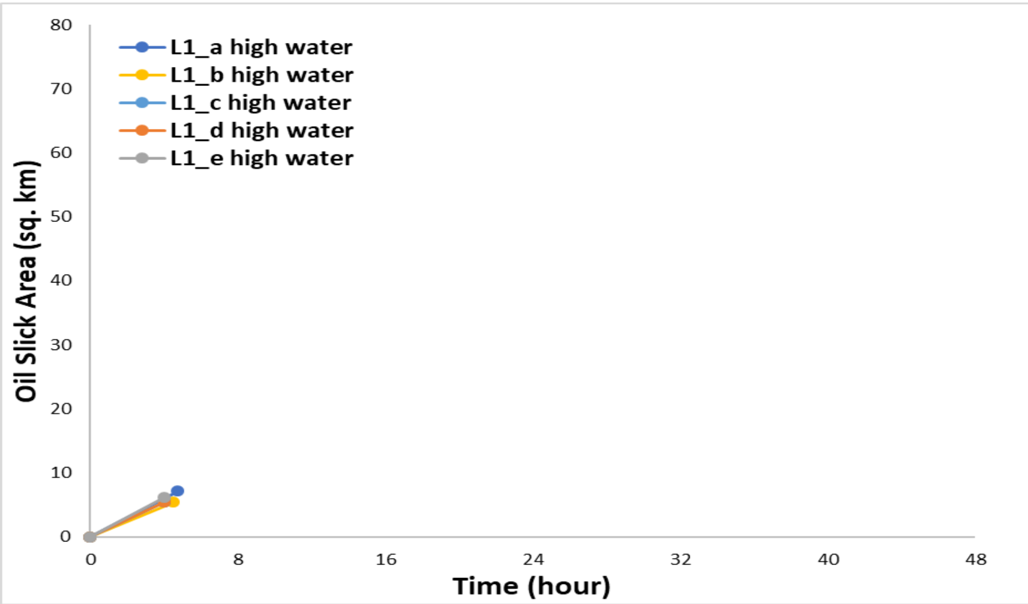

Figure 5.22: Area covered by simulated oil slick over time for spills along L1 at high water

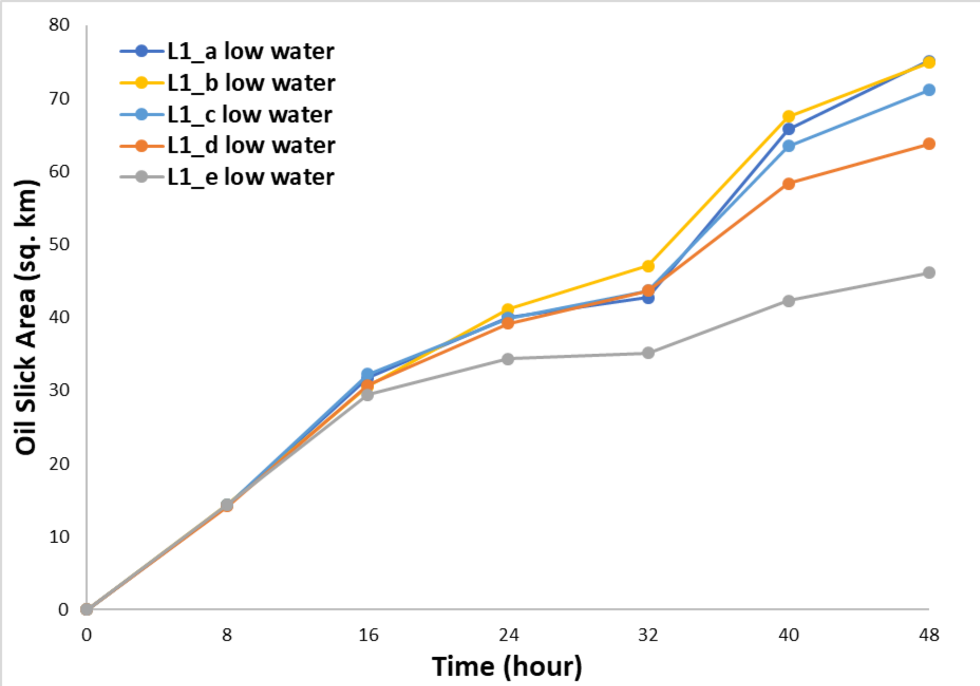

Figure 5.23: Area covered by simulated oil slick over time for spills along L1 at low water

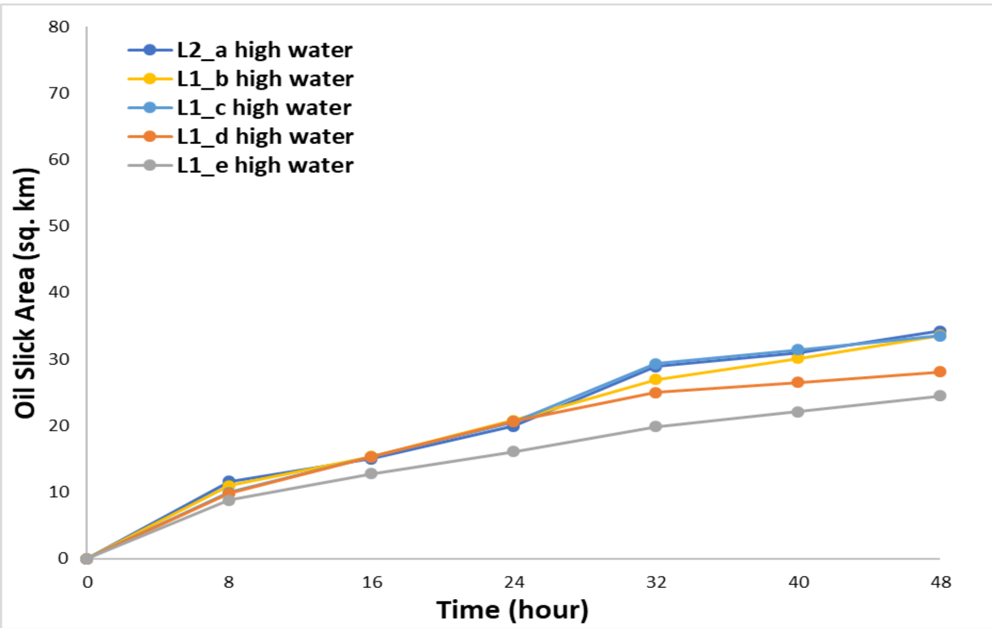

Figure 5.24: Area covered by simulated oil slick over time for spills along L2 at high water

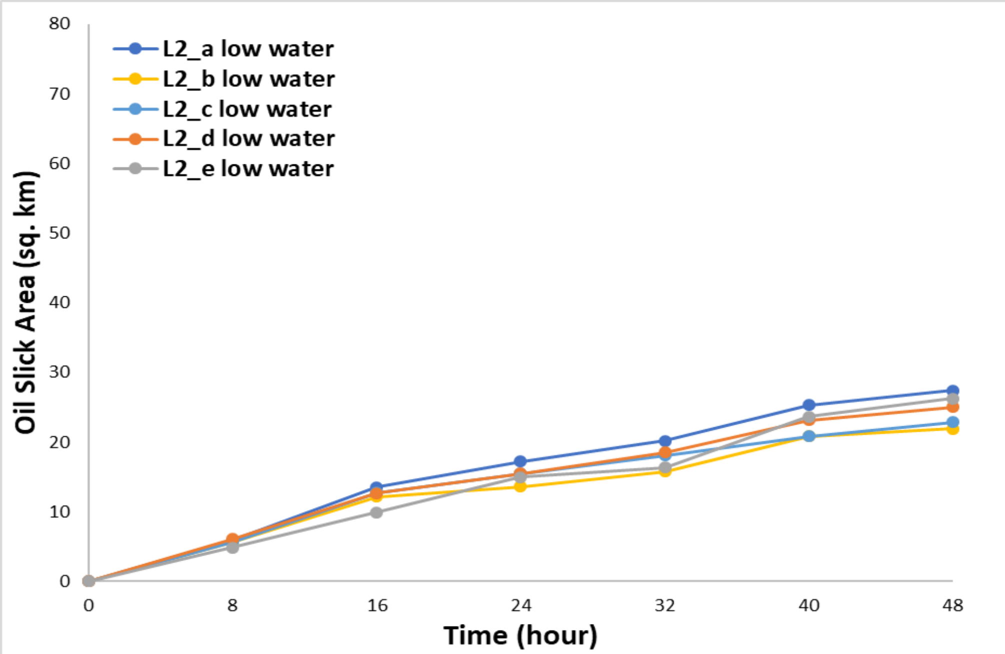

Figure 5.25: Area covered by simulated oil slick over time for spills along L2 at low water

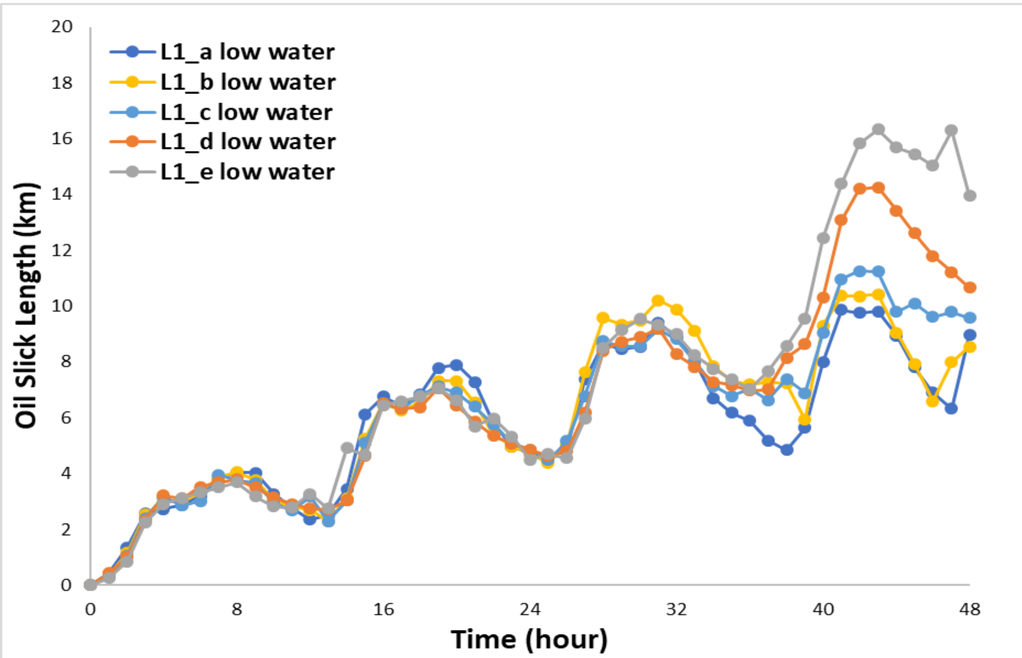

Figure 5.26: Oil slick length over time for spills along L1 at low water

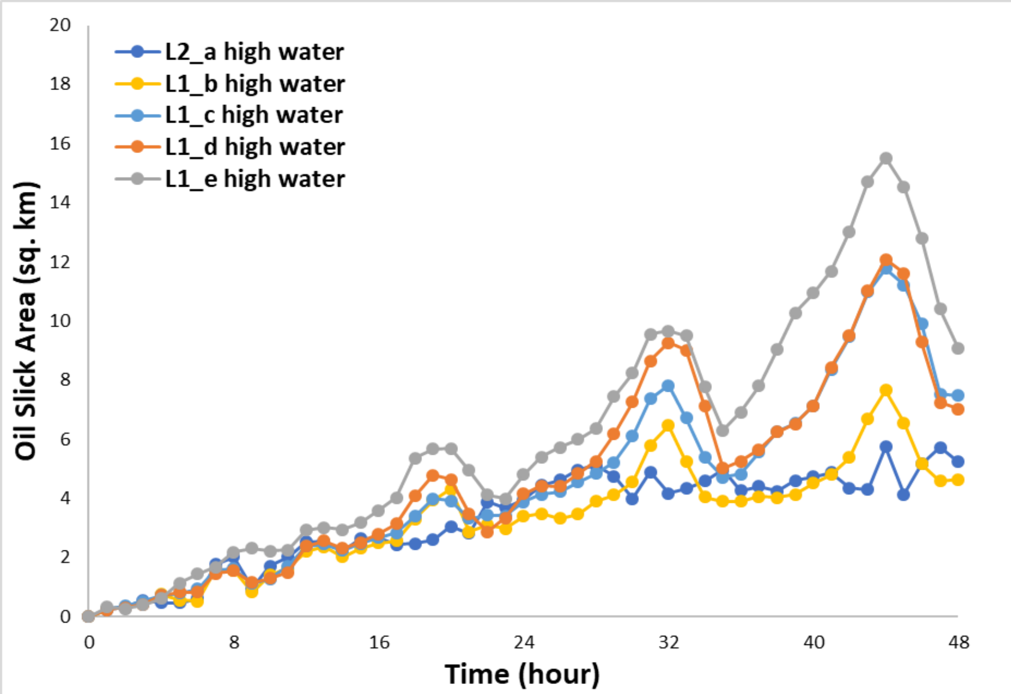

Figure 5.27: Oil slick length over time for spills along L2 at high water

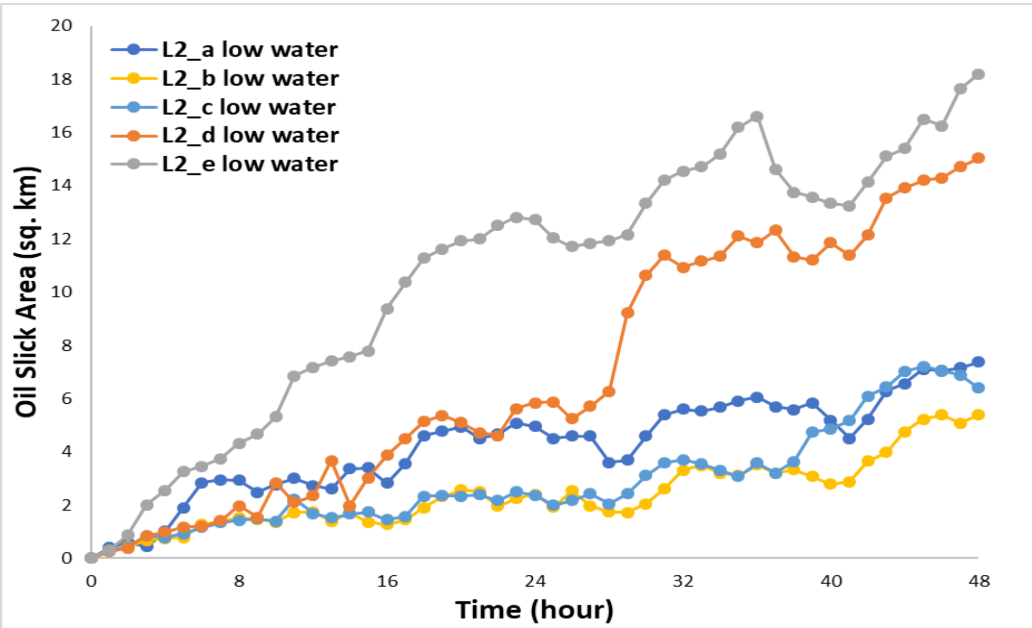

Figure 5.28: Oil slick length over time for spills along L2 at low water

5.4 DISCUSSION

5.4.1 Along the Estuary Length

Results show that the proximity of the oil release location to the estuary mouth influences the oil slick impacted area, as well as, overall distance travelled. At low water, the area covered by oil slicks released near the estuary mouth (along L1; Figure 5.7 – 5.11) was on average 168% larger than oil slicks released further upstream (along L2; Figure 5.17 – 5.21; Table 5.4). While after 48 hours, the overall distance travelled by oil slicks released near the estuary mouth at low water was 56% larger than oil slicks released further upstream (Figure 5.29 – Figure 5.43). This could possibly be explained by stronger currents observed at the estuary mouth (Figure 5.44; Figure 5.45; Table 5.5). We now know that for this macro-tidal estuary, oil slick impacted area and overall travel distance will decrease as the point of release moves further upstream due to decreasing current velocities. Since the amount of oil released is the same in all scenarios, it also suggests that the oil slicks remain denser (more concentrated) as the point of release is further upstream. Oil slicks released at high water could not be compared as slicks released near the estuary mouth leave the computational domain.

Table 5.4: Relative properties of comparable oil slicks released upstream and downstream (ratio = average upstream / average downstream value), as measured 48 hours after the spill.

	Impacted area (sq. km)						Distance (km)
	8 h	**16 h**	**24 h**	**32 h**	**40 h**	**48 h**	**48 h**
L1 LW	14.34	30.95	38.93	42.45	59.45	66.19	28.58
L2 LW	5.64	12.23	15.37	17.78	22.76	24.70	18.32
Ratio	2.54	2.53	2.53	2.39	2.61	2.68	1.56

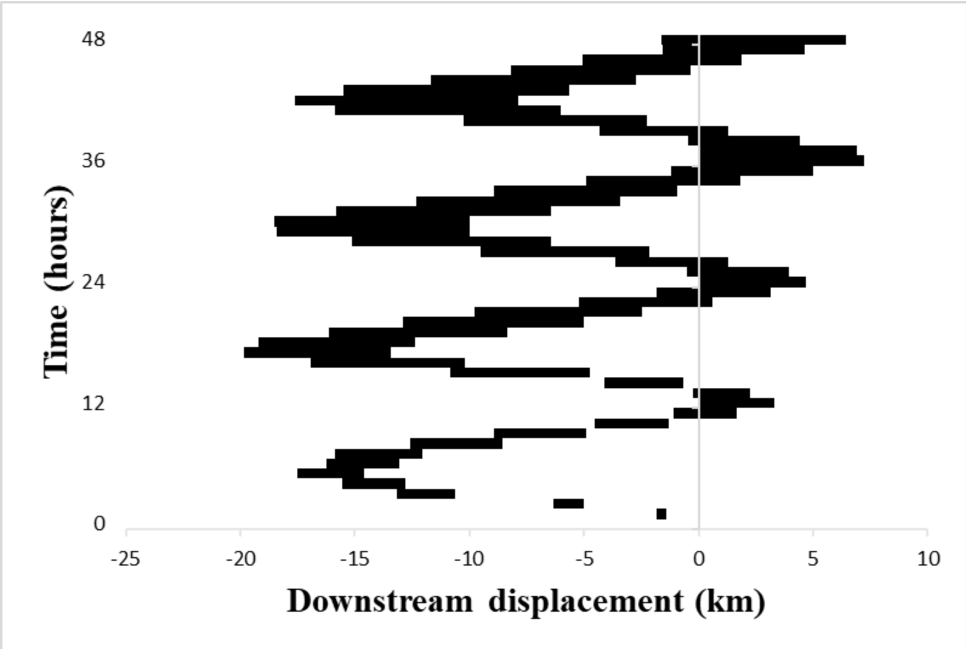

Figure 5.29: Longitudinal position and extent of L1_a oil slicks over time at low water

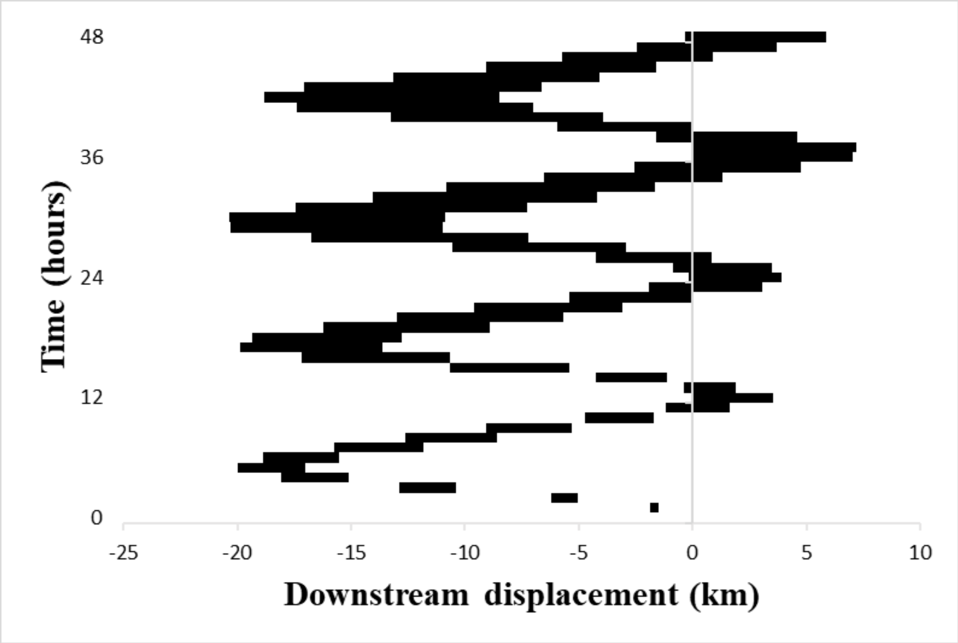

Figure 5.30: Longitudinal position and extent of L1_b oil slicks over time at low water

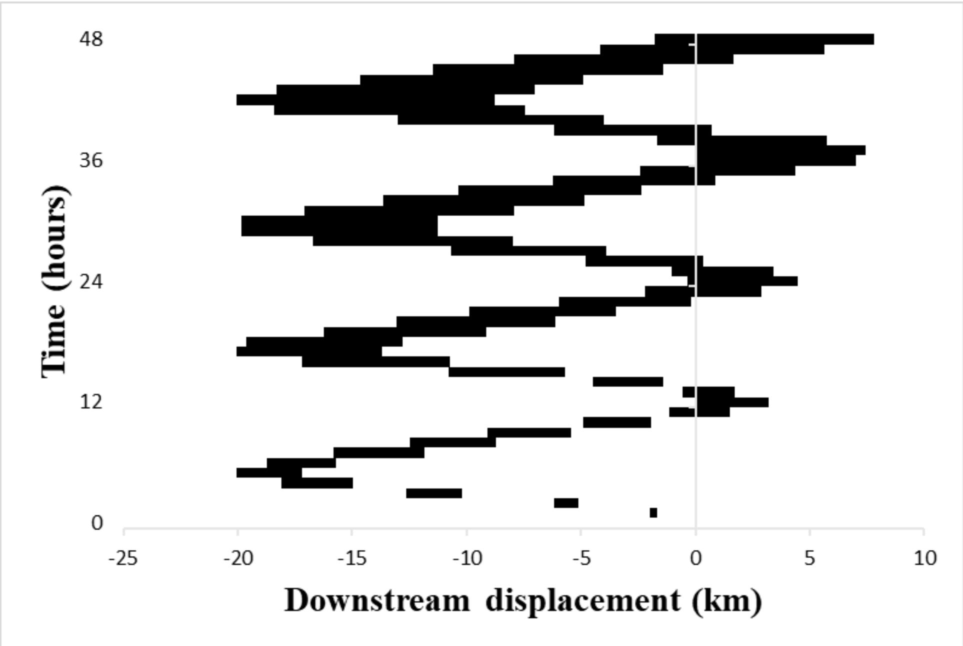

Figure 5.31: Longitudinal position and extent of L1_c oil slicks over time at low water

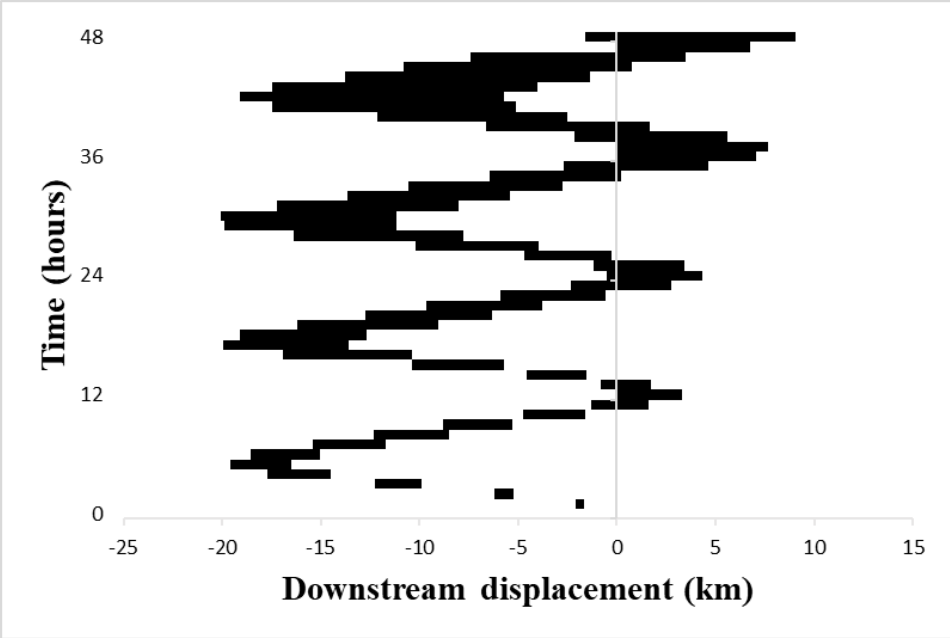

Figure 5.32: Longitudinal position and extent of L1_d oil slicks over time at low water

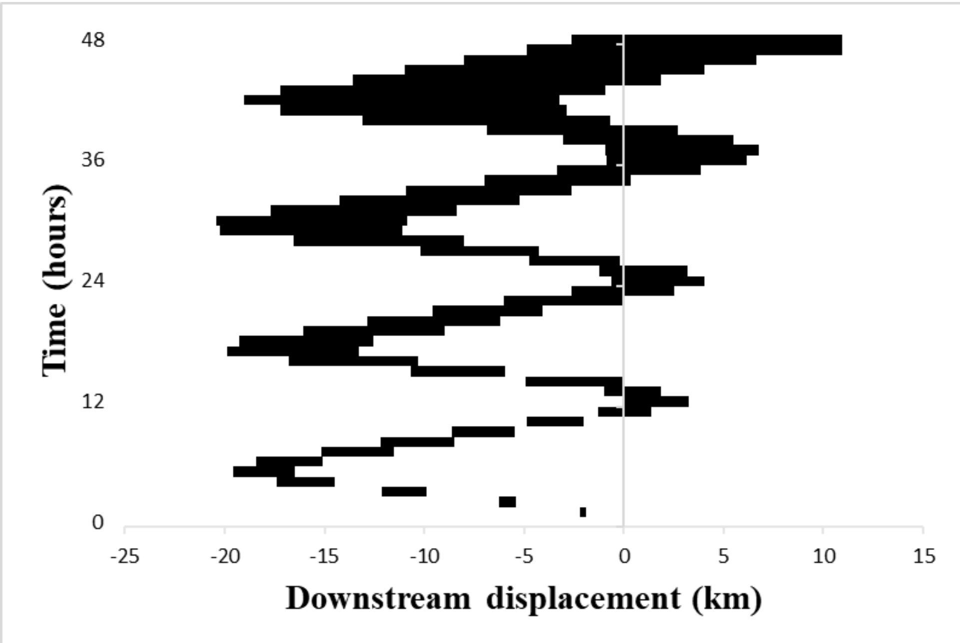

Figure 5.33: Longitudinal position and extent of L1_e oil slicks over time at low water

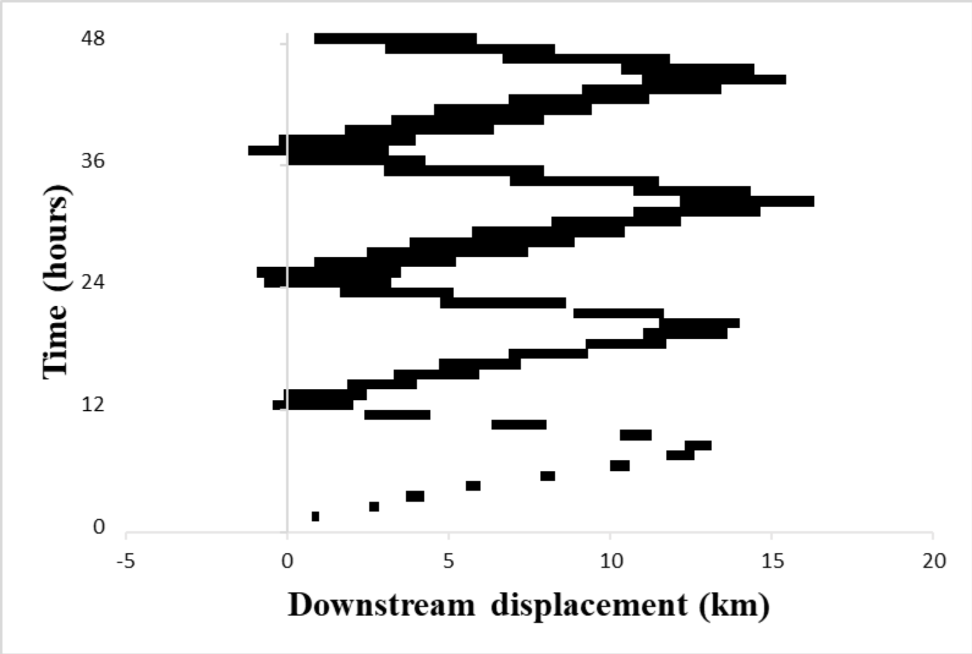

Figure 5.34: Longitudinal position and extent of L2_a oil slicks over time at high water

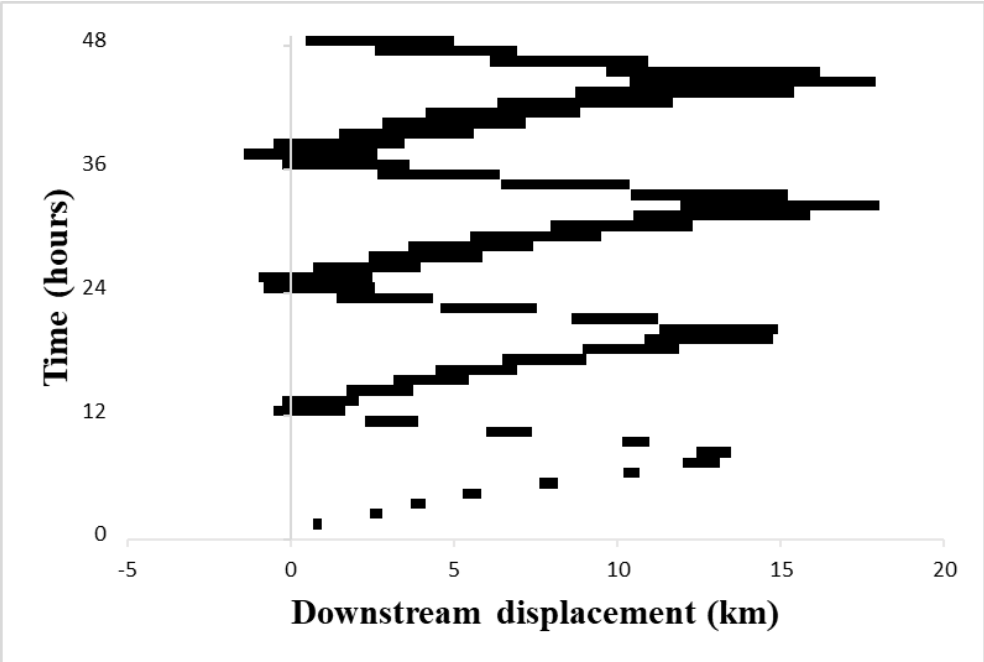

Figure 5.35: Longitudinal position and extent of L2_b oil slicks over time at high water

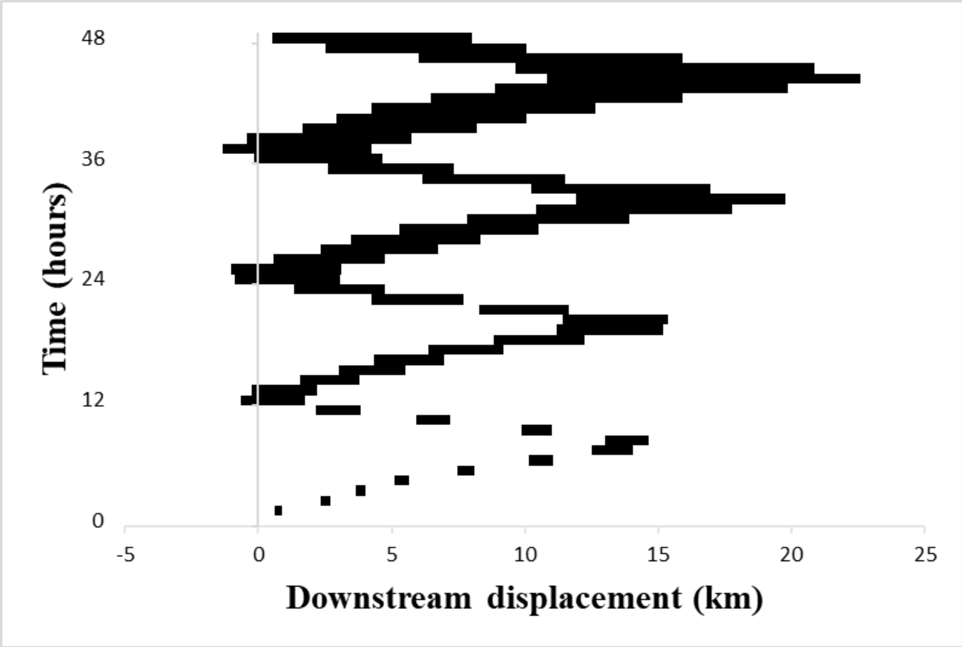

Figure 5.36: Longitudinal position and extent of L2_c oil slicks over time at high water

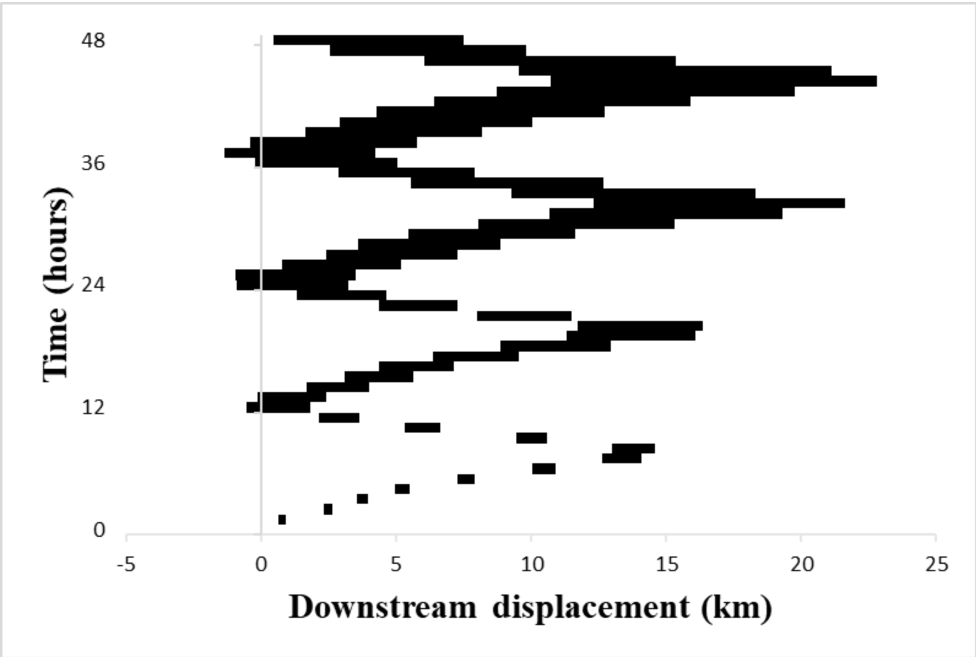

Figure 5.37: Longitudinal position and extent of L2_d oil slicks over time at high water

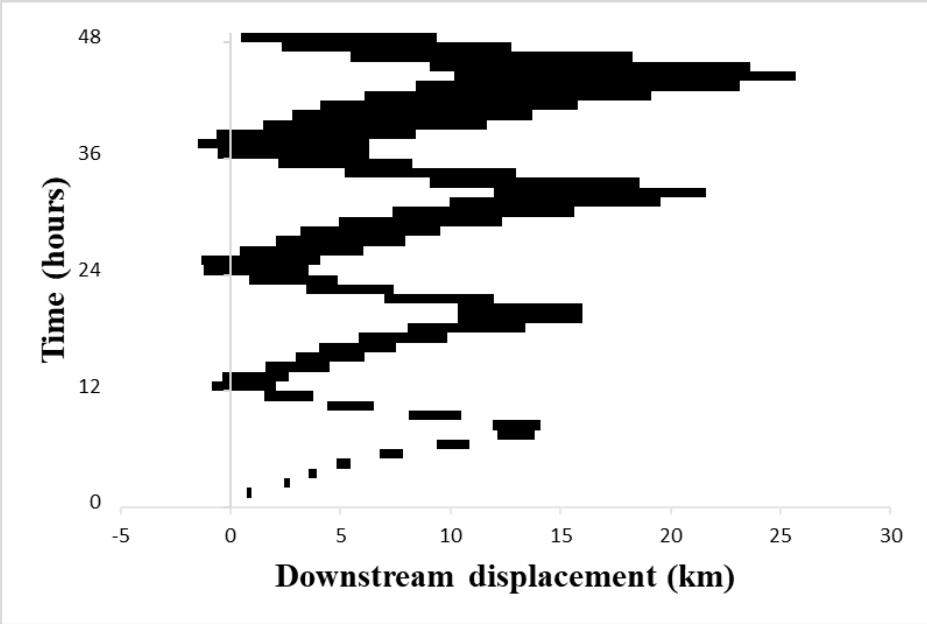

Figure 5.38: Longitudinal position and extent of L2_e oil slicks over time at high water

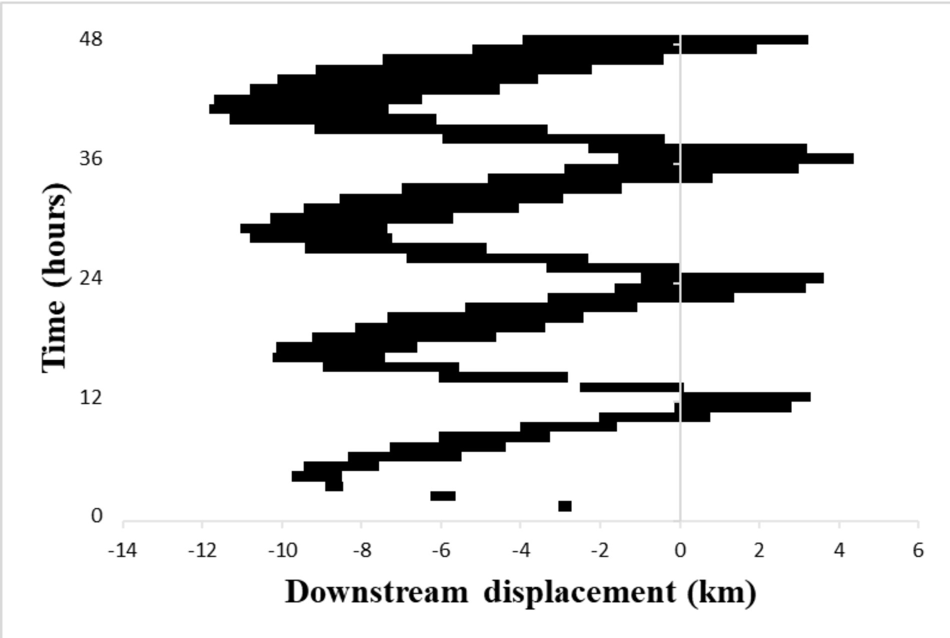

Figure 5.39: Longitudinal position and extent of L2_a oil slicks over time at low water

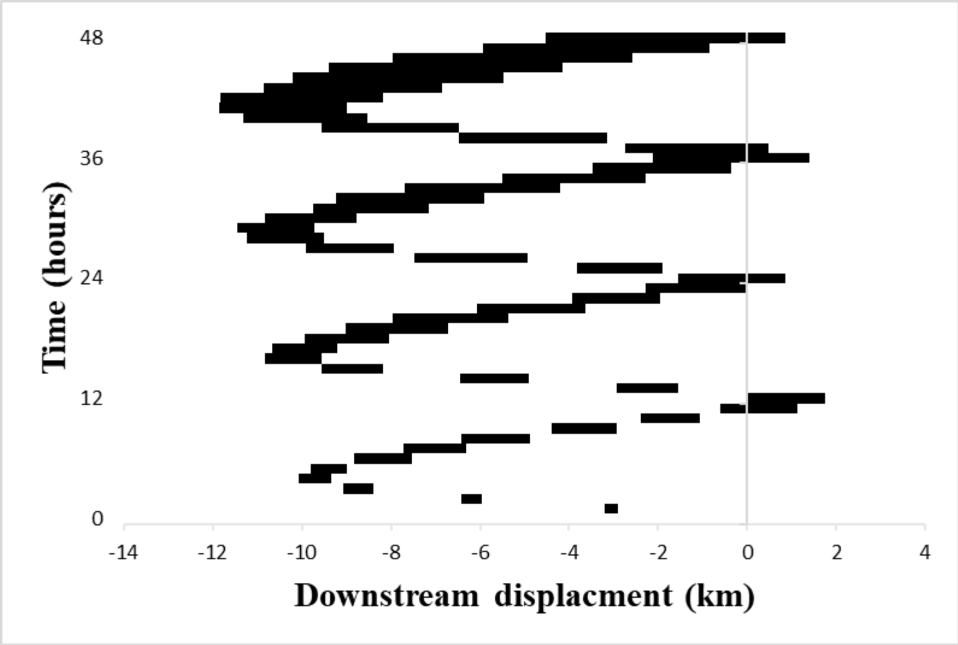

Figure 5.40: Longitudinal position and extent of L2_b oil slicks over time at low water

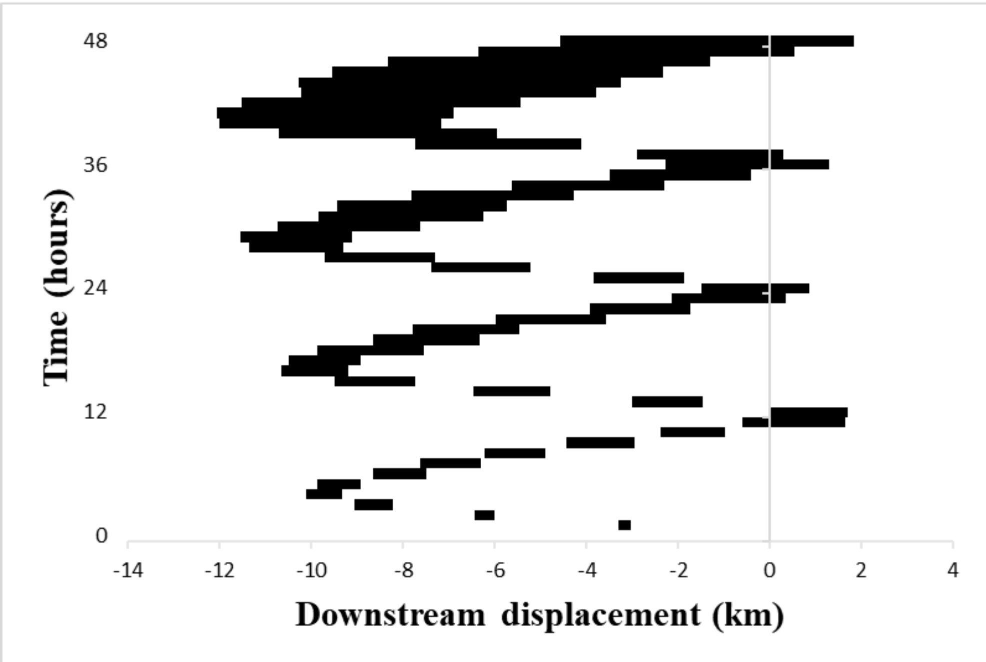

Figure 5.41: Longitudinal position and extent of L2_c oil slicks over time at low water

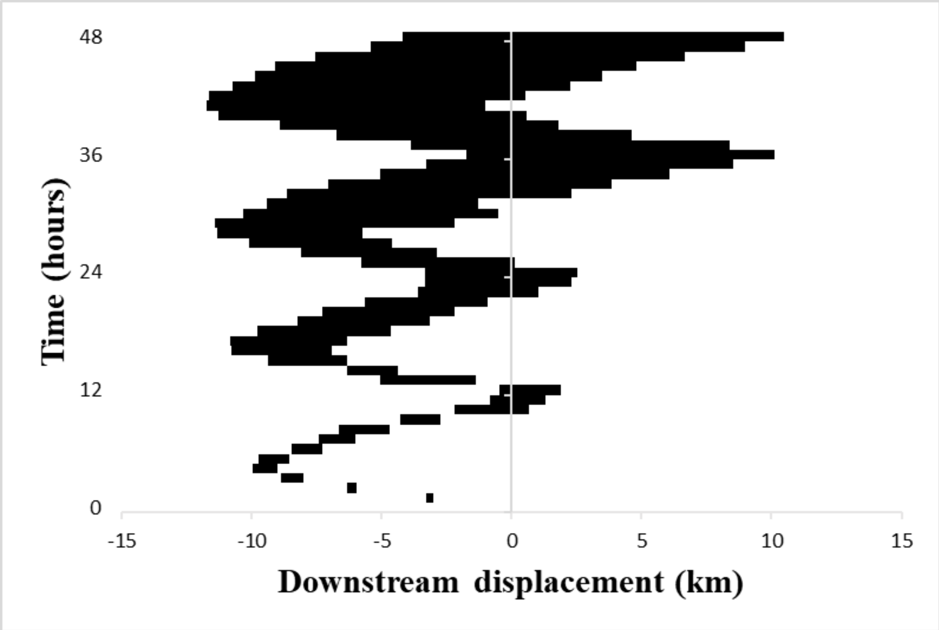

Figure 5.42: Longitudinal position and extent of L2_d oil slicks over time at low water

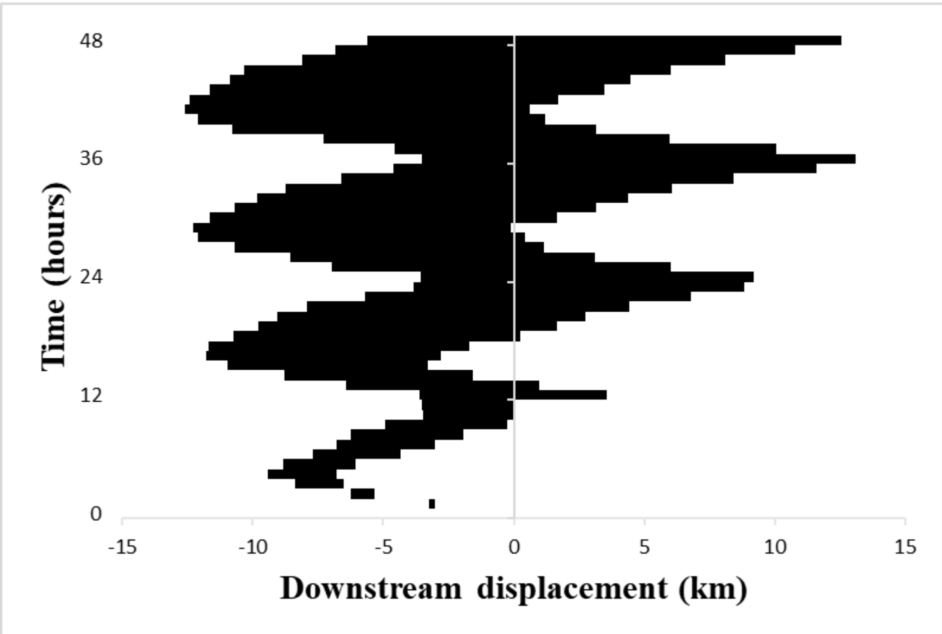

Figure 5.43: Longitudinal position and extent of L2_e oil slicks over time at low water

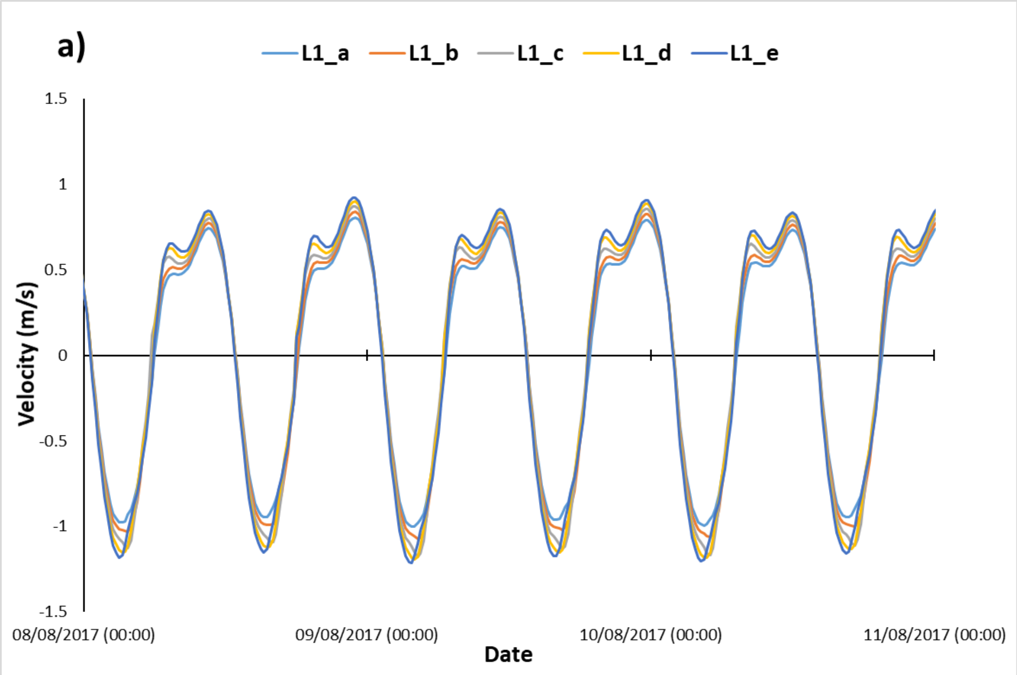

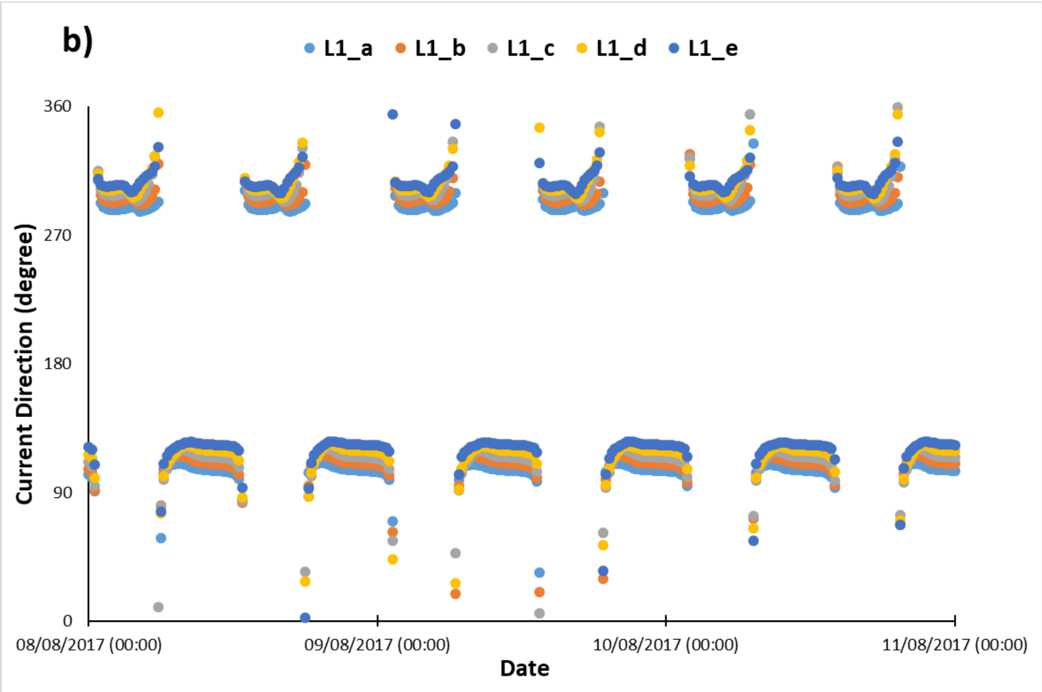

Figure 5.44: (a) Simulated current velocity; and (b) direction (measured from the 5 release locations at L1) covering the duration of oil spill. Note: negative current velocity indicates upstream movement while positive current velocity indicates downstream movement.

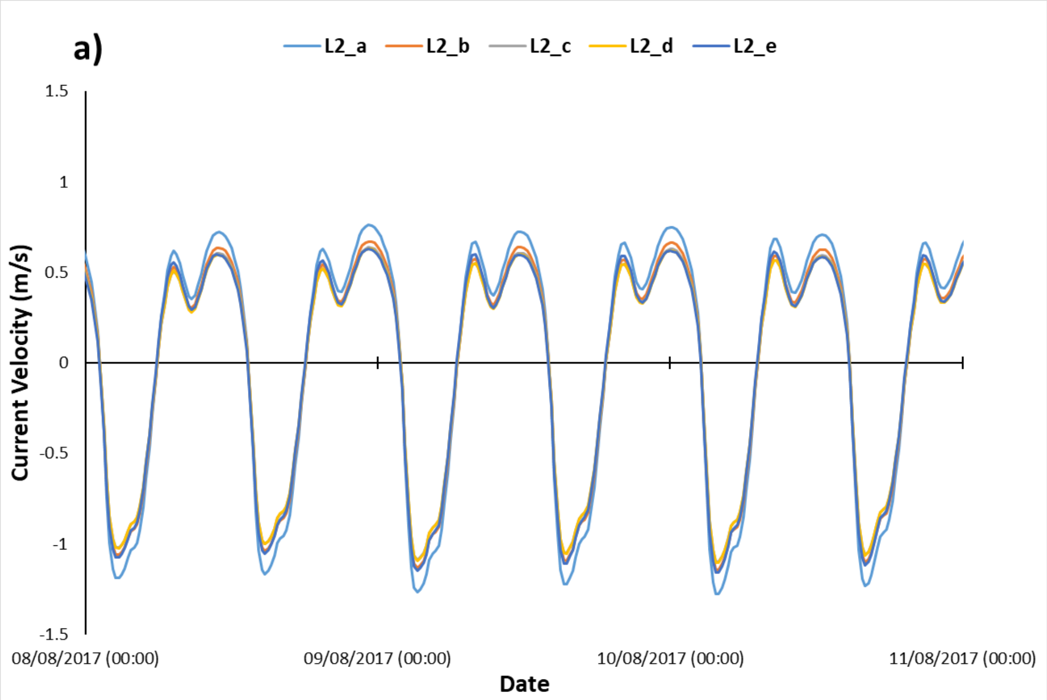

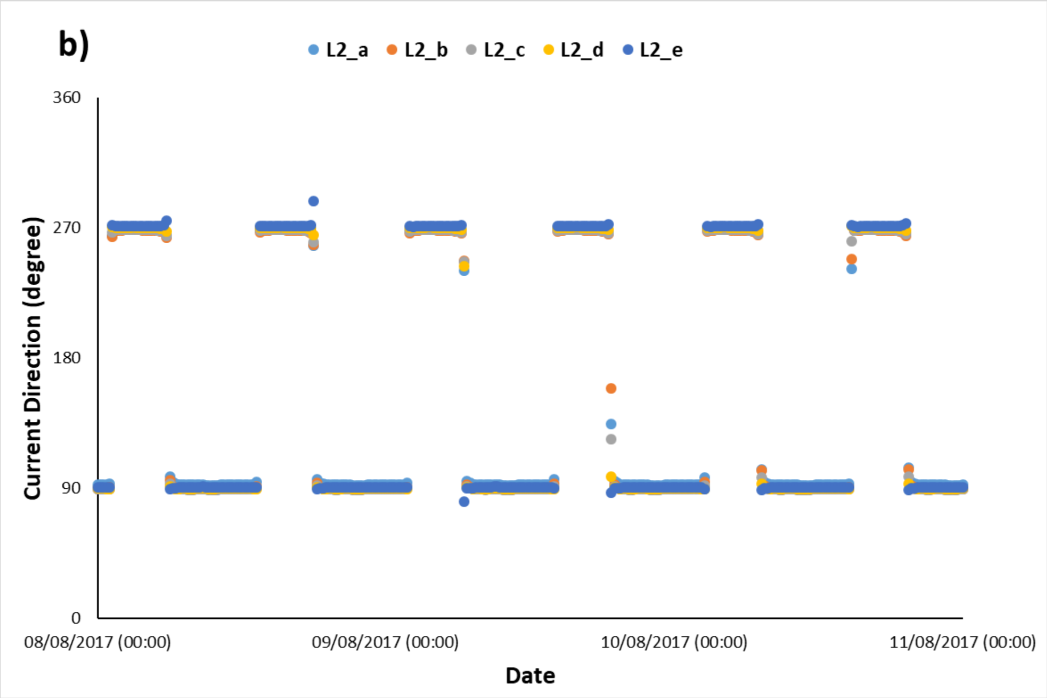

Figure 5.45: (a) Simulated current velocity; and (b) direction (measured from the 5 release locations at L2) covering the duration of oil spill. Note: negative current

velocity indicates upstream movement while positive current velocity indicates downstream movement.

Table 5.5: **Average current speed and direction measured from the 5 lateral release locations along L1 and L2 within the oil slick.**

Oil release location	**Average current speed (m/s)**	**Average flood direction**	**Average ebb direction**
L1_a	0.58	290.50	127.99
L1_b	0.62	296.21	107.46
L1_c	0.65	302.43	109.82
L1_d	0.67	306.57	114.41
L1_e	0.68	308.02	119.28
L1	0.64	300.75	115.79
L2_a	0.64	269.05	92.92
L2_b	0.56	267.36	90.41
L2_c	0.54	267.98	89.65
L2_d	0.53	269.52	89.87
L2_e	0.55	271.31	90.56
L2	0.56	269.04	90.68

5.4.2 Cross-sectional Width

Oil slick released near the mouth of the estuary was observed to travel towards the south bank with the ebb tides (Figure 5.7 – 5.11). To understand the slick transport, current speed and direction were measured from the 5 lateral release locations along L1 and L2

(Figure 5.44; 5.45). Results revealed a lateral variation in current speed and direction (Figure 5.44; 5.45; Table 5.5). Lateral variation of current speed and direction is common in estuaries and is influenced by estuary shape, length, depth, friction factor and river flow (Prandle 2009). Considering the influence of current on oil slick transport (Section 2.2.1.1), the varying current speed (Table 5.5) will be a contributor to the difference in distance travelled by oil slicks (Table 5.6). In the lower half of the estuary, flood currents travelled at 301^o upstream while ebb currents travelled at 116^o towards the mouth of the estuary (Table 5.5). Along L2, flood and ebb currents travelled at 269^o and 91^o respectively (Table 5.5). The direction of flood currents towards the head of the estuary and ebb currents towards its mouth highlights the influence estuary geometry has on the estuarine current direction which in turn affects oil slick transport. In the lower half of the estuary (i.e. considering oil slicks released from L1), the current direction towards the estuary mouth resulted in oil slicks spreading towards the south bank. Upon reaching the south bank, oil slicks were restricted from spreading any further (Figure 5.10; 5.11). The difference in current direction across the estuary cross-sectional width (Table 5.5) can possibly explain the difference in oil slick impacted area (Figure 5.23; Table 5.3). Consequently, the area impacted by the oil slicks can possibly be explained by the southwards direction of ebb currents and proximity of the release location to the south bank. After 48 hours, the area covered by oil slick released at L1_a was 63% larger than oil slick released from L1_e (Table 5.3; Figures 5.7; 5.11). Analysis of the dynamics of oil slicks released further upstream along L2 also suggest that current direction and proximity to estuary bank influences the oil slick impacted area and travel distance. It was observed that the direction of flood and ebb currents along the estuary followed the change in estuary geometry. This might present a challenge for understanding oil slick transport in non-uniform shaped estuaries. To fully understand the difference in oil slick transport, responders will need to be aware of the axial and lateral variations of current speed and direction in different segments of the estuary and how it affects oil slicks from a particular release location.

Under the various release conditions, maximum oil slick length was greater for slicks released close to the south bank (L1_e LW; L2_e_HW; L2_e_LW) (Figure 5.26 – 5.28; Table 5.6). Observation of oil slick transport showed that movement of oil slicks close to the edge of the grid (river bank) was distorted, resulting in the formation of longer slicks (Figure 5.29 – 5.43). For example, movement of part of the oil slicks was observed to be restricted near the edge of the grid possibly due to the lower flow velocities at river banks. This was elongating the oil slick. Currents in the opposite direction were then observed to move the entire oil slick further elongating the oil slick. It is worth noting that lower flow velocities were not consistently observed along the river bank (Appendix P). This is possibly due to the shape of the estuary, which further complicates the estuarine current dynamics. Oil slick farther away from the south bank expanded southwards, forming wider slicks, oil slicks close to the south bank formed longer slicks, due to proximity to the river bank. The interaction between oil slicks and the river bank resulted in an increase in overall distance (Figure 5.29 – 5.43; Table 5.6). To effectively deal with oil slicks, oil spill modellers will need to take cognisance of the interaction between oil slicks and the edge of the computational grid (river bank). In a real-life scenario, the influence of estuary bank will depend on the characteristics of oil slicks and on the type of shoreline (Tri et al. 2015).

Table 5.6: Summary of maximum oil slick length (km) and displacement (km) from point of release, as measured 48 hours after the spill.

Scenario	Maximum slick length	Upstream displacement	Downstream displacement	Overall distance
L1_a LW	9.86	19.85	7.21	27.06
L1_b LW	10.42	20.29	7.21	27.51
L1_c LW	11.26	20.06	7.82	27.88
L1_d LW	14.26	20.06	9.04	29.10
L1_e LW	16.33	20.41	10.92	31.33
L2_a HW	5.74	1.20	16.31	17.51
L2_b HW	7.66	1.42	18.00	19.42
L2_c HW	11.78	1.34	22.59	23.93
L2_d HW	12.08	1.38	22.78	24.16
L2_e HW	15.51	1.49	25.68	27.17
L2_a LW	7.37	11.82	4.36	16.18
L2_b LW	5.39	11.86	1.75	13.61
L2_c LW	7.22	12.06	1.85	13.91

L2_d LW	15.05	11.72	10.48	22.20
L2_e LW	18.20	12.62	13.10	25.72

5.4.3 Interaction with the Edge of the Computational Grid (Oil Beaching)

It was observed that the risk of beaching increases as the estuary becomes narrower. However, the results depict the complexity in predicting the likelihood of beaching in a large macro-tidal estuary (Table 5.3). It is clear that the likelihood of beaching is dependent on the oil release location, the geometry of the estuary and current magnitude and direction. These factors also determine the time of first contact with the bank. Oil spill responders will need to be aware of these factors to effectively deal with oil spills in an estuarine environment.

5.5 LIMITATIONS

To achieve the study aim this chapter assesses the influence of varying lateral oil release locations on oil slick transport in tide-dominated estuaries. Findings from this study may be unique to this environment. Considering the complexity of estuaries, the findings in this chapter may not be suitable for other estuarine environments. Further work can aim to extend results to other estuarine systems.

5.6 CONCLUSION

Until now, the influence of lateral oil release locations on oil slick transport in a large macro-tidal estuary has never been explicitly investigated. To address this gap in knowledge, oil slick transport is simulated for 10 release locations in the Humber Estuary. These simulations show that for this large well-mixed macro-tidal estuary:

(a) oil spills released further downstream develop larger oil slicks and travel greater distances than oil spills released upstream due to the difference in current magnitude (also see Chapter 3);

(b) oil slicks remain denser (more concentrated) as the point of release is further upstream;

(c) current direction plays an important role in the spreading of oil slicks;

(d) estuary geometry influences oil slick transport as it dictates current speed and direction;

(e) current magnitude is the key determinant of difference in dynamics between oil slicks released along the estuary length;

(f) while differences in lateral current speed and direction are key determinants of the differences in the dynamics of oil slicks released along the estuary width;

(g) proximity to the river bank influences oil slick transport, as lower flow velocities distort oil slick movement resulting in the formation of longer slicks. However, in a real-life scenario, the influence of estuary bank will depend on the characteristics of oil slicks and on the type of shoreline; and

(h) the likelihood of beaching is dependent on the oil release location, the geometry of the estuary and current magnitude and direction.

The implications of these findings for operational oil spill response are: (a) the need to be aware of current direction in different segments of the estuary and how it affects oil slicks from a particular release location; (b) need to take cognisance of the interaction between oil slicks and estuary bank and how it influences overall distance travelled by oil slicks; (c) the risk of beaching increases as the estuary becomes narrower; and (d) the need to understand the interaction between oil release location, the geometry of the estuary and current magnitude and direction to effectively deal with oil slicks in a tide-dominated estuary.

Based on the findings in this chapter as well as in Chapter 3 and 4, the next chapter (Chapter 6) will provide answers to the research questions (Section 1.2) and also recommendations for advanced research.

CHAPTER 6

6. CONCLUSION AND RECOMMENDATION

This chapter reviews the findings made in this study and proposes recommendations for advanced research.

6.1 CONCLUSION

Oil spills are a source of worldwide marine pollution due to growing energy demand and consumption. The demand for energy and the importance of estuaries (as they provide a free connection to the open ocean) have resulted in an increased risk of oil spill pollution in estuaries. Despite the significant risk oil spills present to estuaries, a survey of oil spill literature reveal that estuaries have received much less research attention compared to coastal and pelagic environment. Seasonal freshwater discharge variation and projected climatic conditions are common estuarine processes. However, until now, no study has assessed the influence of these processes on oil spill transport in estuaries. To address this gap, this study developed a range of oil spill models to understand the influence of prevailing advection mechanisms on oil spills in a tide-dominated estuary. Due to the unpredictability of oil spills, this study also assessed the influence of oil release location on oil slick transport. Geographically, tide-dominated estuaries are common around the globe. As a result, findings from this study is expected to have a global impact, enabling adequate management and control, and sustainable development.

This study provided insight into the complexities of estuary classification (Section 2.1) and reviewed the processes that influence oil spill behaviour in estuaries (Section 2.2;

2.3). Also, this study evaluated the current state of hydrodynamic and oil spill modelling, as well as, several hydrodynamic tools suitable for modelling natural processes within the estuarine environment (Section 2.4; 2.5). Several oil spill modelling tools were also evaluated. Consequently, this study was able to outline the current state of hydrodynamic modelling of estuarine processes and oil spill modelling as an indication of the areas where future development will occur (Section 2.6).

For the first time, a detailed analysis of oil spill transport in a large tide-dominated estuary was presented. Using the Humber Estuary as a case study, this study aimed to assess the influence of tidal cycles, seasonal freshwater discharge variability, sea level rise, projected 21st century river flow and oil release location on the transport of hypothetical oil spills. The research aim was achieved by providing answers to the following research questions:

1. How will seasonal variability of river discharge influence oil spill trajectory in a tide-dominated estuary?
2. What will be the influence of projected climatic condition on oil spill trajectory in a tide-dominated estuary?
3. How will varying lateral points of release influence oil spill trajectory in a tide-dominated estuary?

TELEMAC3D was employed to develop hydrodynamic models that represent the behaviour of the Humber Estuary in summer and winter. Satisfactory model performance (R^2 = 0.883 and 0.852 for summer and winter respectively) was attained using constant discharge at the river boundary. The models were validated against measured tidal height data at Immingham station for summer and winter, also with a satisfactory agreement (R^2 = 0.912 and 0.848 for summer and winter respectively). The oil spill model for the Humber Estuary was developed with the TELEMAC oil spill module.

In addressing the research gaps (Section 1.2), the following findings were made, some of which have not been demonstrated until now:

1. **How will seasonal variability of river discharge influence oil spill trajectory in a tide-dominated estuary?**
    a. because of seasonal variation in river discharge, winter slicks released at high water did not exhibit any upstream displacement over repeated tidal cycles, while summer slicks travelled upstream into the estuary over repeated tidal cycles (Section 3.4.3);
    b. there is a statistically significant ($P < 0.05$) difference in the influence of hydrodynamic conditions (seasonal discharge variation, water level and tidal range) on oil slick impacted area, length and distance travelled (Section 3.4.4);
    c. the tidal range has a key influence on oil slick impacted area, with spring tide slicks being 125% bigger than neap tide slicks, on average (Section 3.4.2);
    d. seasonal variations in river discharge have a significantly smaller impact on oil slick impacted area, with summer spills covering an area of only 4% larger than winter spills on average (Section 3.4.1);
    e. although smaller in impacted area, winter slicks travel farther (12% on average) and are narrower than summer slicks (Section 3.4.1);
    f. the influence of seasonal discharge on oil slick spreading is dependent on the time of release within a tidal cycle (Section 3.4.1); and

g. the possibility of oil beaching on the banks of the estuary exposes environmental risks, with up to 24.6 km of shoreline affected in the simulations (Section 3.4.5).
h. oil slicks are likely to remain in the estuary within the first 48 hours (Section 3.4.1);
i. oil spills released further downstream develop larger oil slicks and move over greater distances than oil spills released upstream (Section 3.4.2);
j. the farthest upstream displacement of the oil slick occurs for spills released at low water during summer spring tide conditions (e.g. 13 km for L2; Section 3.4.1); and
k. the farthest downstream displacement of the oil slick occurs for spills released at high water during winter spring tide conditions (e.g. 26 km for L2; Section 3.4.1).

2. **What will be the influence of projected climatic condition on oil spill trajectory in a tide-dominated estuary?**
   a. the influence of sea level rise on oil slick impacted area, length and overall distance travelled is relatively insignificant (Section 4.4.1);
   b. the influence of short-term sea level rise on oil slick displacement varies from the influence of long-term sea level rise under summer conditions. This could possibly be due to the complex effect of sea level on tidal dynamics. However, the influence of sea level rise on oil slick displacement is consistent under winter conditions, suggesting that the influence of sea level rise on oil slicks displacement is influenced by seasonal variations (Section 4.4.1);

c. projected changes in river discharge have relatively insignificant influence on oil slick impacted area, length and overall distance travelled (Section 4.4.2); and

d. considering sea level rise and projected river flow (SLR + Flow) scenario, oil slicks were further displaced upstream by 0.35 km and downstream displacement was reduced by 1.33 km in summer while winter slicks were further displaced by 0.4 km. In comparison to the projected flow scenarios, long-term sea level rise mitigates the impact of projected river flow on oil slick spreading (Section 4.4.2).

e. under summer conditions, long-term sea level rise (2100) transports the entire oil slick further upstream, thus encouraging upstream displacement and discouraging downstream displacement (Section 4.4.1);

f. under winter conditions, long-term sea level rise (2100) discourages further downstream displacement of oil sick (Section 4.4.1);

g. an 80% decrease in summer river flow led to oil slicks displacement of 0.6 km further upstream and reduced downstream displacement by 0.14 km (Section 4.4.2); and

h. a 25% increase in winter river flows led to oil slicks displacement of 0.68 km further downstream (Section 4.4.2).

3. **How will varying lateral points of release influence oil spill trajectory in a tide-dominated estuary?**

a. current magnitude is the key determinant of difference in dynamics between oil slicks released along the estuary length (Section 5.4.1);

b. while differences in lateral current speed and direction are key determinants of the differences in the dynamics of oil slick released along the estuary width (Section 5.4.2); and

c. proximity to the river bank influences oil slick transport, as lower flow velocities distort oil slick movement resulting in the formation of longer slicks. However, in a real-life scenario, the influence of estuary bank will depend on the characteristics of oil slicks and on the type of shoreline (Section 5.4.3).

d. oil spills released further downstream develop larger oil slicks and travel greater distances than oil spills released upstream due to the difference in current magnitude (Section 5.4.1);

e. oil slicks remain denser (more concentrated) as the point of release is further upstream (Section 5.4.1);

f. current direction plays an important role in the spreading of oil slicks (Section 5.4.2);

g. estuary geometry influences oil slick transport as it dictates current speed and direction (Section 5.4.2); and

h. the likelihood of beaching is dependent on the oil release location, the geometry of the estuary and current magnitude and direction (Section 5.4.3).

6.2 IMPLICATIONS OF FINDINGS

This study is the first to characterise the influence of environmental factors particularly seasonal freshwater flow variations, projected climatic conditions (sea level rise, projected 21st century river flow) and oil release location on oil spill transport in a tide-dominated estuary. The research findings are expected to have global implications on oil spill response as tide-dominated estuaries as well as these environmental factors are common around the globe.

The implication of this research to operational oil spill response are:

(a) the need to take cognisance of time of oil release within a tidal period (Chapter 3);
(b) the need to understand how the interaction of river discharge and tidal range influences oil slick dynamics, as this will aid responders in assessing the likely oil trajectories (Chapter 3);
(c) the need to be aware of axial and lateral variations in current magnitude and direction in the estuary and how it affects oil slicks from a release location (Chapter 5);
(d) need to take cognisance of the interaction between oil slicks and estuary bank and how it influences oil slicks overall travel distance (Chapter 5);
(e) recognise that the risk of beaching increases as the estuary becomes narrower (Chapter 5); and
(f) the need to understand the interaction between oil release location, the geometry of the estuary and current magnitude and direction to effectively deal with oil slicks in a tide-dominated estuary (Chapter 5).

Furthermore, this study can aid in the preparation of a robust plan for effectively dealing with oil spills in the Humber Estuary.

6.3 RECOMMENDATION FOR FURTHER STUDIES

Despite the research depth, there are more areas that can still be explored.

(a) This study considered instantaneous oil slick release. Further studies can be undertaken with continuous oil spill release.

(b) In some scenarios, oil slicks were observed to leave the computational domain. Further studies can be undertaken with an increased computational domain, to understand the influence of the North Sea current magnitudes and directions on the oil slicks and the likelihood of re-entering the estuary.

(c) Due to limited river discharge data, the hydrodynamic model was developed using constant river discharge data at the fluvial boundaries. Comparative studies can be undertaken using high-resolution river discharge data to drive the hydrodynamic model.

(d) To assess the influence of sea level rise on oil spill dynamics, a sediment model can be coupled to the hydrodynamic model to take cognisance of change in water depth. This might reveal how the relationship between sea level rise and water depth influences oil spill dynamics.

(e) The influence of flooding and storm events on oil slick transport can also be explored.

(f) Findings from this study may be unique to tide-dominated estuaries. Considering the complexity of estuaries, further work can aim to extend results to other estuarine systems.

REFERENCES

Abadie, S., Morichon, D., Grilli, S., and Glockner, S. (2010) 'Numerical Simulation of Waves Generated by Landslides using a Multiple-Fluid Navier–Stokes Model'. *Coastal Engineering* [online] 57 (9), 779-794. available from <http://www.sciencedirect.com/science/article/pii/S0378383910000396>

Abascal, A. J., Castanedo, S., Núñez, P., Mellor, A., Clements, A., Pérez, B., Cárdenas, M., Chiri, H., and Medina, R. (2017) 'A High-Resolution Operational Forecast System for Oil Spill Response in Belfast Lough'. *Marine Pollution Bulletin* 114 (1), 302-314

Abascal, A. J., Castanedo, S., Medina, R., and Liste, M. (2010) 'Analysis of the Reliability of a Statistical Oil Spill Response Model'. *Marine Pollution Bulletin* 60 (11), 2099-2110

Abascal, A. J., Castanedo, S., Mendez, F. J., Medina, R., and Losada, I. (2009) 'Calibration of a Lagrangian Transport Model using Drifting Buoys Deployed during the Prestige Oil Spill'. *Journal of Coastal Research* 25 (1), 80-90

ABPmer, WL, and Delft Hydraulics (2002) *Humber Estuary Shoreline Management Plan - Stage 2*: Hydrodynamic Model Calibration Report, R.1004

Adeboye, O. B., Schultz, B., Adekalu, K. O., and Prasad, K. C. (2019) 'Performance Evaluation of AquaCrop in Simulating Soil Water Storage, Yield, and Water Productivity of Rainfed Soybeans (Glycine Max L. Merr) in Ile-Ife, Nigeria'. *Agricultural Water Management* [online] 213, 1130-1146. available from <http://www.sciencedirect.com/science/article/pii/S0378377418305195>

Afenyo, M., Khan, F., Veitch, B., and Yang, M. (2016b) 'Modeling Oil Weathering and Transport in Sea Ice'. *Marine Pollution Bulletin* 107 (1), 206-215

Afenyo, M., Veitch, B., and Khan, F. (2016a) 'A State-of-the-Art Review of Fate and Transport of Oil Spills in Open and Ice-Covered Water'. *Ocean Engineering* 119, 233-248

Ahlstrom, S. W. (1975) *A Mathematical Model for Predicting the Transport of Oil Slicks in Marine Waters* . Richland, Wash., USA: Battelle Pacific Northwest Laboratories

Al Shami, A., Harik, G., Alameddine, I., Bruschi, D., Garcia, D. A., and El-Fadel, M. (2017) 'Risk Assessment of Oil Spills Along the Mediterranean Coast: A Sensitivity Analysis of the Choice of Hazard Quantification'. *Science of the Total Environment* 574, 234-245

Al-Rabeh, A. H., Lardner, R. W., and Gunay, N. (2000) 'Gulfspill Version 2.0: A Software Package for Oil Spills in the Arabian Gulf'. *Environmental Modelling & Software* 15 (4), 425-442

Al-Rabeh, A. H., Cekirge, H. M., and Gunay, N. (1989) 'A Stochastic Simulation Model of Oil Spill Fate and Transport'. *Applied Mathematical Modelling* 13 (6), 322-329

Amir-Heidari, P. and Raie, M. (2018) 'Probabilistic Risk Assessment of Oil Spill from Offshore Oil Wells in Persian Gulf'. *Marine Pollution Bulletin* [online] 136, 291-299. available from <http://www.sciencedirect.com/science/article/pii/S0025326X1830554X>

Anifowose, B., Lawler, D. M., van der Horst, D., and Chapman, L. (2016) 'A Systematic Quality Assessment of Environmental Impact Statements in the Oil and Gas Industry'. *Science of the Total Environment* [online] 572, 570-585. available from <http://www.sciencedirect.com/science/article/pii/S0048969716315297>

Anifowose, B., Lawler, D. M., van der Horst, D., and Chapman, L. (2014) 'Evaluating Interdiction of Oil Pipelines at River Crossings using Environmental Impact Assessments'. *Area* 46 (1), 4-17

Archer, A. W. (2013) 'World's Highest Tides: Hypertidal Coastal Systems in North America, South America and Europe'. *Sedimentary Geology* [online] 284-285, 1-25. available from <http://www.sciencedirect.com/science/article/pii/S0037073812003326>

Ariana, D., Kusmana, C., and Setiawan, Y. (2017) 'Study of Sea Level Rise using Satellite Altimetry Data in the Sea of Dumai, Riau, Indonesia'. *Journal of Geomatics and Planning* 4 (1), 75-82

ASCE (1996) 'State-of-the-Art Review of Modeling Transport and Fate of Oil Spills'. *Journal of Hydraulic Engineering* 122 (11), 594-609

Ata, R., Goeury, C., and Hervouet, J. (2014) *TELEMAC MODELLING SYSTEM: 2D Hydrodynamics TELEMAC-2D Software Releaase 7.0 User Manual*. National Hydraulics and Environment Laboratory, Numerical and Physical Modelling in River and Coastal Hydrodynamics: EDF R&D, France: EDF R&D

Azevedo, A., Oliveira, A., Fortunato, A. B., Zhang, J., and Baptista, A. M. (2014) 'A Cross-Scale Numerical Modeling System for Management Support of Oil Spill Accidents'. *Marine Pollution Bulletin* 80 (1–2), 132-147

Badejo, O. and Nwilo, P. (2004) 'Management of Oil Spill Dispersal Along the Nigerian Coastal Areas'

Bandara, U. C., Yapa, P. D., and Xie, H. (2011) 'Fate and Transport of Oil in Sediment Laden Marine Waters'. *Journal of Hydro-Environment Research* 5 (3), 145-156

Bárcena, J. F., Camus, P., García, A., and Álvarez, C. (2015) 'Selecting Model Scenarios of Real Hydrodynamic Forcings on Mesotidal and Macrotidal Estuaries Influenced by River Discharges using K-Means Clustering'. *Environmental Modelling & Software* 68, 70-82

Beegle-Krause, C. J. (ed.) (2001) *Internatonal Oil Spill Conference*. 'General Noaa Oil Modeling Environment (Gnome): A New Spill Trajectory Model': American Petroleum Institute

Bernabeu, A. M., Fernández-Fernández, S., and Rey, D. (2016) 'A Theoretical Model to Estimate the Oil Burial Depth on Sandy Beaches: A New Oil Spill Management Tool'. *Marine Pollution Bulletin* 109 (1), 361-372

Berntsen, J., Thiem, Ø., and Avlesen, H. (2015) 'Internal Pressure Gradient Errors in σ-Coordinate Ocean Models in High Resolution Fjord Studies'. *Ocean Modelling* 92, 42-55

Berry, A., Dabrowski, T., and Lyons, K. (2012) 'The Oil Spill Model OILTRANS and its Application to the Celtic Sea'. *Marine Pollution Bulletin* 64 (11), 2489-2501

Bhakta, D., Meetei, W. A., Vaisakh, G., Das, S. K., and Manna, R. K. (2018) 'Impacts of Water Regulation on Tenualosa Ilisha in the Narmada Estuary, Gujarat, India'. *Journal of Fisheries* 6 (1), 563-568

Billy, J., Chaumillon, E., Féniès, H., and Poirier, C. (2012) 'Tidal and Fluvial Controls on the Morphological Evolution of a Lobate Estuarine Tidal Bar: The Plassac Tidal Bar in the Gironde Estuary (France)'. *Geomorphology* [online] 169-170, 86-97. available from <http://www.sciencedirect.com/science/article/pii/S0169555X12001882>

Bindoff, N. L., Willebrand, J., Artale, V., Cazenave, A., Gregory, J. M., Gulev, S., Hanawa, K., Le Quéré, C., Levitus, S. N.,Y., Shum, C. K., Talley, L. D., and Unnikrishnan, A. S. (2007) 'Observations: Oceanic Climate Change and Sea Level'. in *Climate Change 2007: The Physical Science Basis. Contribution of Working Group I to the Fourth Assessment Report of the Intergovernmental Panel on Climate Change*. ed. by Solomon, S., Qin, D., Manning, M., Chen, Z., Marquis, M., Averyt, K. B., Tignor, M., and Miller, H. L. Cambridge, United Kingdom and New York, NY, USA: Cambridge University Press, 387-432

Boehm, P. D., Fiest, D. L., Mackay, D., and Peterson, S. (1982) 'Physical-Chemical Weathering of Petroleum Hydorcarbons from the Ixtoc I Blowout: Chemical Measurements and a Weathering Model'. *Environmental Science & Technology* 16 (8), 498-505

Bolaños, R., Brown, J. M., and Souza, A. J. (2014) 'Wave–current Interactions in a Tide Dominated Estuary'. *Continental Shelf Research* 87, 109-123

Bonilla, S., Conde, D., Aubriot, L., and Pérez, M. (2005) 'Influence of Hydrology on Phytoplankton Species Composition and Life Strategies in a Subtropical Coastal

Lagoon Periodically Connected with the Atlantic Ocean'. *Estuaries* 28 (6), 884-895

Botelho, D., Imberger, J., Dallimore, C., and Hodges, B. R. (2009) 'A hydrostatic/Non-Hydrostatic Grid-Switching Strategy for Computing High-Frequency, High Wave Number Motions Embedded in Geophysical Flows'. *Environmental Modelling & Software* 24 (4), 473-488

Boufadel, M. C., Du, K., Kaku, V., and Weaver, J. (2007) 'Lagrangian Simulation of Oil Droplets Transport due to Regular Waves'. *Environmental Modelling & Software* 22 (7), 978-986

Boyes, S. and Elliott, M. (2006) 'Organic Matter and Nutrient Inputs to the Humber Estuary, England'. *Marine Pollution Bulletin* [online] 53 (1), 136-143. available from <http://www.sciencedirect.com/science/article/pii/S0025326X0500398X>

BP (2011) *Brent* [online] available from <https://www.bp.com/en/global/trading/crude-oil-and-refined-products/crudes/europe/brent.html> [04/10 2018]

Brakstad, O. G. and Faksness, L. (eds.) (2000) *SPE International Conference on Health, Safety and Environment in Oil and Gas Exploration and Production*. 'Biodegradation of Water-Accommodated Fractions and Dispersed Oil in the Seawater Column'. held 26-28 June at Stavanger, Norway: Society of Petroleum Engineers

Brière, C., Abadie, S., Bretel, P., and Lang, P. (2007) 'Assessment of TELEMAC System Performances, a Hydrodynamic Case Study of Anglet, France'. *Coastal Engineering* 54 (4), 345-356

Briggs, G. A. (1984) 'Plume Rise and Buoyancy Effects.'. *In: Randerson, D., (Ed.) Atmospheric Science and Power Production, U.S. Dept. of Energy Technical Information Center, Springfield, VA, USA*

Broomans, P. (2002) *Numerical Accuracy in Solution of the Shallow-Water Equations*. [online] Master thesis or dissertation. Delft, Netherlands: Delft University of Technology

Brown, J. M. and Davies, A. G. (2010) 'Flood/ebb Tidal Asymmetry in a Shallow Sandy Estuary and the Impact on Net Sand Transport'. *Geomorphology* 114 (3), 431-439

Brown, J. M. and Davies, A. G. (2009) 'Methods for Medium-Term Prediction of the Net Sediment Transport by Waves and Currents in Complex Coastal Regions'. *Continental Shelf Research* 29 (11–12), 1502-1514

Brown, J. M., Bolaños, R., and Wolf, J. (2011) 'Impact Assessment of Advanced Coupling Features in a tide–surge–wave Model, POLCOMS-WAM, in a Shallow Water Application'. Journal of Marine Systems [online] 87 (1), 13-24. available from <http://www.sciencedirect.com/science/article/pii/S0924796311000352>

Burn, D. H., Hannaford, J., Hodgkins, G. A., Whitfield, P. H., Thorne, R., and Marsh, T. (2012) 'Reference Hydrologic Networks II. using Reference Hydrologic Networks to Assess Climate-Driven Changes in Streamflow'. *Hydrological Sciences Journal* 57 (8), 1580-1593

Cameron, W. M. and Pritchard, D. W. (1963) 'Estuaries'. in *The Sea. Volume 2*. ed. by Hill, M. N. New York: John Wiley & Sons, 306-324

Candy, A. S. (2017) 'An Implicit Wetting and Drying Approach for Non-Hydrostatic Baroclinic Flows in High Aspect Ratio Domains'. *Advances in Water Resources* 102, 188-205

Carrère, L., Lyard, F., Cancet, M., Guillot, A., and Roblou, L. (eds.) (2013) *FES 2012: A New Global Tidal Model Taking Advantage of nearly 20 Years of Altimetry*. '20 Years of Progress in Radar Altimatry'. held 24-29 September at Venice, Italy: ESA (European Space Agency)

Castanedo, S., Medina, R., Losada, I., Vidal, C., Mendez, F. J., Osorio, A., Juanes, J. A., and Puente, A. (2006) 'The Prestige Oil Spill in Cantabria (Bay of Biscay). Part I: Operational Forecasting System for Quick Response, Risk Assessment, and Protection of Natural Resources'. *Journal of Coastal Research* 22 (6), 1474-1489

Cave, R. R., Ledoux, L., Turner, K., Jickells, T., Andrews, J. E., and Davies, H. (2003) 'The Humber Catchment and its Coastal Area: From UK to European Perspectives'. *Science of the Total Environment* [online] 314-316 (Supplement C), 31-52. available from <http://www.sciencedirect.com/science/article/pii/S0048969703000937>

Cazenave, A. and Nerem, R. S. (2004) 'Present-Day Sea Level Change: Observations and Causes'. *Reviews of Geophysics* 42 (3)

Cekirge, H. M., Koch, M., Long, C., Giammona, C. P., Binkley, K., Engelhardt, R., and Jamail, R. (1995) 'State-of-the-Art Techniques in Oil Spill Modeling'. *International Oil Spill Conference Proceedings* 1995 (1), 66-72

Chai, T. and Draxler, R. R. (2014) 'Root Mean Square Error (RMSE) Or Mean Absolute Error (MAE)? – Arguments Against Avoiding RMSE in the Literature'. *Geoscientific Model Development* 7 (3), 1247-1250

Chao, X., Shankar, N. J., and Cheong, H. F. (2001) 'Two- and Three-Dimensional Oil Spill Model for Coastal Waters'. *Ocean Engineering* 28 (12), 1557-1573

Chassignet, E. P., Hurlburt, H. E., Smedstad, O. M., Halliwell, G. R., Hogan, P. J., Wallcraft, A. J., Baraille, R., and Bleck, R. (2007) 'The HYCOM (HYbrid Coordinate Ocean Model) Data Assimilative System'. *Journal of Marine Systems* 65 (1–4), 60-83

Chassignet, E. P., Hurlburt, H., Smedstad, O. M., Halliwell, G., Wallcraft, A. J., Metzger, E. J., Blanton, B., Lozano, C., Rao, D., Hogan, P., and Srinivasan, A. (2006) 'Generalized Vertical Coordinates for Eddy-Resolving Global and Coastal Ocean Forecasts'. *Oceanography* 19 (1), 118-129

Chen, H., An, W., You, Y., Lei, F., Zhao, Y., and Li, J. (2015) 'Numerical Study of Underwater Fate of Oil Spilled from Deepwater Blowout'. *Ocean Engineering* 110, Part A, 227-243

Chen, J., Zhang, W., Wan, Z., Li, S., Huang, T., and Fei, Y. (2019) 'Oil Spills from Global Tankers: Status Review and Future Governance'. *Journal of Cleaner Production* [online] 227, 20-32. available from <http://www.sciencedirect.com/science/article/pii/S095965261931090X>

Cheng, Y. and Andersen, O. B. (2011) 'Multimission Empirical Ocean Tide Modeling for Shallow Waters and Polar Seas'. *Journal of Geophysical Research: Oceans* 116 (C11)

Cheng, C., Shalabh, , and Garg, G. (2014) 'Coefficient of Determination for Multiple Measurement Error Models'. *Journal of Multivariate Analysis* [online] 126, 137-152. available from <http://www.sciencedirect.com/science/article/pii/S0047259X14000141>

Cheng, P., Valle-Levinson, A., and de Swart, H. E. (2010) 'Residual Currents Induced by Asymmetric Tidal Mixing in Weakly Stratified Narrow Estuaries'. *Journal of Physical Oceanography* 40 (9), 2135-2147

Cheng, Y., Li, X., Xu, Q., Garcia-Pineda, O., Andersen, O. B., and Pichel, W. G. (2011) 'SAR Observation and Model Tracking of an Oil Spill Event in Coastal Waters'. *Marine Pollution Bulletin* 62 (2), 350-363

Chernetsky, A. S., Schuttelaars, H., and Talke, S. A. (2010) 'The Effect of Tidal Asymmetry and Temporal Settling Lag on Sediment Trapping in Tidal Estuaries'. *Ocean Dynamics* 60 (5), 1219-1241

Cheviet, C., Violeau, D., and Guesmia, M. (2002) 'Numerical Simulation of Cohesive Sediment Transport in the Loire Estuary with a Three-Dimensional Model Including New Parameterisations'. Proceedings in Marine Science [online] 5, 529-543. available from <http://www.sciencedirect.com/science/article/pii/S1568269202800389>

Chiu, C., Huang, C., Wu, L., Zhang, Y. J., Chuang, L. Z., Fan, Y., and Yu, H. (2018) 'Forecasting of Oil-Spill Trajectories by using SCHISM and X-Band Radar'. *Marine Pollution Bulletin* [online] 137, 566-581. available from <http://www.sciencedirect.com/science/article/pii/S0025326X18307720>

Choi, Y., Takahashi, K., Abe, A., Nishio, S., and Sou, A. (2013) 'Simulation of Deepwater Horizon Oil Spill using Coupled Atmosphere-Ocean Model'. *Marine Engineering* 48 (1), 105-109

Christierson, B. v., Vidal, J., and Wade, S. D. (2012) 'Using UKCP09 Probabilistic Climate Information for UK Water Resource Planning'. *Journal of Hydrology* [online] 424-425, 48-67. available from <http://www.sciencedirect.com/science/article/pii/S0022169411009036>

Chu-Agor, M. L., Muñoz-Carpena, R., Kiker, G., Emanuelsson, A., and Linkov, I. (2011) 'Exploring Vulnerability of Coastal Habitats to Sea Level Rise through Global Sensitivity and uncertainty Analyses'. *Environmental Modelling & Software* [online] 26 (5), 593-604. available from <http://www.sciencedirect.com/science/article/pii/S136481521000321X>

Church, J. A., Clark, P. U., Cazenave, A., Gregory, J. M., Jevrejeva, S., Levermann, A., Merrifield, M. A., Milne, G. A., Nerem, R. S., Nunn, P. D., Payne, A. J., Pfeffer, W. T., Stammer, D., and Unnikrishnan, A. S. (2013) *2013: Sea Level Change. in: Climate Change 2013: The Physical Science Basis. Contribution of Working Group I to the Fifth Assessment Report of the Intergovernmental Panel on Climate Change [Stocker, T.F., D. Qin, G.-K. Plattner, M. Tignor, S.K. Allen, J. Boschung, A. Nauels, Y. Xia, V. Bex and P.M. Midgley (Eds.)]*. Cambridge, United Kingdom and New York, NY, USA: Cambridge University Press

Cooper, J. A. G. (2002) 'The Role of Extreme Floods in Estuary-Coastal Behaviour: Contrasts between River- and Tide-Dominated Microtidal Estuaries'. *Sedimentary Geology* 150 (1–2), 123-137

Cooper, J. A. G. (2001) 'Geomorphological Variability among Microtidal Estuaries from the Wave-Dominated South African Coast'. *Geomorphology* [online] 40 (1), 99-122. available from <http://www.sciencedirect.com/science/article/pii/S0169555X01000393>

Coppini, G., De Dominicis, M., Zodiatis, G., Lardner, R., Pinardi, N., Santoleri, R., Colella, S., Bignami, F., Hayes, D. R., Soloviev, D., Georgiou, G., and Kallos, G. (2011) 'Hindcast of Oil-Spill Pollution during the Lebanon Crisis in the Eastern Mediterranean, July–August 2006'. *Marine Pollution Bulletin* 62 (1), 140-153

Cowley, P. D., Whitfield, A. K., and Bell, K. N. I. (2001) 'The Surf Zone Ichthyoplankton Adjacent to an Intermittently Open Estuary, with Evidence of Recruitment during Marine Overwash Events'. *Estuarine, Coastal and Shelf Science* [online] 52 (3), 339-348. available from <http://www.sciencedirect.com/science/article/pii/S0272771400907108>

Csanady, G. (1973) *Turbulent Diffusion in the Environment*. Dordrecht, Holland: D. Reidel Publishing Company

Cucco, A., Sinerchia, M., Ribotti, A., Olita, A., Fazioli, L., Perilli, A., Sorgente, B., Borghini, M., Schroeder, K., and Sorgente, R. (2012) 'A High-Resolution Real-Time Forecasting System for Predicting the Fate of Oil Spills in the Strait of Bonifacio (Western Mediterranean Sea)'. *Marine Pollution Bulletin* 64 (6), 1186-1200

Dai, Z., Liu, J. T., Wei, W., and Chen, J. (2014) 'Detection of the Three Gorges Dam Influence on the Changjiang (Yangtze River) Submerged Delta'. *Scientific Reports* 4 (1)

Dalrymple, R. W. and Choi, K. (2007) 'Morphologic and Facies Trends through the fluvial–marine Transition in Tide-Dominated Depositional Systems: A Schematic Framework for Environmental and Sequence-Stratigraphic Interpretation'. *Earth-Science Reviews* [online] 81 (3), 135-174. available from <http://www.sciencedirect.com/science/article/pii/S0012825206001413>

Dalrymple, R. W., Zaitlin, B. A., and Boyd, R. (1992) 'Estuarine Facies Models; Conceptual Basis and Stratigraphic Implications'. *Journal of Sedimentary Research* 62 (6), 1130-1146

Darby, S. E., Alabyan, A. M., and Van de Wiel, M. J. (2002) 'Numerical Simulation of Bank Erosion and Channel Migration in Meandering Rivers'. *Water Resources Research* 38 (9), 2-1-2-21

Davies, J. L. (1964) 'A Morphogenic Approach to World Shorelines'. *Zeitschrift Für Geomorphologie* 8, 27-42

De Dominicis, M., Bruciaferri, D., Gerin, R., Pinardi, N., Poulain, P. M., Garreau, P., Zodiatis, G., Perivoliotis, L., Fazioli, L., Sorgente, R., and Manganiello, C. (2016) 'A Multi-Model Assessment of the Impact of Currents, Waves and Wind in Modelling Surface Drifters and Oil Spill'. *Deep Sea Research Part II: Topical Studies in Oceanography* 133, 21-38

De Dominicis, M., Pinardi, N., Zodiatis, G., and Lardner, R. (2013b) 'MEDSLIK-II, a Lagrangian Marine Surface Oil Spill Model for Short-Term Forecasting – Part 1: Theory'. *Geoscientific Model Development* 6 (6), 1851-1869

De Dominicis, M., Pinardi, N., Zodiatis, G., and Archetti, R. (2013a) 'MEDSLIK-II, a Lagrangian Marine Surface Oil Spill Model for Short-Term Forecasting – Part 2: Numerical Simulations and Validations'. *Geoscientific Model Development* 6 (6), 1871-1888

DeCola, E., Fletcher, S., Higman, B., Mattox, A., Popovich, M., and Robertson, T. (2012) *Oil Spill Response Gap and Response Capacity Analysis for Proposed Northern Gateway Tanker Oil Spills in Open Water and Protected Water Operating Environments*: Nuka Research and Planning Group, LLC

Delgado, L., Kumzerova, E., and Martynov, M. (2006) 'Simulation of Oil Spill Behavior and Response Operations in PISCES'. *WIT Transactions on Ecology and the Environment* 88 (279), 292

Delvigne, G. A. L. and Sweeney, C. E. (1988) 'Natural Dispersion of Oil'. *Oil and Chemical Pollution* [online] 4 (4), 281-310. available from <http://www.sciencedirect.com/science/article/pii/S0269857988800030>

Di Martino, B. and Peybernes, M. (2007) 'Simulation of an Oil Slick Movement using a Shallow Water Model'. *Mathematics and Computers in Simulation* 76 (1-3), 155-160

Dolgopolova, E. N. and Isupova, M. V. (2010) 'Classification of Estuaries by Hydrodynamic Processes'. *Water Resources* 37 (3), 268-284

Dong, L., Su, J., Ah Wong, L., Cao, Z., and Chen, J. (2004) 'Seasonal Variation and Dynamics of the Pearl River Plume'. *Continental Shelf Research* [online] 24 (16), 1761-1777. available from <http://www.sciencedirect.com/science/article/pii/S0278434304001219>

Douglas, G. S., Owens, E. H., Hardenstine, J., and Prince, R. C. (2002) 'The OSSA II Pipeline Oil Spill: The Character and Weathering of the Spilled Oil'. *Spill Science & Technology Bulletin* 7 (3–4), 135-148

Dublin-Green, C. O. (1994) *Benthic Foraminifera as Pollution Indicators in the Bonny Estuary*. Victoria Island, Lagos: Nigeria Institute for Oceanography and Marine Research

Durgut, İ. and Reed, M. (2017) 'Modeling Spreading of Oil Slicks Based on Random Walk Methods and Voronoi Diagrams'. *Marine Pollution Bulletin* 118 (1-2), 93-100

Edwards, A. M. C. and Winn, P. S. J. (2006) 'The Humber Estuary, Eastern England: Strategic Planning of Flood Defences and Habitats'. *Marine Pollution Bulletin* [online] 53 (1), 165-174. available from <http://www.sciencedirect.com/science/article/pii/S0025326X05004005>

Egbert, G. D. and Erofeeva, S. Y. (2002) 'Efficient Inverse Modeling of Barotropic Ocean Tides'. *Journal of Atmospheric and Oceanic Technology* 19 (2), 183-204

Eke, C. D. and Anifowose, B. (eds.) (2017) *Oil Spill Trajectory Simulation for the Clair Oilfield, Faroe Shetland Channel, United Kingdom Continental Shelf*. 'SPE Health, Safety, Security, Environment, & Social Responsibility Conference - North America'. held 18 - 20 April at New Orleans, Louisianna. USA: Society of Petroleum Engineers

Elliott, A. J. (1986) 'Shear Diffusion and the Spread of Oil in the Surface Layers of the North Sea'. *Ocean Dynamics* 39 (3), 113-137

Elliott, A. J., Hurford, N., and Penn, C. J. (1986) 'Shear Diffusion and the Spreading of Oil Slicks'. *Marine Pollution Bulletin* 17 (7), 308-313

English Nature (2003) *The Humber Estuary European Marine Site: Interim Advice*. London: English Nature

Evans, G. P. (1993) A Framework for Marine and Estuarine Model Specification in the UK (Report no FR0374): Foundation for Water Research

Faghihifard, M. and Badri, M. A. (2016) 'Simulation of Oil Pollution in the Persian Gulf Near Assaluyeh Oil Terminal'. *Marine Pollution Bulletin* 105 (1), 143-149

Faksness, L., Brandvik, P. J., Daling, P. S., Singsaas, I., and Sørstrøm, S. E. (2016) 'The Value of Offshore Field Experiments in Oil Spill Technology Development for Norwegian Waters'. *Marine Pollution Bulletin* 111 (1–2), 402-410

Falconer, R. A. and Owens, P. H. (1990) 'Numerical Modelling of Suspended Sediment Fluxes in Estuarine Waters'. *Estuarine, Coastal and Shelf Science* [online] 31 (6), 745-762. available from <http://www.sciencedirect.com/science/article/pii/027277149090080B>

Farzingohar, M., Ibrahim, Z., and Yasemi, M. (2011) 'Oil Spill Modeling of Diesel and Gasoline with GNOME Around Rajaee Port of Bandar Abbas, Iran'. *Iranian Journal of Fisheries Sciences* 10 (1), 35-46

Fay, J. A. (1971) 'Physical Processes in the Spread of Oil on a Water Surface'. *International Oil Spill Conference Proceedings: June 1971* 1971 (1), 463-467

Fernandes, R., Neves, R., and Viesgas, C. (2013) 'Integration of an Oil and Inert Spill Model in A Framework for Risk Management of Spills at Sea - A Case Study for the Atlantic Area'. *Instituto Superior Técnico - MARETEC*

Fernández-Nieto, E. D., Noble, P., and Vila, J. (2010) 'Shallow Water Equations for Non-Newtonian Fluids'. *Journal of Non-Newtonian Fluid Mechanics* [online] 165 (13), 712-732. available from <http://www.sciencedirect.com/science/article/pii/S0377025710000947>

Fingas, M. F. (2015) *Oil Spill Science and Technology*. 1st edn. Hoboken, New Jersey: John Wiley & Sons

Fingas, M. F. (2013) *The Basics of Oil Spill Cleanup*. Third edn. Boca Raton, FL: CRC Press

Fingas, M. F. and Fieldhouse, B. (2012) 'Studies on Water-in-Oil Products from Crude Oils and Petroleum Products'. *Marine Pollution Bulletin* 64 (2), 272-283

Fingas, M. F. (2011) *Oil Spill Science and Technology*. First edn. Burlington, MA: Gulf Professional Pub./Elsevier

Fingas, M. F. and Fieldhouse, B. (2009) 'Studies on Crude Oil and Petroleum Product Emulsions: Water Resolution and Rheology'. *Colloids and Surfaces A: Physicochemical and Engineering Aspects* 333 (1–3), 67-81

Fingas, M. F. and Fieldhouse, B. (eds.) (2006) *Arctic and Marine Oilspill Program (AMOP) Technical Seminar*. 'A Review of Knowledge on Water-in-Oil Emulsions'. held 6-8 Jun 2006 at Vancouver, BC (Canada). Canada: Environment Canada

Fingas, M. F. (2004) 'Modeling Evaporation using Models that are Not Boundary-Layer Regulated'. *Journal of Hazardous Materials* 107 (1–2), 27-36

Fingas, M. F. and Fieldhouse, B. (2004) 'Formation of Water-in-Oil Emulsions and Application to Oil Spill Modelling'. *Journal of Hazardous Materials* 107 (1–2), 37-50

Fingas, M. F. (1998) 'Studies on the Evaporation of Crude Oil and Petroleum Products II. Boundary Layer Regulation'. *Journal of Hazardous Materials* 57 (1–3), 41-58

Fingas, M. F. (1997) 'Studies on the Evaporation of Crude Oil and Petroleum Products: I. the Relationship between Evaporation Rate and Time'. *Journal of Hazardous Materials* 56 (3), 227-236

Fingas, M. F., Fieldhouse, B., and Mullin, J. (eds.) (1996) *Studies of Water-in-Oil Emulsions: The Role of Asphaltenes and Resins*. 'The Nineteenth Arctic and Marine Oilspill Program (AMOP) Technical Seminar, Environment Canada' at Ottawa, Ontario, Canada

Fischer, H. B., List, E. J., Koh, R. C. Y., Imberger, J., and Brooks, N. H. (1979) *Mixing in Inland and Coastal Waters*. New York: Academic Press

Flemming, B. W. (2012) 'Siliciclastic Back-Barrier Tidal Flats'. in *Principles of Tidal Sedimentology*. ed. by Davis Jr, R. and Dalrymple, R. W. Dordrecht: Springer, 231-267

Fok, H. S. (2012) *Ocean Tides Modeling using Satellite Altimetry*. Columbus, Ohio: The Ohio State University

French-McCay, D. P., Schuttenberg, H., and Isaji, T. (eds.) (1999) *22nd Arctic and Marine Oil Spill Program (AMOP) Technical Seminar*. 'Probabilities of Oil Exceeding Thresholds of Concern: Examples from an Evaluation for Florida Power and Light'. held 2-4 June at Calgary, Alberta: Environment Canda

French-McCay, D. P., Reed, M., Jayko, K., Feng, S., Rines, H., Pavignano, S., Isaji, T., Puckett, S., Keller, A., French III, F. W., Gifford, D., McCue, J., Brown, G., MacDonald, E., Quirk, J., Natzke, S., Bishop, R., Welsh, M., Phillips, M., and 'Ingram, B. S. (1996) *The CERCLA Type A Natural Resource Damage Assessment Model for Coastal and Marine Environments (NRDAM/CME), Technical Documentation, Vol. I - Model Description.* Washington DC: Office of Environmental Policy and Compliance, U.S. Dept of the Interior

French-McCay, D. P., Howlett, E. R., and Mendelsohn, D. (eds.) (1994) *17th Arctic and Marine Oil Spill Program, Technical Seminar*. 'Oil and Chemical Impact Model System Description and Application'. held 8-10 June at Vancouver, British Columbia, Canada

Froneman, P. W. (2004) 'Zooplankton Community Structure and Biomass in a Southern African Temporarily open/closed Estuary'. *Estuarine, Coastal and Shelf Science* [online] 60 (1), 125-132. available from <http://www.sciencedirect.com/science/article/pii/S0272771403003548>

Fujii, T. (2012) 'Climate Change, Sea-Level Rise and Implications for Coastal and Estuarine Shoreline Management with Particular Reference to the Ecology of Intertidal Benthic Macrofauna in NW Europe'. *Biology* 1 (3), 597-616

Fujii, T. (2007) 'Spatial Patterns of Benthic Macrofauna in Relation to Environmental Variables in an Intertidal Habitat in the Humber Estuary, UK: Developing a Tool for Estuarine Shoreline Management'. *Estuarine, Coastal and Shelf Science* [online] 75 (1), 101-119. available from <http://www.sciencedirect.com/science/article/pii/S0272771407001801>

Ganju, N. K. and Schoellhamer, D. H. (2009) 'Calibration of an Estuarine Sediment Transport Model to Sediment Fluxes as an Intermediate Step for Simulation of Geomorphic Evolution'. *Continental Shelf Research* [online] 29 (1), 148-158. available from <http://www.sciencedirect.com/science/article/pii/S0278434307002658>

Geveler, M., Ribbrock, D., Göddeke, D., and Turek, S. (2010) 'Lattice-Boltzmann Simulation of the Shallow-Water Equations with Fluid-Structure Interaction on Multi- and Manycore Processors'. in *Facing the Multicore-Challenge: Aspects of New Paradigms and Technologies in Parallel Computing*. ed. by Keller, R., Kramer, D., and Weiss, J. Berlin, Heidelberg: Springer Berlin Heidelberg, 92-104

Gichamo, T. Z., Popescu, I., Jonoski, A., and Solomatine, D. (2012) 'River Cross-Section Extraction from the ASTER Global DEM for Flood Modeling'. *Environmental Modelling & Software* 31, 37-46

Gifford-Miears, C. and Leon, A. (2013) 'Tutorial on the use of TELEMAC-2D Hydrodynamics Model and Pre-/Post-Processing with BlueKenue for Flood-Inundation Mapping in Unsteady Flow Conditions'. *CE 540 Unsteady Flows in Rivers and Pipe Networks, School of Civil and Construction Engineering, Oregon State University*

Gobler, C. J., Cullison, L. A., Koch, F., Harder, T. M., and Krause, J. W. (2005) 'Influence of Freshwater Flow, Ocean Exchange, and Seasonal Cycles on Phytoplankton – Nutrient Dynamics in a Temporarily Open Estuary'. *Estuarine, Coastal and Shelf Science* [online] 65 (1), 275-288. available from <http://www.sciencedirect.com/science/article/pii/S0272771405002039>

Goeury, C., Hervouet, J., Baudin-Bizien, I., and Thouvenel, F. (2014) 'A Lagrangian/Eulerian Oil Spill Model for Continental Waters'. *Journal of Hydraulic Research* 52 (1), 36-48

Goeury, C. (2012) *Modélisation Du Transport Des Nappes d'hydrocarbures En Zone Continentale Et Estuarienne*. [online] PhD thesis or dissertation. France: Université Paris-Est

Goeury, C., Hervouet, J., Benoit, M., Baudin-Bizien, I., and Fangeat, D. (2012) 'Numerical Modeling of Oil Spill Drifts for Management of Risks in Continental Waters'. *Water Pollution XI* 164, 275-286

Gong, Y., Zhao, X., Cai, Z., O'Reilly, S. E., Hao, X., and Zhao, D. (2014) 'A Review of Oil, Dispersed Oil and Sediment Interactions in the Aquatic Environment: Influence on the Fate, Transport and Remediation of Oil Spills'. *Marine Pollution Bulletin* 79 (1–2), 16-33

Griffiths, S. P. (2001) 'Factors Influencing Fish Composition in an Australian Intermittently Open Estuary. is Stability Salinity-Dependent?'. *Estuarine, Coastal and Shelf Science* [online] 52 (6), 739-751. available from <http://www.sciencedirect.com/science/article/pii/S027277140090756X>

Guillou, N., Chapalain, G., and Neill, S. P. (2016) 'The Influence of Waves on the Tidal Kinetic Energy Resource at a Tidal Stream Energy Site'. *Applied Energy* 180, 402-415

Guo, L., van der Wegen, M., Roelvink, D., and He, Q. (2015) 'Exploration of the Impact of Seasonal River Discharge Variations on Long-Term Estuarine Morphodynamic Behavior'. *Coastal Engineering* [online] 95, 105-116. available from <http://www.sciencedirect.com/science/article/pii/S037838391400194X>

Guo, W. J. and Wang, Y. X. (2009) 'A Numerical Oil Spill Model Based on a Hybrid Method'. *Marine Pollution Bulletin* 58 (5), 726-734

Guo, W. J., Wang, Y. X., Xie, M. X., and Cui, Y. J. (2009) 'Modeling Oil Spill Trajectory in Coastal Waters Based on Fractional Brownian Motion'. *Marine Pollution Bulletin* 58 (9), 1339-1346

Guo, W., Jiang, M., Li, X., and Ren, B. (2018) 'Using a Genetic Algorithm to Improve Oil Spill Prediction'. *Marine Pollution Bulletin* [online] 135, 386-396. available from <http://www.sciencedirect.com/science/article/pii/S0025326X18305046>

Guo, W., Wu, G., Jiang, M., Xu, T., Yang, Z., Xie, M., and Chen, X. (2016) 'A Modified Probabilistic Oil Spill Model and its Application to the Dalian New Port Accident'. *Ocean Engineering* 121, 291-300

Guo, W., Hao, Y., Zhang, L., Xu, T., Ren, X., Cao, F., and Wang, S. (2014) 'Development and Application of an Oil Spill Model with wave–current Interactions in Coastal Areas'. *Marine Pollution Bulletin* 84 (1–2), 213-224

Haidvogel, D. B., Arango, H. G., Budgell, W. P., Cornuelle, B. D., Curchitser, E., Di Lorenzo, E., Fennel, K., Geyer, W. R., Hermann, A. J., Lanerolle, L., Levin, J., McWilliams, J. C., Miller, A. J., Moore, A. M., Powell, T. M., Shchepetkin, A. F., Sherwood, C. R., Signell, R. P., Warner, J. C., and Wilkin, J. (2008) 'Ocean Forecasting in Terrain-Following Coordinates: Formulation and Skill Assessment of the Regional Ocean Modeling System'. *Journal of Computational Physics* 227 (7), 3595-3624

Hannaford, J. (2015) 'Climate-Driven Changes in UK River Flows: A Review of the Evidence'. *Progress in Physical Geography: Earth and Environment* 39 (1), 29-48

Hannaford, J. (2015) 'Climate-Driven Changes in UK River Flows: A Review of the Evidence'. *Progress in Physical Geography: Earth and Environment* 39 (1), 29-48

Hashemi, M. R., Neill, S. P., Robins, P. E., Davies, A. G., and Lewis, M. J. (2015) 'Effect of Waves on the Tidal Energy Resource at a Planned Tidal stream array'. *Renewable Energy* 75, 626-639

Hasselmann, K., Barnett, T. P., Bouws, E., Carlson, H., Cartwright, D. E., Enke, K., Ewing, J. A., Gienapp, H., Hasselmann, D. E., Kruseman, P., Meerburg, A., Müller, P., Olbers, D. J., Richter, K., Sell, W., and Walden, H. (1973) *Measurements of Wind-Wave Growth and Swell Decay during the Joint North Sea Wave Project (JONSWAP).*: Deutsches Hydrographisches Institut

Hearn, C. J. and Largier, J. L. (1997) 'The Summer Buoyancy Dynamics of a Shallow Mediterranean Estuary and some Effects of Changing Bathymetry: Tomales Bay, California'. *Estuarine, Coastal and Shelf Science* [online] 45 (4), 497-506. available from <http://www.sciencedirect.com/science/article/pii/S0272771496901973>

Hervouet, J. (2007) *Hydrodynamics of Free Surface Flows, Modelling with the Finite-Element Method*. West Sussex, England: John Wiley & Sons Ltd.

Holm, S. (1979) 'A Simple Sequentially Rejective Multiple Test Procedure'. *Scandinavian Journal of Statistics* 6 (2), 65-70

Hori, K., Saito, Y., Zhao, Q., Cheng, X., Wang, P., Sato, Y., and Li, C. (2001) 'Sedimentary Facies of the Tide-Dominated Paleo-Changjiang (Yangtze) Estuary during the Last Transgression'. *Marine Geology* [online] 177 (3), 331-351. available from <http://www.sciencedirect.com/science/article/pii/S0025322701001657>

Horn, M. and French-McCay, D. P. (2014) *Trajectory Modelling in Support of the Shelburne Basin Exploration Drilling Program: Model Description, Approach and Summary of Results*. South Kingstown, Rhode Island, USA: RPS ASA

Howlett, E. R., Jayko, K., Isaji, T., Anid, P., Mocke, G., and Smit, F. (eds.) (2008) *Copedec Vii*. 'Marine Forecasting and Oil Spill Modeling in Dubai and the Gulf Region' at Dubai, UAE

Hu, K., Ding, P., Wang, Z., and Yang, S. (2009) 'A 2D/3D Hydrodynamic and Sediment Transport Model for the Yangtze Estuary, China'. *Journal of Marine Systems* 77 (1–2), 114-136

Humber Nature Partnership (2015) *Humber Management Scheme: FAQS - Ports, Habours and Commercial Shipping*. United Kingdom: Humber Nature

Hunter, J. R. (1987) *The Application of Lagrangian Particle-Tracking Technique to Modelling of Dispersant in the Sea. in Numerical Modelling: Applications to Marine System*. Holland, Amsterdam, the Netherlands: J. Noye

Iazeolla, G., Mariani, M., Cassina, L., Marconi, M., Deffis, J. M., and Buffagni, M. (eds.) (2016) *SPE International Conference and Exhibition on Health, Safety, Security, Environment, and Social Responsibility*. 'Advanced Oil Spill Modelling in the Offshore Oil & Gas Industry: Improving the Emergency Response Management Along the Project Life-Cycle'. held 11-13 April at Stavanger, Norway: Society of Petroleum Engineers

ITOPF (2002) 'Fate of Marine Oil Spills'. *Technical Information Paper*, 8p

Janeiro, J., Zacharioudaki, A., Sarhadi, E., Neves, A., and Martins, F. (2014) 'Enhancing the Management Response to Oil Spills in the Tuscany Archipelago through Operational Modelling'. *Marine Pollution Bulletin* 85 (2), 574-589

Janeiro, J., Fernandes, E., Martins, F., and Fernandes, R. (2008) 'Wind and Freshwater Influence Over Hydrocarbon Dispersal on Patos Lagoon, Brazil'. *Marine Pollution Bulletin* 56 (4), 650-665

Jia, L., Wen, Y., Pan, S., Liu, J. T., and He, J. (2015) 'Wave–current Interaction in a River and Wave Dominant Estuary: A Seasonal Contrast'. *Applied Ocean Research* 52, 151-166

Johansen, Ø. (1982) 'Dispersion of Oil from Drifting Slicks'. *Spill Technology Newsletter*, 134-149

Johnson, J. A., Edwards, D. A., Blue, D., and Morey, S. J. (2018) 'Physical Properties of Oil-Particle Aggregate (OPA)-Containing Sediments'. *Soil and Sediment Contamination: An International Journal* 27 (8), 706-722

Joly, A., Goeury, C., and Hervouet, J. (2014) *Adding a Particle Transport Module to Telemac-2D with Applications to Algae Blooms and Oil Spills*. National Hydraulics and Environment Laboratory, EDF R&D, France: EDF R&D

Jones, H. F. E., Poot, M. T. S., Mullarney, J. C., de Lange, W. P., and Bryan, K. R. (2016) 'Oil Dispersal Modelling: Reanalysis of the Rena Oil Spill using Open-Source Modelling Tools'. *New Zealand Journal of Marine and Freshwater Research* 50 (1), 10-27

Jones, R. K. (ed.) (1997) *Arctic and Marine Oil Spill Program Technical Seminar*. 'A Simplified Pseudo-Component Oil Evaporation Model'. held 11-13 June at Vancouver (Canada). Ottawa, Ontario, Canada: Emergency Sciences Division, Environment Canada

Kanarska, Y., Shchepetkin, A. F., and McWilliams, J. C. (2007) 'Algorithm for Non-Hydrostatic Dynamics in the Regional Oceanic Modeling System'. *Ocean Modelling* 18 (3-4), 143-174

Kanarska, Y. and Maderich, V. (2003) 'A Non-Hydrostatic Numerical Model for Calculating Free-Surface Stratified Flow'. *Ocean Dynamics* 53, 176-185

Kang, J., Zhang, J., and Bai, Y. (2016a) 'Modeling and Evaluation of the Oil-Spill Emergency Response Capability Based on Linguistic Variables'. *Marine Pollution Bulletin* 113 (1-2), 293-301

Kang, T., Oh, J. H., Hong, J., and Kim, D. (2016b) 'Effect of the Hebei Spirit Oil Spill on Intertidal Meiofaunal Communities in Taean, Korea'. *Marine Pollution Bulletin* 113 (1-2), 444-453

Kang, T., Oh, J. H., Hong, J., and Kim, D. (2016) 'Effect of the Hebei Spirit Oil Spill on Intertidal Meiofaunal Communities in Taean, Korea'. *Marine Pollution Bulletin* 113 (1-2), 444-453

Kankara, R. S., Arockiaraj, S., and Prabhu, K. (2016) 'Environmental Sensitivity Mapping and Risk Assessment for Oil Spill Along the Chennai Coast in India'. *Marine Pollution Bulletin* 106 (1–2), 95-103

Kärnä, T., Baptista, A. M., Lopez, J. E., Turner, P. J., McNeil, C., and Sanford, T. B. (2015) 'Numerical Modeling of Circulation in High-Energy Estuaries: A Columbia River Estuary Benchmark'. *Ocean Modelling* [online] 88, 54-71. available from <http://www.sciencedirect.com/science/article/pii/S1463500315000037>

Kennish, M. J. (2002) 'Environmental Threats and Environmental Future of Estuaries'. *Environmental Conservation* 29 (01)

Khaustov, A. and Redina, M. (eds.) (2012) *Supertoxicants: Modeling of their Formation and Distribution Caused by the Oil Spills on the Objects of Production and Transportation of Oil (Russian)*. 'SPE Russian Oil and Gas Exploration and Production Technical Conference and Exhibition'. held 16-18 October at Moscow, Russia: Society of Petroleum Engineers

Kim, Y. H., Hong, S., Song, Y. S., Lee, H., Kim, H., Ryu, J., Park, J., Kwon, B., Lee, C., and Khim, J. S. (2017) 'Seasonal Variability of Estuarine Dynamics due to Freshwater Discharge and its Influence on Biological Productivity in Yeongsan River Estuary, Korea'. *Chemosphere* 181, 390-399

King, B., Brushett, B., and Lemckert, C. (2010) 'A Case Study of Consensus Modelling for Tracking Oil Spills'. *IOP Conference Series: Earth and Environmental Science* 11

Kirby, J. T. (1986) 'Higher-Order Approximations in the Parabolic Equation Method for Water Waves'. *Journal of Geophysical Research: Oceans* 91 (C1), 933-952

Kirstein, B. E., Clayton, J., Clary, C., Payne, J. R., McNabb, D. G., Fauna, G., and Redding, R. (1987) *Integration of Suspended Particulate Matter and Oil Transportation Study*. Anchorage, Alaska, USA: U.S. Minerals Management Service

Kitheka, J. U., Obiero, M., and Nthenge, P. (2005) 'River Discharge, Sediment Transport and Exchange in the Tana Estuary, Kenya'. *Estuarine, Coastal and Shelf Science* [online] 63 (3), 455-468. available from <http://www.sciencedirect.com/science/article/pii/S0272771404003208>

Kollo, M., Laanearu, J., and Tabri, K. (2017) 'Hydraulic Modelling of Oil Spill through Submerged Orifices in Damaged Ship Hulls'. *Ocean Engineering* 130, 385-397

Korotenko, K. A., Mamedov, R. M., Kontar, A. E., and Korotenko, L. A. (2004) 'Particle Tracking Method in the Approach for Prediction of Oil Slick Transport in the Sea: Modelling Oil Pollution Resulting from River Input'. *Journal of Marine Systems* 48 (1–4), 159-170

Korsah, P. and Anifowose, B. (eds.) (2014) *Abu Dhabi International Petroleum Exhibition and Conference*. 'Oil Spill Trajectory Simulation for the Saltpond Oilfield, Ghana, West Africa'. held 10 - 13 November at Abu Dhabi, UAE: Society of Petroleum Engineers

Kowalewska-Kalkowska, H. and Marks, R. (2016) 'Estuary, Estuarine Hydrodynamics'. in *Encyclopedia of Marine Geosciences*. ed. by Harff, J., Meschede, M., Petersen, S., and Thiede, J. Dordrecht: Springer Netherlands, 235-238

Kumbier, K., Carvalho, R. C., and Woodroffe, C. D. (2018) 'Modelling Hydrodynamic Impacts of Sea-Level Rise on Wave-Dominated Australian Estuaries with Differing Geomorphology'. *Journal of Marine Science and Engineering* 6 (66)

Lamine, S. and Xiong, D. (2013) 'Guinean Environmental Impact Potential Risks Assessment of Oil Spills Simulation'. *Ocean Engineering* 66, 44-57

Lawler, D. M. (2016) 'Turbidity, Turbidimetry, and Nephelometry'. In *Elsevier Reference Module in Chemistry, Molecular Sciences and Chemical Engineering*. ed. by Reedijk, J. Waltham, MA: Elsevier

Lawrie, R. A., Stretch, D. D., and Perissinotto, R. (2010) 'The Effects of Wastewater Discharges on the Functioning of a Small Temporarily open/closed Estuary'. *Estuarine, Coastal and Shelf Science* [online] 87 (2), 237-245. available from <http://www.sciencedirect.com/science/article/pii/S0272771410000351>

Lee, K., Stoffyn-Egli, P., Tremblay, G. H., Owens, E. H., Sergy, G. A., Guénette, C. C., and Prince, R. C. (2003) 'Oil–Mineral Aggregate Formation on Oiled Beaches: Natural Attenuation and Sediment Relocation'. *Spill Science & Technology Bulletin* 8 (3), 285-296

Lee, M. and Jung, J. (2015) 'Pollution Risk Assessment of Oil Spill Accidents in Garorim Bay of Korea'. *Marine Pollution Bulletin* 100 (1), 297-303

Legrand, S. (2015). *A modelling study of the drift and fate of large oil spills in seven sub-regions of the North Sea and the English Channel*. Operational Directorate Natural Environment.

Lehr, W. J., Jones, R., Evans, M., Simecek-Beatty, D., and Overstreet, R. (2002) 'Revisions of the ADIOS Oil Spill Model'. *Environmental Modelling & Software* 17 (2), 189-197

Lehr, W. J. and Simecek-Beatty, D. (2000) 'The Relation of Langmuir Circulation Processes to the Standard Oil Spill Spreading, Dispersion, and Transport Algorithms'. *Spill Science & Technology Bulletin* 6 (3–4), 247-253

Lei, J., Li, F., Zhang, S., Ke, H., Zhang, Q., and Li, W. (2017) 'The International Archives of the Photogrammetry, Remote Sensing and Spatial Information Sciences'. *ISPRS - International Archives of the Photogrammetry, Remote Sensing and Spatial Information Sciences* XLII-2/W7, 1521-1528

Lei, L. and He, W. (2017) 'Simulation of Oil Transport After Oil Spill in the Bohai Sea'. *Applied Mechanics and Civil Engineering VI*, 133-136

Lesser, G. R., Roelvink, D., van Kester, J. A. T. M., and Stelling, G. S. (2004) 'Development and Validation of a Three-Dimensional Morphological Model'. *Coastal Engineering* 51 (8–9), 883-915

Li, F., Dong, H., and Liang, M. (2018) 'Analysis, Treatment and Countermeasures on Oil Spills at Sea'. *IOP Conference Series: Materials Science and Engineering* 397 (012086)

Li, H., Li, Y., Li, C., Wang, G., Xu, S., Song, J., and Zhang, S. (eds.) (2016b) *International Conference on Energy Engineering and Environmental Protection*

(EEEP2016). 'Numerical Simulation Study on Drift and Diffusion of Dalian Oil Spill': IOP Publishing Ltd

Li, P., Cai, Q., Lin, W., Chen, B., and Zhang, B. (2016a) 'Offshore Oil Spill Response Practices and Emerging Challenges'. *Marine Pollution Bulletin* 110 (1), 6-27

Li, Y. S. and Zhan, J. M. (2001) 'Boussinesq-Type Model with Boundary-Fitted Coordinate System'. *Journal of Waterway, Port, Coastal, and Ocean Engineering* 127 (3), 152-160

Liang, D. (2010) 'Evaluating Shallow Water Assumptions in Dam-Break Flows'. *Proceedings of the Institution of Civil Engineers - Water Management* 163 (5), 227-237

Lima, J. A., Sartori, A., Yassuda, E., Pereira, J. E., Anderson, E., and Campos, E. (2003) 'Development of Oil Spill Scenarios for Contingency Planning Along the Brazilian Coast'. *International Oil Spill Conference Proceedings* 2003 (1), 947-953

Lin, B. and Falconer, R. A. (1997) 'Three-Dimensional Layer-Integrated Modelling of Estuarine Flows with Flooding and Drying'. *Estuarine, Coastal and Shelf Science* [online] 44 (6), 737-751. available from <http://www.sciencedirect.com/science/article/pii/S0272771496901584>

Lin, B. and Falconer, R. A. (1995) 'Modelling Sediment Fluxes in Estuarine Waters using a Curvilinear Coordinate Grid System'. *Estuarine, Coastal and Shelf Science* [online] 41 (4), 413-428. available from <http://www.sciencedirect.com/science/article/pii/0272771495900020>

Lindim, C., Pinho, J. L., and Vieira, J. M. P. (2011) 'Analysis of Spatial and Temporal Patterns in a Large Reservoir using Water Quality and Hydrodynamic Modeling'. *Ecological Modelling* [online] 222 (14), 2485-2494. available from <http://www.sciencedirect.com/science/article/pii/S0304380010003741>

Little, D. I. (1987) 'Oil in Sediments of the Humber Estuary Following the ‘sivand’ Oilspill Incident'. in *Fate and Effects of Oil in Marine Ecosystems*. ed. by Kuiper, J. and Van Den Brink, W. J. Dordrecht: Springer, 79-81

Liu, T. and Sheng, Y. P. (2014) 'Three Dimensional Simulation of Transport and Fate of Oil Spill Under Wave Induced Circulation'. *Marine Pollution Bulletin* 80 (1–2), 148-159

Liu, X., Guo, M., Wang, Y., Yu, X., Guo, J., Tang, C., Hu, X., Wang, C., and Li, B. (2016b) 'Assessing Pollution-Related Effects of Oil Spills from Ships in the Chinese Bohai Sea'. *Marine Pollution Bulletin* 110 (1), 194-202

Liu, X., Guo, J., Guo, M., Hu, X., Tang, C., Wang, C., and Xing, Q. (2015) 'Modelling of Oil Spill Trajectory for 2011 Penglai 19-3 Coastal Drilling Field, China'. *Applied Mathematical Modelling* 39 (18), 5331-5340

Liu, X. and Wirtz, K. W. (2009) 'The Economy of Oil Spills: Direct and Indirect Costs as a Function of Spill Size'. *Journal of Hazardous Materials* 171 (1–3), 471-477

Liu, Y., Roy-Engel, A. M., Baddoo, M. C., Flemington, E. K., Wang, G., and Wang, H. (2016a) 'The Impact of Oil Spill to Lung health—Insights from an RNA-Seq Study of Human Airway Epithelial Cells'. *Gene* 578 (1), 38-51

Liu, Z., Lin, L., Xie, L., and Gao, H. (2016c) 'Partially Implicit Finite Difference Scheme for Calculating Dynamic Pressure in a Terrain-Following Coordinate Non-Hydrostatic Ocean Model'. *Ocean Modelling* 106, 44-57

Liubartseva, S., Coppini, G., Pinardi, N., De Dominicis, M., Lecci, R., Turrisi, G., Creti, S., Martinelli, S., Agostini, P., Marra, P., and Palermo, F. (2016) 'Decision Support System for Emergency Management of Oil Spill Accidents in the Mediterranean Sea'. *Natural Hazards and Earth System Sciences* 16 (8)

Llebot, C., Rueda, F. J., Solé, J., Artigas, M. L., and Estrada, M. (2014) 'Hydrodynamic States in a Wind-Driven Microtidal Estuary (Alfacs Bay)'. *Journal of Sea Research* 85, 263-276

Lowe, J. A., Bernie, D., Bett, P. E., Bricheno, L., Brown, S., Calvert, D., Clark, R. T., Eagle, K. E., Edwards, T., Fosser, G. G., Fung, F., Gohar, L., Good, P., Gregory, J., Harris, G. R., Howard, T., Kaye, N., Kendon, E. J., Krijnen, J., Maisey, P., McDonald, R. E., McInnes, R., McSweeny, C. F., Mitchell, J. F. B., Murphy, J. M., Palmer, M., Roberts, C., Rostron, J., Sexton, D. M. H., Thorton, H. E., Tinker, J., Tucker, S., Yamazaki, K., and Belcher, S. (2018) *UKCP18 Science Overview Report*. United Kingdom: Met Office

Lyard, F., Lefevre, F., Letellier, T., and Francis, O. (2006) 'Modelling the Global Ocean Tides: Modern Insights from FES2004'. *Ocean Dynamics* 56 (5), 394-415

Lynch, D. R., Greenberg, D. A., Bilgili, A., McGillicuddy, D. J., Manning, J. P., and Aretxabaleta, A. L. (2015) *Particles in the Coastal Ocean: Theory and Applications*. New York: Cambridge University Press

MacCready, P. and Geyer, W. R. (2010) 'Advances in Estuarine Physics'. *Annual Review of Marine Science* 2 (1), 35-58

Mackay, D., Shiu, W., Hossain, K., Stiver, W., McCurdy, D., Petterson, S., and Tebeau, P. (1982) *Development and Calibration of an Oil Spill Behavior Model.* Groton, Conn., USA: United States Coast Guard Office of Research and Development

Mackay, D., Paterson, S., and Trudel, K. (1980) *A Mathematical Model of Oil Spill Behaviour*. Ottawa,Canada: Report to Research and Development Division, Environment Emergency Branch, Environmental Impact Control Directorate, Environmental Protection Service, Environment Canada

Mackay, D., Buist, I., Mascarenhas, R., and Paterson, S. (1979) *Oil Spill Processes and Models*. Ottawa, Canada: Report to Research and Development Division, Environment Emergency Branch, Environmental Impact Control Directorate, Environmental Protection Service, Environment Canada

Mackay, D. and Leinonen, P. J. (1977) *Mathematical Model of the Behavior of Oil Spills on Water with Natural and Chemical Dispersion*. Canada: Economic and Technical Review Report. Prepared for Fisheries and Environment Canada.

Magnier, B., Claude, N., Villaret, C., Rodrigues, S., and Tassi, P. (eds.) (2013) *XXth TELEMAC-MASCARET User Conference*. 'Numerical Simulation of Flow Structures in the Presence of Alternate and Transverse Bars: Application to the Loire River (France)'. held 16–18 October, 2013 at Karlsruhe, Germany: BAW

Mahgoub, M., Hinkelmann, R., and La Rocca, M. (2015) 'Understanding the Behaviour of Gravity Currents in Tideless Estuaries and Considering the Impact of Sea Level Rise within the Nile Estuary'. Journal of Coastal Research 313 (3), 714-722

Mantovanelli, A., Marone, E., da Silva, E. T., Lautert, L. F., Klingenfuss, M. S., Prata, V. P., Noernberg, M. A., Knoppers, B. A., and Angulo, R. J. (2004) 'Combined Tidal Velocity and Duration Asymmetries as a Determinant of Water Transport and Residual Flow in Paranaguá Bay Estuary'. *Estuarine, Coastal and Shelf Science* [online] 59 (4), 523-537. available from <http://www.sciencedirect.com/science/article/pii/S0272771403002531>

Marsh, T. and Dixon, H. (eds.) (2012) *'Hydrology for a Changing World', Proceedings of the Eleventh National BHS Symposium*. 'The UK Water Balance: How Much has it Changed in a Warming World?'. held August 2012 at Dundee: British Hydrological Society

Marshall, J., Hill, C., Perelman, L., and Adcroft, A. (1997) 'Hydrostatic, Quasi-Hydrostatic, and Nonhydrostatic Ocean Modeling'. *Journal of Geophysical Research: Oceans* 102 (C3), 5733-5752

Marta-Almeida, M., Ruiz-Villarreal, M., Pereira, J., Otero, P., Cirano, M., Zhang, X., and Hetland, R. D. (2013) 'Efficient Tools for Marine Operational Forecast and Oil Spill Tracking'. *Marine Pollution Bulletin* 71 (1–2), 139-151

Martin, J. L. and McCutcheon, S. C. (1999) *Hydrodynamics and Transport for Water Quality Modeling*. Boca Raton, Florida: CRC Press Inc.

McLusky, D. S. and Elliott, M. (2004) *The Estuarine Ecosystem: Ecology, Threats and Management*. 3rd edn. New York: Oxford University Press

Mearns, A., Watabayashi, G., and Lankford, J. (2011) 'Dispersing Oil Near Shore in the California Region'. *CalCOFl Report* 42, 97-109

Mehra, A. and Rivin, I. (2010) 'A Real Time Ocean Forecast System for the North Atlantic Ocean'. *Terrestrial, Atmospheric and Oceanic Sciences* 21 (1), 211-228

Meinshausen, M., Smith, S. J., Calvin, K., Daniel, J. S., Kainuma, M. L. T., Lamarque, J., Matsumoto, K., Montzka, S. A., Raper, S. C. B., Riahi, K., Thomson, A., Velders, G. J. M., and van Vuuren, D. P. P. (2011) 'The RCP Greenhouse Gas Concentrations and their Extensions from 1765 to 2300'. *Climatic Change* 109 (1), 213

Mellor, G. L. (2004) *User Guide for a Three-Dimensional, Primitive Equation, Numerical Ocean Model*. Princeton University, Princeton, NJ: Program in Atmospheric and Oceanic Sciences

Mendes, R., Dias, J. M., and Pinheiro, L. M. (2009) 'Numerical Modeling Estimation of the Spread of Maritime Oil Spills in Ria De Aveiro Lagoon'. *Journal of Coastal Research* 56 (56), 1375-1379

Merrifield, M. S., Hines, E., Liu, X., and Beck, M. W. (2011) 'Building Regional Threat-Based Networks for Estuaries in the Western United States'. *Plos One* 6 (2), 1-10

Met Office Hadley Centre (2018) *UKCP18 21st Century Time-Mean Sea Level Projections Around the UK for 2007-2100*: Centre for Environmental Data Analysis

Michel, C., Quiniou, V., and Vigan, X. (eds.) (2012) *Metocean and Oil Spill Modelling*. 'SPE/APPEA International Conference on Health, Safety, and Environment in Oil and Gas Exploration and Production'. held 11 - 13 September at Perth, Australia: Society of Petroleum Engineers

Mishra, A. K. and Kumar, G. S. (2015) 'Weathering of Oil Spill: Modeling and Analysis'. *Aquatic Procedia* 4, 435-442

Mitchell, S. B. (2013) 'Turbidity Maxima in Four Macrotidal Estuaries'. *Ocean & Coastal Management* [online] 79 (Supplement C), 62-69. available from <http://www.sciencedirect.com/science/article/pii/S0964569112001457>

Mitchell, S. B., Couperthwaite, J. S., West, J. R., and Lawler, D. M. (2003b) 'Measuring Sediment Exchange Rates on an Intertidal Bank at Blacktoft, Humber Estuary, UK'. *Science of the Total Environment* [online] 314-316 (Supplement C), 535-549. available from <http://www.sciencedirect.com/science/article/pii/S004896970300072X>

Mitchell, S. B., Lawler, D. M., West, J. R., and Couperthwaite, J. S. (2003a) 'Use of Continuous Turbidity Sensor in the Prediction of Fine Sediment Transport in the Turbidity Maximum of the Trent Estuary, UK'. *Estuarine, Coastal and Shelf Science* [online] 58 (3), 645-652. available from <http://www.sciencedirect.com/science/article/pii/S0272771403001768>

Mitchell, S. B., West, J. R., Arundale, A. M. W., Guymer, I., and Couperthwaite, J. S. (1998) 'Dynamics of the Turbidity Maxima in the Upper Humber Estuary System, UK'. *Marine Pollution Bulletin* [online] 37 (3), 190-205. available from <http://www.sciencedirect.com/science/article/pii/S0025326X98001787>

Miththapala, S. (2013) Lagoons and Estuaries: Coastal Ecosystems Series (Volume 4). Colombo, Sri Lanka: International Union for Conservation of Nature, Sri Lanka Country Office

Moffatt and Nichol (2005) *Hydrodynamic Modeling Tools and Techniques South Bay Salt Pond Restoration Project*. Oakland, Carlifonia: California State Coastal Conservancy

Morris, R. and Mitchell, S. B. (2013) 'Has Loss of Accommodation Space in the Humber Estuary Led to Elevated Suspended Sediment Concentrations?'. *Journal of Frontiers in Construction Engineering* 2 (1), 1-9

Moss, R. H., Edmonds, J. A., Hibbard, K. A., Manning, M. R., Rose, S. K., van Vuuren, D. P., Carter, T. R., Emori, S., Kainuma, M., Kram, T., Meehl, G. A., Mitchell, J. F. B., Nakicenovic, N., Riahi, K., Smith, S. J., Stouffer, R. J., Thomson, A. M., Weyant, J. P., and Wilbanks, T. J. (2010) 'The Next Generation of Scenarios for Climate Change Research and Assessment'. *Nature* 463, 747-756

Moulinec, C., Denis, C., Pham, C., Rouge, D., Hervouet, J., Razafindrakoto, E., Barber, R. W., Emerson, D. R., and GU, X. (2011) 'TELEMAC: An Efficient Hydrodynamic Suite for Massively Parallel Architectures'. *Computers & Fluids* 51 (1), 30-34

Murphy, D., Gemmell, B., Vaccari, L., Li, C., Bacosa, H., Evans, M., Gemmell, C., Harvey, T., Jalali, M., and Niepa, T. H. R. (2016) 'An in-Depth Survey of the Oil Spill Literature since 1968: Long Term Trends and Changes since Deepwater Horizon'. *Marine Pollution Bulletin* [online] 113 (1), 371-379. available from <http://www.sciencedirect.com/science/article/pii/S0025326X1630844X>

Muschenheim, D. K. and Lee, K. (2002) 'Removal of Oil from the Sea Surface through Particulate Interactions: Review and Prospectus'. *Spill Science & Technology Bulletin* 8 (1), 9-18

Nagheeby, M. and Kolahdoozan, M. (2010) 'Numerical Modeling of Two-Phase Fluid Flow and Oil Slick Transport in Estuarine Water'. *International Journal of Environmental Science & Technology* 7 (4), 771-784

Najjar, R. G., Pyke, C. R., Adams, M. B., Breitburg, D., Hershner, C., Kemp, M., Howarth, R., Mulholland, M. R., Paolisso, M., Secor, D., Sellner, K., Wardrop, D., and Wood, R. (2010) 'Potential Climate-Change Impacts on the Chesapeake Bay'. *Estuarine, Coastal and Shelf Science* [online] 86 (1), 1-20. available from <http://www.sciencedirect.com/science/article/pii/S0272771409004582>

Neill, S. P. and Hashemi, M. R. (2013) 'Wave Power Variability Over the Northwest European Shelf Seas'. *Applied Energy* [online] 106, 31-46. available from <http://www.sciencedirect.com/science/article/pii/S0306261913000354>

Nelson, J. R., Grubesic, T. H., Sim, L., Rose, K., and Graham, J. (2015) 'Approach for Assessing Coastal Vulnerability to Oil Spills for Prevention and Readiness using GIS and the Blowout and Spill Occurrence Model'. *Ocean & Coastal Management* 112, 1-11

Nepstad, R., Størdal, I. F., Brönner, U., Nordtug, T., and Hansen, B. H. (2015) 'Modeling Filtration of Dispersed Crude Oil Droplets by the Copepod Calanus Finmarchicus'. *Marine Environmental Research* 105, 1-7

Nerem, R. S. and Mitchum, G. T. (2002) 'Estimates of Vertical Crustal Motion Derived from Differences of TOPEX/POSEIDON and Tide Guage Sea Level Measurements'. *Geophysical Research Letters* 29 (19), 40-1-40-4

Nguyen, A. D. (2008) *Salt Intrusion, Tides and Mixing in Multi-Channel Estuaries*. Unpublished Master of Science thesis or dissertation. Delft, The Netherlands: Delft University of Technology

NOAA (2017) *Webgnome* [online] available from <Gnome-stage.orr.noaa.gov> [June/23 2017]

NOAA (2002) *GNOME User's Manual*: Hazardous Materials Response Division (HAZMAT), Office of Response and Restoration, National Oceanic and Atmospheric Administration

Noh, S. R., Kim, J., Cheong, H., Ha, M., Jee, Y., Park, M., Choi, K., Kim, H., Cho, S., Choi, K., and Paek, D. (2019) 'Hebei Spirit Oil Spill and its Long-Term Effect on Children's Asthma Symptoms'. *Environmental Pollution* [online] 248, 286-294. available from <http://www.sciencedirect.com/science/article/pii/S0269749118341794>

North, E. W., Adams, E. E., Thessen, A. E., Schlag, Z., He, R., Socolofsky, S. A., Masutani, S. M., and Peckham, S. D. (2015) 'The Influence of Droplet Size and Biodegradation on the Transport of Subsurface Oil Droplets during the Deepwater Horizon Spill: A Model Sensitivity Study'. *Environmental Research Letters* 10 (2), 024016

Nozais, C., Perissinotto, R., and Mundree, S. (2001) 'Annual Cycle of Microalgal Biomass in a South African Temporarily-Open Estuary: Nutrient Versus Light Limitation'. *Marine Ecology Progress Series* 223, 39-48

NRC Canada (2011) *Blue Kenue Reference Manual*. Ottawa, Ontario, Canada: Canadian Hydraulics Centre, National Research Council

Nzualo, T. N. M., Gallo, M. N., and Vinzon, S. B. (2018) 'Short-Term Tidal Asymmetry Inversion in a Macrotidal Estuary (Beira, Mozambique)'. *Geomorphology* [online] 308, 107-117. available from <http://www.sciencedirect.com/science/article/pii/S0169555X16308893>

Ohlberger, J., Buehrens, T. W., Brenkman, S. J., Crain, P., Quinn, T. P., and Hilborn, R. (2018) 'Effects of Past and Projected River Discharge Variability on Freshwater Production in an Anadromous Fish'. *Freshwater Biology* 63 (4), 331-340

Omotoso, O. E., Munoz, V. A., and Mikula, R. J. (2002) 'Mechanisms of Crude Oil–Mineral Interactions'. *Spill Science & Technology Bulletin* 8 (1), 45-54

Otero, P., Ruiz-Villarreal, M., Allen-Perkins, S., Vila, B., and Cabanas, J. M. (2014) 'Coastal Exposure to Oil Spill Impacts from the Finisterre Traffic Separation Scheme'. *Marine Pollution Bulletin* 85 (1), 67-77

Overstreet, R., Lewandowski, A., Lehr, W. J., Jones, R., Simecek-Beatty, D., and Calhoun, D. (eds.) (1995) *International Oil Spill Conference*. 'Sensitivity Analysis in Oil Spill Models: Case Study using ADIOS'. held February - March at Washington DC. Washington DC: American Petroleum Institute

Özgökmen, T., Chassignet, E. P., Dawson, C., Dukhovskoy, D., Jacobs, G., Ledwell, J., Garcia-Pineda, O., MadDonald, I., Morey, S., Olascoaga, M., Poje, A., Reed, M., and Skancke, J. (2016) 'Over what Area did the Oil and Gas Spread during the 2010 Deepwater Horizon Oil Spill?'. *Oceanography* 29 (3), 96-107

Palmer, M., Howard, T., Tinker, J., Lowe, J. A., Bricheno, L., Calvert, D., Edwards, T., Gregory, J., Harris, G. R., Krijnen, J., Pickering, M., Roberts, C., and Wolf, J. (2018) *UKCP18 Marine Report*. United Kingdom: Met Office

Pan, J. and Gu, Y. (2016) 'Cruise Observation and Numerical Modeling of Turbulent Mixing in the Pearl River Estuary in Summer'. *Continental Shelf Research* [online] 120, 122-138. available from <http://www.sciencedirect.com/science/article/pii/S027843431630142X>

Parsapour-Moghaddam, P. and Rennie, C. (eds.) (2014) *International Conference on Fluvial Hydraulics (River Flow 2014)* . 'Morphodynamics Modelling of a Turtuous Meandering Clay Bed River using Delft3d: Stillwater Creek, Ottawa'. held 3-5 September at Switzerland. The Netherlands: CRC Press

Payne, J. R., Kirstein, B. E., McNabb, D. G., Lambach, J. L., Oliveira, C., Jordan, R. E., and Hom, W. (1983) 'Multivariate Analysis of Petroleum Hydrocarbon Weathering in the Subarctic Marine Environment'. *International Oil Spill Conference Proceedings: February 1983* 1983 (1), 423-434

Pelling, H. E., Uehara, K., and Green, J. A. M. (2013) 'The Impact of Rapid Coastline Changes and Sea Level Rise on the Tides in the Bohai Sea, China'. Journal of Geophysical Research: Oceans 118 (7), 3462-3472

Pérez-Ortiz, A., Pescatore, J., and Bryden, I. (eds.) (2013) *A Systematic Approach to Undertake Tidal Energy Resource Assessment with Telemac-2D*. 'European Wave and Tidal Energy Conference (EWTEC) '. held September 2013 at Aalborg, Denmark

Pezy, J., Baffreau, A., and Dauvin, J. (2017) 'What are the Factors Driving Long-Term Changes of the Suprabenthos in the Seine Estuary?'. *Marine Pollution Bulletin* 118 (1–2), 307-318

Pham, C., Goeury, C., and Joly, A. (2016) *TELEMAC MODELLING SYSTEM: 3D Hydrodynamics TELEMAC-3D Software Releaase 7.0 Operating Manual*. National Hydraulics and Environment Laboratory, EDF R&D, France: EDF R&D

Pietrzak, J. D., de Boer, G. J., and Eleveld, M. A. (2011) 'Mechanisms Controlling the Intra-Annual Mesoscale Variability of SST and SPM in the Southern North Sea'. *Continental Shelf Research* [online] 31 (6), 594-610. available from <http://www.sciencedirect.com/science/article/pii/S0278434310003882>

Pinet, P. R. (2019) *Invitation to Oceanography*. 8th edn. Burlington, MA: Jones & Bartlett Learning

Pittaluga, M. B.., Tambroni, N., Canestrelli, A., Slingerland, R., Lanzoni, S., and Seminara, G. (2015) 'Where River and Tide Meet: The Morphodynamic Equilibrium of Alluvial Estuaries'. *Journal of Geophysical Research: Earth Surface* 120 (1), 75-94

Pontee, N. I., Whitehead, P. A., and Hayes, C. M. (2004) 'The Effect of Freshwater Flow on Siltation in the Humber Estuary, North East UK'. *Estuarine, Coastal and Shelf Science* [online] 60 (2), 241-249. available from <http://www.sciencedirect.com/science/article/pii/S0272771404000174>

Prandle, D. (2009) *Estuaries Dynamics, Mixing, Sedimentation and Morphology*. Cambridge; New York: Cambridge University Press

Prasad, S., Balakrishnan, N., Francis, P., and Vijayalaksmi, T. (2014) 'Hindcasting and Validation of Mumbai Oil Spills using GNOME'. *International Research Journal of Environment Sciences* 3 (12), 18-27

Pritchard, D. W. (1955) 'Estuarine Circulation Patterns.'. *Proceedings of the American Society of Civil Engineers* 81, 717/1-717/11

Priya, K. L., Jegathambal, P., and James, E. J. (2012) 'Hydrodynamic Modeling of Estuaries - A-State-of-Art'. *International Journal of Environmental Science* 3 (1), 233-240

Pu, X., Shi, J. Z., and Hu, G. (2016) 'Analyses of Intermittent Mixing and Stratification within the North Passage of the Changjiang (Yangtze) River Estuary, China: A Three-Dimensional Model Study'. *Journal of Marine Systems* [online] 158, 140-

164. available from <http://www.sciencedirect.com/science/article/pii/S0924796316000403>

Pye, K. and Blott, S. J. (2014) 'The Geomorphology of UK Estuaries: The Role of Geological Controls, Antecedent Conditions and Human Activities'. *Estuarine, Coastal and Shelf Science* [online] 150 (Part B), 196-214. available from <http://www.sciencedirect.com/science/article/pii/S0272771414001425>

Quinn, N., Lewis, M., Wadey, M. P., and Haigh, I. D. (2014) 'Assessing the Temporal Variability in Extreme Storm-Tide Time Series for Coastal Flood Risk Assessment'. *Journal of Geophysical Research: Oceans* 119 (8), 4983-4998

Rahman, A. and Venugopal, V. (2017) 'Parametric Analysis of Three Dimensional Flow Models Applied to Tidal Energy Sites in Scotland'. *Estuarine, Coastal and Shelf Science* 189, 17-32

Rahman, A. and Venugopal, V. (eds.) (2015) *Proceedings of the 11th European Wave and Tidal Energy Conference*. 'Inter-Comparison of 3D Tidal Flow Models Applied to Orkney Islands and Pentland Firth'. held 6-11th Sept 2015 at Nantes, France

Ranasinghe, R., Duong, T. M., Uhlenbrook, S., Roelvink, D., and Stive, M. (2012) 'Climate-Change Impact Assessment for Inlet-Interrupted Coastlines'. *Nature Climate Change* 3, 83

Ranieri, A., Lyra, A. P., Lemos, B., Lutz, G., and Andrade, F. (eds.) (2013b) *SPE Latin-American and Caribbean Health, Safety, Environment and Social Responsibility Conference*. 'Oil Spill Response Equipment and Techniques for Waxy Oils in Brazil'. held 26 - 27 June at Lima, Peru: Society of Petroleum Engineers

Ranieri, A., Lyra, A. P., Lutz, G., Andrade, F., Santos, F., and Pellegrini, J. (eds.) (2013a) *SPE Latin-American and Caribbean Heath, Safety, Environment and Social Responsibility Conference*. 'Introducing Resources in Oil Spill Trajectory Modeling - Contingency Analysis'. held 26-27 June at Lima, Peru: Society of Petroleum Engineers

Ranji, Z., Hejazi, K., Soltanpour, M., and Allahyar, M. R. (2017) 'Inter-Comparison of Recent Tide Models for the Persian Gulf and Oman Sea'. *Coastal Engineering Proceedings* 1 (35)

Ray, R. D., Egbert, G. D., and Erofeeva, S. Y. (2011) 'Tide Predictions in Shelf and Coastal Waters: Status and Prospects'. in *Coastal Altimetry* . ed. by Vignudelli, S., Kostianoy, A. G., Cipollini, P., and Benveniste, J. Berlin: Springer-Verlag, 191-216

Reed, M., Johansen, Ø., Leirvik, F., and Brørs, B. (2009) 'Numerical Algorithm to Compute the Effects of Breaking Waves on Surface Oil Spilled at Sea'. *A Final Report Submitted to NOAA/UNH Coastal Response Research Center* MK 800704, 1-75

Reed, M., Daling, P. S., Brakstad, O. G., Singsaas, I., Faksness, L., Hetland, B., and Ekrol, N. (eds.) (2000) *Proceedings of the 23. Arctic and Marine Oilspill Program (AMOP) Technical Seminar*. 'OSCAR2000: A Multi-Component 3-Dimensional Oil Spill Contingency and Response Model'. held 14-16 June at Vancouver, Canada: Environment Canada

Reed, M., Johansen, Ø., Brandvik, P. J., Daling, P. S., Lewis, A., Fiocco, R., Mackay, D., and Prentki, R. (1999) 'Oil Spill Modeling Towards the Close of the 20th Century: Overview of the State of the Art'. *Spill Science & Technology Bulletin* 5 (1), 3-16

Reed, M., French-McCay, D. P., Rines, H., and Rye, H. (1995b) 'A Three-Dimensional Oil and Chemical Spill Model for Environmental Impact Assessment'. *International Oil Spill Conference Proceedings* 1995 (1), 61-66

Reed, M., Aamo, O. M., and Daling, P. S. (1995a) 'Quantitative Analysis of Alternate Oil Spill Response Strategies using OSCAR'. *Spill Science & Technology Bulletin* [online] 2 (1), 67-74. available from <http://www.sciencedirect.com/science/article/pii/1353256195000205>

Reed, M., Gundlach, E., and Kana, T. (1989) 'A Coastal Zone Oil Spill Model: Development and Sensitivity Studies'. *Oil and Chemical Pollution* [online] 5 (6), 411-449. available from <http://www.sciencedirect.com/science/article/pii/S026985798980019X>

Rehitha, T. V., Ullas, N., Vineetha, G., Benny, P. Y., Madhu, N. V., and Revichandran, C. (2017) 'Impact of Maintenance Dredging on Macrobenthic Community Structure of a Tropical Estuary'. *Ocean & Coastal Management* 144, 71-82

Restrepo, J. C., Ortíz, J. C., Pierini, J., Schrottke, K., Maza, M., Otero, L., and Aguirre, J. (2014) 'Freshwater Discharge into the Caribbean Sea from the Rivers of Northwestern South America (Colombia): Magnitude, Variability and Recent Changes'. *Journal of Hydrology* [online] 509, 266-281. available from <http://www.sciencedirect.com/science/article/pii/S002216941300869X>

Reynaud, J., Witt, C., Pazmiño, A., and Gilces, S. (2018) 'Tide-Dominated Deltas in Active Margin Basins: Insights from the Guayas Estuary, Gulf of Guayaquil, Ecuador'. *Marine Geology* [online] 403, 165-178. available from <http://www.sciencedirect.com/science/article/pii/S0025322718300598>

Reynolds, C., Kim, Y. H., Isaji, T., Jayko, K., and Comerma, E. (2009) *Oil Spill, Produced Water, Drilling Mud and Drill Cuttings Discharge Modeling, Ghana*: ASA

Rice, K. C., Hong, B., and Shen, J. (2012) 'Assessment of Salinity Intrusion in the James and Chickahominy Rivers as a Result of Simulated Sea-Level Rise in Chesapeake Bay, East Coast, USA'. *Journal of Environmental Management* [online] 111, 61-69. available from <http://www.sciencedirect.com/science/article/pii/S0301479712003519>

Robins, P. E., Skov, M. W., Lewis, M. J., Giménez, L., Davies, A. G., Malham, S. K., Neill, S. P., McDonald, J. E., Whitton, T. A., Jackson, S. E., and Jago, C. F. (2016) 'Impact of Climate Change on UK Estuaries: A Review of Past Trends and Potential Projections'. *Estuarine, Coastal and Shelf Science* [online] 169, 119-135. available from <http://www.sciencedirect.com/science/article/pii/S0272771415301669>

Robins, P. E., Lewis, M. J., Simpson, J. H., Howlett, E. R., and Malham, S. K. (2014) 'Future Variability of Solute Transport in a Macrotidal Estuary'. *Estuarine, Coastal and Shelf Science* [online] 151, 88-99. available from <http://www.sciencedirect.com/science/article/pii/S0272771414002716>

Robins, P. E., Neill, S. P., Giménez, L., Jenkins, S., and Malham, S. K. (2013) 'Physical and Biological Controls on Larval Dispersal and Connectivity in a Highly Energetic Shelf Sea'. *Limnology and Oceanography* 58 (2), 505-524

Ross, L. and Sottolichio, A. (2016) 'Subtidal Variability of Sea Level in a Macrotidal and Convergent Estuary'. *Continental Shelf Research* [online] 131, 28-41. available from <http://www.sciencedirect.com/science/article/pii/S0278434316305970>

RPS (2016b) *The OILMAP Suite*: RPS Group

RPS (2016a) *OILMAP Release Notes Version: 7.0 (July 2016)*. South Kingstown, Rhodes Island: RPS Group

RPS ASA (2019) *Software - OILMAP* [online] available from <http://www.asascience.com/software/oilmap/> [June/26 2019]

Rudder, A. C. (1992) 'An Explicit Hamiltonian Formulations of Surface Waves in Water of Finite Depth'. *Journal of Fluid Mechanics* 237, 435-455

Rutherford, R., Moulitsas, I., Snow, B. J., Kolios, A. J., and De Dominicis, M. (2015) 'CranSLIK v2.0: Improving the Stochastic Prediction of Oil Spill Transport and Fate using Approximation Methods'. *Geoscientific Model Development* 8 (10), 3365-3377

Samaras, A. G., De Dominicis, M., Archetti, R., Lamberti, A., and Pinardi, N. (2014) 'Towards Improving the Representation of Beaching in Oil Spill Models: A Case Study'. *Marine Pollution Bulletin* 88 (1–2), 91-101

Samuels, W. B., Huang, N. E., and Amstutz, D. E. (1982) 'An Oilspill Trajectory Analysis Model with a Variable Wind Deflection Angle'. *Ocean Engineering* [online] 9 (4), 347-360. available from <http://www.sciencedirect.com/science/article/pii/0029801882900282>

Savcenko, R. and Bosch, W. (2012) *EOT11A - Empirical Ocean Tide Model from Multi-Mission Satellite Altimetry*. München, Germany: Deutsches Geodätisches Forschungsinstitut (DGFI)

Savenije, H. H. G. (2005) *Salinity and Tides in Alluvial Estuaries*. 1st ed.. edn. Amsterdam: Amsterdam : Elsevier

Savenije, H. H. G. (2001) 'A Simple Analytical Expression to Describe Tidal Damping Or Amplification'. *Journal of Hydrology* [online] 243 (3), 205-215. available from <http://www.sciencedirect.com/science/article/pii/S0022169400004145>

Sayed, M., Serrer, M., and Mansard, E. (2008) 'Oil Spill Drift and Fate Model'. in *Oil Spill Response: A Global Perspective*. ed. by Davidson, W. F., Lee, K., and Cogswell, A. Netherlands: Springer Science & Business Media, 205-220

Scharler, U. M. (2012) 'Ecosystem Development during Open and Closed Phases of Temporarily open/closed Estuaries on the Subtropical East Coast of South Africa'. *Estuarine, Coastal and Shelf Science* [online] 108, 119-131. available from <http://www.sciencedirect.com/science/article/pii/S0272771411003416>

Schettini, C. A. F., Valle-Levinson, A., and Truccolo, E. C. (2017) 'Circulation and Transport in Short, Low-Inflow Estuaries Under Anthropogenic Stresses'. *Regional Studies in Marine Science* 10, 52-64

Schettini, C. A. F. and Miranda, L. B. d. (2010) 'Circulation and Suspended Particulate Matter Transport in a Tidally Dominated Estuary: Caravelas Estuary, Bahia, Brazil'. *Brazillian Journal of Oceanography* 58 (1), 1-11

Schiller, R. and Kourafalou, V. H. (2010) 'Modeling River Plume Dynamics with the Hybrid Coordinate Ocean Model'. *Ocean Modelling* 33 (1-2), 101-117

Scholz, D., Kucklick, J., Pond, R., Walker, A., Bostrom, A., and Fischbeck, P. (1999) *Fate of Spilled Oil in Marine Waters: Where does it Go? what does it do? how do Dispersants Affect it?*: American Petroleum Institute

Sebastião, P. and Guedes Soares, C. (2007) 'Uncertainty in Predictions of Oil Spill Trajectories in Open Sea'. *Ocean Engineering* 34 (3–4), 576-584

Sebastião, P. and Guedes Soares, C. (1995) 'Modeling the Fate of Oil Spills at Sea'. *Spill Science & Technology Bulletin* [online] 2 (2), 121-131. available from <http://www.sciencedirect.com/science/article/pii/S1353256196000096>

Seenath, A., Wilson, M., and Miller, K. (2016) 'Hydrodynamic Versus GIS Modelling for Coastal Flood Vulnerability Assessment: Which is Better for Guiding Coastal Management?'. *Ocean & Coastal Management* 120, 99-109

Seifi, F., Deng, X., and Baltazar Andersen, O. (2019) 'Assessment of the Accuracy of Recent Empirical and Assimilated Tidal Models for the Great Barrier Reef, Australia, using Satellite and Coastal Data'. *Remote Sensing* 11 (1211)

Sharpe, J. D., Kaufman, J. A., Goldman, Z. E., Wolkin, A., and Gribble, M. O. (2019) 'Determinants of Oil-Spill Cleanup Participation Following the Deepwater Horizon Oil Spill'. *Environmental Research* [online] 170, 472-480. available from <http://www.sciencedirect.com/science/article/pii/S001393511930009X>

Shchepetkin, A. F. and McWilliams, J. C. (2003) 'A Method for Computing Horizontal Pressure-Gradient Force in an Oceanic Model with a Nonaligned Vertical Coordinate'. *Journal of Geophysical Research* 108 (C3)

Sigleo, A. C. and Frick, W. E. (2007) 'Seasonal Variations in River Discharge and Nutrient Export to a Northeastern Pacific Estuary'. *Estuarine, Coastal and Shelf Science* [online] 73 (3), 368-378. available from <http://www.sciencedirect.com/science/article/pii/S0272771407000388>

Simecek-Beatty, D. and Lehr, W. J. (2016) '23 - Forensic Trajectory Modeling of Marine Oil Spills'. in *Standard Handbook Oil Spill Environmental Forensics (Second Edition)*. ed. by Stout, S. A. and Wang, Z. Boston: Academic Press, 1015-1037

Simecek-Beatty, D. (2011) '*Oil Spill Trajectory Forecasting - Uncertainty and Emergency Response*'. in *Oil Spill Science and Technology.* ed. by Fingas, M. F. Burlington, MA: Elsvier/Gulf Professional Pub., 275-299

Singsaas, I., Reed, M., and Daling, P. S. (eds.) (2000) *Use of a Recently Developed Model System in Oil Spill Response Analysis*. 'SPE International Conference on Health, Safety and Environment in Oil and Gas Exploration and Production, 26-28 June' at Stavanger, Norway: Society of Petroleum Engineers

Skinner, C. J., Coulthard, T. J., Parsons, D. R., Ramirez, J. A., Mullen, L., and Manson, S. (2015) 'Simulating Tidal and Storm Surge Hydraulics with a Simple 2D Inertia Based Model, in the Humber Estuary, U.K'. *Estuarine, Coastal and Shelf Science* [online] 155 (Supplement C), 126-136. available from <http://www.sciencedirect.com/science/article/pii/S0272771415000402>

Slinger, J. H. (2017) 'Hydro-Morphological Modelling of Small, Wave-Dominated Estuaries'. *Estuarine, Coastal and Shelf Science* [online] 198, 583-596. available from <http://www.sciencedirect.com/science/article/pii/S0272771416305467>

Smolders, S., Tatiana, M., Joris, V., and Teles, M. J. (eds.) (2014) 21st Telemac Mascaret User Conference. 'Implementation of Controlled Reduced Tide and Flooding Areas in the TELEMAC 3D Model of the Scheldt Estuary'. held 15-17 October at Grenoble, France. France

Snow, G. C. (2016) 'Determining the Health of River-Dominated Estuaries using Microalgal Biomass and Community Composition'. *South African Journal of*

Botany [online] 107, 21-30. available from <http://www.sciencedirect.com/science/article/pii/S0254629916002374>

Snowden, R. J. and Ekweozor, I. K. E. (1987) 'The Impact of a Minor Oil Spillage in the Estuarine Niger Delta'. *Marine Pollution Bulletin* [online] 18 (11), 595-599. available from <http://www.sciencedirect.com/science/article/pii/0025326X87902797>

Sobey, R. J. and Barker, C. (1997) 'Wave-Driven Transport of Surface Oil'. *Journal of Coastal Research* 13 (2), 490-496

Socolofsky, S. A., Adams, E. E., Boufadel, M. C., Aman, Z. M., Johansen, Ø., Konkel, W. J., Lindo, D., Madsen, M. N., North, E. W., Paris, C. B., Rasmussen, D., Reed, M., Rønningen, P., Sim, L. H., Uhrenholdt, T., Anderson, K. G., Cooper, C., and Nedwed, T. J. (2015) 'Intercomparison of Oil Spill Prediction Models for Accidental Blowout Scenarios with and without Subsea Chemical Dispersant Injection'. *Marine Pollution Bulletin* 96 (1–2), 110-126

Sorgente, R., Tedesco, C., Pessini, F., De Dominicis, M., Gerin, R., Olita, A., Fazioli, L., Di Maio, A., and Ribotti, A. (2016) 'Forecast of Drifter Trajectories using a Rapid Environmental Assessment Based on CTD Observations'. *Deep Sea Research Part II: Topical Studies in Oceanography* 133, 39-53

Sotillo, M. G., Fanjul, E. A., Castanedo, S., Abascal, A. J., Menendez, J., Emelianov, M., Olivella, R., García-Ladona, E., Ruiz-Villarreal, M., Conde, J., Gómez, M., Conde, P., Gutierrez, A. D., and Medina, R. (2008) 'Towards an Operational System for Oil-Spill Forecast Over Spanish Waters: Initial Developments and Implementation Test'. *Marine Pollution Bulletin* 56 (4), 686-703

Souli, M. and Benson, D. J. (2010) *Arbitrary Lagrangian Eulerian and Fluid-Structure Interaction: Numerical Simulation*. 1st edn. London: ISTE

Spaulding, M. L. (2017) 'State of the Art Review and Future Directions in Oil Spill Modeling'. *Marine Pollution Bulletin* 115 (1-2), 7-19

Stansby, P., Chini, N., and Lloyd, P. (2016) 'Oscillatory Flows Around a Headland by 3D Modelling with Hydrostatic Pressure and Implicit Bed Shear Stress Comparing with Experiment and Depth-Averaged Modelling'. *Coastal Engineering* 116, 1-14

Sterling, M. C., Bonner, J. S., Ernest, A. N. S., Page, C. A., and Autenrieth, R. L. (2004) 'Characterizing Aquatic sediment–oil Aggregates using in Situ Instruments'. *Marine Pollution Bulletin* [online] 48 (5), 533-542. available from <http://www.sciencedirect.com/science/article/pii/S0025326X03004545>

Stiver, W. and Mackay, D. (1984) 'Evaporation Rate of Spills of Hydrocarbons and Petroleum Mixtures'. *Environmental Science & Technology* 18 (11), 834-840

Stronach, J. and Hospital, A. (eds.) (2014) *37th Arctic and Marine Oil Spill Program Technical Seminar on Environmental Contamination and Response*. 'The Implementation of Molecular Diffusion to Simulate the Fate and Behaviour of a Diluted Bitumen Oil Spill and its Application to Stochastic Modelling'. held June 2014 at Canmore, Alberta, Canada

Syvitski, J. P. M. (2008) 'Deltas at Risk'. *Sustainability Science* 3 (1), 23-32

Syvitski, J. P. M. and Saito, Y. (2007) 'Morphodynamics of Deltas Under the Influence of Humans'. *Global and Planetary Change* 57 (3–4), 261-282

Taguchi, E., Stammer, D., and Zahel, W. (2014) 'Inferring Deep Ocean Tidal Energy Dissipation from the Global High-Resolution Data-Assimilative HAMTIDE Model'. *Journal of Geophysical Research: Oceans* 119 (7), 4573-4592

Tessier, B. (2012) 'Stratigraphy of Tide-Dominated Estuaries'. in *Principles of Tidal Sedimentology*. ed. by Davis Jr, R. and Dalrymple, R. W. Dordrecht: Springer, 109-128

Tessier, B., Billeaud, I., Sorrel, P., Delsinne, N., and Lesueur, P. (2012) 'Infilling Stratigraphy of Macrotidal Tide-Dominated Estuaries. Controlling Mechanisms: Sea-Level Fluctuations, Bedrock Morphology, Sediment Supply and Climate Changes (the Examples of the Seine Estuary and the Mont-Saint-Michel Bay, English Channel, NW France)'. *Sedimentary Geology* 279, 62-73

Tkalich, P., Huda, K., and Gin, K. Y. H. (2003) 'A Multiphase Oil Spill Model'. *Journal of Hydraulic Research* 41 (2), 115-125

Tkalich, P. and Chan, E. S. (2002) 'Vertical Mixing of Oil Droplets by Breaking Waves'. *Marine Pollution Bulletin* 44 (11), 1219-1229

Townend, I. and Whitehead, P. (2003) 'A Preliminary Net Sediment Budget for the Humber Estuary'. *Science of the Total Environment* [online] 314-316 (Supplement C), 755-767. available from <http://www.sciencedirect.com/science/article/pii/S0048969703000822>

Toz, A. C. and Koseoglu, B. (2018) 'Trajectory Prediction of Oil Spill with Pisces 2 Around Bay of Izmir, Turkey'. *Marine Pollution Bulletin* [online] 126 (Supplement C), 215-227. available from <http://www.sciencedirect.com/science/article/pii/S0025326X17307269>

Tri, D. Q., Don, N. C., Ching, C. Y., and Mishra, P. K. (2015) 'Application of Environmental Sensitivity Index (ESI) Maps of Shorelines to Coastal Oil Spills: A Case Study of Cat Ba Island, Vietnam'. *Environmental Earth Sciences* 74 (4), 3433-3451

Tweedley, J. R., Warwick, R. M., and Potter, I. C. (2016) 'The Contrasting Ecology of Temperate Macrotidal and Microtidal Estuaries'. in *Hughes, R.,Hughes, D.,* *Hughes ,R., Dale, A. and Smith, I. Oceanography and Marine Biology: An Annual Review, Volume 53.* ed. by Anon: CRC Press, 73-171

Umrao, R. K., Sharma, L. K., Singh, R., and Singh, T. N. (2018) 'Determination of Strength and Modulus of Elasticity of Heterogenous Sedimentary Rocks: An ANFIS Predictive Technique'. *Measurement* [online] 126, 194-201. available from <http://www.sciencedirect.com/science/article/pii/S026322411830455X>

Uncles, R. J., Easton, A. E., Griffiths, M. L., Harris, C. B., Howland, R. J. M., King, R. S., Morris, A. W., and Plummer, D. H. (1998c) 'Seasonality of the Turbidity Maximum in the Humber–Ouse Estuary, UK'. *Marine Pollution Bulletin* [online] 37 (3), 206-215. available from <http://www.sciencedirect.com/science/article/pii/S0025326X98901576>

Uncles, R. J., Howland, R. J. M., Easton, A. E., Griffiths, M. L., Harris, C. B., King, R. S., Morris, A. W., Plummer, D. H., and Woodward, E. M. S. (1998b) 'Seasonal Variability of Dissolved Nutrients in the Humber–Ouse Estuary, UK'. *Marine Pollution Bulletin* [online] 37 (3), 234-246. available from <http://www.sciencedirect.com/science/article/pii/S0025326X98901175>

Uncles, R. J., Easton, A. E., Griffiths, M. L., Harris, C. B., Howland, R. J. M., Joint, I., King, R. S., Morris, A. W., and Plummer, D. H. (1998a) 'Concentrations of Suspended Chlorophyll in the Tidal Yorkshire Ouse and Humber Estuary'. *Science of the Total Environment* 210-211, 367-375

Vale, L. M. and Dias, J. M. (2011) 'Coupling of a Lagrangian Particle Tracking Module to a Numerical Hydrodynamic Model: Simulation of Pollution Events Inside an Estuarine Port Area'. *Journal of Coastal Research* SI (64), 1609-1613

Valle-Levinson, A. (2010) *Contemporary Issues in Estuarine Physics* [online] . Cambridge: Cambridge University Press. available from <https://www.cambridge.org/core/books/contemporary-issues-in-estuarine-physics/5D204C31934B0B3E87EB1B7D0325DA2D> [2019/08/12]

van der Wal, D., Wielemaker-van den Dool, A., and Herman, P. M. J. (2010) 'Spatial Synchrony in Intertidal Benthic Algal Biomass in Temperate Coastal and Estuarine Ecosystems'. *Ecosystems* 13 (2), 338-351

van Griensven, A., Popescu, I., Abdelhamid, M. R., Ndomba, P. M., Beevers, L., and Betrie, G. D. (2013) 'Comparison of Sediment Transport Computations using Hydrodynamic Versus Hydrologic Models in the Simiyu River in Tanzania'. *Physics and Chemistry of the Earth, Parts A/B/C* 61–62, 12-21

van Maren, D. S. and Hoekstra, P. (2004) 'Seasonal Variation of Hydrodynamics and Sediment Dynamics in a Shallow Subtropical Estuary: The Ba Lat River, Vietnam'. *Estuarine, Coastal and Shelf Science* [online] 60 (3), 529-540. available from <http://www.sciencedirect.com/science/article/pii/S0272771404000599>

van Maren, D. S., Hoekstra, P., and Hoitink, A. J. F. (2004) 'Tidal Flow Asymmetry in the Diurnal Regime: Bed-Load Transport and Morphologic Changes Around the Red River Delta'. *Ocean Dynamics* 54 (3-4), 424-434

Vethamony, P., Sudheesh, K., Babu, M. T., Jayakumar, S., Manimurali, R., Saran, A. K., Sharma, L. H., Rajan, B., and Srivastava, M. (2007) 'Trajectory of an Oil Spill Off Goa, Eastern Arabian Sea: Field Observations and Simulations'. *Environmental Pollution* 148 (2), 438-444

Vidmar, P. and Perkovič, M. (2018) 'Safety Assessment of Crude Oil Tankers'. *Safety Science* [online] 105, 178-191. available from <http://www.sciencedirect.com/science/article/pii/S0925753517313772>

Villaret, C., Hervouet, J., Kopmann, R., Merkel, U., and Davies, A. G. (2013) 'Morphodynamic Modeling using the Telemac Finite-Element System'. *Computers & Geosciences* 53, 105-113

Villoria, C., Anselmi, A., and Garcia, F. (eds.) (1991) *SPE Health, Safety and Environment in Oil and Gas Exploration and Production Conference*. 'An Oil Spill Fate Model Including Sinking Effect'. held 11-14 November at The Hague, Netherlands. The Hague, Netherlands: Society of Petroleum Engineers

Violeau, D., Bourban, S., Cheviet, C., Markofsky, M., Petersen, O., Roberts, W., Spearman, J., Toorman, E., Vested, H. J., and Weilbeer, H. (2002) 'Numerical Simulation of Cohesive Sediment Transport : Intercomparison of several Numerical Models'. *Proceedings in Marine Science* [online] 5, 75-89. available from <http://www.sciencedirect.com/science/article/pii/S1568269202800092>

Vitousek, S. and Fringer, O. B. (2014) 'A Nonhydrostatic, Isopycnal-Coordinate Ocean Model for Internal Waves'. *Ocean Modelling* 83, 118-144

Wang, C., Chen, B., Zhang, B., He, S., and Zhao, M. (2013) 'Fingerprint and Weathering Characteristics of Crude Oils After Dalian Oil Spill, China'. *Marine Pollution Bulletin* 71 (1–2), 64-68

Wang, J. and Shen, Y. (2010) 'Modeling Oil Spills Transportation in Seas Based on Unstructured Grid, Finite-Volume, Wave-Ocean Model'. *Ocean Modelling* 35 (4), 332-344

Wang, S., Shen, Y., Guo, Y., and Tang, J. (2008) 'Three-Dimensional Numerical Simulation for Transport of Oil Spills in Seas'. *Ocean Engineering* 35 (5–6), 503-510

Wang, S., Shen, Y., and Zheng, Y. H. (2005) 'Two-Dimensional Numerical Simulation for Transport and Fate of Oil Spills in Seas'. *Ocean Engineering* 32 (13), 1556-1571

Wang, Z. B. and Townend, I. (2012) 'Influence of the Nodal Tide on the Morphological Response of Estuaries'. *Marine Geology* [online] 291-294 (Supplement C), 73-82. available from <http://www.sciencedirect.com/science/article/pii/S0025322711002647>

Warluzel, A. and Benque, J. P. (1981) 'Un Modèle Mathématique De Transport Et d'étalement d'une Nappe d'hydrocarbure'. Airh 17, 199-212

Warner, J. C., Geyer, W. R., and Lerczak, J. A. (2005) 'Numerical Modeling of an Estuary: A Comprehensive Skill Assessment'. *Journal of Geophysical Research: Oceans* 110 (C5), 1-13

Watts, G., Battarbee, R. W., Bloomfield, J. P., Crossman, J., Daccache, A., Durance, I., Elliott, J. A., Garner, G., Hannaford, J., Hannah, D. M., Hess, T., Jackson, C. R., Kay, A. L., Kernan, M., Knox, J., Mackay, J., Monteith, D. T., Ormerod, S. J., Rance, J., Stuart, M. E., Wade, A. J., Wade, S. D., Weatherhead, K., Whitehead, P. G., and Wilby, R. L. (2015) 'Climate Change and Water in the UK – Past Changes and Future Prospects'. *Progress in Physical Geography: Earth and Environment* 39 (1), 6-28

Wei, Q. F., Mather, R. R., Fotheringham, A. F., and Yang, R. D. (2003) 'Evaluation of Nonwoven Polypropylene Oil Sorbents in Marine Oil-Spill Recovery'. *Marine Pollution Bulletin* 46 (6), 780-783

Whitehead, P. G., Wilby, R. L., Battarbee, R. W., Kernan, M., and Wade, A. J. (2009) 'A Review of the Potential Impacts of Climate Change on Surface Water Quality'. *Hydrological Sciences Journal* 54 (1), 101-123

Whitman, W. G. (1923) 'The Two-Film Theory of Absorption'. Chemical and Metallurgical Engineering

Williams, A. K., Bacosa, H. P., and Quigg, A. (2017) 'The Impact of Dissolved Inorganic Nitrogen and Phosphorous on Responses of Microbial Plankton to the Texas City "Y" Oil Spill in Galveston Bay, Texas (USA)'. *Marine Pollution Bulletin* 121 (1-2), 32-44

Winterwerp, J. C. (2011) 'Fine Sediment Transport by Tidal Asymmetry in the High-Concentrated Ems River: Indications for a Regime Shift in Response to Channel Deepening'. *Ocean Dynamics* 61 (2-3), 203-215

Wirtz, K. W., Baumberger, N., Adam, S., and Liu, X. (2007) 'Oil Spill Impact Minimization Under Uncertainty: Evaluating Contingency Simulations of the Prestige Accident'. *Ecological Economics* 61 (2–3), 417-428

Woodroffe, C. D., Nicholls, R. J., Saito, Y., Chen, Z., and Goodbred, S. L. (2006) 'Landscape Variability and the Response of Asian Megadeltas to Environmental Change'. in *Global Change and Integrated Coastal Management, Volume 10*. ed. by AnonDordrecht, The Netherlands: Springer, 277-314

Woodruff, J. D., Geyer, W. R., Sommerfield, C. K., and Driscoll, N. W. (2001) 'Seasonal Variation of Sediment Deposition in the Hudson River Estuary'. *Marine Geology* [online] 179 (1), 105-119. available from <http://www.sciencedirect.com/science/article/pii/S0025322701001827>

Wu, X. and Parsons, D. R. (2019) 'Field Investigation of Bedform Morphodynamics Under Combined Flow'. *Geomorphology* [online] 339, 19-30. available from <http://www.sciencedirect.com/science/article/pii/S0169555X19301850>

Wu, Y., Falconer, R. A., and Uncles, R. J. (1999) 'Modelling of Water Flows and Cohesive Sediment Fluxes in the Humber Estuary, UK'. *Marine Pollution Bulletin* [online] 37 (3), 182-189. available from <http://www.sciencedirect.com/science/article/pii/S0025326X99001034>

Xie, H., Yapa, P. D., and Nakata, K. (2007) 'Modeling Emulsification After an Oil Spill in the Sea'. *Journal of Marine Systems* 68 (3–4), 489-506

Xu, H., Chen, J., Wang, S., and Liu, Y. (2012) 'Oil Spill Forecast Model Based on Uncertainty Analysis: A Case Study of Dalian Oil Spill'. *Ocean Engineering* 54, 206-212

Yamanaka, T., Raffaelli, D., and White, P. C. L. (2010) 'Physical Determinants of Intertidal Communities on Dissipative Beaches: Implications of Sea-Level Rise'. *Estuarine, Coastal and Shelf Science* [online] 88 (2), 267-278. available from <http://www.sciencedirect.com/science/article/pii/S0272771410001204>

Yan, Y., Zheng, J., and Huang, H. (eds.) (2012) *The Tenth ISOPE Pacific/Asia Offshore Mechanics Symposium*. 'Numerical Simulation of Accidental Oil Spill in Min River Estuary'. held 3-5 October at Vladivostok, Russia: The International Society of Offshore and Polar Engineers

Yang, S. and You, X. (2016) 'Determination of the Oil Spill Removal Area by Oil Particle Tracking in a Harbor'. *Oceanological and Hydrobiological Studies* 45 (2), 230-238

Young, G. C. and Potter, I. C. (2002) 'Influence of Exceptionally High Salinities, Marked Variations in Freshwater Discharge and Opening of Estuary Mouth on the Characteristics of the Ichthyofauna of a Normally-Closed Estuary'. *Estuarine, Coastal and Shelf Science* [online] 55 (2), 223-246. available from <http://www.sciencedirect.com/science/article/pii/S0272771401908996>

Zanier, G., Petronio, A., and Armenio, V. (2017) 'The Effect of Coriolis Force on Oil Slick Transport and Spreading at Sea'. *Journal of Hydraulic Research* 55 (3), 409-422

Zawadzki, L., Ablain, M., Carrère, L., Ray, R. D., Zelensky, N. P., Lyard, F., Guillot, A., and Picot, N. (2016) 'Reduction of the 59-Day Error Signal in the Mean Sea Level Derived from TOPEX/Poseidon, Jason-1 and Jason-2 Data with the Latest FES and GOT Ocean Tide Models'. *Ocean Science Discussions*, 1-20

Zeinstra-Helfrich, M., Koops, W., and Murk, A. J. (2016) 'How Oil Properties and Layer Thickness Determine the Entrainment of Spilled Surface Oil'. *Marine Pollution Bulletin* 110 (1), 184-193

Zelenke, B., O'Connor, C., Barker, C., Beegle-Krause, C. J., and Eclipse, L. (2012) *General NOAA Operational Modeling Environment (GNOME) Technical Documentation. U.S. Dept. of Commerce, NOAA Technical Memorandum NOS OR&R 40*. Seattle, WA: Emergency Response Division, NOAA

Zhai, W., Dai, M., Cai, W., Wang, Y., and Wang, Z. (2005) 'High Partial Pressure of CO2 and its Maintaining Mechanism in a Subtropical Estuary: The Pearl River Estuary, China'. *Marine Chemistry* [online] 93 (1), 21-32. available from <http://www.sciencedirect.com/science/article/pii/S030442030400218X>

Zhang, B., Zhang, C., and Ozer, J. (eds.) (1991) *SURF -A Simulation Model for the Behaviour of Oil Slicks at Sea*. 'In: Ozer, J. (Ed.) (1991) *Oil Pollution: Environmental Risk Assessment (OPERA)*. 'Proceedings of the Final Workshop'. Held 9-10 December at Dalian - China. Brussel: European Economic Communit'. held 9-10 December

Zhang, D. (2017) 'A Coefficient of Determination for Generalized Linear Models'. *The American Statistician* 71 (4), 310-316

Zhang, H., Yin, X., Zhou, H., Wang, J., and Han, L. (2015) 'Weathering Characteristics of Crude Oils from Dalian Oil Spill Accident, China'. *Aquatic Procedia* 3, 238-244

Zhang, H., Sun, T., Xue, S., Yang, W., and Yin, X. (2017) 'Environmental Flow Assessment in Estuaries Taking into Consideration Species Dispersal in Fragmented Potential Habitats'. *Ecological Indicators* 78, 541-548

Zhang, M., Townend, I., Cai, H., He, J., and Mei, X. (2018) 'The Influence of Seasonal Climate on the Morphology of the Mouth-Bar in the Yangtze Estuary, China'. *Continental Shelf Research* [online] 153, 30-49. available from <http://www.sciencedirect.com/science/article/pii/S0278434317302807>

Zhang, Y. J., Ateljevich, E., Yu, H., Wu, C. H., and Yu, J. C. S. (2015) 'A New Vertical Coordinate System for a 3D Unstructured-Grid Model'. *Ocean Modelling* 85, 16-31

Zhang, Y. J. and Baptista, A. M. (2008) 'SELFE: A Semi-Implicit Eulerian–Lagrangian Finite-Element Model for Cross-Scale Ocean Circulation'. *Ocean Modelling* 21 (3–4), 71-96

Zhao, L., Torlapati, J., Boufadel, M. C., King, T., Robinson, B., and Lee, K. (2014) 'VDROP: A Comprehensive Model for Droplet Formation of Oils and Gases in Liquids - Incorporation of the Interfacial Tension and Droplet Viscosity'. *Chemical Engineering Journal* [online] 253, 93-106. available from <http://www.sciencedirect.com/science/article/pii/S1385894714005142>

Zhao, X., Liang, D., and Martinelli, M. (2017) 'MPM Simulations of Dam-Break Floods'. *Journal of Hydrodynamics, Ser.B* 29 (3), 397-404

Zheng, L. and Yapa, P. D. (2000) 'Buoyant Velocity of Spherical and Non-Spherical Bubbles/ Droplets.'. *Journal of Hydraulic Engineering* 126 (11), 852-854

Zhou, J. G. (2013) *Lattice Boltzmann Methods for Shallow Water Flows*.: Springer Berlin Heidelberg

Zhu, L., He, Q., Shen, J., and Wang, Y. (2016) 'The Influence of Human Activities on Morphodynamics and Alteration of Sediment Source and Sink in the Changjiang Estuary'. *Geomorphology* 273, 52-62

Zigic, S. (2004) 'Ocean Modelling - Systems Available for the Environment and Scientific Coordinator'. *13th National Plan: Environment and Scientific Coordinators Workshop*, 49-71

APPENDICES

APPENDIX A: WIND–WAVE MODELLING TOOLS

The hydrodynamics in estuaries become extremely complex with the interaction between tides and waves (Jia et al. 2015; Xu and You 2017). In most oil spill models the wave and wind-induced current are added together and represented as an empirically based drift factor of local wind (Section 2.2.1.3). However, the sea state of any water body is not only made up of waves generated because of local wind but also of waves propagating over a large distance (Guo et al. 2014). The propagation of surface gravity waves across shallow water is affected by bathymetry (reflection, diffraction, shoaling and trapping), dissipation (bottom friction and wave breaking) and nonlinear wave-wave interactions (triad and quadruplet wave-wave interaction) (Gorrell et al. 2011). The Doppler shifting on wave frequency is the simplest and well-known effect of a current on the waves (Dong and Kirby 2012). Other effects are wave breaking, shoaling, fraction, focusing and defocusing (Dong and Kirby 2012). While the effect of waves on current can be understood as either vortex force or radiation stress based on the computation of the wave advection terms (Dong and Kirby 2012; Jia et al. 2015). To determine the effect of waves on currents, a wave model will need to be coupled to the hydrodynamic model (Hashemi et al. 2015; De Dominicis et al. 2016). Studies by Wang and Shen (2010), Guo et al. (2014) and Liu and Sheng (2014) proved that the accuracy of oil spill models is significantly increased when hydrodynamic models are coupled with wind–wave models (i.e. when wave-current interaction is taken into account).

Waves can be simulated with phase-averaged wave models based on spectral action balance equation or spectral energy balance equation (Brière et al. 2007; Hoque et al. 2017). An alternative approach is the phase-resolving models based on Boussinesq equation (Madsen and Sørensen 1992; Li and Zhan 2001), Hamilton equation (Rudder 1992) or mild-slope equation (Berkhoff 1972; Kirby 1986). While phase-averaged models are based on the spectrum concept (which solve the evolution of wave energy spectrum in time, geographical and spectral spaces (Rusu and Guedes Soares 2009)), phase-resolving models are based on the momentum concept (Rusu and Guedes Soares 2013). Furthermore, the phase-averaged model is designed for deepwater modelling while phase-resolving models are ideal for small scale modelling such as a harbour where the effect of diffraction is predominant (Adytia et al. 2012; Thomas and Dwarakish 2015).

Phase-averaged (spectral) wave models account for wave generation, propagation and dissipation (Rusu and Guedes Soares 2013). However, a drawback of phase-averaged models is its inability to compute diffraction (Holthuijsen 2007). The inability of phase-averaged wave models to compute the effects of diffraction reduces the accuracy of the wave model (Jin and Ji 2001). Holthuijsen et al. (2003) pointed out that phase-resolving methods compute the effects of diffraction however, are limited in their capabilities to compute the effect of generation, dissipation and wave-wave interactions of the waves.

The evolution of wave modelling has been driven by the understanding of the processes that contribute to the generation of waves as well as an increase in computing power (van Vledder 2006; Janssen 2008). First-generation models are based on simple wind fields, neglecting dissipation and nonlinear wave-wave interaction while second-generation models are based on simplified nonlinear wave-wave interactions and varying wind fields (Thomas and Dwarakish 2015). Hasselmann et al.'s (1985) development of Discrete Interaction Approximation (DIA) for computing nonlinear four-wave interaction gave rise to third-generation wave models such as WAM model (The WAMDI Group 1988), WaveWatch (Tolman 1991), the SWAN model (Booij et al. 1999) and TOMAWAC (Benoit et al. 1996) (Tolman 2013; Akpinar and Ponce de León 2016). While the DIA is considered to be efficient (Janssen 2008), it is limited in its accuracy of exact nonlinear four-wave interaction (Tolman 2004; Tolman and Grumbine 2013).

The challenge of modelling transportation within Computational Fluid Dynamics can be solved either by using a Eulerian, Lagrangian or semi-Lagrangian approach (Lauritzen et al. 2010). Third-generation wave spectral models are based on the semi-Lagrangian or Eulerian approach (Sørensen et al. 2005). Lagrangian models avoid numerical diffusion (Ardhuin et al. 2001). However, the Lagrangian approach is inefficient for solving nonlinear effects such as wave-wave generation or wave breaking, as a result, key processes that contribute to wave generation and dissipation cannot be accounted for (Booij et al. 1999). While the Eulerian approach can efficiently solve all relevant processes except diffraction (Booij et al. 1999). Explicit schemes have severe time step restrictions due to CFL stability conditions (Zerroukat et al. 2002; Staniforth and Thuburn 2011). Additional numerical diffusion is a resultant effect when finite-difference approximations are employed in Eulerian models (Ardhuin et al. 2001). Ardhuin et al. (2001) point out that the computational cost of Eulerian models is too large with regards to larger shelf areas (i.e. greater than 100 km^2). The semi-Lagrangian approach combines the advantage of the Eulerian and Lagrangian approach (Lauritzen et al. 2010). This approach enables relatively longer time steps to be employed, thereby decreasing the model's computational time (Nair and Machenhauer 2002; Lentine et al. 2011). As a result, less error accumulates and the accuracy of propagation is increased (Cavaleri et al. 2007). Compared to Eulerian models, semi-Lagrangian models require much more memory per grid point. Eulerian models store only the spectrum while semi-Lagrangian models also need larger memory space to store the interpolation coefficients (Ardhuin et al. 2001). Eulerian structured grid is employed by the majority of existing wave models (Tolman 2008). An overview of popular tools employed for wind-wave modelling in the estuarine environment is further discussed.

A.1 SWAN MODEL

The SWAN (Simulating WAves Nearshore) model is an open-source third-generation numerical model to compute random, short-crested wind-generated waves in coastal areas (Pallares et al. 2014; Hashemi et al. 2015). SWAN describes the evolution of 2D wave energy spectrum (Ris et al. 1999) using a finite-difference formulation that implements either a structured (rectilinear or curvilinear) computational grid (Zubier et al. 2003) or an unstructured (triangular) computational grid (Zijlema 2010; The SWAN Team 2016a). SWAN is a phase-averaged model based on the action density spectrum (action balance equation) (N) rather than the energy density spectrum (energy transport equation) (E) as wave action density is conserved in the presence of current whereas energy density is not (Guo et al. 2014). The relationship between action density and energy density can be written as (Booij et al. 1999; Rusu and Guedes Soares 2009):

$$N(\sigma, \theta) = \frac{E(\sigma,\theta)}{\sigma} \qquad \text{(A.1)}$$

where:

σ is the intrinsic frequency; θ is the wave direction; and $N(\sigma, \theta)$ is the action density as a function of intrinsic frequency.

SWAN resolves the numerical propagation scheme using a fully implicit scheme (Booij et al. 1999). While the implicit scheme allows a large time step to be employed, a large time step may result in an increase in numerical dispersion and dissipation errors (Hsu et al. 2005). Consequently, SWAN employs an action density limiter to ensure numerical stability at relatively large time steps (The SWAN Team 2016b). An alternative to the limiter within SWAN is the frequency-dependent under-relaxation proposed by Zijlema and van der Westhuysen (2005), which improves accuracy and convergence properties. The source/sink terms are resolved using explicit and implicit schemes based on the stability of the formulation (Booij et al. 1999). SWAN is an extension of deepwater models to shallow water (i.e. coastal regions with water depth less than 20 – 30 m and horizontal scales less than 20 – 30 km e.g. tidal inlets, channels, barrier islands, tidal flats, estuaries etc.) by adding deep water source terms in WAve Model (WAM) to additional terms in other to model shallow water (Booij et al. 1999; Rusu and Guedes Soares 2011; Adytia et al. 2012). Hence the total source/sink terms employed in SWAN for shallow water (Rusu, Gonçalves and Guedes Soares 2011) becomes:

$$S_{total} = S_{in} + S_{dis,w} + S_{nl4} + S_{dis,b} + S_{dis,br} + S_{nl3} \quad \text{(A.2)}$$

Where the terms on the right-hand side represent wind input, whitecapping and quadruplet wave-wave interactions which are deep water processes of wave generation; and shallow water processes bottom friction, depth-induced breaking wave and triad wave-wave interactions respectively. SWAN employs the explicit scheme to resolve the positive source terms and negative quadruplet wave-wave interaction while an implicit scheme to resolve negative source/sink terms (Booij et al. 1999). SWAN also has an option to include other source/sink processes, these include; obstacle transmission, wave-induced set-up, vegetation dissipation. Mud dissipation and turbulence dissipation (The SWAN Team 2016b).

SWAN accounts for refraction, generation and dissipation in shallow and deep water (Jin and Ji 2001). The more recent version of SWAN (SWAN Cycle III version 41.10) also accounts for diffraction using a phase-decoupled approach based on the Berkhoff (1972) equation i.e. mild-slope equation (Holthuijsen et al. 2003; Rusu and Guedes Soares 2011). However, the phase-decoupled approach within SWAN poorly handles diffraction in harbours or in front of reflecting obstacles (The SWAN Team 2016a).

SWAN is a robust model as users have the options of activating alternative formulations for computing key parameters (Table A.1) (Rusu and Guedes Soares 2009). SELFE-SWAN model (Guo et al. 2014), POM-SWAN model (Guo and Wang 2009) and ROMS-SWAN model (Berry et al. 2012) are examples of studies that have employed SWAN in oil spill modelling. The full details of SWAN are described in Booij et al. (1999).

Table A.1: Third generation SWAN options for source terms (adapted from The SWAN Team 2016a, 2016b)

Source/Sink Term	**Option 1 (Default option)**	**Option 2**	**Option 3**
Linear wind growth	Cavaleri and Malanotte-Rizzoli (1981)		
Exponential wind growth	Snyder et al. (1981)	Janssen (1989, 1991)	Yan (1987) (modified)
Whitecapping	Komen et al. (1984)	Janssen (1991)	van der Westhuysen, Zijlema and Battjes (2007)
Quadruplet wave-wave interactions	Hasselmann et al. (1985)		
Bottom friction	Hasselmann et al. (1973)	Collins (1972)	Madsen et al. (1988)
Depth-induced breaking wave	Battjes and Janssen (1978)		
Triad wave-wave interactions	Eldeberky (1996)		

Vegetation dissipation	Dalrymple et al. (1984)		
Obstacle transmission	Seelig (1979); d’Angremond et al. (1996)		
Mud dissipation	Ng (2000)		
Wave-induced set-up			
Turbulence dissipation			

A.2 TOMAWAC

TOMAWAC (TELEMAC-based Operational Model Addressing Wave Action Computation) is an open-source third-generation phased-averaged spectral wave model dedicated to resolving deep water to shallow water applications such as estuaries (Moulinec et al. 2011; Hashemi et al. 2015). TOMAWAC describes the evolution of 2D wave energy spectrum using an unstructured finite element formulation (Brière et al. 2007) making TOMAWAC ideal for irregular shorelines and complex bathymetry (Kuang and Stansby 2006; Mattarolo and Benoit 2010). TOMAWAC resolves the numerical propagation scheme using a method of characteristic (piece-wise ray method) (Benoit et al. 1996). The method of characteristic enables TOMAWAC to revoke the CFL stability conditions, as a result save computational time (Ardhuin, et al.

2001; Fouquet 2016). However, in the general case, the method of characteristic has a significant level of numerical diffusion and is not conservative (Fouquet 2016). The source/sink terms within TOMAWAC represents contributions from wind input Q_{in}; energy dissipation by whitecapping Q_{wc}, bottom friction Q_b and depth induced breaking wave Q_{br}; quadruple Q_{nl4} and triad wave-wave interactions Q_{nl3}; as well as other source/sink processes: enhanced breaking dissipation of waves on a current Q_{cur}; dissipation due to vegetation Q_{veg} (Equation A.3) (Fouquet 2016). However, Brière et al. (2007) and Jia et al. (2015) study on the Adour River mouth and Modaomen estuary respectively reveal that wave propagation model in regions where the length of the modelled area is relatively small can ignore wind input, non-linear wave-wave interactions and whitecapping. The influence of these processes can be ignored where the length of the modelled area is relatively small as the time residence of the waves is short and the wind forcing is weak (Brière et al. 2007). TOMAWAC employs an implicit scheme to resolve source/sink terms dominant in medium and large water depth while an explicit scheme is employed to resolve source/sink terms dominant in shallow water depth (Fouquet 2016). The formulation options available to resolve the source/sink terms within TOMAWAC is summarised in Table A.2.

$$Q = Q_{in} + Q_{wc} + Q_{nl4} + Q_b + Q_{br} + Q_{nl3} + Q_{cur} + +Q_{veg} \qquad (A.3)$$

Table A.2: TOMAWAC options for source terms (adapted from Fouquet 2016)

Source/Sink Terms	Option 1 (Default value)	Option 2	Option 3	Option 4	Option 5
Q_{in} (Exponential wind growth)	No wind input	Janssen 1989, 1991	Snyder et al. (1981)	Yan (1987)	
Q_{in} (Linear wind growth)	Cavaleri and Malanotte-Rizzoli (1981)				
Q_{wc}	No whitecapping-induced dissipation	Komen, Hasselmann and Hasselmann (1984) Janssen (1991)	van der Westhuysen et al. (2007)		

Q_{nl4}	No non-linear quadruplet interaction	Hasselmann et al. (1985)	Tolman (2004)	Lavrenov (2001); Gagnaire-Renou et al. (2010)	
Q_b	No bottom friction-induced dissipation	Hasselmann et al. (1973)			
Q_{br}	No breaking-induced dissipation	Battjes and Janssen (1978)	Thornton and Guza (1983)	Roelvink (1993)	Izumiya and Horikawa (1984)
Q_{nl3}	No non-linear triad interaction	Eldeberky and Battjes (1995)	Becq 1998		
Q_{cur}	No wave-blocking effect	Hedges et al. (1985)	van der Westhuysen (2012)		
Q_{veg}	No vegetation-induced dissipation	Suzuki et al. (2011)			

TOMAWAC accounts for refraction, generation and dissipation (Chini et al. 2010; Jia et al. 2015). The recent version of TOMAWAC (release 7.1), enables users to incorporate diffraction by choosing between Holthuijsen et al. (2003) model based on the Berkhoff (1972) equation i.e. Mild-Slope Equation or a revised Mild-Slope Equation proposed by Porter (2003) (Fouquet 2016).

A.3 MIKE21 SW

MIKE21 SW (Spectral Wave) is a third-generation spectral model that simulates growth decay and transformation of wind-generated waves and swells in coastal and offshore areas (Moeini and Etemad-Shahidi 2007). MIKE21 SW has two different formulations: 1) a directional decoupled parametric formulation; 2) fully spectral formulation (DHI 2008). The directional decoupled parametric formulation is based on Holthuijsen et al. (1989) study and is suitable only for nearshore applications while the fully spectral formulation based on action balance equation as described in Komen et al. (1994) and Young (1999) is suitable for nearshore and offshore applications (Aboobacker et al. 2014). MIKE21 SW is formulated in Cartesian co-ordinates for small scale applications and polar spherical co-ordinates for large scale application (Arı Güner et al. 2013). The model's description of the action balance equation is similar to the SWAN model formulated as a function of wave frequency and direction (Moeini and Etemad-Shahidi 2007; Aboobacker et al. 2014). The source terms employed in MIKE21 SW for shallow water can be expressed as (Liang 2017):

$$S_{total} = S_{in} + S_{nl} + S_{ds} + S_{bot} + S_{surf} \qquad \text{(A.4)}$$

where:

S_{in} is wind generation energy; S_{nl} is nonlinear wave-wave interaction; S_{ds} is energy dissipation by whitecapping; S_{bot} is energy dissipation by bottom friction; and S_{surf} is energy dissipation by depth induced breaking wave.

Sørensen et al. (2005) describe source terms within MIKE21 SW. Wind input is based on Janssen (1989, 1991) formulation. Nonlinear wave-wave interaction is based on DIA developed by Hasselmann et al. (1985). Energy dissipation by whitecapping is based on Hasselmann (1974) modified according to Janssen (1989, 1992). Energy dissipation by bottom friction is based on Johnson and Kofoed-Hansen (2000) approach, which is dependent on sediment and wave properties (DHI 2008). A detailed description of the energy dissipation by bottom friction is contained in Hoque et al. (2017). Energy dissipation by depth induced breaking wave is based on Battjes and Janssen (1978) approach and Elderberky and Battjes (1996) dissipation source term is employed.

MIKE SW is a Eulerian model based on an unstructured finite volume method (Sørensen et al. 2005). MIKE21 SW resolves the numerical propagation scheme using an explicit method. Considering the severe time-step restrictions due to CFL stability conditions, MIKE21 SW employs a multisequence explicit integration scheme based on Vilsmeier and Hanel (1996) idea in other to relax the restriction and speed-up the computation (Sørensen et al. 2005). The source terms are resolved using implicit explicit schemes (Hoque et al. 2017). A summary of the wave modelling tools is presented in Table A.3.

Table A.3: Summary of popular wave modelling tools (adapted from Aboobacker et al. 2014; Hashemi et al. 2015; Fouquet 2016; The SWAN Team 2016a, 2016b; Hoque et al. 2017)

	Year of Inception	General Model Availability	Numerical Solution Method	Equation	Formulations For Resolving Diffraction	Source Term Formulation
SWAN	1999	Open Source Code	Finite Difference	Action balance equation (formulated as a function of wave frequency and direction)	Holthuijsen, Herman and Booij (2003) model	Provides formulation options to resolve each source/sink terms
TOMAWAC	1996	Open Source Code	Finite Element	Action balance equation (formulated as a	• Holthuijsen, Herman and Booij (2003) model • Porter (2003) model	Provides formulation options to resolve

				function of wave-number)		each source/sink terms
MIKE21 SW		Proprietary Software (with a wide variety of license type)	Finite Volume	Action balance equation (formulated as a function of wave frequency and direction)	Holthuijsen, Booij and Herbers (1989) study	Default Formulations for source/sink terms (does not explicitly represent triad wave-wave interaction)

REFERENCES

Aboobacker, V. M., Seemanth, M., Samiksha, S. V., Sudheesh, K., Kerkar, J., and Vethamony, P. (2014) 'Sea Breeze-Induced Wind Sea Growth in the Central West Coast of India'. *Ocean Engineering* 84, 20-28

Adytia, D., Ramdhani, M., and Groesen, E. V. (eds.) (2012) *The 6th Asia-Pacific Workshop on Marine Hydrodynamics (APHydro2012)*. 'Phase Resolved and Averaged Wave Simulatons in Jakarta Habour'. held September 3-4 at Malaysia

Akpinar, A. and Ponce de León, S. (2016) 'An Assessment of the Wind Re-Analyses in the Modelling of an Extreme Sea State in the Black Sea'. Dynamics of Atmospheres and Oceans 73, 61-75

Ardhuin, F., Herbers, T. H. C., and O'Reilly, W. C. (2001) 'A Hybrid Eulerian–Lagrangian Model for Spectral Wave Evolution with Application to Bottom Friction on the Continental Shelf'. *Journal of Physical Oceanography* 31 (6), 1498-1516

Arı Güner, H. A., Yüksel, Y., and Özkan Çevik, E. (2013) 'Estimation of Wave Parameters Based on Nearshore wind–wave Correlations'. *Ocean Engineering* [online] 63, 52-62. available from <http://www.sciencedirect.com/science/article/pii/S0029801813000450>

Battjes, J. A. and Janssen, P. A. E. M. (eds.) (1978) *16th International Conference on Coastal Engineering*. 'Energy Loss and Set-Up due to Breaking of Random Waves'. New York: American Society of Civil Engineering

Becq, F. (1998) 'Extension De La Modélisation Spectrale Des États De Mer Vers Le Domaine Côtier'. *Thèse Présentée à l'université De Toulon*

Benoit, M., Marcos, F., and Becq, F. (1996) 'Development of a Third Generation Shallow-Water Wave Model with Unstructured Spatial Meshing'. *Proceedings 25th International Conference on Coastal Engineering, ASCE*, 465-478

Berkhoff, J. C. W. (ed.) (1972) *Proc. 13th Int. Conf. Coastal Engineering*. 'Computations of Combined refraction–diffraction' at New York: ASCE

Berry, A., Dabrowski, T., and Lyons, K. (2012) 'The Oil Spill Model OILTRANS and its Application to the Celtic Sea'. *Marine Pollution Bulletin* 64 (11), 2489-2501

Booij, N., Ris, R. C., and Holthuijsen, L. H. (1999) 'A Third-Generation Wave Model for Coastal Regions: 1. Model Description and Validation'. *Journal of Geophysical Research: Oceans* 104 (C4), 7649-7666

Brière, C., Abadie, S., Bretel, P., and Lang, P. (2007) 'Assessment of TELEMAC System Performances, a Hydrodynamic Case Study of Anglet, France'. *Coastal Engineering* 54 (4), 345-356

Cavaleri, L., Alves, J. H. G. M., Ardhuin, F., Babanin, A., Banner, M. L., Belibassakis, K., Benoit, M., Donelan, M., Groeneweg, J., Herbers, T. H. C., Hwang, P. A., Janssen, P. A. E.

M., Janssen, T., Lavrenov, I. V., Magne, R., Monbaliu, J., Onorato, M., Polnikov, V., Resio, D., Rogers, W. E., Sheremet, A., McKee Smith, J., Tolman, H. L., van Vledder, G. P., Wolf, J., and Young, I. R. (2007) 'Wave Modelling – the State of the Art'. Progress in Oceanography 75 (4), 603-674

Cavaleri, L. and Rizzoli, P. M. (1981) 'Wind Wave Prediction in Shallow Water: Theory and Applications'. *Journal of Geophysical Research: Oceans* 86 (C11), 10961-10973

Chini, N., Stansby, P., Leake, J., Wolf, J., Roberts-Jones, J., and Lowe, J. (2010) 'The Impact of Sea Level Rise and Climate Change on Inshore Wave Climate: A Case Study for East Anglia (UK)'. *Coastal Engineering* 57 (11–12), 973-984

Collins, J. I. (1972) 'Prediction of Shallow-Water Spectra'. *Journal of Geophysical Research* 77 (15), 2693-2707

Dalrymple, R., A., Kirby, J. T., and Hwang, P. A. (1984) 'Wave Diffraction due to Areas of Energy Dissipation'. *Journal of Waterways, Ports, Harbours and Coastal Engineering* 110 (1), 67-79

De Dominicis, M., Bruciaferri, D., Gerin, R., Pinardi, N., Poulain, P. M., Garreau, P., Zodiatis, G., Perivoliotis, L., Fazioli, L., Sorgente, R., and Manganiello, C. (2016) 'A Multi-Model Assessment of the Impact of Currents, Waves and Wind in Modelling Surface Drifters and Oil Spill'. Deep Sea Research Part II: Topical Studies in Oceanography 133, 21-38

Dong, Z. and Kirby, J. T. (2012) 'Theoritical and Numerical Study of Wave-Current Interaction in Strongly-Sheared Flows'. Coastal Engineering Proceedings 33, 1-7

d'Angremond, K., van der Meer, J. W., and de Jong, R. J. (1996) 'Wave Transmission at Low-Crested Structures'. *Proceedings 25th International Conference Coastal Engineering*

DHI (2008) *MIKE 21 Wave Modelling - MIKE 21 Spectral Waves FM - Short Description*. Høsholm, Denmark: DHI Water and Environment.

Eldeberky, Y. (1996) *Nonlinear Transformation of Wave Spectra in the Nearshore Zone, PhD Thesis*. Delft, Netherlands: Dep. of Engineering, Delft University of Technology

Eldeberky, Y. and Battjes, J. A. (1995) 'Parameterisation of Triads Interactions in Wave Energy Models'. *Proc. Coastal Dynamics*, 140-148

Fouquet, T. (2016) *TELEMAC MODELLING SYSTEM: TOMAWAC Software Release 7.1 Operating Manual*. National Hydraulics and Environment Laboratory, EDF R&D, France: EDF R&D

Gagnaire-Renou, E., Benoit, M., and Forget, P. (2010) 'Ocean Wave Spectrum Properties as Derived from Quasi-Exact Computations of Nonlinear Wave-Wave Interactions'. *Journal of Geophysical Research* 115 (C12)

Gorrell, L., Raubenheimer, B., Elgar, S., and Guza, R. T. (2011) 'SWAN Predictions of Waves Observed in Shallow Water Onshore of Complex Bathymetry'. Coastal Engineering 58 (6), 510-516

Guo, W. J. and Wang, Y. X. (2009) 'A Numerical Oil Spill Model Based on a Hybrid Method'. *Marine Pollution Bulletin* 58 (5), 726-734

Guo, W., Hao, Y., Zhang, L., Xu, T., Ren, X., Cao, F., and Wang, S. (2014) 'Development and Application of an Oil Spill Model with wave–current Interactions in Coastal Areas'. *Marine Pollution Bulletin* 84 (1–2), 213-224

Hashemi, M. R., Neill, S. P., Robins, P. E., Davies, A. G., and Lewis, M. J. (2015) 'Effect of Waves on the Tidal Energy Resource at a Planned Tidal stream array'. *Renewable Energy* 75, 626-639

Hasselmann, K., Barnett, T. P., Bouws, E., Carlson, H., Cartwright, D. E., Enke, K., Ewing, J. A., Gienapp, H., Hasselmann, D. E., Kruseman, P., Meerburg, A., Müller, P., Olbers, D. J., Richter, K., Sell, W., and Walden, H. (1973) *Measurements of Wind-Wave Growth and Swell Decay during the Joint North Sea Wave Project (JONSWAP)*.: Deutsches Hydrographisches Institut

Hasselmann, S., Hasselmann, K., Allender, J. H., and Barnett, T. P. (1985) 'Computations and Parameterization of the Nonlinear Energy Transfer in a Gravity-Wave Spectrum. Part II: Parameterizations of the Nonlinear Energy Transfer for Application in Wave Models'. *Journal of Physical Oceanography* 15, 1378-1391

Hedges, T. S., Anatasiou, K., and Gabriel, D. (1985) 'Interaction of Random Waves and Currents'. *Journal of Waterway, Port, Coastal, and Ocean Engineering* 111 (2), 275-288

Holthuijsen, L. H. (2007) Waves in Oceanic and Coastal Waters. 1st edn. Cambridge: Cambridge University Press

Holthuijsen, L. H., Booij, N., and Herbers, T. H. C. (1989) 'A Prediction Model for Stationary, Short-Crested Waves in Shallow Water with Ambient Currents'. *Coastal Engineering* [online] 13 (1), 23-54. available from <http://www.sciencedirect.com/science/article/pii/0378383989900318>

Holthuijsen, L. H., Herman, A., and Booij, N. (2003) 'Phase-Decoupled refraction–diffraction for Spectral Wave Models'. *Coastal Engineering* 49 (4), 291-305

Hoque, M. A., Perrie, W., and Solomon, S. M. (2017) 'Evaluation of Two Spectral Wave Models for Wave Hindcasting in the Mackenzie Delta'. *Applied Ocean Research* 62, 169-180

Hsu, T. W., Ou, S. H., and Liau, J. M. (2005) 'Hindcasting Nearshore Wind Waves using a FEM Code for SWAN'. *Coastal Engineering* 52 (2), 177-195

Izumiya, T. and Horikawa, K. (1984) 'Wave Energy Equation Applicable in and Outside the Surf Zone'. *Coastal Engineering in Japan* 27, 119-137

Janssen, P. A. E. M. (2008) 'Progress in Ocean Wave Forecasting'. Journal of Computational Physics 227 (7), 3572-3594

Janssen, P. A. E. M. (1991) 'Quasi-Linear Theory of Wind-Wave Generation Applied to Wave Forecasting'. *Journal of Physical Oceanography* 21 (11), 1631-1642

Janssen, P. A. E. M. (1989) 'Wave-Induced Stress and the Drag of Air Flow Over Sea Waves'. *Journal of Physical Oceanography* 19 (6), 745-754

Jia, L., Wen, Y., Pan, S., Liu, J. T., and He, J. (2015) 'Wave–current Interaction in a River and Wave Dominant Estuary: A Seasonal Contrast'. *Applied Ocean Research* 52, 151-166

Jin, K. and Ji, Z. (2001) 'Calibration and Verification of a Spectral wind–wave Model for Lake Okeechobee'. *Ocean Engineering* 28 (5), 571-584

Johnson, H. K. and Kofoed-Hansen, H. (2000) 'Influence of Bottom Friction on Sea Surface Roughness and its Impact on Shallow Water Wind Wave Modeling'. *Journal of Physical Oceanography* 30 (7), 1743-1756

Komen, G. J., Calaveri, L., Donelan, K., Hasselmann, K., Hasselmann, S., and Janssen, P. A. E. M. (1994) *Dynamics and Modelling of Ocean Waves*. 1st edn. New York: Cambridge University Press

Komen, G. J., Hasselmann, S., and Hasselmann, K. (1984) 'On the Existence of a Fully Developed Wind-Sea Spectrum'. *Journal of Physical Oceanography* 14 (8), 1271-1285

Kuang, C. and Stansby, P. (2006) *Sandbanks for Coastal Protection: Implications of Sea-Level Rise. Part 3: Wave Modelling*. Manchester, UK: Tyndall Centre for Climate Change Research

Lauritzen, P. H., Nair, R. D., and Ullrich, P. A. (2010) 'A Conservative Semi-Lagrangian Multi-Tracer Transport Scheme (CSLAM) on the Cubed-Sphere Grid'. Journal of Computational Physics 229 (5), 1401-1424

Lavrenov, I. V. (2001) 'Effect of Wind Wave Parameter Fluctuation on the Nonlinear Spectrum Evolution'. *Journal of Physical Oceanography* 31 (4), 861-873

Lentine, M., Grétarsson, J. T., and Fedkiw, R. (2011) 'An Unconditionally Stable Fully Conservative Semi-Lagrangian Method'. Journal of Computational Physics 230 (8), 2857-2879

Liang, B., Shao, Z., Wu, Y., Shi, H., and Liu, Z. (2017) 'Numerical Study to Estimate the Wave Energy Under Wave-Current Interaction in the Qingdao Coast, China'. *Renewable Energy* 101, 845-855

Liu, T. and Sheng, Y. P. (2014) 'Three Dimensional Simulation of Transport and Fate of Oil Spill Under Wave Induced Circulation'. Marine Pollution Bulletin 80 (1–2), 148-159

Madsen, O. S., Poon, Y., and Graber, H. C. (eds.) (1988) *21th International Conference on Coastal Engineering*. 'Spectral Wave Attenuation by Bottom Friction: Theory'. New York: American Society of Civil Engineering

Madsen, P. A. and Sørensen, O. R. (1992) 'A New Form of the Boussinesq Equations with Improved Linear Dispersion Characteristics. Part 2. A Slowly-Varying Bathymetry'. Coastal Engineering [online] 18 (3), 183-204. available from <http://www.sciencedirect.com/science/article/pii/037838399290019Q>

Mattarolo, G. and Benoit, M. (eds.) (2010) *3rd International Conference on Ocean Energy*. 'Development of a Nearshore Sea-State Database Off Reunion Island for Wave Energy Resource Assessment'. held 6th October at Bilbao

Moeini, M. H. and Etemad-Shahidi, A. (2007) 'Application of Two Numerical Models for Wave Hindcasting in Lake Erie'. *Applied Ocean Research* 29 (3), 137-145

Moulinec, C., Denis, C., Pham, C., Rouge, D., Hervouet, J., Razafindrakoto, E., Barber, R. W., Emerson, D. R., and GU, X. (2011) 'TELEMAC: An Efficient Hydrodynamic Suite for Massively Parallel Architectures'. *Computers & Fluids* 51 (1), 30-34

Nair, R. D. and Machenhauer, B. (2002) 'The Mass-Conservative Cell-Integrated Semi-Lagrangian Advection Scheme on the Sphere'. Monthly Weather Review 130 (3), 649-667

Ng, C. (2000) 'Water Waves Over a Muddy Bed: A Two-Layer Stokes' Boundary Layer Model'. *Coastal Engineering* 40 (3), 221-242

Pallares, E., Sánchez-Arcilla, A., and Espino, M. (2014) 'Wave Energy Balance in Wave Models (SWAN) for Semi-Enclosed domains–Application to the Catalan Coast'. *Continental Shelf Research* 87, 41-53

Porter, D. (2003) 'The Mild-Slope Equations'. *Journal of Fluid Mechanics* 494, 51-63

Ris, R. C., Holthuijsen, L. H., and Booij, N. (1999) 'A Third-Generation Wave Model for Coastal Regions: 2. Verification'. *Journal of Geophysical Research* 104 (C4), 7667-7681

Roelvink, D. (1993) 'Dissipation in Random Wave Groups Incident on a Beach'. *Coastal Engineering* [online] 19 (1), 127-150. available from <http://www.sciencedirect.com/science/article/pii/037838399390021Y>

Rusu, E. and Guedes Soares, C. (2013) 'Modeling Waves in Open Coastal Areas and Harbors with Phase-Resolving and Phase-Averaged Models'. Journal of Coastal Research 292, 1309-1325

Rusu, E. and Guedes Soares, C. (2011) 'Wave Modelling at the Entrance of Ports'. *Ocean Engineering* 38 (17–18), 2089-2109

Rusu, E. and Guedes Soares, C. (2009) 'Numerical Modelling to Estimate the Spatial Distribution of the Wave Energy in the Portuguese Nearshore'. *Renewable Energy* 34 (6), 1501-1516

Seelig, W. N. (1979) 'Effect of Breakwaters on Waves: Laboratory Tests of Wave Transmission by Overtopping'. *Coastal Structures* 79ASCE, 941

Snyder, R. L., Dobson, F. W., Elliot, J. A., and Long, R. B. (1981) 'Array Measurements of Atmospheric Pressure Fluctuations Above Surface Gravity Waves'. *Journal of Fluid Mechanics* 102, 1-59

Sørensen, O. R., Kofoed-Hansen, H., Rugbjerg, M., and Sørensen, L. S. (2005) 'A Third-Generation Spectral Wave Model using an Unstructured Finite Volume Technique'. *Coastal Engineering*

Staniforth, A. and Thuburn, J. (2011) 'Horizontal Grids for Global Weather and Climate Prediction Models: A Review'. Quarterly Journal of the Royal Meteorological Society 138 (662), 1-26

Suzuki, T., Zijlema, M., Burger, B., Meijer, M. C., and Narayan, S. (2012) 'Wave Dissipation by Vegetation with Layer Schematization in SWAN'. *Coastal Engineering* 59 (1), 64-71

The SWAN Team (2016b) *SWAN Scientific and Technical Documenation: SWAN Cycle III Version 41.10*. Delft, The Netherlands: Delft University of Technology

The SWAN Team (2016a) *SWAN User Manual: SWAN Cycle III Version 41.10*. Delft, The Netherlands: Delft University of Technology

The Wamdi Group (1988) 'The WAM Model—A Third Generation Ocean Wave Prediction Model'. Journal of Physical Oceanography 18 (12), 1775-1810

Thomas, T. J. and Dwarakish, G. S. (2015) 'Numerical Wave Modelling – A Review'. Aquatic Procedia [online] 4, 443-448. available from <http://www.sciencedirect.com/science/article/pii/S2214241X15000607>

Thornton, E. B. and Guza, R. T. (1983) 'Transformation of Wave Height Distribution'. *Journal of Geophysical Research* 88 (C10), 5925

Tolman, H. L. and Grumbine, R. W. (2013) 'Holistic Genetic Optimization of a Generalized Multiple Discrete Interaction Approximation for Wind Waves'. Ocean Modelling 70, 25-37

Tolman, H. L. (2013) 'A Generalized Multiple Discrete Interaction Approximation for Resonant Four-Wave Interactions in Wind Wave Models'. Ocean Modelling 70, 11-24

Tolman, H. L. (2008) 'A Mosaic Approach to Wind Wave Modeling'. Ocean Modelling 25 (1–2), 35-47

Tolman, H. L. (2004) 'Inverse Modeling of Discrete Interaction Approximations for Nonlinear Interactions in Wind Waves'. *Ocean Modelling* 6 (3–4), 405-422

Tolman, H. L. (1991) 'A Third-Generation Model for Wind Waves on Slowly Varying, Unsteady, and Inhomogeneous Depths and Currents'. Journal of Physical Oceanography 21 (6), 782-797

van der Westhuysen, A. J. (2012) 'Spectral Modeling of Wave Dissipation on Negative Current Gradients'. *Coastal Engineering* 68, 17-30

van der Westhuysen, A. J., Zijlema, M., and Battjes, J. A. (2007) 'Nonlinear Saturation-Based Whitecapping Dissipation in SWAN for Deep and Shallow Water'. *Coastal Engineering* 54 (2), 151-170

van Vledder, G. P. (2006) 'The WRT Method for the Computation of Non-Linear Four-Wave Interactions in Discrete Spectral Wave Models'. Coastal Engineering 53 (2–3), 223-242

Vilsmeier, R. and Hanel, D. (1996) 'Adaptive Solutions for Unsteady Laminar Flows on Unstructured Grid'. *International Journal for Numerical Methods in Fluids* 22 (2), 85-101

Wang, J. and Shen, Y. (2010) 'Modeling Oil Spills Transportation in Seas Based on Unstructured Grid, Finite-Volume, Wave-Ocean Model'. Ocean Modelling 35 (4), 332-344

Xu, T. and You, X. (2017) 'Numerical Simulation of Suspended Sediment Concentration by 3D Coupled Wave-Current Model in the Oujiang River Estuary, China'. Continental Shelf Research 137, 13-24

Yan, L. (1987) *An Improved Wind Input Source Term for Third Generation Ocean Wave Modelling*. De Bilt, The Netherlands: Koninklijk Nederlands Meteorologisch Instituut

Young, I. R. (1999) *Wind Generated Ocean Waves*. 1st edn. Amsterdam: Elsevier

Zerroukat, M., Wood, N., and Staniforth, A. (2002) 'SLICE: A Semi-Lagrangian Inherently Conserving and Efficient Scheme for Transport Problems'. Quarterly Journal of the Royal Meteorological Society 128 (586), 2801-2820

Zijlema, M. (2010) 'Computation of Wind-Wave Spectra in Coastal Waters with SWAN on Unstructured Grids'. *Coastal Engineering* 57 (3), 267-277

Zijlema, M. and van der Westhuysen, A. J. (2005) 'On Convergence Behaviour and Numerical Accuracy in Stationary SWAN Simulations of Nearshore Wind Wave Spectra'. *Coastal Engineering* 52 (3), 237-256

Zubier, K., Panchang, V., and Demirbilek, Z. (2003) 'Simulation of Waves at Duck (North Carolina) using Two Numerical Models'. *Coastal Engineering Journal* 45 (03), 439-469

APPENDIX B: SEDIMENT TRANSPORT MODELLING TOOLS

Sediment transport is driven by currents and waves (Jin and Ji 2001; Jia et al. 2015; Hashemi et al. 2015). Sediments are stirred and transported by currents while waves enhance stirring (Brown and Davies 2009), this is typical in estuarine areas (Xu and You 2017). It is important to understand the complex interaction between these processes as sediment transport drives morphodynamic processes in rivers, estuaries and seas (Garel et al. 2014; Villaret et al. 2016; Lopez and Baptista 2017). To accurately assess the evolution of an estuary, it is necessary to consider sediment transport (Knaapen and Joustra 2012; Luan et al. 2017).

Coastal engineers and scientist have employed empirical, physical and data-driven model types to understand morphological evolution (Fortunato et al. 2009). Morphological evolution models are generally categorised into behaviour-based and process-based models (Amoudry and Souza 2011). Simple parameterization descriptions based on the long term morphological system's general behaviour is the basis of behaviour-based models (Amoudry and Souza 2011). However, the development of process-based models has shown the capability of adequately predicting morphological evolution making them increasingly attractive (Elias et al. 2006; Fortunato et al. 2009). A drawback of process-based models is their requirement of high-quality input data which cannot always be guaranteed by measurements (van der Wegen and Jaffe 2013).

Process-based sediment transport models are governed by physical laws which describe the water motion (hydrodynamics and waves), sediment transport and bathymetry updates implemented in a loop system to ensure feedback and dynamic interaction (Figure B.1) (Cayocca 2001; van Rijn et al. 2003). Within process-based models, sediment transport is computed by decomposing the total sediment transport into suspended sediment transport and bedload sediment transport (Lesser et al. 2004; Villaret et al. 2013). The influence of sediment sizes on the total sediment transport, spatial variation of sediment size across the model area and sediment fractions changes within the bed at a computing point are important aspects of sediment transport (Luo et al. 2013). Bed evolution is computed by solving the conservation of sediment mass between the sediment load and water column expressed by the Exner equation (Amoudry and Liu 2009; Villaret et al. 2013). Details of popular tools employed for sediment transport modelling in the estuarine environment are further discussed and summarised in Table B.1.

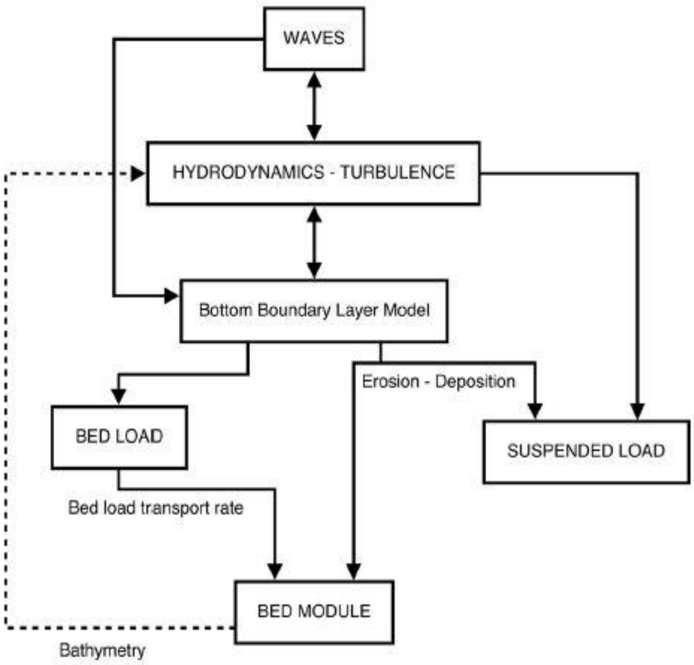

Figure B.1: General structure of process-based models (Amoudry and Souza 2011)

Table B.1: Summary of popular sediment modelling tools (adapted from Lesser et al. 2004; Warner et al. 2008; Amoudry and Souza 2011; Villaret and Tassi 2014)

	General Model Availability	Model Type	Numerical Solution Method	Cohesive Sediment
SISYPHE	Open Source	Two-dimensional horizontal	Finite Element	No
DELFT3D	Open Source	Three-dimensional	Finite Difference	Yes
ROMS	Open Source (Limited Distribution)	Three-dimensional	Finite Difference	Yes

B.1 SISYPHE

SISYPHE (version 6.3) is an open-source two-dimensional sediment transport and bed evolution model of the TELEMAC suite that employs a finite element system (Villaret and Tassi 2014). SISYPHE solves 10 different sediment classes characterised by settling density, grain density and means diameter applicable to non-cohesive sediment either as uniform (single-sized) or graded (multiple-sized) and cohesive sediments (Amoudry and Souza 2011; Villaret et al. 2013; Villaret and Tassi 2014). The suspended load is computed from the depth-averaged sediment concentration (advection/diffusion) equation. SISPHYE provides users with four options to treat the diffusion terms (i.e. the diffusion coefficients) and four numerical methods (method of characteristics; distributive schemes (PSI); conservative N-scheme; and method of Streamline Upwind Petrov Galerkin SUPG) to treat the advection terms (Villaret and Tassi 2014). The pros and cons of the numerical schemes available in SISYPHE are highlighted by Villaret and Tassi (2014).

Bedload transport rate can be computed by a wide option of semi-empirical formulas (Villaret et al. 2013). The recommended choice of formula is dependent on the sediment type and range of particle size (Table B.2) (Villaret and 2014).

Table B.2: Bedload transport formulae and recommended parameters (adapted from Villaret and Tassi 2014)

Formula	Recommendation
Meyer-Peter and Muller formula (Meyer-Peter and Muller 1948)	Coarse sediments (0.4 mm < d50 < 29 mm)
Einstein-Brown formula (Einstein 1950)	Gravel (d50 > 2 mm) Large bed shear stress (θ > θc)
Engelund-Hansen formula (Eugelund and Hansen 1967)	Fine sediment (0.2 mm < d50 < 2 mm)
Modified Engelund-Hansen formula (Chollet and Cunge 1980)	Fine sediment (0.2 mm < d50 < 2 mm)
van Rijn’s formula (van Rijn 1984)	Particles (0.2 mm < d50 < 2 mm)

*Bijker's formula (Bijker 1968)	
*Soulsby-van Rijn formula (Soulsby 1997)	
*Bailard's formula (Bailard 1981)	
*Dibajnia and Watanabe (1992) formula	

The formulae marked with "*" within Table B.2 are wave sediment transport formulae implemented to account for the effect of waves on sediment transport while the other formulae are implemented when considering current only (i.e. no wave effect) (Brown and Davies 2009; Luo et al. 2013; Villaret and Tassi 2014). Bedload transportation in SISYPHE includes bedslope effects and bedload transport in curved channels (Villaret and Tassi 2014).

B.2 DELFT3D

Delft3D sediment module is an open-source three-dimensional tool that utilises a finite-difference representation to compute sediment transport processes (Chatzirodou et al. 2016). Delft3D computes up to five different sediment classes, either classified as "mud" or "sand" as different algorithms are implemented settling velocity and bed-exchange based on the sediment type (mud or sand) (Amoudry and Souza 2011). Computation of suspended sediment takes into account settling velocity, bed exchange, density effects, vertical diffusion coefficient for sediment and suspended correction vector (Dan et al. 2011). For sand transport class, settling velocity and bed-exchange is computed using van Rijn (1993) method (Lesser et al. 2004). For mud transport class, bed-exchange is computed using Parthenaides (1965) and Krone (1962) formulations (Lesser et al. 2004; Amoudry and Souza 2011).

Bedload transportation is computed using van Rijn (1993) approach (Amoudry and Souza 2011). Delft3D simulates sediment transport without waves using van Rijn et al. (2001) formulation and sediment transport including waves using van Rijn et al. (2001) formulations (Lesser et al. 2004). Delft3D also considers bed slope effects (Boudet et al. 2016).

B.3 COMMUNITY SEDIMENT TRANSPORT MODELING SYSTEM (CSTMS-ROMS)

CSTMS-ROMS hereafter referred to as ROMS is an open-source three-dimensional sediment transport model integrated into the ROMS model (Amoudry and Souza 2011). ROMS computes an unlimited number of user-defined non-cohesive sediment class described by settling velocity, grain density, grain diameter, erodibility constant and critical stress for erosion (Warner et al. 2008).Suspended load transport is computed by solving the advection-diffusion equation for tracers (Haas and Warner 2009). However, a source/sink term for bed exchange and vertical settling is added (Warner et al. 2008). Bedload transport is computed using Meyer-Peter and Muller (1948) to simulate sediment transport without waves and Soulsby and Damgaard (2005) formula to simulate sediment transport including waves (Warner et al. 2008). Amoudry and Souza (2011) point out that both formulas have been modified to include bed slope effect.

REFERENCES

Amoudry, L. O. and Liu, P. L. (2009) 'Two-Dimensional, Two-Phase Granular Sediment Transport Model with Applications to Scouring Downstream of an Apron'. *Coastal Engineering* 56 (7), 693-702

Amoudry, L. O. and Souza, A. J. (2011) 'Deterministic Coastal Morphological and Sediment Transport Modeling: A Review and Discussion'. *Reviews of Geophysics* 49 (2)

Bailard, J. (1981) 'An Energetics Total Load Transport Model for a Plane Sloping Beach'. *Journal of Geophysical Research* 86 (C11), 10938-10954

Bijker, E. W. (1968) 'Mechanics of Sediment Transport by the Combination of Waves and Current.'. *In: Design and Reliability of Coastal Structures, 23rd Int. Conf. on Coastal Engineering*, 147-173

Boudet, L., Sabatier, F., and Radakovitch, O. (2016) 'Modelling of Sediment Transport Pattern in the Mouth of the Rhone Delta: Role of Storm and Flood Events'. *Estuarine, Coastal and Shelf Science*

Brown, J. M. and Davies, A. G. (2009) 'Methods for Medium-Term Prediction of the Net Sediment Transport by Waves and Currents in Complex Coastal Regions'. *Continental Shelf Research* 29 (11–12), 1502-1514

Cayocca, F. (2001) 'Long-Term Morphological Modeling of a Tidal Inlet: The Arcachon Basin, France'. *Coastal Engineering* 42 (2), 115-142

Chatzirodou, A., Karunarathna, H., and Reeve, D. E. (2016) 'Investigation of Deep Sea Shelf Sandbank Dynamics Driven by Highly Energetic Tidal Flows'. *Marine Geology* 380, 245-263

Chollet, J. P. and Cunge, J. A. (1980) 'New Interpretation of some Head Loss-Flow Velocity Relationships for Deformable Beds'. *Journal of Hydraulic Research* 17 (1), 1-13

Dan, S., Walstra, D. R., Stive, M. J. F., and Panin, N. (2011) 'Processes Controlling the Development of a River Mouth Spit'. *Marine Geology* 280 (1–4), 116-129

Dibajnia, M. W.,A. (1992) 'Sheet Flow Under Non-Linear Waves and Currents'. *Coastal Engineering*, 2015-2029

Einstein, H. B. (1950) *The Bed Load Function for Sediment Transportation in Open Channel Flow*. Washington D.C.: Technical Bulletin No. 1026, US Deot. of Agriculture

Elias, E. P. L., Cleveringa, J., Buijsman, M. C., Roelvink, D., and Stive, M. J. F. (2006) 'Field and Model Data Analysis of Sand Transport Patterns in Texel Tidal Inlet (the Netherlands)'. *Coastal Engineering* 53 (5-6), 505-529

Engelund, F. and Hansen, E. (1967) *A Monograph on Sediment Transport in Alluvial Streams*. Copenhagen: Teknisk Forlag

Fortunato, A. B., Bertin, X., and Oliveira, A. (2009) 'Space and Time Variability of Uncertainty in Morphodynamic Simulations'. *Coastal Engineering* 56 (8), 886-894

Garel, E., Sousa, C., Ferreira, Ó., and Morales, J. A. (2014) 'Decadal Morphological Response of an Ebb-Tidal Delta and Down-Drift Beach to Artificial Breaching and Inlet Stabilisation'. *Geomorphology* 216, 13-25

Haas, K. A. and Warner, J. C. (2009) 'Comparing a Quasi-3D to a Full 3D Nearshore Circulation Model: SHORECIRC and ROMS'. *Ocean Modelling* 26 (1–2), 91-103

Hashemi, M. R., Neill, S. P., Robins, P. E., Davies, A. G., and Lewis, M. J. (2015) 'Effect of Waves on the Tidal Energy Resource at a Planned Tidal stream array'. *Renewable Energy* 75, 626-639

Jia, L., Wen, Y., Pan, S., Liu, J. T., and He, J. (2015) 'Wave–current Interaction in a River and Wave Dominant Estuary: A Seasonal Contrast'. *Applied Ocean Research* 52, 151-166

Jin, K. and Ji, Z. (2001) 'Calibration and Verification of a Spectral wind–wave Model for Lake Okeechobee'. *Ocean Engineering* 28 (5), 571-584

Knaapen, M. and Joustra, R. (eds.) (2012) *XIXth TELEMAC-MASCARET User Conference*. 'Morphological Acceleration Factor: Usability, Accuracy and Run Time Reductions'. held 18-19 October at Oxford, UK. Oxford, UK: HR Wallingford

Krone, R. B. (1962) *Flume Studies of the Transport of Sediment in Estuarial Shoaling Processes; Final Report*. Berkeley, California: Hydraulic Engineering Laboratory and Sanitary Engineering Research Laboratory, University of California

Lesser, G. R., Roelvink, D., van Kester, J. A. T. M., and Stelling, G. S. (2004) 'Development and Validation of a Three-Dimensional Morphological Model'. *Coastal Engineering* 51 (8–9), 883-915

Lopez, J. E. and Baptista, A. M. (2017) 'Benchmarking an Unstructured Grid Sediment Model in an Energetic Estuary'. *Ocean Modelling* 110, 32-48

Luan, H. L., Ding, P. X., Wang, Z. B., and Ge, J. Z. (2017) 'Process-Based Morphodynamic Modeling of the Yangtze Estuary at a Decadal Timescale: Controls on Estuarine Evolution and Future Trends'. *Geomorphology* 290, 347-364

Luo, J., Li, M., Sun, Z., and O'Connor, B. A. (2013) 'Numerical Modelling of Hydrodynamics and Sand Transport in the Tide-Dominated Coastal-to-Estuarine Region'. *Marine Geology* 342, 14-27

Meyer-Peter, E. and Müller, R. (1948) *Formulae for Bed-Load Transport*. Stockholm, Sweden.: IAHR

Partheniades, E. (1965) 'Erosion and Deposition of Cohesive Soils'. *Journal of the Hydraulics Division* 91, 105-139

Soulsby, R. L. and Damgaard, J. S. (2005) 'Bedload Sediment Transport in Coastal Waters'. *Coastal Engineering* 52 (8), 673-689

van der Wegen, M. and Jaffe, B. E. (2013) 'Towards a Probabilistic Assessment of Process-Based, Morphodynamic Models'. *Coastal Engineering* 75, 52-63

van Rijn, L. C., Roelvink, D., and Horst, W. t. (2001) *Approximation Formulae for Sand Transport by Currents and Waves and Implementation in DELFT-MOR*. Delft Hydraulics, Delft, The Netherlands: Deltares (WL)

van Rijn, L. C., Walstra, D. J. R., Grasmeijer, B., Sutherland, J., Pan, S., and Sierra, J. P. (2003) 'The Predictability of Cross-Shore Bed Evolution of Sandy Beaches at the Time Scale of Storms and Seasons using Process-Based Profile Models'. *Coastal Engineering* 47 (3), 295-327

van Rijn, L. C. (1993) *Principles of Sediment Transport in Rivers, Estuaries and Coastal Seas*. 1st edn. Amsterdam: Aqua Publications

van Rijn, L. C. (1984) 'Sediment Transport, Part I: Suspended Load Transport'. *Journal of Hydraulic Engineering* 110 (11)

Villaret, C. and Tassi, P. (2014) *Sisyphe v6.3 User's Manual - Part II: Non-Cohesive Sediments*. National Hydraulics and Environment Laboratory, EDF R&D, France: EDF R&D

Villaret, C., Hervouet, J., Kopmann, R., Merkel, U., and Davies, A. G. (2013) 'Morphodynamic Modeling using the Telemac Finite-Element System'. *Computers & Geosciences* 53, 105-113

Villaret, C., Kopmann, R., Wyncoll, D., Riehme, J., Merkel, U., and Naumann, U. (2016) 'First-Order Uncertainty Analysis using Algorithmic Differentiation of Morphodynamic Models'. *Computers & Geosciences* 90, Part B, 144-151

Warner, J. C., Sherwood, C. R., Signell, R. P., Harris, C. K., and Arango, H. G. (2008) 'Development of a Three-Dimensional, Regional, Coupled Wave, Current, and Sediment-Transport Model'. *Computers & Geosciences* 34 (10), 1284-1306

Xu, T. and You, X. (2017) 'Numerical Simulation of Suspended Sediment Concentration by 3D Coupled Wave-Current Model in the Oujiang River Estuary, China'. *Continental Shelf Research* 137, 13-24

APPENDIX C: HYDRODYNAMIC MODELLING TOOLS

C.1 POM

POM (Princeton Ocean Model) is a three-dimensional finite-difference explicit model which employs the hydrostatic and Boussinesq equation to solve the shallow-water equation (Blumberg and Mellor 1987; Mellor 2004). POM employs a sigma coordinate to resolve the vertical and curvilinear orthogonal coordinates to resolve the horizontal grid (Wang et al. 2008; Xu et al. 2012). To minimise POM's pressure gradient errors over steep topography, different pressure gradient schemes have been implemented within POM, but they are more computationally expensive and sophisticated (Ezer et al. 2002). POM employs an explicit scheme. Therefore, the external model basic equations (vertically integrated equations) are derived by integrating the internal model basic equations over the vertical using the boundary coordinates (see Mellor 2004). POM employs Smagorinsky formula to resolve the horizontal diffusion coefficients and the Mellor-Yamada (MY) level 2.5 turbulence model to resolve the vertical diffusivity (Guo and Wang 2009). Examples of estuarine hydrodynamic models developed with POM include the Pearl River Estuary, China (Wong et al. 2003), Yangtze Estuary, China (Zhang et al. 2016), Bangpakong Estuary, Thailand (Buranapratheprat and Yanagi 2003) and Cape Fear River Estuary, United States (Xia et al. 2008) (Table A.1). The full details of POM are described in Blumberg and Mellor (1987) and Mellor (2004).

C.2 ROMS

ROMS (Regional Oceanic Modeling System) is a 3D-finite difference, free-surface model that solves the Reynolds-averaged Navier-Stokes equations using the hydrostatic and Boussinesq approximation (Haidvogel et al. 2000; Shchepetkin and McWilliams 2005). ROMS employs sigma coordinates to resolve the vertical and curvilinear orthogonal coordinates to resolve the horizontal grid and employs an explicit time-stepping scheme (Warner et al. 2013). There are a lot of similarities between POM and ROMS, but ROMS employ polynomial fits in new pressure gradient schemes and a new time-stepping algorithm to reduce the numerical errors (Ezer at al. 2002; Shchepetkin and McWilliams 2003;2005) that arise from the application of sigma coordinates and mode splitting scheme respectively. Within ROMS, a predictor-corrector time-stepping algorithm is employed which applies a filter to every external time step in other to correct the vertically averaged velocity of the baroclinic mode (Shchepetkin and McWilliams 2005; Lazure and Dumas 2008). The time-stepping algorithm enables ROMS to employ an external time step of about twice the time step restriction due to CFL condition and 1.5 times larger than the internal time steps in POM (Ezer et al. 2002). To reduce the pressure gradient errors, ROMS employs an algorithm that reconstructs the density field (Shchepetkin and McWilliams 2003). Comparison of various numerical aspects of POM and ROMS was undertaken by Ezer et al. (2002). ROMS provides users with several turbulent closure models; these include: 1) the GLS method; 2) the MY level 2.5 method; 3) the K-profile parametrization (KPP); 4) Brunt-Vaisala frequency mixing; 5) user-defined analytical expressions for K_H and K_M (Haidvogel et al. 2008). Examples of estuarine hydrodynamic models developed with ROMS include the Hudson River Estuary, United States (Warner et al. 2005a); Yangtze Estuary, China (Fan and Song 2014); Pearl River Estuary, China (Pan and Gu 2016. The full details of ROMS are described in Haidvogel et al. (2000), Shchepetkin and McWilliams (2005); Haidvogel et al. (2008); Shchepetkin and McWilliams (2009) and a summary is presented in Table A.1.

C.3 DELFT3D-FLOW

Delft3D-FLOW is an open-source finite-difference model that solves the 2D/3D shallow-water equations using the hydrostatic and Boussinesq approximations (Chatzirodou and

Karunarathna 2014; Abascal et al. 2017). Delft3D-FLOW employs a sigma terrain-following (sigma) coordinate in the vertical and provides the user with the choice between Cartesian rectangular, orthogonal curvilinear or spherical grid in the horizontal. Delft3D-FLOW employs a semi-implicit method; Alternating Direction Implicit (ADI) method to solve the horizontal momentum and continuity equations (Lesser et al. 2004). The ADI method is only implicit with respect to the computation direction while the barotropic (external) mode equations are derived by integrating the momentum equations over the vertical using the boundary coordinates (see Lazure and Dumas 2008). Delft3D-FLOW employs several turbulent closure models (Lesser et al. 2004; Yuill et al. 2016). These models include: (1) constant coefficient; (2) k-L turbulence closure model; (3) k-ε turbulent closure model; (4) Algebraic Eddy viscosity closure Model (AEM); while the constant coefficient model is based on a constant value specified by the user, the other three methods are based on the "eddy viscosity" concept of Kolmogorov (1942) and Prandtl (1945) (Deltares 2014). Examples of estuarine hydrodynamic models developed with Delft3D-FLOW include the Shenzhen River Estuary, China (Zhang and Mao 2015) and Yangtze Estuary, China (Jie et al. 2014). The full details of Delft3D-FLOW are described in Lesser et al. (2004) and a summary is presented in Table A.1.

C.4 SELFE

SELFE (Semi-implicit Eulerian-Lagrangian Finite-Element) is a three-dimensional open-source hydrodynamic model which employs the hydrostatic and Boussinesq approximations to solve shallow-water equations; and employs the transport equation for salt and heat (Zhang and Baptista 2008; Chen and Liu 2014). SELFE employs hybrid SZ coordinates to resolve the vertical and unstructured triangular grid in the horizontal direction (Roland et al. 2012). Zhang and Baptista (2008) point out that bottom boundary layer and processes such as the intrusion of salinity into the estuary and frictional losses are best represented by terrain-following S coordinates while the Z coordinates are best used to represent thin surface plume.

SELFE adopts a semi-implicit time stepping in the computation of all equations, this enhances stability and maximises efficiency (Casulli and Walter 2000; Liu et al. 2008). SELFE implicitly computes vertical viscosity and barotropic-pressure gradient in the momentum equations and divergence term in the continuity equations while the other terms are treated explicitly (Zhang and Baptista 2008). The errors that are generated due to the splitting of internal and external modes (Shchepetkin and McWilliams 2005) are eliminated within SELFE, as no mode splitting is employed (Chen et al. 2015b). Furthermore, advection within the momentum equation is treated with the Eulerian-Lagrangian method while advection within the transport equations can be computed with the Eulerian-Lagrangian method, a Total Variation Diminishing (TVD) scheme or a finite-volume upwind method (Azevedo et al. 2009). Turbulence closure model of SELFE is based on Umlauf and Burchard (2003) Generic Length Scale (GLS) turbulence closure. An advantage of this model is the incorporation of most of the 2.5 closure models ($k-\omega$ (Wilcox 1998); $k-\varepsilon$ (Rodi 1984); Mellor and Yamada 1982) in a single numerical model (Warner et al. 2005b; Chen et al. 2015b). Examples of estuarine hydrodynamic models developed with SELFE include the Tamsui River Estuary, Taiwan (Chen and Liu 2017) and Danshui River Estuary, Taiwan (Chen et al. 2015b). The full details of SELFE are described in Zhang and Baptista (2008) and a summary is presented in Table A.1.

C.5 FVCOM

FVCOM (Finite-volume coastal ocean model) is a three-dimensional open-source finite-volume model that solves the primitive equation under hydrostatic or non-hydrostatic approximation (Chen et al. 2003; Chen et al. 2011; Lai et al. 2010). Chen et al. (2007) purport that the finite-volume method within FVCOM was developed to combine the best attributes of the finite-difference method (i.e. computational efficiency) and finite-element method (i.e. resolving complex geometry). FVCOM employs a terrain-following sigma coordinate scheme to resolve the vertical and an unstructured triangular grid in the horizontal direction (Bruder et al. 2014). Within the hydrostatic approximation, FVCOM employs an explicit time splitting approach (Huang et al. 2008). However, the non-hydrostatic FVCOM provides users with the option to choose between an explicit or semi-implicit time splitting approach (Chen et al. 2011). By default, FVCOM employs the MY level 2.5 turbulence method as modified by Galperin et al. (1988) and provides the k-ε turbulent closure model and General Turbulence Model (GOTM) (a modification of the k-ε turbulent closure model (Burchard 2001)) as a turbulence closure model option (Lai et al. 2010; Chen et al. 2011; Zheng and Weisberg 2012). The development of GOTM aimed at modelling wave-enhanced layer dynamic near the surface, which are not included in two-equation turbulence models (such as k-ε turbulent closure model and the MY level 2.5 turbulence method) (Burchard 2001). However, Aleynik et al. (2016) purport that there is no significant difference in accuracy performance between the MY level 2.5 turbulence method and GOTM scheme. The horizontal diffusion coefficient can be resolved using a constant value of the Smagorinsky eddy parameterization method (Chen et al. 2011). Chen et al. (2007) compared FVCOM with POM while Huang et al. (2008) compared FVCOM with ROMS. Both studies agree that FVCOM obtains higher numerical accuracy as FVCOM is capable of better resolving irregular coastlines. Examples of estuarine hydrodynamic models developed with FVCOM include the Satilla River Estuary, United States (Chen et al. 2008) and Changjiang Estuary, China (Ma et al. 2011). Chen et al. (2011) contain a detailed description of FVCOM and a summary is presented in Table A.1.

Table C.1: Summary of hydrodynamic modelling tools (adapted from: Blumberg and Mellor 1978; Haidvogel 2000; Chen et al. 2003; Lesser et al. 2004; Hervouet 2007; Wang et al. 2008; Zhang and Baptista 2008; Lai et al. 2010; Chen et al. 2011; Deltares 2014; Pham et al. 2016)

	Year of Inception	**General Model Availability**	**Numerical Solution Method**	**Equation**	**Turbulence Closure Model Options**	**Ocean and Sea Oil Spill Modelling**	**Estuary numerical modelling**	**Estuary Oil Spill Modelling**
POM	1977	Open Source Code	Finite Difference	Shallow Water Equations	Mellor-Yamada level 2.5	Wang et al. 2005; Wang et al. 2008; Guo et al. 2009; Xu et al. 2012	Wong et al. 2003; Zhang et al. 2016; Buranaprathep rat and Yanagi 2003); Xia et al. 2008	

ROMS	2000	Open Source Code	Finite Difference	Shallow Water Equations	• Mellor–Yamada level 2.5 • GLS • K-profile parameterization (KPP) • Brunt-Vaisala frequency mixing • User-defined analytical expressions for K_H and K_M	González et al. 2008; Berry et al. 2012; Kim et al. 2013; Otero et al. 2014; Chen et al. 2015a	Warner et al. 2005a; Fan and Song 2014; Pan and Gu 2016	

Deflt3D-FLOW	2004	Open Source Code	Finite Difference	Shallow Water Equations	• constant coefficient • *k*-*L* model • *k*-ε model • Algebraic Eddy viscosity	Abascal 2017	Zhang and Mao 2015; Jie et al. 2014	
SELFE	2005	Open Source Code	Finite Element	Shallow Water Equations	Generic Length Scale (GLS) turbulence Closure	Azevedo et al. 2014	Chen et al. 2015b; Chen and Liu 2017	
TELEMAC-3D	Original version in 1987	Open Source Code	Finite Element	Reynolds-Averaged Navier-Stokes Equations	• Constant viscosity • Mixing length mode • *k*-ε model	Stringari et al. 2013; Marques et al. 2017	Cheviet et al. 2014; Smolders et al. 2014; Mahgoub et al.	

	The non-hydrostatic version in 2008				• Smagorinsky model		2015; Pu et al. 2016; Ross and Sottolichio 2016	
FVCOM	Original version in 2003 The non-hydrostatic version in 2008	Open Source Code	Finite Volume	Reynolds-Averaged Navier-Stokes Equations	• MY level 2.5 turbulence • k-ε model • General Turbulence Model (GOTM)	Li et al. 2016b; Weisberg et al. 2016; Weisberg et al. 2017	Chen et al. 2008; Ma et al. 2011	

REFERENCES

Abascal, A. J., Castanedo, S., Núñez, P., Mellor, A., Clements, A., Pérez, B., Cárdenas, M., Chiri, H., and Medina, R. (2017) 'A High-Resolution Operational Forecast System for Oil Spill Response in Belfast Lough'. *Marine Pollution Bulletin* 114 (1), 302-314

Aleynik, D., Dale, A. C., Porter, M., and Davidson, K. (2016) 'A High Resolution Hydrodynamic Model System Suitable for Novel Harmful Algal Bloom Modelling in Areas of Complex Coastline and Topography'. *Harmful Algae* 53, 102-117

Azevedo, A., Oliveira, A., Fortunato, A. B., Zhang, J., and Baptista, A. M. (2014) 'A Cross-Scale Numerical Modeling System for Management Support of Oil Spill Accidents'. *Marine Pollution Bulletin* 80 (1–2), 132-147

Azevedo, A., Oliveira, A., Fortunato, A. B., and Bertin, X. (2009) 'Application of an Eulerian-Lagrangian Oil Spill Modeling System to the Prestige Accident: Trajectory Analysis'. *Special Issue no. 56. Proceedings of the 10th International Coastal Symposium ICS 2009* I, 777-781

Blumberg, A. F. and Mellor, G. L. (1987) 'A Description of a Three-Dimensional Coastal Ocean Circulation Model'. *American Geophysical Union*, 1-16

Bruder, B., Bomminayuni, S., Haas, K. A., and Stoesser, T. (2014) 'Modeling Tidal Distortion in the Ogeechee Estuary'. *Ocean Modelling* 82, 60-69

Buranapratheprat, A. and Yanagi, T. (2003) 'Seasonal Variations in Circulation and Average Residence Time of the Bangpakong Estuary, Thailand'. *Mer* 41 (4), 199-213

Burchard, H. (2001) 'Simulating the Wave-Enhanced Layer Under Breaking Surface Waves with Two-Equation Turbulence Models'. *Journal of Physical Oceanography* 31 (11), 3133-3145

Carafa, R., Marinov, D., Dueri, S., Wollgast, J., Ligthart, J., Canuti, E., Viaroli, P., and Zaldívar, J. M. (2006) 'A 3D Hydrodynamic Fate and Transport Model for Herbicides in Sacca Di Goro Coastal Lagoon (Northern Adriatic)'. *Marine Pollution Bulletin* 52 (10), 1231-1248

Casulli, V. and Walters, R. A. (2000) 'An Unstructured Grid, Three-Dimensional Model Based on the Shallow Water Equations'. *International Journal for Numerical Methods in Fluids* 32, 331-348

Chatzirodou, A. and Karunarathna, H. (2014) 'Impacts of Tidal Energy Extraction on Sea Bed Morphology'. *Coastal Engineering* 1 (34), 1-10

Chen, C., Beardsley, R. C., Cowles, G. W., Qi, J., Lai, Z., Gao, G., Stuebe, D., Xu, Q., Xue, P., Ge, J., Ji, R., Hu, S., Tian, R., Huang, H., Wu, L., and Lin, H. (2011) *An Unstructured Grid, Finite-Volume Coastal Ocean Model: FVCOM User Manual*. 3rd edn. Cambridge, Massachusetts 02139: Project No. 2010-R/RC-116

Chen, C., Qi, J., Li, C., Beardsley, R. C., Lin, H., Walker, R., and Gates, K. (2008) 'Complexity of the flooding/drying Process in an Estuarine Tidal-Creek Salt-Marsh System: An Application of FVCOM'. *Journal of Geophysical Research: Oceans* 113 (C07052)

Chen, C., Huang, H., Beardsley, R. C., Liu, H., Xu, Q., and Cowles, G. W. (2007) 'A Finite Volume Numerical Approach for Coastal Ocean Circulation Studies: Comparisons with Finite Difference Models'. *Journal of Geophysical Research* 112 (C3)

Chen, C., Liu, H., and Beardsley, R. C. (2003) 'An Unstructured Grid, Finite-Volume, Three-Dimensional, Primitive Equations Ocean Model: Application to Coastal Ocean and Estuaries'. *Journal of Atmospheric and Oceanic Technology* 20 (1), 159-186

Chen, H., An, W., You, Y., Lei, F., Zhao, Y., and Li, J. (2015b) 'Numerical Study of Underwater Fate of Oil Spilled from Deepwater Blowout'. *Ocean Engineering* 110, Part A, 227-243

Chen, W. and Liu, W. (2017) 'Investigating the Fate and Transport of Fecal Coliform Contamination in a Tidal Estuarine System using a Three-Dimensional Model'. *Marine Pollution Bulletin* 116 (1–2), 365-384

Chen, W., Liu, W., Hsu, M., and Hwang, C. (2015a) 'Modeling Investigation of Suspended Sediment Transport in a Tidal Estuary using a Three-Dimensional Model'. *Applied Mathematical Modelling* 39 (9), 2570-2586

Chen, W. and Liu, W. (2014) 'Modeling Flood Inundation Induced by River Flow and Storm Surges Over a River Basin'. *Water* 6 (10), 3182-3199

Cheviet, C., Violeau, D., and Guesmia, M. (2002) 'Numerical Simulation of Cohesive Sediment Transport in the Loire Estuary with a Three-Dimensional Model Including New Parameterisations'. Proceedings in Marine Science [online] 5, 529-543. available from <http://www.sciencedirect.com/science/article/pii/S1568269202800389>

Deltares (2014) *DELFT3D User Manual: 3D/2D Modelling Suite for Integral Water Solutions*. Delft, The Netherlands: Deltares

Ezer, T., Arango, H. G., and Shchepetkin, A. F. (2002) 'Developments in Terrain-Following Ocean Models: Intercomparisons of Numerical Aspects'. *Ocean Modelling* 4 (3–4), 249-267

Fan, W. and Song, J. (2014) 'A Numerical Study of the Seasonal Variations of Nutrients in the Changjiang River Estuary and its Adjacent Sea Area'. *Ecological Modelling* [online] 291, 69-81. available from <http://www.sciencedirect.com/science/article/pii/S0304380014003639>

Galperin, B., Kantha, L. H., Hassid, S., and Rosati, A. (1988) 'A Quasi-Equilibrium Turbulent Energy Model for Geophysical Flows'. *Journal of the Atmospheric Sciences* 45 (1), 55-62

González, M., Ferrer, L., Uriarte, A., Urtizberea, A., and Caballero, A. (2008) 'Operational Oceanography System Applied to the Prestige Oil-Spillage Event'. *Journal of Marine Systems* 72 (1–4), 178-188

Guo, W. J. and Wang, Y. X. (2009) 'A Numerical Oil Spill Model Based on a Hybrid Method'. *Marine Pollution Bulletin* 58 (5), 726-734

Haidvogel, D. B., Arango, H. G., Hedstrom, K., Beckmann, A., Malanotte-Rizzoli, P., and Shchepetkin, A. F. (2000) 'Model Evaluation Experiments in the North Atlantic Basin: Simulations in Nonlinear Terrain-Following Coordinates'. *Dynamics of Atmospheres and Oceans* 32 (3–4), 239-281

Hervouet, J. (2007) *Hydrodynamics of Free Surface Flows, Modelling with the Finite-Element Method*. West Sussex, England: John Wiley & Sons Ltd.

Huang, H., Chen, C., Cowles, G. W., Winant, C. D., Beardsley, R. C., Hedstrom, K., and Haidvogel, D. B. (2008) 'FVCOM Validation Experiments: Comparisons with ROMS for Three Idealized Barotropic Test Problems'. *Journal of Geophysical Research* 113 (C7)

Jie, H., Leicheng, G., van der Wegen, M., and Roelvink, D. (eds.) (2014) *IAHS-AISH Proceedings and Reports*. 'Hindcasting Morphodynamic Evolution with Sand-Mud Interactions in the Yangtze Estuary'. held 24 - 27 August at Guangzhou; China

Kim, C., Cho, Y., Choi, B., Jung, K. T., and You, S. H. (2013) 'Improving a Prediction System for Oil Spills in the Yellow Sea: Effect of Tides on Subtidal Flow'. *Marine Pollution Bulletin* 68 (1–2), 85-92

Kolmogorov, A. N. (1942) 'Equations of Turbulent Motion of an Incompressible Fluid.'. *IZV Akad. Nauk. USSR, Ser. Phys.* 6, 56-58. (translated into English by D.B. Spalding, as Imperial College, Mechanical Engineering Department Report ON/6, 1968, London, U.K.);

Lai, Z., Chen, C., Cowles, G. W., and Beardsley, R. C. (2010) 'A Nonhydrostatic Version of FVCOM: 1. Validation Experiments'. *Journal of Geophysical Research* 115 (C11), 1-23

Lazure, P. and Dumas, F. (2008) 'An external–internal Mode Coupling for a 3D Hydrodynamical Model for Applications at Regional Scale (MARS)'. *Advances in Water Resources* 31 (2), 233-250

Lesser, G. R., Roelvink, D., van Kester, J. A. T. M., and Stelling, G. S. (2004) 'Development and Validation of a Three-Dimensional Morphological Model'. *Coastal Engineering* 51 (8–9), 883-915

Li, H., Li, Y., Li, C., Wang, G., Xu, S., Song, J., and Zhang, S. (eds.) (2016b) *International Conference on Energy Engineering and Environmental Protection (EEEP2016)*. 'Numerical Simulation Study on Drift and Diffusion of Dalian Oil Spill': IOP Publishing Ltd

Liu, W., Chen, W., Kuo, J., and Wu, C. (2008) 'Numerical Determination of Residence Time and Age in a Partially Mixed Estuary using Three-Dimensional Hydrodynamic Model'. *Continental Shelf Research* 28 (8), 1068-1088

Ma, G., Shi, F., Liu, S., and Qi, D. (2011) 'Hydrodynamic Modeling of Changjiang Estuary: Model Skill Assessment and Large-Scale Structure Impacts'. *Applied Ocean Research* 33 (1), 69-78

Mahgoub, M., Hinkelmann, R., and La Rocca, M. (2015) 'Understanding the Behaviour of Gravity Currents in Tideless Estuaries and Considering the Impact of Sea Level Rise within the Nile Estuary'. Journal of Coastal Research 313 (3), 714-722

Marques, W. C., Stringari, C. E., Kirinus, E. P., Möller Jr, O. O., Toldo Jr, E. E., and Andrade, M. M. (2017) 'Numerical Modeling of the Tramandaí Beach Oil Spill, Brazil—Case Study for January 2012 Event'. *Applied Ocean Research* 65, 178-191

Mellor, G. L. (2004) *User Guide for a Three-Dimensional, Primitive Equation, Numerical Ocean Model*. Princeton University, Princeton, NJ: Program in Atmospheric and Oceanic Sciences

Mellor, G. L. and Yamada, T. (1982) 'Development of a Turbulence Closure Model for Geophysical Fluid Problems'. *Reviews of Geophysics* 20 (4), 851

Otero, P., Ruiz-Villarreal, M., Allen-Perkins, S., Vila, B., and Cabanas, J. M. (2014) 'Coastal Exposure to Oil Spill Impacts from the Finisterre Traffic Separation Scheme'. *Marine Pollution Bulletin* 85 (1), 67-77

Pan, J. and Gu, Y. (2016) 'Cruise Observation and Numerical Modeling of Turbulent Mixing in the Pearl River Estuary in Summer'. *Continental Shelf Research* [online] 120, 122-138. available from <http://www.sciencedirect.com/science/article/pii/S027843431630142X>

Pham, C., Goeury, C., and Joly, A. (2016) *TELEMAC MODELLING SYSTEM: 3D Hydrodynamics TELEMAC-3D Software Releaase 7.0 Operating Manual*. National Hydraulics and Environment Laboratory, EDF R&D, France: EDF R&D

Prandtl, L. (1945) 'Uber Ein Neues Formelsystem Fur Die Ausgebildete Turbulenz (on a New Formation for Fully Developed Turbulence)'. *Nachrichten Der Akademie Der Wissenschaften (Report of Academy of Sciences, Gottingen, Germany)*, 6-19

Pu, X., Shi, J. Z., and Hu, G. (2016) 'Analyses of Intermittent Mixing and Stratification within the North Passage of the Changjiang (Yangtze) River Estuary, China: A Three-Dimensional Model Study'. *Journal of Marine Systems* [online] 158, 140-164. available from <http://www.sciencedirect.com/science/article/pii/S0924796316000403>

Rodi, W. (1984) *Turbulence Models and their Application in Hydraulics*. 2nd edn. Delft, The Netherlands: International Association for Hydraulics Research

Roland, L. A., Zhang, Y. J., Wang, H. V., Meng, Y., Teng, Y., Maderich, V., Brovchenko, I., Dutour-Sikiric, M., and Zanke, U. (2012) 'A Fully Coupled 3D Wave-Current Interaction Model on Unstructured Grids.'. *Journal of Geophysical Research: Oceans* 117 (C00J33)

Ross, L. and Sottolichio, A. (2016) 'Subtidal Variability of Sea Level in a Macrotidal and Convergent Estuary'. *Continental Shelf Research* [online] 131, 28-41. available from <http://www.sciencedirect.com/science/article/pii/S0278434316305970>

Shchepetkin, A. F. and McWilliams, J. C. (2009) 'Correction and Commentary for "Ocean Forecasting in Terrain-Following Coordinates: Formulation and Skill Assessment of the Regional Ocean Modeling System" by Haidvogel Et Al., J. Comp. Phys. 227, Pp. 3595–3624'. *Journal of Computational Physics* 228 (24), 8985-9000

Shchepetkin, A. F. and McWilliams, J. C. (2005) 'The Regional Oceanic Modeling System (ROMS): A Split-Explicit, Free-Surface, Topography-Following-Coordinate Oceanic Model'. *Ocean Modelling* 9 (4), 347-404

Smolders, S., Tatiana, M., Joris, V., and Teles, M. J. (eds.) (2014) 21st Telemac Mascaret User Conference. 'Implementation of Controlled Reduced Tide and Flooding Areas in the TELEMAC 3D Model of the Scheldt Estuary'. held 15-17 October at Grenoble, France. France

Stringari, C. E., Corrêa da Silva Machado, M. I., Kirinus, E. P., and Marques, W. C. (eds.) (2013) *Application of TELEMAC System at the Southern Brazilian Shelf: Case Study of Tramandaí Beach Oil Spill*. 'XXth TELEMAC-MASCARET User Conference'. held 16–18 October, 2013 at Karlsruhe, Germany: BAW

Umlauf, L. and Burchard, H. (2003) 'A Generic Length-Scale Equation for Geophysical Turbulence Models'. *Journal of Marine Research* 61 (2), 235-265

Wang, S., Shen, Y., Guo, Y., and Tang, J. (2008) 'Three-Dimensional Numerical Simulation for Transport of Oil Spills in Seas'. *Ocean Engineering* 35 (5–6), 503-510

Warner, J. C., Defne, Z., Haas, K. A., and Arango, H. G. (2013) 'A Wetting and Drying Scheme for ROMS'. *Computers & Geosciences* 58, 54-61

Warner, J. C., Sherwood, C. R., Arango, H. G., and Signell, R. P. (2005b) 'Performance of Four Turbulence Closure Models Implemented using a Generic Length Scale Method'. *Ocean Modelling* 8 (1–2), 81-113

Warner, J. C., Geyer, W. R., and Lerczak, J. A. (2005a) 'Numerical Modeling of an Estuary: A Comprehensive Skill Assessment'. *Journal of Geophysical Research: Oceans* 110 (C5), 1-13

Weisberg, R. H., Lianyuan, Z., and Liu, Y. (2017) 'On the Movement of Deepwater Horizon Oil to Northern Gulf Beaches'. *Ocean Modelling* 111, 81-97

Weisberg, R. H., Zheng, L., Liu, Y., Murawski, S., Hu, C., and Paul, J. (2016) 'Did Deepwater Horizon Hydrocarbons Transit to the West Florida Continental Shelf?'. *Deep Sea Research Part II: Topical Studies in Oceanography* 129, 259-272

Wilcox, D. C. (1988) 'Reassessment of the Scale-Determining Equation for Advanced Turbulence Models'. *AIAA Journal* 26 (11), 1299-1310

Wong, L. A., Chen, J. C., Xue, H., Dong, L. X., Guan, W. B., and Su, J. L. (2003) 'A Model Study of the Circulation in the Pearl River Estuary (PRE) and its Adjacent Coastal Waters: 2. Sensitivity Experiments'. *Journal of Geophysical Research: Oceans* 108 (5), 26-1 - 26-12

Xia, M., Xie, L., Pietrafesa, L. J., and Peng, M. (2008) 'A Numerical Study of Storm Surge in the Cape Fear River Estuary and Adjacent Coast'. *Journal of Coastal Research* 24 (4 SUPPL.), 159-167

Xu, H., Chen, J., Wang, S., and Liu, Y. (2012) 'Oil Spill Forecast Model Based on Uncertainty Analysis: A Case Study of Dalian Oil Spill'. *Ocean Engineering* 54, 206-212

Yuill, B. T., Khadka, A. K., Pereira, J., Allison, M. A., and Meselhe, E. A. (2016) 'Morphodynamics of the Erosional Phase of Crevasse-Splay Evolution and Implications for River Sediment Diversion Function'. *Geomorphology* 259, 12-29

Zhang, S. and Mao, X. -. (2015) 'Hydrology, Sediment Circulation and Long-Term Morphological Changes in Highly Urbanized Shenzhen River Estuary, China: A Combined Field Experimental and Modeling Approach'. *Journal of Hydrology* 529, 1562-1577

Zhang, W., Gong, Z., Zhang, C., and Tan, W. (2016) 'Response of Nearshore Circulation Outside Yangtze Estuary to El Niño Events'. *Water Science and Engineering* [online] 9 (2), 145-154. available from <http://www.sciencedirect.com/science/article/pii/S1674237016000065>

Zhang, Y. J. and Baptista, A. M. (2008) 'SELFE: A Semi-Implicit Eulerian–Lagrangian Finite-Element Model for Cross-Scale Ocean Circulation'. *Ocean Modelling* 21 (3–4), 71-96

Zheng, L. and Weisberg, R. H. (2012) 'Modeling the West Florida Coastal Ocean by Downscaling from the Deep Ocean, Across the Continental Shelf and into the Estuaries'. *Ocean Modelling* 48, 10-29

APPENDIX D

Table D.1: TIDAL HARMONICS AT THE HUMBER ESTUARY MOUTH (EXTRACTED FROM FES2014 MODEL)

S/N	Tidal Constituents	Frequency (deg/hr)	541049, 402468		540841, 409420	
			Amplitude (cm)	Phase Lag (deg)	Amplitude (cm)	Phase Lag (deg)
1	2N2	27.895	5.784	93.664	5.740	93.061
2	EPS2	27.423	0.204	32.407	0.162	33.657
3	J1	15.585	1.345	-100.303	1.360	-100.468
4	K1	15.041	14.883	-87.498	14.873	-87.798
5	K2	30.082	20.517	-171.043	20.276	-171.704
6	L2	29.528	8.773	156.118	8.626	155.397
7	La2	29.456	2.547	143.383	2.541	142.804
8	M2	28.984	209.702	147.123	206.835	146.354

9	M3	43.476	0.909	17.956	0.872	16.681
10	M4	57.968	4.393	149.235	3.906	149.902
11	M6	86.952	6.020	-61.413	6.637	-59.295
12	M8	115.936	0.373	50.087	0.442	54.026
13	Mf	1.098	1.221	-159.503	1.201	-160.094
14	MKS2	29.066	1.242	-49.340	1.193	-50.294
15	Mm	0.544	0.834	-163.770	0.797	-165.932
16	MN4	57.423	2.249	174.206	2.165	173.322
17	MS4	58.984	2.179	-84.081	1.750	-88.063
18	MSf	1.015	0.292	-128.548	0.190	-123.312
19	MSqm	2.113	0.030	-160.923	0.037	-148.407
20	Mtm	1.633	0.209	-167.224	0.207	-166.875
21	Mu2	27.968	2.894	170.036	5.740	93.061

22	N2	28.439	40.568	123.689	2.878	169.216
23	N4	56.879	0.318	125.946	40.223	123.121
24	Nu2	28.512	8.679	125.808	0.307	125.158
25	O1	13.943	15.974	111.058	8.602	125.026
26	P1	14.958	5.052	-98.774	15.946	110.722
27	Q1	13.398	5.414	52.239	4.998	-98.842
28	R2	30.041	0.615	-173.329	5.414	52.080
29	S1	15	2.549	171.742	0.609	-174.330
30	S2	30	70.229	-155.653	2.543	171.997
31	S4	60	0.811	-92.242	69.353	-167.711
32	Sa	0.041	0.014	93.489	0.794	-96.671
33	Ssa	0.082	0.839	-179.063	0.008	115.642
34	T2	29.958	4.503	-174.516	0.842	-179.441

APPENDIX E

C script modified to extract 15-minutes tidal height data from the FES2014 model from January 1st 2017 – December 31st 2017 at 541049, 402468 (Lat. 53.625; Long 0.1250).

```
/* This file is part of FES library.

   FES is free software: you can redistribute it and/or modify
   it under the terms of the GNU LESSER GENERAL PUBLIC LICENSE as published by
   the Free Software Foundation, either version 3 of the License, or
   (at your option) any later version.

   FES is distributed in the hope that it will be useful,
   but WITHOUT ANY WARRANTY; without even the implied warranty of
   MERCHANTABILITY or FITNESS FOR A PARTICULAR PURPOSE.  See the
   GNU LESSER GENERAL PUBLIC LICENSE for more details.

   You should have received a copy of the GNU LESSER GENERAL PUBLIC LICENSE
   along with FES.  If not, see <http://www.gnu.org/licenses/>.
*/

#include <stdlib.h>
#include <stdio.h>

#include "fes.h"
```

```
// Path to the configuration file and data used to test the library
// Change these settings to your liking.
#define INI "/home/chijioke/Downloads/fes/data/fes2014/ocean_tide_extrapolated.ini"
#define FES_DATA "/home/chijioke/Downloads/fes/data/fes2014/ocean_tide_extrapolated"


int main(void) {
  // The return code
  int rc = 0;
  // The hour of the estimate.
  double hour;
  // Latitude and longitude of the point where the ocean tide will be
  // evaluated.
  double lon = 0.1250;
  double lat = 53.5625;
  // Short tides (semi_diurnal and diurnal tides)
  double tide;
  // Time in CNES Julian days, defined as Modified Julian Day minus 33282.
  // Thus CNES 0 is at midnight between the 31 December and 01 January 1950
  // AD Gregorian.
  double time;
  // Long period tides
  double lp;
  // Loading effects for short tide
  double load;
```

```
  // Loading effects for long period tides (is always equal to zero)
  double loadlp;
  // FES handlers
  FES short_tide;
  FES radial_tide = NULL;

#ifdef _WIN32
  _putenv_s("FES_DATA", FES_DATA);
#else
  setenv("FES_DATA", FES_DATA, 1);
#endif

  // Creating the FES handler to calculate the ocean tide
  if (fes_new(&short_tide, FES_TIDE, FES_IO, INI)) {
    printf("fes error : %s\n", fes_error(short_tide));
    goto error;
  }

  // Creating the FES handler to calculate the loading tide
  if (fes_new(&radial_tide, FES_RADIAL, FES_IO, INI)) {
    printf("fes error : %s\n", fes_error(radial_tide));
    goto error;
  }

  printf("%12s %9s %9s %9s %9s %9s %9s %9s %9s\n", "JulDay", "Hour", "Latitude",
      "Longitude", "Short_tid", "LP_tid", "Pure_Tide", "Geo_Tide",
```

```
      "Rad_Tide");

for (hour = 0, time = 2457754.5; hour < 8760; hour=hour+0.25, time += 0.25/ 24.0) {
  // Compute ocean tide
  if (fes_core(short_tide, lat, lon, time, &tide, &lp)) {
    // If the current point is undefined (i.e. the point is on land), the
    // tide is not defined.
    if (fes_errno(short_tide) == FES_NO_DATA)
      continue;
    else {
      fprintf(stderr, "%s\n", fes_error(short_tide));
      goto error;
    }
  }

  // Compute loading tide
  if (fes_core(radial_tide, lat, lon, time, &load, &loadlp)) {
    // If the current point is undefined (i.e. the point is on land), the
    // loading tide is not defined.
    if (fes_errno(radial_tide) == FES_NO_DATA)
      continue;
    else {
      fprintf(stderr, "%s\n", fes_error(radial_tide));
      goto error;
    }
  }
```

```
    // tide + lp        = pure tide (as seen by a tide gauge)
    // tide + lp + load = geocentric tide (as seen by a satellite)
    printf("%12.5f %9.2f %9.3f %9.3f %9.3f %9.3f %9.3f %9.3f %9.3f\n", time, hour,
        lat, lon, tide, lp, tide + lp, tide + lp + load, load);
  }

  goto finish;

  error:
    rc = 1;

  finish:
    // Release the memory used by the FES handlers.
    fes_delete(short_tide);
    fes_delete(radial_tide);

    return rc;
}
```

APPENDIX F

F.1 STEERING FILE DESCRIBING THE INITIAL CONDITIONS OF THE TELEMAC3D SIMULATION FOR THE SUMMER MONTH, AUGUST 2017.

```
/
/
 ADVECTION-DIFFUSION SCHEME WITH SETTLING VELOCITY     = 1
/
/VALIDATION              = YES
/REFERENCE FILE          = 'r3d_tidal_flats_set1.ref'
/
/ These options also work with the same time step,
/ but with more mass error
/
/ADVECTION-DIFFUSION SCHEME WITH SETTLING VELOCITY     = 0
/ADVECTION-DIFFUSION SCHEME WITH SETTLING VELOCITY     = 2
/
3D RESULT FILE                          : 'r3d_summer_run1.slf'
2D RESULT FILE                          : 'r2d_summer_run1.slf'
LIQUID BOUNDARIES FILE                  : 'summer1_cal.txt'
BOUNDARY CONDITIONS FILE                : 'bc_humber3OD.cli'
GEOMETRY FILE                           : 'humber_geometry3OD.slf'
/---------------------------------------------------------------------/
/ COMPUTATION CONTINUED                 = YES
/ PREVIOUS COMPUTATION FILE             = 'T3DHYD'
/---------------------------------------------------------------------/
/
 PARALLEL PROCESSORS  = 0
/
/---------------------------------------------------------------------/
/                   OPTIONS GENERALES
/---------------------------------------------------------------------/
 TITLE                          = 'Humber Estuary - Summer'
 ORIGINAL DATE OF TIME          = 2017; 8; 1
/
 VARIABLES FOR 2D GRAPHIC PRINTOUTS = 'U,V,S'
 VARIABLES FOR 3D GRAPHIC PRINTOUTS = 'Z,U,V,W'
 /
 NUMBER OF HORIZONTAL LEVELS= 5
 /
/DURATION                       = 2677500
 TIME STEP                      = 45
 NUMBER OF TIME STEPS           = 59500
 GRAPHIC PRINTOUT PERIOD        = 20
 LISTING PRINTOUT PERIOD        = 20
/---------------------------------------------------------------------/
 LAW OF BOTTOM FRICTION                       = 2
 FRICTION COEFFICIENT FOR THE BOTTOM          = 60
 TURBULENCE MODEL FOR THE BOTTOM              = 2
 HORIZONTAL TURBULENCE MODEL                  = 4
 VERTICAL TURBULENCE MODEL                    = 2
/
 MIXING LENGTH MODEL            = 3 / Nezu and Nakagawa
```

```
 DAMPING FUNCTION              = 0    / no damping
/
 COEFFICIENT FOR HORIZONTAL DIFFUSION OF VELOCITIES = 0.1D0
 COEFFICIENT FOR VERTICAL DIFFUSION OF VELOCITIES       = 1.E-6
 COEFFICIENT FOR HORIZONTAL DIFFUSION OF TRACERS      = 0.1D0
 COEFFICIENT FOR VERTICAL DIFFUSION OF TRACERS          = 1.E-6
/
 CORIOLIS                          = YES
 CORIOLIS COEFFICIENT          = 1.172E-4 /lattitude 53.72
/-------------------------------------------------------------------------/
 INITIAL CONDITIONS             = 'CONSTANT ELEVATION'
 INITIAL ELEVATION              = 6
 PRESCRIBED FLOWRATES       = 30.0; 0.0; 25.0
 PRESCRIBED ELEVATIONS      = 0.0; 13.096; 0.0
/-------------------------------------------------------------------------/
/
/ NON-HYDROSTATIC VERSION                              = YES
 SCHEME FOR ADVECTION OF VELOCITIES                = 1
 ACCURACY FOR DIFFUSION OF VELOCITIES             = 1.E-6
 MAXIMUM NUMBER OF ITERATIONS FOR DIFFUSION OF VELOCITIES= 500
 PRECONDITIONING FOR DIFFUSION OF VELOCITIES  = 34
 SOLVER FOR PROPAGATION                                 = 2
 PRECONDITIONING FOR PROPAGATION                  = 2
/
 SCHEME FOR ADVECTION OF DEPTH                       = 5
 IMPLICITATION FOR DEPTH                                 = 0.55
 IMPLICITATION FOR VELOCITIES                          = 0.60
 MASS-LUMPING FOR DEPTH                                = 1.0
FREE SURFACE GRADIENT COMPATIBILITY              = 0.9     / to smooth surface levels
 MATRIX STORAGE                                               = 3
/
/-------------------------------------------------------------------------/
 MASS-BALANCE                                                                                            = YES
 INFORMATION ABOUT MASS-BALANCE FOR EACH LISTING PRINTOUT         = YES
 TREATMENT OF FLUXES AT THE BOUNDARIES                                           =2;2;2
/-------------------------------------------------------------------------/
/
/ tidal flats
/
 TIDAL FLATS                                    = YES
 TREATMENT OF NEGATIVE DEPTHS   = 2
 STABILIZED INITIAL CONDITION        = NO
/
/-------------------------------------------------------------------------/
/ TRACERS
/-------------------------------------------------------------------------/
/
  NUMBER OF TRACERS                                = 2
  NAMES OF TRACERS              = 'TEMPERATURE     °C            '; 'SALINITY       KG/M3
'
  INITIAL VALUES OF TRACERS                      = 17.4473; 29.2832
  PRESCRIBED TRACERS VALUES                    = 0.0; 0.0; 17.4473; 29.2832; 0.0; 0.0
  DENSITY LAW                                             = 3
  SCHEME FOR ADVECTION OF TRACERS          = 14
/-------------------------------------------------------------------------/
/
&ETA
&FIN
```

F.2 STEERING FILE DESCRIBING THE INITIAL CONDITIONS OF THE TELEMAC3D SIMULATION FOR THE WINTER MONTH, FEBRUARY 2010.

```
/
/
 ADVECTION-DIFFUSION SCHEME WITH SETTLING VELOCITY     = 1
/
/VALIDATION                = YES
/REFERENCE FILE            = 'r3d_tidal_flats_set1.ref'
/
/ These options also work with the same time step,
/ but with more mass error
/
/ADVECTION-DIFFUSION SCHEME WITH SETTLING VELOCITY     = 0
/ADVECTION-DIFFUSION SCHEME WITH SETTLING VELOCITY     = 2
/
3D RESULT FILE                          : 'r3d_winter_run1.slf'
2D RESULT FILE                          : 'r2d_winter_run1.slf'
LIQUID BOUNDARIES FILE                  : 'winter_cal.txt'
BOUNDARY CONDITIONS FILE                : 'bc_humber3OD.cli'
GEOMETRY FILE                           : 'humber_geometry3OD.slf'
/----------------------------------------------------------------------/
/ COMPUTATION CONTINUED                 = YES
/ PREVIOUS COMPUTATION FILE             = 'T3DHYD'
/----------------------------------------------------------------------/
/
 PARALLEL PROCESSORS  = 0
/
/----------------------------------------------------------------------/
/                 OPTIONS GENERALES
/----------------------------------------------------------------------/
 TITLE                           = 'Humber Estuary - Winter'
 ORIGINAL DATE OF TIME           = 2010; 2; 1
/
 VARIABLES FOR 2D GRAPHIC PRINTOUTS = 'U,V,S'
 VARIABLES FOR 3D GRAPHIC PRINTOUTS = 'Z,U,V,W'
 /
 NUMBER OF HORIZONTAL LEVELS = 5
 /
/DURATION                        = 2418300
 TIME STEP                       = 45
 NUMBER OF TIME STEPS            = 53740
 GRAPHIC PRINTOUT PERIOD         = 20
 LISTING PRINTOUT PERIOD         = 20
/----------------------------------------------------------------------/
 LAW OF BOTTOM FRICTION                        = 2
 FRICTION COEFFICIENT FOR THE BOTTOM           = 60
 TURBULENCE MODEL FOR THE BOTTOM               = 2
 HORIZONTAL TURBULENCE MODEL                   = 4
 VERTICAL TURBULENCE MODEL                     = 2
/
 MIXING LENGTH MODEL             = 3 / Nezu and Nakagawa
 DAMPING FUNCTION                = 0    / no damping
/
 COEFFICIENT FOR HORIZONTAL DIFFUSION OF VELOCITIES = 0.1D0
 COEFFICIENT FOR VERTICAL DIFFUSION OF VELOCITIES       = 1.E-6
```

```
 COEFFICIENT FOR HORIZONTAL DIFFUSION OF TRACERS      = 0.1D0
 COEFFICIENT FOR VERTICAL DIFFUSION OF TRACERS        = 1.E-6
/
 CORIOLIS                        = YES
 CORIOLIS COEFFICIENT            = 1.172E-4 /latitude 53.72
/----------------------------------------------------------------------/
 INITIAL CONDITIONS              = 'CONSTANT ELEVATION'
 INITIAL ELEVATION               = 6
 PRESCRIBED FLOWRATES            = 400.0;0.0;800.0
 PRESCRIBED ELEVATIONS           = 0.0; 9.279; 0.0
/----------------------------------------------------------------------/
/
/ NON-HYDROSTATIC VERSION                              = YES
 SCHEME FOR ADVECTION OF VELOCITIES                    = 1
 ACCURACY FOR DIFFUSION OF VELOCITIES                  = 1.E-6
 MAXIMUM NUMBER OF ITERATIONS FOR DIFFUSION OF VELOCITIES= 500
 PRECONDITIONING FOR DIFFUSION OF VELOCITIES           = 34
 SOLVER FOR PROPAGATION                                = 2
 PRECONDITIONING FOR PROPAGATION                       = 2
/
 SCHEME FOR ADVECTION OF DEPTH                         = 5
 IMPLICITATION FOR DEPTH                               = 0.55
 IMPLICITATION FOR VELOCITIES                          = 0.60
 MASS-LUMPING FOR DEPTH                                = 1.0
FREE SURFACE GRADIENT COMPATIBILITY                    = 0.9    / to smooth surface levels
 MATRIX STORAGE                                        = 3
/
/----------------------------------------------------------------------/
 MASS-BALANCE                                                       = YES
 INFORMATION ABOUT MASS-BALANCE FOR EACH LISTING PRINTOUT           = YES
 TREATMENT OF FLUXES AT THE BOUNDARIES                              =2; 2; 2
/----------------------------------------------------------------------/
/
/ tidal flats
/
 TIDAL FLATS                          = YES
 TREATMENT OF NEGATIVE DEPTHS         = 2
 STABILIZED INITIAL CONDITION         = NO
/
/----------------------------------------------------------------------/
/ TRACERS
/----------------------------------------------------------------------/
/
  NUMBER OF TRACERS                   = 2
  NAMES OF TRACERS               = 'TEMPERATURE     °C              '; 'SALINITY        KG/M3
'
  INITIAL VALUES OF TRACERS           = 6.6234; 27.1978
  PRESCRIBED TRACERS VALUES           = 0.0; 0.0; 6.6234; 27.1978; 0.0; 0.0
  DENSITY LAW                         = 3
  SCHEME FOR ADVECTION OF TRACERS          = 14
/----------------------------------------------------------------------/
/
&ETA
&FIN
```

APPENDIX G

SENSITIVITY ANALYSIS ON THE OIL SPILL MODEL TO MESH RESOLUTION.

Tablee G.1: Properties of Computational Domain.

Selected Edge Length	Nodes	Elements	Mean Edge Length	Minimum Edge Length	Maximum Edge Length
50 m	92,369	183,925	54.57	11	803
75 m	41,190	81,625	81.69	13	889
100 m	23,528	46,329	108.20	18	960

Tablee G.2: Simulated oil slick area, A (sq. km), for oil slick released at L2 during low water spring tide

Scenarios	0 - 8h	8 - 16h	16 - 24h	24 - 32h	32 - 40h	40 - 48h
L2 LW ST summer	A	A	A	A	A	A
Edge Length = 50 m	7.47	13.59	19.84	27.03	29.77	32.67
Edge Length = 75 m	7.16	14.93	18.71	22.69	29.20	30.23
Edge Length = 100 m	7.32	14.76	18.89	24.44	29.80	31.15

Note: L2 = release points; LW = low water; ST = spring tide.

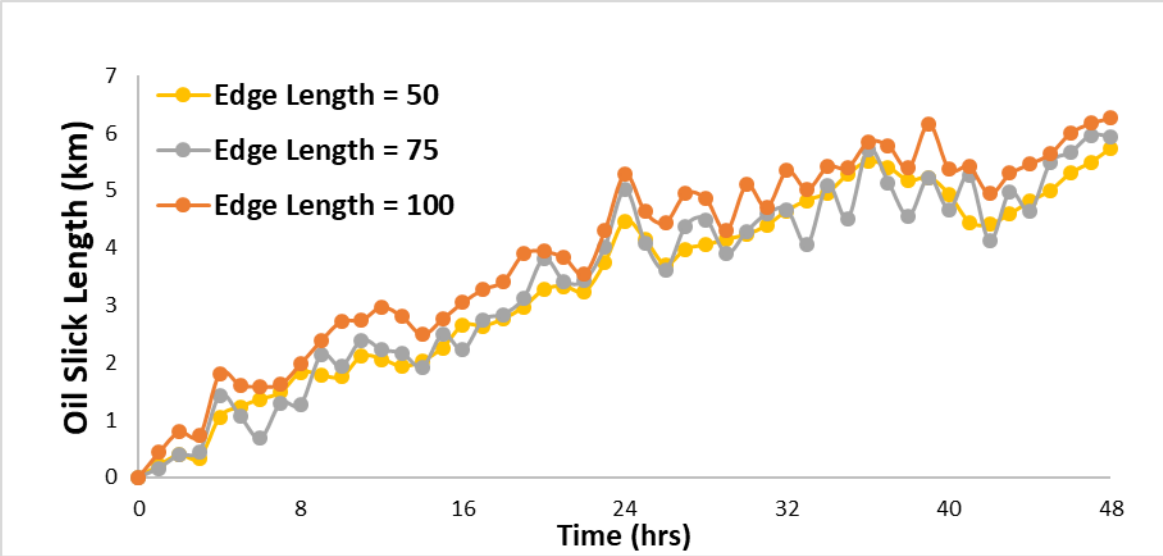

Edge Length = 50
Edge Length = 75
Edge Length = 100
Oil Slick Length (km)
Time (hrs)
0
1
2
3
4
5
6
7
0
8
16
24
32
40
48

APPENDIX H

MATLAB CODE EMPLOYED TO CONVERT BATHYMETRY POINT DATA FROM CHART DATUM TO ORDNANCE DATUM

```
xy=[539698, 410406; ... %1 Spurn
521432, 416166; ... %2 Immingham
506201, 426283; ...%3 Humber Bridge
496219, 423025; ...%4 Ferriby
493109, 426556; ...%5 Brough
483757, 424265; ...%6 Blacktoft
485880, 414661; ...%7 Flixborough
483589, 411572]; %8 Keadby

bif=[486426.5457 ,423236.1076];
dz=-[3.9,3.9,3.3,2.7,2.5,1.5,0.9,0.4];

for i=1:Humber1.NPOIN2

   if Humber1.XYZ2(i,1)>xy(2,1)
       Humber2.RESULT(i)=Humber1.RESULT(i)-dz(2);

   elseif Humber1.XYZ2(i,1)>xy(3,1)
      Humber2.RESULT(i)=Humber1.RESULT(i)-(dz(3)+(dz(2)-
dz(3))*(Humber1.XYZ2(i,1)-xy(3,1))/(xy(2,1)-xy(3,1)));

   elseif Humber1.XYZ2(i,1)>xy(4,1)
      Humber2.RESULT(i)=Humber1.RESULT(i)-(dz(4)+(dz(3)-
dz(4))*(Humber1.XYZ2(i,1)-xy(4,1))/(xy(3,1)-xy(4,1)));

   elseif Humber1.XYZ2(i,1)>xy(5,1)
      Humber2.RESULT(i)=Humber1.RESULT(i)-(dz(5)+(dz(4)-
dz(5))*(Humber1.XYZ2(i,1)-xy(5,1))/(xy(4,1)-xy(5,1)));

   elseif Humber1.XYZ2(i,1)>xy(6,1)&Humber1.XYZ2(i,2)>bif(2)
      Humber2.RESULT(i)=Humber1.RESULT(i)-(dz(6)+(dz(5)-
dz(6))*(Humber1.XYZ2(i,1)-xy(6,1))/(xy(5,1)-xy(6,1)));

   elseif Humber1.XYZ2(i,1)<xy(6,1)&Humber1.XYZ2(i,2)>bif(2)
       Humber2.RESULT(i)=Humber1.RESULT(i)-dz(6);

   elseif Humber1.XYZ2(i,2)>xy(7,2)&Humber1.XYZ2(i,2)<bif(2)
       dzbif=(dz(6)+(dz(5)-dz(6))*(bif(1)-xy(6,1))/(xy(5)-xy(6,1)));

      Humber2.RESULT(i)=Humber1.RESULT(i)-(dzbif-(dzbif-dz(7))*(bif(2)-
Humber1.XYZ2(i,2))/(bif(2)-xy(7,2)));
```

```
   elseif Humber1.XYZ2(i,2)<xy(7,2)
       Humber2.RESULT(i)=Humber1.RESULT(i)-(dz(8)+(dz(7)-
dz(8))*(Humber1.XYZ2(i,1)-xy(8,1))/(xy(7,1)-xy(8,1)));

   end

end

fid=telheadw(Humber2,'C:\Users\ekec4\Desktop\humber_sim2\humber_geometry3O
D.slf');
fid=telstepw(Humber2,fid);

fclose all
```

APPENDIX I

MODIFIED STEERING FILE DESCRIBING THE CONFIGURATION OF THE TELEMAC3D SIMULATION FOR OIL SPILL SCENARIO "SUMMER_HIGH WATER_NEAP TIDE"

```
/
/
 ADVECTION-DIFFUSION SCHEME WITH SETTLING VELOCITY     = 1
/
/VALIDATION                = YES
/REFERENCE FILE            = 'r3d_tidal_flats_set1.ref'
/
/ These options also work with the same time step,
/ but with more mass error
/
/ADVECTION-DIFFUSION SCHEME WITH SETTLING VELOCITY     = 0
/ADVECTION-DIFFUSION SCHEME WITH SETTLING VELOCITY     = 2
/
FORTRAN FILE                              : 'sum_oil_flot.f'
3D RESULT FILE                            : 'r3d_summer_run1.slf'
2D RESULT FILE                            : 'r2d_summer_run1.slf'
LIQUID BOUNDARIES FILE                    : 'summer1_cal.txt'
BOUNDARY CONDITIONS FILE                  : 'bc_humber3OD.cli'
GEOMETRY FILE                             : 'humber_geometry3OD.slf'
/---------------------------------------------------------------------/
/ COMPUTATION CONTINUED                   = YES
/ PREVIOUS COMPUTATION FILE               = 'T3DHYD'
/---------------------------------------------------------------------/
/
 PARALLEL PROCESSORS  = 0
/
/---------------------------------------------------------------------/
/                    OPTIONS GENERALES
/---------------------------------------------------------------------/
 TITLE                            = 'Humber Estuary - Summer'
 ORIGINAL DATE OF TIME            = 2017; 8; 1
/
 VARIABLES FOR 2D GRAPHIC PRINTOUTS = 'U,V,S'
 VARIABLES FOR 3D GRAPHIC PRINTOUTS = 'Z,U,V,W'
 /
 NUMBER OF HORIZONTAL LEVELS= 5
 /
/DURATION                         = 266400
 TIME STEP                        = 45
 NUMBER OF TIME STEPS             = 5920
 GRAPHIC PRINTOUT PERIOD          = 20
 LISTING PRINTOUT PERIOD          = 20
/---------------------------------------------------------------------/
 LAW OF BOTTOM FRICTION                        = 2
 FRICTION COEFFICIENT FOR THE BOTTOM           = 70
 TURBULENCE MODEL FOR THE BOTTOM               = 2
 HORIZONTAL TURBULENCE MODEL                   = 4
```

```
 VERTICAL TURBULENCE MODEL                    = 2
/
 MIXING LENGTH MODEL         = 3 / Nezu and Nakagawa
 DAMPING FUNCTION            = 0    / no damping
/
 COEFFICIENT FOR HORIZONTAL DIFFUSION OF VELOCITIES = 0.1D0
 COEFFICIENT FOR VERTICAL DIFFUSION OF VELOCITIES       = 1.E-6
 COEFFICIENT FOR HORIZONTAL DIFFUSION OF TRACERS      = 0.1D0
 COEFFICIENT FOR VERTICAL DIFFUSION OF TRACERS           = 1.E-6
/
 CORIOLIS                          = YES
 CORIOLIS COEFFICIENT         = 1.172E-4 /lattitude 53.72
/--------------------------------------------------------------------/
 INITIAL CONDITIONS             = 'CONSTANT ELEVATION'
 INITIAL ELEVATION              = 6
 PRESCRIBED FLOWRATES       = 30.0; 0.0; 25.0
 PRESCRIBED ELEVATIONS      = 0.0; 13.096; 0.0
/--------------------------------------------------------------------/
/
/ NON-HYDROSTATIC VERSION                                = YES
 SCHEME FOR ADVECTION OF VELOCITIES                  = 1
 ACCURACY FOR DIFFUSION OF VELOCITIES               = 1.E-6
 MAXIMUM NUMBER OF ITERATIONS FOR DIFFUSION OF VELOCITIES= 500
 PRECONDITIONING FOR DIFFUSION OF VELOCITIES  = 34
 SOLVER FOR PROPAGATION                                   = 2
 PRECONDITIONING FOR PROPAGATION                    = 2
/
 SCHEME FOR ADVECTION OF DEPTH                       = 5
 IMPLICITATION FOR DEPTH                                 = 0.55
 IMPLICITATION FOR VELOCITIES                          = 0.60
 MASS-LUMPING FOR DEPTH                                = 1.0
FREE SURFACE GRADIENT COMPATIBILITY               = 0.9     / to smooth surface levels
 MATRIX STORAGE                                              = 3
/
/--------------------------------------------------------------------/
 MASS-BALANCE                                                                                      = YES
 INFORMATION ABOUT MASS-BALANCE FOR EACH LISTING PRINTOUT          = YES
 TREATMENT OF FLUXES AT THE BOUNDARIES                                       =2;2;2
/--------------------------------------------------------------------/
/
/ tidal flats
/
 TIDAL FLATS                                   = YES
 TREATMENT OF NEGATIVE DEPTHS   = 2
 STABILIZED INITIAL CONDITION       = NO
/
/--------------------------------------------------------------------
/                         OIL SPILL
/--------------------------------------------------------------------
OIL SPILL MODEL                              : YES
OIL SPILL STEERING FILE                  : oilspill.txt
NUMBER OF DROGUES                       : 2500
PRINTOUT PERIOD FOR DROGUES        : 20
DROGUES FILE                                   : SU_N_HW.dat
/--------------------------------------------------------------------/
/ WIND
/--------------------------------------------------------------------/
WIND                                                = YES
```

```
WIND VELOCITY ALONG X                    = -4.07D0
WIND VELOCITY ALONG Y                    = -3..59D0
COEFFICIENT OF WIND INFLUENCE     = 0.565E-6
/OPTION FOR WIND                           = 1
/
/-----------------------------------------------------------------------/
/-----------------------------------------------------------------------/
/ TRACERS
/-----------------------------------------------------------------------/
/
NUMBER OF TRACERS                                                         : 1
SCHEME FOR ADVECTION OF TRACERS                                :14
INITIAL VALUES OF TRACERS                                               : 0.
STANDARD VALUES FOR TRACERS                                        : 0.
ACCURACY FOR DIFFUSION OF TRACERS                             : 1.E-22
COEFFICIENT FOR VERTICAL DIFFUSION OF TRACERS           : 0.
COEFFICIENT FOR HORIZONTAL DIFFUSION OF TRACERS       : 0.75
MAXIMUM NUMBER OF ITERATIONS FOR DIFFUSION OF TRACERS     : 5000
PRECONDITIONING FOR DIFFUSION OF TRACERS                  : 34
/-----------------------------------------------------------------------/
/
&ETA
&FIN
```

APPENDIX J:

OIL SPILL STEERING FILE

NUMBER OF UNSOLUBLE COMPONENT IN OIL
9
UNSOLUBLE COMPONENT PARAMETERS (FRAC MASS,TEB)
8.66D-02 , 368.15D0
1.052D-01 , 422.15D0
5.18D-02 , 448.15D0
9.19D-02 , 505.15D0
2.098D-01 , 615.15D0
4.48D-02 , 642.15D0
2.212D-01 , 782.15D0
4.42D-02 , 823.15D0
1.445D-01 , 858.15D0
NUMBER OF SOLUBLE COMPONENT IN OIL
1
SOLUBLE COMPONENT PARAMETERS (FRAC MASS,TEB,SOLU,KDISS,KVOL)
0, 0, 0, 0, 0
OIL DENSITY
836.9D0
OIL VISCOSITY
6.377D-6
VOLUME OF OIL SPILL
1D+04
WATER TEMPERATURE
290.597
SPREADING MODEL (1=FAY'S MODEL, 2=MIGRHYCAR'S MODEL, 3=CONSTANT AREA)
1

APPENDIX K

FORTRAN FILE SHOWING THE MODIFIED *OIL_FLOT* SUBROUTINE FOR OIL SPILL RELEASED AT L1 DURING HIGH WATER, SPRING TIDE.

```
!                  ******************
                   SUBROUTINE OIL_FLOT
!                  ******************
!
     &(PARTICULES,NFLOT,NFLOT_MAX,MESH,LT,VOLDEV,RHO_OIL,NB_COMPO,
     &NB_HAP,FMCOMPO,TBCOMPO,FMHAP,TBHAP,SOLU,ETAL,AREA,NPLAN,GRAV)
!
!***********************************************************************
! TELEMAC2D & TELEMAC3D  V6P3                          21/08/2010
!***********************************************************************
!
!brief    THE USER MUST GIVE :
!+
!+
!+   1) THE TIMESTEP WHEN THE FLOATING BODY IS RELEASED.
!+
!+
!+   2) THE TIME WHEN THE COMPUTATION IS STOPPED FOR THIS FLOATING BODY.
!+
!+
!+   3) THE INITIAL POSITION OF THE FLOATING BODY AT THE TIME OF RELEASE.
!
!history  J-M JANIN (LNH)
!+        17/08/1994
!+        V5P2
!+
!
!history  N.DURAND (HRW), S.E.BOURBAN (HRW)
!+        13/07/2010
!+        V6P0
!+   Translation of French comments within the FORTRAN sources into
!+   English comments
!
!history  N.DURAND (HRW), S.E.BOURBAN (HRW)
!+        21/08/2010
!+        V6P0
!+   Creation of DOXYGEN tags for automated documentation and
!+   cross-referencing of the FORTRAN sources
!
!history  CEDRIC GOEURY (LHSV)
!+        28/06/2013
!+        V6P3
!+   First version
!+
!Edited by Chijioke Eke
!March 2019
!Edited portion in red highlight
!~~~~~~~~~~~~~~~~~~~~~~~~~~~~~~~~~~~~~~~~~~~~~~~~~~~~~~~~~~~~~~~~~~~~~~~
!~~~~~~~~~~~~~~~~~~~~~~~~~~~~~~~~~~~~~~~~~~~~~~~~~~~~~~~~~~~~~~~~~~~~~~~
```

```
!| ELTFLO         |<->| NUMBERS OF ELEMENTS WHERE ARE THE FLOATS
!| ETAFLO         |<->| LEVELS WHERE ARE THE FLOATS
!| LT             |-->| CURRENT TIME STEP
!| MESH           |<->| MESH STRUCTURE
!| NFLOT          |-->| NUMBER OF FLOATS
!| NFLOT_MAX      |-->| MAXIMUM NUMBER OF FLOATS
!| NIT            |-->| NUMBER OF TIME STEPS
!| NPLAN          |-->| NUMBER OF PLANES
!| NPOIN          |-->| NUMBER OF POINTS IN THE MESH
!| SHPFLO         |<->| BARYCENTRIC COORDINATES OF FLOATS IN THEIR
!|                |   | ELEMENTS.
!| SHZFLO         |<->| BARYCENTRIC COORDINATES OF FLOATS IN THEIR LEVEL
!| X              |-->| ABSCISSAE OF POINTS IN THE MESH
!| Y              |-->| ORDINATES OF POINTS IN THE MESH
!| Z              |-->| ELEVATIONS OF POINTS IN THE MESH
!| XFLOT          |<->| ABSCISSAE OF FLOATING BODIES
!| YFLOT          |<->| ORDINATES OF FLOATING BODIES
!| ZFLOT          |<->| ELEVATIONS OF FLOATING BODIES
!~~~~~~~~~~~~~~~~~~~~~~~~~~~~~~~~~~~~~~~~~~~~~~~~~~~~~~~~~~~~~~~~~~~~~~~~~
!
      USE BIEF
      USE STREAMLINE, ONLY : ADD_PARTICLE
!
      IMPLICIT NONE
      INTEGER LNG,LU
      COMMON/INFO/LNG,LU
!
!+-+-+-+-+-+-+-+-+-+-+-+-+-+-+-+-+-+-+-+-+-+-+-+-+-+-+-+-+-+-+-+-+-+-+-+-+-+
!
      INTEGER, INTENT(INOUT)          :: NFLOT
      INTEGER, INTENT(IN)             :: NFLOT_MAX,LT,NPLAN
      INTEGER, INTENT(IN)             :: NB_COMPO,NB_HAP
      INTEGER, INTENT(IN)             :: ETAL
      DOUBLE PRECISION, INTENT(IN)    :: GRAV
      DOUBLE PRECISION, INTENT(IN)    :: VOLDEV,RHO_OIL,AREA
      DOUBLE PRECISION, INTENT(IN)    :: FMCOMPO(NB_COMPO)
      DOUBLE PRECISION, INTENT(IN)    :: TBCOMPO(NB_COMPO)
      DOUBLE PRECISION, INTENT(IN)    :: FMHAP(NB_HAP)
      DOUBLE PRECISION, INTENT(IN)    :: TBHAP(NB_HAP)
      DOUBLE PRECISION, INTENT(IN)    :: SOLU(NB_HAP)
      TYPE(BIEF_MESH), INTENT(INOUT)  :: MESH
      TYPE(OIL_PART), INTENT(INOUT)   :: PARTICULES(NFLOT_MAX)
!
!+-+-+-+-+-+-+-+-+-+-+-+-+-+-+-+-+-+-+-+-+-+-+-+-+-+-+-+-+-+-+-+-+-+-+-+-+-+
!
      INTEGER                         :: K,J,NUM_GLO,NUM_LOC,NUM_MAX,I
      INTEGER                         :: NFLOT_OIL
      DOUBLE PRECISION                :: RHO_EAU,PI,COEF1
      DOUBLE PRECISION                :: COEF2,DELTA,NU,NU2
      DOUBLE PRECISION                :: COORD_X, COORD_Y
      DOUBLE PRECISION                :: XFLOT(1), YFLOT(1),ZFLOT(1)
      DOUBLE PRECISION                :: SHPFLO(3,1)
      DOUBLE PRECISION                :: SHZFLO(1)
      INTEGER                         :: TAGFLO(1)
      INTEGER                         :: ELTFLO(1)
      INTEGER                         :: ETAFLO(1)
!
!+-+-+-+-+-+-+-+-+-+-+-+-+-+-+-+-+-+-+-+-+-+-+-+-+-+-+-+-+-+-+-+-+-+-+-+-+-+
```

```
!
!    THIS IS AN EXAMPLE !!!!!!!!!!!!!!!!!!!
!
     RHO_EAU=1000.D0
     PI=ACOS(-1.D0)
!    HARDCODED WATER MOLECULAR VISCOSITY
     NU=1.D-6
     NU2=NU**2
!
     COEF1=1.21D0**4
     COEF2=COEF1/1.53**2
     DELTA=(RHO_EAU-RHO_OIL)/(RHO_EAU)
!
     IF(LT.EQ.14880) THEN
      NUM_GLO=0
      NUM_MAX=0
      NUM_LOC=0
      COORD_X=0.D0
      COORD_Y=0.D0
      NUM_MAX=INT(SQRT(REAL(NFLOT_MAX)))
      DO K=0,NUM_MAX-1
       DO J=0,NUM_MAX-1
        COORD_X=536230.938D0+REAL(J)
        COORD_Y=409680.750D0+REAL(K)
        NUM_GLO=NUM_GLO+1
        NFLOT_OIL = 0
        IF(MESH%DIM.EQ.3)THEN
         CALL ADD_PARTICLE(COORD_X,COORD_Y,COORD_Y,NUM_GLO,
    &         NFLOT_OIL,1,XFLOT,YFLOT,ZFLOT,TAGFLO,SHPFLO,SHZFLO,
    &         ELTFLO,ETAFLO,MESH,NPLAN,0.D0,0.D0,0.D0,0.D0,0,0)
        ELSEIF(MESH%DIM.EQ.2)THEN
         CALL ADD_PARTICLE(COORD_X,COORD_Y,0.D0,NUM_GLO,
    &         NFLOT_OIL,1,XFLOT,YFLOT,YFLOT,TAGFLO,SHPFLO,SHPFLO,
    &         ELTFLO,ELTFLO,MESH,NPLAN,0.D0,0.D0,0.D0,0.D0,0,0)
        END IF
        IF(NFLOT_OIL.EQ.1)THEN
         NUM_LOC = NUM_LOC+1
!=======================================================================
!----INITIALIZATION PARAMETERS FOR THE CALCULATION OF PARTICULE MOTION----
!=======================================================================
         PARTICULES(NUM_LOC)%XOIL = XFLOT(1)
         PARTICULES(NUM_LOC)%YOIL = YFLOT(1)
         PARTICULES(NUM_LOC)%ID = TAGFLO(1)
         PARTICULES(NUM_LOC)%SHPOIL(1) = SHPFLO(1,1)
         PARTICULES(NUM_LOC)%SHPOIL(2) = SHPFLO(2,1)
         PARTICULES(NUM_LOC)%SHPOIL(3) = SHPFLO(3,1)
         PARTICULES(NUM_LOC)%ELTOIL = ELTFLO(1)
         IF(MESH%DIM.EQ.3)THEN
          PARTICULES(NUM_LOC)%ZOIL = ZFLOT(1)
          PARTICULES(NUM_LOC)%ETAOIL = ETAFLO(1)
          PARTICULES(NUM_LOC)%SHZOIL = SHZFLO(1)
         END IF
!=======================================================================
!-----------INITIALIZATION PARAMETERS FOR THE CALCULATION OF OIL----------
!---------------------------WEATHERING PROCESSES--------------------------
!=======================================================================
         PARTICULES(NUM_LOC)%STATE=1
         PARTICULES(NUM_LOC)%TPSECH=0
```

```
          IF(ETAL.EQ.1)THEN
            PARTICULES(NUM_LOC)%SURFACE=PI*COEF2*
     &          (DELTA*GRAV/(VOLDEV*NU2))**(1.D0/6.D0)
     &          *VOLDEV/NFLOT_MAX
          ELSEIF(ETAL.EQ.3)THEN
            PARTICULES(NUM_LOC)%SURFACE = AREA
          ELSEIF(ETAL.EQ.2) THEN
            PARTICULES(NUM_LOC)%SURFACE = 0.D0
          ELSE
            IF(LNG.EQ.1) THEN
              WRITE(LU,*) 'ETAL=',ETAL,' INCONNU DANS OIL_FLOT'
            ENDIF
            IF(LNG.EQ.1) THEN
              WRITE(LU,*) 'ETAL=',ETAL,' UNKNOWN IN OIL_FLOT'
            ENDIF
            CALL PLANTE(1)
            STOP
          END IF
          PARTICULES(NUM_LOC)%MASS0 = (VOLDEV*RHO_OIL)/NFLOT_MAX
          PARTICULES(NUM_LOC)%MASS_EVAP=0.D0
          PARTICULES(NUM_LOC)%MASS_DISS=0.D0
          DO I=1,NB_COMPO
            PARTICULES(NUM_LOC)%COMPO(I)%MASS=
     &          PARTICULES(NUM_LOC)%MASS0*FMCOMPO(I)
            PARTICULES(NUM_LOC)%COMPO(I)%TB=TBCOMPO(I)
            PARTICULES(NUM_LOC)%COMPO(I)%SOL=0.D0
            PARTICULES(NUM_LOC)%MASS=PARTICULES(NUM_LOC)%MASS+
     &          PARTICULES(NUM_LOC)%COMPO(I)%MASS
          END DO
          DO I=1,NB_HAP
            PARTICULES(NUM_LOC)%HAP(I)%MASS=
     &          PARTICULES(NUM_LOC)%MASS0*FMHAP(I)
            PARTICULES(NUM_LOC)%HAP(I)%TB=TBHAP(I)
             PARTICULES(NUM_LOC)%HAP(I)%SOL=SOLU(I)
            PARTICULES(NUM_LOC)%MASS=PARTICULES(NUM_LOC)%MASS+
     &          PARTICULES(NUM_LOC)%HAP(I)%MASS
          END DO
          NFLOT = NUM_LOC
        END IF
      END DO
    END DO
  ENDIF
!
!-----------------------------------------------------------------------
!
  RETURN
  ENDNDIF
```

APPENDIX L

PYTHON SCRIPT EMPLOYED TO CONVERT TELEMAC OIL DISPLACEMENT OUTPUT FILE (TECPLOT .dat FORMAT) TO ARCMAP (.XYZ) READABLE FORMAT.

L.1 Class definition

```
import re
class OilDrogue(object):
    def __init__(self, line):
        self.id, self.x, self.y, self.mass, self.color = self.parse(line)

    def parse(self, line):
        """
        parse the line into class variables
        """
        lt = re.split(',|\n', line)
        id = int(lt[0])
        x = float(lt[1])
        y = float(lt[2])
        mass = [float(lt[i]) for i in range(3, len(lt)-1)]
        color = int(lt[-1])
        return id, x, y, mass, color

    def __str__(self):
        return '{0},{1},{2}'.format(self.x, self.y, self.color)
```

L.2 Python script for oil slicks released at “low water neap tide summer” – 01/08/2017 18:45 (Release time step = 67500).

```
# (c) Hailiang Shen, Ph.D., P.Eng. hlshen2005@gmail.com
# 2018-05-02
# Modified by Chijioke Eke to output oil slick displacement at every 15-minutes time step
import os
import sys
from struct import pack
import datetime
from collections import defaultdict
from OilDrogue import OilDrogue

class OilParticle2Pcl(object):
    def __init__(self, displacement_file, Nmass=1):
        self.Ddrogues = defaultdict(list)
        self.times = []
        self.read_displacement_file(displacement_file)
        self.Nmass = Nmass
```

```
        self.pcl = None

    def read_displacement_file(self, placement_file):
        """
        read displacement file into class variables
        """
        if not os.path.exists(placement_file):
            print ('{0} does not exist'.format(placement_file))
            return

        current_time = -99
        for line in open(placement_file, 'rt'):
            line = line.strip()
            if line == '':
                continue
            if 'ZONE' in line:    # parse the time in second
                k = line.rfind('=')
                current_time = float(line[k+1:])
                self.times.append(current_time)
            elif current_time != -99:
                self.Ddrogues[current_time].append(OilDrogue(line))

    def to_xyz_file(self, xyz_file, current_time):
        """
        convert to xyz file, only contains the results in one single time step
        """
        with open(xyz_file, 'wt') as f:
            for od in self.Ddrogues[current_time]:
                f.write('{0}\n'.format(str(od)))

def test():
    i = 67500.0000
    c = OilParticle2Pcl(r"SU_L1_N_LW.dat")
    c.to_xyz_file(r'01.xyz', i)
    c.to_xyz_file(r'02.xyz', i + 900)
    c.to_xyz_file(r'03.xyz', i + 1800)
    c.to_xyz_file(r'04.xyz', i + 2700)
    c.to_xyz_file(r'05.xyz', i + 3600)
    c.to_xyz_file(r'06.xyz', i + 4500)
    c.to_xyz_file(r'07.xyz', i + 5400)
    c.to_xyz_file(r'08.xyz', i + 6300)
    c.to_xyz_file(r'09.xyz', i + 7200)
    c.to_xyz_file(r'10.xyz', i + 8100)
    c.to_xyz_file(r'11.xyz', i + 9000)
    c.to_xyz_file(r'12.xyz', i + 9900)
    …
    …
    …
    c.to_xyz_file(r'191.xyz', i + 171900)
    c.to_xyz_file(r'192.xyz', i + 172800)
    c.to_xyz_file(r'193.xyz', i + 173700)

if __name__ == '__main__':
    test()
```

APPENDIX M

SENSITIVITY ANALYSIS OF MODEL TO FLOW

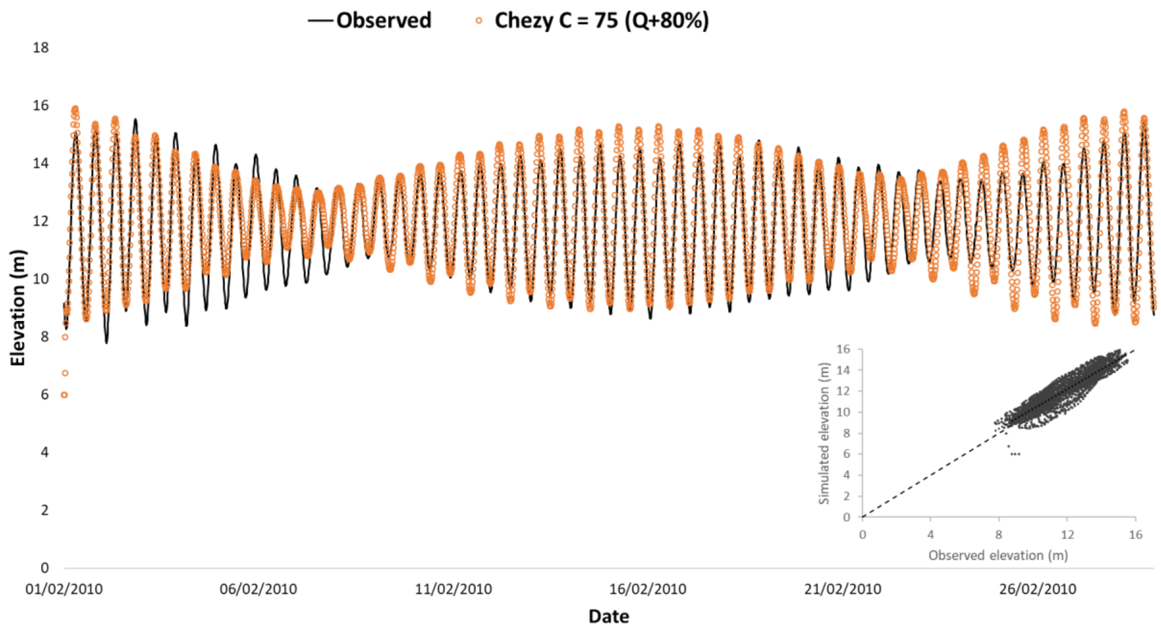

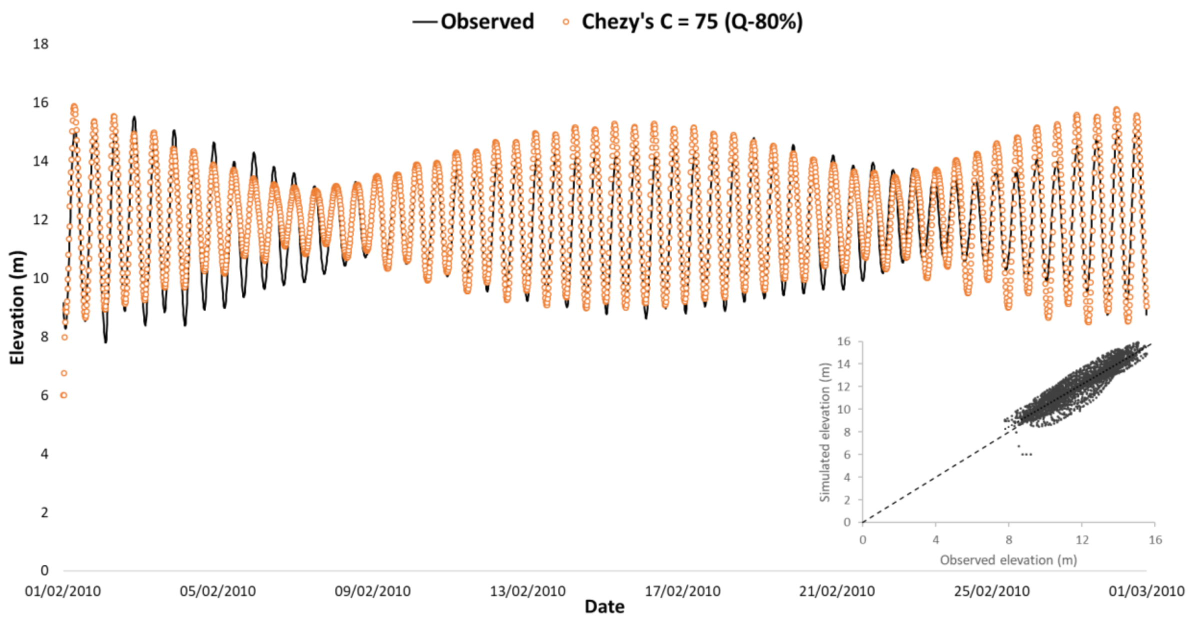

Table M.1: Calibration metrics comparing observed and simulated tidal heights as a function of Chezy C. Best values for each metric are indicated as underlined italics.

Season (representative month)	**Chezy C = 75**	**RMSE** (m)	**R^2**	**b**
Winter (February 2010)	Q + 80%	<u>*0.707*</u>	<u>*0.853*</u>	<u>*0.938*</u>
	Q – 80%	0.711	0.852	0.935

APPENDIX N

ONE WAY ANOVA (P<0.05) FOLLOWED BY HOLM-SIDAK TEST

N.1 OIL SLICK IMPACTED AREA

season (summer/winter)	water level (high water/low water)	tide (spring tide/neap tide)
1.12	1.69	2.44
0.81	1.23	2.31
1.18	1.74	2.37
1.04	1.53	1.86

Anova: Single Factor

SUMMARY

Groups	*Count*	*Sum*	*Average*	*Variance*
season	4	4.15	1.0375	0.026291667
water level	4	6.19	1.5475	0.052825
tide	4	8.98	2.245	0.0687

ANOVA

Source of Variation	*SS*	*df*	*MS*	*F*	*P-value*	*F crit*
Between Groups	2.93955	2	1.469775	29.82968768	0.00010689	4.256495
Within Groups	0.44345	9	0.049272			
Total	3.383	11				

alpha	0.05
i	rank
m (level)	3

		t test	Rank (i)	root (m+1-i)	1 - alpha		Holm-Sidak
season	water level	0.013254	3	1	0.9500	0.95	0.050000
water level	tide	0.007356	2	2	0.9500	0.974679	0.025321
tide	season	0.000542	1	3	0.9500	0.983048	0.016952

N.2 OIL SLICK LENGTH

season (summer/winter)	water level (high water/low water)	tide (spring tide/neap tide)
0.96	1.57	2.08
0.76	1.24	2.22
0.90	1.64	1.99
0.88	1.61	1.71

Anova: Single Factor

SUMMARY

Groups	*Count*	*Sum*	*Average*	*Variance*
season	4	3.5	0.875	0.00703333
water level	4	6.06	1.515	0.03443333
tide	4	8	2	0.04633333

ANOVA

Source of Variation	*SS*	*df*	*MS*	*F*	*P-value*	*F crit*
Between Groups	2.54726667	2	1.273633	43.5182232	2.36118E-05	4.256495
Within Groups	0.2634	9	0.029267			
Total	2.81066667	11				

alpha	0.05
i	rank
m (level)	3

		t test	Rank (i)	root (m+1-i)	1 - alpha		Holm-Sidak
season	water level	0.00282692	2	2	0.95	0.974679	0.025320566
water level	tide	0.01474891	3	1	0.95	0.95	0.05
tide	season	0.00071283	1	3	0.95	0.983048	0.016952428

N.3 OIL SLICK DISTANCE TRAVELLED

season (summer/winter)	water level (high water/low water)	tide (spring tide/neap tide)
0.98	1.71	1.74
0.73	1.26	1.71
1.01	1.53	1.95
0.83	1.26	1.72

Anova: Single Factor

SUMMARY

Groups	*Count*	*Sum*	*Average*	*Variance*
season	4	3.55	0.8875	0.017225
water level	4	5.76	1.44	0.0486
tide	4	7.12	1.78	0.013

ANOVA

Source of Variation	*SS*	*df*	*MS*	*F*	*P-value*	*F crit*
Between Groups	1.623216667	2	0.811608	30.88899461	9.3229E-05	4.256495
Within Groups	0.236475	9	0.026275			
Total	1.859691667	11				

alpha	0.05
i	rank
m (level)	3

		t test	Rank (i)	root (m+1-i)	1 - alpha		Holm-Sidak
season	water level	0.008062239	2	2	0.95	0.974679	0.025320566
water level	tide	0.045698315	3	1	0.95	0.95	0.05
tide	season	5.63128E-05	1	3	0.95	0.983048	0.016952428

APPENDIX O

BOXPLOTS OF RELATIVE INFLUENCES OF HYDRODYNAMIC PROPERTIES

O.1 OIL SLICK IMPACTED AREA

	season (summer/winter)	water level (high water/low water)	tide (spring tide/neap tide)
	1.12	1.69	2.44
	0.81	1.23	2.31
	1.18	1.74	2.37
	1.04	1.53	1.86
average	1.04	1.55	2.25
percentile			
0.00	0.81	1.23	1.86
0.05	0.86	1.29	1.94
0.25	1.04	1.53	2.25
0.50	1.04	1.55	2.31
0.75	1.12	1.69	2.37
0.95	1.17	1.73	2.43
1.00	1.18	1.74	2.44
differences			
0.25-0.00	0.23	0.30	0.39
0.25-0.05	0.18	0.24	0.31
0.50-0.25	0.00	0.02	0.06
0.75-0.50	0.08	0.14	0.06
0.95-0.75	0.05	0.04	0.06
1.00-0.75	0.06	0.05	0.07

O.2 OIL SLICK LENGTH

	season (summer/winter)	water level (high water/low water)	tide (spring tide/neap tide)
	0.96	1.57	2.08
	0.76	1.24	2.22
	0.90	1.64	1.99
	0.88	1.61	1.71
average	0.88	1.52	2.00
percentile			
0.00	0.76	1.24	1.71
0.05	0.78	1.30	1.77
0.25	0.88	1.52	1.99
0.50	0.88	1.57	2.00
0.75	0.90	1.61	2.08
0.95	0.95	1.63	2.19
1.00	0.96	1.64	2.22
differences			
0.25-0.00	0.12	0.28	0.28
0.25-0.05	0.09	0.22	0.22
0.50-0.25	0.01	0.05	0.01
0.75-0.50	0.02	0.04	0.08
0.95-0.75	0.05	0.02	0.11
1.00-0.75	0.06	0.03	0.14

O.3 OIL SLICK DISTANCE TRAVELLED

	season (summer/winter)	water level (high water/low water)	tide (spring tide/neap tide)
	0.98	1.71	1.74
	0.73	1.26	1.71
	1.01	1.53	1.95
	0.83	1.26	1.72
average	0.89	1.44	1.78
percentile			
0.00	0.73	1.26	1.71
0.05	0.75	1.26	1.71
0.25	0.83	1.26	1.72
0.50	0.89	1.44	1.74
0.75	0.98	1.53	1.78
0.95	1.00	1.67	1.92
1.00	1.01	1.71	1.95
differences			
0.25-0.00	0.10	0.00	0.01
0.25-0.05	0.08	0.00	0.01
0.50-0.25	0.06	0.18	0.02
0.75-0.50	0.09	0.09	0.04
0.95-0.75	0.02	0.14	0.14
1.00-0.75	0.03	0.18	0.17

APPENDIX P

MEASUREMENT OF CURRENT VELOCITY ACROSS THE LENGTH AND WIDTH OF THE HUMBER ESTUARY SIMULATION.

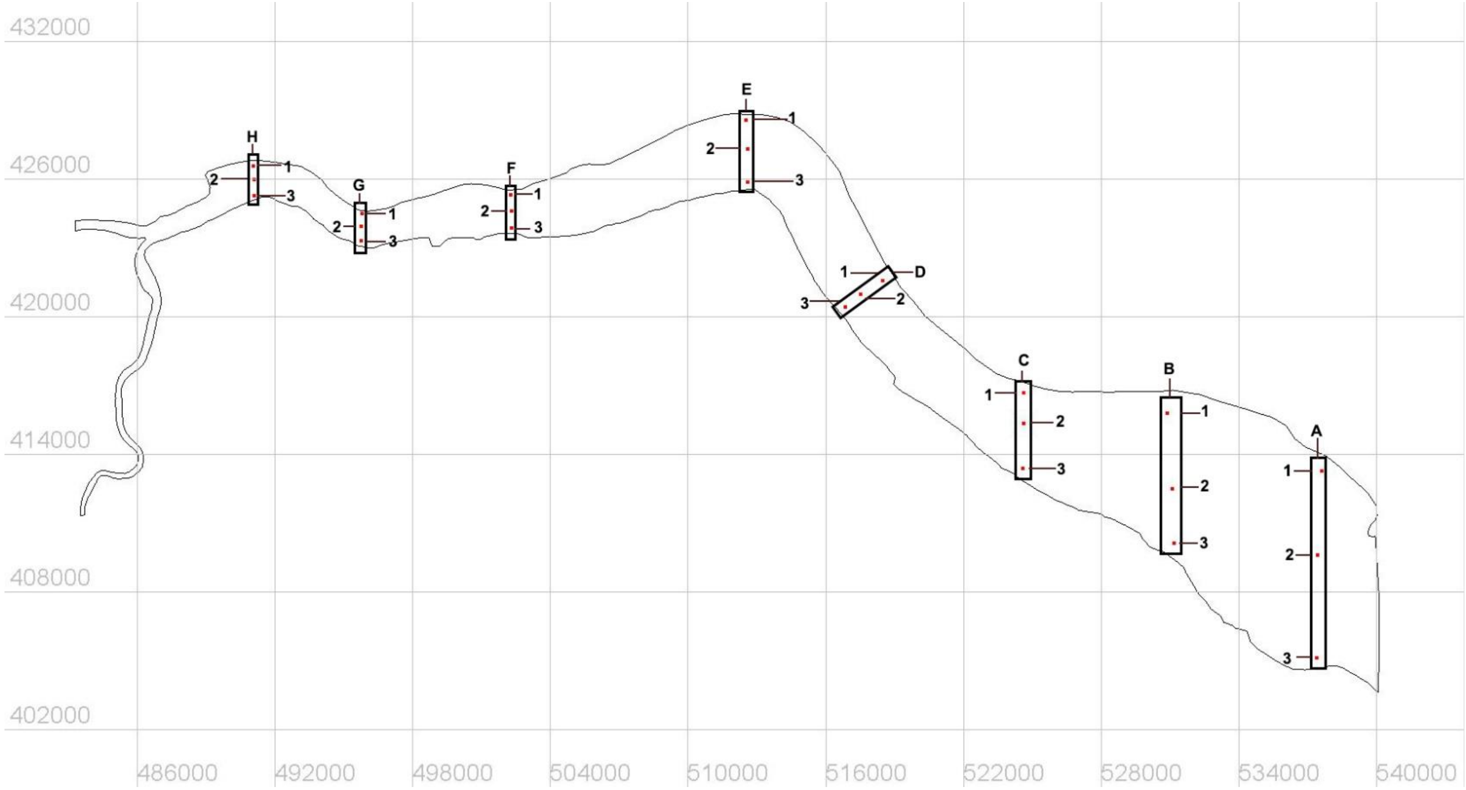

Figure P.1: Outline for the computational domain with red dots showing points were current velocity was extracted.

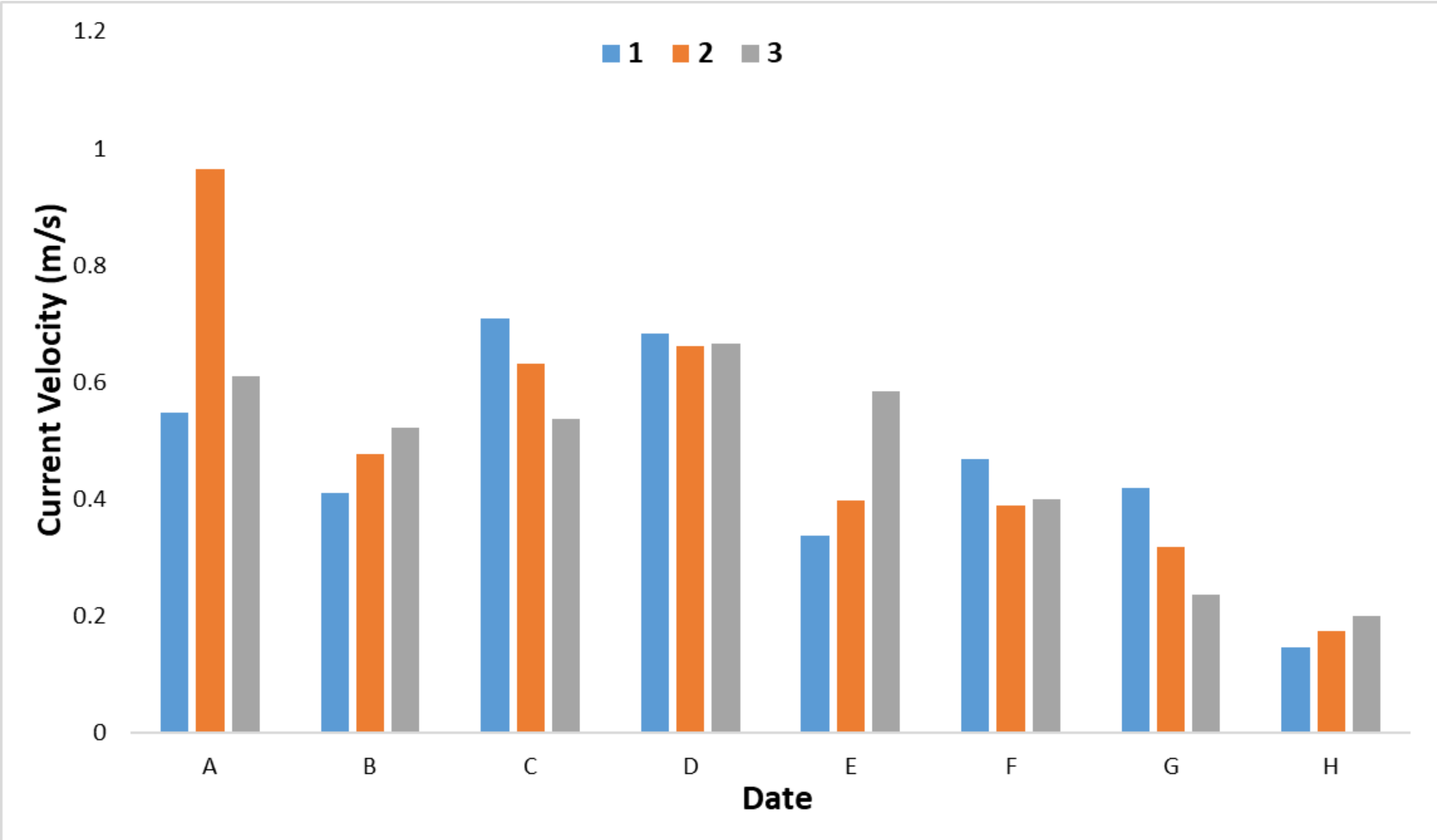

Figure M.2: Average free surface velocities covering the duration of the oil spill (08/08/2017 – 11/08/2017)

Low Risk Research Ethics Approval

Content removed on data protection grounds

Content removed on data protection grounds

Content removed on data protection grounds

Content removed on data protection grounds

Content removed on data protection grounds

Content removed on data protection grounds

Content removed on data protection grounds

Content removed on data protection grounds

Content removed on data protection grounds

Content removed on data protection grounds

Content removed on data protection grounds